International Scientific-Technical and Production Journal

CONTENTS

CURRENT PROBLEMS IN WELDING AND LIFE OF STRUCTURES

GLORIOUS JUBILEE

The staff of the E.O. Paton Electric Welding Institute are extending heartfelt greetings to their leader, outstanding scientist in the field of electric welding, metallurgy and technology of metals, on the occasion of his 85th birthday anniversary and 50th anniversary of his activity as Director of the Institute. Boris E. Paton has adequately followed up and further developed the cause of his farther, Evgeny Oskarovich Paton, the founder of the Institute, turning the Institute into a world-renowned science and technology center on welding and allied technologies. Many technologies emerged at the Institute, which were accepted not only in Ukraine, but also in many countries of the world.

Prof. B. Paton has also done a lot for consolidation of the Academy of Sciences of Ukraine, where he has been president since 1962 without interruption. Over the past years the Academy has grown immensely, and became an authoritative organization in the most diverse areas of modern science.

Boris Paton has proved to be a talented scientist and outstanding organizer, capable of managing the research conducted by large teams of scientists. The most important thing for him is achievement of significant results in the priority areas of R&D. He never tries to emphasize his role and prefers to promote talented staff members full of initiative, enthralling them with new ideas. Such a leader's style creates ideal conditions for productive creativity, and the basis for establishing a sound atmosphere in a working team.

Boris Paton started his scientific-technical activity during the Second World War at the Electric Welding Institute, which became actively involved in the work to satisfy the needs of the defense industry in the Nizhny Tagil Tank-Building Factory, where the famous T-34 tanks were made. This was where he began studying automatic regulation of the processes of welding with continuous feed of filler wires into the arc zone. It resulted in determination of the basic requirements to the static and dynamic characteristics of the drives of automatic regulation systems, which formed the basis for development of the first generation of semi-automatic machines, using thin electrode wire in combination with shielding fluxes and gases. Later on B. Paton began studying the physical processes in the arc, responsible for transfer of electrode metal into the molten pool, in order to find the methods to reduce spattering. He established a significant influence on this process of the external characteristics of the power source, and demonstrated the rationality of applying the sources with a flat external characteristic for semi-automatic and automatic welding. These research results formed the basis for development of the processes of welding in CO_2 and gas mixtures, pulsed-arc welding, which still predominate in the technologies of welding fabrication. The first work of B. Paton essentially formed the scientific basis for development of modern welding equipment.

Dealing with welded bridges, Evgeny Paton dreamed about a method of mechanized welding of joints in different positions in space. Such a welding process with forced formation of the metal was developed with Boris E. Paton participation and first used in construction of a bridge in Kyiv, which is named after Evgeny Paton.

When selecting research subjects, B. Paton is often guided by the needs of a particular industry, so that the work results could be further effectively used in practice. He came to the conclusion that development of a number of mechanical engineering sectors in the Soviet Union was restrained by the difficulties of fabrication of large-sized equipment, and in order to overcome these difficulties it was necessary to develop an inexpensive and simple enough process of welding thick-walled parts. This science and technology challenge was solved by development of electroslag welding technology, which was used in manufacture of powerful hydraulic turbines, presses, chemical reactors and other vessels.

Studying various welding processes as control objects was first outlined by B. Paton as one of the most important fields in the theory of welding processes and thus became the research subject for many specialists. In addition to the problems of control of arc and electroslag welding, he also dealt with electrical engineering methods of improvement of various welding processes. B. Paton made a considerable contribution to development of flash-butt and spot welding, where the systems of automatic control of the process are the key elements, determining the technological parameters and reliability of welding equipment. He guided the development of generations of unique machines for flash-butt welding of parts of large cross-sections of high-strength steels and alloys, in particular, for welding components of high-strength aluminium alloys used in aerospace industry and aircraft engineering, and for welding the main pipelines. This equipment is used in various industrial sectors and has no analogs in the world practice. B. Paton's contribution to study of physical principles of electron beam and microplasma welding and development of up-to-date equipment for these processes is substantial.

B. Paton was the first to suggest application of welding in space. His ideas, warmly supported by Sergey Korolyov in mid-60s, initiated investigations in this promising field of modern engineering, which demonstrated the possibility of construction and subsequent operation of large-sized manned facilities in

space. A special research unit «Vulkan» was developed for the first space welding experiment with direct participation and guidance of B. Paton, which was used in space in 1969. The attractiveness of applying the electron beam for welding, cutting, brazing and coating deposition of metallic materials under the conditions of space was demonstrated. Versatile manual hardware «Universal» was also developed and tested in open space by cosmonauts V. Dzhanibekov and S. Savitskaya in 1984. The hardware is suitable for the above technological processes. In the USA, Japan and Germany investigations on welding in space started much later.

By B. Paton's initiative the Institute began working on underwater welding, for which purpose a special laboratory was set up and fitted, where underwater arc welding can be performed at different pressures. This work resulted in development of self-shielded flux-cored wire and a semi-automatic machine for welding under the water at a sufficiently high pressure.

B. Paton attached a lot of importance to explosion welding and cutting. By his initiative and with his participation, special testing grounds were set up, where metal welding and cutting with cumulative charges can be performed, and manufacturing of batches of charges for welding and cutting under special conditions, for instance under the water, was established.

It is impossible to enumerate all the fields of research and inventor's activity of B. Paton, which over half a century formed the basis of the activity of a large scientific-technical team, led by him.

Work related to welding application in medicine can be noted as some of the original research of the recent years. This is primarily joining the incisions of various soft live tissues, instead of stitching them. It is has been proved that electric welding by high frequency currents is possible in this case, and that it has advantages over the traditional method of stitching by many indices. Pilot samples of equipment with control devices, which provide feedback from the process of joint formation, have been developed. More than 1000 patients have been operated on with positive results with participation of a large team of Kyiv surgeons, using the new procedure. There is every ground to believe, that welding of soft live tissues will become accepted in many clinics eventually, as an effective surgical technique.

B. Paton is the originator of new ideas, he has an exceptional sense of all the new developments, which emerge in the allied fields of science and technology, and which may be used for welding. He was the initiator of application of beam heating sources (electron beam, laser) for welding. His unyielding support resulted in electron beam welding becoming widely accepted in our country from the very first years of introduction of this heating source. Now B. Paton is giving special attention to outlining new fields of laser application.

B. Paton may be rightfully regarded as the founder of a number of new special metallurgical technologies. Weld metal after electroslag processing turned out to have higher physical properties than that produced by regular melting processes. Profound study of this phenomenon led to development of the technology of electroslag metallurgy. Special shops were set up with the capacity of several tons of metal per year, designed for fabrication of critical items. Work of B. Paton and his staff in this field was recognized in many countries, including the USA, Germany, France, Japan, etc.

Processes of plasma and electron beam welding formed the basis of other special electrometallurgical processes of steel making. The areas of their application were established, where they are the most effective and useful. In particular, it was possible to develop the electron beam technology of producing composite materials from metals, immiscible in the molten condition. This technology was called physical vapour deposition technology due to the fact that formation of the final product is achieved by vapour deposition and their solidification on a substrate without liquid pool formation. It is anticipated that this new technology will become applied in the future.

B. Paton initiated investigations on various methods of coating deposition by spraying at the Institute, beginning from the 1980s. These studies resulted in improvement of the plasma and flame processes of spraying, development of filler materials, providing coatings with special higher service characteristics. Work in this field is successfully carried on.

In connection with the fact that the design life of the main pipelines, reactors (including nuclear), railway bridges, large volume tanks and other critical structures and constructions is over, technical diagnostics and non-destructive testing methods of quality control are becoming particularly important. B. Paton takes part in development of methods and means for this purpose, as well as procedures for evaluation of the performance of critical constructions, which have been in service for a long time. He performs a tremendous amount of work on coordination of programs and measures, aimed at determination of the technical condition and extension of the life of highly hazardous facilities, being Chairman of the Interdepartamental Commission on Scientific-Technical Safety at the Council of National Security and Defense of Ukraine and Chairman of the Science-Coordination and Expert Council on Residual Life and Safe Operation of Structures, constructions and machines at the Presidium of the National Academy of Sciences of Ukraine.

In 1958 by the decision of the Government, PWI was entrusted with the functions of the head research organization on welding in the country. B. Paton became the Head of the Coordination and Scientific Councils set up at the Institute, which included the most prominent welding scientists and specialists. In addition to coordination of research and design developments, the head institute was putting together

and coordinating the fulfillment of government approved integrated programs of development of welding science, engineering and material-technical basis of welding fabrication in the USSR. B. Paton's activity in this field is simply invaluable ---- welding fabrication, science and engineering acquired the necessary dynamism and exceeded the world level as to some indices.

One may have the impression that one person, no matter how talented he is, cannot cope with intensive activity addressing such a multitude of problems, just a fraction of which was enumerated above. However, such an impression would be incorrect. A characteristic trait of B. Paton consists in his ability to see the essence of each problem, to clearly and precisely outline the ways to solve it, and to involve his staff as deeply as he himself is fascinated by it. B. Paton shows real passion in searching for problems, where he and his team could be useful. He is author of many patents and in his every day activity he gives a lot of his attention to inventor's efforts. Many of the inventions emerged in his study during meetings and discussions of urgent problems in the field of welding.

At present the Institute, similar to other research institutions, is going through a difficult transition period. However, through the efforts of B. Paton, the Institute has been preserved and is functioning actively. Traditions are unchanged and the main scientific staff continue working fruitfully. Over the recent years a number of companies were set up, based at the Institute, which are improving the developments to meet customer requirements and are promoting the Institute's developments in industry and construction. Production and innovation firms with different forms of property established the E.O. Paton Electric Welding Institute Science and Technology Park.

B. Paton's role in organizing the activity of the Academy of Sciences of Ukraine in certainly great. B. Paton sees his main goal in preserving the Academy institutions and their staff in the active condition, training a new generation of scientists and as far as possible, creating proper conditions for their work. Considering the very limited funding, all this is difficult but necessary to implement. As in the previous times, the Academy's staff are relying on the energy and unyielding determination of B. Paton, needed to overcome the temporary difficulties.

B. Paton is a fervent supporter of preservation and consolidation of the creative and business contacts between scientists and representatives of industry from different countries, he develops such new forms of scientific-technical co-operation, as integrated implementation of international programs, organizing joint laboratories and ventures, and extensive information exchange. PWI is a member of the International Institute of Welding and European Welding Federation.

B. Paton is a member of the International Committee on Scientific-Technological Development of CIS countries, Head of Interstate Council on Welding and Allied Technologies, he is Chairman of the Co-ordination Council of Interstate Program «Highly Reliable Pipeline Transport», Board Member of International Fuel-Energy Association and member of Board of Trustees of the International Nuclear Safety Foundation.

The scope of international and public activity of Boris E. Paton is represented by his being President of the International Association of the Academy of Sciences, Honorary President of the International Engineering Academy, member of the European Academy and International Academy of Technological Sciences, Honorary Member of the International Academy of Sciences, Education, Industry and Art, International Aeronautical Academy, Roman Club, Honorary Doctor of a number of major universities and Foreign Member of Academies and Scientific-Technical Societies of many countries.

B. Paton is winner of Lenin and State Prizes of the USSR, Honoured Worker of Science and Technology of Ukr. SSR, Honoured Inventor of the USSR, twice Hero of Socialist Labour, Hero of Ukraine; his awards include the Order of Lenin, Labour Red Banner, Friendship of the Peoples, «For Services to Homeland», Order of Prince Yaroslav the Wise and other local and foreign orders and medals.

He was granted numerous scientific awards and diploma, including M.V. Lomonosov Gold Metal of the USSR Academy of Sciences, Gold Medal of Lausanne Association of Italian Metallurgists, Acad. S.I. Vavilov medal of USSR Academy of Sciences, V.G. Shukhov Gold Medal of the Union of Engineers and Scientific-Technical Societies of Russia, Gold Medal of the World Organization of Intellectual Property V. Vernadsky Award of «Ukraine ---- XXI Century» Foundation for Intellectual Co-operation, etc.

We are happy that Boris E. Paton is full of energy and creative ideas and are sincerely wishing him new outstanding achievements in his titanic activity for the benefit of science, sound health and great personal happiness for many years to come.

E.O. Paton Electric Welding Institute
Editorial Board «The Paton Welding Journal»

CURRENT TRENDS OF RESEARCH AND DEVELOPMENT IN THE FIELD OF WELDING AND STRENGTH OF STRUCTURES

B.E. PATON

E.O. Paton Electric Welding Institute, NASU, Kyiv, Ukraine

The paper presents some developments made lately by the E.O. Paton Electric Welding Institute, such as hybrid welding methods, activation of processes occurring in the weld pool under the effect of minor additions of chemicals, electric arc welding using an embedded electrode, machines for flash butt and electron beam welding, new filler alloys and fluxes for brazing, and new structural materials. It is noted that structures, constructions and equipment that approach their critical age have substantially increased in number. In this connection, the pressing problem is reliable estimation of residual life of structures using non-destructive testing and technical diagnostics methods. Technology and instruments for welding of live tissues are considered.

Continuous increase in science intensity of welding production leads to improvement of the quality of products, rise in their effectiveness and competitiveness. At present welding is applied for making permanent joints in a very wide range of metallic, non-metallic and composite structural materials under conventional conditions of earth atmosphere, in ocean and in space. Volumes of the world welding fabrication amount to hundreds of millions of tons.

Steel continues to be the main structural material in welding production, despite a progressively increasing amount of light alloys, polymeric and composite materials applied for the fabrication of welded structures. World manufacturers have materially ruled out forecasts of futurologists concerning replacement of steel by alternative materials. So far, metallurgists are winning a competition in the market of structural materials owing to the development and production of new steel grades, primarily the high-strength ones, and revolutionary modifications of the production processes. The world production and consumption of steel, despite some cases of decline, are characterised by a steady growth. While in 1995 the world output of steel was 750 mln t, by 2005 it will be over 900 mln t, as predicted by the International Institute of Welding.

It is a known fact that fabrication of welded parts, structures and constructions constitutes up to 70 % of the world consumption of metal rolled products. Given that welded metal structures, owing to their good recycling ability, are compatible with the environment, they have a high potential for wide application in the near future.

The above peculiarities determine the general positive trend in the world welding fabrication, dynamic development of the world and regional welding markets, as well as scopes of the R&D activity in development and improvement of welding and related technologies. The E.O. Paton Electric Welding Institute is involved in a wide range of activities in the field of welding and strength of structures.

A new area, i.e. hybrid welding processes, has been formed in the last years in the field of high technologies. A new method for welding thin sections of aluminium alloys was offered. It consists in a simultaneous utilisation of laser beam and microplasma arc burning in a mode of different-polarity pulses of the electric current. The combined effect on metal by the two heat sources enables a substantial increase in the efficiency of utilisation of energy of each of them. As a result, the factor of utilisation of the microplasma arc power may grow from 50 % (in conventional microplasma welding) to 75 % (in the hybrid process).

In hybrid welding of aluminium alloy AMg3, 3 mm thick, at a speed of 0.25 m/min using no filler, the full penetration is achieved at a laser power of 1.2 kW and arc current of 35 A. The penetration depth in microplasma and laser welding under the same conditions is 0.7 and 0.4 mm, respectively. The cross section area of the weld in hybrid welding is 4 times as large as the sum of the corresponding areas in laser and microplasma welding (Figure 1).

One of the promising lines of development of welding is activation of processes occurring in the weld pool and arc burning in inert gases using minor additions of chemical elements. The level of understanding of the nature of the activation phenomenon makes it possible to use it for increasing the efficiency and improvement of the plasma and MIG welding processes. As shown by investigations, the penetration depth in this case increases by a factor of 2 and 4, respectively. That is, the activation creates preconditions for performing welding in inert gases at decreased heat input.

The new process of electric arc welding using a special embedded electrode covered with a thin layer
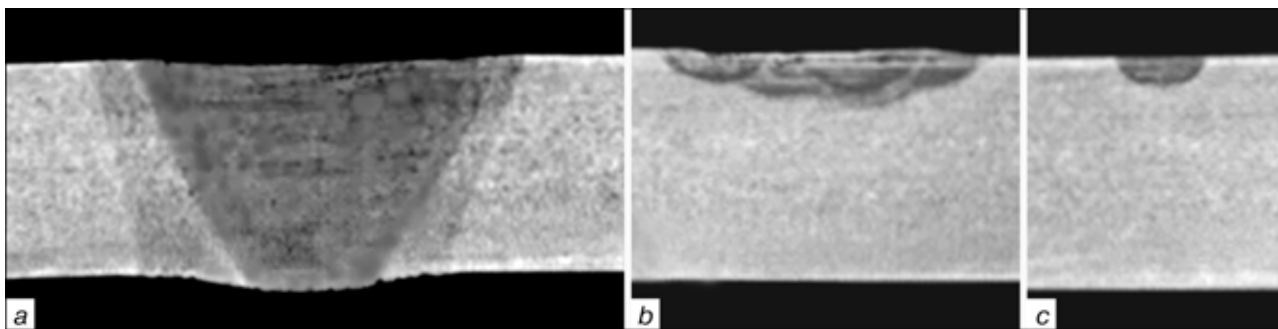
Figure 1. Penetration of metal in hybrid (*a*), microplasma (*b*) and laser (*c*) welding of aluminium alloy AMg3

(about 1 mm thick) of the insulation coating, which is preliminarily introduced into the narrow gap between the parts welded, has been developed for joining thick sections. Welding is performed in a vertical position in single pass. This enables avoidance of devices for movement of the welding arc. The latter moves on its own over the tip of a flat electrode within the entire width of the gap, providing the desirable penetration of edges. Figure 2 shows a butt joint in rails made by this method. Welding using the embedded electrode is carried out in the automatic mode. Compared with other methods intended for joining thick sections, it offers a number of advantages, such as the possibility of welding under field conditions and in hard-to-reach locations, as well as high productivity.

Flash butt welding is one of the most efficient methods for joining metals. This area is progressing with advantage, and capabilities of this process are far from being exhausted. A new modification of the continuous flash butt welding method, termed the pulsed flash butt welding, has been developed. This method, patented in the leading world countries, enables a substantial improvement in the indicators of

flash butt welding and widening of its application field. In particular, the time of welding can be reduced 2--3 times, and metal losses as well as power consumption can be decreased. At the same time, the process allows metal to be heated to high temperatures, which is required for welding high-strength steels and alloys. The new method has a guaranteed application owing to the development of the welding process control systems using the advanced automation and computer facilities. Such systems provide not only a multifactorial automatic control of the welding process, but also a simultaneous diagnostics of the quality of welded joints. The new method served as the basis for the development of technologies for joining high-strength rails, dissimilar materials, such as Hatfield steel to rail steel, tools steels, and rolled billets with a large cross section area.

New generations of machines for flash butt welding of rails, railway frogs (Figure 3) and rolled products are available. The Kakhovka Plant for Electric Welding Equipment manufactures these machines on a mass scale and exports them to many countries all over the world.

Rapid progress takes place in the field of EBW: equipment is upgraded, and new techniques and designs are developed. Efforts in upgrading the equipment are aimed mostly at realisation of the possibility of joining parts of complex configurations by EBW, which is achieved through using the computer-aided control for all the sub-systems of the machine and the course of the technological process.

Figure 2. Butt joint in rail of the R-65 steel made by electric arc welding using embedded electrode
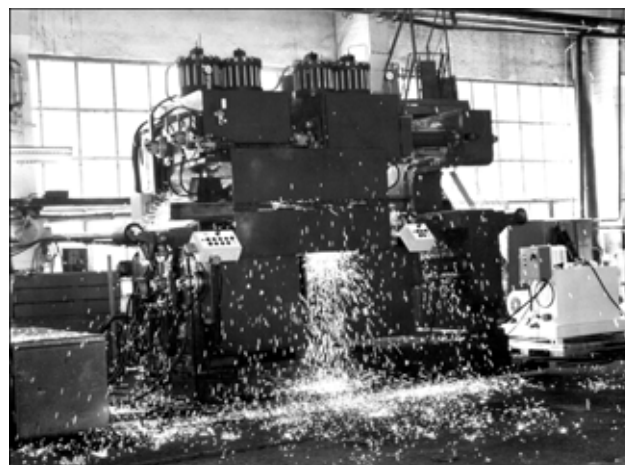
Figure 3. Machine for flash butt welding of railway frogs
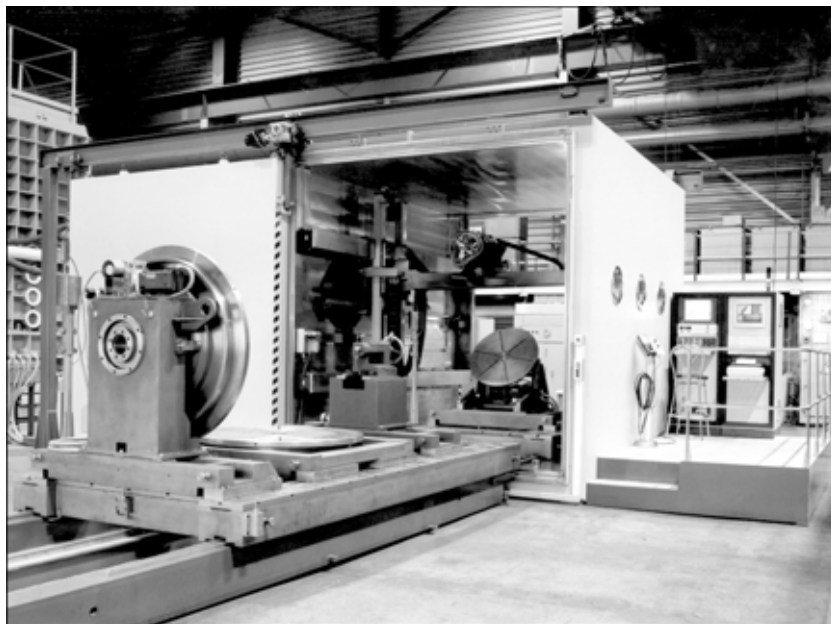
Figure 4. General view of computerised machine KL-115 for EBW of large-size parts

In the KL-115 EBW machine (Figure 4) the computer control provides movement of the welding gun along seven axes: three linear axes, turning and rotation of the gun along two axes, and turning and rotation of the workpiece manipulator. It is possible to simultaneously control movement along any four axes and all the welding process parameters, which enables welding of parts of any configuration. The secondary-emission seam tracking system RASTR eliminates any deviation of the beam from the joint, which may be caused by thermal distortions of a workpiece during welding.

Mastering of the process of a pulsed impact on the weld pool by electron beam led to a substantial improvement in the shape of welds. In particular, the welded joints in steel 60 mm thick made in flat position with the molten zone about 1 mm wide and the weld aspect ratio equal to 40 (Figure 5) were provided owing to the use of longitudinal serrated scanning of the electron beam. Compared with penetration by a static beam, the weld aspect ratio in this case increases more than twice. Rounding in the weld root (with a radius of 0.5 mm), favourable for eliminating the root defects, was achieved on blind welds. It should be noted that these welds are hardly inferior in their geometry to the welds made by using equipment with an accelerating voltage of 150 kV.

The technology and equipment developed allow the electron beam to be used for the fabrication of different-application structures, such as billets for passenger aircraft wings of high-strength aluminium alloy (Figure 6).

In view of an increasing variety of combinations of hard-to-weld dissimilar materials, much consideration is given to basic and applied research in the field of brazing. New filler metals for brazing high nickel alloys, such as those based on the Ni--Cr--Zr system, have been developed. These brazing filler metals have a new quality level, compared with traditional ones.

They make it possible to considerably widen the scope of application of manufacturing and repair brazing in modern engine construction.

Much progress has been achieved in the field of development of filler metals for brazing alloys on the base of intermetallics, such as γ-TiAl, which is the alternative to high nickel alloys. Joints produced by using the developed filler metals exhibit strength close to that of base metal at room and high temperatures (700 °C), and in testing to long-time strength (Table).
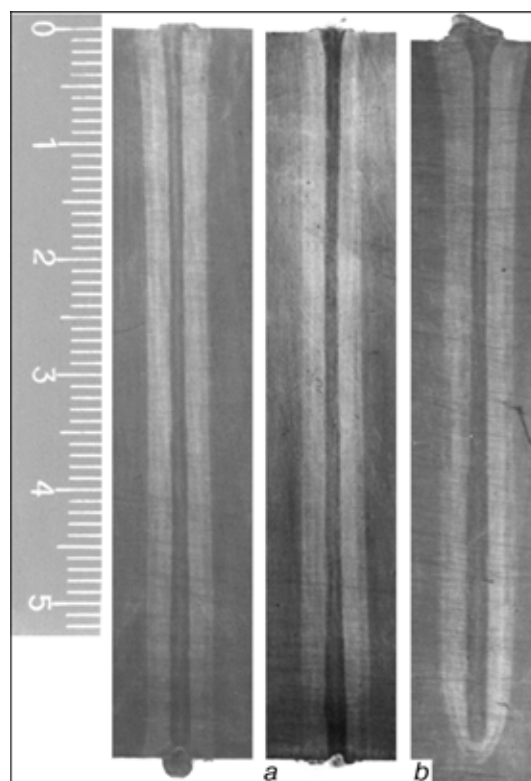
Figure 5. Welds on steel made with through (*a*) and blind (*b*) penetration in flat position (U_{acc} = 60 kV, I_b = 235 mA, v_w = = 18 m/h, serrated scanning of the beam of special configuration)
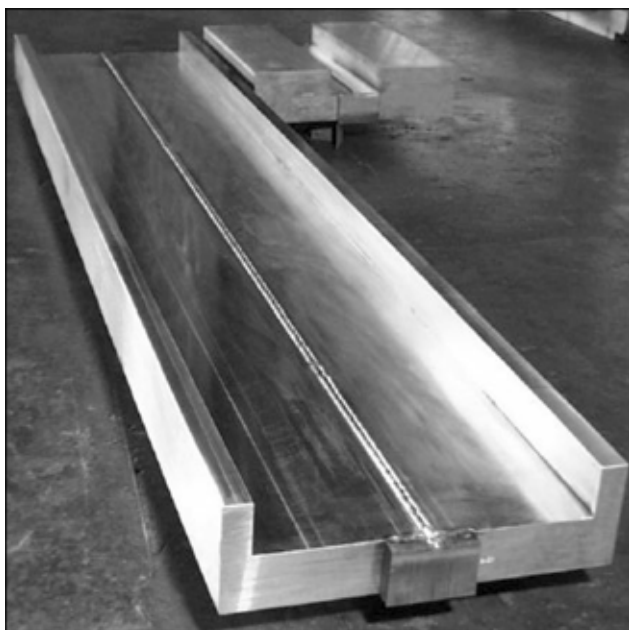
Figure 6. EB welded billet of a passenger plane wing 100 mm thick made from high-strength aluminium alloy

The new flux for brazing aluminium has been developed. A distinctive feature of this flux is that brazing can be performed without filler metal. The latter is formed due to reaction of the flux components with aluminium. This flux is good for development of highly efficient technological processes for mass production of aluminium radiators, emitting aerials and other different-application products.

Rational utilisation of new structural materials with high mechanical properties offers an efficient solution to the problems of reduction of metal consumption and improvement in reliability and durability of welded structures. High-strength sparsely alloyed steels of the 06G2B and 09G2SYuch grades were developed for the fabrication of building structures. The steels have yield point of more than 440 MPa and tensile strength of 590 MPa, and are characterised by high cold resistance at temperatures down to --70 °C, which was demonstrated on sharp-notched specimens of the Charpy type (KCV 150--

Figure 7. Variations in values of fatigue limit σ_{max} at $N = 1 \cdot 10^6$ cycles depending upon the method of treatment of a AMg6 joint and cycle asymmetry R_σ of alternating stresses

Properties of intermetallic alloy γ-TiAl and its brazed joints using brazing filler metal of the Ti--Zr system

Test piece	Strength, MPa			
	at room temperature	at 700 °Ñ	Long-time strength at Ò = 700 °Ñ	
			Load 140 MPa	Load 200 MPa
Alloy γ-TiAl	650--700	320--350	--	--
Brazed joint	650--690	280--315	500 h*	300 h*

*Specimen did not fracture.

300 J∕cm^2). High strength, ductility and cold resistance of the HAZ metal of these steels are provided by the welding thermal cycles with wide ranges of cooling rates. To reduce the probability of delayed fracture of welded joints in steels 06G2B and 09G2SYuch, the welding parameters for them should be selected on a condition that the diffusible hydrogen content of the deposited metal be $[H]_{dif} < < 10$ ml∕100 g, and that the rate of cooling of the HAZ metal be $w_{6/5} < 30$ °C∕s.

Aluminium and aluminium alloys rank second after steel in volumes of production and consumption. High-strength Al--Li alloys, alloys with a maximum permissible degree of alloying, as well as alloys containing efficient modifiers, such as scandium, zirconium and others, providing a simultaneous improvement in weldability of materials and mechanical properties of welded joints, find currently an increasingly wide application.

Widening of the fields of application of aluminium alloys for welded structures depends upon ensuring the required resistance of the joints to fatigue fracture. Cyclic fatigue life of welded joints in aluminium alloys is about 40 % of that of the joints in structural steels. Therefore, aluminium welded structures need postweld treatment more than steel ones.

As shown by investigations, surface plastic deformation of the weld to base metal transition zone by ultrasonic peening may be an efficient method for postweld treatment of welded joints in aluminium alloys. This is well illustrated in Figure 7, which shows results of fatigue tests of butt welded joints in aluminium alloy AMg6 in the as-welded condition, after machining and after ultrasonic peening using equipment with a comparatively low power consumption (no more than 0.3 kW), comprising piezoceramic transducer. Increase in fatigue resistance of butt welded joint in aluminium alloy AMg6 after the treatment, compared with the as-welded condition, was 45--100 %, depending upon the cycle asymmetry.

The work is in progress on development of new structural weldable titanium alloys for aerospace and chemical engineering, medicine and other applications. Developed was the experimental alloy T-100 (Ti--5.5Al--1.2Mo--1.2V--4.0Nb--1.8Fe), which is not inferior in the level of strength to the well-known alloy VT22 and, at the same time, has good weldabi-

lity when using both arc and EBW methods. Welded joints in alloy T-110 after heat treatment have satisfactory ductile properties, the strength level being not less than 95 % of that of the base metal (1100 MPa), and durability of welded joints under a load of 600 MPa being $5 \cdot 10^5$ cycles.

Resistance to aggressive environment is one of the most important characteristics of titanium that determine its wide application in chemical engineering. Commercial-purity titanium and its alloys with palladium exhibit the highest corrosion resistance. However, strength of these alloys is no more than 500 MPa. Corrosion resistance of high-strength titanium alloys used in industry is inferior to that of commercial-purity titanium.
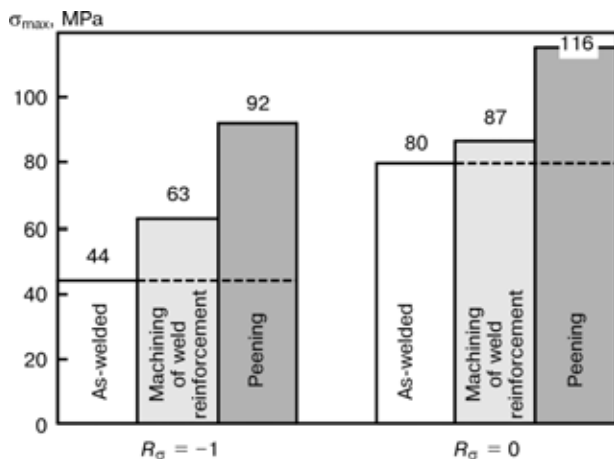
As shown by investigations, strength of titanium can be increased without any loss in its corrosion resistance through using isomorphic β-stabilisers, such as molybdenum, vanadium and niobium, as alloying elements. On this base, a new titanium alloy of the Ti--4.5Al--2.5V--2.5Mo--3.5Nb--1.5Zr system was developed. Strength of this alloy (950 MPa) is almost twice as high as that of commercial titanium, and its stress corrosion resistance is not inferior to that of commercial titanium.

Resalts of theoretical and experimental studies in the field of chemically pure halide fluxes for welding titanium and Ti-base alloys were used for elaboration of welding methods which were fundamentally new for titanium. They include submerged-arc MIG welding, electroslag welding, argon-arc TIG welding over the flux layer (A-TIG), and magnetically impelled arc narrow-gap welding.

Flux-cored titanium wires and technologies for argon-arc TIG welding of titanium were developed. This welding process allows making single-pass square-groove welds on titanium up to 16 mm thick. Technologies for mechanised TIG welding of titanium and appropriate equipment for performing welding under field and factory conditions are available. Studies are underway on activation of metallurgical processes during EBW of titanium through applying corresponding fluxes.

The Institute developed technologies for electron beam remelting and facilities for production of titanium ingots and semi-finished products (Figure 8), using less expensive raw materials, e.g. titanium sponge. These facilities installed at the Research-Production Centre «TITAN» allow production of commercial batches of titanium ingots in an amount of to 1500 tons a year. Welded structures are the end product of welding fabrication. The major challenge for scientists and technologists is building of reliable and durable structures for operation under the most different conditions.

Currently there is a substantial increase in the number of structures, constructions and equipment that are approaching their critical age or that have already exhausted their design lifetime. According to estimates of specialists, exhaustion of lifetime of ma-
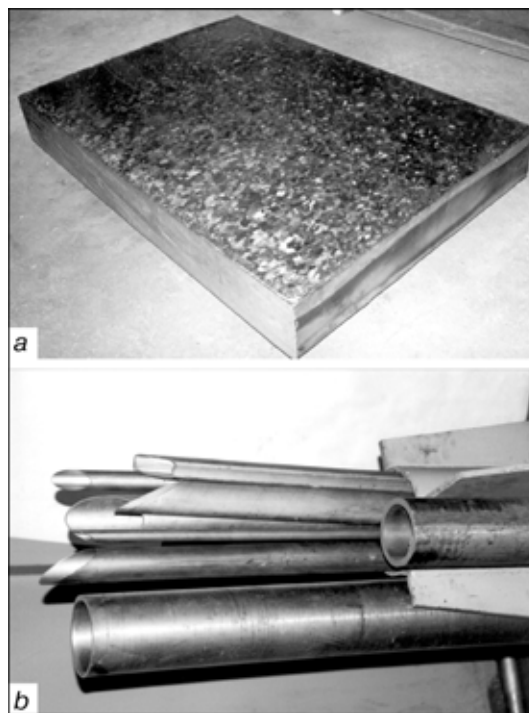
Figure 8. Titanium ingot (*a*) and semi-finished pipe products (*b*) produced by electron beam remelting

chines is in excess of 50 % in CIS countries. This put a number of industries (power generation, transport, petrochemical, chemical, main pipelines etc.) in a difficult situation.

So, the top-priority task under the current conditions is to provide safe operation of structures and constructions. Therefore, the hottest problem at present is ensuring a reliable estimation of residual life of structures and its guaranteed extension. Much has been done in the last years for advancement of strength design of welded structures. Methods and equipment for technical diagnostics of welded joints, intended not only for revealing the shape and size of defects, but also for quantitative estimation of degradation of strength properties of structural materials have been intensively developed. New approaches to estimation of residual life of structures have been formed on the basis of the knowledge derived. One of such approaches, based on the probability-economic statement of the problem, is the risk analysis. It allows elaboration of a well-grounded strategy for ensuring safe operation of durable structures, where increase in severity of their service conditions outpaces investigation and evaluation of their performance.

Much consideration is given to estimation of life of structures and equipment in oil-refining industry, the characteristic features of which are diversity of aggressive media affecting the equipment and wide variety of service defects, starting from corrosion-erosion damages and ending with degradation of service properties of structural materials. Figure 9 shows some typical examples of variations in strength characteristics of metal of vessels that have been in operation in hydrocarbon-containing medium for 20 years. Strength properties decreased by about 11 %
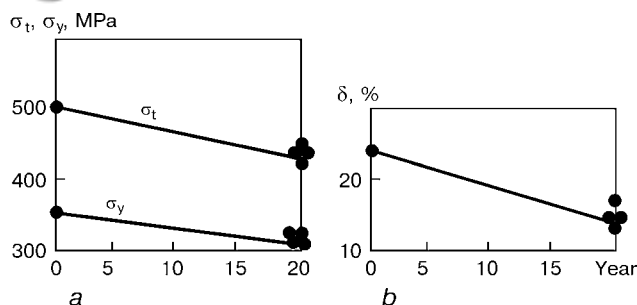
Figure 9. Variation in strength properties (*a*) and elongation (*b*) of metal (17GS grade) of oil-refining equipment with service time

and elongation ---- by 35 % during that period. Further development of notions of the mechanisms and rates of development of typical service defects and damages through estimation of limiting states will enable working out of more perfect regulatory documents for optimisation of repair operations and improvement of reliability of welded structures.

Technology for acoustic emission (AE) diagnostics, based on analysis of signals generated in deformation of structure materials, finds an increasingly wide application now. It provides the possibility of operating structures on the basis of their actual state, avoiding the planned preventive testing operations and repair. Wide acceptance of the AE technology is attributable to the possibility of 100 % control of facilities using a comparatively small number of transducers, and estimation of fracture loads at early stages of formation of dangerous situations. These benefits allow the AE technology to be applied now for monitoring of technical state of structures during operation. For example, the AE diagnostic system employed at the Odesa Port Factory is designed for ensuring continuous monitoring of the state of the isometric ammonia storage tank with a surface area of 4500 m^2 for 15 years using 56 transducers.

The work is underway on upgrading systems for NDT of main pipelines. The electromagnetic-acoustic flaw detector was developed for construction and operation of main oil and gas pipelines. The detector has successfully passed industrial tests. Excitation of ul-

trasonic waves is done using the electromagnetic-acoustic transducer that requires no contact liquid. This method is not critical to the quality of the pipe surface and shape of the weld reinforcement bead. Transducer scanning over the pipe surface and introduction of the ultrasonic waves in different directions provide identification of type, size and location of internal defects in welded joints and pipe material.

Methods for laser interferometry were developed for investigation of stress-strain states and inspection of quality of welded joints and structures. Compact holographic devices are available, applied for diagnostics of structures from non-metallic and composite materials. The shearography method, based on electronic processing of optical information, outgrew from the optical holography. An important advantage of this method is that it allows contactless measurements and the possibility of real-time observation of the interference fringe patterns on the display screen, avoiding any photographic recording. Electron shearography is applied to advantage for NDT of the quality of welded cylinders for compressed air used as fuel for internal combustion engines in motor transport (Figure 10).

Design, construction and putting into operation within the minimum possible terms ---- this is the trend in civil and industrial engineering involving welded structures. The prominent example of this fact is construction in Kyiv of the International Exhibition Centre. Characteristic feature of an engineering design of structures (Figure 11) is the system of lattice girders of roofing with the immediately adjacent tubular elements in units extending to 24, 35 and 54 m.

The capabilities of welding seem to be unlimited. The confirmation of this is welding of tissues of living organisms. In the former Soviet Union it was Prof. G.A. Nikolaev who was the first to get interested in this issue for welding of bones. Known are the works carried out by Ukrainian scientists on gluing surgical wounds, as well as studies performed at the Cornell University (USA).

The E.O. Paton Electric Welding Institute, in collaboration with the Institute of Surgery of the Academy of Medical Sciences and the Ministry of Health of Ukraine, as well as with participation at
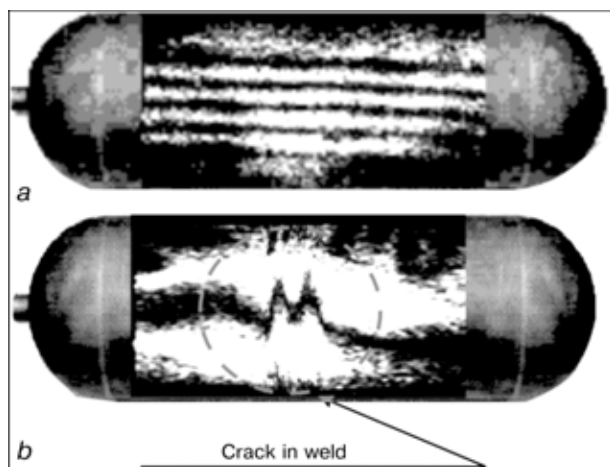
Figure 10. Monitoring of quality of welded cylinders for compressed air by the electron shearography method: *a* — defect-free structure; *b* ---- cylinder with a weld containing hair-line crack

Figure 11. Lattice girders of roofing of the International Exhibition Centre in Kyiv
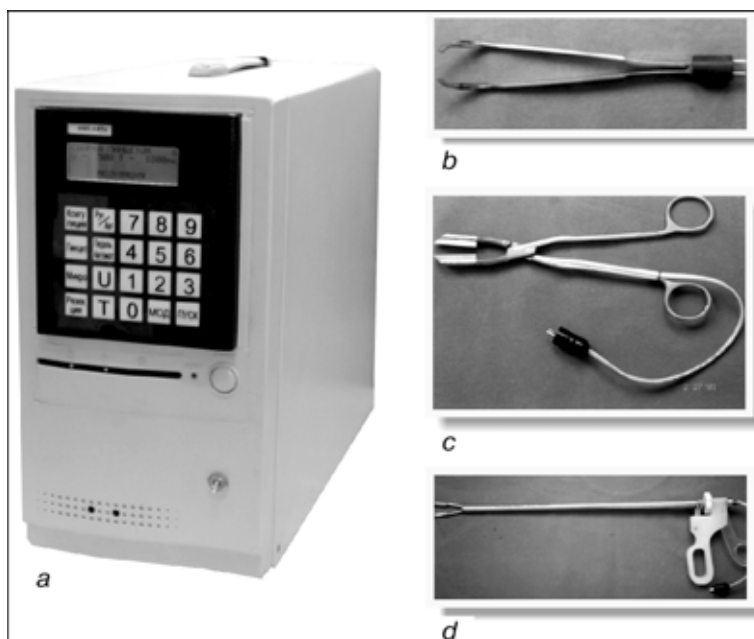
Figure 12. Equipment and instruments for welding live tissues: *a* — high-frequency welding power unit; *b* — welding forceps; *c* ---- welding clamp; *d* ---- welding laparoscopic clamp

the initial stage of the work by the Association OKhMATDIT of the Ministry of Health of Ukraine, and at a later stage by involving the Central Hospital of the Security Council of Ukraine, developed a new medical technology for joining soft tissues by welding, avoiding surgical threads, metal stirrups, glues, solders or other materials or products foreign for a living organism. The new welding technology was recognised as ingenious, which is documented by patents.

It was found that under certain conditions the cuts in tissues could be joined by thermal denaturation of proteins, leading to their coagulation. This can be done by using high-frequency currents safe for an organism.

Pioneering experiments on applying this technology, conducted on small laboratory animals, proved a promising future for this area and laid the basis for the development of prototypes of equipment for further research. Experiments on animals led to using welding for joining cuts in different organs of a large batch of pigs. The consistent positive experimental results are especially valuable because tissues of pigs are close in their structure and composition to human tissues. Therefore, this made it possible to verify the method on the latter. Initially, the experiments were conducted on ablated organs. Then, after obtaining positive results, the experiments were gradually made more sophisticated, involving welding directly during surgical operations. This served as the ground for the Ministry of Health of Ukraine to give permission to use the new surgical equipment in clinical practice.

The device for welding soft tissues consists of a power unit and control computer (Figure 12). The computer does not only control the power unit, but also adapts the welding process to specific properties of the tissues of the cut regions being joined. About a thousand of patients have been operated using welding in two Kyiv clinics during the last two years. The experience gained proves that welding holds promise for general surgery, operative gynecology, urology, otolaryngology and other field of medicine related to violation of integrity of tissues.

It is likely that in the future welding will allow the new approaches to be developed and procedures of some complex operations to be improved. Plenty of exciting research will be done in the future in this very important area. For the time being, it is necessary to widen the range of clinics that use welding in order to employ the experience accumulated for bringing the experimental equipment up to mass production and common application.

As seen from the above brief review, which is far from being exhaustive, welding and related technologies continue to be developed both extensively and intensively in a comprehensive way. Theoretical and technological preconditions are being created for manufacture of new products in traditional fields of welding industry, as well as for mastering of increasingly wide spheres of its application which before were considered exotic. Welding and related processes will continue to be the leading and mass-production technology in all the fields of manufacturing during the 21st century.

FIFTY YEARS OF THE E.O. PATON BRIDGE

L.M. LOBANOV[1], **V.I. KIRIAN**[1] and **O.I. SHUMITSKY**[2]
[1]E.O. Paton Electric Welding Institute, NASU, Kyiv, Ukraine
[2]V.N. Shimanovsky UkrNIIPSK, Kyiv, Ukraine

Problems of welded bridge construction, solved under the supervision of E.O. Paton, are considered at the initial stage of its development and finally 50 years ago by the construction of unique all-welded bridge across the Dnieper river in Kyiv. The ways of assurance of rated service life of all-welded bridges are shown on the base of major principles of design, used in E.O. Paton bridge designing, and established main causes of earlier initiation of fatigue cracks in elements of standardized spans. Design solutions of spans and welded connections, preventing the occurrence of secondary stresses and vibrations in them, were recognized determinant. Selection of steel, welding technology and treatment of welded joints plays an important role in the prevention of fractures.

Keywords: *span, welded joint, stress, vibration, fatigue crack, steel, service life*

During 50 years the E.O. Paton all-welded bridge across the Dnieper river in Kyiv serves people reliably (Figure 1). In this grand unique construction the long-standing dream of its creator about «electric welding meeting with bridge construction» is embodied. Since the completion of construction (movement along the bridge was opened on November 5, 1953), the initial and most responsible stage in the development of welded bridge construction was realized. Soon (on December 18, 1953), the bridge was named after Evgeny Oskarovich Paton, and in 1995 it was recognized by the American Welding Society as the outstanding welded structure and the E.O. Paton Electric Welding Institute of the NAS of Ukraine was awarded with Honorable Plate of AWS (Figure 2).

It is known that before construction of E.O. Paton bridge many attempts to create welded bridges both in the former USSR and other countries were not successful. The cracks were initiated in them not only during shop and site welding, but also in the process of service. The number of fractures of welded spans was growing. Due to this, the welded bridges in many countries were regarded with a great distrust. The problem covered the wide scales, it became general for all the metal structures. But these were only attempts and trials, check-outs or risk for success. The simple replacement of riveted joints by welds (and using the technology of welding and materials of those times) could not guarantee the reliable operation of structure, bridges in particular, operating under the conditions of low climatic temperatures and complex alternating loads. It was necessary to review thoroughly all the approaches and statements related to

Figure 1. General view of the E.O. Paton all-welded bridge across the Dnieper river in Kyiv

designing, fabrication and erection of metal spans (and, as a matter of fact, welded structures as a whole), being more economic as compared with riveted, but not always meeting the requirements for strength, life and adaptability to manufacture.

This circumstance was used actively by opponents as a major argument against realization of idea of the welded bridge in Kyiv. Only owing to high prestige of Evgeny Oskarovich Paton and his engineering courage it was managed to receive positive decision of authorized bodies.

In 1946--1951 Evgeny Paton, the acknowledged leader in the field of welding and bridge construction, united and organized the joint work of bridge designers and staff members of the Electric Welding Institute. They carried out a large complex of research and designing works to develop further the major principles of designing of welded bridges, made by E.O. Paton as early as 1933 [1]. As a result of this large work:

• the new design of the bridge was made. Instead of the lattice principal girders of a high height, designed before the war, four solid-wall continuous girders with chords of thin-sheet metal and economic thin wall were designed. Their height was in the limits of railway dimensions for feasibility of fabrication and transportation by large blocks. To provide a local stability of the wall, a system of horizontal stiffeners, included into composition of section of principal beams, adaptable to manufacture and welding, was used. This allowed designers to reach a record thickness of walls of principal beams 1 / 250, at a minimum consumption of steel which is concentrated in chords. The latter were reinforced with second sheets under supports and in the middle of spans in accordance with bending moments. Principal beams over the bridge supports were reinforced from beneath by blocks in the form of support reinforcement;

• special grade of low-carbon steel «MSt3 for welded bridges», low-sensitive to the thermodeformational cycle of welding, was developed. It was produced by control of the chemical composition (≤ 0.20 % C; 0.12--0.25 % Si; 0.36--0.60 % Mn; ≤ 0.05 % S; ≤ 0.045 % P). Silicon and aluminium were used as deoxidizers, and the set thermal condition of rolling provided a fine-grain structure. Some experimental welded spans of railway bridges were fabricated from this steel;

• improved grades of electrode wires (manganese grade A, Sv-10GA) and fluxes (AN-348, AN-348A, OSTs-45) were developed and tested under the industrial conditions;

• equipment was updated and simplified for automatic and mechanized welding of structures in shop conditions, providing stability of the preset welding condition under the industrial conditions and accuracy of electrode direction along the weld (welding tractor TS-17-M, semi-automatic machine PSh-5, holder DSh-27);

• new methods and equipment for automatic welding of vertical butt welds with their forced formation were developed for erection of spans;

Figure 2. Honorable plate of the American Welding Society awarded to the E.O. Paton Electric Welding Institute of the NAS of Ukraine in 1995

• technology of shop and site welding was developed;

• design solutions of welded connections of spans and sequence of their welding were determined using criterion of assurance of preset level of strength and ductility of welded joints. These characteristics were determined from the results of testing large-sized specimens of real defect-free welded joints at minimum temperature of service (in the given case--40 °C) with a record of tension diagram. It was assumed that the satisfactory operation of welded joint under the service conditions will be guaranteed if the rupture stresses σ_r reach the level of ultimate strength σ_t ($\sigma_r = \sigma_t$), which is not lower than that of the parent metal. Another important requirement was the development of a high plastic deformation ($\sigma_t > \sigma_y$) before the specimen rupture.

The metal susceptibility to strain ageing and transition to brittle state was evaluated on specific large-sized specimens with a natural stress raiser in the zone of welding (narrow slot in a longitudinal composite stiffener, welded up to the plate using fillet welds).

These and other developments served as scientific grounds for designing, fabrication and construction of the first large all-welded bridge in Europe [1, 2]. The shop fabrication of metal structures of bridge of a total mass of about 10000 t was realized since December 1951 to April 1952, and the site works were made since April 1952 to October 1953. The total length of the bridge is 1543 m. It has 24 spans, 20 by 58 m, and four fairway arches of 87 m (Figure 3, *a*). In transverse section the span has four principal I-beams with a solid wall, located at 7.6 m distance from each other (Figure 3, *b*). They are joined by transverse braces. Longitudinal braces are available only in the lower chord between middle principal beams along the entire length of the bridge. Over the supports the longitudinal braces were mounted between all four principal beams. Upper chords are joined by transverse rolled braces to a reinforced plate of the bridge road, operating with them for bending. The total width of the bridge is 27 m (roadway is 21 m and two pedestrian ways by 3 m). There are two tram lines in the middle of the roadway.
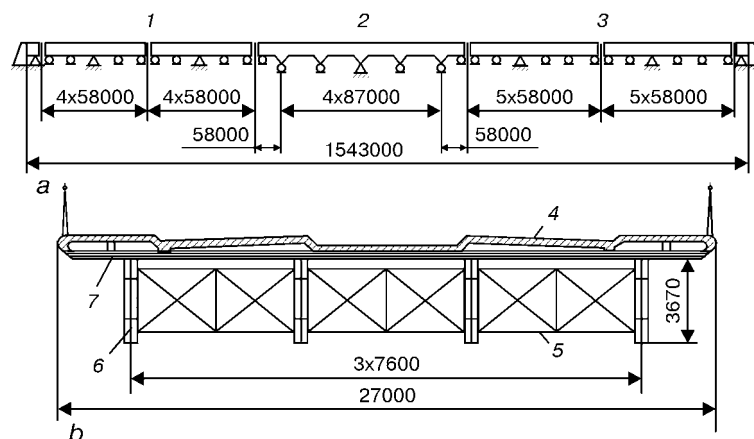
Figure 3. General scheme (*a*) and cross section (*b*) of the E.O. Paton bridge across the Dnieper river in Kyiv: *1* — left-bank area (two continuous four-span stiffening beams); *2* — middle area (the same, one six-span girder); *3* — right-bank area (the same, two six-span girders); *4* — reinforced-concrete plate of passageway; *5* — transverse braces between principal beams; *6* — principal welded I-beam with a solid wall; *7* — transverse rolled I-beam

Due to earlier existing fractures of welded spans, the great attention was paid to the quality of welds, except using such design solutions of welded joints, which mostly satisfied the above-mentioned requirements for strength. Therefore, designing was based on the principle of maximum use of automatic and mechanized submerged arc welding in shop and site conditions. For this purpose, the principal beams were designed in the form of a I-beam with a solid wall having long longitudinal welds. Vertical stiffeners were replaced mainly by horizontal stiffeners. At the plant the erection elements of principal beams were manufactured in large blocks. Their length was 27--29 m and mass of about 38 t. In addition, a special design of a site butt with inserts for a vertical wall was developed that made it feasible to weld the lower chord butts by the automatic machine using run-out tabs, then their cutting and flush machining with a lower chord sheet. Butts of the vertical wall insert were designed for the automatic welding with a forced weld formation. Welding of butts with inserts of the upper chord was also provided by the automatic machines using run-out tabs, their subsequent cutting and flush machining with a chord. All this allowed 93 % of shop and 88 % of site welds of principal beams to be made by the automatic and mechanized submerged arc welding, that guaranteed their high quality.

Over the fifty years the E.O. Paton bridge is under the intensive service without capital repair. It is important to note here that during recent decades the loads on bridge (up to class N-30) and intensity of traffic (71000 cars per day) have been greatly increased as compared with design values (class N-30, 10000 cars per day). At regular inspection of its joints and members, the cracks, tears and fractures of elements were not observed.

At the same time, as the experience showed, in modern welded spans of motor-road and railway bridges, whose design service life is 80--100 years, the fatigue cracks are initiated after a short period of service [3, 4]. As was established during study of stress-strain state of span elements, prone to an earlier initiation of fatigue cracks, the main causes of their occurrence are local secondary alternating stresses and vibration of span elements, stipulated mainly by imperfectness of structure and design of welded members [5]. Therefore, the design way of prevention of fatigue fractures of bridge spans is one of the main ways. Moreover, the rates of designing should include such rules of designing and preparation of welded joints which could avoid the appearance of inadmissible levels of vibrations and local alternating stresses, thus providing the preset life.

In this respect, the design solutions of stiffening beam of E.O. Paton bridge are basic and used in modern approaches to designing of welded spans not prone to the formation of fatigue cracks. Principal design feature in this case is the inclusion of transverse beams of reinforced concrete roadway into a joint operation. This was provided by joining of upper chords of principal and transverse beams to a reinforced-concrete plate of the bridge road.

This principle found a wide spreading in modern high-way bridges. The solid-wall principal beams are joined by design and technology to a roadway part [6]. Here, the use of box-type spans was most promising. In this case the system of separate principal I-beams with a solid wall, joined by transverse and longitudinal angle braces, is replaced by one or several (up to three) box-type beams. Transverse sections of two Kyiv rope bridges across the Dnieper river (Moscow bridge for motor-cars and South bridge for motor-cars and metro trains) which were included into Collection «Famous bridges in the world», are shown in Figure 4 [7, 8]. In these box-type spans, one of the main elements, alongside with principal I-beams, is a steel orthotropic plate. The modern design of the orthotropic plate represents a steel sheet, reinforced with longitudinal stiffeners and transverse beams. It is used as a roadway and serves simultaneously a widened upper chord of principal beams. Lower parts of principal beams (widened lower chord) are joined by a similar orthotropic plate, thus forming a stiffening box-type beam.

In these comparatively rigid structures the stresses in main elements are distributed more uniformly. In
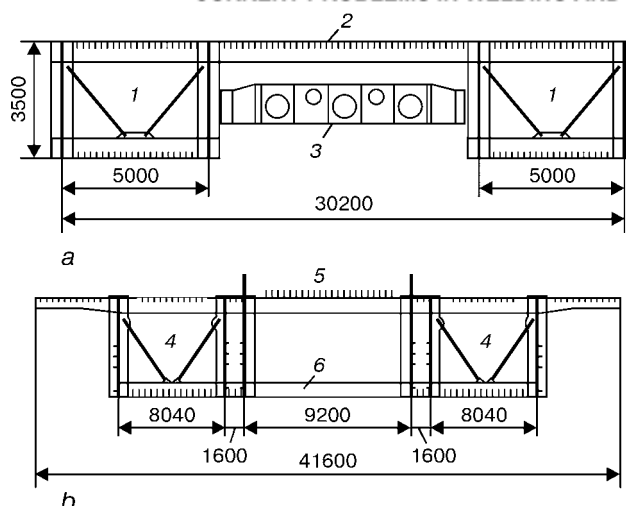
Figure 4. Transverse section of metallic rope spans of Moscow (*a*) and South (*b*) bridges across the Dnieper river in Kyiv: *1* — box-type principal beams; *2* — orthotropic plate of passageway; *3* — diaphragms; *4* — three-wall box-type principal beams with cantilevers; *5* ---- orthotropic plate of special design for passage of metro trains; *6* — braces-distance pieces

addition, there are no basic causes of occurrence of secondary stresses and vibrations leading to the initiation of fatigue cracks. Detail inspection of metal stiffening beam of a rope span of the Moscow bridge in 1999 (after 23-year service) and South bridge in 2002 (after 12-year service) confirmed that fatigue cracks were not formed in their elements.

As to the railway bridge spans of 18.6 and 33.6 m length, manufactured until now by standard projects of the 1960--1970s, then the fatigue cracks are occurred in them after 1--7 years of service. They damage elements, in which their appearance was not expected and fatigue was not calculated. Among the most widely spread damages, the cracks in shaped sections and elements of braces, welded joints of vertical stiffeners with chords and horizontal stiffeners, walls of principal beams in places of breaking of vertical stiffeners, zone of fusion of upper chord weld in junction with vertical stiffeners should be noted.

One of the main causes of formation of fatigue cracks are the secondary local stresses and vibration of elements of span due to a non-centered transmission of circulating load from rolling stock to principal beams. It is assumed that the distance between middle planes of walls of principal beams is equal to 2000 mm, and the width of the railway track is 1530 mm. When designing under the supervision of E.O. Paton in the 1950s, everything possible was made to reduce the effect of eccentricity of load applying. In these all-welded spans the external sheets of upper chords on which the bridge fenders are fastened, had width of 200 mm, braces were arranged at the level of chords, and vertical stiffeners were welded up to chords with a complete penetration. Life of these spans is 15--20 times higher as compared with standard spans of the 1960--1970s. Such significant decrease in life of spans of the 1960--1970s was due to negligible, for the first glance, changes in the project. They consisted in increase of width of upper chord sheets to 420 mm, and in some cases, depending on span length (18.2--33.6 m) to 520 mm and even

to 620 mm, in transfer of braces fastening from chords to beam wall and mating of vertical stiffeners with upper chords through «sliding blocks». In the presence of a gap in the joint of vertical stiffeners and chords (in practice it reaches 0.5--1.0 mm) the passage of each carriage (even axle) of the rolling stock causes the turning of the chord and deflection of wall from its plane in the zone of recess of vertical stiffeners, i.e. wall bending in all its height. The latter causes the turning of the lower chord and promotes the occurrence of vibrations of the wall section. Braces, fastened to walls, are also greatly vibrated. At definite rates of the rolling stock these vibrations can be resonance. In case of increase in width of upper chords (420--620 mm) a single-side support of bridge fender on them is greatly increased and, respectively, the eccentricity of load transmission from the rail track to the principal beam is increased. Moreover, the secondary stresses from torsion occur in chords, while in braces and upper parts of wall they appear from bending.

As to the level, the secondary stresses are negligible and cannot themselves cause the initiation of fatigue cracks. However, they are superimposed on the main train stresses and, in addition, those stresses are added to them, which occur as a result of vibration of the span--train system, and also vibration of the span elements. In this case the life of span elements is determined by amplitude and frequency ratios of added stresses [5]. Negative influence of vibration is increased with increase in relative values of its amplitude and frequency.

In addition, it is important to outline here that spans of the 1960--1970s (standard projects) became bolted-welded. First bolts appeared in them in the 1960s. With their use the longitudinal and transverse braces were fastened to shaped section. Then the bolts were used for fastening braces to shaped sections. During recent time the fastening of vertical stiffeners to walls of principal beams is also realized by high-strength bolts. Welded were only butts of sheets of principal beams and chord welds.

Meanwhile, the experience of service showed that replacement of welds by joints using high-strength bolts does not guarantee the prevention of fatigue fractures, as the main source of their initiation, i.e. non-centered transmission of load to principal beams and other causes of occurring local alternating stresses and vibration, is remained. In this case the labour-intensity in manufacture and erection of bolted-welded spans was greatly increased as compared with all-welded spans, which were welded completely in shops and transported in a ready form by railway to the site.

Thus, the design way of prevention of fatigue fracture of elements of spans is determinant. The used design solutions should be directed, first of all, to the increase in eccentricity of load transmission from the rolling stock to the principal beams. This can be attained, for example, using special centering devices, welded up to upper chords of the principal beams, which contact bridge fenders rails at a small area. Its central axis should coincide with a middle plane of the principal beam wall. Known are, for example, cases of rails fastening directly to upper chords of principal beams without fenders. In this case the distance between the principal beams is decreased to the width of the railway track. The mounting of bridge roadway on ballast is sufficiently effective method [9]. The ballast pocket, made of reinforced concrete, is included into operation of upper chords of principal beams.

To extend the service life of solid-wall spans being under service, a number of new methods of their reinforcement, reducing the level of vibration of elements, is suggested [10]. They are based on using an orthotropic plate (with traffic on ballast, cross-pieces) or reinforcement of upper chords of principal beams with longitudinal stiffeners.

The above-given methods of updating standard projects and reconstruction of spans under service make it possible to increase their life. However, to guarantee the rated service life of 80--100 years for welded spans of railway bridges, not labour-consuming in fabrication, the radically new design solutions are necessary, preventing the main causes of earlier initiation of fatigue cracks.

For this purpose, experimental investigations of stress-strain state of elements and welded members of spans, fabricated by standard projects and using offered new design solutions were carried out under the service conditions (at test ground). At the selection of these design solutions the main principle about the combined operation of the span main elements, suggested as far back as the 1950s by E.O. Paton, was determinant.

On the basis of these data the initial statements of creation of all-welded spans of the railway bridges of the new type, not prone to the fatigue crack formation, were formulated [5, 11, 12], the main of which is the joining of principal beams at the level of upper chords by a system of such braces which could improve the three-dimensional operation of span at the expense of a uniform distribution of forces between the elements and reduction of the vibration level in them.

For this purpose, a replacement of longitudinal and transverse braces of angle section by, respectively, sheets-inserts and sheet diaphragms of closed or open type was suggested. Here, the method of welding up of the above-described elements is very important. The main difference consists in the fact that the sheets-inserts, diaphragms and stiffeners are welded up to the upper chords of principal beams with a complete penetration. Vertical stiffeners and diaphragms are welded to the upper part of walls of principal beams at the distance of 200 mm from chords also with a complete penetration, and in other places ---- with fillet welds.

The offered sheets-inserts and diaphragms, forming rigid structural stands together with walls of principal beams, prevent the mutual displacement of principal beams, improve the span rigidity for bending (in horizontal and vertical directions) and torsion, contribute to a uniform distribution of service stresses. This greatly reduces a local torsion of the upper chord and, associated with it, secondary alternating stresses in span elements, thus leading also to the decrease in vibration of elements.

Full-scale tests of the offered span at experimental section of railway road, being 60 years under the service, showed its high resistance to fatigue fractures. Fatigue cracks were not observed in its welded members. Tests were not performed until exhaustion of the life margin, however, it is quite evident that the suggested design of the span can serve as a reliable base for the creation of standardized spans of the new type, resistant against fatigue damages.

OJSC «UkrNIIPSK» named after V.N. Shimanovsky and the E.O. Paton Electric Welding Institute of the NAS of Ukraine have developed a project of experimental all-welded span of railway bridge (design length is 23.6 m) which is planned to be erected in one of branches of railways of Ukraine.

In parallel with improvement of design of spans of bridges, it is necessary to perform the treatment of welded joints to improve their cyclic life. Here, it is important to outline, that design measures are primary, as the treatment of welded joints under the unfavourable conditions (the presence of secondary stresses and vibrations) cannot lead always to the desirable results. Among the many methods of improvement of fatigue resistance of welded joints (mechanical, TIG remelting, surface plastic deformation (SPD)), the most promising methods of treatment are those, whose positive effect is based on the decrease in coefficient of stress concentration in the zone of transition from parent metal to weld metal, where the fatigue cracks are more often initiated, and creation there of the favourable residual compression stresses [5, 13, 14]. Such method of SPD, as ultrasonic peening treatment with magnetostriction transducer

Effect of high-frequency mechanical peening on properties of steels of different strength

	Materials and joints investigated			Conditions of loading	
Steel grade	Ultimate strength, MPa	Thickness, mm	Type of joint	Kind of loading	Coefficient of asymmetry
St3 (killed)	458	20	Butt	Tension	0
Å460	589	10	T-joints	Bending	0.1
WELDOX 420	573	20	Transverse stiffener, welded with fillet welds		0.1
	573	20			0.1
TMCP	560	20			0.1
St3 (killed)	460	30		Bending	0
	460	30			0
	460	30			0
09G2SYuch	550	14	Longitudinal stiffener		0
15KhSND	520	14			0
G235B	436	8	Butt		0.1
	436	8	Cruciform	Four-point bending	0.25
	436	8			--0.5

(Cont.)

Steel grade	Fatigue strength at $N = 2 \cdot 10^6$ cycles, MPa		Increase in fatigue strength, +		References
	In initial state	After treatment	MPa	%	
St3 (killed)	140	220	80	57	[16]
Å460	168	290	122	73	[19]
WELDOX 420	198	327	129	65	[20] (different technologies of treatment)
	198	341	143	72	
TMCP	178	351	173	97	[21]
St3 (killed)	113	167	54	49	Data of PWI
	113	164	51	48	Data of PWI (different technologies of treatment)[*]
	113	226	113	100	
09G2SYuch	96	156	60	62	Data of PWI
15KhSND	86	180	94	110	
G235B	148	234	86	57	[22][*]
	142	234	92	64	
	165	282	117	71	

[*]Tool with a piezo-ceramic transducer.

for conversion of electrical oscillations into mechanical vibrations, was developed in the 1980s [15, 16]. Over the recent years the E.O. Paton Electric Welding Institute of the NAS of Ukraine began to use a compact equipment for SPD, the high-frequency mechanical peening (HFMP) using a transducer based on reverse piezo-electric effect [17, 18]. In the first case the output capacity of ultrasonic generator, initiating the oscillations, is 1 kW and more, and in the second case it reaches 0.4 kW.

The general tendency of improving the effectiveness of HFMP is known with increase in steel strength providing the use of the same HFMP condition. The data about the effectiveness of HFMP of main types of welded joints of structural steels, including also materials, recommended for bridge construction (15KhSND, 09G2SYuch), are given in the Table. They show the feasibility of obtaining the significant increase in fatigue strength (up to 100 %) also for the above-mentioned steels. Here, it is important to establish the optimum condition of HFMP depending on the class of steel strength and type of welded joint.

Thus, the data obtained about the effectiveness of HFMP, its high efficiency and relatively low consumed power allow HFMP to be considered as the most challenging method of improving fatigue resistance of welded joints. HFMP is simple in realization, its cost is lower as compared with other methods of
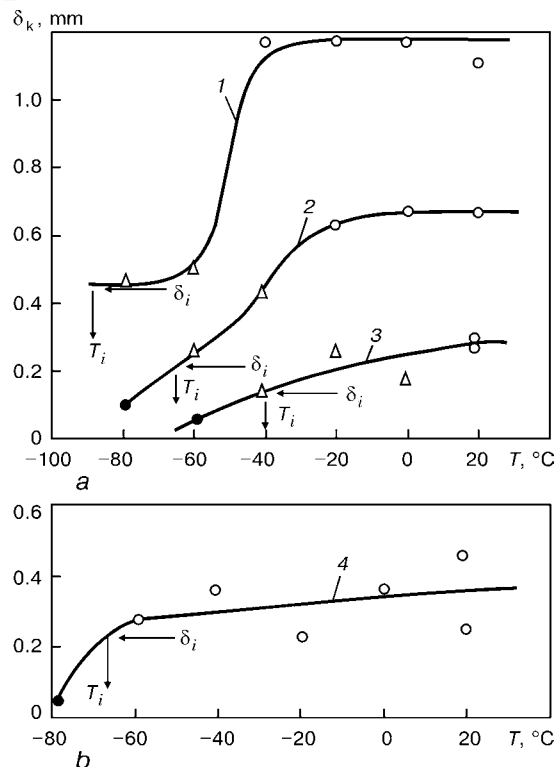
Figure 5. Temperature relationship of fracture toughness δ_k (δ_c, δ_i, δ_u, δ_m) of steel 09G2SYuch in initial state (*1*) and after strain ageing (*2*), tweld metal (*3*) and heat-affected zone (*4*): ● ---- δ_c; Δ — δ_u; ○ — δ_m

treatment (mechanical, TIG remelting, shot blasting).

Except the above-described design and technological ways of assurance of long life of bridge spans, the selection of steels for their fabrication is of a great importance. The level of service properties of structural materials for bridges should be sufficient to prevent brittle, tough and lamellar fractures. At present the steels of a rather limited assortment with a maximum rated resistance (yield strength) up to 390 MPa are used in bridge construction [23, 24]. Undoubtedly, this list of steels should be widened as regards to strength and other service properties of rolled metal.

New compositions and technologies of production of structural materials opened up the wide opportunities. At the same time it is necessary to take into account that sparsely-alloyed steels of increased and high strength are more sensitive to the technological processing. This requires comprehensive investigations of parent material and metal of welded joints using advanced methods, including the criteria of fracture mechanics at the stage of their mastering [25].

There are examples in foreign practice of using materials with 600--800 MPa yield strength [26, 27]. During recent years a domestic steel 09G2SYuch ($\sigma_{0.2} \geq 450$ MPa) [23], developed on the base of a widely used steel 09G2S is used for fabrication of motor-car, city and pedestrian bridges. A favourable combination of increased content of manganese, microalloying (aluminium, cerium) and ladle processing provides high stable service properties. Thus, at a guaranteed value of yield strength 450 MPa and ul-

timate strength 580 MPa the impact strength of steel 09G2SYuch on specimens with a sharp notch *KCV* at temperature --70 °C is equal to 55--69 J∕cm².

Requirements for bridge steels and their welded joints, designed for prevention of brittle, tough and lamellar fractures, should be based on modern approaches and criteria of fracture mechanics using conceptions «fitness for purpose». To control the fulfillment of these requirements under the shop conditions in manufacture of materials and metal structures, the characteristics *KCV* are determined, which are established in accordance with correlation relationships KCV--δ_{IC} (δ_{IC} is the critical crack tip opening) [28].

On the example of steel 09G2SYuch, the basic statements of establishing requirements for parent material and metal of welded joints, directed to prevention of brittle and tough fractures, were considered. Evaluation of fracture toughness of steel 09G2SYuch (12 mm thickness of sheet) and its welded joint (shop mechanized welding in CO_2, wire Sv-08G2S) was realized at different temperatures using a deformation criteria of fracture mechanics δ_k (Figure 5). Depending on the nature and stage of fracture the following designations are accepted: δ_c ---- initiation of brittle or quasi-brittle fracture ($T < T_i$, T_i ---- temperature of transition from quasi-brittle to tough fracture); δ_u ---- the same, after initiation and stable growing of tough crack ($T \geq T_i$); δ_i ---- initiation of tough fracture ($T \geq T_i$); δ_m ---- transition of stable propagating tough crack into unsteady state ($T > T_i$).

Value δ_i was determined using curves δ_R (Figure 6). Investigations showed that δ_i does not depend on temperature and rate of loading [29, 30]. In addition, in fulfillment of condition of plane deformation

$$t > \delta_i E / \lambda \sigma_y$$

(E is the modulus of elasticity; λ is the coefficient equal to 4--5), the value δ_i becomes independent of metal thickness t. In other words, it can be considered as characteristics of material and used for evaluation of «fitness for purpose» of elements of welded structures.

To prevent the most hazardous brittle fractures the temperature of transition from quasi-brittle to tough initiation of crack T_i of the parent material and metal of welded joints should be lower that the minimum temperature of service T_s ($T_i > T_s$). It is important that the conditions for determination of T_i in the laboratory tests were similar to those of metal operation in real structure. Here, the basic importance is the rate of loading and degree of three-dimensionality of stress-strain state which is determined mainly by thickness of the specimen and size of initial crack-like defect. Taking this into account, the values T_i, acceptable for most practical cases, can be obtained in testing standard specimens of a full thickness at the rate of metal deforming in defect apex, corresponding to service conditions. These data, depending on the rate of crack tip opening δ' for some structural materials and welded joints, are given in Figure 7.
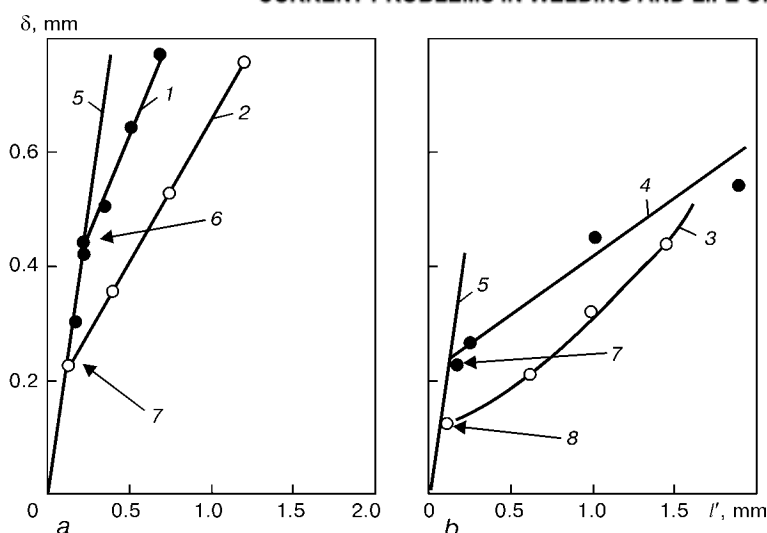
Figure 6. Dependence of crack tip opening δ on stable increment of its length l' in tough state (curves δ_R) for steel 09G2SYuch: *1* —— initial state; *2* — after strain ageing; *3* — weld metal; *4* — heat-affected zones; *5* ---- line of crack tip blunting ($\delta = 2l'$) (points ---- experimental data)

Conditions of metal operation in a tough state ($T_i < T_s$) should be considered as determinant. This is stipulated by a basic change in the nature of crack propagation. Below T_i it is instable from the moment of initiation, while in the temperature interval above T_i the fracture is preceded by the stage of a stable propagation of crack after its initiation.

Except the inequality $T_i < T_s$, the need in introducing of one more additional condition, which refers to the level of fracture toughness δ_i at the stage of initiation of a tough crack to limit its size by a preset value, is quite evident. It is written $\delta_i > \delta_i^*$, where δ_i^* is the required (minimum) level of fracture toughness, designed to guarantee the integrity of structure in the presence in it of an assumed (hypothetical) crack-like defect. Value δ_i^* is established coming from the «fitness for purpose» conception.

Thus, the selection of steel and technology of welding with conditions

$$T_i > T_s, \quad \delta_i > \delta_i^*$$

will guarantee the safe service of metal structure, preventing the occurrence of brittle and tough fractures.

In addition, steel for bridge construction should have a sufficient level of resistance against initiation of lamellar fractures. It is known that the service characteristics of rolled metal, including ductility and toughness, are significantly decreased in transition from longitudinal to transverse direction and can reach low enough values in the direction of thickness (direction Z). As a result, the hazard of occurrence of lamellar cracks under the action of negligible stresses directed normal to the sheet plane is appeared. Further, these cracks can serve as the beginning of initiation of brittle, tough and fatigue fractures in structure elements under the action of main stresses [31].

At present, to evaluate the susceptibility of steels to lamellar fracture, the characteristic of reduction in area ψ_Z of flat standard specimen with an axis oriented to the direction Z is widely used. As to its level, then, in accordance with technical specifications for plate rolled stock for bridge construction, ψ_Z at room temperature should be more than 20 %. The practice showed that this value ψ_Z is optimum from the point of view of prevention of formation of lamellar cracks in the process of technological operations (welding, surfacing and others) in manufacture of metal structures, when the temperature is equal to room or higher temperature.

With decrease in temperature the characteristics of ductility and fracture toughness of metal in the direction Z can be abruptly deteriorated. This is associated not only with usual temperature embrittlement of metal, but also with its susceptibility to «low-temperature» lamellar fracture, stipulated by a crystallographic texture and weakening of boundaries of subgrains [32]. It concerns to a larger extent to modern steels with a negligible content of non-metallic inclusions and high enough level of isotropy of properties at room and increased temperatures. Therefore, the high values ψ_Z at positive temperatures are the necessary condition, but not far sufficient to prevent
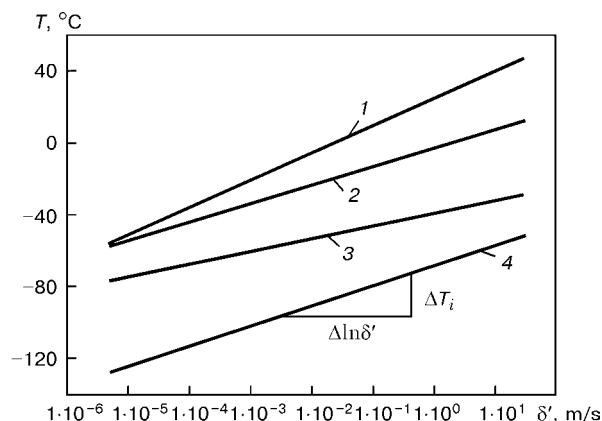

Figure 7. Dependence of transition temperature T_i on rate of crack tip opening δ' in semi-logarithmic system of coordinates: *1* — steel 09G2S; *2* — weld metal St3; *3* — the same (Mn–Ti); *4* — microalloyed (Mn–Ni–Mo–Nb) steel of a controllable rolling

the lamellar fractures in service of welded metal structures.

In this connection, in parallel with determination of ψ_Z at room temperature, it is necessary to introduce testing of structural steels in the direction Z at minimum design temperature using criteria of fracture mechanics. Here, the optimum requirements to fracture toughness should be established on the basis of «fitness for purpose» conception. These requirements can be given directly by rated values of characteristics of fracture mechanics or in appropriate characteristics of standard impact strength tests of specimens with sharp notch KCV.

It should be outlined in conclusion that the creation of the first large all-welded bridge a half of century ago with fulfillment of a complex of research and design works to provide its reliable service opened up the wide way for the electric welding in bridge construction and came beyond the frames of solution of a private problem of the separate object. At that time a number of basic approaches and design-technological solutions was developed for a wide application of electric welding in metal construction in general.

As a result of experience of a collaborative work of designers, scientists, researchers and technologists, E.O. Paton school of welded engineering structures has been created in principle, resulted in the creation of a number of outstanding constructions, and also in further progress in this field.

1. Shevernitsky, V.V., Novikov, V.I., Zhemchuzhnikov, G.V. et al. (1951) *Static strength of low-carbon welded joints.* Ed. by E.O. Paton. Kyiv: AN Ukr. SSR.
2. Paton, E.O., Lebed, D.P., Radzevich, E.N. et al. (1954) *Application of automatic welding in erection of large all-welded town bridge.* Kyiv: AN Ukr. SSR.
3. Mirolyubov, Yu.P., Panin, E.M., Frolov, V.V. et al. (1983) Fatigue cracks in solid-walled span structures. In: *Transact. of NII of Bridges on Problems of Design and Operation of Artificial Constructions.* Leningrad: V.N. Obraztsov IRTE.
4. Fisher, J., Mertz, D. (1985) Cracking in steel bridges. *Grazhd. Stroitelstvo*, **2**, 9--13.
5. Trufyakov, V.I. (1998) Increase of fatigue strength of welded joints and structures. *Avtomatich. Svarka*, **11**, 11--19.
6. (1997) *Welded engineering structures.* Vol. 2. Types of structures. Ed. by L.M. Lobanov. Kyiv: PWI.
7. Fuks, G.B., Korneev, M.M. (1998) Rope bridges by the Ukrainian projects. Present and future. In: *Proc. of 2nd Meeting of Ukrainian Inter-Branch Sci.-Pract. Seminar on Current Problems of Construction and Operational Buildings in the Railway Lines*, Kyiv, June 30--July 1, 1998. Kyiv: Kyivorgstroj.
8. Virola, Yu. (2001) *World-wide known bridges.* Ed. by A.I. Lantukh--Leshchenko. Kyiv: NTU.
9. Belenya, E.I., Streletsky, N.N., Vedenikov, G.S. et al. (1991) *Metal structures.* Spec. Course. Ed. by E.I. Belenya. Moscow: Strojizdat.
10. Orlov, V.G., Doroshkevich, A.A., Zenkin, A.I. (1997) New methods of reinforcement of solid-walled span structures. *Put i Put. Khozyajstvo*, **8**, 9--10.
11. Trufyakov, V.I., Dvoretsky, V.I., Lobanov, L.M. (1996) Fatigue failures of welded bridges in CIS: Results of inspection, investigation and experimental tests. In: *Proc. of Int. Conf. on Welded Structures in Particular Welded Bridges*, Budapest, Sept. 2--3, 1996.
12. Trufyakov, V.I., Dvoretsky, V.I., Orlov, V.G. et al. (1995) New approach to the creation of solid-walled welded span structures of railway bridges. *Welded Structures*, **1**, 249--255.
13. Kudryavtsev, I.V., Naumchenkov, I.E. (1976) *Fatigue of welded structures.* Moscow: Mashinostroenie.
14. Trufyakov, V., Mikheev, P., Kudryavtsev, Yu. (1995) Fatigue strength of welded structures. Residual stresses and strengthening treatments. *Welding and Surfacing Rev.*, **2**, 100.
15. Statnikov, E.Sh., Shevtsov, E.M., Kulikov, V.F. (1977) Ultrasonic peening tool for strengthening of welds and decrease of residual stresses. In: *New physical methods of intensification of technological process.* Moscow: Metallurgiya.
16. Mikheev, P.P., Nedoseka, A.Ya., Parkhomenko, I.V. et al. (1984) Efficiency of application of ultrasonic peening to improve the fatigue strength of welded joints. *Avtomatich. Svarka*, **3**, 4--7.
17. Prokopenko, G.I., Krivko, V.P. *Ultrasonic multibit tool.* USSR author's cert. 601143. Int. Cl. B 24 B 39/04. Publ. 05.03.78.
18. Trufyakov, V.I., Shonin, V.A., Mashin, V.S. et al. (2001) Application of high-frequency peening to increase the fatigue resistance of butt welded joints in aluminium alloys. *The Paton Welding J.*, **7**, 7--11.
19. Yanosch, I., Koneczny, N., Debiez, S. et al. (1995) Improvement of fatigue strength in welded joints (in HSS and aluminium alloy). *IIW Doc. XIII-1594--95.*
20. Blomquist, A., Statnikov, E.Sh., Muktepavee, V.O. et al. (2000) Comparison of ultrasonic impact treatment (UIT) and other fatigue life improvement methods. *IIW Doc. XIII-1870--00.*
21. Trufyakov, V.I., Statnikov, E.Sh., Mikheev, P.P. et al. (1998) The efficiency of ultrasonic impact treatment for improving the fatigue strength of welded joints. *IIW Doc. XIII-1745--98.*
22. Lixing, X., Dongpo, W., Yufeng, Z. et al. (2000) Investigation on improving fatigue properties of welded joints by ultrasonic peening method. *IIW Doc. XIII-1812--00.*
23. (1985) *SniP 2.05.03--84.* Bridges and tubes. Moscow: TsITP GS SSSR.
24. (1992) *GOST 6713--91.* Low-alloy structural rolled metal for bridge engineering. Specifications. Moscow: Standart.
25. Kirian, V.I., Mikhoduj, L.I. (2002) Problems in application of new steels of increased and high strength in welded structures. *The Paton Welding J.*, **3**, 10--17.
26. Fisher, J.W., Dexter, R.I. (1994) High-performance steel for American bridges. *Welding J.*, **1**, 35--43.
27. Tani, S., Kaneko, V., Ishiguro, M. et al. (1996) Recently developed structure steel for use in civil engineering and constructions. *NKK Technical Rev.*, **74**, 17--25.
28. Girenko, V.S., Dyadin, V.P. (1986) Relationship between impact strength and fracture mechanics criteria of structural materials and their welded joints. *Avtomatich. Svarka*, **10**, 61--62.
29. Kirian, V.I. (1984) Procedure of evaluation of structural steel resistance to tough fractures. *Ibid.*, **11**, 1--6.
30. Kirian, V.I., Vashchenko, A.P., Volgin, L.A. et al. (1993) Evaluation of structural steel fracture toughness in high-speed strain conditions. *Problemy Prochnosti*, **5**, 51--59.
31. Girenko, V.S., Bernatsky, A.V., Rabkina, M.D. et al. (1987) Lamellar, lamellar-brittle and lamellar-tough fractures of welded joints. *Ibid.*, **3**, 70--76.
32. (1993) *Welded engineering structures.* Vol. 1. Principles of structure design. Ed. by L.M. Lobanov. Kyiv: Naukova Dumka.

SPACE TECHNOLOGIES ON THE THRESHOLD OF THE CENTURIES: RESULTS AND PROSPECTS

Yu.P. SEMYONOV

S.P. Korolyov Rocket-Space Corporation «Energiya», Korolyov, Russia

The paper presents the main scientific-technical achievements of S.P. Korolyov RSC «Energiya» over the last decade as an illustration of the successes of the rocket-space industry in the international market of advanced science-intensive technologies for space mastering in the XXI century. These achievements would be unthinkable without solving the diverse problems of welding to together with the leading organization in this field — the E.O. Paton Electric Welding Institute.

Despite all the economic and political difficulties of the last decade of the XX century, S.P. Korolyov Rocket-Space Corporation «Energiya» managed to not only preserve the profile of the company, the basis of scientific-technical potential of the Russian aerospace industry, but also initiate totally new directions and technologies in the field. Let me describe just the large-scale projects, which without exaggeration can be regarded as advanced breakthrough science-intensive technologies of the XXI century: manned orbital complexes «Mir» and ISS, «Sea Launch» aerospace complex, «Yamal» communications satellites, large-sized space structures, project of manned expedition to the Mars, power units for submarines and cars.

All the above-mentioned work was conducted by S.P. Korolyov RSC «Energiya» together with other organizations, specifically with involvement of research institutes of the Russian Academy of Sciences and CIS countries. And, certainly, one of the examples of such a fruitful co-operation is interaction of the team, formed by S.P. Korolyov in mid-fifties of the last century, with the E.O. Paton Electric Welding Institute. As far back as 1958--1959 the technology of electron beam welding of engines in vacuum was introduced in our enterprise together with PWI. This unit is still operable, and is used to weld refractory bronze and titanium alloys. Our co-operation, which over the almost half a century period, spread also to other areas of development of aerospace systems, for instance, development of large-sized transformable structures, is still bearing fruit now.

The program of manned orbital station «Mir» turned out to be unprecedented in terms of the diversity and complexity of the work performed (Figure 1). This project was the focus of the greatest achievements of Russian (Soviet) science and technology of the XX century. Its implementation provided priceless experience of solving the most diverse applied problems in space, which ensured further progress and enhancement of the available space potential for the entire world community on the threshold of the new millenium.

The program of «Mir» station (1986--2001), which incorporated the experience of operation of orbital stations of «Salyut» series, laid the foundations of the classical approach to erection of the future long-term manned complexes in the near-earth orbit, namely modular design and stage-by-stage construction, repairability of on-board systems and structures, regular transportation-logistics service, safety of continuous operation of the crew, adaptability to changes in the flight program, technology of periodical maintenance of freely flying vehicles, multi-faceted purpose-oriented use and controlled de-orbiting.

The station was continuously improved and developed during operation. All together seven modules were taken to orbit, their total weight being 135 t. Modular design enabled a prompt variation of the direction of investigations during the mission, as required by experiment directors, and the method of construction in stages allowed a rational distribution of financial and material resources. The ability to perform fast repair and preventive maintenance operations was envisaged already at the design stage, which enabled eliminating the most complex, also
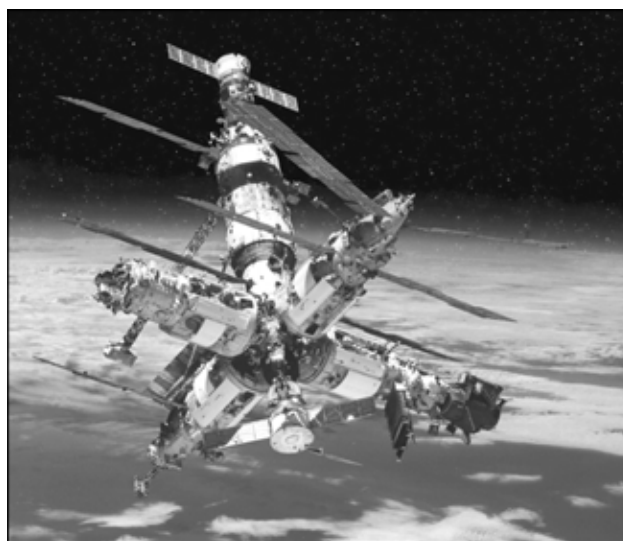
Figure 1. Manned orbital station «Mir»

Figure 2. Three transporting vehicles docked to the «Mir» station

unforeseen failures during the flight. The super long fifteen year mission of the space station, which was 3 times longer than its design life, as well as overcoming a number of serious emergency and failure situations provided priceless experience of operation of orbital space complexes.

Fundamentally new scientific-engineering solutions, promising in terms of further development of the space vehicles, were used in designing practically all the on-board systems. More than 100 new unique structural materials were developed and applied, and advanced technologies were mastered.

The high effectiveness of transport-logistics system of the «Mir» station is indicated by the fact that the total stream of supply «Earth--board» was equal to more than 150 t of fuel and payloads. 31 «Soyuz» and 64 «Progress» vehicles were launched to the station, 9 dockings of the Space Shuttle were conducted. The system of teleoperator control of the cargo ships at their docking to the station became an integral part of all the unmanned space vehicles (SV), interacting with the orbital complex SV, this improving the reliability of performing the orbital manoeuvres of approach and docking (Figure 2).

The experience of many years of large-scale co-operation in space may rightfully regarded as the main achievement. 104 cosmonauts and astronauts from Russia, USA, European and Asian countries worked

Figure 4. Docking of the Space Shuttle to the «Mir» station

on board «Mir» station, where more that 31200 experimental sessions were conducted in various scientific programs.

«Mir» station became practically the first international orbital scientific laboratory, as well as a kind of testing grounds for trying out under the real conditions many engineering solutions and technological processes, used in the International Space Station (ISS) (Figure 3):

• modular principle of erection in orbit of space constructions of large overall dimensions and weight (up to 240 t) was implemented for the first time in world practice;

• «Soyuz», «Progress» and Space Shuttle spaceships were tried out as vehicles for delivery of crews, as well as for material-technical supply of manned complexes (Figure 4);

• technology has been optimized of maintaining the station in a working condition during a long term (15 years) flight and experience has been acquired of coping with emergency situations, providing crew safety and station viability;

• interaction of international crews in long-term fights has been tested, as well as the technology of joint control of manned space vehicles from two Flight

Figure 3. International Space Station

Figure 5. International crew in the «Mir» station consisting of 10 persons

Main parameters of orbital rocket space complex based on «Proton-M» carrier-rocket

Launcher*	«Proton-M», 2 launches	
Acceleration module	11S861-03-A	1S861-03-P
Space vehicle	No	Yes
Payload mass, t: $H_{p.w}/H_{SV} = 200/245$ km, $i = 51.6$ $H_{p.w}/H_{SV} = 200/350$ km, $i = 51.6$ Geostationary orbit	21.85 – 5.5	– 21.6 5.5
*Bajkonur launching site; launch cost is about 1500 mln roubles.		

Proton-M-I Proton-M-II

Figure 6. Docking of two acceleration modules to assemble a 5.5 t space vehicle in the geostationary orbit

Control Centers in the town of Korolyov (Russia) and in Houston (USA). All this permitted successfully completing the initial stage of deployment of ISS of more than 180 t weight in near-earth orbit.

Speaking of «Salyut», «Mir», and ISS manned orbital stations, we should emphasize the fundamental importance of the accumulated experience of conducting in orbit about 200 automatic docking operations of SV and modules of various weights and dimensions. This opens up new prospects for development of orbital rocket-space complexes with tremendous power capabilities, which may be regarded as a serious alternative to use of the currently developed rockets of «heavy» class of the type of «Arian-5». Use of the technology of docking in orbit allows delivering to a geostationary orbit SV of the total weight of about 5.5 t, by applying a two-launch scheme with a reliable «Proton» carrier-rocket (Figure 6). It should be noted that Europe just started studying the problem of delivery to orbit of vehicles of the above-mentioned weight. When the two-launch scheme is used, this problem is solved in a much more reliable manner, than in the case of conducting a single launch, using a not well enough tried out heavy-class carrier-rocket. A sad example of that was «Arian-5» accident in December 12, 2002, when a satellite of more than US\$ 500 mln value was lost at launch.

Mastering the proposed fundamentally new technology of taking heavy SV to orbit in parts with their subsequent assembly in any working orbits, including a geostationary orbit, can now be undertaken only by RSC «Energiya». The work can be conducted in a short time at minimum risk to reach practically any goal in the next decade.

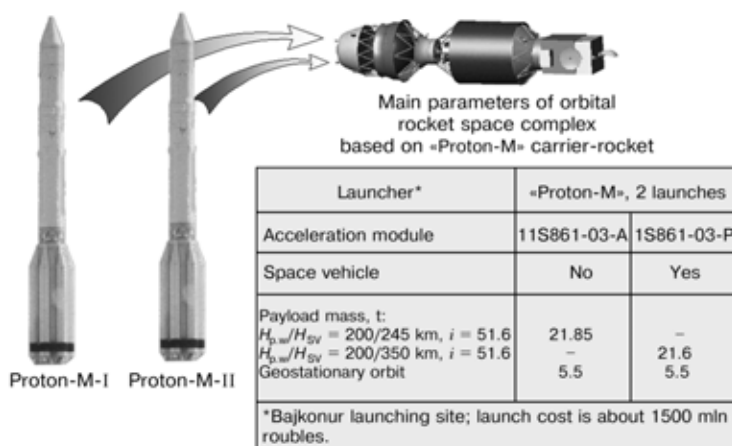Another successfully implemented project was construction of the «Sea Launch» aerospace complex based at sea, which was recognized to be the most ambitious project of the end of the XX century (Figure 7).

The space complexes, the weights of which reach, as a rule, several hundred tons, and the linear dimensions are several tens of meters, are traditionally based in the ground launching sites. Those of them, that are located in-depth of the continents should have considerable areas of unused land. Russia now, for instance, removes from utilization more than 13 mln ha area for dropping of the first stages, and Kazakhstan more than 5 mln ha. In addition, the launching sites should also have a very substantial social infrastructure. The countries of the world now have 15 ground launching sites. Some of them established launching sites for carrier-rockets closer to the equator or the ocean: Kuru cosmodromes in Guiana (France), on Cape Canaveral (USA), Tanegashima (Japan), Shriharikota (India). However, nobody was prepared to take the risk of completely moving the launching site to the Ocean water area, because of concern for the problems, involved in basing a launching site on a floating structure.

Use of floating platforms, located in the Ocean water area as the launching sites, offers great advantages: it is possible to perform SV launches in different directions, including the geostationary and sun-synchronous orbits; there is no need to allocate areas for «laying» the first stages. «Launch power parameters» are much improved due to rotation of the Earth. Under these conditions a middle-class rocket «Zenit», capable of taking 1 t SV to a geostationary orbit, when launched from Bajkonur launching site, carries an almost 3 t vehicle from a floating platform, i.e. its capabilities increase 3 times, when launched from the

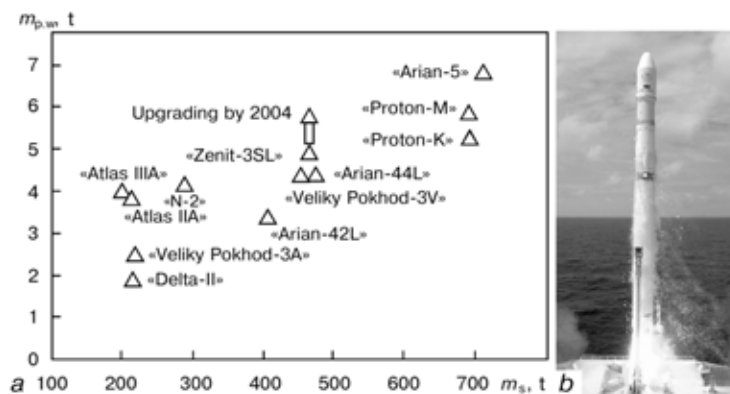**Figure 7.** Aerospace complex «Sea Launch»

Figure 8. Schematic of the launcher (*a*) and place of the carrier-rocket «Zenit-3SL» in the series of launching means (*b*): m_s — starting mass; $m_{p.w}$ — payload weight in an orbit of transition to geostationary orbit

equator and using a two-launch scheme, it will be possible to take to the geostationary orbit a satellite of 6 t weight, as in the case of application of the same scheme for heavy-class «Proton» carrier-rocket, launched from Bajkonur launching site.

The main problem was the need to adapt the already existing ground-based and rocket complexes to floating facilities of a limited area, as well as to operation under the sea conditions (presence of moisture and salt). It is necessary to be able to perform the rocket launch from the platform, oscillating on the water surface, accurately aim and determine the coordinates of the start point. Presence of the launch-control team on the floating facility from which the launch is performed, is inadmissible at the moment of the launch. Hence another mandatory requirement: everything should be done in the automatic mode by commands, sent from another vessel. After studying such an attractive idea, the conclusion was invariably the same: «the idea is good, but difficult-to-implement, in view of a host of technical problems to be solved».

When at the start of 1990s, in connection with disintegration of the Soviet Union, we faced a real threat of loosing the Bajkonur launching site, RSC «Energiya» again came back to the idea of establishing

Figure 9. Launching «Zenit-3SL» rocket

a floating launching site. In 1993 the conceptual design of the complex was released, which was called «Sea Launch». In the period from 1993 to 1995 reports were made several times for the country's leaders on the rationality of deploying such work in Russia. Having found no support in our homeland, we focused our efforts on organizing international co-operation to fulfill the project. Numerous meetings and heated discussions allowed us convincing our future partners of the correctness and rationality of accepting the concept of construction of «Sea Launch» complex. In 1995 an international company was formed, which included the following firms: S.P. Korolyov RSC «Energiya» (Russia), «Boeing» (USA), «Kvarner» (Norway) and «KB Yuzhnoe» (Ukraine).

The platform, built in Norway and fitted with start facilities in Vyborg shipbuilding plant, left for the base port at Long-Beach in June, 1998. About 2000 t of start facilities and electronic instrumentation were mounted on the platform. RSC «Energiya» was entrusted with its mounting. About 30 organizations worked in co-operation with us.

The complex also includes an assembly-command ship (ACS), which is used as a floating assembly-testing facility in the port, and in the start region is the center of remote control of pre-start preparation and of conducting the start. The engineering complex in ACS provides acceptance of rocket stages, accelerating modules and space vehicles, their docking and testing, and reloading of the assembled «Zenit-3SL» rocket to the start platform.

The ship was built in the yard in Glasgow (Scotland), and its fitting with rocket systems of the total weight of about 1500 t was performed in St.-Petersburg in Kanonersky Shipbuilding Plant. ACS accommodates first-class erection-assembly and testing complex for preparation of three carrier rockets «Zenit-3SL» for start. The mounting-testing facility includes halls for preparation of space vehicles, acceleration modules and a fueling station. Also located here is the flight control center, which is excellently equipped and has up-to-date display means and everything that is required for a launch. A totally new three-stage non-polluting carrier-rocker «Zenit-3SL» was actually developed under this project. After completion of preparation of the rocket-space complex,
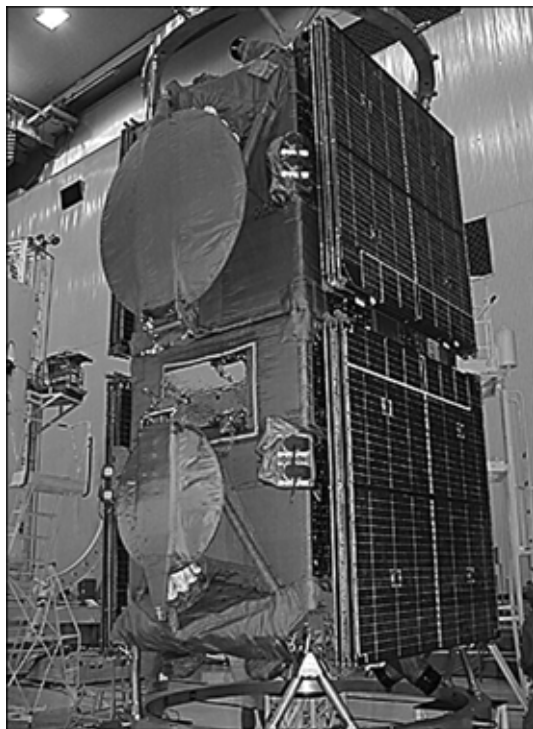
Figure 10. Two «Yamal-100» satellites

Figure 11. Examples of application of three-layer composite materials

the ACS and the platform go over to the start area on the equator at the longitude of 0°1′54″ w.l. (near the Christmas Island).

By the scope of the resolved problems «Sea Launch» project may only be compared with «Energiya--Buran» complex, developed in the USSR in the period from 1978 to 1988.

On March 28, 1999 a demonstration launch and taking «Demosat» vehicle to a working orbit were conducted, which proceeded without any serious remarks at the highest level of accuracy, thus marking the commissioning of the complex. By now eight SV launches have already been performed from the «Sea Launch» rocket-space complex (Figure 9). This rocket-space complex took a fitting place among the effective up-to-date launching facilities.

A not less vivid example of a project with introduction of advanced technological solutions implemented over the last years certainly is development of «Yamal» telecommunication platforms of a new generation.

At the start of 1990s RSC «Energiya» has returned to this manufacturing sector after a thirty year pause, since the time of development of the first communications satellite «Molniya-1». We immediately tried to rise to the current level of technology in development of communication satellites, and in terms of some design solutions implemented in «Yamal-100» SV (Figure 10), we even surpassed the foreign analogs. This took more than six years of intensive work. When developing new SV, we moved away from the classical approach, including the US one of upgrading a vehicle by not more than 30 %. In this case the satellite was developed as 100 % new one, i.e. we took a great risk.

What does the concept of advanced technologies mean today in the field of development of telecommunications satellites? First of all, this is unitizing, which allows separately retrofitting individual elements and achieving a high reliability and adaptability to fabrication in assembly operations.

We have fully eliminated the use of sealed compartments and associated systems of thermoregulation with hydroblocks, pumping the liquid (heat carrier). This allowed us to move from a 3-year to a 10--15 year life of the satellite, as the hydroblocks are mechanisms. which have a limit operating life of 3 to 5 years. We started applying three-layer composite materials (Figure 11) for the structures of the case and solar batteries, with heat pipes built into the case panels. The heat pipes were made without applying light-weight and high-strength composites, but just high-strength light-weight metal.

Figure 12. «Yamal-200» satellite
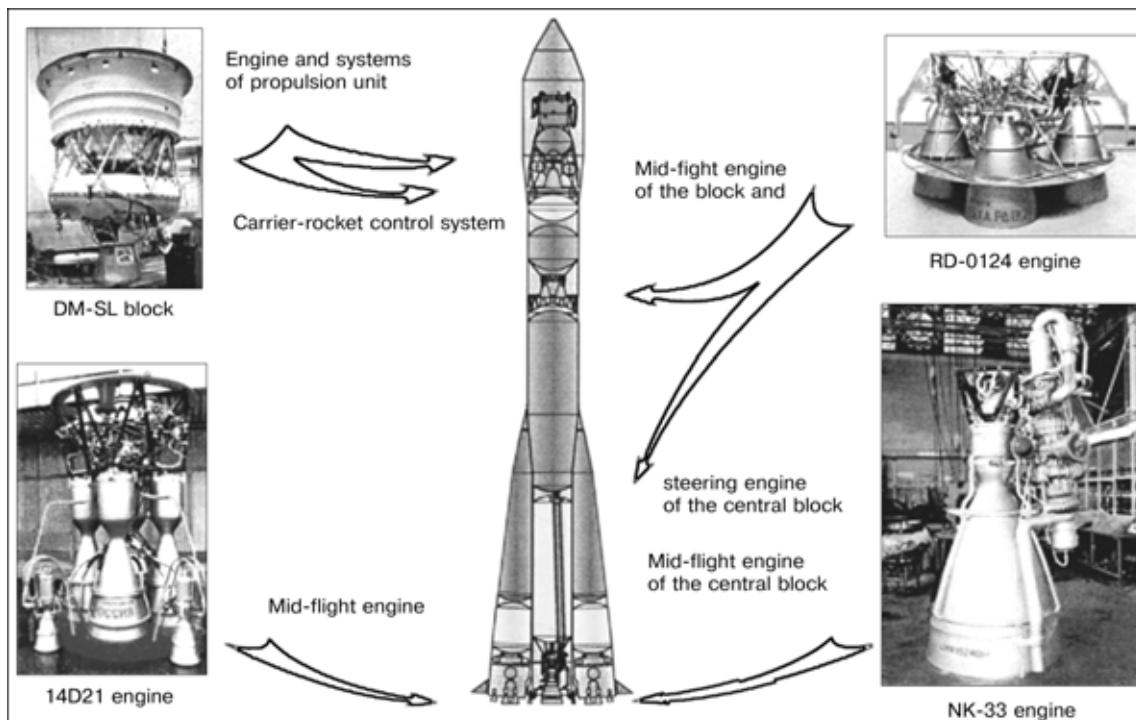
Figure 13. Rocket-space complex «Avrora»

Introduction of these new design and technological processes allowed obtaining up to 120 kg gain in weight in each vehicle. Considering that two «Yamal-100» vehicles are taken to orbit by one launch of «Proton» carrier-rocket, the total gain was 240 kg. Based on the already developed «Yamal-100» platform more powerful variants of this vehicle are being developed ---- two «Jamal-200» SV (Figure 12).

It is quite real to take vehicles of this class to a geostationary orbit with the most inexpensive, reliable and non-polluting carrier-rocket of «Soyuz» type, which was developed as far back as in the 1950s. More than 2 thousand launches of rockets of this type were conducted over the past 40 years. A modification of this famous carrier-rocket, suited to perform the posed task, was called «Avrora». Issuing documentation for this rocket is now going on, but so far just using the funds of S.P. Korolyov RSC «Energiya» (Figure 13).

Work on development of large-sized solar reflectors in near-earth orbit should be further mentioned. This is a purely Russian technology, which will certainly write a bright page in the history of cosmonautics of the XXI century. Effective use of such reflectors for lighting individual regions of the Earth is possible, provided their area is equal to 5000--10000 m^2. The main problems in their development are minimizing their weight and ensuring automatic deployment from the transportation into the working position. This problem was referred to the category of fantastic up to very recent time. However, technological achievements in the field of materials science led to development of such mirrors of polymer metallized film, deployed into the working position and maintaining the required form due to centrifugal forces, arising in the reflector revolution around its axis, normal to its plane.

At the start of 1990s RSC «Energiya» began practical implementation of this idea. In 1993 during demonstration experiment «Znamya-2» on «Progress M-15» spaceship (Figure 14) a twenty meter thin-film reflector was deployed, which was used for lightning selected regions of the Earth before sunrise. Analysis of TV and telemetry information, downlinked to the Earth, confirmed the correctness of the accepted engineering solutions and developed calculation procedures. Space experiment with the film reflector was repeated in 1999. Today RSC «Energiya» is working to develop reflectors of already 60 and 200 m diameter. Implementation of the task of re-reflection of the sun light to individual regions of the Earth is of tremendous practical importance for high-altitude regions of
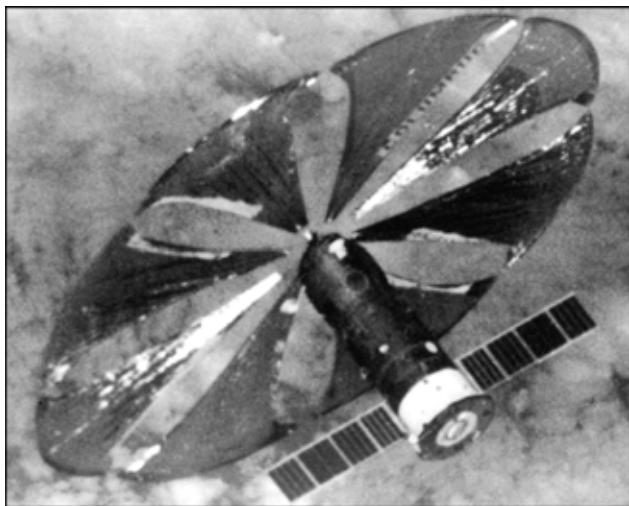
Figure 14. «Znamya-2» experiment

Figure 15. Hinged truss developed by PWI and shown as part of the reusable solar battery of «Mir» station

Figure 17. Antenna of 6 m diameter in a free flight

the Earth, as well as for the work, conducted in emergencies.

Another vivid example of application of the unique space technologies, tried out in the manned complexes, is erection of heavy large-sized platforms on the geostationary orbit, both for solving the telecommunications tasks, and for comprehensive studies of the Earth. By their purpose such vehicles should include large antennaes (of up to 30 m diameter) and extended truss structures of up to 100 m length. Development of technical proposals, and for a number of vehicles of this class of draft projects, was only made possible by the extensive experience of development together with the E.O. Paton Electric Welding Institute of transformable truss structures of hinge-lever type up to 15 m long in the «Salyut-7» and «Mir» stations (Figure 15). Successfully performed work on deployment and folding of such structures, also in the automatic mode, gives us confidence

of the correctness of the selected design-technological solutions and realizability of projects, which still seem to be «exotic».

Good results were also obtained in the field of development of deployable antennae of a large diameter from 6 to 30 m, which have no analogs in the world (Figure 16). For instance, packing dimensions of an antennae of 30 m diameter are just 1500 mm (diameter) for 2000 mm (length), and its weight is not more than 200 kg.

This joint work with Georgian colleagues, which was completed in 1999 by an impressive space experiment «Reflektor» in the «Mir» station (Figure 17), opened up a great prospect for development of not only various antennae, operating in the radio- and submillimeter ranges of wave lengths, but also large-diameter concentrator mirrors of solar gas-turbine units for large-sized orbital complexes such as, for instance, ISS.

Gaining unique experience of development of large-sized orbital complexes, we for many years have worked to study also the concepts of man's flight to Mars. No other country has similar experience of development of a project of a mission to Mars. The main problem in implementation of a manned mission to Mars (Figure 18) consists in provision of an acceptable level of crew safety both due to a high level of duplication of the systems and units, and due to multiple retrofitting, also under the conditions of Mars.

High effectiveness of electric jet engines allows implementing another very valuable advantage of the

Figure 16. Deployment of a space reflector in «Mir» station
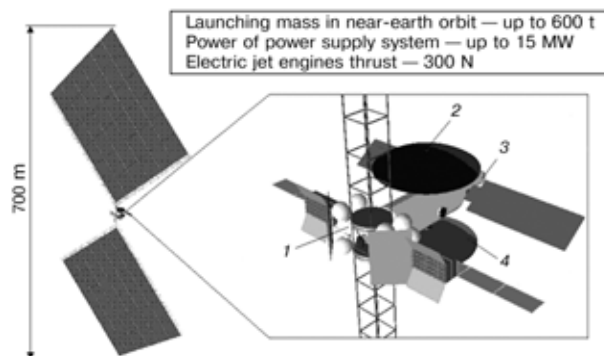
Figure 18. Schematic of interplanetary mission complex for a mission to Mars: *1* — solar tug; *2* — shuttle; *3* — interplanetary ship; *4* — landing module

TESTED SPACE TECHNOLOGIES AND MEANS

«Energiya» rocket, developed in 1987, has passed space flight testing
1987–1988

Long-term flight experience — a procedure of supporting long-term flights was optimized, several flights of more than 1–1.5 years duration were conducted
1971–2000

Systems of assembly in orbit (system of assembly of ship elements has been tried out, more than 200 dockings have been conducted)
1965–2000

Control systems — multimachine systems have been designed and tried out, system prototypes are available
1987–2000

Experience of truss structure development (experiments with different variants of trusses and reflectors were conducted in «Salyut» and «Mir» stations)
1982–2000

Life support systems — systems have been optimized with oxygen and water closed-loop cycle
1982–2000

Film solar batteries (a thin-film solar battery with amorphous silicon with layer of 20 μm thickness was exposed in «Mir» station)
1998

Electric jet engines — DAS engines have been optimized; DAS-66 has operated in orbit; (STEX)
1972

Experimental modules (a series of modules has been developed, which are the prototypes of Martian vehicles, taken to orbit by «Progress» vehicles; the first «Module-M» is being tested now)
1998–2001

Figure 19. Preparation for a mission to Mars in Russia

project, namely not only the crew in a capsule returns to the Earth, but also the entire spaceship comes back to the near-earth orbit for re-use. The service life of the ship is 15 years. It only uses 15 % of its service life in one mission, and after the required preventive replacements of the hardware it will be fit for a mission again.

A considerable part of the path to implementation of a mission to Mars has already been covered. Engineering solutions for the future mission were tried out during the flights of «Salyut» and «Mir» stations (Figure 19). A tremendous scope of experiments has been performed on studying the behaviour of the human body in a long-term space flight. Valery Polyakov, cosmonaut-doctor, worked for almost a year and a half in orbit. The mission to Mars will take about the same time.

A system of automatic docking has been developed and is operating in an excellent manner. This system is required for successive assembly of individual parts of the Martian ship by a multi-launch system. Various variants of deployable trusses («Mayak», «Opora», «Sofora», «Rapana», «Topol»), the prototypes of truss structures for the solar tug, were studied in the orbital stations (Figure 20).

Systems of life support by a closed-loop cycle by water and oxygen have been retrofitted. It is now possible to produce these important components from water and carbon dioxide gas evolved by man, instead of bringing them from the Earth. In other words, the technical readiness for development of an interplanetary ship is very high and attractive in terms of both crew safety and cost.

It is also necessary to mention those advanced science-intensive breakthrough technologies, which
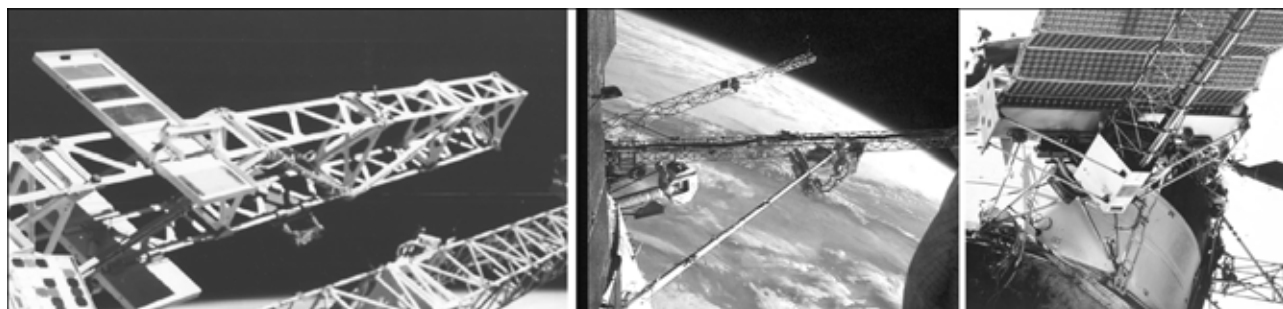
Figure 20. Prototypes of deployable truss structures for the solar tug tested in the «Mir» station
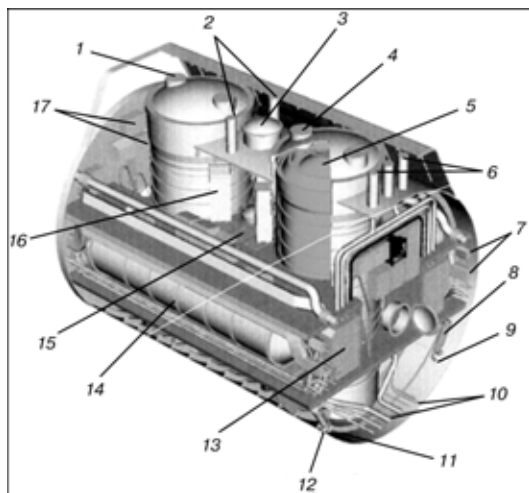
Figure 21. Electrochemical generator for a diesel submarine: *1* — structural access door; *2* — ventilation hatches of enclosures; *3* — cargo port; *4* ---- hydrogen filling hatch; *5* — hydrogen storage module; *6* — oxygen filling hatches; *7* — through cables; *8* — module for emergency drain of hydrogen; *9* — block for controllable drain of hydrogen; *10* — transit piping; *11* ---- module for controllable drain of oxygen; *12* — module for emergency drain of oxygen; *13* — oxygen fitting module; *14* — oxygen storage module; *15* — ECG power unit; *16* — ECG control unit; *17* — control system consoles


Figure 22. Presentation of electromobile with an electrochemical generator

we are actively «bringing down to the Earth» today. There are a lot of such cases. For instance, we are doing joint work with «Rubin» Design Bureau, headed by Prof. I.D. Spassky on development of a power unit for diesel submarines, using as the basis an electrochemical generator, developed by us for the reusable «Energiya--Buran» space system (Figure 12); with AVTOVAZ team we have worked to develop an electric vehicle, based on electrochemical generators (Figure 22). This is a highly promising area of work.

And, finally, it would be unfair not to mention the long-term and fruitful co-operation between S.P. Korolyov RSC «Energiya» and E.O. Paton Electric Welding Institute in the field of the main subject of this International Conference ---- welding and life of structures. All specialists are well aware of the world's first «Vulkan» unit, which was tested in 1969, as well as other pioneering experiments on optimizing the electron beam welding technologies, using a versatile hand tool in «Salyut-7» station. These results were reported several times in detail in many conferences. It is most unfortunate that we were not actually able to conduct in the «Mir» station the «Flagman» experiment, which is impressive in its complexity and posed goals, and which involved the use of the new generation «Universal» welding hardware.

Special mention should be made of the extremely important role that PWI had in development of the technologies of welding fuel tanks 10.6 mm thick and 12.8 m in diameter for N-1 carrier-rocket, which was developed in our enterprise (Figures 23 and 24). This unique work was conducted in 1965, and since that time we have never had any more problems with welding either in space or on the Earth, due to cooperation with the specialists of PWI.
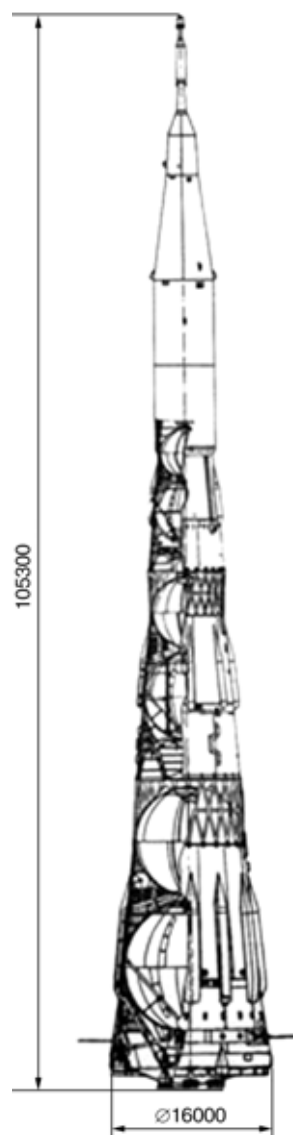
Figure 23. N-1 rocket-carrier
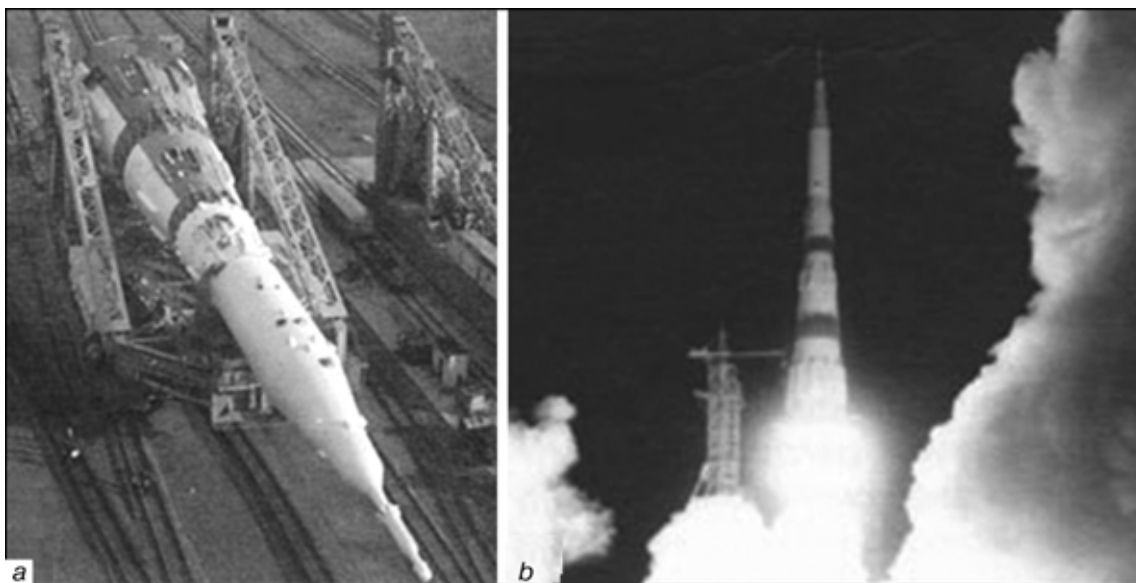
Figure 24. Rocket-space system N1-L3 on its way to the launching site (*a*) and in flight (*b*)

The following welding processes have been accepted and are widely used in our plant now: laser welding for sealed cases of instruments and fittings; argon-arc welding in inert gases in a controlled atmosphere; automatic welding in a vacuum chamber of high pressure cylinders of titanium alloys; friction welding of dissimilar bimetal materials.

Argon-arc welding is used for fabrication of manned and transporting spacecraft, accelerating modules and other products from aluminium alloys.

In conclusion it should be emphasized that all the above-mentioned projects have been implemented and are being implemented not in an economically stable country with a comprehensive support of the state, but under the conditions of a crisis in economy. This was made possible only due to the high potential of the production facilities, created already in the Soviet Union, preserved and developing due to dedicated efforts of the teams, working under the conditions, close to the extremal ones. The aerospace industry now is one of the few (if not the only one), which not only demonstrates examples of survival in the formed economic conditions in Russia, and maintaining the traditional links with organizations, which turned out to be abroad on the threshold of the centuries, but is also laying the foundations for development of the most advanced science-intensive technologies of the XXI century.

DEVELOPMENTS IN PROPERTY PREDICTIONS FOR WELD METAL

D.L. OLSON[1], **E. METZBOWER**[2], **S. LIU**[1] and **Y.D. PARK**[1]

[1]Colorado School of Mines, Golden, USA

[2]U.S. Naval Research Laboratory, Washington, D.C., USA

With the introduction of higher strength low-carbon steels, which have properties that are based on strengthening mechanisms other than the austenitic decomposition, new predictive expressions are required. As new welding processes increase productivity, it also becomes essential to present the cooling rate, $\Delta t_{8/5}$, into predictive expressions. Furthermore, the oxygen content must be included to make these expressions useful in predicting weld metal properties. In addition to the elemental consideration, influences from solidification and second phase particles, such as inclusions, affecting the weld metal solid-state transformation reactions are discussed. Empirical expressions have been developed to predict hardness, yield and ultimate tensile strength, as well as ductility and toughness for low-carbon and low-alloy higher strength steel weld metal. The difficulty introduced by multiple pass welding on weld property predictions is recognized. Various approaches, based on either deterministic analyses with numerical calculations or experimental correlations have been attempted, and these approaches are also discussed. With the availability of new analytical approaches, such a neural net regression analysis, more rapid and compatible selection of the welding consumable composition for a specific alloy and welding thermal experience can be achieved.

Introduction to property prediction expressions. After half a century in the development of methods to predict weld properties and to select welding parameters, analytical approaches and practices are now achieving more reliable results. The first analytical expressions were based primarily on composition and had a «rule of thumb» usefulness in achieving the selection for the degree of preheat and ⁄ or postweld heat treatment that would be required for a specific steel composition [1, 2]. These compositional tools would only correlate to results for the same class of carbon steel, plate thickness and welding parameters, usually for SMA welding. With the introduction of higher strength low-carbon steels, which have properties that are based on strengthening mechanisms other than the austenitic decomposition, new predictive expressions were required. As new welding processes increase productivity, it also becomes essential to incorporate processing parameters, such as the cooling rate into these expressions [3].

With new understanding of the interrelationships between welding process parameters, weld metal composition, microstructure and properties, as well as the new availability of statistical and neural net analytical approaches as discussed by Metzbower et al. [4, 5] and Blackburn et al. [6], the selection of welding consumables can be based on a quantitative footing. It is desirable to be able to rapidly select the welding consumable composition for a specific alloy and welding thermal experience. To better understand the evolution of the development in properties prediction, the necessary features for these analytical methods are described.

Formulation of carbon equivalent expressions. Carbon equivalent equations are hardenability type expressions which were originally developed for use with medium-carbon steels where eutectoidal decomposition is the primary phase transformation with martensite as the major product during fast cooling. They are empirically determined to explain the influence of alloying elements on the transformation behavior of steels. They have also been successfully used for predicting weldability of various types of steel plates by correlating alloy content and cracking susceptibility during welding. A commonly used carbon equivalent equation, the IIW expression, is given below to illustrate a weldability prediction equation:

$$CE = C + \frac{Mn}{6} + \frac{Cr + Mo + V}{5} + \frac{Ni + Cu}{15}. \qquad (1)$$

Alloys with carbon equivalent greater than 0.45 wt.% are usually welded with a preheat. When carbon equivalent is greater than 0.55 wt.%, both pre- and postweld heat treatment are recommended to obtain a sound weld. Another carbon equivalent type expression that relates weld cracking susceptibility to alloy composition is the Ito--Bessyo P_{cm} equation. It is included in the AWS D1.1 Structural Welding Code [1, 2] as a means to assist in hydrogen control:

$$P_{cm} = C + \frac{Si}{30} + \frac{Mn + Cu + Cr}{20} + \frac{Ni}{60} + \frac{Mo}{15} + \frac{V}{10} + 5B. \quad (2)$$

The P_{cm} equation correlates well with the steels that have low carbon contents, usually < 0.1 wt.%. Steels with P_{cm} values of 0.2 wt.% or lower have shown good resistance to weld cracking.

Even though the above equations are commonly applied for HAZ in wrought materials it is questionable if these expressions have the ability to predict properties and transformation behavior of weld me-

tals. Plate martensite of high carbon content is not expected to predominate in the weld metal microstructure and microalloy precipitates may form during the welding thermal cycle. Additionally, influences from solidification and second phase particles, such as inclusions, will also affect the weld metal solid-state transformation reactions. Oxide inclusions are known to promote intragranular ferrite nucleation and should reduce the hardenability. The existing carbon equivalent expressions do not sufficiently incorporate the role (effect) of oxide weld metal inclusions into the formulation, which needs to be done before the carbon equivalent equations can be reliably used for prediction of weld metal microstructure and properties. Also, if carbon equivalent equations are to become effective in predicting weld metal properties, they must also address the influence of welding parameters, for example, cooling rate in the form of $\Delta t_{8/5}$.

Fundamentally derived forms of the predictive equations have been suggested by Liu et al. [7] considering both thermodynamic and kinetic approaches in their formulation. For athermal transformations, such as martensite formation, in which phase stability can be expressed by $\Delta G_{\gamma-\alpha}$, a microstructural sensitive property, such as CE, can be given by the following:

$$CE = K_0\,[C + K_{Mn}Mn + K_{Si}Si + \ldots + K_{C'}ClnC + \\ + K_{Mn'}MnlnMn + K_{Si'}SilnSi + \ldots], \quad (3)$$

where K_0 is the proportionality constant and K_i are coefficients for the various alloying additions and are subject to fundamental interpretation. Mn, Si, C, … are the concentrations of the different elements expressed in weight percent. This expression is based on the assumption that microstructural sensitive properties are directly related to the amount of alloying elements present in the initial and transformed phases. Notice the presence of both linear and non-linear terms in (3). Omission of the non-linear terms will simplify the equation to a form similar to the IIW carbon equivalent equation. In the case of low-alloy steels, omission of the non-linear terms may be acceptable since the coefficients can be manipulated to compensate for the omission. However, it becomes apparent that in high alloy systems, some of the information about alloying behavior may be lost without the non-linear terms.

Assuming that the carbon equivalent can be directly related to the thermodynamic driving force for carbon transport, a new form of the equation for CE can be obtained and expressed as

$$CE = K_0'C\,[1 + K_C'C + K_{Mn}'Mn + K_{Si}'Si + \ldots]. \quad (4)$$

Notice that equation (4) is different from equation (3) and the form suggests a multiplication relationship to the interaction between carbon and other alloying elements. The presence of interaction terms is reasonable because each alloy addition influences the carbon behavior and, thus, should be a product term with carbon. This form of the carbon equivalent equa-

tion should better fit the low-carbon microalloyed steels, in which there is carbonitride precipitation.

For para-equilibrium conditions, in which carbon is observed to partition, the following expression is developed:

$$CE = K_0''C \begin{bmatrix} 1 + K_C''C + K_{Mn}''Mn + K_{Si}''Si + \ldots + \\ + K_{LC}''lnC + K_{LC}''ClnC + \\ + K_{LMn}''MnlnMn + K_{LSi}'K_{Si}lnSi + \ldots \end{bmatrix}. \quad (5)$$

This equation is again different from the commonly used form of carbon equivalent expressions as seen in (3) and (4). Terms expressing the interaction between elements contain the natural logarithm of element concentration. The last three terms are a major concern when there are orders of magnitude variations for minor alloying additions. The lack of these terms may cause problems in the efforts to correlate microalloyed HSLA steel properties to composition.

Prediction of weld metal properties. Although the above equations are commonly applied for HAZ in wrought materials, it is questionable whether these expressions have the ability to predict properties and transformation behavior of weld metals. Influences from solidification and second phase particles, such as inclusions, will also affect the weld metal solid-state transformation reactions. In addition to the elements considered in (1) to (5), the oxygen content must be included to make these expressions useful in predicting weld metal properties.

Role of weld metal oxygen. Welds typically pick up oxygen to levels of several hundred ppm then deoxidize to oxygen levels of around 200 ppm with the formation of oxide inclusions. Weld metal inclusions, resulting from oxidation of alloying elements, are an important factor in influencing weld metal microstructure in low-carbon and high-strength steels. The type, size distribution, and density of weld metal inclusions are all important variables to control in order to achieve the desired weld metal microstructures and properties. An oxygen term (or terms) needs to be added to the carbon equivalent expressions, and the magnitude of the coefficient(s) will be dependent on the type of inclusions being formed (the type of consumable being used). An adjusted P_{cm} called P_{cmo} is given in [8]:

$$P_{cmo} = C + \frac{Si}{30} + \frac{Mn + Cr + Cu}{20} + \\ + \frac{V}{10} + \frac{Mo}{15} + \frac{Ni}{60} + 5B - \frac{3}{4}O. \quad (6)$$

Compared to the original P_{cm} equation, equation (6) includes an oxygen term which is minus 0.75 times the weld metal oxygen concentration.

Liu and Olson [9, 10] suggested that for low-carbon microalloyed steel weld metals, the desirable size distribution of inclusions would be when the maximum in size distribution is greater than the Zener particle diameter. In high-strength steel weld metals, Ramsay et al. [11] found that a bimodal inclusion size distribution would be best to achieve the smallest

Table 1. Equilibrium partition ratios of various solute elements in low-alloy steel

Element	C	Si	Mn	Al	Ti	B	O	S	N
κ	0.17	0.80	0.70	0.95	0.50	0.001	0.01	0.20	0.04

austenite grain size and the smallest packets of lath martensite. This condition would allow optimum weld metal toughness at a given strength level. A fundamental understanding of weld pool chemistry is essential if the proper inclusion type, size distribution, and quantity are going to be produced consistently over a specific heat input range.
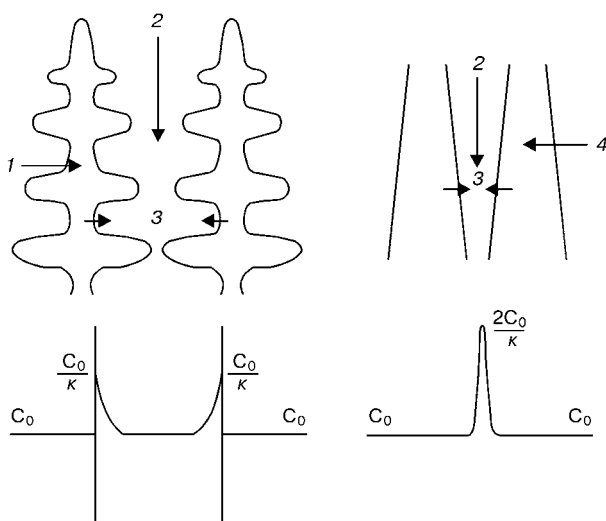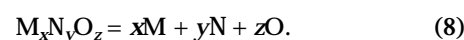
Role of solidification on inclusion formation. During cellular or dendritic solidification commonly observed in steel weldments, solute elements segregate to the liquid at the solid--liquid interface, and the liquid concentration of specific solute elements can reach high levels in the interdendritic spaces, as illustrated in Figure 1. For dendritic solidification, it can be assumed that diffusion in the liquid is complete over the interdendritic space, and that diffusion in the solid occurs only for high diffusivity solutes. Neglecting solid diffusion, the composition in the liquid at the solid--liquid interface can be modeled [12] by the non-equilibrium lever rule or Scheil equation:

$$C_L = C_0 f_L^{\kappa - 1}, \qquad (7)$$

where C_0 is the bulk concentration in the weld pool; C_L is the concentration in the liquid at the interface; and κ is the equilibrium partition ratio. This equation can be modified to account for diffusion in the solid if so desired.

The equilibrium partition ratio, κ, controls the direction and the extent of segregation. For most alloy elements in steel the partition ratio is less than one and the element segregates to the interdendritic liquid. Table 1 gives some approximate values of κ for various solutes in low-alloy steel [13].

Consider the deoxidation equilibrium as represented by the dissolution reaction for an oxide:

$$M_xN_yO_z = xM + yN + zO. \qquad (8)$$

The free energy change associated with the dissolution of the $M_xN_yO_z$ oxide can be written as

$$\Delta G = \Delta G^o + RT\ln\frac{[M]^x[N]^y[O]^z}{[M_xN_yO_x]}, \qquad (9)$$

where [M], [N] and [O] are the solute activities in the liquid; and *x, y* and *z* are the stoichiometric constants from (8); $[M_xN_yO_z]$ is the activity for the specific inclusion and can be assumed to have the value of one.

The free energy as a function of the remaining liquid fraction:

$$\Delta G = \Delta G^o + RT\ln\frac{[\gamma_M M_o f_L^{\kappa_M - 1}]^x\,[\gamma_N N_o f_L^{\kappa_N - 1}]^y\,[\gamma_O O_o f_L^{\kappa_O - 1}]^z}{[M_xN_yO_x]}, \qquad (10)$$

where $[M_o]$, $[N_o]$ and $[O_o]$ are the bulk concentrations of M, N, and O in the melt; and $[\gamma_M]$, $[\gamma_N]$ and $[\gamma_O]$ are the activity coefficients for the solutes. It is this free energy expression (10) that allows for the prediction of the intragranular weld metal inclusion formation.

Figure 2 also illustrates the influence of microsegregations in low-carbon steel weld metal with high oxygen content and shows rows of intragranular oxide inclusions which formed in the solute with interdendritric regions. It is these «last to form» oxides that serve to establish the fine acicular ferrite in the weld metal, as seen in Figure 3. This microsegregation must be accounted for in future predictive expressions for weld metal microstructure and properties.

The sequence of deoxidation reactions can be predicted based on the assumptions that the weld pool comes to equilibrium with the strongest deoxidant and that the intradendritic concentrations of oxygen

Figure 1. Solute concentration enrichment of interdendritic region of the weld pool: *1* ---- primary dendrite arm; *2* — interdendritic spacing; *3* — dendrites thickening; *4* — dendrite arm

Figure 2. Light micrograph showing aligned non-metallic inclusions in the interdendritic regions [30]

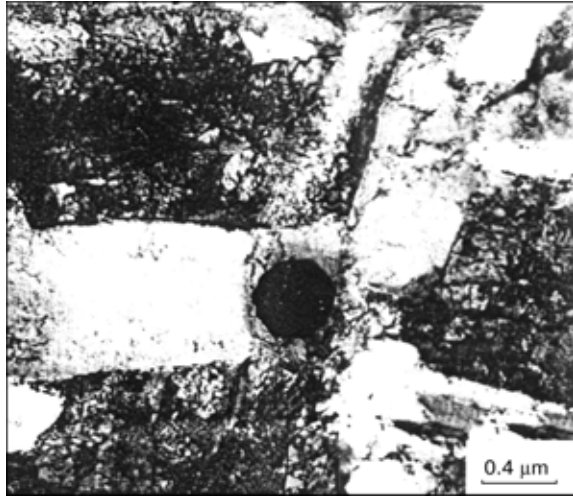**Figure 3.** Oxides formed in the liquid and nucleate acicular ferrite in high-strength low-alloy steel weld metal

Figure 4. Changes in the martensite start temperature, M_s, due to local solute concentration variation ($M_s(c) = 521–14.3Cr–17.5Ni–28.9Mn–37.6Si–350C–39.5Mo–1.19(CrNi)+23.1(Cr+Mo)C$) [15]

and deoxidants will be increased by microsegregation during solidification to a point where the solubility product is exceeded. As solidification progresses from 0 to 95 % solid (liquid fraction from 1.0 to 0.05): the interdendritic silicon concentration increases by about 50 %, manganese by about 100 %, oxygen increases by a factor of 8, and the aluminum concentration shows a very small increase. The dramatic increase in the interdendritic oxygen concentration as solidification progresses will cause additional oxides to precipitate in the weld metal on as discussed by Frost et al. [14]. Table 2 shows the compositional changes caused by microsegregation as determined by the Scheil equation.

Figure 4 is a schematic of the intragranular variation of alloy content in weld metal. The expression for martensite start in weld metal [15] is also given. With the compositional variation across the weld metal grain there should be correlatable variation in martensite. Figure 5 illustrates on micrographs the streaks of untempered and tempered martensite in interdendritic AISI 4340 steel weld metal. These micrographic features are clear evidence of the influence of microsegregations of solute in high-strength steel weld metal.

Influences of thermal experience. Most carbon equivalent expressions are only a function of composition and do not consider thermal experience and severity of quench. The thickness of plate, edge preparation, preheat, and heat input of the process will influence the cooling rate. The time to cool from 800 to 500 °C, $\Delta t_{8/5}$, is an alternate way to describe the cooling rate of a weldment and has been used to compare the welding thermal cycle to the acceptable thermal experience that would achieve specified properties. Property predicting expressions that contain a $\Delta t_{8/5}$, have been introduced.

A formula devised by Lorenz and Duren [16] for calculating HAZ hardness, which takes into consideration both alloy composition and cooling rate, is shown in the following equation:

$$HV = 2019[(1 – 0.5\log\Delta t_{8/5})C + 0.3(CE – C)] + \\ + 66(1 – 0.8\log\Delta t_{8/5}). \tag{11}$$

Yurioka [17] also introduced a carbon equivalent type expression to describe low-carbon steel weldability that has $\Delta t_{8/5}$ as a contributing term. The maximum HAZ hardness was related to both the alloy composition and cooling rate:

$$H_{\max} = 442C + 99CE_{II} + 206 – \\ – (402C – 90CE_{II} + 80)\operatorname{arctg}(x), \tag{12}$$

where

$$x = \frac{(\log\Delta t_{8/5} – 2.30CE_I + 1.35CE_{III} + 0.882)}{(1.15CE_I – 0.673CE_{III} – 0.601)}; \tag{13}$$

$$CE_I = C + \frac{Si}{24} + \frac{Mn}{6} + \frac{Cu}{15} + \frac{Ni}{12} + \frac{Cr}{8} + \frac{Mo}{4} + \Delta H;$$

$$CE_{II} = C + \frac{Si}{24} + \frac{Mn}{5} + \frac{Cu}{10} + \frac{Ni}{18} + \frac{Cr}{5} + \frac{Mo}{2,5} + \frac{V}{5} + \frac{Nb}{3};$$

$$CE_{III} = C + \frac{Mn}{3.6} + \frac{Cu}{20} + \frac{Ni}{9} + \frac{Cr}{5} + \frac{Mo}{4};$$

$\Delta H = 0$ at B ≤ 1 ppm; $\Delta H = 0.03fn$ at B = 2 ppm; $\Delta H = 0.06fn$ at B = 3 ppm; $\Delta H = 0.09fn$ at B ≥ 4 ppm; $fn = (0.02 – N)/0.02$; N is the nitrogen content (wt.%).

This set of equations proposed by Yurioka was found to best fit HAZ properties in a comprehensive

Table 2. Composition changes caused by microsegregation in low-alloy steel

Element	κ	$f_s = 0$	$f_s = 0.2$	$f_s = 0.4$	$f_s = 0.6$	$f_s = 0.8$	$f_s = 0.9$	$f_s = 0.95$
Al	0.95	0.040	0.040	0.041	0.043	0.043	0.045	0.047
Ti	0.50	0.030	0.034	0.039	0.067	0.067	0.095	0.134
Si	0.80	0.500	0.523	0.554	0.690	0.690	0.797	0.910
B	0.001	0.005	0.006	0.008	0.025	0.025	0.050	0.100
Mn	0.70	0.150	1.600	1.750	2.430	0.243	2.990	3.680
O	0.01	0.0006	0.0008	0.0015	0.0030	0.0030	0.0059	0.0117
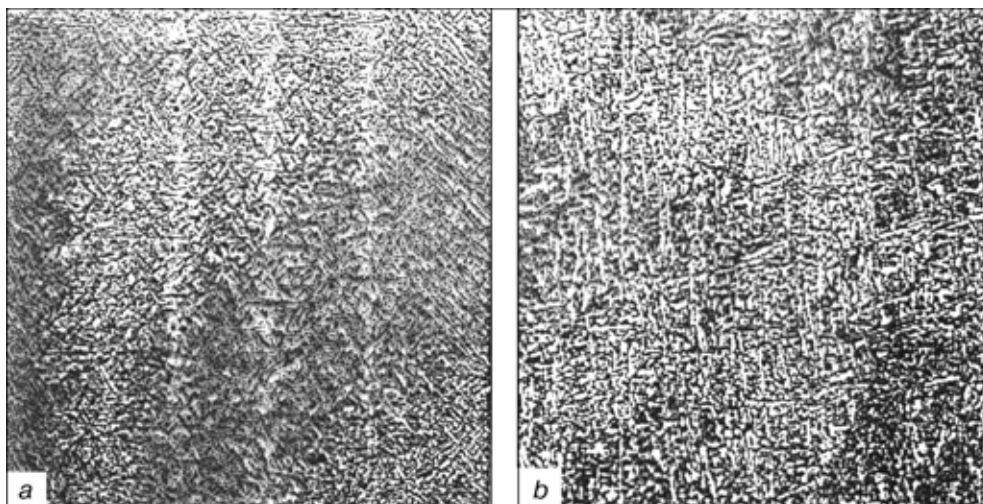
Figure 5. Light micrographs of untempered (*a*) and tempered (*b*) AISI 4340 steel welds made with $40SiO_2$--$20MnO$--$40CaO$ flux ($\times 500$) [31]

investigation involving over twenty-five reported carbon equivalent expressions [3, 18]. Both hardenability and weld thermal cycle, $\Delta t_{8/5}$, in predicting weld metal mechanical behavior were considered.

An approximate calculation for $\Delta t_{8/5}$ can be obtained from the Rosenthal solution for welding heat behavior [19]. $\Delta t_{8/5}$ is directly related to the heat input, H, by the following equations:

$$\Delta t_{8/5} = 8.149 \cdot 10^{-4} \left(\frac{\eta H}{2\pi\kappa} \right) \qquad (14)$$

and

$$\Delta t_{8/5} = 2.767 \cdot 10^{-6} \left\{ \frac{\eta H^2}{4h^2 \pi\kappa\rho\, C_p} \right\} \qquad (15)$$

where η and H are the process efficiency and heat input of the welding process, respectively; κ, ρ and C_p are the thermal conductivity, specific gravity and specific heat of the material, respectively; h is the thickness of the plate. Equation (14) is for three dimensional heat transfer conditions such as those found in thick plate welding, while equation (15) is intended for two dimensional heat flow in thin plate welding. It is clear that to describe the microstructure and mechanical behavior of a high-strength low-alloy steel weld metal, the effects of alloying elements, oxygen, welding parameters and cooling rate need to be considered.

Multipass weld deposition. A significant fraction of the structural welds are multiple passes. This situation results in depositing weld metal onto prior weld deposits producing a HAZ in the prior deposited weld metal. The resulting macrostructure is best characterized for large section welding as metallic composite. The variations of composition and microstructure do not severely alter the bead-to-bead properties in the lower strength steel and the resulting properties, even though they vary, still maintain an acceptable properties across the multipass weld metal. The situation is remarkably different in the higher and high-strength multiple passes steel weldments resulting in potentially significant variation in hardness across the multipass weld metal.

Ramirez et al. [20] has shown for the low-alloy high-strength steels that properly selecting alloy additions to the welding consumable can produce a weld deposits with the potential of forming weld metal precipitates at different time-temperature cycles. Thus, when one precipitate is over aging in the steel due to a subsequent weld pass, another precipitate is in the initial forming state. This arrangement in precipitation maintains a sufficient concentration and proper size distribution of the precipitates to achieve a fairly uniform hardness, and thus strength, level across the multiple pass weldment. Evans [21--23] has produced a large property database on multiple pass steel weld deposits with systematic variations of specific allying additions. The development of methodologies for weld property prediction must address this non-uniform microstructural behavior across the multipass welds. The need to introduce and apply composite material concepts to assist in selecting consumable compositions that maintains approximately uniform weld metal properties needs to be advanced.

Deterministic analysis with numerical calculations. International efforts have also engaged in developing numerical deterministic analyses with calculations which model the various welding atomic mechanistic processes (pyrochemistry, solidification, solid-state phase transformations) that occur in the welding environment, from the weld pool behavior to the solid-state phase transformations [24]. These efforts have added insight into the atomic processes involved and will eventually lead to more comprehensive methods to predict microstructure and properties. However, this fundamental approach is still limited, firstly, due to insufficient chemical and physical information as to elemental compound and material properties and, secondly, due to the complex computational methodology which is difficult for its transfer to an industrial welding practitioner. The use of further refined experimental correlation methodologies for weld metal microstructure and property predictions is still the most workable approach. With a sufficient collection of experimental correlatable
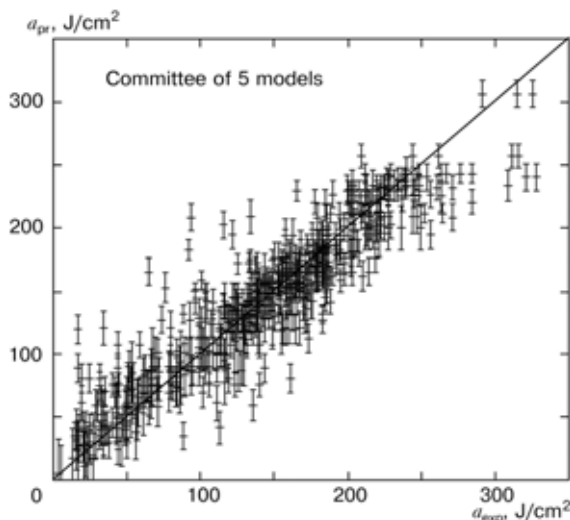
Figure 6. Comparison of predicted and measured Charpy V-notch energy at --51 °C based on a committee of 5 models

Figure 7. Variations in yield strength as a function of carbon content at two different cooling rates

data, the use of neural net regression analyses has made significant improvements in property predictability. Special efforts are needed to obtain more experimental correlatable data for high-strength steel weld metals.

Prediction of weld metal properties. Empirical expressions have been developed to predict hardness [25], yield and ultimate tensile strength [6, 26], as well as ductility and toughness [4, 5] for low-carbon and higher strength low-alloy steel weld metal. Various approaches, including statistical and neural net analyses, have been attempted and compared.

Extensive experimental data for the welding of high-strength steels for naval platforms has been utilized by Metzbower et al. [4, 5] to develop artificial neural networks for their strength and toughness. This data provided an opportunity for creating a quantitative model for the estimation of steel weld metal mechanical properties. A neural network is capable of realizing a great variety of non-linear relationships. Data are presented to the network in the form of input

(composition and cooling rate) and output (desired property) parameters, and the optimum non-linear relationship found by minimizing the difference between the measured value and the predicted value. As in regression analysis, the results then consist of a series of coefficients (called weights) and a specification of the kind of function, which in combination with the weight, relates the inputs to the output. The predictability of the neural net analysis is further enhanced by using a committee of the best models to make predictions. The best models are ranked using the values of their test errors. The committee is formed by combining the predictions of the best models that result in the lowest test error. An example of the predictions from the best model can be seen in Figure 6, where the predicted and experimental data for the Charpy V-notch energy measured at --51 °C for a low-carbon steel weld metal is shown [4, 5]. Once a neural network has been established, predictions for that particular property can be made as a function of each input parameter individually or in combination with other input parameters. For exam-

Figure 8. Iso-hardness (*a*) and iso-strength (*b*) diagram for low-alloy steels [28]

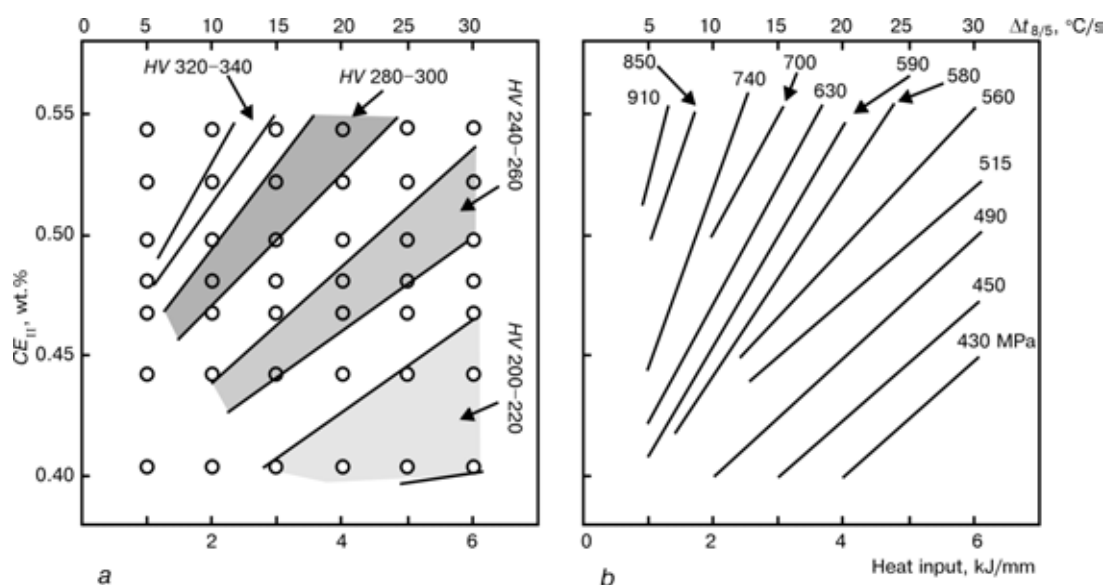ple, Figure 7 shows the variation in yield strength as a function of carbon content at two different cooling rates and clearly indicates the non-linearity of the prediction and the interdependence of the variables.

Isoproperty diagrams. An isoproperty diagram, which correlates the thermal experience and hardenability to weld metal microstructure, can be very useful in the selection of welding consumables for different welding conditions, heat input, and alloy composition. Carbon equivalent--$\Delta t_{8/5}$ diagrams have been used by Liu et al. [27] to predict weld properties. Figure 8 illustrates an iso-hardness diagram and iso-strength diagram for low-alloy steels [28]. The lines on this diagram represent welds with equal property that resulted from different sets of welding conditions and alloy composition. Welding engineers can adjust process parameters according to material property fluctuations to always obtain consistent weld properties. The best carbon equivalent expression to be used with the isoproperty diagrams needs to be determined.

Selection of resilient welding parameters. Acceptable welds can be achieved with a large range of combinations of weld compositions and welding parameters, but some combinations are more robust to process parameter variation. With the evolution of more reliable constitutive equations and / or neural net procedures to predict weld properties, analytical methods may become available to select a resilient set of welding parameters that will reduce the rejection rate. A method based on calculus of variations has been proposed to examine the sensitivity of weld properties to fluctuations in processing and chemical composition [29].

CONCLUSION

An international effort to expand the data pool of experimentally determined correlations between various weld properties and weld composition and thermal experience, $\Delta t_{8/5}$, needs to be promoted and performed. The resulting data bank should be made available to the international welding metallurgy research community. This effort will promote collaboration between investigators and more rapidly introduce new and refine existing approaches for weld property predictability.

1. Granjon, H. (1967) Notes on the carbon equivalent. *IIW Doc. IX-555--67.*
2. Ito, Y., Bessyo, K. (1968) Weldability formula of high strength steels related to heat affected zone cracking. *IIW Doc IX-567.*
3. Lundin, C.D., Gill, T.P.S., Qiao, C.Y.P. et al. (1989) Validity of conventional carbon equivalent formulae to the weldability of low-carbon microalloyed steels for marine structures. *Ship Structure Committee Report.* DTCG-23-C-20035, April 14, 1989.
4. Metzbower, E.A., Deloach, J.J., Lalam, S.H. et al. (2001) Neural network analysis of strength and ductility of welding alloys for high-strength low-alloy shipbuilding steels. *Sci. and Techn. Welding and Joining,* 6 (**2**), 116--124.
5. Metzbower, E.A., Deloach, J.J., Lalam, S.H. et al. (2001) Analysis of toughness of welding alloys for high-strength low-alloy shipbuilding steels. *Ibid.,* 6 (**4**), 368--374.
6. Blackburn, J., Deloach, J.J., Brandemarte, A. (1997) A strength model for low-carbon, ferritic, GMA weld metal. In: *Proc. of Nat. Welding Seminar.* Bangalove: Ind. IW.
7. Liu, S., Olson, D.L., Matlock, D.K. (1986) A thermodynamic and kinetic approach in the development of expressions for alloy behavior prediction. *J. Heat Treat.,* 4 (**4**), 309--316.
8. Onsoien, M.I., Liu, S., Olson, D.L. (1996) Shielding gas oxygen equivalent in weld metal microstructure optimization. *Welding J.,* 75 (**7**), 216--224.
9. Liu, S., Olson, D.L. (1986) The role of inclusions in controlling HSLA steel weld microstructures. *Welding J.,* 65 (**6**), 139--149.
10. Liu, S., Olson, D.L. (1987) The influence of inclusion chemical composition on weld metal microstructure. *J. Materials for Energy Systems,* 9 (**3**), 237--251.
11. Ramsay, C.W., Olson, D.L., Matlock, D.K. (1990) The influence of inclusions on the microstructures and properties of a high-strength steel weld metal. In: *Proc. of Gatlinburg Int. Conf. on Recent Trends in Welding Research,* May 14--18, 1989. Materials Park.
12. Scheil, E. (1942) BemerKungen zur Schichtkristallbildung. *Zeitschrift fur Metallkunde,* **34**, 70--72.
13. Olson, D.L., Liu, S., Edwards, G.R., (1990) Role of solidification of HSLA steel weld metal chemistry. In: *Weldability of Materials.* Materials Park.
14. Frost, R.H., Olson, D.L., Liu, S. (1992) Influence of solidification on inclusion formation in welds In: *Proc. of 3rd Int. Conf. on Int. Trends in Welding Science and Technology,* Gatlinburg. ASM Int., Materials Park.
15. Self, J.A., Carpenter, B.F., Olson, D.L. et al. (1987) Phase transformation and alloy stability. In: *Alternate alloying for environmental resistance.* Warrendale: TMS.
16. Lorenz, K., Duren, C. (1982) *IIW Doc. IX-B--82.*
17. Yurioka, N., Ohkita, S., Tamehiro, H. (1981) Study on carbon equivalents to access cold cracking tendency and hardness in steel welding. In: *Proc. of AWMI Symp. on Pipeline Welding in the 80's.*
18. Devletian, J.H. (2000) Carbon equivalent (P_{cm}) limits for thick carbon and low alloy steels. *National Shipbuilding Research Project Report NSRP 0530, U.S. Navy, Carderock Det.*
19. Rosenthal, D. (1946) The theory of moving sources of heat and its application to metal treatment. In: *Transact. of ASME,* **68**, 819--866.
20. Ramirez, E., Liu, S., Olson, D.L. (1996) Dual precipitation strengthening effect of copper and niobium in high-strength steel weld metal. *Materials Science and Engineering A,* A216, 91--103.
21. Evans, G.M. (1980) The effect of manganese on the microstructure and properties of weld metal deposits. *Welding J.,* 59 (**3**), 65--75.
22. Evans, G.M. (1991) The effect of aluminum in shielded metal and C--Mn steel multi-run deposits. *Ibid.,* 70 (**1**), 32--39.
23. Evans, G.M. (1993) The effect of micro-alloying elements in C--Mn steel weld metal. *Welding in the World,* 31 (**1**), 12--19.
24. Cerjak, H. (2002) *Mathematical modelling of weld phenomena 5.* Materials Modeling Series. London: IOM Com.
25. Hart, P.H.M. (1986) Resistance to hydrogen cracking in steel weld metals. *Welding J.,* 65 (**1**), 14--22.
26. Yurioka, N. (2002) Prediction of strength of weld metal. Report II. *IIW Doc. IX-2026--02.*
27. Liu, S., Ibarra, S., Olson, D.L. (1994) Assessment of microstructural and property prediction equations in structural welding. *OTC 7497.*
28. Kluken, A.O., Liu, S., Olson, D.L. (1992) Use of predictive equations for arctic steel heat affected zone properties. In: *Proc. of 11th Int. Conf. on Offshore Mechanics and Arctic Energy.* N.Y.: ASME.
29. Olson, D.L., Ibarra, S., Liu, S. (1991) Selection of resilient welding parameters for arctic fabrications and repair. In: *Proc. of 10th Int. Conf. OMAE.* N.Y.: ASME.
30. Indacochea, J.E., Olson, D.L. (1983) Relationship of weld metal microstructure and penetration to weld metal oxygen content. *J. Materials for Energy Systems,* 5 (**3**), 139--148.
31. Burke, P.A., Indacochea, J.E., Olson, D.L. (1990) The effects of welding flux additions on 4340 steel weld metal composition. *Welding J.,* 69 (**3**), 115--122.

METALLURGY OF STEEL:
SPECIFICS OF PRODUCTION IN THE XX CENTURY, PROBLEMS AND PREDICTION
OF FUTURE DEVELOPMENT

N.P. LYAKISHEV and **A.V. NIKOLAEV**

A.A. Bajkov Institute of Metallurgy and Materials Science, RAS, Moscow, Russia

Major stages of development of metallurgical production of steel in the XX century are considered and geopolitical factors, defining its progress, are formulated. A determinant role of energy consumption in aggloblast furnace production is shown in the energy balance of the integrated works. Alternative processes of steel production are described. The significant decrease in energy consumption can be attained in combination of several technologies. Steel melting and generation of commercial heat and electric energy using the technology of plasma-electrometallurgical complex are challenging. The ways of metallurgy progress in the XXI century are outlined.

Production of iron in the XX century. The XX century was called «cast iron century», as the cast iron melting in the world exceeded the steel production and in 1913 it was 78.5 mln t (steel ---- 72.4 mln t). By the end of the XX century the steel production reached 800 mln t, while the iron production was about 500 mln t (≈ 63 %), that allowed the century to be called «steel century» (Figure 1) [1]. The main manufacturers of cast iron and steel were integrated works, functioning on the base of aggloblast furnace technology. In steel melting production in the first half of the XX century the decisive role was played by open-hearth process and, partially, basic oxygen converter process. Electric steel melting process was used for melting quality steels. The second half of the XX century was characterized by almost complete refusal from the open hearth process and a wide spreading of the converter process.

Over the past century an enormous metal stock has been accumulated, that required the development of industrial methods of its utilization. To solve the mentioned problem, an electric furnace became the optimum metallurgical unit that stimulated the rapid development of the electric steel melting process (Figure 2).

A method of continuous steel casting, developed in the former USSR, found a wide spreading, thus increasing the efficient metal output by 15 %, and also improving its quality. However, as to the volumes of application of the continuous casting, the domestic metallurgy is now greatly behind the advanced countries of the world: at present it amounts to about 50 %, while in industrialized countries it is more than 90 %.

Changes occurring in the metallurgical production reflected the global processes, forming the progress in the world industry. Essential changes took place
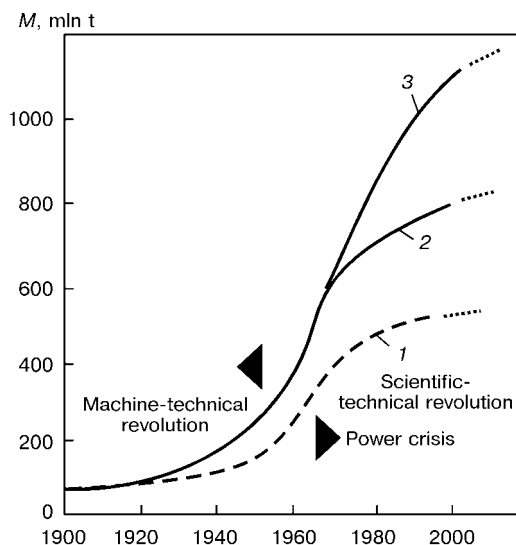

Figure 1. World production M of cast iron (1 — physical tons) and steel (2 — physical tons; 3---- qualitons) [2] in the XX century
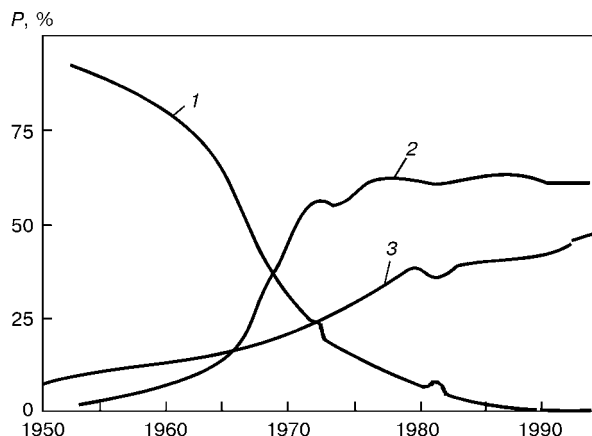

Figure 2. Structural modification of electric steel-melting processing P at the second half of the XX century: 1 ---- open-hearth furnace; 2 — converters; 3 — electric-arc furnaces

in power and raw material base, where the ecological problem was clearly manifested.

Geopolitical factors of the present development of world industry. At the second half of the XX century the transition from machine-technical revolution to scientific-technical revolution, characterized by a wide use of high technologies, was occurred. The industrial process was intensified, its specific parameters were increased, the quality of products was improved, the power and material consumption was reduced and the labour productivity was increased.

In this period the world industry was rapidly progressing as a whole and the rates in growth of steel production were also increased. The power consumption was drastically increased and in the 1970s the energy crisis began to be manifested, which is continued until now in not so distinct form.

A large work has been done in the industrialized countries for the decrease in energy-content of internal gross production (IGP). Unfortunately, the energy-content of IGP in Russia 3 times exceeds, as a whole, the same parameter in the industrialized countries. Except the non-perfectness of the technologies proper, the climatic conditions of Russia have also negative influence on this parameter.

The important feature of the last century was the appearance of a clearly expressed world ecological crisis in this period. Antropogeneous effect on «Earth» system is manifested in an intensive exhaustion of raw resources and fossil fuels, increase in concentration of hothouse gases in atmosphere, thus leading to the change in climate. The average temperature of the Earth surface is changed adequately to the content of carbon dioxide in atmosphere (Figure 3). In spite of recommendations of Kioto Protocol the increase in carbon dioxide emissions and its concentration over three recent years is continued. This is stipulated by the fact that to reduce the carbon dioxide emissions it is necessary to replace old traditional technologies by the radically new technologies, that will require significant capital investments. Thus, the expenses for modification of the USA industry to reduce the carbon dioxide emission by 20 % (as compared with 1990) can amount up to 3.6 trillion dollars [3].

Under the influence of global processes, occurring in the XX century, the development of conception of «steady progress» was begun, consisting in the creation of such conditions on Earth which will allow mankind to survive [4].

Metallurgy is closely related to all the above-mentioned. Coming from the described positions, let us consider changes occurring in the metallurgical production (Figure 4).

STR and metallurgy of steel. In spite of the fact that scientific-technical revolution (STR) in Russia was passing, as a whole, somewhat slowly, the great achievements were remarkable in ferrous metallurgy. Alongside with enlargement of blast furnaces and modification of their design, and also increase in quality of coke and ore raw materials, such innovations
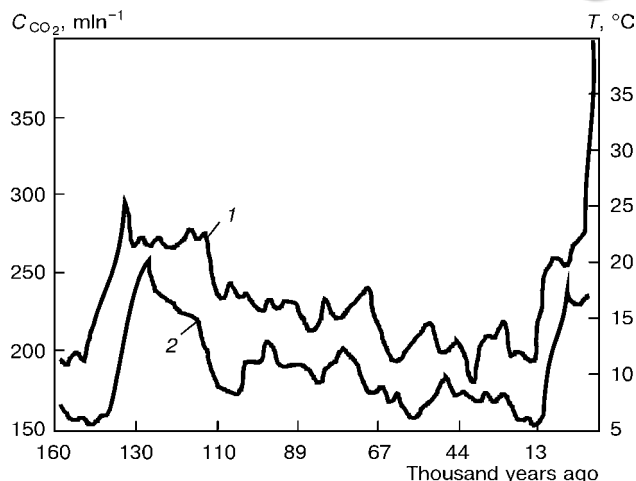
Figure 3. Change in concentration C of carbon dioxide in atmosphere (1) and mean global temperature of Earth surface (2): 1 — $C = 280$ mln^{-1} at the beginning of machine-technical revolution; 2 — $C = 353$ mln^{-1} at present

found a wide application as wet blasting, increased gas pressure at the top, enrichment of blasting with oxygen, blowing-in of gaseous, liquid and solid fuels, etc. into a hearth. All this made it possible to decrease the consumption of coke from 1.5--2.7 to 0.7--0.9 t per ton of cast iron by the middle of the century that corresponded to energy-content of cast iron production at the level of 40--50 GJ/t. By the end of the century the coke consumption in the industrialized countries was decreased to 250--500 kg per ton and provided the energy consumption at the level of 20--25 GJ per ton of cast iron (Figure 5).

Over the recent decades the most remarkable achievements in the field of electric melting in steel-making production are as follows: design of furnaces was updated, their specific electric capacity is greatly increased, application of various forms of arc discharge, such as DC and AC arc, plasma arc with a hollow electrode, burning in a foamed slag, and others. All this increased the efficiency of furnaces, the annual capacity factor, power and technological characteristics of melting steel and improved the labour conditions.

Such high technologies as vacuum-arc remelting, electron beam melting, plasma remelting, electroslag
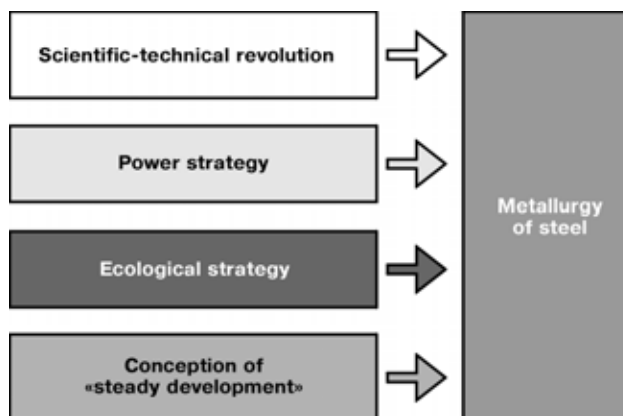
Figure 4. Geopolitical factors defining the modern metallurgical production
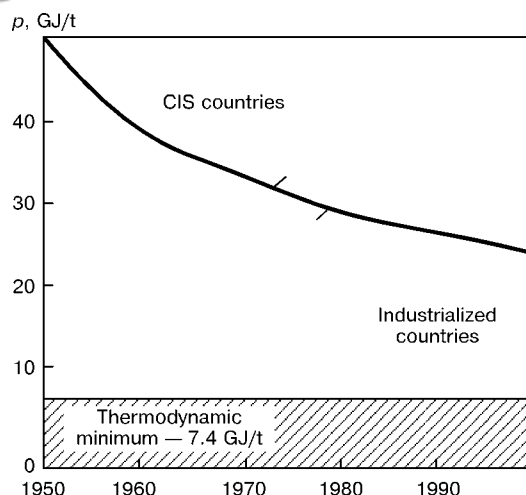
Figure 5. Dynamics of energy-content *p* of cast iron production in blast furnaces at the second half of the XX century: *1* — CIS countries; *2* — industrialized countries

and induction melting were developed and implemented at the second half of the XX century. The development of these processes, especially in our country, was stimulated also by the requirements of the defence complex, which required the high-quality metal to solve its problems. At this period the non-ferrous metallurgy and chemical industry, related to ferrous metallurgy, were rapidly developed. Owing to the intensification of their production, a highly-competitive medium in the sphere of production and application of structural and functional materials was created. Though the steel keeps its leading position in the market, 90 wt.% and 70 vol.% (aluminium, plastics and polymers press its positions), however, the composites and ceramics are now slowly introduced into production. Thus, in the USA the use of steel in the 1971--1991 period was reduced by 15 %, and the consuming of aluminium products was increased by 55 %, while those of plastic materials ---- almost by 3 times (Figure 6). The similar situation was observed in Japan, Germany and other countries.

Due to the situation occurred, the manufacturers of steels began to pay more attention to assurance of the production quality. Dynamics of growth of world
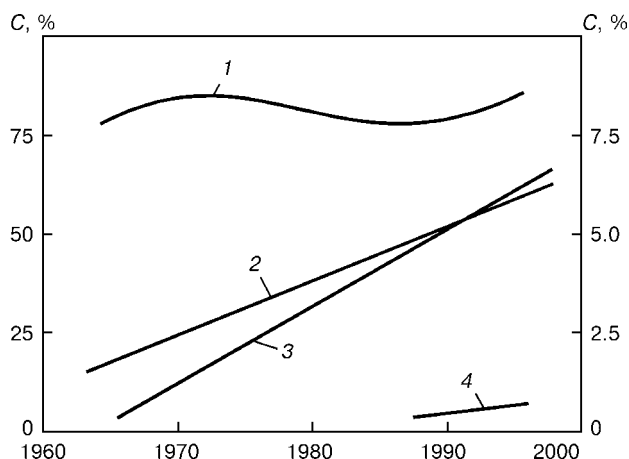
Figure 6. Dynamics of volume of consumption *C* of structural materials in the USA: *1* — steel; *2* — aluminium; *3* — plastics; *4* ---- titanium, ceramics and others
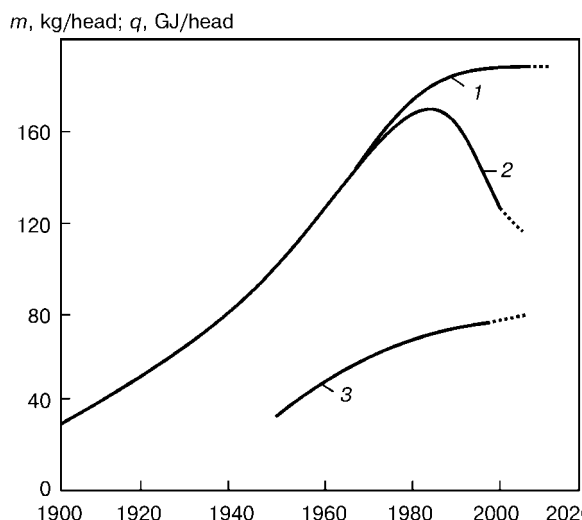
Figure 7. Dynamics of growth of world production of steel per head *m* (*1* ---- physical tons; *2* — qualitons) and power generation *q* (*3*) in the XX century

production of steel per head in this period is worthy of note. Since the 1970s some decrease in the above-mentioned characteristic was noted (Figure 7).

The demand for steel at the second half of the XX century was satisfied not only due to a physical volume, but also, to a great extent, owing to its quality. At the end of the century the demand for steel was satisfied by about 40 % owing to the latter [4]. The reduction in actual consumption of steel per head was due mainly to the increase in output of the quality steels (low-alloy steels in particular).

Power problem in steel production. The steel production is a high-power-consuming technology, because metallurgy consumes, as a whole, about 20 %, while ferrous metallurgy consumes about 10 % of all the power resources. The cost of power in iron production in most countries is approximately a half of cost of the steel billet. The energy-content of products both at the present time and also in the nearest future should be considered as a main characteristic defining the position of steel at the market of materials [5].

The above-mentioned level of power consumption in metallurgy is typical almost of all the industrialized countries. It stimulates the creation of lower energy-consuming structural materials, including also those, being not on iron base.

At present, the major manufacturers of steel are the integrated works. Blast furnace with its infra-structure (cake and by-product process, agglomeration and electric energy production) consumes about 79 % of total power consumption (Figure 8). During the last half of the XX century the power consumption in the industrialized countries for the cast iron production decreased approximately 2 times and amounts to 20--25 GJ/t [6]. This was attained by improving the quality of coke, ore raw material and some new technological solutions, which were above-described.

In determination of reserves of energy saving the real technological process is compared with its «ideal» analog. As is known, the thermodynamic minimum (minimum energy consumption) in iron reduction
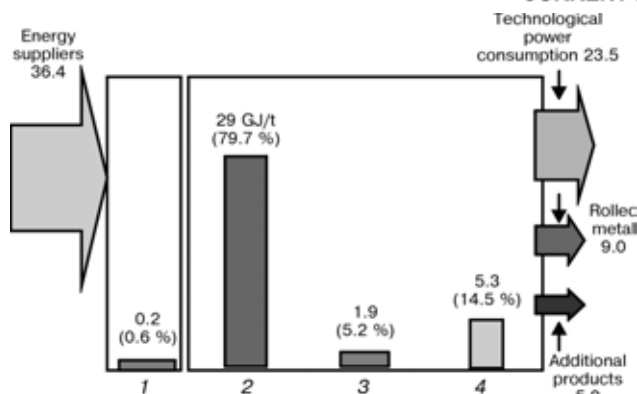
Figure 8. Structure of power consumption in production of steel rolled metal using blast-furnace-converter technology: *1* — ore preparation; *2* — aggloblast-furnace production; *3* — steel-melting; *4* — rolling

Figure 9. Global (*1*) and world (*2*) emissions *E* of carbon dioxide in cast iron production at the second half of the XX century

from oxide (Fe_2O_3) is equal to 7.4 GJ / t (energy of oxide dissociation). The level of power consumption in production of iron (cast iron), attained at present, about 3 times exceeds the thermodynamic minimum.

High power consumption of steel metal production of the integrated works is stipulated by the imperfection of utilization and use of the secondary energy, which in the total energy balance of the enterprise is approximately a half, and at the present technology is used approximately by 10--20 %.

It should be noted that the energy-content in producing aluminium, the main alternative material of iron, exceeds at present by more than twice the similar parameter of iron (cast iron) and is about 57 GJ / t, that 1.7 times (33.1 GJ / t) exceeds the thermodynamic minimum of producing aluminium and 7.7 times (7.4 GJ / t) exceeds the thermodynamic minimum of iron production. However, it should be taken into account that the coefficient of replacement steel by aluminium in some spheres of its application is equal approximately to 3.

In the course of accumulation of the metal stock, the share of the native iron in the steel production is decreased. In the industrialized countries the cast iron share in the 1990s was about 50 % in the USA, in France and Great Britain ---- about 65 %, in Italy ---- approximately 45 % and in Russia ---- about 75 %.

Steel production and ecology. As the metallurgy is the high power-consuming branch, the energy factor could not but influence its ecological characteristics. Thus, as to the harmful pollution into atmosphere, the metallurgy occupies the second place after the power engineering. The metallurgical enterprises consume about 20 % of all fossil hydrocarbon energy resources, transforming them mainly into carbon dioxide, thus contributing to the increase in total industrial pollution. As is followed from the results of calculations, the carbon dioxide emissions in cast iron melting using a blast furnace technology can amount approximately to 15 % of carbon dioxide emission of the world industry (Figure 9).

In the whole world the ways are searched for the reduction of carbon dioxide emission, including also the methods of iron production, at which the harmful
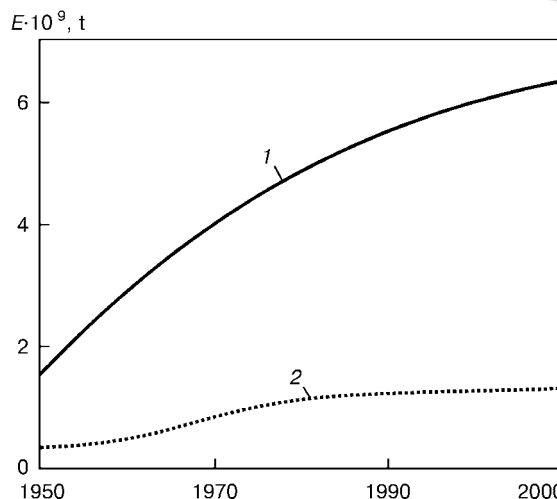
pollution into environment is decreased. Thus, for the countries, used widely the high-technology processes (USA, Japan, Great Britain, China), the tendency of reducing the carbon dioxide emission into atmosphere per a unity of IGP is clearly observed (Figure 10).

The main consumer of energy and a source of emission of harmful substances into environment at the traditional method of iron (cast iron) production from mineral raw material is an aggloblast furnace complex. The highest contribution (more than 60 %) to the environment pollution is made by an agglomeration production. Therefore, the radical change in technology in this area of the production cycle can provide the most significant effect.

At present two main types of reduction processes are being developed, i.e. solid- and liquid-phase. In the blast-furnace process a solid-phase reduction is prevailed. The essential drawback of this process is the use of scarce reducing agents, such as coke, natural gas and specially prepared ore raw material of the sufficiently high quality. One of the most important directions in the solution of problems related to pro-
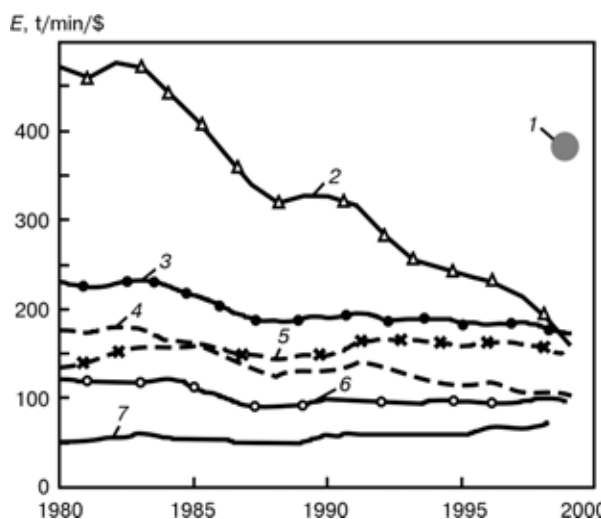
Figure 10. Dynamics of changing emissions *E* of carbon dioxide related to IGP (US dollars) in different countries of the world: *1* ---- Russia; *2* — China; *3* — USA; *4* — Great Britain; *5* ---- India; *6* — Japan; *7* — Brasil
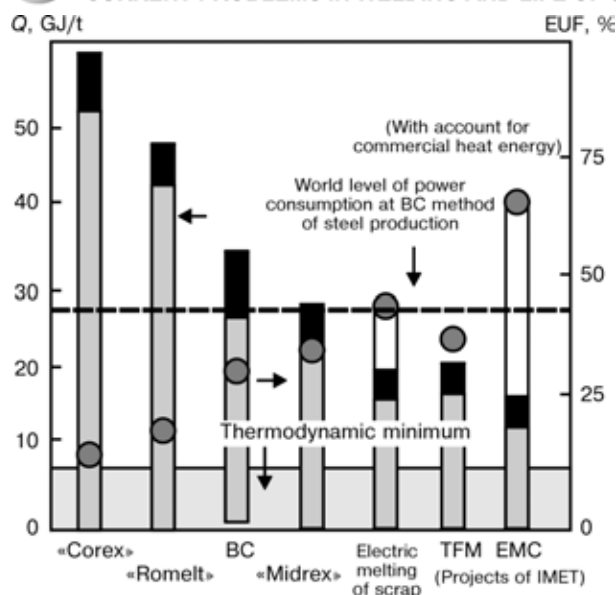
Figure 11. Power consumption Q (*1*) and EUF (*2*) of different technological processes of steel rolled metal production: EUF — efficient utilization factor; BC — blast-furnace-converter process; TFM ---- technology free of metal melting; EMC ---- electrometallurgical complex, EUF I_s 100 / ΣI (I_s — chemical energy of steel; ΣI ---- total power consumption); specific power consumption in rolling is 5.3 GJ / t; consumption coefficient — 1.2

duction and application of coke, is the use of the powdered-coal fuel (PCF). Owing to this, the harmful effect on environment is decreased (the volume of cake and by-product process is reduced), but here the energy-content of aggloblast-furnace complex is somewhat increased. In the metallurgy of the former USSR the PCF began to be used earlier than abroad (for example, in steel works of Donetsk, Ukraine). However, as a result of a low price for the natural gas this direction of development in domestic metallurgy was delayed. In future, it is necessary to make these works on use of PCF more active.

At present many technologies of solid- and liquid-phase reduction have been developed using both different kinds of energy and also various ore materials and reducing agents. Processes of the solid-phase reduction, most typical and mastered in industry, are «Midrex» and several modifications of process «Hill». Typical liquid-phase process is «Romelt». «Corex» is a combined process, it includes a solid-phase stage (reduction) and liquid-phase (cast iron).

In this technologies the ecological problems of steel production are solved in different degrees. Thus, in the process «Midrex» there is no cake and by-product process. The energy-content of iron production in use of this technology is approximately 1.5 times lower than in the blast-furnace process (Figure 11). However, when the above-mentioned technology is used, a scarce and expensive source of energy and reducing agent is required, i.e. natural gas. It means that the carbon dioxide emission into atmosphere will occur as before, though it is significantly (2 times approximately) decreased as compared with the blast-furnace process.

The main advantage of the process «Corex» is the cast iron production using only a power-generating

coal. However, this technology has also drawbacks. Energy-content of cast iron melting by the «Corex» technology is about 2 times higher than in the blast-furnace production. Therefore, the volume of emission (kg / t) of hothouse gases is not decreased, but increased [7]:

blast-furnace-converter process 2010
electric arc melting of metal scrap 640
«Midrex» in combination with electric melting 1870
«Corex» in combination with converter process 3090

Decrease in energy-content of the process «Corex» is possible only in case of filtration and complete use of heat and chemical energy of exhausting gases.

In the «Romelt» the power-generating coal, ore raw materials are used also as a source of energy and reducing agent and, here, no special preparation is required. As to the energy-content and emission of carbon dioxide into atmosphere the «Romelt» process is greatly superior to the blast-furnace production.

To provide acceptable power and ecological characteristics in the technological structure of the process «Romelt», the same as in «Corex» process, the problem of trapping of hothouse gases and complete utilization of chemical and heat energy of exhausting gases should be solved. These processes are formed as power-metallurgical complexes where metal and energy (heat and electric) are the products. Creation of these complexes is at the initial stage.

The blast-furnace and above-mentioned processes are also characteristic of emissions of sulphur and nitrogen compounds, whose hazard is not less than that of carbon dioxides. Thus, there is no complete enough solution of power and ecology problems in already existing and developing reduction processes.

The evident alternative process is an electrometallurgy of steel which is progressing rapidly over the recent years. The major premise for this is a large metal stock accumulated in the world (in the USA is about 3 bln t, in Europe ---- about 2.5 bln t and in Russia ---- about 2 bln t). In use of about 3 % of metal stock as a scrap, the metallurgical industry of Russia can melt about 50 mln t of steel annually.

Mini-works, in which the electric steel-making on scrap base is realized, are greatly superior in all the technical characteristics to the integrated works. The energy-content of production of steel rolled metal in them is almost 2.5 times lower as compared with the energy-content at the integrated enterprises, and the labour productivity is 3--5 times higher than at the traditional integrated works. The important feature of the mini-works is the fact that electricity, the most technological and ecologically clean power source is the only power base.

When the charge, consisting of 30 % of cast iron and 70 % of scrap (Figure 12) is used, the energy-content of steel production in electric furnaces is approximately 1.5 times lower than that in blast-furnace-converter method and equal to about 16 GJ / t [8].

One of the problems, which arise in the development and creation of highly-effective electric steel-

Table 1. Share of electric melting in a total volume of steel production, %

Country-manufacturer	1970	2001
USA	15.5	47
EC countries	14.0	41
Japan	16.8	28
Russia	13.0	15

Figure 12. Effect of scrap content S in charge on change in power consumption p (1) and EUF (2) of energy in steel production from cast iron and scrap: EUFI_s 100 / ($I_b + I_s + I_e$) (I_b — energy-content of cast iron production; I_s ---- chemical energy of scrap; I_e — electric energy)

melting equipment, is the use, except electricity, of other power sources, for example, organic fuel. In electric furnaces of company «Danieli», supplied from transformer of 55 MW and consuming the active power of 43 MW, there are seven fuel torches of 5 MW capacity each.

In blast-furnace steel-making, using the fuel heating, the efficiency of power as a whole is approximately 2 times lower than in use of the electricity only, in spite of great economy of electric energy (up to 200 kW·h / t). This is explained by a low (about 20--60 %) value of effective efficiency factor of fuel heat sources.

The effectiveness of power of fuel torches for scrap heating is low and is 40--50 %. In combustion of additional fuel the ecological problems also arise due to a neutralizing harmful emissions in the form of SO_x, NO_x, CO, furan, etc.

In spite of this, the use of the fossil hydrocarbon fuel in melting scrap in electric steel-melting units is justified in many cases, as it contributes to acceleration of melting and to the decrease in steel cost at relatively high cost of electric power.

Now, in the whole world more 40 % of steel is melted in electric furnaces. Electric processes of melting are very rapidly implemented in the USA (Table 1).

At present the problem of presence of harmful impurities (nickel, copper, chromium, etc.) in the scrap of non-ferrous metals is remained still actual. Taking into account that at a multiple use of the scrap the content of harmful impurities in it is increased, there arises a need in use of the native iron, cast iron and direct-reduced iron, in the charge. Even now, a reduction part, as a rule, direct reduction, is included into the technological process at the mini-works. It should be noted that at these enterprises the continuous casting of steel is made into thin sheets, that also saves the energy. This method finds the more and more spreading.

The major technological parameters of installation for continuous casting of a thin sheet at the «Krupp Thyssen Nirosta» Works in Crefield are as follows:

```
diameter of rolls, mm  ..........................................  1500
rate of pouring, m / min  .....................................  60–150
sheet size, mm:
    thickness  ...............................................  1.5--4.5
    width  ....................................................  1100--1450
steel assortment  .......................  austenitic, stainless steels
efficiency, t / year  ...........................................  400000
```
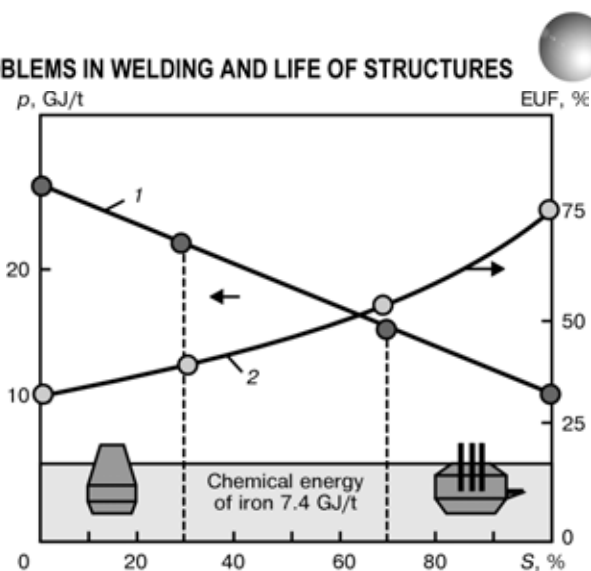
Great changes in the technology and assortment are occurred in rolling process. Production of hot-rolled strips is continuously increased (Figure 13).

The progress of electrometallurgy (construction of mini-works) influenced greatly the structure of cast iron production. In many countries of the world the number of blast furnaces, first of all of a small volume, is decreased (Table 2) and their technology is significantly updated [9]. Thus, in the USA with decrease in number of furnaces by 34 % (1998 ---- 38 furnaces and 2015 ---- 25) the cast iron melting is scheduled to be decreased only by 13 % (from 53 to 44 mln t / year, respectively). Here, the consumption of coke is decreased to 320 kg / t, and PCF is increased up to 200 kg / t, while the specific efficiency will increase to 2.9 t / (m^3·day). This should be considered as the new radical change in the development of the metallurgy.

Within the scope of creation of ecologically safe electrometallurgical complex (EMC) the interest can be attracted to a reduction module with a superhigh (about 100 MW / m^3) power intensity reached as a result of using a highly-concentrated power source, a plasma arc, which is developing at the Institute of
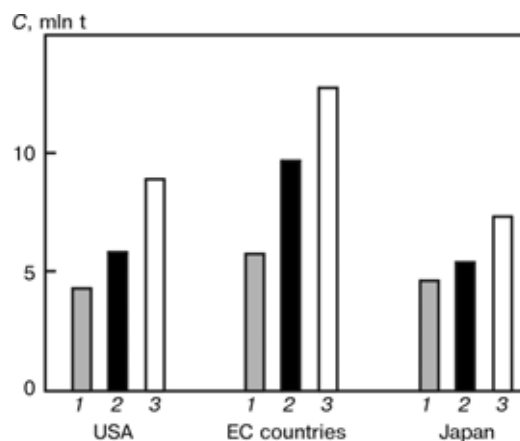
Figure 13. Consumption C of thin hot-rolled strips in industrialized countries of the world: 1 ---- 1997; 2 — 2002; 3 — prediction for 2007
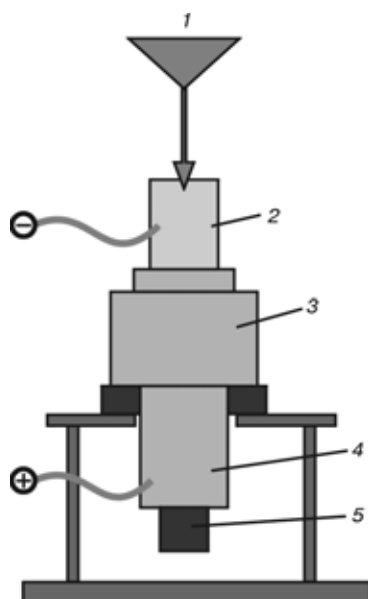
Figure 14. Design scheme of a semi-industrial plasma reduction module (5--8 MW capacity; arc current 10 kA; voltage 400–800 V; efficiency 1.5–3.0 t ∕ h of iron; specific efficiency 200 t ∕ (m^3·day); electrode diameter 300 mm; ingot diameter 500 mm; gas consumption ---- up to 2000 nm^3∕h; consumption of ore concentrate 4.5 t ∕ h): *1* ---- ore concentrate (reducing agent); *2* ---- plasmatron; *3* ---- reactor; *4* — mould; *5* ---- ingot

Metallurgy and Materials Science of RAS (Figure 14). Due to a high power density in a reaction volume, the specific efficiency of the plasma furnace at liquid-phase reduction can reach 200 t ∕ (m^3·day), and that of blast furnace ---- up to 2--3 t ∕ (m^3·day). Fi-gure 14 shows the structure of power flows of EMC. The synthesis gas, purified from sulphur, produced in coal gasification is directed for the reduction to a metallurgical unit, and then, as a fuel, to a vapour-gas unit of a power unit [10].

EMC produces three types of commercial products: metal products, heat and electrical energy. Complex does not use a coke and does not consume the electrical power from the external power system. This technology is characteristic by that the ore raw and reducing agent are used in a dispersed state. The
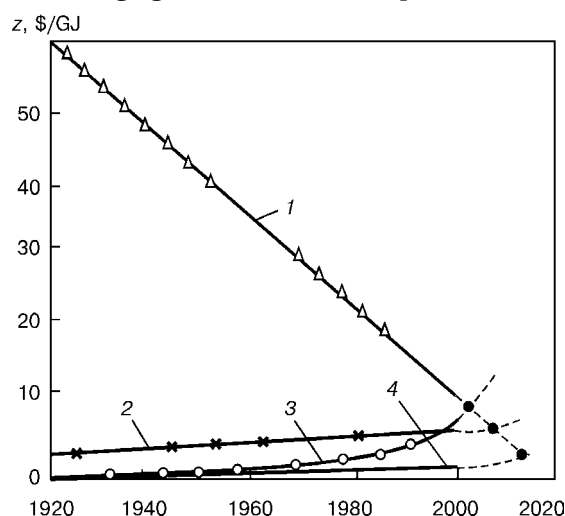
**Figure 15.** Dynamic of growth of prices *z* (averaged) for energy of different energy suppliers in the XX century: *1* ---- electricity; *2* ---- oil; *3* — gas; *4* — coal

Table 2. Dynamics of use of blast furnaces in the industrialized countries of the world by years

Country	1975	1980	1990	1996	2001
USA	197	--	--	40	36
EC countries	–	154	--	--	58
Japan	–	--	34	--	30

primary source of power is the power-generating coal. The calculations made showed that energy-content of production of metal products using the EMC technology is 1.5--2 times lower than that of traditional aggloblast-furnace technology. Technology of EMC in the given variant does not eliminate the carbon dioxide emissions into environment, but it is reduced by the decrease in energy-content in steel production, as a whole.

The reduction module of the metallurgical unit of EMC can function using only a gaseous reducing agent, for example, hydrogen. Thus, an ecologically clean electric hydrogen metallurgy of steel can be created, eliminating the carbon dioxide emission into atmosphere.

The continuous decrease in electric energy cost will promote the wide progress in electrical technology, including electrometallurgy (Figure 15) [11].

Metallurgy of steel and strategy of «steady development». At the end of the XX century the stabilization and some decay in steel production is observed in the industrialized countries, while in the countries of Asia, South America and some other regions of the world is vice versa, the rapid development of the ferrous metallurgy is observed. In this respect, China is distinguished, where the modern metallurgical industry was created for a short period and China occupied the first place in the world on the steel production. Thus, in 2002, about 150 mln t of steel was planned to be produced.

At the end of the 1980s in such industrialized countries as the USA, Germany, Great Britain and France, the steel consumption was stabilized at the level of about 400--500 kg ∕ head and the tendency in some reduction of production appeared. Russia at present produces about 50 mln t, being behind China, Japan and the USA. More than half of the metal, produced in Russia, is exported. Actual consumption of steel (rolled metal) in Russia is at the level of 225 kg ∕ head. Steel is exported mainly in the form of billets, for which the power consumption per a cost unit (i.e. dollar or rouble of metal product cost) is most important (Figure 16). The power consumption per dollar of billet cost is approximately 1.7 times exceeds the similar characteristic for the cold-rolled sheet and more than 2.5 times for zinc-plated sheet. It means that the metallurgy of Russia at the world market plays objectively a role of manufacturer of energy-consuming not-highly technological and inexpensive metal products.

Metallurgy of steel in future. Production of steel in the world in the third century takes place under

the conditions of more redoubling STR, intensified ecological and power crisis. It seems, that in the XX century the production of steel products by its importance in the world industry reached its culmination. Further, the steel metallurgy will develop in an acute competitive struggle with manufacturers of alternative materials (aluminium, plastics, ceramics and composite materials).

The most important factor in the solution of problems of metallurgy in the XXI century will be ever-growing role of the scientific-technical progress. In the USA over the recent twenty years the expenses for research and design works were increased in material-production branches, such as metallurgy, chemical industry, etc., almost 5 times and amount to 16 billion dollars, and, as a whole, the internal expenses for research and developments of the USA are about 160 billion dollars. In Russia the total investments into the science over the recent decade was abruptly decreased and amount to about 2 billion dollars [12].

In spite of great achievements in the field of development of metallurgical processes, especially, in electrotechnologies, the main source of iron (cast iron) production, at least at the beginning of the new century, will remain blast furnace. Research works directed to the increase in power and ecological characteristics, implementation of inexpensive energy suppliers can extent the dominating role of blast-furnace-converter production. However, it is already evident that the aggloblast-furnace production of iron will not withstand competition by energy-material-content and ecological characteristics and will pass its dominating role, at least at the second half of the XXI century. Electrotechnology on the base of iron scrap and direct-reduced iron will be major even at the end of the first half of the XXI century in steel production. This will require the development of effective methods of scrap preparation and purification it from harmful impurities. Many things, related to this process, have not been yet solved.

From all the above-described, it may be concluded that the considered tendencies in the development of metallurgy and alternative metallurgical processes, making it possible to reduce the power consumption, to implement non-traditional power and raw material resources into production, to reduce the harmful effect on environment, are still at the initial stage of developments and industrial implementation, in spite of
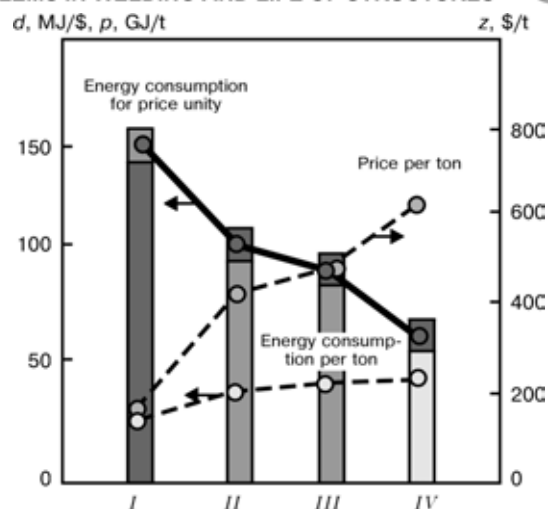
Figure 16. Energy consumption for price unity d, energy-content p and price z of different types of metal products: I — cast iron, ingots; II, III ---- thin hot-rolled and cold-rolled sheets, respectively; IV — zinc-plated sheet

a great interest shown to them. The successful development of new and newest power and ecologically perfect processes will be defined by capital investments for the carrying out research of high technologies and their industrial testing. The Russian metallurgical science has high potentials, but at insufficient financing, they will be quickly decreased.

1. Lyakishev, N.P., Nikolaev, A.V. (2002) Metallurgy of steel at the threshold of the 3rd millenium. *Elektrometallurgiya*, **1**, 3--13.
2. Shevelev, L.N. (1999) *World ferrous metallurgy of the 1950-2000s.* Moscow: Mashinostroenie.
3. Inozemtsev, V.L. (2002) Crisis of Kioto Conventions and problem of global climate warming. *Priroda*, January.
4. Kondratiev, K.Ya., Losev, K.S. (2002) Illusions and reality of strategy of steady development. *Vestnik RAN*, **7**, 592--601.
5. Lyakishev, N.P. (1982) Main tendencies in development of ferrous metallurgy and problem of energy saving. In: *Metallurgy, steels, alloys, processes.* Moscow: Metallurgiya.
6. Nikolaev, A.V. (1993) System analysis of energy-material structure of steel production. *Stal*, **11**, 14--18.
7. (2001) Eurofer and the Kioto Protocol. *Steel Times*, March, 96.
8. Lyakishev, N.P., Nikolaev, A.V. (2002) Power aspects of steel metallurgy. *Stal*, **3**, 66–73.
9. (1996) Fewer blast furnaces, but higher productivity. *New Steel*, November.
10. Tsvetkov, Yu.V., Nikolaev, A.V. (1998) Plasma processes in metallurgy of the future (Problems of creation of power-metallurgical complex). *Stal*, **10**, 55--60.
11. Kholdren, D.P. (1990) Power industry at the transition stage. *V Mire Nauki*, **11**, 113--121.
12. Strakhov, V.N. (2001) Necessity in public movement «For revival of Russian science», its aims and problems. *Nauka i Tekhnologiya v Rossii*, **4/5**, 2--5.

THE NEW ISO 3834 ---- QUALITY REQUIREMENTS FOR FUSION AND RESISTANCE WELDING OF METALLIC MATERIALS

D. von HOFE[1] and **B. SCHAMBACH**[2]
[1]DVS, Germany,
[2]DIN, Germany

History of development of the quality management system standards of the ISO 9000 series a nd degree of their conformity with later standards ISO 3834:1994 and EN 729:1994 are considered. Priorities related to revision of standard ISO 3834 in terms of acceptance of improved standard ISO TC44 SC «Unification of Requirements in the Field of Metal Welding» are noted.

Keywords: *fusion welding, resistance welding, quality standard, revision of standard, welding production, quality level*

Origin of ISO 3834: past history. Nowadays, plants which manufacture metallic welded products and would like to prove their competence to their customers have in a lot of cases introduced a quality management system and have had this certified according to the International Standard ISO 9001:2000 [1].

In the International Standard ISO 9000:2000 [2] which includes the definitions of terms for ISO 9001:2000, it is stated in Section 3.4.1, Remark 3:

«A process where the conformity (3.6.1) of the resulting product (3.4.2) cannot be readily or economically verified is frequently referred to as a «special process»».

As the proper execution of such special processes in most cases cannot be checked on the finished product at all or at economically justifiable expense it necessitates the precise definition and particular monitoring of such processes and of their parameters relevant to quality.

According to interpretations of experts, welding is such a special process. It was already customary in many industrialised countries prior to the introduction of ISO 9000ff in its earlier version dated 1994 to stipulate requirements on the welding processes and on plants performing welding work. In many cases these were fixed in standards, e.g. in Germany, in an absolutely general form in the DIN 8563, Parts 1 and 2 [3, 4] standards or in a product-related form in DIN 18800, Part 7 [5] for steel structures or in the AD guidelines for pressure vessels.

The International Institute of Welding (IIW) has also dealt with these problems and, in 1986, published its own document IIW-902--86 «Guidelines for Quality Assurance in Welding Technology» [6] from IIW Commission V, which became the basis for the subsequent standardisation in CEN and ISO.

ISO 3834 applicable at present. With the stipulation in the European Union that in harmonised

European product directives reference should be made to European standards, it became necessary to harmonise the different regulations in the member countries of the EU also with regard to the requirements on welding plants. This resulted in the series of European standards EN 729 «Quality Requirements for Welding ---- Fusion Welding of Metallic Materials», Parts 1 to 4, which was first published in 1994.

This series of standards covers as well common welding practice as all the quality influencing factors in a three level set of requirements and had been elaborated with close reference to the series of standards of ISO 9000ff from the year 1994.

Objectives of the series of standards were:
• to lay down quality requirements for welding production as well in shops as on sites;
• to describe suitable requirements to manufacturers, which use welding in production;
• to assure / guarantee the applicability to all kinds of constructions by graduated requirements;
• to present instructions for the description of manufacturers capability to produce welded constructions in the defined quality;
• to prepare requirements for rules and contracts;
• to describe for the manufacturers management welding requirements to a Quality Management System.

After completion of the European series of standards EN 729 it was adopted identical as International Standard ISO 3834 (Parts 1 to 4) at the same year.

In 2000, revised versions of ISO 9000, ISO 9001 and ISO 9004 [7] were published and ISO 9002 [8] and ISO 9003 [9] were deleted. Thereafter, it was necessary to decide whether this had to have consequences for the ISO 3834:1994 and EN 729:1994 standards and, if yes, what consequences.

One absolutely fundamental change in the new ISO 9001 is that the previous ISO 9002 and ISO 9003 standards dated 1994, are also covered by the new ISO 9001:2000 standard. This was achieved by the fact that ISO 9001:2000 no longer recognises any graduated requirements on Quality Management Systems. This standard leaves it up to the system operator

Summary comparison of ISO 3834-2, ISO 3834-3 and ISO 3834-4

No	Element	ISO 3834-2	ISO 3834-3	ISO 3834-4
1	Requirements review	Necessary		
		Documentation is required	Documentation may be required	Documentation is not required
2	Technical review	Necessary		
		Documentation is required	Documentation may be required	
3	Sub-contracting	Treat like a manufacturer for the specific sub-contracted product, services and/or activities, however final responsibility for quality remains with the manufacturer		
4	Welders and welding operators	Qualification is required		
5	Welding co-ordination personnel	Required		No specific requirement
6	Inspection and testing personnel	Qualification is required		
7	Production and testing equipment	Suitable and available as required for preparation, process execution, testing, transport, lifting in combination with safety equipment and protective clothes		
8	Equipment maintenance	Necessary as applicable to provide, maintain and achieve product conformity, documented plans, and records are required	Necessary as applicable to provide, maintain and achieve product conformity, records are recommended	As necessary to assure equipment is suitable and available, no specific requirements for records
9	List of equipment	Required		No specific requirement
10	Production planning	Required. Documented plans and records are required	Required. Documented plans and records are recommended	No specific requirement
11	Welding procedure specifications	Required		Appropriate welding technique required
12	Qualification of the welding procedures	Required		No specific requirement
13	Batch testing	If required	No specific requirement	
14	Storage and handling of welding consumables	A procedure is required in accordance with supplier recommendations		In accordance with supplier recommendations
15	Storage of parent material	Protection required from influence by environment; identification shall be maintained through storage		No specific requirement
16	Postweld heat treatment	Confirmation that the requirements according to product standard or specifications are fulfilled		No specific requirement
		Procedure, record and traceability of the record to the product are required	Procedure and record are required	
17	Inspection and testing before, during and after welding	Necessary		If required
18	Non-conformance and corrective actions	Measures of control are implemented procedures for repair and/or rectification are required		Measures of control are implemented
19	Calibration and validation of measuring, inspection and testing equipment	Necessary	If required	No specific requirement
20	Identification during process	If required		No specific requirement
21	Traceability	If required		No specific requirement
22	Quality records	If required		

to stipulate, within the framework of the general requirements, the requirements chosen by him.

In the following the consequences on that for the definition of requirements on welding shops will be discussed.

Revision status of ISO 3834. In the responsible European and International standards committees of CEN and ISO, the following was decided.

• The series of standards ISO 3834 and EN 729 will be worked out in future according to the Vienna agreement between ISO and CEN, ISO leading.

• The previous graduation of the quality requirements:

a. Comprehensive quality requirements;

b. Standard quality requirements;

c. Elementary quality requirements should be retained.

• The series of standards ISO 3834 should cover as in the past fusion welding processes and get the title «Quality Requirements for Fusion Welding of Metallic Materials».

• The standards ISO 14554, Parts 1 and 2 «Quality Requirements for Welding ---- Resistance Welding of Metallic Materials» [10, 11] will have to be revised as well.

• The future parts of the standard ISO 3834 Parts 2 to 4 [12--15] will not include normative references to other ISO Standards related to quality requirements in welding. For that a separate part will be worked out (ISO 3834, Part 5 [16]).

Although of the adherence of three quality levels, certification according to ISO 9001 is now possible at all three levels. The manufacturer must himself specify the level chosen by him if this does not result from application standards, e.g. in Europe for unfired pressure devices from EN 13445:2002 «Unfired Pressure Vessels ---- Part 4: Fabrication» [17], or in Germany for steel structures from DIN 18800-7:2002 «Steel Structures ---- Part 7: Execution and Constructor's Qualification» and for railway vehicles from DIN 6700 «Welding of Railway Vehicles and Parts---- Part 2: Qualification of Manufacturers of Welding Rolling Stock Materials ---- Quality Assurance» [18].

Priorities for the further discussion to process ISO 3834. *Quality levels.* After a combination of the certification according to ISO 9001 with all parts of ISO 3834 had been made possible by the amendments in ISO 9001:2000, the question to be asked was whether three levels of requirements for welding plants are still necessary in ISO 3834. The current status of the discussion (May 2003) is that the existing system should be retained for the following reasons:

• the three-level system has gained acceptance since the introduction of EN 729 and ISO 3834, and

• with regard to the application of ISO 3834 in product standards, reference is made to all three levels depending on the stresses and the safety requirements, e.g. in EN 13445:2002 to the level according to Part 3, in DIN 18800-7:2002 to levels according to Parts 2 to 4, and in DIN 6700 to levels according to Parts 3 and 4.

This results to a division into three levels, their selection and use, which are very near to those of the former ISO 3834. In the new Part 1 of ISO 3834 «Quality Requirements for Fusion Welding of Metallic Materials ---- Part 1: Guidelines for Selection and Use» the requirements of the three levels are listed clearly arranged in the Table.

The working group of ISO TC44 SC10 responsible for the revision of ISO 3834 did not decide on product related definitions of the three quality levels. That has to be left to the manufacturers and users of welded products and to the related directives and product standards.

A proposal for the following definitions was not excepted:

Part 2 «Comprehensive Quality Requirements»: application to structures in which the failure of welds may lead to the failure of the structure and to highly complex structures whose failure effects can hardly be limited, if at all.

Part 3 «Basic Quality Requirements»: application to structures in which the failure of welds fundamentally impairs the intended use of the structure and to structures whose failure effects do have only minor effects on the safety of people and on other goods.

Part 4 «Elementary Quality Requirements»: application to structures in which the failure of welds does not fundamentally impair the intended use of the structure and to structures whose failure effects do not have any effects on the safety of people and other goods.

Normative references. One additional change in the revised ISO 3834 needs to be discussed and relates to references to standards which are also applicable to fulfill the welding quality requirements or have to be considered.

It is planned to make indirect reference to standards which are also applicable via a new Part 5 «Normative References to Fulfill the Requirements of ISO 3834-2, ISO 3834-3 and ISO 3834-4», in which the standards which are also applicable are listed tabular according to the processes of arc welding, electron beam and laser beam welding and gas welding in a summarized form.

The purposes of this measure are to incorporate the contents of Parts 1 to 4 into regional sets of standards without any amendments in the text and, in a regional Part 5 deviating from ISO 3834-5, to be able to refer to regional standards instead of to ISO standards. This should allow ISO 3834 to be introduced also into those countries which have not yet been able to modify their regional sets of standards to ISO standards or only in part, e.g. USA and Japan.

In any case, it must be pointed out that certification according to ISO 3834 is only possible if the standards, to which reference is made, are ISO standards or standards with contents which are confirmed as identical by the certifier.

The concept presented here was worked out by the responsible working group WG 3 «Revision of ISO 3834» under German secretariat and excepted by ISO TC44 SC10 «Unification of Requirements in the Field of Metal Welding» for publication as Committee Draft. An urgent request now is being made for the comments of the expert world on this subject.

1. *ISO 9001:2000.* Quality management system. Requirements.
2. *ISO 9000:2000.* Quality management system. Fundamentals and vocabulary.
3. *DIN 8563-1:1986.* Quality assurance of welded structures. Part 1. Fundamentals.
4. *DIN 8563-2:1978.* Quality assurance of welding operations. Part 2. Requirements regarding the firm.
5. *DIN 18800-7:2002.* Steel structures. Part 7. Execution and constructer's qualification.
6. *Document IIW-902--86.* Guidelines for quality assurance in welding technology.
7. *ISO 9004:2000.* Quality management system. Guidelines for performance improvements.
8. *ISO 9002:1994.* Quality systems. Model for quality assurance in production, installation and servicing.
9. *ISO 9003:1994.* Quality systems. Model for quality assurance in final inspection and test.
10. *ISO 14554-1:2000.* Quality requirements for welding. Resistance welding of metallic materials. Part 1. Comprehensive quality requirements.
11. *ISO 14554-2:2000.* Quality requirements for welding. Resistance welding of metallic materials. Part 2. Elementary quality requirements.
12. *Committee Draft ISO/CD 3834-1.* Quality requirements for fusion welding of metallic materials. Part 1. Guidelines for selection and use (ISO/CD 3834-1:2003).
13. *Committee Draft ISO/CD 3834-2.* Quality requirements for fusion welding of metallic materials. Part 2. Comprehensive quality requirements (ISO/CD 3834-2:2003).
14. *Committee Draft ISO/CD 3834-3.* Quality requirements for fusion welding of metallic materials. Part 3. Standards quality requirements (ISO/CD 3834-3:2003).
15. *Committee Draft ISO/CD 3834-4.* Quality requirements for fusion welding of metallic materials. Part 4. Elementary quality requirements (ISO/CD 3834-4:2003).
16. *Committee Draft ISO/CD 3834-5.* Quality requirements for fusion welding of metallic materials. Part 5. Normative references to fulfil the requirements of ISO 3834-2, ISO 3834-3 and ISO 3834-4 (ISO/CD 3834-5:2003).
17. *EN 13445-4:2002.* Unfired pressure vessels. Part 4. Fabrication.
18. *DIN 6700-2:2001.* Welding of railway vehicles and parts. Part 2. Qualification of manufacturer of welded rolling stock materials. Quality assurance.

PROBLEMS OF GUARANTEEING THE STRENGTH AND DESIGN LIFE OF SLEET-PROOF OFF-SHORE PLATFORMS IN THE ARCTIC SHELF

I.V. GORYNIN, A.V. ILIIN, A.V. BARANOV and **V.P. LEONOV**

Central R&D Institute of Structural Materials «Prometej», St.-Petersburg, Russia

A set of requirements to the quality of welded joints, guaranteeing prevention of cyclic and brittle fractures should be satisfied, in order to provide service reliability of hull structures in off-shore platforms in the Russian shelf. The paper analyzes the problems, arising in application of foreign approaches to substantiation of these requirements, and suggests ways to solve these problems, based on the methods of physical modelling of fracture processes. Investigation results are implemented in standards and procedures of RF Register and are used in certification of materials and welding technologies for shelf structures.

Keywords: *off-shore platforms, welded joints, stress raisers, cyclic strength, crack resistance*

Provision of service reliability of casings of sleet-proof off-shore platforms (SPOSP), exposed to a combination of low climatic temperatures (down to --50 °C) and a high-cycle icing (up to 10^7) and wave-wind (up to 10^8) loading in service is an engineering challenge. Such conditions carry a high risk of brittle fractures, resulting from initial technological defects or fatigue cracks developing in service. The weakest links of the structure are welded joints, containing stress raisers, namely sources of fatigue crack initiation, zones with a lower brittle fracture resistance and a high level of residual welding stresses (RWS). In this connection, the main means of ensuring the serviceability is meeting certain requirements to the quality of welded joints, which include requirements to material toughness and cold resistance, guaranteeing prevention of brittle fractures, and requirements to the design-technological features, guaranteeing prevention of fatigue damage.

The procedural base for a substantiated specifying of these requirements has been absent up to now, which made the designers use foreign standards and procedures [1--3, etc.]. Such a practice could not be regarded as satisfactory, because of a lack of the ability to allow for the specific features of materials, welding technologies and methods to improve the fatigue strength, applied in Russia, as well as of much more difficult conditions of service in the Russian shelf, compared to non-freezing sea basins (on mastering which the foreign standards are mostly focused). Considering the system of provision of reliability of shelf structures, established abroad, the following should be emphasized.

• *Fatigue design is mandatory for these structures.* The actual load spectrum based on the principle of linear summation of damage is replaced by the impact of equivalent stress of $\Delta\sigma_{ev}$ range. Further on two design models (or their combination) are used, which may be conditionally called Nominal Stress

method and Hot Spot Stress method. In the first model the welded joints are subdivided into classes (C, D, E, F, F2, G, W, etc. by an international classification) by the level of cyclic strength, and each class is characterized by a certain curve of admissible cyclic stresses (*S--N* curve) of the following form:

$$\lg N = \lg \alpha - m \lg \Delta\sigma_{ev}, \qquad (1)$$

where N is the number of cycles to fracture; α and m are the curve parameters.

Thus, the position of the curve in the integral form allows for all the factors, determining the cyclic strength of a joint, namely stress concentration, RWS level, and structural inhomogeneity. In the second model a common «basic» *S--N* curve is introduced, which also integrally allows for all the factors, related to the presence of a weld, and the scale factor and joint configuration are incorporated by calculation of the hot spot stress magnitude, namely of stresses in the hot spot, considered as nominal in formula (1).

Practical application of both the models leads to the conclusion that it is difficult to reveal within them the influence of individual factors on cyclic strength (namely of the dimensions and configuration of the elements being welded, loading conditions, features of welding technology, determining RWS level and geometry of the concentrators) and, therefore, solve the problem of selection of the welding technology, depending on the required cyclic fatigue life. Hot spot stress method seems to allow separating the design factors from the technological ones, but it involves additional numerical studies and uses a highly disputable idea of separation of stress concentration into that «related to the presence of a weld» and that «related to mating of elements of different rigidity».

• *Requirements to the toughness and cold resistance of off-shore structure material,* in addition to specifying the common for shipbuilding impact energy of a specimen with a sharp notch *KCV*, depending on yield point $\sigma_{0.2}$: KCV $(J / mm^2) > 0.1\sigma_{0.2}$ (MPa), also incorporate much more stringent limitations on the thickness of materials, being used. They, on the

whole, are reduced to satisfying the following inequality:

$$T_d \geq T_i + \Delta T(S), \qquad (2)$$

where T_d and T_i are the design temperature of the structure and temperature to determine the impact energy, respectively; $\Delta T(S)$ is the temperature margin, dependent on thickness S and reaching 25--35 °C at $S < 40$ mm.

In addition to that, control of crack resistance parameter of crack tip opening displacement (CTOD) is introduced for the first time as mandatory in shipbuilding: for welded joint material at $S > 40$--50 mm, and for the base metal at $S > 60$--70 mm. Specified level of CTOD in different documents varies from 0.10 to 0.35 mm, but it is often left at the discretion of the customer, ordering the equipment.

Adaptation of these principle for the Russian shelf structures is made difficult by the fact, that at $T_d = = -40 -- -50$ °C satisfying condition (2) with the used temperature margins turns out to be impossible already at the thickness above 20--30 mm, even for steels of the most cold-resistant category F, and respective welding consumables. In such a case introduction of a procedure to determine applicability of a material by the criterion of brittle fracture prevention and substantiation of crack resistance criterion in terms of fracture mechanics become particularly urgent.

Problems of elaboration of requirements to cyclic and brittle strength of SPOSP welded joints are closely interrelated, as limit dimensions of a fatigue crack, admissible in cyclic strength evaluations, should be safe also by the criterion of brittle fracture prevention, and the factor of cyclic loading is one of the principal ones in determination of material toughness requirements. It is obvious, that solution of these problems requires applying physical methods of fracture analysis. The main results of research, conducted in Institute «Prometej» in these areas are given below.

Forecasting the cyclic fatigue strength of typical SPOSP welded components. The main areas of investigations were: analysis of the stress-strain state (SSS) in the zones of the most probable initiation of fatigue cracks, shape stress raisers and geometrical weld defects, determination of the characteristics of material fatigue resistance, theoretical evaluations, based on the selected model of fracture. In prediction of fatigue life of structural elements with concentrators, the most widely accepted is the approach, which determines the number of cycles N_Σ to formation of a crack of size (depth) a_f in the following form:

$$N_\Sigma = N_i(e_a) + \int_{a_0}^{a_f} \frac{da}{V_k(\Delta K_1, K_{1max})}, \qquad (3)$$

where $N_i(e_a)$ is the dependence of the number of cycles to appearance of a crack on deformation amplitude e_a; a, a_0 are the current and initial dimensions (depth) of a crack; $V_k(\Delta K_1, K_{1max})$ is the dependence of crack growth rate on the range of stress intensity factor ΔK_1 and its maximum value in the cycle, K_{1max}. When

applied to welded joints, such an approach requires determination of the following SSS parameters: e_a, ΔK_1 and K_{1max} dependencies on a, as well as determination of functions, characterizing fracture resistance of a material: $N_i(e_a)$ and $V_k(\Delta K_1, K_{1max})$. However, there exists a more complex problem, related to absence of definiteness in selection of the initial crack dimension a_0, when representing the fatigue life as a sum of two addends. It is particularly urgent exactly for welded joints with sharp stress raisers, where radius R should be regarded as a random value.

The main method of SSS analysis was a numerical method of finite elements (FEM). Based on numerous FEM solutions, it is proposed to describe the distribution of local stresses in the zones of their concentration by the following relationship [4--6]:

$$K_l(r) = 1 + \frac{A}{\sqrt{R + nr}}, \qquad (4)$$

where $K_l(r)$ is the stress intensity factor at distance r to the point of their maximum; $n = 4.5 + C(r/A)^2$; $C = 2$--6, depending on the considered direction. «Macrogeometry parameter» A (mm$^{0.5}$) depends on the type, dimensions and loading conditions of a joint, and may be regarded as a generalized characteristic of a concentrator SSS. This allows separating the technological factor (determining r statistics) from the design factor, which is to be evaluated at the design stage. A number of interpolation formulas have been proposed for A evaluation for the case of 2D joint (butt, tee, etc.), as well as for spatial (3D) components [6]. The most general relationship has the form of

$$A = f(\theta)\left(\frac{a_1}{S^*} + \frac{a_2}{t^*} + \frac{a_3}{h^*}\right)^{-0.5},$$

where $f(\theta)$ is the function of the angle of weld transition to base metal (may be assumed to be $\sin^{0.5}\theta$); S^*, t^*, h^* are the dimensions of the joint in its projection to a plane, normal to weld axis; a_1--a_3 are the coefficients, found by processing solution files by the least squares method. Transition from local stresses to intensity of local deformations e_i is performed by the following formula:

$$K_{ti}(r) = K_t(r) f_1 f_2,$$

where K_{ti} is the ratio of $e_i E$ to nominal stress component normal to weld axis [7].

Correction f_1 allows for the presence of a biaxial nominal stressed state, correction f_2 for the possibility of elastoplastic deformation, taking into account the mechanical inhomogeneity of the base and weld metal.

Method of recording the variation of potential energy in FEM modelling of crack propagation was used to derive dependencies of ΔK_1 and K_{1max} on a in the fields of summary (residual + service) stresses. For cracks, propagating from weld shape stress concentrators, the following interpolation formulas are recommended:

$$\Delta K_1 = \sigma^s Y_1 Y_3 \pi a;$$
$$K_{1max} = [\sigma_{0\bar{o}} Y_4(1 - \sigma_s/\sigma_y) + \sigma_s] Y_1 Y_3 \pi a, \qquad (5)$$

where $Y_1 = 1 + \dfrac{0.44A}{a(1 + 3a/A^2)} \, (\sqrt{\rho + 4.5a} - \sqrt{\rho})$ is the correction function, allowing for stress concentration; Y_3 is the Sneddon correction for crack shape (ratio of its half-axes); σ_{0x} is the average level of RWS in the concentrator; $Y_4 = \exp[-0.2(a/Z)^2]$ is the correction function, allowing for RWS gradient.

Generalization of the results of solving thermodeformational (welding) problems by FEM allowed suggesting differentiation of welded joints by the level of RWS normal component σ_{0x}, depending on the number of passes in welding, availability of limited shrinkage displacements, and temperatures of $\gamma \to \alpha$ phase transition.

A series of investigations of fatigue fracture resistance of the local hull steels was performed in order to determine the dependencies included into (3). It was found that $N_i(e_a)$ dependence at the coefficient of cycle asymmetry $\rho = -1$ can be assigned in the following form:

$$\dot{e}_a \dot{A} = 11640 N_i^{-0.390} + 0.5 \sigma_t, \qquad (6)$$

where σ_t is the ultimate strength, MPa.

Impact of a corrosive environment, r rising up to limit high values, simulating the presence of RWS, presence of the rough rolled stock surface, lead to practical neutralizing of the influence of material strength on N_i magnitude to a similar degree.

Practically coinciding $V_k(\Delta K_1, K_{1max})$ dependencies (cyclic crack resistance diagrams) were obtained for all the hull materials. Data for the welded joint metal in as-welded condition is characterized by greater scatter, but after application of specimen swaging by plastic deformation (up to 0.5--1.0 %) to relieve RWS, it practically coincides with the data for base metal. Influence of loading cycle asymmetry of positive terms on the crack kinetics is very pronounced only in the near-threshold region of the diagram (at $V_k < 10^{-8}$ m/cycle) and may be modeled by variation of threshold values of $\Delta K_1(\Delta K_{th})$ as function of ρ. Finally, the following relationship is recommended to describe the kinetics of the crack in the metal of unheat-treated welded joints:

$$V_k \text{ (m/cycle)} = 8.6 \cdot 10^{-11} (\Delta K_1 \text{ (MPa}\sqrt{m}) - - 7.0 (1 - 0.85r))^{2.3}. \qquad (7)$$

In connection with the problems of applying formula (3) to predict fatigue life of welded joints with «sharp» concentrators, a model of fatigue fracture propagation was proposed, which treats the rate of its propagation as a sum of two components, namely macrocrack growth rate V_k, found from (7), and additional damage rate V_i, determined by the amplitude of plastic deformations $e_{a.pl}$ in the considered point [7]:

$$N = \int_{a_0}^{a_f} \frac{da}{V_i + V_k}. \qquad (8)$$

Function $V_i(e_{a.pl})$ was determined by the results of testing smooth specimens (formula (6)). When $e_{a.pl}$ was calculated, lowering of material strength properties in near-surface layers of the metal was taken into account:

$$e_{a.pl} = e_a - S_{st}^y [1 - \exp(-k\dot{a})]/E,$$

where S_{st}^y is the cyclic yield point in the steady-state straining mode; k is the material characteristic.

Numeric integration (8) was performed by a special computer program, where the algorithm included the above-defined functions $e_a(a)$ and $K_1(a)$. Model validity was checked by comparing the results of calculation and testing specimens with mechanically introduced concentrators with different relationships of parameters A, ρ and at r variation. Unlike the known empirical relationships (Peterson, Ziebel--Stiller), the model allows a sufficiently accurate prediction of the combined influence of stress concentration and cycle asymmetry of positive terms on fatigue life.

Positive results of model verification allowed it to be used as a tool for numerical studies of the process of fracture of welded joints with geometrically heterogeneous concentrators of weld shape. Characteristics of distribution of the radius of weld transition to the base metal, namely ρ_a as mathematical expectation and ρ_σ as standard deviation, were determined by the replica method for the principal welding technologies. When the process was modeled, crack propagation in the local stress field, determined by the statics of the stress concentrator microgeometry, was considered. Theoretical investigations showed that for a limit high RWS level and the most unfavourable distribution parameters the design $S–N$ curves coincide well with the above standard curves (in case of coincidence of the thickness of elements being welded). This is in agreement with the method of deriving the latter as lower envelopes of large experimental values.

A possibility was demonstrated of reducing the theoretical evaluations of cyclic fatigue strength of welded joints to the following procedures:
• determination of the «basic» S--N curve in the form of an analytical expression (1), depending on the anticipated RWS level (lowering of RWS level leads to a larger m coefficient in the formula);
• determination of the effective stress concentration factor of a welded joint relative to this curve by the following formula:

$$K_{ef} = 1 + \dot{A}/\sqrt{\rho_{ef}},$$

where ρ_{ef} is the characteristic of the technological process of welding ($\rho_{ef} = \rho_a - \rho_\sigma$).

This methodology permits making satisfactory predictions also of the effectiveness of additional technological treatments, improving the concentrator geometry (argon-arc surface melting, machining), or inducing compressive residual stresses (surface-plastic deformation).

It should be noted that the position of the introduced basic S--N curves has a complex physical nature, reflecting the prevalence of the deformation process of welded joint damage in the low-cycle loading region, and the conditions of microcrack initiation in the high-cycle region.

Evaluation of resistance of SPOSP welded joints to brittle fractures. Investigation of SSS in this direction included prediction of fracture mechanics parameters for cracks in the field of RWS and service stresses at their random orientation, dimensions and position in space. It is shown that in order to obtain limit evaluations, summation of the residual and service stresses should be performed by the principle of summation of *J*-integrals. In this case, redistribution of plastic deformations at crack propagation leads to the fact that the dimension of the «process zone» in welding or joint thickness should used instead of crack length, allowing for RWS, with the numeric coefficients found during the study. For instance, limit evaluations for a crack oriented across the weld, yield the following formula:

$$J_I^{\Sigma} = 1.2\sigma_y^2 S/E' + (\sigma^s + \sigma_R)^2 Y_2^2 Y_3^2 \pi a, \qquad (9)$$

where Y_2 is the correction function, allowing for the influence of free surfaces in a plate of a limited thickness; and σ_R is the anticipated maximum level of reactive stresses.

The high level of total stresses, characteristic for the SPOSP welded components, determines the need to use the non-linear fracture mechanics parameters in material certification, namely CTOD parameter used in foreign shipbuilding, or critical value of *J*-integral. These sections of GOST 25.506--85 are different from the current foreign standards, and it does not cover the material with RSW. Therefore, the accepted procedure of testing for crack resistance was based on the use of the main procedures of BS 7448 standard, pp. 1, 2, including the method of side swaging to relieve RWS and a procedure of metallographic examination to determine the correctness of testing individual structural components of the metal of welded joints.

Results of determination of temperature dependencies of crack resistance allowed revealing for all the considered hull materials three regions with different types of fracture, namely high-temperature (where fracture proceeds completely as a result of stable tough growing of the crack); intermediate (where a stable growth of the crack is completed by unstable fracture with an abrupt transition from fibrous fracture to crystalline fracture) and low-temperature (where there is no stable crack growth, and the fracture is fully crystalline) (Figure 1). In the latter case only the fracture conditions are characterized by just one parameter of crack resistance. In the intermediate region the critical parameters at crack initiation and unstable fracture are different, and a stable crack growth is described by the so-called *R*-curve. Highly sensitive to the structural condition of the material and thickness of the specimen being tested are the temperature limits of different types of fracture, and for the intermediate region also the crack resistance, determined by the moment of unstable fracture. Apart from that, the crack initiation characteristics and *R*-curves are not structure sensitive, and *R*-curves are independent on temperature. Its lowering influences
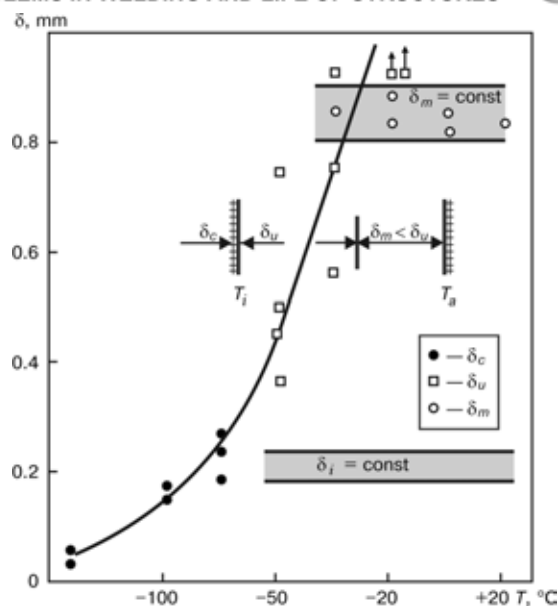

Figure 1. Types of fracture in crack resistance testing and determined parameters (δ_m ---- CTOD at overloading maximum)

the shortening of the region of tough growing of the crack and drawing of the points of instability and crack initiation closer to each other.

For hull steels, corresponding to the requirements of the current specifications [8, etc.], CTOD level for to --50 °C temperatures meets the highest requirements. It is more complicated to reach it for the metal of the HAZ and weld of welded joints. For the HAZ metal the most critical is the coarse-grained structural constituent at the fusion boundary, and increase of welding heat input leads to decrease of its crack resistance. For the weld metal the biggest problem is ensuring the high cracking resistance in automatic submerged-arc welding. In manual welding CTOD of 0.1--0.2 mm at the temperature below --40 °C is achieved by applying electrodes with nickel content of up to 3 %, in gas-shielded welding ---- by application of a mixture of $Ar + CO_2$. In automatic welding this is done by using agglomerated fluorite-basic fluxes with limitation of weld metal strength and lowering of welding heat input (Figure 2).

Analysis of the features of brittle fracture allows defining more precisely the problem of substantiation of the strength criterion. Foreign standards use the so-called CTOD Design Curve method [9, etc.], where the results of CTOD determination are compared to the design crack opening in the strength condition for a selected «design» defect. Application of this procedure raises the following problems:

• selection of the size of the «design» defect for cyclically-loaded structures. If we take into account the possibility of defect growth with its initial dimensions assumed proceeding from the detecting ability of means of NDT (as it is done in nuclear engineering), then the requirements on crack resistance for the welded joint material are difficult to meet;

• theoretical substantiation of the transition from the results of specimen testing to predicting the fracture of structures with another defect configuration and different loading conditions. Known is the non-invariance of crack resistance parameters, determined
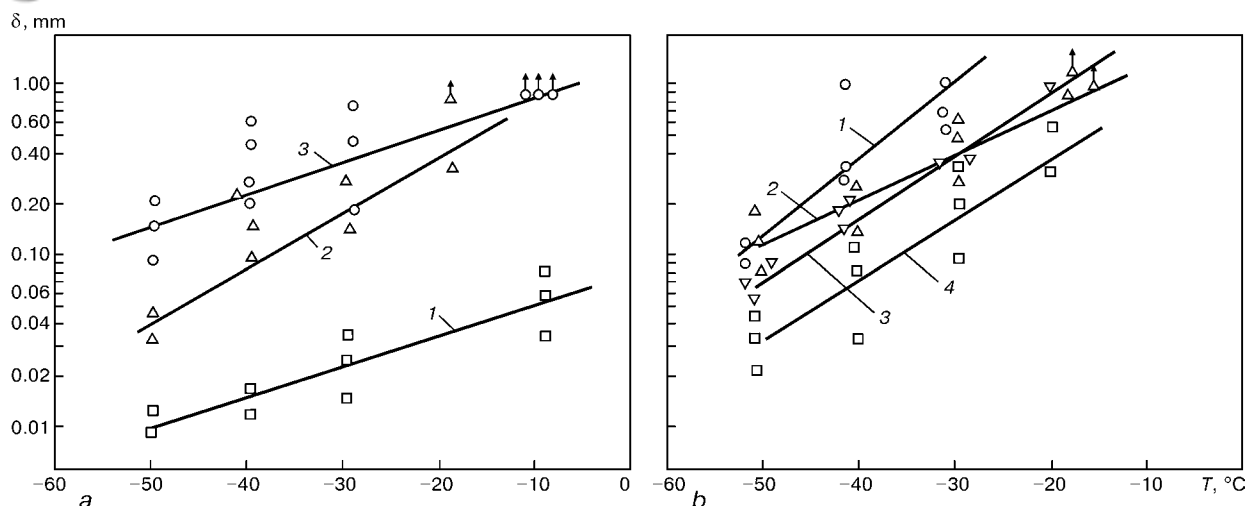
Figure 2. Results of testing weld metal for crack resistance: *a* — manual welding (*1* — UONI-13/45R; *2* ---- 48KhN2; *3* — 48KhN5); *b* ---- automated welding (*1* — Sv-10GNA + 48AF51; *2* — Sv-08GN2MDTA, Ar + CO_2; *3* — Sv-04N3GMTA + 48AF50; *4* ---- Sv-04N3MGA + FIMS20P

by the moment of unstable fracture, namely such is the practice of CTOD determination in certification testing. It is rational to analyze also the possibility of allowing for the margin of material resistance to fracture propagation due to a stable crack growth.

Thus, in order to substantiate the strength criterion, it is necessary to compare the conditions for a stable crack growth and unstable fracture in a specimen and an element of a full-scale structure. The known condition of instability ($\partial J/\partial a > \partial Jc/\partial a$ [10]) does not describe the observed fractures, as it does not take into account the possibility of an abrupt change of the fracture micromechanism observed experimentally.

In order to solve these theoretical and applied problems, a physical model was proposed of a stable crack growth, «stable crack growth--unstable brittle fracture» transition and reverse transition, namely crack retardation [11--13]. A stable crack growth is considered to be the result of achieving a critical SSS in its tip at the deficit of intensity of the released elastic energy. With the assumption of constant specific work of plastic deformation in crack growth, equations were derived, which describe the found *R*-curves for small- and full-scale flow, under the conditions of planar deformation and in case of deviation from them (mode of cleavage crack tunneling). Energy condition of unstable fracture at an abrupt change of its micromechanism was suggested and experimentally substantiated, which is confirmed by the methods of electron microscopy, X-ray analysis, crack resistance testing with variation of compliance of the loading system, specimen dimensions and configuration.

The developed theoretical concepts allow

• substantiation of the observed correlation dependencies of the temperature of brittle crack retardation and different critical temperatures of tough-brittle transition;

• describing the influence of specimen scale and configuration on unstable fracture conditions. Practically important is the experimentally confirmed conclusion (Figure 3) that testing of standard specimens in bending or off-centre tension is more stringent in terms of the relationship between the elastic constituent of *J*-integral and its full value, compared to possible variants of crack location in a full-scale element of a structure of the same thickness.

As a result, an approach is substantiated, which considers as a critical event the moment of transition to an unstable fracture (unlike the existing ones, considering the moment of crack initiation). This permits defining the condition of brittle strength in a form, not requiring entering the specific dimensions of a «design defect», namely variation of the defect dimension and position allows determination of the most dangerous situation by a combination of the full value of *J*-integral and its elastic component. Obtained evaluations of loading parameters were used to substantiate the requirements to the level of relative (dimensionless) crack resistance $\beta = J_{ct}E/(\sigma_{0.2}S)^2$ by the «absolute» criterion of brittle fracture prevention (cyclically loaded structures) for cracks in the field of total stresses, and those for cracks with dimensions limited by the zone of high tensile RWS (for structures exposed mostly to static loads). When going over to specifying the absolute level of CTOD parameter the required value turns out to be proportional to the thickness and yield point of the material.

Implementation of research findings. The main research resulted in development of standards and procedures of RF Register, which supervises the design and construction of off-shore facilities.

Work on prediction of the cyclic fatigue life of welded elements was generalized in the form of an approved by the Register «Procedure for Determination of Curves of Admissible Cyclic Stresses and Selection of Optimal Design-Technological Features of Welded Joints». It enables selection of the thicknesses of the main structural elements, determination of the scope of additional technological treatments, increasing the fatigue resistance, of the ability to use components with structural lacks-of-penetration, and of the need to lower the structural stress concentration. Relationships for calculation of the endurance of a structure include the characteristics of Weibull distribution for a non-stationary service load and pa-

rameters of *S*--*N* curves for a welded joint at stationary loading, which depend on a set of structural and technological factors. The procedure incorporates the following sequence for selection of the basic *S*--*N* curve, proceeding from the anticipated level of RWS and loading cycle asymmetry, calculation of K_{ef} value, allowing for the design features, dimensions and loading conditions of a joint (determination of *A* parameter) and technology of weld performance (ρ_{ef} determination). In addition, a procedure was incorporated for evaluation of the life at the stage of fatigue crack growth for structural elements of the type of «bond breaking up» and joints with initial geometrical defects.

The procedure was used to perform evaluations of cyclic fatigue life of the base and ice lining of «Prirazlomnaya» SPOSP project, which demonstrated the reality of initiation of premature cyclic fractures at ice loading on the ice lining elements and the need to take additional technological measures during construction.

The results of substantiation of the criteria of toughness and cold resistance were incorporated in the «Materials», «Welding» and «Casing» sections of the Register «Rules of Classification, Construction and Fitting of OSP / DR», released in the year 2000. This document for the first time in local shipbuilding establishes the scope of additional testing of materials to substantiate the areas of their applicability, basic principles of testing procedures, requirements to CTOD value for the base and welded joint metal. The level of requirements depends on the category of the structural element by the degree of its criticality (seriousness of consequences in case of failure) and its loading conditions, namely cyclic or static, as well as possibility of a dynamic nature of load application.

The defined requirements were used in development of specifications for materials and technologies of welding for the projects of SPOSP «Prirazlomnaya», «Malekpak», «Sakhalin-2», as well as for addressing a number of specific issues, for instance, that of admissibility of elimination of post-weld heat treatment of joints on thick metal.

Procedural developments in the field of testing for crack resistance were incorporated in the «Procedure for Determination of Crack Resistance Parameters at Static Loading for Welded Joint Metal», approved by the Register. Over the last years it was widely tried out in certification testing of materials and technologies of welding, conducted under the supervision of the Register and foreign classification societies (DnV, Lloyd, etc.), as well as in performance of purpose-oriented programs of RF Ministry of Science and of contract work with the Russian Shipbuilding Agency. Certification testing has been performed of sheet rolled stock of a number of Russian metallurgical enterprises, and welding technologies, being developed for Arctic structures. On the whole, experience of performing this work demonstrates that the results of additional crack resistance testing usually allow a significant widening of the area of applicability of the certified material, despite the limitations specified in foreign standards, by increasing the information content of the data on a material.
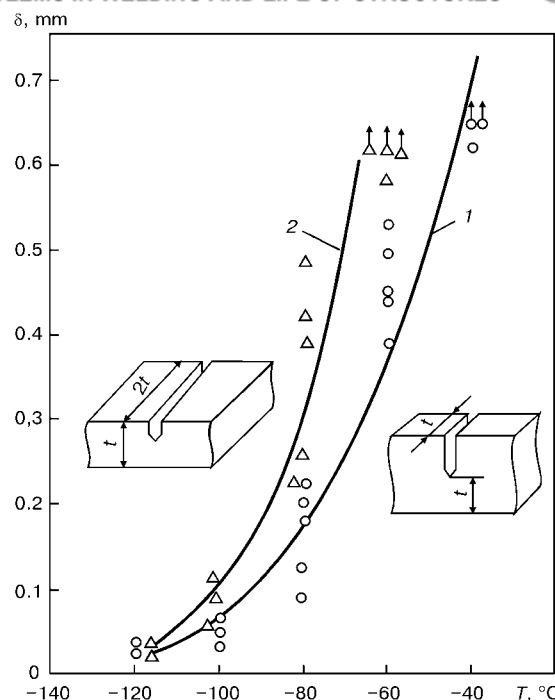

Figure 3. Comparison of the results of testing samples of standard (*1*) and non-standard (*2*) geometry

Thus, the results of the performed theoretical and experimental investigations of welded joint strength enabled development of a mutually coordinated package of codes and procedures, allowing current problems of design and construction of off-shore structures for shelf facilities to be solved.

1. (1984) *Fatigue strength analysis for mobile off-shore unit.* DnV, Det Norske Veritas. Classification notes No. 30.2.
2. (1989) *BS 7191--1989.* British Standard Specification for weldable structural steels for fixed off-shore structures. BSI.
3. (1990) *Canadian Standard Association. Preliminary standard S473-M1989. Steel structures.* Part III of the code for the design, construction and installation of fixed off-shore structures.
4. Iliin, A.V., Leonov, V.P., Manninen, T.P. (1981) Influence of welded joint geometry on elastic stress concentration. *Voprosy Sudostroen.*, Series Welding. Issue 32.
5. Gorynin, I.V., Iliin, A.V., Leonov, V.P. et al. (1990) Design determination of fatigue life of welded joints, allowing for the influence of technological factors. *Sudostroit. Promyshl.*, Series Materials Science, Welding. Issue 10.
6. Iliin, A.V., Leonov, V.P. (2000) Improvement of design procedures for evaluation of fatigue life of welded joints in structures of off-shore platforms, based on simulation of cyclic fracture processes. In: *Transact. of the Russian Register of Shipping*, 23.
7. Iliin, A.V., Leonov, V.P., Mizetsky, A.V. (1996) Method of numerical simulation of the initial stage of cyclic damage in welded joints. Construction of *S*--*N* curves. *Voprosy Materialoved.*, **2** (5), 62--76.
8. (2002) *TU 5.961-11804--2002.* Plate rolled stock of higher strength steel with improved weldability.
9. (1980) *WES 2815.* Method of assesment for defects in fusion-welded joints with respect to brittle fracture. *J. Jap. Weld. Eng. Soc.*
10. Siratori, M., Migoshi, T., Matsushita, X. (1986) *Computational fracture mechanics*. Moscow: Mir.
11. Iliin, A.V., Mizetsky, A.V. (2000) Conditions of stable crack growth and unstable fracture in materials with a quasibrittle temperature transition. *Voprosy Materialoved.*, **2** (22), 84--104.
12. Iliin, A.V. (2001) Prediction of the form of *J*--*R* curves and conditions of stable growth of a crack at a stressed state uniform at the crack front. *Zav. Laboratoriya*, **9**, 46--53.
13. Iliin, A.V., Leonov, V.P. (2002) Features of using CTOD parameter as a characteristic for transition from the mode of stable crack growth to that of unstable fracture in structural steels. *Ibid.*, **2**, 28–36.

DEVELOPMENT OF HIGH EFFICIENCY ARC WELDING METHODS

N. KIJI, K. KOBAYASHI, J. ISHII and **H. YAMAOKA**
Ishikawajima-Harima Heavy Industries Co., Ltd., Japan

The high efficiency twin arc TIG welding method and the high AC MAG welding method have been developed and applied into various structures. Those welding methods can weld in the higher current conditions and achieve the higher deposition rate than the other conventional welding methods. About A-TIG welding, the efficient welding procedure for thick plate welding has been developed.

In the manufacture field, various welding processes are used. With the quality and the performance which are required of products, those welding processes are used properly. The TIG welding is capable of producing high quality welds and is particularly well suited to positional welding, where consistent penetration can be achieved in all welding positions. Consequently, the technique has been widely applied to sheet, plate and pipe welding in various materials. On the other hand, the MAG welding using CO_2 or the mixture of CO_2 and Ar as shielding gas is a low cost, and is a high efficiency welding process. This welding process is used widely in manufacture fields such as shipbuilding and bridge construction.

As compared with other welding processes, the deposition rate of the TIG welding is low, and its weld penetration is shallow. In order to apply the TIG welding for thick plate structures, the increase in the deposition rate is required. The high efficiency twin arc TIG welding method which has two electrodes in single torch has been developed. In the twin arc welding, the sound weld is obtained also on high welding-current conditions.

MAG welding process is a high efficient method as compared with TIG welding. However, in welding of heavy thick plate which exceeds 50 mm, generally submerged arc welding (SAW) is used. In SAW, because of the feeding of flux and disposal of slag, the increase in efficiency is prevented. A narrow-gap MAG welding is performed in the limited field. In this technique, a special welding equipment and advanced skill are required. Moreover, general MAG welding is direct current arc welding. In direct current arc welding, the magnetic blow occurs in high-current conditions, and the lack of fusion tends to produce because of the weld penetration profile like a finger.

Accordingly, authors have developed the high alternating current (AC) MAG welding process which is high efficiency and easy handling. In this welding method, because the thick metal-cored wire which includes a little flux is used, the stable AC arc can continue, high-current welding is possible and the slag forms very little as compared with SAW.

The A-TIG process using activating flux was developed by the E.O. Paton Electric Welding Institute in the early 1960s. In this process, the activating flux applied to the surface of material increases the weld penetration depth of TIG welding. The A-TIG process is capable of welding up to 12 mm in a single pass without filler material. For greater plate thickness, a multi-pass welding technique is necessary. For thick plate welding, the welding procedure combined the A-TIG process with conventional MAG welding has been developed.

High efficiency TIG welding method. *Characteristics of the method.* Generally, in high electric current regions in TIG welding method, arc power becomes excessive, making big hollow in a weld pool, and this prevents the formation of sound weld. So, there was a limit to improve welding efficiency by adopting high current in TIG welding. The developed welding method employs two electrodes within a single torch, and pulse current is supplied independently to each electrode from two power sources, as shown in Figure 1. Two pulsed arcs generate from electrodes alternatively, and by controlling each arc power, it became possible to weld with high current without big hollow in weld pool. Moreover, welding wire is sent to the molten pool from torch front by heating with introducing direct current, and this makes it possible to obtain high deposition rate. Appearance of the arcs is shown in Figure 2. The two arcs from the separate electrodes were pulled together to form one large arc.

Pulse current control in accordance with welding positions. In this developed welding method, pulsed current is applied to two electrodes from two welding power sources, and each pulse current can be set up individually. Moreover, by synchronizing of mutual pulse control, and current controlling method synchronized with weaving, it is capable of giving characteristics in accordance with welding positions.

In the horizontal position, two electrodes are arranged in perpendicular to the welding direction and the current values of upper and lower electrodes are set up individually. By applying appropriate pulse
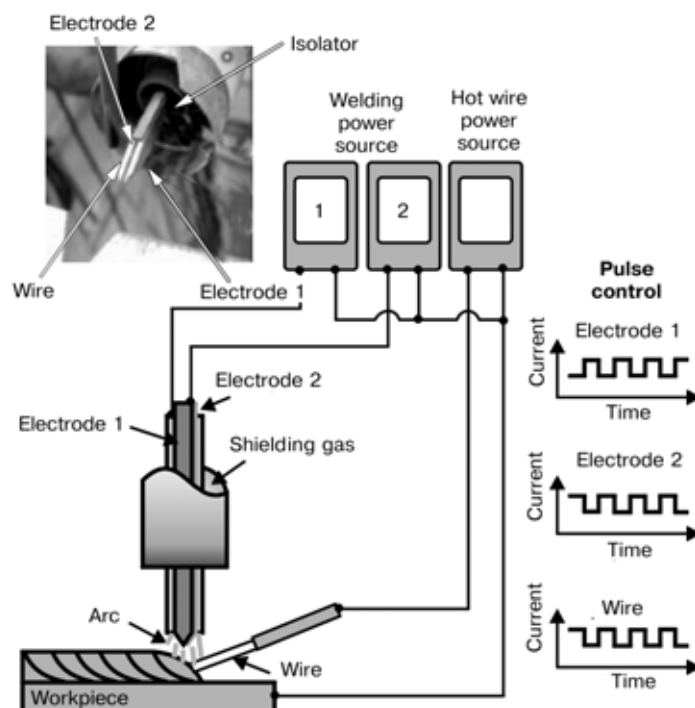
Figure 1. High efficiency twin arc TIG welding method

current to each electrode alternatively, good bead shape of less undercut and overlap can be achieved even with high deposition rate (Figure 3).

On the other hand, in the vertical position two electrodes are arranged in perpendicular to the welding direction as same as in horizontal position, and pulsed currents is applied to both electrodes (right and left) alternatively. Consistent penetration can be achieved by weaving the electrodes in the groove and applying the peak current to the groove wall at the stopping time. Heat input can be controlled by applying the lower pulse current in the weaving movement (Figure 4).

Examples of welding. Examples of narrow-gap welding in the horizontal and vertical positions are shown in Figure 5. Low alloy steel (SF340A or SQV-2A) plates and carbon steel (SM490A) plates were used for the test. Long rectangular electrodes were used, and welding was performed without weaving.

Horizontal welding. Welding was performed without weaving with U-groove (bevel angle of 2°, root radius of 6 mm, groove depth of 150 mm). Only long rectangular section tungsten electrodes were inserted into the groove and nozzle skirt was set at the tip of a torch nozzle in order to cover the groove surface and hold the shielding gas appropriately. In horizontal welding, it is necessary to prevent hanging down of a molten pool by arc power and to prevent undercut in upper side groove with keeping consistent penetration in upper and lower groove walls.

Figure 3. Control of pulse current for horizontal welding

Torch position	Left groove wall	Weaving movement	Right groove wall
Left current / right current	I_p/I_b	I_m/I_m	I_b/I_p

Figure 4. Control of pulse current for vertical welding: I_p — peak current; I_b ---- base current; I_m ---- movement current

Figure 2. Appearance of twin arc

Welding current   300–600 A
Arc voltage   9–12 V
Travel speed   10–16 cm/min
Deposition rate   17–23 g/min

Test piece — SQV-2A steel

a

Welding current   300–600 A
Arc voltage   10–11 V
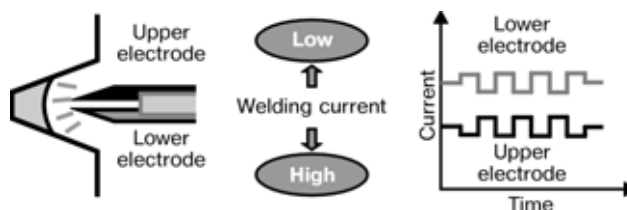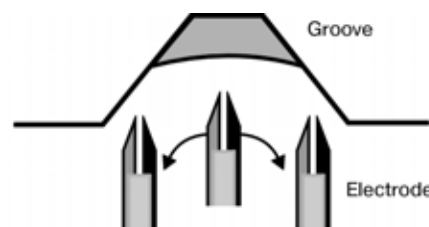Travel speed   6 cm/min
Deposition rate   18–27 g/min

Test piece — SM490A steel

b
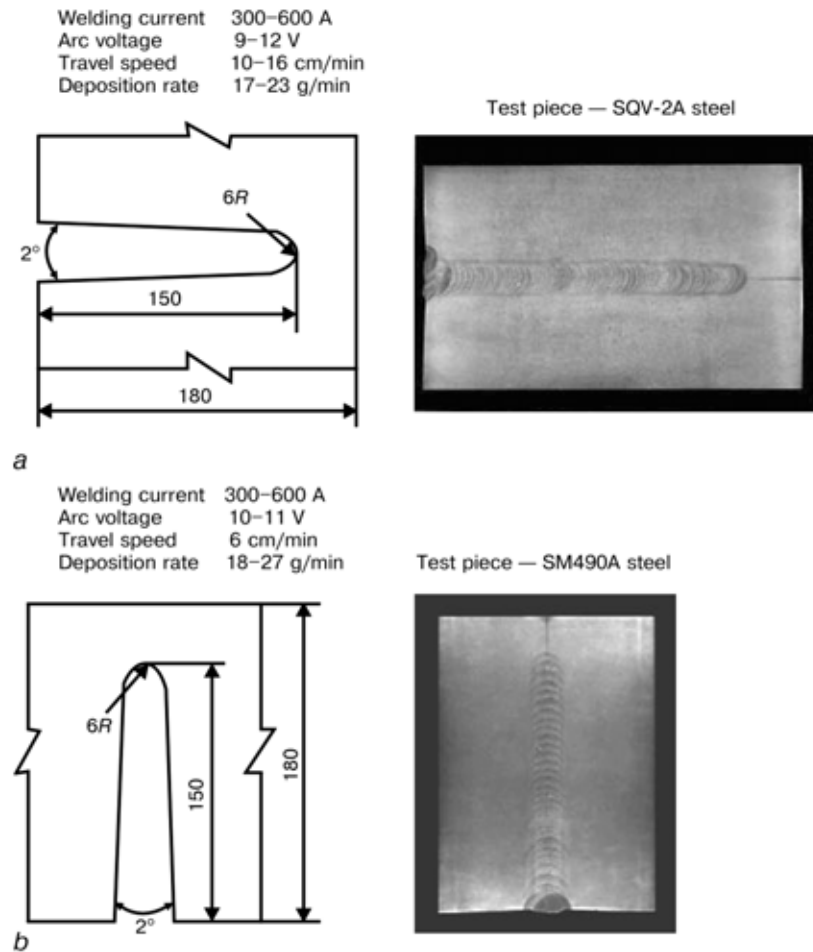
Figure 5. Examples of macrosection and welding condition for horizontal narrow-gap welding of low alloy steel plate (*a*) and vertical narrow-gap welding of carbon steel plate (*b*)

For these purposes, welding was performed by applying different welding current to upper and lower electrode, higher current to lower electrode. The welding current applied for upper electrode was 250 A and that of lower electrode was 350 A (totally 600 A), and travel speed was 10 cm/min. One pass per layer welding was adopted except final layer, and was welded with 69 passes. A good-shaped bead without hanging down of a molten pool was obtained for each pass. In addition, consistent penetration was achieved, as shown in the macrosection in Figure 5, *a*.

Vertical welding. Vertical up welding was performed with using the same U-groove used in horizontal welding. Welding was carried out at the current of 300 A at each electrodes (totally 600 A) and travel speed of 6 cm/min, maximum deposition rate

Figure 6. Property of alternating current arc: U_{reign} — reignition voltage; $U_{\text{o.-c}}$ — open-circuit voltage of power source

Figure 7. High AC MAG welding method

Figure 8. Cross section of metal-cored wire 4.8 mm in diameter

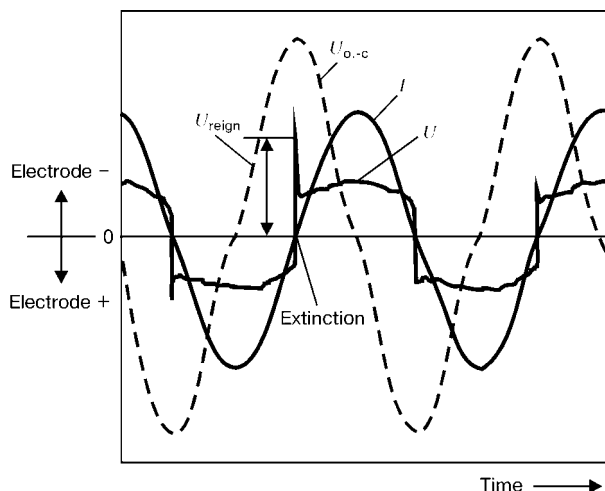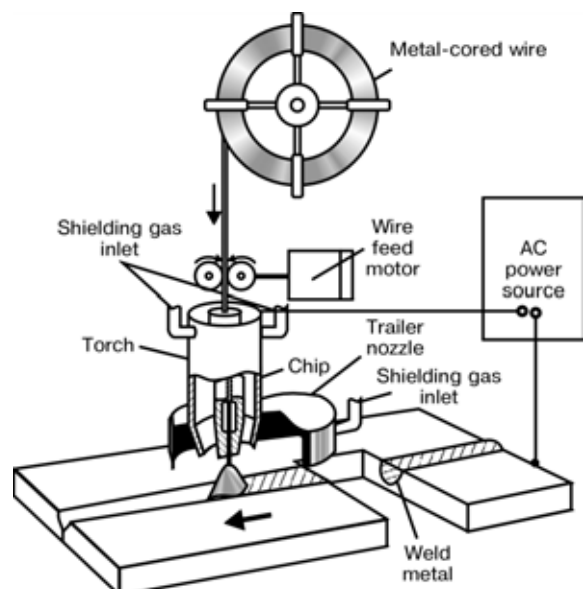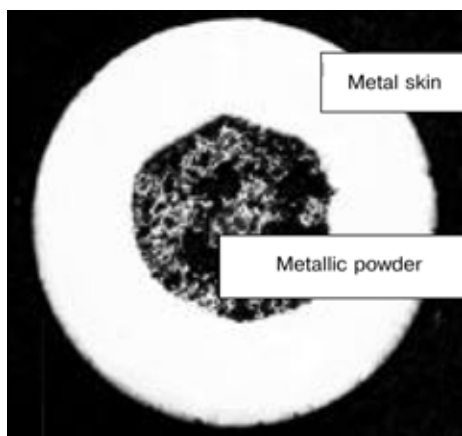**Figure 9.** Change of current (*a*) and voltage (*b*) in high AC MAG welding with metal-cored wire at welding current of 800 A in shielding gas mixture Ar + 10 % CO_2

was 27 g/min for 36 passes. One pass per layer welding method without weaving was applied.

Also in narrow-gap welding, it was confirmed that consistent penetration to in a groove wall could be achieved with each pass, as shown in the macrosection in Figure 5, *b*.

High AC MAG welding method. *Characteristics of the method.* The change of welding current, arc voltage and open-circuit voltage of a welding source is shown in Figure 6. In AC arc welding when the polarity of current is reversed, the arc extinguishes. In order to keep AC arc stably, reignition of arc at the time of a polarity being reversed needs to be done. Therefore, in order to ignite arc again, it is necessary to use the welding source with open-circuit voltage higher than reignition voltage. The welding source with a high open-circuit voltage has a possibility of receiving an electric shock. In order to use a general AC power source, the metal-cored wire which includes a little flux and reduces the reignition voltage, has been developed. The metal-cored wire has a large diameter like SAW wire. The high AC MAG welding equipment is shown in Figure 7, and the cross section of the metal-cored wire is shown in Figure 8. In case Ar + 10 % CO_2 mixture is used for shielding gas and the welding current is set to 800 A by actual value, the measurement result of current and voltage during welding is shown in Figure 9. The average reignition voltage is 65 V and is lower than the open-circuit voltage of the welding source. Reignition of arc can be done certainly, and the AC arc continues stably.

The relationship between the welding current and the deposition rate in the high AC MAG welding is shown in Figure 10. Because the wire of more than 3.2 mm diameter is used, the welding process can be carried out in the high current range of 400--1000 A, and obtained about 3 times higher deposition rate (200--300 g/min) compared with a conventional MAG welding.

Examples of welding. Examples of butt welding and corner welding in flat position are shown in Figure 11. Carbon steel plates were used for the test. The wire 4.8 mm in diameter and Ar + 10 % CO_2 mixed gas were used, and welding tests were carried out with a flat torch.
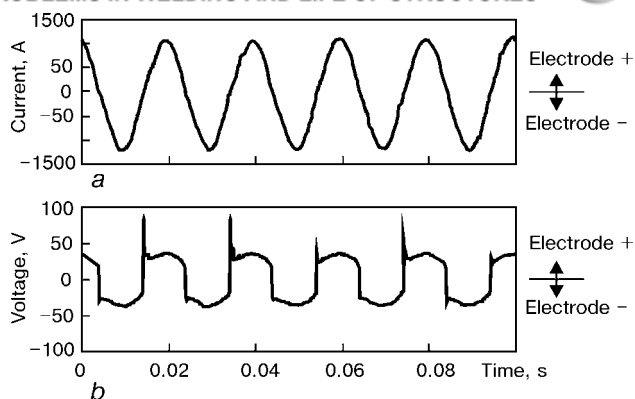
The one side welding of thick plates was performed with V-groove (bevel angle of 20°, root gap of 8 mm, groove depth of 65 mm). Penetration welding was possible using the flat torch that can be inserted into groove. The plate of 65 mm thickness was welded with 10 passes. One pass per layer welding can be carried out except final layer.

The corner welding with single bevel groove was also performed (bevel angle of 15°, root gap of 10 mm, groove depth of 70 mm). In the welding of root pass, the weld penetration to backing metal was obtained enough. The plate of 70 mm thickness was welded with 11 passes. Also in the corner welding, one pass per layer welding can be carried out except final layer.

Trial of the A-TIG process. *Butt welding of stainless steel.* In the A-TIG process, because the deep weld penetration is obtained, the groove with a thick root face can be used. For thick root face, the limits of linear misalignment and root gap were investigated. The activating flux FASTIG™ SS-7 and 6 mm thick stainless steel plates were used for the welding test. The results of the welding test are shown in the Table. The butt welding of 6 mm thick stainless steel without burn through is possible up to 2.5 mm linear misalignment and/or 2 mm root gap. As compared with the

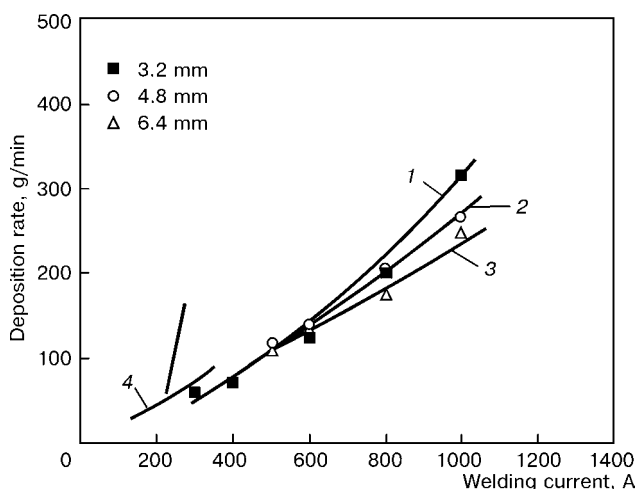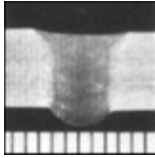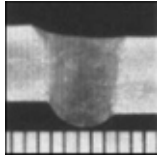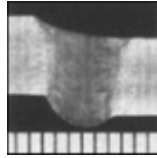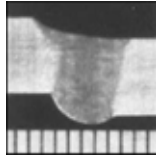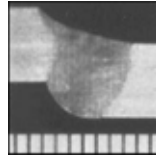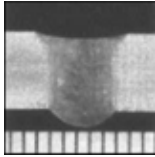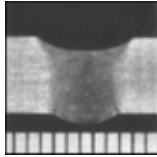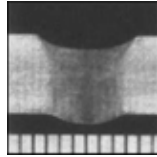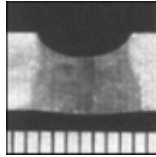**Figure 10.** Relationships between welding current and deposition rate in high AC MAG welding with wires of different diameter (*1--3*) and conventional MAG welding with wire 1.2 mm in diameter (*4*) (shielding gas Ar + 10 % CO_2, wire extension 30 mm, voltage 30 V)

The characteristic weld bead profiles in 6 mm thick stainless steel made using A-TIG welding

	0.5 mm	1.0 mm	1.5 mm	2.0 mm	2.5 mm
Linear misalignment					
Root gap				Burn through	
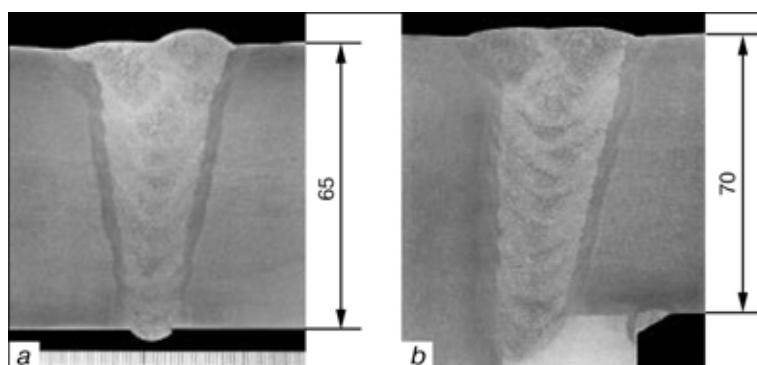
Figure 11. Examples of macrosection for butt (*a*) and corner (*b*) welding in flat position of low alloy steel plate at welding current 700--900 A, voltage 23--29 V, speed 25--35 cm ⁄ min, heat input 23-63 kJ ⁄ cm, with 10 passes (*a*) and at welding current 900--1050 A, voltage 25--31 V, speed 22--35 cm ⁄ mm, heat input 34–89 kJ ⁄ cm, with 11 passes (*b*)
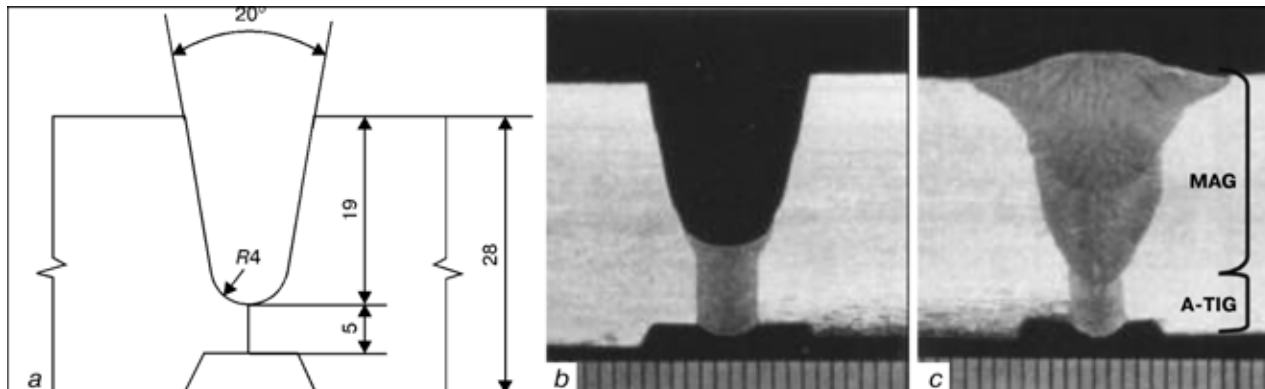
Figure 12. Configuration of groove (*a*), and cross sections of 28 mm thick stainless steel with 5 mm thick root face welded using A-TIG process with root pass (*b*) and conventional MAG process with two passes (*c*)

conventional TIG welding with the V-groove which has a thin root face, the required tolerance of groove alignment is easy in A-TIG process.

Examples of welding. The butt welding of 28 mm thick stainless steel was conducted using the A-TIG process and the conventional MAG welding. The groove configuration and the cross sections of weld bead are shown in Figure 12 (the root face of 5 mm thickness, bevel angle of 20°, groove depth of 19 mm and root radius of 4 mm.

Firstly, the penetration welding with A-TIG process was carried out, and then the welding was completed with the conventional MAG process. As compared with conventional welding procedure (conventional TIG welding + SAW), the total welding cost is reduced by 25 %.

CONCLUSION

The high efficiency twin arc TIG welding method and the high AC MAG welding method have been developed and the fundamental weld examinations were carried out. Using these welding methods, the substantial efficiency is achieved in various manufacturing field. The high efficiency twin arc TIG welding has been applied to the construction of a LNG storage tank, and the high AC MAG welding has been applied to the construction of bridges and ships.

Moreover, the application trial to stainless steel was carried out about the A-TIG process. It is possible to carry out thick plate welding with the high efficiency by combining with another welding process, especially MAG welding.

NEW INFORMATION SYSTEMS FOR NON-DESTRUCTIVE TESTING AND DIAGNOSTICS OF WELDED STRUCTURES

N.P. ALYOSHIN

N.E. Bauman Moscow State Technical University, Moscow, Russia

New devices providing information on internal structure of a part and its defects are described. Acoustic-emission systems allow identification of such dangerous sources as plastic deformation, initiation and propagation of cracks and corrosion damages. Ultrasonic tomograph registers information on configuration, size and orientation of defects. Spectral-acoustic monitoring systems are suggested for measuring volumetric two-axial stresses. New solution to a practical problem of development of technology and equipment for NDT of austenitic welds in joints from 5 to 100 mm thick is described.

Keywords: *welded structures, life of structures, non-destructive testing, diagnostics, acoustic-emission systems, spectral-acoustic systems, devices*

Diagnostics is an integral part of any technological process of manufacture of materials and parts. Availability of high-quality materials and technologies used for the fabrication of structures does not guarantee their trouble-free operation at the absence of efficient diagnostics methods.

Importance of NDT and diagnostics methods is particularly high now, as wear of the process equipment stock in some cases is higher than 65 %. Therefore, to avoid accidents at the most critical objects in operation, it is imperative to develop technologies and equipment for evaluation of their residual life.

Good results have been obtained in Russia in terms of development of highly informative flaw detection equipment and methods for estimation of residual life of some objects. The instruments and devices developed are based on the latest achievements in the field of ultrasonic inspection, information science and radio electronics, and they are not in the least inferior in their performance to the best world standards.

Model of a defect in the form of ellipsoid with known semi-axes is most suitable for estimation of residual life and operational reliability. In this case the ellipsoid should interpolate an actual loss of integrity of the object material with a sufficient accuracy. It is impossible to determine semi-axes of such an ellipsoid from the data of ultrasonic inspection without an accurate solution of the problem of scattering of an ultrasound from such reflectors. This problem in its most general form can be formulated as follows. A wave characterised by shift vector U_0 falls on the ellipsoid confined by surface S with semi-axes a, b and c, the mechanical properties of the surface of which are described by impedance tensor Z. Interaction of this wave with the ellipsoid results in formation of a new field characterised by shift vector $U_0 + U$, its component U being called the scattered wave. Then it is necessary to construct the

field of U which would meet the equation of steady-state oscillations of a linearly elastic medium

$$(\lambda + 2\mu) \text{ grad div} U - \mu \text{ rot rot } U + \rho\omega^2 U = 0,$$

the radiation conditions and, together with the incident wave field, one of the following boundary conditions:

$$D_n[U_0(M) + U(M)] = 0, \quad M \in S, \tag{1}$$

$$U_0(M) + U(M) = 0, \quad M \in S, \tag{2}$$

$$D_n[U_0(M) + U(M)] + \mathbf{Z}(M) \times \\ \times [U_0(M) + U(M)] = 0, \quad M \in S, \tag{3}$$

where λ, μ are the Lame's constants; ρ is the density of a space material; M is the point of the space; and D_n is the differentiation operator of type

$$D_n = (\ldots) = 2\mu \text{ grad } (\ldots)\mathbf{n} + \lambda\mathbf{n} \text{ div } (\ldots) + \mu\mathbf{n} \text{ rot } (\ldots);$$

$\mathbf{n}$ is the vector of an external normal to surface S of the scattering body, and boundary conditions (1) through (3) correspond to scattering at the acoustically soft, acoustically hard and impedance (inclusion of a foreign material) boundaries, respectively.

To make the calculations substantially simpler, we suggest that the scattered field sources be removed outside the range of solution of the boundary problem. Thus, the new calculation method can be called the method of removal of sources. Intensity of each of the sources remains finite, as well as the number of the sources, whereas the field induced along the scattering surface by each of them is a smooth function.

Calculation by the method of removal of sources consists in the following. Like with any other numerical methods, it is assumed here that the solution obtained precisely meets the specified conditions at the finite quantity of the scattering surface points. As these points increase in number, the resulting approximations converge to the precise solution. As this solution is not known beforehand, it is assumed that the convergence criterion is the accuracy of meeting the above approximated conditions on the scattering
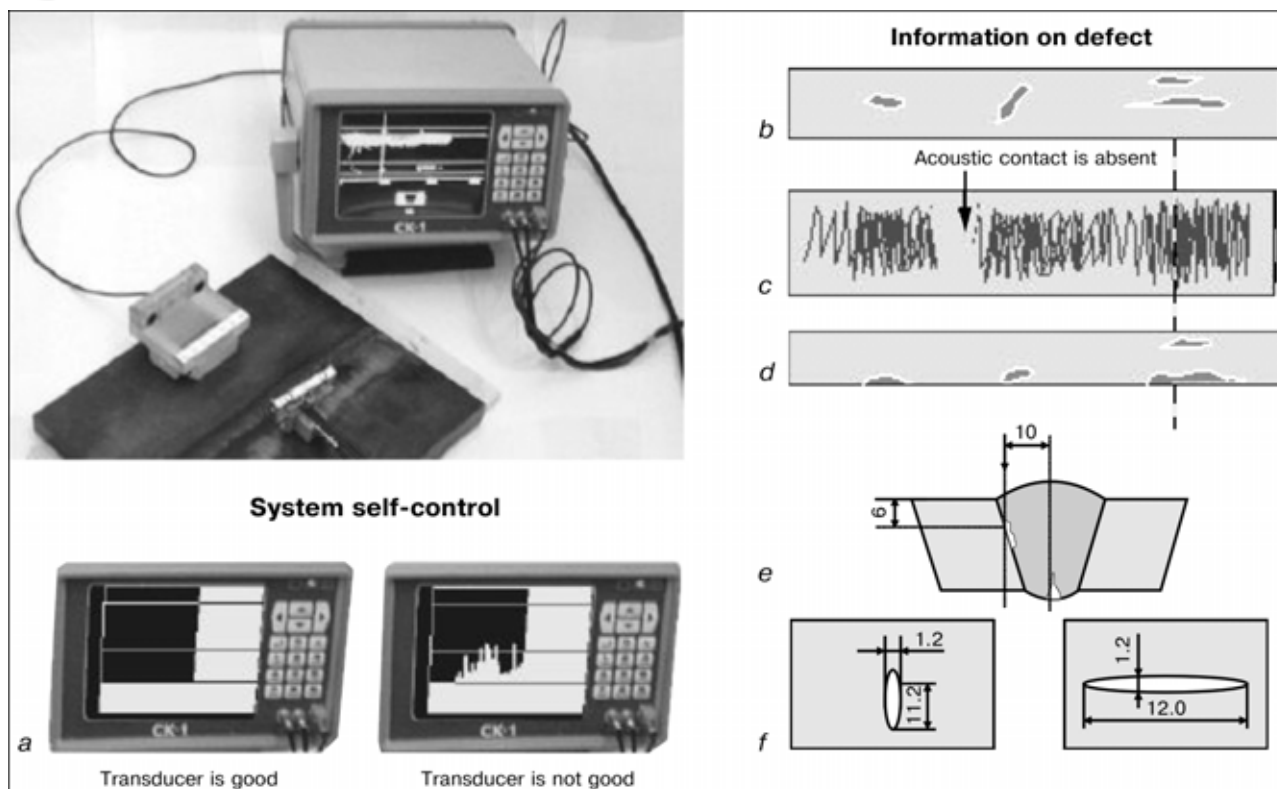
Figure 1. Multi-program portable ultrasonic flaw detector-tomograph SK-1 (*a*) and possibilities of using it to several defects (*b--d*): *b* — top view; *c* — scan trace; *d* — longitudinal section of weld; *e* — transverse section of weld; *f* ---- tomographic image of defect

surface, which in fact is the accuracy of interpolation of the solution on surface *S* with respect to its values in the system of the selected points.

Comparison of the suggested calculation method with other methods and experimental data allows a conclusion of the efficiency of the method of removal of sources for solving the problems of scattering of longitudinal and transverse waves in an elastic medium from different reflectors.

Solution of this problem made it possible to develop such an algorithm of data processing which enabled the 3D image to be reconstructed by scanning only in one plane. The theoretical results obtained were embodied in an ultrasonic flaw detector, i.e. tomograph SK-1 (Figure 1), the ingenious part of which is a 3D coordinate system, in addition to the algorithms of processing the generated information.

This provides a comprehensive information about defects. The weld is displayed on the screen of the flaw detector, i.e. tomograph, from the top (similar to the X-ray pattern) (Figure 1, *b*), from the side (section along the weld) (Figure 1, *d*) and from the end (section across the weld) (Figure 1, *e*), with an indication of equivalent sizes and coordinates of defects. The device also performs automatic measurements of semi-axes of the interpolation ellipsoid (Figure 1, *f*). In addition, the scan trace is displayed on the screen, showing the quality of the acoustic contact, path and velocity of the transducer moved by an operator (Figure 1, *c*). Furthermore, the SK-1 device is intended to perform the following functions:

- automatic adjustment of sensitivity;
- measurement of parameters and certification of transducers used together with the flaw detector;
- accumulation and storage of the test results during the testing process to be subsequently entered into the database or represented in the form of a document.

The testing procedure in the case of using SK-1 consists in movement of the transducer over the surface of an object along the weld with two receiving microphones located on its reverse side, and measurement of function $F(x, t)$ of voltage at the output of the transducer in each position x within a range of $x_0 \leq x \leq x_1$ and at each moment of time t within a range of $t_0 \leq t \leq t_1$, where x_0 and x_1 are the initial and final readings of the position sensor of the transducer, respectively; t_0 to t is the time range of a probable formation of echo signals within the test zone. The results obtained are processed using the following formula:

$$\varphi(x, z) = \int_{x_0}^{x_1} F(x - x_1') \frac{2}{c} \sqrt{(x - x_1')^2 + z^2} \, d_0 \times$$

$$\times \left(\frac{x - x_3'}{\sqrt{(x - x_1')^2 + z^2}} \right) dx_1',$$

where d_0 is the matching factor of the beam.

Then follow construction and display of the image on the screen according to the following algorithm:

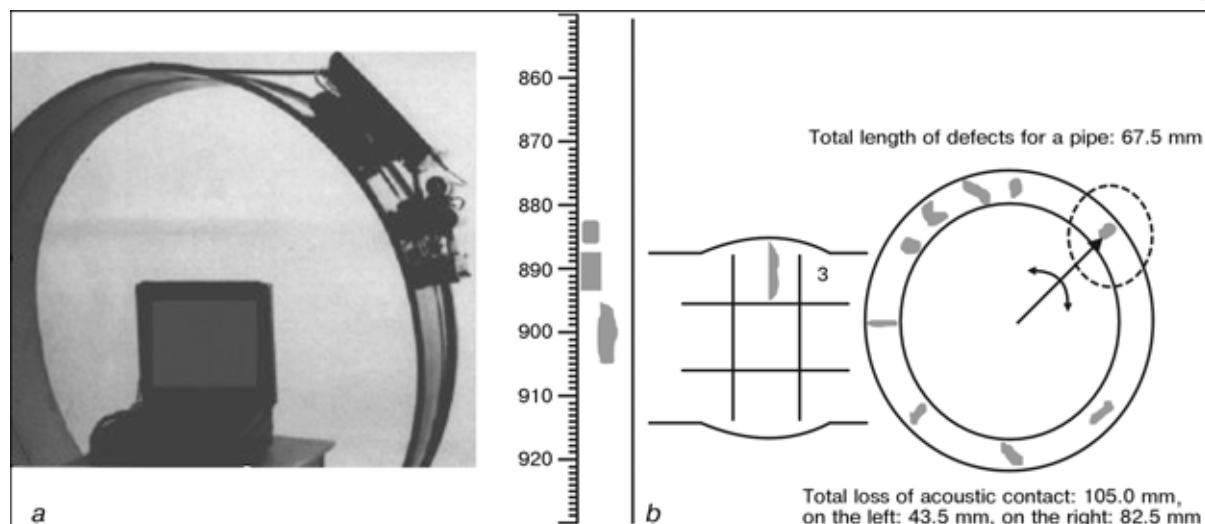**Figure 2.** Automated ultrasonic inspection system «Avtokon-MGTU»: *a* ---- general view of the system; *b* — display of test results on the monitor screen

$$
\begin{cases}
\text{light the point if} & \dfrac{|\varphi(x,\, z)|}{\max|\varphi(x,\, z)|} \geq \dfrac{1}{2}; \\[2mm]
\text{extinguish the point if} & \dfrac{|\varphi(x,\, z)|}{\max|\varphi(x,\, z)|} < \dfrac{1}{2}.
\end{cases}
$$

The device operates at frequencies ranging from 1 to 5 MHz. Resolution of the image is approximately $(1.0\text{--}1.2)\lambda$.

Permanent memory of the device can contain up to 180 settings for testing different objects. The device can be applied to test objects made from metals and plastics over a wide range of thicknesses.

In the case of extended parts, it is advisable to use the automated ultrasonic inspection system «Avtokon-MGTU», which has a productivity of more than 1 m / min (Figure 2, *a*).

The system consists of three main parts: robotic scanner on magnetic wheels, electronic unit and connecting cable 20 m long. The acoustic unit of eight piezo-transducers is fixed on the scanner. The transducers provide testing of a weld section from 4 to 20 mm thick at a uniform sensitivity (± 2 dB) without transverse scanning. These transducers are used also for monitoring the quality of the acoustic contact. Owing to the presence of magnetic wheels there is no need to perform an extremely labour-consuming operation, i.e. installation of extra flexible guides for movement of the scanner.

Characteristic feature of the system is the presence of the weld tracking sensors which provide an accuracy of ± 1 mm with respect to the weld axis at the presence of edge displacements and bends. The electronic unit screen displays information on the weld for its top and transverse section views (Figure 2, *b*).

The algorithm of processing of the incoming signals provides the high accuracy of identification of plane and volumetric defects. The «Avtokon-MGTU» system is intended for testing of pipes or tanks with a diameter of 500 mm and larger at a wall thickness of 4--20 mm. The operating temperature range is from --40 to +40 °C. Weight of the scanner is 8 kg, and total weight of the system is 18 kg.

The N.E. Bauman Moscow State Technical University (MGTU) has recently developed a new modification of the versatile system SK-2 (Figure 3). Unlike other known multi-channel systems, it allows high-accuracy measurements of oscillations of the amplitude of the acoustic contact separately for each channel using no additional acoustic transducers. This leads to a substantial improvement in reliability of the automated inspection owing to compensation for losses of the acoustic contact in each of the channels. The system operates at a temperature from --40 to +60 °C. Weight of the electronic unit is 5 kg.

It is not always enough to know shape and sizes of local defects in an object to evaluate its performance. Residual stresses in different elements of structure of an object have a high effect on its residual life. There is a great number of devices designed for evaluation of residual stresses, based on measurement of different characteristics of magnetic, electromagnetic or ultrasonic fields. The drawback they share is a low accuracy of the measurements (20--25 %). The «Welding and Testing» Centre of MGTU developed a prototype of the automated acoustic system for estimation of structural and strength characteristics of

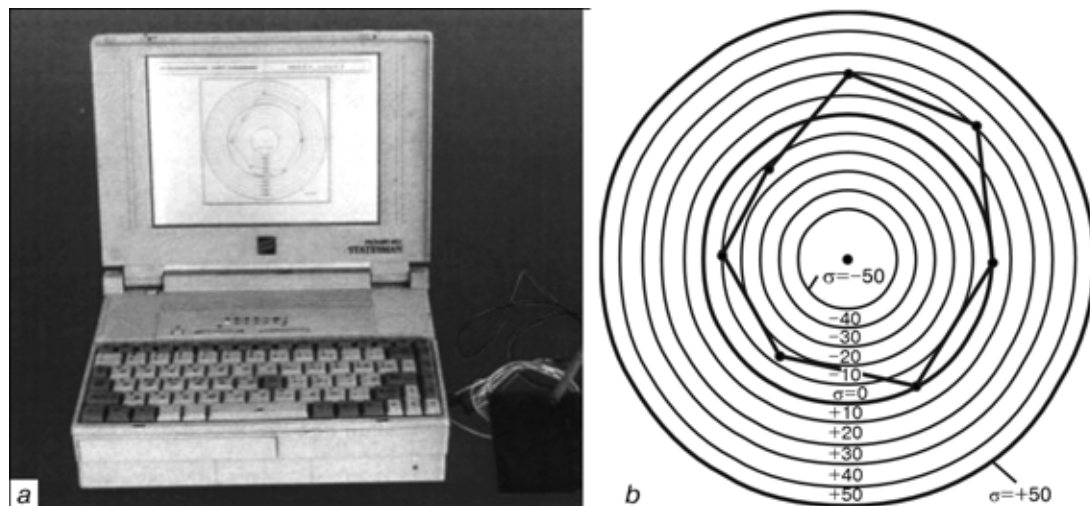**Figure 3.** Multi-program 8-channel ultrasonic flaw detector SK-2

Figure 4. Spectral acoustic system «Astron» for monitoring of mechanical stresses: *a* — general view of the system; *b* — determination of stresses on the pipe diameter

materials (Figure 4). Operation of the system is based on analysis of relationships between parameters of spectra of pulses of elastic waves propagating in a material studied, its physical-mechanical and structural characteristics.

Elastic wide-band acoustic pulses are emitted into the material of a part or element to be studied. The central frequency of a spectrum is selected from a range of 1--15 MHz, depending upon the type of the material. Either bulk or surface waves are used for analysis, depending upon the thickness of the material studied.

While propagating, an acoustic pulse interacts with the main components of structure of the material, i.e. grains, microcracks, micropores or internal stresses, which affect the spectrum of a signal. Correlation or functional relationships between the spectral-acoustic parameters and structural-mechanical characteristics of the material of a test object are established while performing the set of learning experiments. The measurement algorithm is based on the method of determination of time delays appearing in the equations which relate velocities of propagation of the elastic waves to the effective elastic stresses. Two pulses which passed different acoustic paths are selected. The delay used in the acoustic-elasticity algorithm is calculated from the following formula:

$$\tau = \tau_0 - \frac{1}{2K} \sum_{i=1}^{k} \frac{1}{f_1} \times$$

$$\times \{ \operatorname{arctg} [B_2(f_i)/A_2(f_i)] - \operatorname{arctg} [B_1(f_1)/A_1(f_1)] \},$$

where τ_0 is the delay of the leading front of the second pulse being analysed; A and B are the sine and cosine terms of the Fourier transform, respectively; f_i is the i-th spectral frequency from the selected informative frequency range; and K is the total number of spectral frequencies.

Stresses in an object tested are determined by measuring the required delays and taking stresses from the database on the basis of the acoustic-elastic relationships established earlier. An error of determination of variations in stresses is 5--10 MPa. The system developed performs the following functions:

• measurement of stresses formed in erection or assembly of plane elements of structures by riveting, welding, gluing, etc.;

• measurement of redistribution of stresses formed in elements of complex, statically indeterminate systems due to repair, e.g. by replacement of elements;

• monitoring of the stressed state of critical load-carrying elements of machines and structures during their tests or operation;

• evaluation of spatial heterogeneity of stresses in a material of plane elements of structures by surface scanning;

• monitoring and remote-medium recording of time diagrams of dynamic stresses induced in critical structural elements by service loads.

The acoustic emission (AE) method is dominant among methods of diagnostics of welded structures available in the world practice. Methodology of the AE diagnostics developed by MGTU is based on the use of new complex energy parameters of AE, spectral and regression analysis, as well as individual wave components to identify the type of a defect, estimate the extent of its development and stage of pre-fracture of a structure due to a propagating crack. It is possible to use the AE diagnostics for the mechanism of plastic deformation, micro- and macrocracking, different types of corrosion and corrosion cracking.

The vector-energy analysis and experimental studies of distribution of the energy flow density, power of the AE signals and their energy spectra for longitudinal and transverse waves, as well as the total field around a crack, proved the promising character of the AE flaw detection based on registration of individual wave components. Identity of the energy spectrum of the longitudinal and transverse waves and the total AE field from one disturbance source (deformation

due to slip, propagation of cracks) was established for the objects studied. The linear relationship was revealed between mechanical deformation energy and acoustic energy of the total field, as well as the longitudinal and transverse waves. The distribution of energy of the total AE field and its individual components around the crack apex was shown to be similar to configuration of the plastic deformation zone. The probability ranges of indicators of the processes being diagnosed (AE sources), plotted by statistical processing of parameters of the AE signal flow were proved to be efficient to identify the AE sources.

For example, with the scattering ellipses (mean energy of signals B and median frequency) used as the informative indicators, identification of plastic deformation and propagating microcrack performed by this method is characterised by a high reliability. An error of classification of a microcrack against plastic deformation was 3 % (Figure 5).

High-sensitivity strip and wide-band AE transducers were developed, having a frequency range of 20--5000 kHz and sensitivity of $2 \cdot 10^8$ V/m.

The scientific and methodical developments were used as the basis for building the 16-channel AE measurement system, providing real-time localisation, identification and diagnostics of the degree of danger of a developing defect.

Development of reliable means for NDT of welded joints in austenitic stainless steels is a topical problem. MGTU carried out the work resulting in the development of a new approach to the technology of ultrasonic inspection of coarse-grained materials. Macrostructure of the weld or casting is estimated and solidification model is constructed on the basis of analysis of the metal solidification process. Then propagation of the ultrasonic waves through a heterogeneous anisotropic polycrystalline medium is studied and the acoustic model is developed, allowing for the main weakening factors, such as attenuation, refraction at the fusion line and transparency of the fusion line, deviation of the beam path from the wave normal and deformation of the sound beam.

Calculation of the scattered fields V_j^s in coarse-grained media modelled as the set of grains disoriented with respect to each other was made by using the bulk integral equation of the type of Lippmann--Schwinger
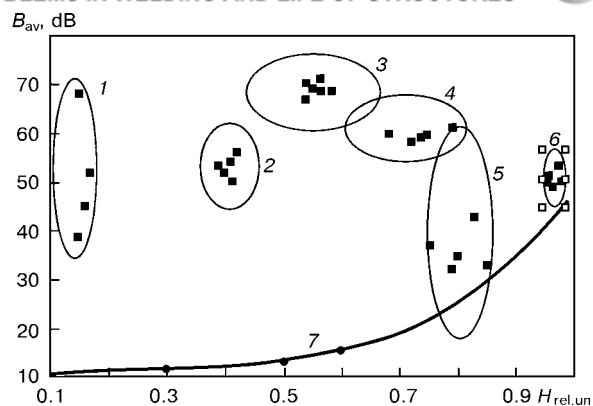
Figure 5. Results of AE tests of large specimens in diagnostics diagram: *1* — unstable crack, lack of penetration; *2* ---- growing crack; *3* — propagating delamination; *4* — multiple bulk defects; *5* — plastic deformation, stable crack; *6* — corrosion cracking; *7* — level of soundness

(its Born's approximation) with Green's function $G_{ij}(\overrightarrow{r}\,', \overrightarrow{r}\,'')$:

$$V_j^s(\overrightarrow{r}\,'', V_i^0) = \int\limits_V G_{ij}(\overrightarrow{r}\,' - \overrightarrow{r}\,'') \, f_i(\overrightarrow{r}\,'', V_i^0) \, d\overrightarrow{r}\,'',$$

where $f_i(\overrightarrow{r}\,'', V_i^0)$ is the function which depends upon the amplitude of an incident wave and describes the effect of heterogeneities; $\overrightarrow{r}\,'$ is the radius vector of the observation point; $\overrightarrow{r}\,''$ is the radius vector of the source; and V is the volume of a scatterer (superscript s means a scattered field). Analytical expressions were derived and scattering coefficients were calculated as a result of this solution for a coarse-crystalline structure, which is a transversally isotropic medium at frequencies used in ultrasonic inspection, as well as for a coarse-grained structure, which is an isotopic medium.

The problem of passage through the fusion line is very important for ultrasonic inspection of austenitic welded joints, because finding of directions and determination of intensities of the waves transformed at the fusion line are required for correct interpretation of the inspection results. It was suggested that the coordinate system related to the wave vector should be used to simplify the calculations. This allowed sufficiently simple expressions to be derived to determine velocities of the longitudinal, $v_r(\theta)$, and
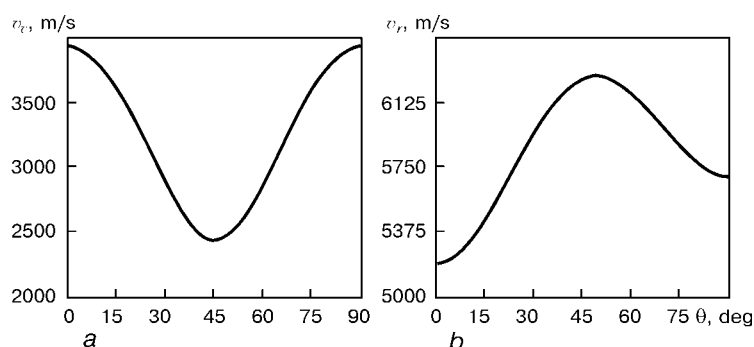
Figure 6. Dependencies of velocities of the vertically polarised transverse (*a*) and longitudinal (*b*) waves in a transversally isotropic medium upon the angle of incidence on crystals, θ
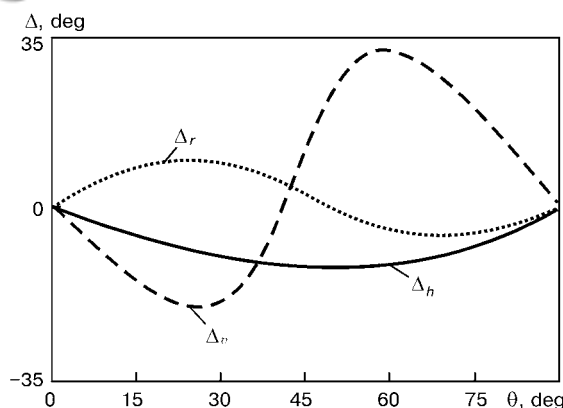
Figure 7. Deviation of acoustic axis from the wave normal in metal of the austenitic weld depending upon the direction of incidence on a crystal

vertically-polarised transverse, $v_v(\theta)$, waves in a transversally isotropic medium (Figure 6):

$$v_r(\theta) = \sqrt{C_{11} - 0.25A\,[\sin^4\theta + 2\sin^2(2\theta)]}\;\frac{1}{\sqrt{\rho}};$$

$$v_v(\theta) = \sqrt{C_{44} - 0.44A\,\sin^2(2\theta)]}\;\frac{1}{\sqrt{\rho}},$$

where θ is the angle of incidence on crystals; $A = C_{11} + C_{12} - 2C_{44}$; C_{11}, C_{12} and C_{44} are the elastic constants of a cubic-system crystal, as well as the coefficients to be calculated for the different-polarisation waves passing through the boundary between the isotropic (heat-affected zone) and transversally isotropic (weld metal) media.

In anisotropic materials the direction of propagation of energy does not coincide with the direction of an ultrasonic wave. This leads to deviation of the ultrasonic beam from the wave normal. Maximum

amplitudes of shifts of particles in a wave registered by the transducers were revealed in the direction of the Umov's vector. Relationships were derived on the basis of analysis of directions of transfer of the wave energy, these relationships establishing dependence of the deviations of beams, Δ, upon the direction of the wave vector and elastic constants of a single crystal (Figure 7):

$$\Delta_r(\theta) = \mathrm{arctg}\left\{\frac{[A\,\sin2\theta\,(\cos^2\theta - 0.75\sin^2\theta)]}{[2C_{11} - A(\cos^4\theta + 2\sin^2\theta)/2]}\right\};$$

$$\Delta_v(\theta) = \mathrm{arctg}\left\{\frac{[A\,\sin2\theta\,(\sin^2\theta - 0.75\cos^2\theta)]}{[2C_{44} + 7A\,\sin^2 2\theta/8]}\right\};$$

$$\Delta_h(\theta) = \mathrm{arctg}\left\{\frac{A\,\sin2\theta}{(8C_{44} + 2A\sin^2\theta)}\right\},$$

where θ is the angle between the wave vector and crystal axis; subscripts r, v and h relate to the longitudinal, vertically polarised and horizontally polarised transverse waves, respectively.

Analysis of variation of velocities of the ultrasonic waves and deviation of the acoustic beam from the wave normal showed refraction of ultrasound fixed in a crystalline structure, leading to deformation of the sound beam and distortion of the wave fronts.

The developed acoustic-crystalline model was realised in the form of a package of the PC applied programs intended for evaluation of optimal parameters and interpretation of results of inspection of coarse-grained materials with a differing crystalline structure. Generality and accuracy of the model allows using it with modern ultrasonic flaw detectors.

TECHNOLOGICAL APPLICATIONS
OF ELECTRON AND LASER BEAM

J. PILARCZYK and **M. BANASIK**

Welding Institute, Gliwice, Poland

In the paper it has been discussed the scientific-research and technological works in the field of electron beam welding and laser cutting and welding conducted at the Welding Institute in Gliwice. The characteristics of the equipment applied in the works have been presented. It has been given a number of application examples of technology developed at the Institute and implemented to machine-building and automotive industry. The collaboration of the Institute with another institutions and industrial companies on the area of implementation of these technologies has been discussed.

Keywords: *investigations, electron beam technologies, laser technologies, equipment development, technology application*

Electron and laser beam technologies at the Welding Institute in Gliwice. The work within the EBW, as well as the laser cutting and welding technologies are one of the major areas of the Institute's activities.

The following activities within the EBW, as well as laser cutting and welding technologies, are carried on at the Institute:

• R&D;

• education and training;

• supporting the industrial companies in implementation of these technologies.

The work within R&D is directed, first of all, on as fast as possible transfer of EBW and laser technologies to industrial companies and practical use of them. The work focuses on testing of electron and laser beam weldability of modern construction materials.

The essential task of the Welding Institute within the educational and training activities is concentrated on forming the training base for industrial needs through organizing of scientist seminary meetings, training workshops, post-graduated courses (e.g. European Welding Engineer courses) for welding engineers or those specialized in allied techniques. The programme of the courses comprises the lectures and

Figure 1. EBW machines designed and built at the Welding Institute in Gliwice: *a* — EB Welder SE60∕10: chamber interior dimensions of 1500×1000×1000 mm, with *X, Y* axis work envelope (650×500 mm), rotary axis (*A* and *C* rotary table with jaw chuck), triode type gun (direct heating, 10 kW∕60 kV), optics, beam oscillation generator, pumping system (mechanical pump + Root's + diffusion pump, automatic control) and work cycle of 10 min × $5 \cdot 10^{-3}$ hPa, vacuum in chamber of $2 \cdot 10^{-3}$ hPa and gun space vacuum of $2 \cdot 10^{-5}$ hPa; *b* ---- EB Welder SE60∕15: system with three-position rotary table and programming of welding parameters, triode type gun (direct heating, 15 kW∕60 kV), optics, work envelope (*Y* axis moving gun of 110 mm, *h* = 50 mm, ring $\varnothing$ = 220 mm max and *h* = 300 mm, shaft $\varnothing$ = = 40 mm max), pumping system (mechanical pump + Root's + diffusion pump, automatic control), work cycle of 15 s × $2 \cdot 10^{-3}$ hPa, vacuum in chamber of $2 \cdot 10^{-3}$ hPa and gun space vacuum of $2 \cdot 10^{-5}$ hPa

© J. PILARCZYK and M. BANASIK, 2003
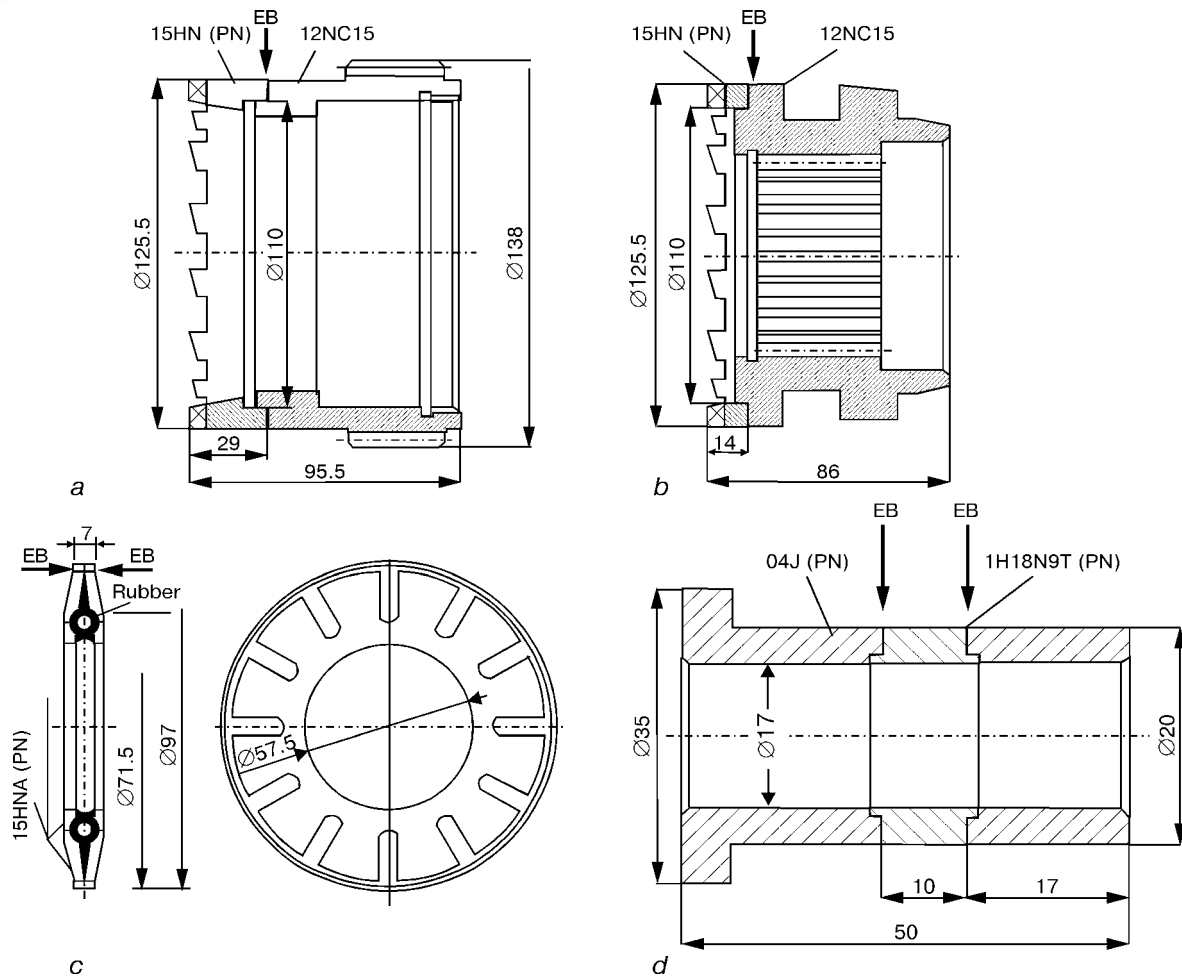
Figure 2. EBW application: *a, b* ---- sleeves of claw clutch of case hardening steel for semi-automatic lathe machines Amtec-657 type made using EB Welder SE60∕15 at *t* = 5 mm, *U* = 60 kV, *I* = 50 mA, *v* = 2.7 m∕min; *c* ---- contact wheels of case hardening steel to grinding machines for gears material made using EB Welder SE15∕60 at *t* = 2 mm, *U* = 60 kV, *I* = 30 mA, *v* = 3 m∕min; *d* — steel sleeves of electromagnets for hydraulic valves made using EB Welder SE 60∕10-L at *t* = 1.5 mm, *U* = 60 kV, *I* = 10 mA, *v* = 0.9 m∕min
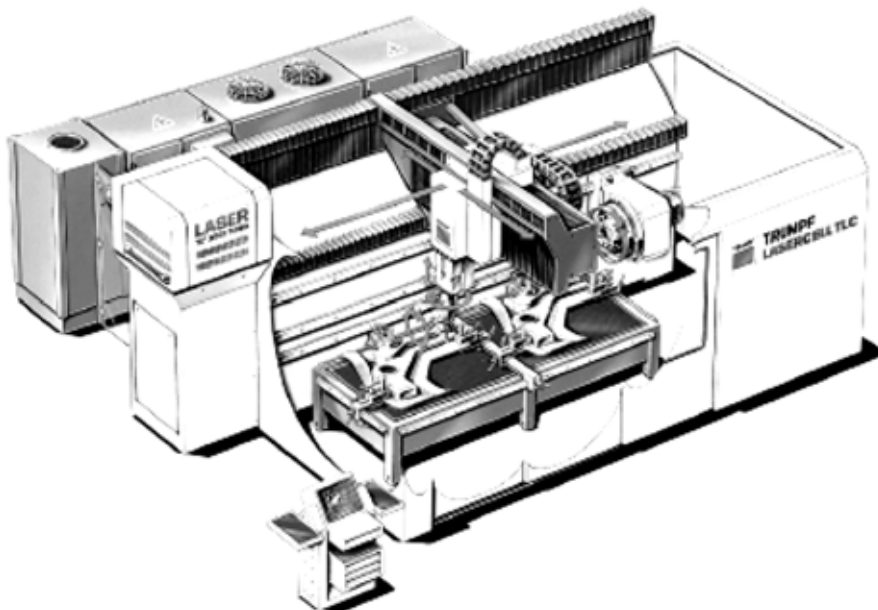
Figure 3. Multiaxis machine system TRUMPF LASERCELL 1005 for cutting, welding and surface treatment at the Welding Institute in Gliwice: working range: *X* ---- 3000 mm, *Y* ---- 1500 mm, *Z* ---- 500 mm, *C* ---- N·360°, *B* ---- ±120°; speed: *X*-axis ---- 50 m∕min, *Y*-axis — 50 m∕min, *Z*-axis ---- 30 m∕min, *C*-axis — 360°∕s, *B*-axis — 360°∕s; accuracy: smallest programmable increment ---- ±0.01 mm, positioning accuracy — ±0.1 mm; repeatability — ±0.03 mm; control: Sinumerik 840D; RF-excited CO_2 laser TLF series 3800 W; power variation 5–100 %; frequency modulation 100 Hz to 100 kHz; option: rotary axis, diameter at center 93 mm, axial load 300 kg; CNC rotary axis with rotation max 60 rpm, rotary table with defined hole array ∅ 400 mm
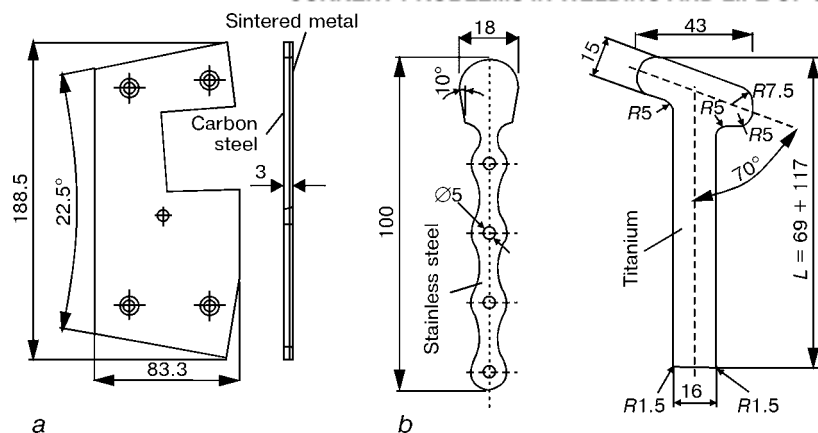
Figure 4. Laser 2D cutting application: *a* — plates of sliding followers for machine producing the tyres made using Lasercell TLC 1005 (2D, *f* = 5"; *P* = 3800 W, *v* = 2.7 m ⁄ min, cutting gas N_2 4.6 and 17 bar); *b* — body implants made using Lasercell TLC 1005 (2D, *f* = 5") at *P* = 3800 W, *v* = 2.7 m ⁄ min, cutting gas N_2 5.0 and 17 bar for stainless steel 3 mm thick, and *P* = 2600 W, *v* = = 5.6 m ⁄ min, cutting gas Ar 4.6 and 16 bar for titanium 2 mm thick

shows within the electron beam and laser technologies.

In the field of implementation of these technologies to industrial practice, the Institute acts the role of professional centre of «job-shop» type provided with the complete R&D base. The centre is able to support industrial companies in solution of many issues related to implementation of electron beam and laser technologies. The role of the Institute within this scope consists in working out the process procedures and making the pilot ⁄ prototype production, especially for small and medium enterprises; production analysis in the chosen industrial plants considering a possibility to turn the existing processes of manufacturing into the highly efficient and material-saving electron beam and laser technologies and preparation of engineering-economical analyses.

Such a type of activities is especially important for Polish industry, because in many cases the possibility of application of these technologies, particularly in small and medium enterprises, is also a condition to obtain and perform the large contracts concluded with customers from Western Europe. The contracts include the manufacture of advanced products, in which domestic intermediate products are applied. The purchase of specialistic equipment to perform the contracts, often single and short ones, cannot be taken into account due to high cost of the equipment, installation and training of personnel, as well as the later use of this equipment in such enterprises. These Institute's activities, especially within the laser technology, creates for domestic manufacturers the unique opportunity to discover and test the laser technology possibilities and to introduce them step by step, whereas a number of serious technical-economical problems connected with the implementation of laser welding technology can be avoided.

The Welding Institute has got two research-technological laboratories: Electron Beam Welding Laboratory and Laser Technologies Laboratory. The research and technological works are carried out in both laboratories with taking advantage of the whole research base of the Institute, which is composed of Mechanical Testing and Metallography Laboratory, which is fitted out, among the others, with the following equipment: the testing machine INSTRON 4210 ⁄ 600 kN, simulator of thermal cycles, spectrometer Perkin-Elmer 3300 with its control system

Figure 5. Laser 3D cutting application: various elements of car armchair and body of deep-drawing, Zn-coated and carbon steel 0.8 + 3 mm (3D, *f* = 5")

The Paton WELDING JOURNAL

Digital PC and the Omnimet Express Image Analysis System. The Laboratory carries on the complex testing of joint properties including also such a testing as CTOD and *J*-integral, as well as it works out the diagrams of microstructural changes under conditions of welding thermal cycles; Non-Destructive Testing Laboratory that is equipped, among the other devices, with the X-ray apparatus ERESCO 200MF (Seifert & Co.), flexible endoscope SMW 200/12 (Olympus Optical), magnetic flaw detector TK-1280E (Tiede) and the supersonic flaw detector UKS-7D (Krautkramer). The Laboratory carries on the complex testing and quality assessment of joints by means of non-destructive methods.

The both Laboratories have got the accreditation of numerous classification societies.

Electron beam welding. The work within the EBW technology has been carried on at the Welding Institute in Gliwice for 20 years. In this time it has been carried out the investigations aimed at both the technology and equipment development. During this time, the construction was developed and the prototypes of electron beam welders of three different types were made. They were the multipurpose electron beam welder (Figure 1, *a*) and two small-chamber electron beam welders, namely the welder provided with a three-position rotary table (Figure 1, *b*) and the welder provided with the twenty-position manipulator situated inside its chamber. The former two items were made with the use of only domestic components, systems and sub-assemblies, whereas in the third case, the gun and power source supplied by the Leybold Hereus (ALD) company were applied.

In that time, among other research, it was carried out the following investigations:

• weldability of numerous bimetallic compositions, among the others high speed steels + carbon steels, hot-work steels + carbon steels, sintered materials + carbon steels;

• weldability of higher-hardenability steel and research on the possibility of modification of the weld chemical composition by the introduction of consumables in different form;

• possibility to apply mathematical methods in order to forecast the hardness of electron beam welded joints;

• possibility of radiographic detection of welded joint flaws characteristic for the EBW method.

At that time, a number of welding processes were worked out to meet the needs of industry. The components that are often manufactured in many countries by the application of the EBW method, were considered, e.g. elements of electromagnetic clutches, elements of gear boxes or bimetallic tools.

During the last years, the Institute carried out many investigations into the possibility of application
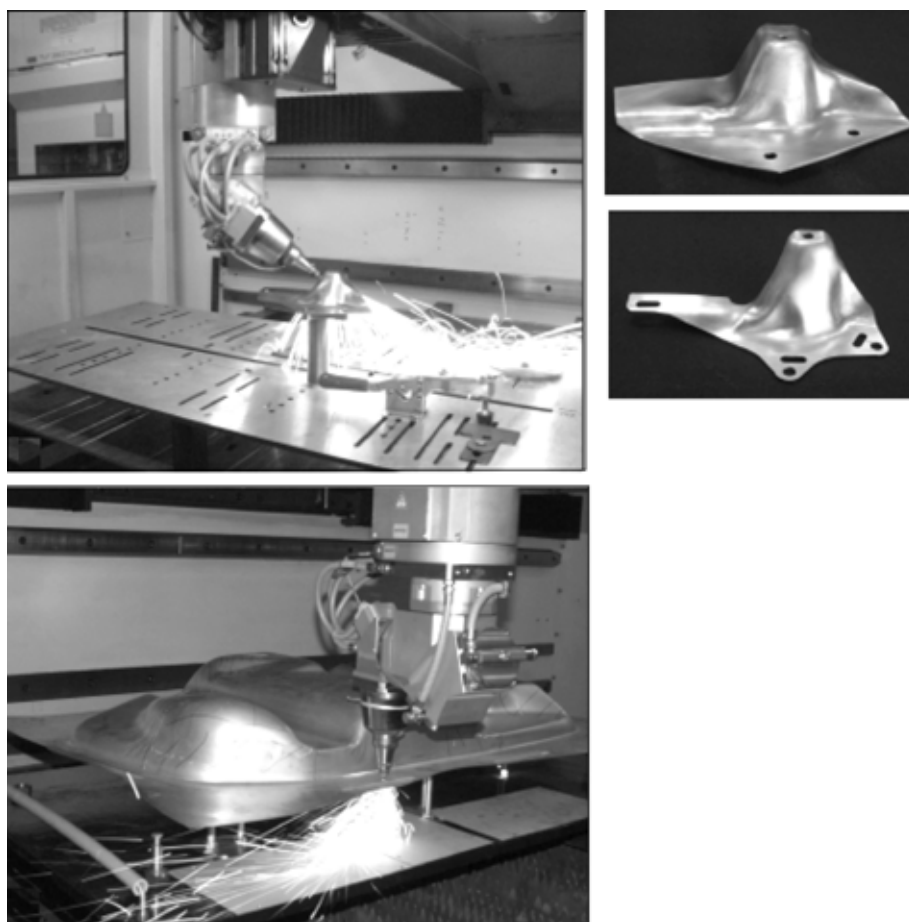
Figure 6. Laser 3D cutting application: element of car armchair and car fuel container of deep-drawing steel and carbon steel 3 mm thick (3D, $f = 5''$)
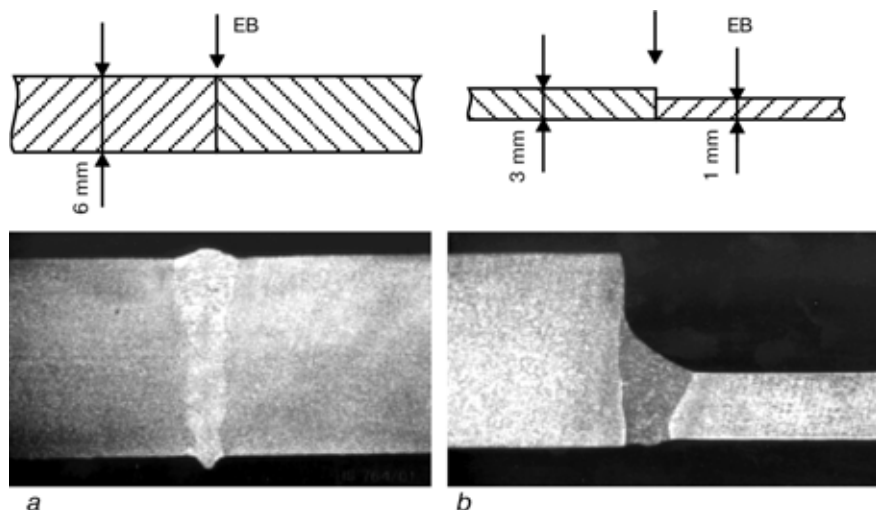
Figure 7. Investigations into weldability of large-sized carbon steel (*a*) and stainless steel plates (*b*) different in thickness (2D, *f* = = 270 mm)

of the EBW for regeneration and repair of wearing specialistic components, which decide about serviceability of the whole machine or production line. The purchase of such components as spare parts or making them just as quite new ones, requires often the using unobtainable machines and tooling or is very expensive. The examples of application of EBW for regeneration of the elements of such a type that are the elements of machines operating in production lines in the automotive industry, are shown in Figure 2. This method is also used for the manufacture of the elements, in which a change of magnetic properties in different zones of material over a section of the element is required (Figure 2, *d*).

Laser beam technology. At present the laser beam technology is developed basing on the laser equipment of the latest generation, namely TRUMPF LASER-CELL 1005 with CO_2 laser 3800 W in capacity (Figure 3). This equipment is a laser machining centre appropriated for 3D cutting and welding of large-sized elements and machining of 2D elements, as well as elements having rotational symmetry. This equipment

has got three inter-changeable operating heads: two ones for cutting provided with the lens objective 5" and 7", and one for welding provided with the mirror objective 270 mm and the cross-jet system. It is furnished with the modern gas installation with the mixer for shielding gases.

The TRUMPF LASERCELL 1005 is an equipment having the modular construction. This conception enables to configure the equipment in a differentiated way and to adapt it to the definite needs, first of all, due to the dimensions of the work table and the number of controlled axes. The simultaneous control of five axes is possible in the 3D machining system. The equipment enables to machine large sheets 1.5×3.0 m in area in the 2D (flat elements) machining system. The highly rigid supporting structure enables to obtain very high speeds of auxiliary motions, as well as the high accuracy of setting up the laser head. The control system based on the postprocessor supplied by Siemens-Sinumerik 840D is conducive to this purpose, considerably. Owing to this system the change of the 3D machining programme takes place in short
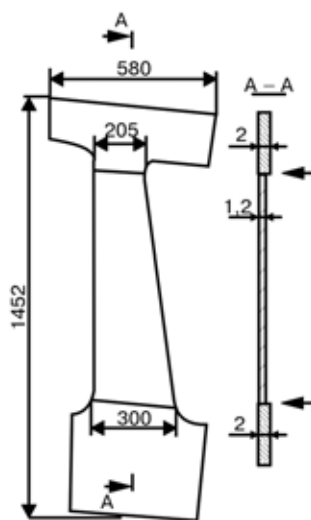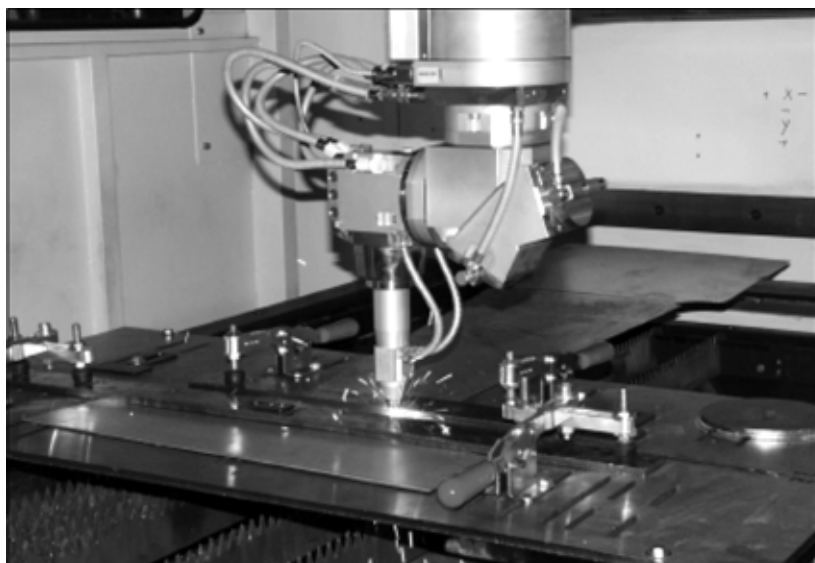
Figure 8. Welding process of tailored blanks using Lasercell TLC 1005 (welding head mirror 270 mm, cross jet system, shielding gas — helium)

The Paton WELDING JOURNAL

time and the adaptation in the equipment the «Teach in» module is possible, that allows creating, in the on-line system, the control program for the work head motion and parameters of the machining process.

2D and 3D laser beam cutting. The research and process work in the field of laser cutting of flat elements comprise all grades of carbon and alloy steels, as well as some special materials as titanium, clad plates and others. The majority of work focuses on optimisation of cutting process parameters to achieve the best quality of cut surface. During the last 2 years the laser cutting procedures were developed and the pilot lots of elements were made for more than 50 industrial companies. The examples of laser cutting application for shaped cutting of steel sheet, titanium and clad plates are shown in Figure 4.

The work within cutting of 3D elements is connected with co-operation between the Institute and subsidiaries supplying some parts to the automotive industry, the factories of furniture, companies making
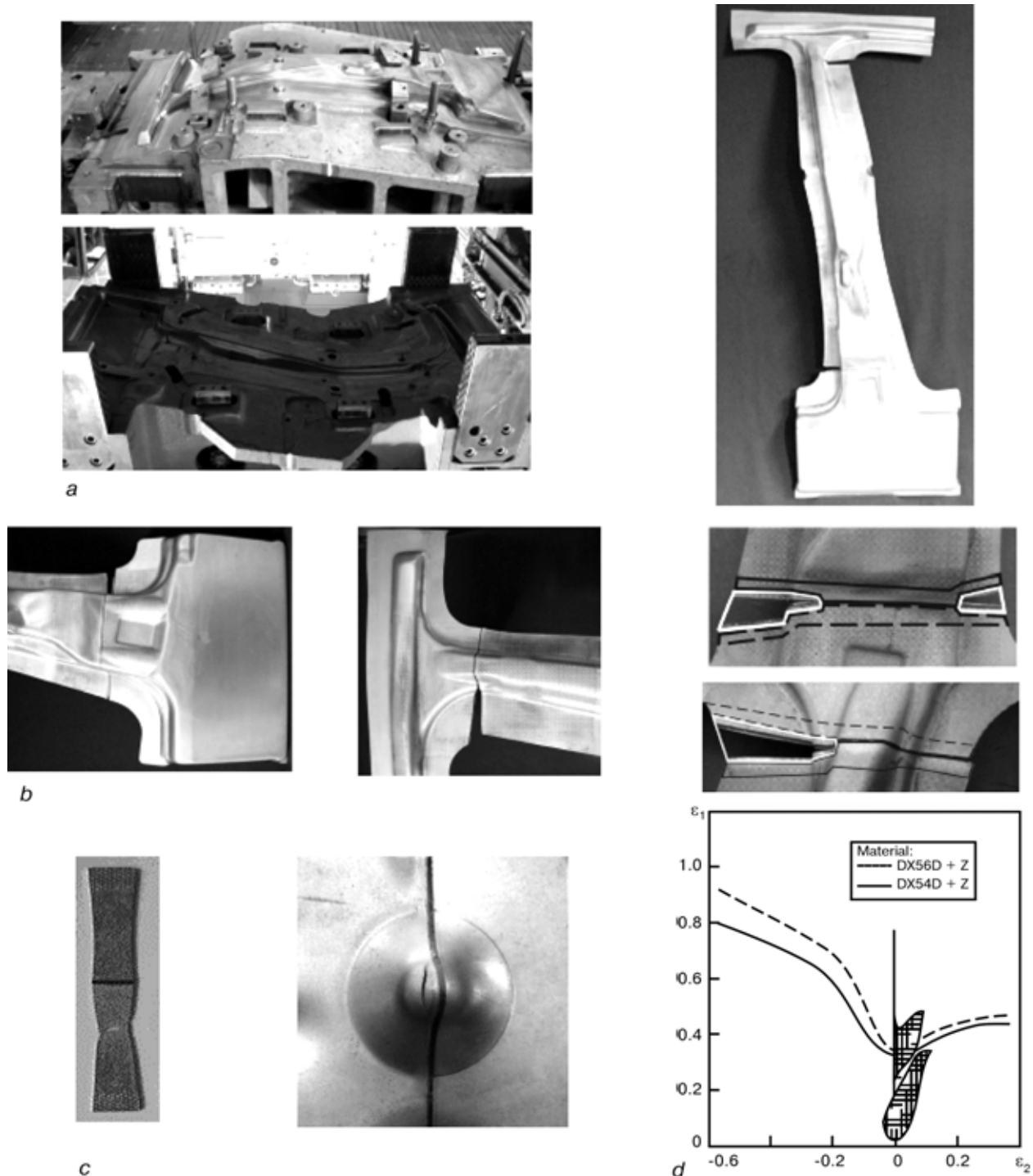
Figure 9. Investigations on technology of laser welding of tailored blanks: tool set (lower and upper tool) for press-forming of central pillars in Audi A3 car (*a*); investigations into deformations and defects in press-forming process (*b*); testing of mechanical properties (tensile and Erichsen test) (*c*); distribution of local strains on selected areas of an industrial draw piece from a laser welded charge on the background of the forming limit diagram of car body sheets (*d*)
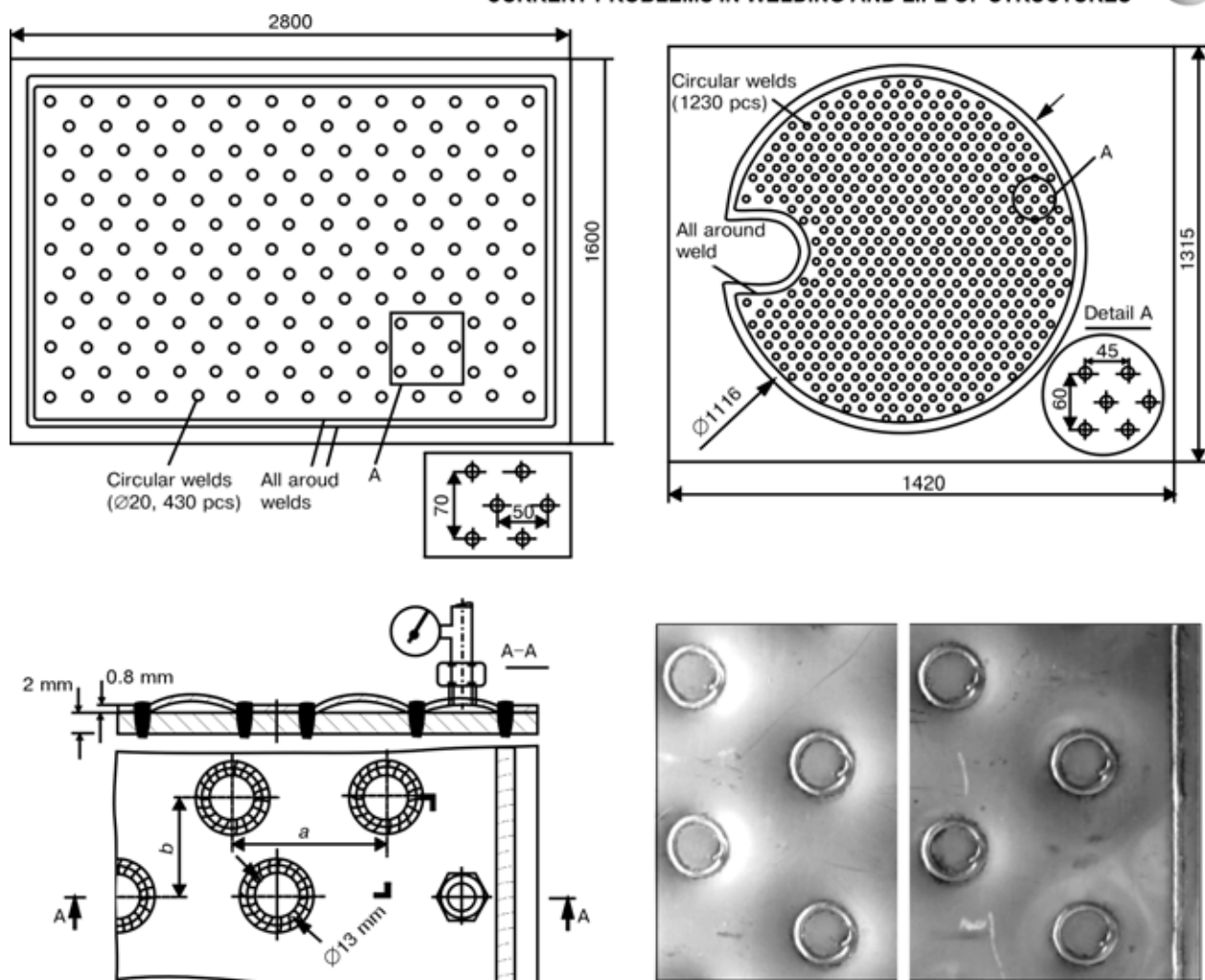
Figure 10. Laser welding of heat exchangers of stainless steel for food industry using Lasercell TLC 1005 (2D, f = 270 mm)

advertising boards and components for decoration of room interiors. The co-operation with these companies comprises the development of process procedures, NC programs and cutting of pilot elements made of carbon steel and aluminium alloys. The example of application of LASERCELL TLC 1005 system for shaped cutting of steel elements is illustrated in Figures 5--6.

Laser beam welding. The research started lately at the Institute, in the field of laser welding with application of CO_2 laser and LASERCELL 1005 equipment focuses on:

• comparative testing of electron beam and laser welded joints quality in low alloy steels, as well as on investigations into welding of large-sized plates made of carbon and stainless steels (Figure 7);

• development of welding technology for tailored blank type sheets and different joint designs together with testing of drawability characteristics (Figures 8 and 9);

• development of welding technology for heat exchangers used in food industry (Figure 10);

• practical application of laser welding in manufacture of alloy steel pipes on production lines for continuous pipe welding.

CONCLUSION

Co-operating very closely with Polish industrial companies and other domestic research centres, the Welding Institute in Gliwice has simultaneously maintained and developed numerous international links with R&D units located in Western and Eastern European countries, which are interested in the application of high-energy beams to welding technology. The Institute has remained open for the wide European co-operation in the field of welding technology.

PRELIMINARY STUDY ON PENETRATION MECHANISM OF DOUBLE-SIDED GTAW PROCESS

H. GAO, L. WU and **H. DONG**

State Key Laboratory of Advanced Welding Production Technology, Harbin Institute of Technology, China

How increasing the productivity and lowering the costs are always a serious problem in the welding production. Large amounts of research were done, and many new welding processes were presented, the double-sided arc welding (DSAW) process is one of them. Experiments show that this new process has many advantages in contrast with conventional processes, especially the penetration ability. Up till now, many characteristics of the process are not well known, so deep research into its mechanism is needed, and it is significant for its application. In this paper, through theoretical analysis, experimentation and numerical simulation, the penetration mechanism of double-sided GTAW process is probed. Results show that, firstly, the welding current flows straight through the weld zone, leads to a concentrated current distribution, forms a stronger electromagnetic force field, and causes a stronger fluid flow in the weld pool, which is in favor of the penetration. Secondly, during double-sided GTAW process, when the weld is partially penetrated, there is a heat-concentration zone between the bottoms of the two weld pools, where the temperature can increase quickly even though only a small amount of heat is applied. Thirdly, the buoyancy force caused an inward flow in the bottom weld pool, which can drive the hot liquid on the surface to the bottom of the pool, and then form deep weld pool.

Increasing the productivity and lowering the costs are always an important problem in the welding production. To solve it, the first step is to popularize the high-efficiency welding processes, such as SAW or GMAW, decreasing the use of SMAW. Then improving the automation and intelligence level, e.g. using welding robot station, the productivity can be increased rapidly. Also on the basis of the basic welding processes, developing various new kinds of high-efficency welding processes, improving the welding quality [1].

During the manufacturing of medium thickness metal structures, owing to the penetration ability of the welding arc, it is generally grooved on one or two sides, and then filled with filler metal. Then a series of problem comes, lower productivity, higher cost, more filler metal consumed etc. Because the multi-beads are used, the weld is tended to have defects, such as inclusion, poor fusion condition, big HAZ etc. With the increase of the structure thickness, these problems become more serious. So, it has become a «hot spot» for the welding researchers to increase the penetration ability of the arc.

To solve the problem, much research work had been done, and many progresses are achieved, double-sided arc welding (DSAW) process is one of them. «Double-sided arc» means that there is another gun on the opposite side of the workpiece. According to the number of power supply and the wiring mode, this process can be classified as two kinds: double power supply mode and single power supply mode. For double power supply DSAW, there had been many applications. For example, at Harbin Boiler Factory and the Easten Boiler Factory of China, double-sided pulsed GMAW process was used in the pipe screen

manufacturing, where less welding distortions, higher productivity were achieved [2].

In 1998, Dr. Y.M. Zhang of Kentucky University put forward the single power supply DSAW process [3–5]. His original intention is to enhance the penetration ability of the arc, increase the welding productivity, and the costs don't go up. In the process another gun is placed on the opposite of the workpiece, and the two guns are connected directly to the welding power supply, so there is no connection to the workpiece. The welding current goes from one arc, through the workpiece, then into another arc, it is concentrated in the weld area, and higher heat efficency is obtained. Not only the penetration ability of the arc increases at the same welding current, but also narrower HAZ is obtained, and then the weld quality is improved. In this process, various kinds of conventional arcs can be mixed together, and the conventional welding power supply can be used. So it is worthy to popularize this process in the practice.

In DSAW process, it doesn't equal to the simply addition of the two heat sources, there are complex interactions among the electromagnetism, the heat and the forces, which is different from the conventional welding process. Up till now, these relations are not clear, so it is needed to probe into the penetration mechanism of the process, then give guidance to the applications.

In this paper, the foundamental experiments of aluminum alloy are done; the welding method is Double-Sided Gas Tungsten Arc Welding; the penetration mechanism of double-sided GTAW process is discussed.

Experiments. *Experimental system.* Figure 1 shows the schematic diagram of the experimental system. In the system, gun *1* and gun *2* are general GTAW guns, and the welding power supply is COMPA500P made by Japanese company, it can output AC squared waves, and has built-in HF arc ignition set.
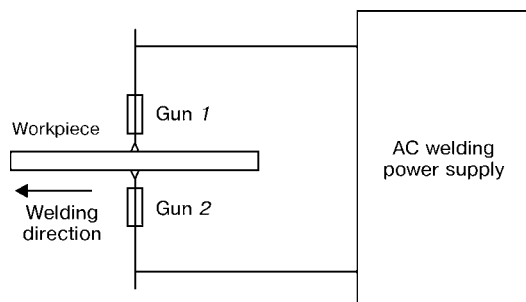
Figure 1. Schematic diagram of experimental system

Experimental results and discussions. The material is LY12 and LF6 aluminum alloys; both tungsten electrodes are of 3 mm in diameter; the shielding gas is pure argon.

Bead-on-plate experiments, without filler metal are done. During the welding, the stability of process, the profile of the arc and the weld pool are observed. Figures 2 and 3 show the macrograph of the weld cross section.

From the experiments, with contrast with conventional single-side GTAW process, the following characteristics of double-sided GTAW process can be concluded.

Stronger penetration ability. Figure 4 shows a conventional weld of 4 mm LF6 aluminum alloy, the welding current is 120 A, and the travel speed is 5 mm/s. It can be seen that the weld is partial penetrated, the top weld width is about 8 mm, and penetration is about 3.3 mm. If a full penetrated weld is needed, you must increased the welding current or lower the travel speed, also you can weld it again on the backside of the workpiece at almost the same parameters. With DSAW process, you can obtain full penetration under relative low welding current. Figure 3 shows the result, the welding current is 60 A, the other parameters keep the same with Figure 4. It is full penetrated, both top and bottom weld width is about 4.7 mm, the difference is obvious.

Lower energy input and higher productivity. Compared with conventional GTAW process, double-sided GTAW process expends less energy, and uses less time. Let's make a comparison, the task is to weld
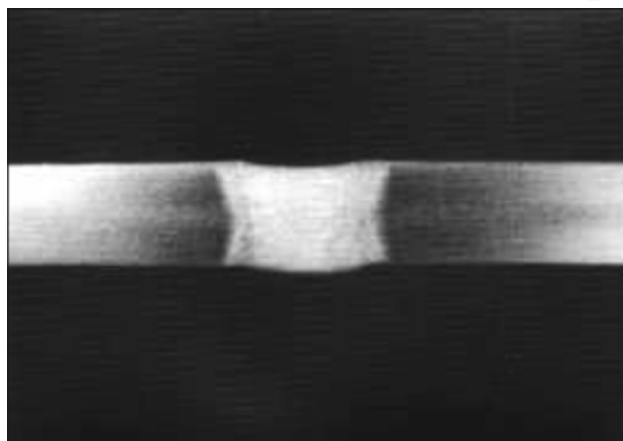
Figure 3. Macrograph of weld cross section for double-sided GTAW process (aluminum alloy LF6 4 mm thick, 65 A, 5 mm/s)

an aluminum alloy butt joint of 1000 mm long, the thickness is 6 mm. When weld it with single GTAW process, the grooves or gaps are needed, and it must be welded on both sides, normally the welding current is 200--270 A, the travel speed is 150--250 mm/min [1]. Here we take the mean values, welding current I_w = 235 A, travel speed v_w = 200 mm/min. So, the welding time of the task can be calculated ($2 \cdot 1000/200$ = 10 min), the time of preparing the grooves is not included. We assume that the arc voltage U = 15 V, so the energy input is IUt = = $235 \cdot 15 \cdot 10 \cdot 60$ = 2115 kJ. If weld this joint with double-sided GTAW process, the welding current is 100 A, the travel speed is 300 mm/min (see Figure 2). The welding time is $1000/300$ = 3.33 min, here we also assume the arc voltages are both 15 V, so the energy input is $2 \cdot 100 \cdot 15 \cdot 3.33 \cdot 60$ = 600 kJ.

From the points of view of time and energy, the welding productivity can be increased several times.

Less distortions. It is found that there is less transverse angular distortion on the workpiece during double-sided GTAW process. According to the theory of welding distortion, the non-uniform distributions of weld transverse shrinkage along the thickness cause angular distortion. During welding process, the high-temperature metal near the weld pool will expand, and it is impeded by the cold metal, so the deformation

Figure 2. Macrograph of weld cross section for double-sided GTAW process (aluminum alloy LY12 6 mm thick, 100 A, 5 mm/s)

Figure 4. Macrograph of weld cross section for conventional GTAW process (aluminum alloy LF6 4 mm thick, 120 A, 5 mm/s)

Figure 5. Transverse forces on weld joint: *a* ---- conventional GTAW; *b* — double-sided GTAW

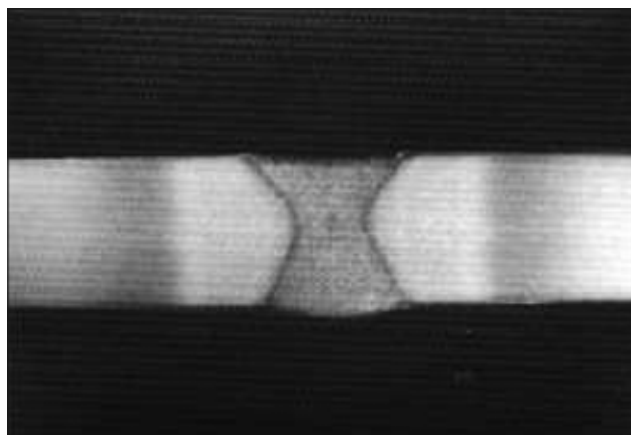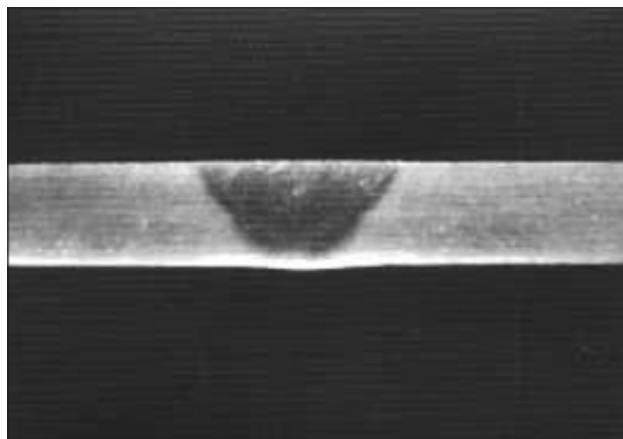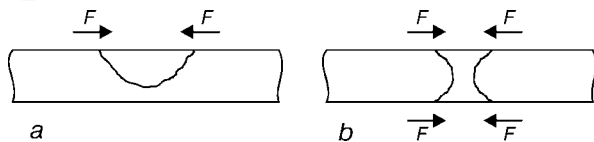forms. When the metal cooled, the transverse shrinkage occurs. For single-side weld, the transverse shrinkage is large on the top side, and it is less on the back side, so there forms angular deflexion on the joint. The angular distortions will affect the quality of the joint, measures must be taken to minimize or correct the distortion.

During double-sided GTAW processs, there are heat sources on both sides of the joint, and the transverse shrinkages are symmetrical, so there is less angular distortion. Meanwhile, the weld is narrower than single weld, the high-temperature zone also becomes narrow, which is in favor of reducing the angular distortion. Figure 5 shows the transverse forces on the weld joint.

Longer the electrode life. When welding aluminum alloys with GTAW process, the clean action must be considered. So normally alternating current is adopted; the electrode wastes very fast; frequent correction is needed, especially in automatic welding.

The wastage of the electrode has direct relation with the welding current, the bigger the current, the faster the electrode wastes. As mentioned above, compared with conventional GTAW process, using relative low current, the joint can be completed by double-sided GTAW process, so the electrode life is prolonged.

Limitation. Because the second welding gun is placed on the opposite side, the additional space is needed. This will limit its application. Owing to the extensive usage of welding process, there must be many occasions for double-sided GTAW process.

Penetration mechanism of double-sided GTAW process. It is desired to obtain the weld with big depth/width ratio; thus the mechanical properties and the microstructure of the weld can be improved.

In order to increase the depth/width ratio, the process of high power density can be used, such as EBW and LBW. Owing to their high costs, the applications are limited. From the above analysis, we know that when using DSAW process, the high depth/width ratio can be obtained with less energy input. Why does this process possess the above characteristics?

Through theoretical analysis, the following reasons may be possible:

• because there are heat sources on both sides, a heat congregated zone forms between the two weld pools, where fewer heat can cause higher temperature increase;

• the welding current goes straight through the weld zone, stronger electromagnetic forces will be generated, thus causing stronger convection flow in the weld pool, which can improve the penetration;

• in double-sided GTAW process, the buoyancy force in the bottom weld pool will take a positive action to the penetration.

It will be analyzed through experiments and numerical simulations in the followed sections.

Influence of the welding current direction. In conventional GTAW process, the welding current flows from one terminal of the power supply through the welding gun, arc and workpiece, then return to another terminal of the power supply. But in double-sided GTAW process, the welding current goes straight through the weld zone on the workpiece, then via another torch to the power supply. Owing to the stronger welding current density in the weld zone, especially in the weld pool, causes a stronger electromagnetic force field and a different convention.

Figure 6 shows the electromagnetic force distribution in double-sided GTAW process of one and two sets of power supply [6]. It can be seen that the electromagnetic force is stronger when one set of power supply is applied, especially in the middle part of the workpiece.

Formation of heat congregation zone. There are many factors that affect the weld penetration, generally, the bigger the welding current, the deeper the
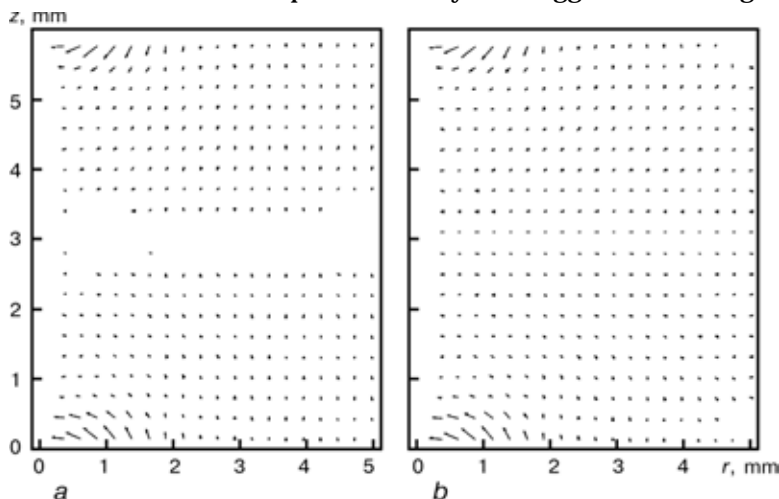

Figure 6. Electromagnetic force distribution in the workpiece under double-sided GTAW process at 110 A: *a* ---- two sets of power supply; *b* — one set of power supply

Figure 7. Macrograph of weld cross section in case of 5 mm offset between the guns

weld penetration. Meanwhile, the penetration is related with the material and the thickness of the workpiece, when the material thermal capacity is bigger, more heat is needed to rise to the same temperature for the same volume of the metal, and a shallow and narrow weld pool is obtained. The thickness of the workpiece will affect the heat conduction in the workpiece, the thicker the workpiece, the shallower and narrower the weld pool. When the penetration depth exceeded 60 % of the thickness of the workpiece, heat congregation phenomena will occur at the bottom of the weld, and then the penetration depth will increase. This is the case for single-side GTAW process, when the metal under the weld pool becomes thin enough, the heat input is more than the heat dissipation, the heat is accumulated there, the temperature raises rapidly, also the penetration increases quickly. For double-sided GTAW process, with the heat transferring into the workpiece, two weld pools form on each side of the workpiece. In the region between the two weld pools, heat is inputed from the two arcs, and is accumulated; the temperature raises rapidly, the heat congregation zone forms. The metal in the heat congregation zone has high temperature; only a little heat is needed to become molten, which makes the two weld pools become deep. Finally the heat congregation zone disappeared, the two weld pools merged together, the weld is full penetrated.

In order to prove the above analysis, the following experiments are done. Take an offset between the guns along the perpendicular direction of the weld seam. If the heat congregation zone exists, the weld pools will grow up along the line between the two arcs center. Figure 7 shows the macrograph of the weld cross section in the case of 5 mm offset. The material is LY12 aluminum alloy, workpiece thickness is 6 mm, travel speed is 5 mm/s, welding current is 110 A, and arc voltages are both 15 V. The guns have 5 mm offset along the perpendicular direction of the weld seam. Figure 8 shows the simulation result with the same parameters.

It can be seen that the weld is partial penetrated, and the two weld pools grow along the centerline of the arcs, showing that the heat congregation zone
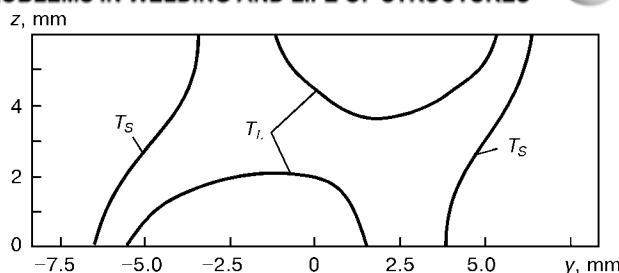
Figure 8. Calculated result in case of 5 mm offset between the guns

forms between the weld pools. The existence of the heat congregation zone will expedite the growing of the weld pool. Figure 9 shows another weld cross section macrograph, the welding current is 120 A, other parameters remain the same as in Figure 7.

Influence of the buoyancy force. The buoyancy force is a kind of body force, which is induced by the density difference in the fluid. In the weld pool, the density difference is caused by temperature gradient. It will cause natural convection in the fluid metal, and normally it appears in the momentum equation as a source item.

In conventional welding process, the buoyancy force also plays an important role in driving the fluid flow, just less important than surface tension and electromagnetic force. There the buoyancy force causes an upward flow along the centerline of the weld pool, which goes against the weld penetration.

When the weld is partial penetrated in double-sided GTAW process, on the top weld pool, the buoyancy force has the similar effect with single-side GTAW process, which makes against to the penetration. But in the bottom weld pool, the effect is different, the buoyancy force also causes an upward flow along the centerline of the weld pool, but an inward flow is formed on the bottom surface, which can take the high-temperature fluid to the interior of the weld pool. Just like the effect of the electromagnetic force, it is in favor of the penetration.

Figure 10 shows the fluid flow field of double-sided GTAW process with only the buoyancy force in action.

In the two weld pools, the buoyancy force causes different fluid flow, the top and bottom weld pool
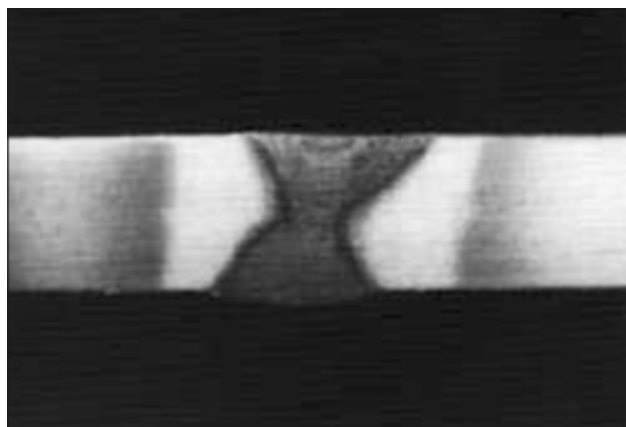
Figure 9. Macrograph of weld cross section in case of two guns offset of 5 mm
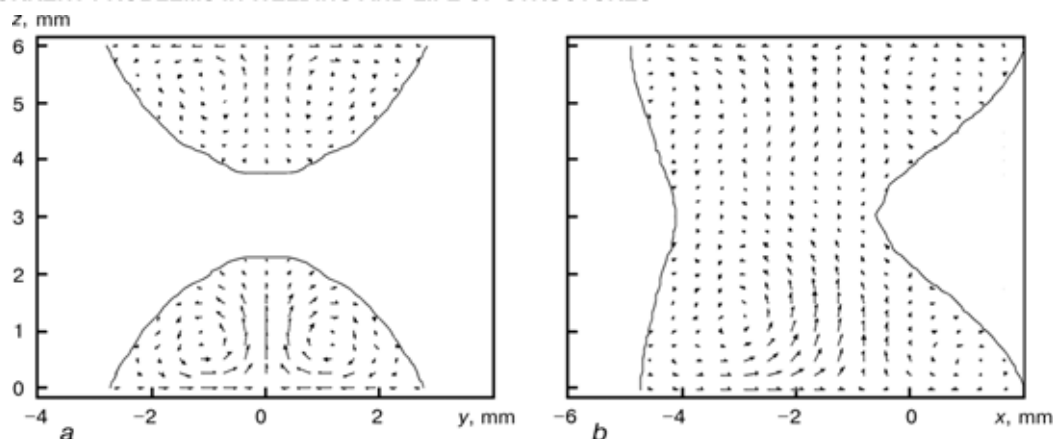
Figure 10. Fluid flow field at the moment of 4 s with only the buoyancy force in action (110 A, 15 V, 10 mm/s): *a* ---- cross section; *b* — longitudinal section

will grow in different ways. According to above analysis, the bottom weld pool will develop more fast, so at the same moment, the bottom weld pool will be deeper than the top one, and the top weld pool will be wider and longer (see Figure 10).

CONCLUSIONS

In this paper, through theoretical analysis, experimentation and numerical simulation, the penetration mechanism of double-sided GTAW process is probed.

1. The welding current goes straight through the weld zone, leads to a concentrated current distribution, forms a stronger electromagnetic force field, and causes a stronger fluid flow in the weld pool, which is in favor of the penetration.

2. During DSAW process, when the weld is partial penetrated, there is a heat-congregated zone between the bottoms of the two weld pools, in which the temperature can increase more, even though only a small amount of heat is increased.

3. The buoyancy force causes an inward flow in the bottom weld pool, which can drive the hot liquid on the surface to the bottom of the pool, and forms deep weld pool.

1. (1995) *Welding handbook*. Vol. 1. Welding process and equipment. Chinese Machine Press.
2. Chen Yuchuan (1993) New welding techniques development in boiler manufacturing. In: *Proc. of 7th Nat. Annual Welding Conf.*, Qingdao, China, 1993. Vol. 1. 26–36.
3. Zhang, Y.M., Zhang, S.B. (1998) Double-sided arc welding increases weld joint penetration. *Welding J.*, June, 57–61
4. Zhang, Y.M., Zhang, S.B. (1999) Welding aluminum alloy 6061 with the opposing dual-torch GTAW process. *Ibid.*, June, 202--206.
5. Zhang, Y.M., Pan, C., Male, A.T. (2000) Improved micro-structure and properties of 6061 aluminum alloy weldments using a double-sided arc welding process. *Metall. and Mater. Transact.*, 31A, 2537–2543.
6. Gao, H.M. (2001) *Research on the mechanism of double-sided arc welding process and the numerical simulation of temperature and fluid flow fields*. Dr. Ph. Thesis. Harbin Institute of Technology.

INFLUENCE OF MICROSTRUCTURE ON CORROSION RESISTANCE OF WELDED JOINTS OF DUPLEX STAINLESS STEEL

M. BELOEV[1], **F. HARTUNG**[2], **N. LOLOV**[3] and **B. ALEXANDROV**[3]

[1]KZU Holding Ltd., Sofia, Bulgaria
[2]Technical Institute of Trier, Germany
[3]Technical University of Sofia, Bulgaria

Properties and applications of a comparatively new group of high-alloyed stainless steels that has been introduced in practice since 1970s are reviewed in this report. These are so called duplex stainless steels, the structure of which consists of approximately equal quantities of austenite and ferrite. These steels have many advantages compared to the traditional austenitic stainless steels. Their advantages result in increasingly wider use of duplex stainless steels in many industry branches as petrochemical industry, especially in off-shore installations, in chemical industry in installations for pulp and paper, in installation for fertilizers etc., in energetic industry for fuel gas desulphurisation, in shipbuilding for chemical tankers, in mining industry in installations for extracting of different ores, in pharmaceutics and so on. The present report represents a first stage of research project for implementation of duplex stainless steels in the Bulgarian industry, performed jointly by the Technical University of Sofia and KZU Holding Ltd. Under the current stage of the project the optimal implementation of pulsed gas metal arc process for welding of duplex stainless steels is being investigated.

Keywords: *duplex stainless steels, designation, alloying elements, microstructure, phase share, intermetallic phases, weldability, mechanical properties, corrosion resistance*

The duplex stainless steels (DSS) form a comparatively new group of high-alloy stainless steels, which has been practically applied since 1970s. Typical for these steels is their microstructure, composed of almost equal quantities of austenite and ferrite with slightly prevailing amount of austenite. DSS possess particular advantages over the traditional austenitic stainless steels (ASS) and ferrite stainless steels (FSS), main of which are listed below:

• much higher corrosion resistance, especially when the localised corrosion is considered, such as pitting and crevice corrosion in chlorine and fluoride containing aggressive media;

• much higher mechanical properties with yield strength almost twice higher as that of ASS, which can be utilised for considerable reduction in weight of welded structures and for attainment of significant savings;

• less technological problems during fabrication of welded structures, due to the very good weldability of DSS;

• good compatibility to the C--Mn structural steels, due to the close thermal expansion coefficients of these two dissimilar groups of steels, which provides for lower level of thermal stresses in the welded structures.

Due to the above advantages, the DSS have been finding widening application in many industrial branches such as the oil industry and particularly for offshore structures; the chemical industry ---- in the installations of paper and pulp plants and in the in-stallation for production of artificial fertilisers; the power industry ---- in the installations for purification of S-containing gases; the shipbuilding ---- for construction of tankers for transportation of aggressive chemical compounds; the mining industry ---- in the equipment for extraction of minerals from ores; the pharmaceutical industry, etc.

Designation of DSS. There is not a unified system for designation of DSS yet. AISI has introduced in USA a 3-digit designation system, similar to that used with the ASS, for example AISI 304, AISI 316, etc. Later on, for the designation of the new grades of DSS, SAE and ASTM have introduced the one letter (S) plus 5-digit designation. The whole range of standardised stainless steels is covered by the «Steel Products Manual for Stainless Steels» and by the SAE / ASTM Unified Numbering System (UNS). It is a usual practice to replace the letter S and the first digit by the word «Duplex», for example, Duplex 2304 instead of S32304 or Duplex 2205 instead S32205, or to skip at all the word «Duplex» ---- 2304, 2205.

According to the European Norms (EN), the steels are designated by 5 digits, first of which is 1 for steel. There is a dot after the first digit, followed by 4-digit designation of the particular steel.

Besides the standard designations, DSS are also given by their producers various trade names.

Groups of DSS. The modern DSS are divided in 4 groups:

• DSS with reduced alloying content (lean duplex), which are not alloyed with mîlybdenum;

• 2205 ---- almost 80 % of the practically used DSS belong to this grade;

• 25Cr duplex, such as Alloy 255 and DP-3;

Table 1. Chemical composition of the most widely used DSS

Standard		Trade name	Typical chemical content, wt.%						PRE_N^*	PRE_W^{**}
UNS	EN 10088		Cr	Ni	Mo	N	Cu	W		
S32304	1.4362	SAF 2304 UR 35 N	23.0	4.0	0.1	–	–	–	24	–
S31803	1.4462	UR 45 N SAF 2205	22.0	5.0	2.8	0.15	–	–	32/33	–
S32205		UR 45 N+	22.8	6.0	3.3	0.18	–	–	36/36	–
S32550	1.4507	UR 52 N Ferralium 255	25.0	6.5	3.0	0.22	1.5	–	38/39	
S31200		UR 47 N	25.0	6.5	3.0	0.22	–	–	38/39	
S31260		DP 3	27.0	7.0	3.0	0.16	0.5	0.3	37	38
S32550	1.4507	UR 52 N+	25.0	7.0	3.5	0.25	1.5	–	41	–
		SAF 2507	25.0	7.0	3.8	0.28	–	–	41	–
S32750	1.4410	UR 45 N+	25.0	7.0	3.0	0.27	–	2.0	39	42.5
S39274		DP 3W	25.0	7.0	3.5	0.24	0.7	0.7	40	41.5
S32760	1.4501	Zeron 100	27.0	7.5	3.8	0.27	0.7	0.7	44	45
		DTS 25.7 NW DTS 25.7 NWCu	25.0	7.5	4.0	0.27	1.7	1.0	42.5	44

$^*PRE_N = Cr + 3.3Mo + 16N.$

$^{**}PRE_W = Cr + 3.3(Mo + 0.5W) + 16N.$

- superduplex stainless steels (SDSS) with 25--26 % Cr and increased content of molybdenum and nitrogen, compared to the 25Cr duplex grades.

The chemical composition and designation, according to SAE/ASTM and EN, of the most widely used DSSÂ together with some trade names, are given in Table 1.

Role of the alloying elements. The interaction between the main alloying elements, in particular Cr, Mî, N and Ni, is rather complicated. In order to obtain a stable duplex microstructure, it is important to ensure a correct content of any of the alloying elements. The chemical content determines the phase balance and strongly influences the formation of the harmful intermetallic compounds at high temperatures.

The influence of alloying elements on the mechanical, physical and corrosion properties is as follows.

Chromium. A minimum of 10.5 % Cr content is sufficient to form a stable passive film of chromium oxide, that protects steel from atmospheric corrosion. The corrosion resistance of stainless steels increases with increasing the chromium content. The chromium is a ferrite former and when its content is higher more nickel is needed in order to obtain duplex microstructure. The higher chromium content also provokes the precipitation of intermetallic phases. As long as the minimal chromium content in ASS is 18 %, in DSS it reaches 22 %.

Molybdenum. Molybdenum complements chromium concerning the corrosion resistance in chlorine environment. The molybdenum is also a ferrite former and increases the tendency to formation of intermetallic phases. In DSS the molybdenum content is limited to 4 %.

Nitrogen. Nitrogen increases the resistance to pitting and crevice corrosion. It significantly increases the strength of DSS and is in fact the most effective alloying element in solid solution strengthening point of view. Except high strength, the nitrogen enriched DSS possess also higher toughness. The nitrogen impedes precipitation of the harmful intermetallic phases. Nitrogen is a strong austenite former which partly replacing nickel and that is why its amount is kept close to the solubility limit, thus allowing to obtain the desired phase balance.

Nickel. Nickel stabilises the austenite. In DSS the nickel content is between 3 and 7 %, when its content in ASS is minimum of 8 %. The lower nickel content in DSS compared to ASS, reduces the influence of worldwide escalation of the nickel price on the price of DSS. Alloying with nickel impedes the formation of intermetallic phases in ASS, but is much less effective in DSS. Because of its bcc crystalline lattice, austenite possesses high toughness. The presence of about 50 % austenite significantly increases toughness, compared to the FSS.

The correlation between the different groups of high alloy steels is shown in Figure 1, based on their chemical content.

Metallurgy of DSS. The metallurgical behaviour of DSS could be investigated through the phase diagram of the triple system Fe--Cr--Ni. A section of this diagram, corresponding to 68 % Fe, is shown in Figure 2. It is seen that DSS solidify as ferrite, part of which then transforms to austenite. The particular transformation temperature depends on the alloy composition. The obtained equilibrium between austenite and ferrite almost does not change at lower temperatures. The influence of the increased amount of nitrogen is also shown on this diagram.

The relative amounts of ferrite and austenite in roll products depend on the chemical composition, but also on the thermal history of the steel. Small variations of the steel composition may significantly
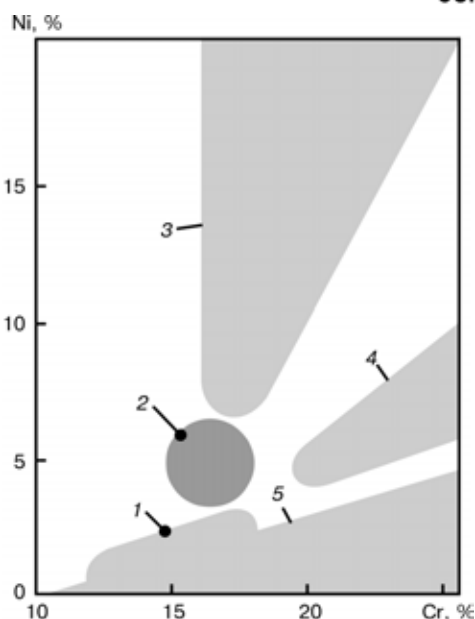
Figure 1. Simplified Schaeffler diagram: *1* — martensitic steels; *2* — precipitation hardening steels; *3* — austenitic steels; *4* — duplex steels; *5* — ferritic steels

Figure 2. Phase diagram of the triple system Fe--Cr--Ni

affect the relative amounts of the two phases, as shown on the constitutional diagram.

During further cooling or subsequent heat treatment, various second phases may precipitate in DSS in the temperature range between 1000 and 300 °Ñ. The tendency to precipitation is strongly influenced by the content of alloying elements and consequently is considerably differing among the various steel grades. The precipitation is stronger in SDSS and weld metal due to their higher alloying content. The time-temperature-precipitation (TTP) diagram is shown in Figure 3, summarizing the approximate temperature ranges where secondary phases precipitate in DSS. This diagram also shows the influence of the different alloying elements, demonstrating that the higher alloying content in SDSS makes them more prone to precipitation. The most important secondary phases precipitating during fabrication and welding are the σ- and χ-phases, secondary austenite and chromium carbides, all of them formed above 500° Ñ. The decomposition of ferrite to α′ determines the upper service temperature. Below 500 °Ñ the precipitation reactions are comparatively slow and insignificant, concerning the embrittlement during welding. The secondary phases known to precipitate in DSS HAZ and weld metal above 500 °Ñ, are shown in Table 2.

Secondary austenite. The austenite precipitating below 900 °Ñ is usually called secondary austenite. It precipitates when the steel or weld metal (WM) is cooled rapidly from high temperatures, where the share of equilibrium ferrite is greater, and then is heated again during welding or heat treatment. The austenite formed at lower temperatures contains less N, Cr and Mo, compared to the primary high-temperature austenite. The secondary austenite morphology varies, depending on the site and mechanism of formation, from Widmanstätten type with sharp
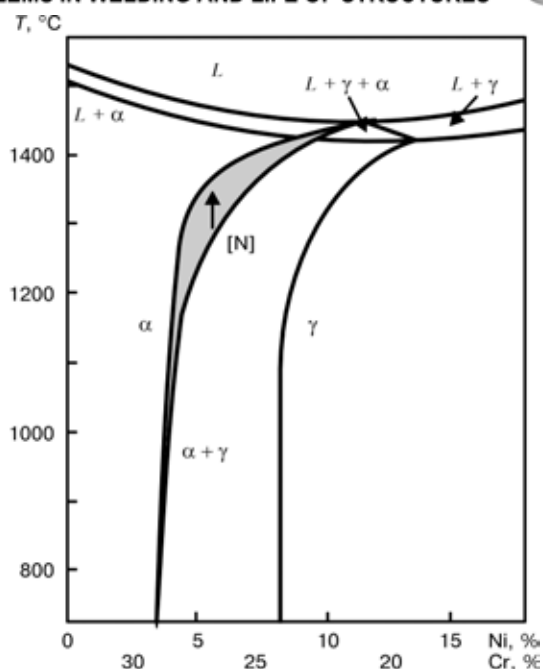
edges, frequently found in WM, to globular type, found in both WM and HAZ. In both cases, due to the low content of N, Cr and Ì î, it has negative influence on the pitting corrosion resistance. It is also considered that precipitation of secondary austenite facilitates the formation of nuclei of phases, rich of chromium and poor of nickel, such as the σ-phase.

Intermetallic phases. The most common intermetallic phase is the σ-phase, frequently precipitating in significant amounts. In many DSS and welded joints of DSS are observed χ- and *R*-phases, but usually they precipitate in smaller amounts. In many cases the σ-phase is used as a synonym of the intermetallic phases.

s-*phase.* The tetragonal σ-phase is an intermetallic Fe--Cr--Mo compound. It is thermodynamically stable in the temperature range between approximately 600 and 1000 °Ñ, depending on the alloying content. The
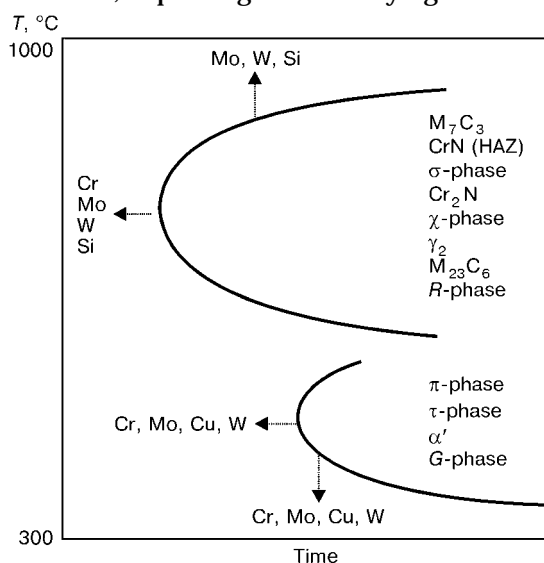
Figure 3. TTP diagram

Table 2. Secondary phases formed in DSS and in weld metal at temperatures above 500 °Ñ

Type of precipitation	Nominal chemical formula	Temperature range, $^i\tilde{N}$	Space group	Lattice parameter, nm
α-ferrite	--	–	$Im3m$	$a = 0.286$--0.288
γ-austenite	--	–	$Fm3m$	$a = 0.358$--0.362
Chromium nitride	Cr_2N	700–900	$P31m$	$a = 0.480$; $c = 0.447$
Chromium nitride	CrN	~ 1000	$Fm3m$	$a = 0.413$--0.447
Phases:				
σ	Fe–Cr--Mo	600--1000	$P4_2/mnm$	$a = 0.879$; $c = 0.454$
χ	$Fe_{36}Cr_{12}Mo_{10}$	700–900	$I43m$	$a = 0.892$
R	Fe–Cr--Mo	550–800	$R3$	$a = 1.090$; $c = 1.934$
π	$Fe_7Mo_{13}N_4$	550–600	$P4_132$	$a = 0.647$
τ	--	550–650	$Fmmm$	$a = 0.405$; $b = 0.484$; $c = 0.286$
M_7C_3	--	950--1050	$Pnma$	$a = 0.452$; $b = 0.699$; $c = 1.211$
$M_{23}C_6$	--	–	$Fm3m$	

σ-phase is enriched of such elements as Cr, Mo, Si and W, and is poor of Ni and Mn.

χ-phase. The cubic χ-phase is an intermetallic phase rich of mîlybdenum, that usually is found in DSS after dwelling in the temperature range between 700 and 900 °Ñ. It is believed that this phase is metastable and is replaced by the σ-phase during longer heat treatments.

R-phase. The thrigonal intermetallic *R*-phase precipitates in DSS in the temperature range 550--800 °Ñ.

α′. The embrittlement at 475 °Ñ is caused by the spinodal decomposition of ferrite α-Fe and α′-Cr rich areas during ageing at 300--550 °Ñ. The formation of α′ may occur as a process of nuclei formation and growth. However it is always connected to significant reduction of the impact toughness.

Chromium nitrides. The precipitation of hexagonal chromium nitrides Cr_2N may occur in DSS into the temperature range between 700 and 900 °Ñ. The precipitation may be a result of over-saturation of ferrite with nitrogen at high cooling rates from high temperatures, during isothermal heat treatment, and also during welding. These precipitates may negatively influence the corrosion resistance and also the impact toughness.

Carbides. The carbides play limited role in the modern DSS, due to their very low carbon content. It is supposed that the carbides provoke precipitation of other harmful phases, such as the σ-phase, by providing sites for nucleation.

Kinetics of intermetallic phase precipitation. The precipitation in DSS or in WM occurs either inside ferrite grains or at the ferrite--austenite or ferrite--ferrite grain boundaries. This, in its essence, is a result from the ferrite instability at temperatures below ≈ 1000 °Ñ and is assisted by the higher diffusion rate in ferrite compared to that in austenite. Consequently, the factors influencing the precipitation kinetics and precipitation temperature range are the composition of ferrite and the number and nature of available nucleation sites, both inside the grains and among them. Other aspects that should be discussed, are the effects of particular alloying elements on the precipitation reactions and the material thermal history.

Composition of ferrite. The composition of ferrite depends on the composition of steel or WM and on the ferrite content. The temperature of heat treatment, the cooling rate and heating by the subsequent welding passes significantly influence the composition of ferrite.

✧ *Content of ferrite and distribution of alloying elements.* A higher ferrite content, for a given chemical composition, results in less alloyed ferrite, while lower ferrite content results in ferrite containing more of the ferrite stabilising alloying elements, such as Cr, Mo and Si. The rapid cooling of welded joints, particularly of the single pass welds, gives shorter time for distribution of the alloying elements, causing more uniform composition of ferrite and austenite, while multipass welding and higher heat input allow longer time for distribution. The rapid cooling results also in higher ferrite contents, thus providing for higher amounts of alloying elements in the ferrite.

Due to a similar reasons, the heat treatment at higher temperatures leads to increase of the volume part of ferrite and to more homogeneous distribution of the alloying elements. Due to these reasons the ferrite will be less sensitive to intermetallic precipitation, but the risk of secondary austenite formation and, at given circumstances, of nitrides precipitation, will increase. It is also found out that formation of intermetallic phases during cooling is slower for the higher temperatures of annealing. More precisely, it is found that the velocity of nucleation decreases with increasing the annealing temperature, but the final amount of the σ-phase after longer ageing times remains unaffected.

Significant variations of the ferrite content and of the composition of ferrite may occur in the welds. It

is found out that the narrow ferrite arms frequently are more enriched of elements, assisting the formation of intermetallic phases, and the precipitation is more likely to occur in these areas.

Influence of the alloying elements. The principle effects of the alloying elements on the ÒÒÐ curves of secondary phases precipitation in DSS and WM are illustrated in Figure 3. The higher contents of alloying elements, and in particular of Mo, W and Si, increase the range of stability of the precipitates and shift the curve towards shorter times. The influence of the typical alloying elements on precipitation is as follows.

• *Chromium and mîlybdenum*. The increase Cr and Ì î content increases the rate of precipitation. Another effect is the widening of temperature range of σ-phase precipitation particularly due to Ì î and also due to Si;

• *Silicon*. Si provokes precipitation of σ-phase, enriched with this element;

• *Nickel*. The increase of Ni content reduces the amount of ferrite and respectively the maximal content of the σ-phase. However, as discussed above, the reduction of ferrite content makes the ferrite richer of Cr and Ì î, which accelerate precipitation of the σ-phase. Ni extends the range of σ-phase stability towards higher temperatures.

• *Nitrogen*. N is an extremely important alloying element in modern DSS. It delays the occurrence of intermetallic compounds, such as σ-phase. It is also supposed that the exchanging part of Ni by N would decrease the precipitation velocity of σ-phase, although the increased risk of nitrides formation should be taken into consideration.

Nucleation.

✧ *Effect of the deformation*. The formation of intermetallic phase nuclei is easier in a deformed metal, for example into the hot rolled or cold worked material. The reason for this is the higher dislocation density, which provide nucleation sites, and also the presence of faster diffusion paths.

✧ *Influence of the solidification types*. The efficiency of phase boundaries as nucleation sites depends on their coherency. The duplex WM usually solidifies as completely ferrite with insignificant segregation, occurring during solidification. Afterwards, the austenite is formed in solid state, frequently with Kurdyumov--Sachs orientation relationship to ferrite, causing formation of low energy ferrite--austenite boundaries.

However this orientation relationship is less frequently found in WM with mixed ferrite-austenite solidification. High-energy boundaries are formed and significant segregation occurs during the mixed solidification. Consequently when the ferrite is highly alloyed in some areas, the nucleation is easier and the precipitation will occur faster.

✧ *Nuclei*. The intermetallic precipitates, remaining after inappropriate heat treatment, or after insufficient treatment for solving the components into the solid solution, have determining effect on the precipitation velocities, because of the shortening of nucleation stage. Consequently, the annealing should be performed at a high enough temperature, in order to avoid precipitation and obtain solving of all intermetallic phases. The annealing at temperatures higher than 1100 °Ñ easily solves the intermetallic phases in most of DSS. Lower annealing temperatures could be used for the lower alloyed grades, while the higher alloyed SDSS may require higher temperatures. The WM should be solution treated at slightly higher temperature than the temperature for the corresponding steel grade, because nickel extends the range of σ-phase stability to higher temperatures. The presence of carbides or nitrides can also facilitate the nucleation.

Influence of the thermal cycle. Formation of intermetallic phases is faster during heating than during cooling, which delays precipitation in the ÑÑÒ diagrams, compared to the ÒÒÒ diagrams. The reason is that the driving force for nucleation is higher at lower temperatures, while the diffusion is faster at higher temperatures. As a result of this, the nucleation is fast during heating and is followed of fast growth during the second stage at higher temperatures. The conditions for precipitation are a little bit more favourable during cooling, when the temperature range of the fastest growth is reached before the temperature range of the fastest nucleation, or during the isothermal heat treatments, where the nucleation and growth occur at a same temperature.

σ-phase. The σ-phase is stable in a temperature range, which depending on the steel composition is somewhere between 600 and 1100 °Ñ. In this range the ferrite is thermodynamically metastable and is prone to decompose into a mixture of austenite and σ-phase. The fact that σ-phase is formed slowly, due to its big tetragonal unit cell of 32 atoms, is favourable.

The ferrite--austenite boundaries are the usual nucleation sites and the carbide particles at grain boundaries facilitate the nucleation. The grain boundary carbides deplete the surrounding ferrite matrix of chromium and provoke a transformation of ferrite in austenite, which locally enriches ferrite with chromium and molybdenum and facilitates the nucleation of σ-phase. The σ-phase also easily nucleates at the grain boundary triple points.

Influence on the properties. It is well known that the precipitation of intermetallic phases unfavorably influences the mechanical properties of parent metal and of WM as well. The main problem, particularly for the qualification of welding procedures, is related to the detrimental influence of the intermetallic phases on the impact toughness and resistance to pitting. It is obvious that the potential risk of corrosion resistance and impact toughness loss should be registered, especially for the SDSS, which are intended for more responsible applications. It is not clear enough though, how to relate the results obtained by
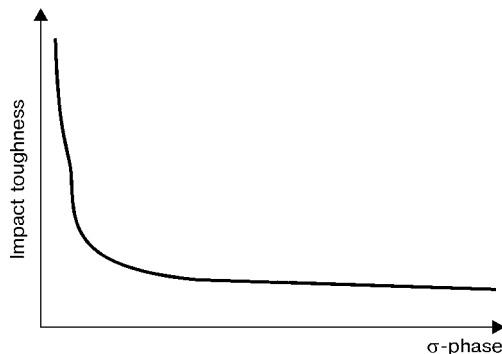
Figure 4. Influence of intermetallic content on impact toughness

short-term testing in strongly aggressive media to the long-term service behaviour in less aggressive media.

Impact toughness. The precipitation of intermetallic phases influences negatively the impact toughness of DSS after dwelling in the temperature range between 600 and 1100 °Ñ. A clear correlation between the ÒÒÐ and impact toughness curves is found for the both parent and weld metal. This correlation fits well to the rapid impact toughness drop with increasing of intermetallic phases content (Figure 4). Even the presence of 1 % intermetallic phase influences the impact toughness, and the material becomes extremely brittle when the intermetallic phase content approaches 10 %.

Corrosion resistance. Pitting and crevice corrosion. The intermetallic precipitates reduce the resistance to pitting and crevice corrosion of both DSS and WM (Figure 5). The intermetallic phases are highly alloyed with chromium and mîlybdenum, and that is why they are resistant to direct corrosion for wide range of aggressive media. The detrimental effect of the precipitates is due to the matrix depletion of alloying elements, similarly to that at formation of carbides and nitrides. As a result of this, preferentially corrodes the poor of chromium and mîlybdenum austenite, which is formed closely to the already precipitated σ-phase. It is believed that the resistance to pitting depends more on the maximal size of intermetallic particles, than to their volume content in the metal. The corrosion test results of isothermally treated specimens show that the lower temperature
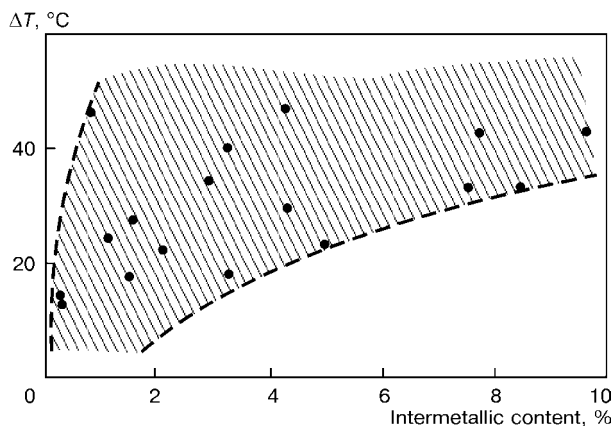
Figure 5. Influence of intermetallic content on corrosion resistance

precipitates are more harmful than the higher temperature ones.

Precipitates related to the welding process. The precipitation of intermetallic phases in WM and HAZ is a little bit faster compared to the precipitation time, which is predicted from the isothermal ageing curves, for two reasons: welding generates significant stress, that accelerates precipitation; and precipitation of intermetallic phases is faster during heating than during cooling or isothermal treating.

However, these two effects are quite small for the WM and HAZ of DSS. There is more significant difference between WM and base metal in distribution of alloying elements between austenite and ferrite, which difference is bigger in WM. The most important factor, however, is the applied welding procedure, through which the too slow cooling or excessive multiple heating should be avoided.

Influence of the chemical composition of WM. The WM is usually alloyed with more nitrogen compared to the parent metal, in order to provide for the formation of enough austenite. For that reason is important to ensure completely ferrite type solidification of WM. The introduction of nitrogen in DSS improves their weldability by increasing the austenitic content in HAZ, thus allowing welding with lower heat input values in order to reduce the risk of precipitation.

Welding thermal cycle. The total dwell time of WM and HAZ in the critical temperature range during single- or multi-run welding is determined by the heat input, number of passes, inter-pass temperature, thickness and geometry of welded joint. Most critical are the areas of repeated (multiple) heating to a maximal temperature that reaches closely the upper limit of the intermetallic phase stability. The dwell times in the intermetallic phase precipitation ranges are accumulated in such cases, frequently leading to reduction of corrosion resistance in multi-run welds.

Usually the dwell time in the critical temperature range is relatively short. That is why there is no risk for participation of intermetallic phases during welding of the regular DSS if the recommended heat inputs and inter-pass temperatures are not exceeded. The SDSS however, may turn to be more difficult for welding at particular conditions. Such conditions may occur in welding of thin wall or small diameter tubes of SDSS.

Welding procedure qualification. Information concerning the problem of intermetallic phase precipitation at the stages of qualification and application of welding procedures is rarely found in literature due to obvious reasons. There is information for precipitation of intermetallic phases during welding of 25 % Cr DSS and of SDSS. Sometimes such problems can also appear during welding of 22 % Cr steels. Areas of welded joints with disobeyed procedures for shielded metal arc welding or with unsuitable microstructure, could easily be found, resulting from improperly developed welding procedures that impose excessively high heat input values. These problems

are mostly expressed in welding of thin (below 5 mm) and thick (above 20 mm) wall joints. For the thin wall tubes the most critical area is HAZ, while for the thick wall joints it is WM.

The most frequent negative results during qualification of welding procedures are obtained by hardness measurements, impact and corrosion resistance tests and metallographic examinations, and are due by intermetallic phases. It should be mentioned, however, that in many cases the corrosion resistance and impact toughness requirements were fulfilled, independently on the presence of intermetallic phases, found by the metallographic examinations.

CONCLUSION

Welding can cause precipitation of intermetallic phases in HAZ and WM of DSS. Precipitation of such phases during welding of SDSS could hardly be avoided. The intermetallic phases can significantly reduce the corrosion resistance and impact toughness, thus not fulfilling the requirements of the welding procedure. In many cases, however, presence of some amount of intermetallic phases could be allowed.

The presence of intermetallic phases is only one of the factors, influencing the properties of welded joints. The other factors are type and state of delivery of parent metal, the welding procedure, surface oxidation and postweld heat treatment.

Welding of DSS 2205 or of DSS with reduced alloying content without exceeding the recommended heat inputs and inter-pass temperatures virtually eliminates the risk of intermetallic phase precipitation. DSS of the 25Cr type could also be welded without intermetallic phase precipitation, but it is especially important to obey strictly the welding procedures. The repeated thermal cycles during multi-pass welding can cause accumulation effect that facilitates the precipitation of intermetallic phases. The critical areas in particular are the root passes in multi-pass welding and HAZ in thin wall or small diameter tubes.

The state of delivery of parent metal has significant role because the residual intermetallic phases, formed during improper heat treatment, have substantial influence on the precipitates.

DETERMINATION OF STRENGTH, SERVICE LIFE AND SURVIVABILITY OF STRUCTURES

K.V. FROLOV, N.A. MAKHUTOV and **M.M. GADENIN**

A.A. Blagonravov Institute of Engineering Science, RAS, Moscow, Russia

Fundamentals of methods and systems of determination of characteristics of strength, service life, survivability and safety of complex technical systems at combined action of service damaging factors are described. In construction of systems of analysis and monitoring of scheduled and emergency situations, it is offered to take into consideration design, technological and service parameters of shapes, sizes, materials, methods of manufacture, control and conditions of operation of load-carrying elements of highly-hazardous objects. One of them is the wide application of welding in the creation of these objects.

Keywords: *technical systems, damaging factors, systems of analysis, monitoring, generalized models*

The aim of developing investigations for determination of strength, service life and survivability is to create the fundamentals of theory of catastrophes and risks in a technogeneous sphere, new principles, technologies and technical complexes, forming the systems of scheduled and express diagnostics and monitoring of normal, emergency and catastrophic situations with most grave consequences [1--32]. These situations in the scope of existing standardized approaches and methods remained, as a rule, little-studied from the scientific and applied points of view due to their complexity, hardly possible prediction and repetition [1--5].

The solution of the put problem includes the creation of generalized mathematical and physical models of complex technological, operating and emergency processes in technical systems for analyzing conditions of transition from conventional states to the conditions of initiation and propagation of accidents and catastrophes. These models are characterized by a multilevel structure, including global, local and object aspects of safety. Developments have an interdisciplinary nature and are the basis of standardization of safety and risks. It is very important here that the initiation of accidents and catastrophes is often connected with zones of welding and surfacing.

Fundamental and basic developments on the theory of catastrophes and safety, scientific bases of engineering and technologies, development of methods of experimental mechanics of machines and structures are intended for use in analysis of initiation and propagation of emergency situations. They were reflected in published articles and papers of journal «Problems of safety in emergency situations» and in some volumes of series «Safety of Russia» [1, 2, 7, 10, 11].

Theory, engineering and technologies of prediction and prevention of accidents and catastrophes include, alongside with modelling, the analysis of new limiting states at most complicated scenarios of development of emergency situations with allowances for primary and secondary factors of damages in parent metal, weld metal and deposits, development of methods and creation of systems of express diagnostics of emergency situations and damaged conditions of technical systems in case of occurrence of technogeneous and natural accidents and catastrophes, having a global, national, regional, local and object nature.

If to take into account all the growing losses from large accidents and catastrophes [1--4, 7--12], it can be seen that there are no actually until now both generally-accepted methods of analysis, calculations and modelling of accidents and catastrophes and standardized quantitative base to provide the survivability and safety at combined actions of damaging factors in national and international practice. This circumstance can be explained by the fact that, as a whole, the complication of created technical objects and conditions of their operation was much faster than the investigation and standardization of their performance. Moreover, the state, interbranch and branch expertises of the largest accidents and catastrophes revealed often the non-conformity of their consequences, causes, conditions and characteristics to really existing standardized fundamentals of designing, manufacture and service of complex and potentially hazardous technical systems.

Fundamentals of stage-by-stage analysis of strength and safety. Formation of trends in development of standardizing, defining the performance and safety of complex technical systems (CTS) was made by specifying and complicating the used methods and criteria [5, 6, 13--32]. Here, the accidents and catastrophes themselves served as initial information base (as an element of feedback) for such development of standardized materials.

As a whole, at traditional solution of the safety problem the following approaches are used (Figure 1):

• from the positions of strength (in its multicriterial expression through stress σ);

• from positions of service life (with time τ and by the cycle N statements);

• from positions of reliability (in multifactorial probability P conception).

In most cases the technogeneous accidents and catastrophes were accompanied by failures of load-carrying elements of potentially hazardous objects (independent of causes and sources of this failure). This has led to the fact that the practice of top priority grounding of strength of the objects created became the most routine during decades and centuries. The traditional methods of grounding strength were based on a complex of characteristics and criteria of fracture (σ_y, σ_t, σ_{-1}, σ_{1-t}), which became standard. On the basis of parameters of strength and fractures the conceptions were formulated about safety factor (n_σ, n_N, n_τ) included to reference, educational and standardizing literature. At present a whole system of criteria and safety factors has been created, which guarantees the non-failure of objects with keeping preset service conditions. For welded structures, the specifics of stress-strain states, criteria of strength and service life in potentially hazardous zones of welding were taken into account in these calculations.

However, these traditional structures and standardized materials did not contain often the direct data determining quantitatively the service and survivability of CTS. Over the recent decades this lack of information was filled and the theory and criteria of service life and reliability, and then survivability and safety were included into the sphere of traditional analysis of the performance of objects [1--6, 13--32].

The new methods and criteria of the following groups are the more oriented to the quantitative solution of the problem of safety of complex objects, creating severe accidents and catastrophes:

• risk (in probability-economic statement);

• survivability (capability and stability of functioning in occurrence of accidents at different stages of propagation of accidents and catastrophes, inadmissible by standards);
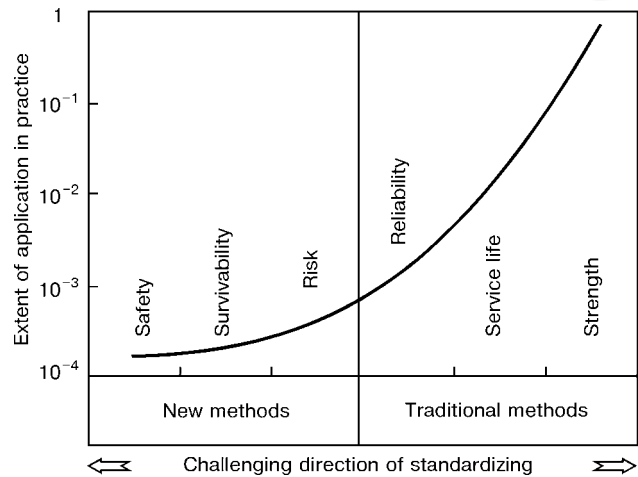
Figure 1. Structure and development of standardizing methods

• safety (with allowance for criteria and characteristics of accidents and catastrophes).

At the same time, volume and degree of evaluation, standardizing and calculation of new characteristics of safety in real engineering practice for large accidents, national and global catastrophes even during recently remain extremely small, i.e. less than 0.1 % (Figure 2). This refers especially to unique military and civil objects manufactured using welding and surfacing technologies. Thus, the task is reduced to the challenging change in the direction of development of standardizing (see Figure 1), namely from basic analysis of safety, survivability and risk to the traditional determination of reliability, service life and strength.

The creation of methods and systems of determination of basic parameters in the entire chain «strength--safety» should be lined up relative to the following priority of analysis of accidental and cata-
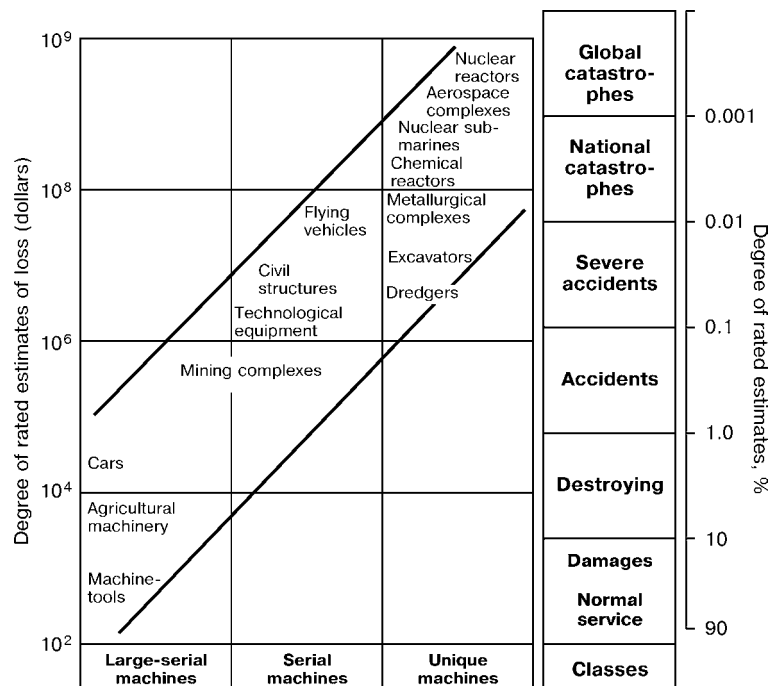
Figure 2. Distribution of economical losses from non-provided reliability and safety of different types of machines

strophic situations in the technogeneous sphere (by the degree and feasibility of their realization):

• hypothetical, which can occur in non-predicted variants and scenarios of development with maximum possible losses and victims (protection from them is low and the objects are not subjected to a direct restoration; feasibility of emergency diagnostics and monitoring are reduced to the determination of portents of these situations and operation of systems of emergency notification);

• out-project, occurring in irreversible damages of critical elements with high losses and human victims (degree of protection from them is insufficient; need in conductance of subsequent restoration works; feasibility of emergency diagnostics and monitoring in addition to hypothetical situations should provide the connection of systems of automated protection);

• project, occurring at coming out beyond the scheduled conditions with predicted and acceptable consequences (protection from them is sufficient; the combined interaction of conventional and emergency systems of diagnostics, monitoring and protection should be provided);

• routine, occurring at scheduled functioning of potentially hazardous objects (consequences from them are predictable, protection from them is high; conventional systems of diagnostics and monitoring are advantageous in this case).

List of classes of accidents and catastrophes, types of emergency and catastrophic situations and levels of a potential hazard of CTS, given in [12], indicates the great scientific and practical need in their arrangement for the solution of problems of reduction of risks of accidents and catastrophes in nature-technogeneous sphere.

Formation of general principles and requirements to the analysis of strength and safety. Definition of strength, service life and survivability in the theory, engineering and technologies of prediction and prevention of accidents and catastrophes includes, in parallel with modelling, analysis of limiting states at most complex scenarios of development of emergency situations with allowance for primary and secondary factors of damages, development of methods and creation of systems of express diagnostics of emergency situations and damaged states of CTS, including those with welded elements of structures. Here, natural hazard, technogenous threats and ever growing role of a human factor can be factors for the technogenous sphere, initiating accidents and catastrophes.

The scientific direction of fundamental and applied investigations on the problems of determination and improvement of strength, service life, survivability and safety of machines with allowance for complex effects of non-linearity was formed [1, 5, 12, 13] over the recent years on the base of a large number of research works made earlier during many decades [5, 12--32].

The significant role in the development of investigations on non-linear mechanics of deforming and fracture (Figure 3), as a scientific basis of grounding initial strength, service life and survivability, is belonged to constantly collaborating scientific centres and schools: academic, branch and higher educational [13--32]. The basic developments referred mainly to the first stage of a life cycle of objects, i.e. stage of their designing, taking into account the technological inheritance and service conditions.

At the first stages the solution of linear problems of theory of elasticity, theory of oscillations, theory of plates and shells were reduced to the determination of static and dynamic nominal and local stresses σ^s from service loads P^s. As criterial parameters of initial deformativity and strength of structural materials the elasticity modulus E, σ_y and σ_t strengths were used:

$$\sigma^y = f(P^y) \leq \left\{ \frac{\sigma_y}{n_y}, \frac{\sigma_t}{n_t} \right\}, \tag{1}$$

where n_y, n_t are the appropriate safety factors.

Taking into account that the welded joints in loading-carrying elements were made with allowance for their equal strength with parent metal elements, the direct reproduction of specifics of welding in equation (1) was not found. This equation is used in manufacture of cars, agricultural machinery, power and technological equipment, widely-used objects of building structures.

In the war and first post-war years the investigations on fatigue and fatigue life were started. Stresses σ^s and number of loading cycles N^s were referred to main parameters of service loading. In addition to equation (1) the conditions of initial cyclic strength were formulated:

$$\sigma_a^y = f(P^y, N^y) \leq \left\{ \frac{\sigma_{-1}}{n_\sigma(K_\sigma \sigma_a^y)\varepsilon_\sigma + \psi_\sigma \sigma_m^y} \right\}, \tag{2}$$

where σ_a^y, σ_m^y are the amplitude and mean stress of cycle; σ_{-1} is the fatigue limit of structural material; K_σ, ε_σ, ψ_σ are the characteristics of material sensitivity to the stress concentration, absolute sizes and cycle asymmetry, respectively.

For welded joints the values σ_{-1} were introduced for different zones of welding, and the residual stresses after welding changed the value of mean stresses σ_m^y. According to equations (1) and (2) the strength and fatigue life of load-carrying elements in aviation, transport and hydropower engineering were calculated. To analyze the local stresses the methods of photoelasticity and tensometry were developed.

Exploration of regions of Siberia and North, and also the creation of objects of the cryogenic engineering put forward the problem in the 1950--1960s for investigation of low-temperature strength with a determination of cold-shortness characteristics. Characteristics of low-temperature local rupture strength S_K were introduced additionally into the analysis of initial strength:
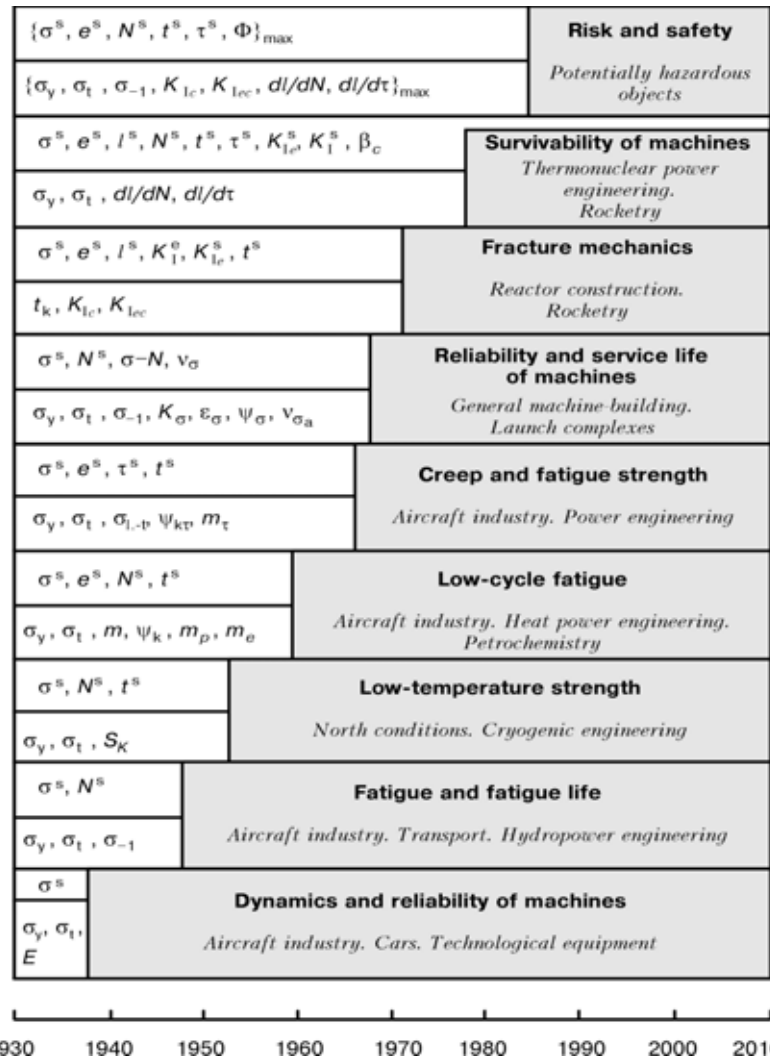
$\{\sigma^s, e^s, N^s, t^s, \tau^s, \Phi\}_{max}$	**Risk and safety**
$\{\sigma_y, \sigma_t, \sigma_{-1}, K_{1c}, K_{1ec}, dl/dN, dl/d\tau\}_{max}$	*Potentially hazardous objects*
$\sigma^s, e^s, l^s, N^s, t^s, \tau^s, K_{1e}^s, K_1^s, \beta_c$	**Survivability of machines**
$\sigma_y, \sigma_t, dl/dN, dl/d\tau$	*Thermonuclear power engineering. Rocketry*
$\sigma^s, e^s, l^s, K_1^e, K_{1e}^s, t^s$	**Fracture mechanics**
t_k, K_{1c}, K_{1ec}	*Reactor construction. Rocketry*
$\sigma^s, N^s, \sigma{-}N, \nu_\sigma$	**Reliability and service life of machines**
$\sigma_y, \sigma_t, \sigma_{-1}, K_\sigma, \varepsilon_\sigma, \psi_\sigma, \nu_{\sigma a}$	*General machine-building. Launch complexes*
$\sigma^s, e^s, \tau^s, t^s$	**Creep and fatigue strength**
$\sigma_y, \sigma_t, \sigma_{l\text{-}t}, \psi_{k\tau}, m_\tau$	*Aircraft industry. Power engineering*
σ^s, e^s, N^s, t^s	**Low-cycle fatigue**
$\sigma_y, \sigma_t, m, \psi_k, m_p, m_e$	*Aircraft industry. Heat power engineering. Petrochemistry*
σ^s, N^s, t^s	**Low-temperature strength**
σ_y, σ_t, S_K	*North conditions. Cryogenic engineering*
σ^s, N^s	**Fatigue and fatigue life**
$\sigma_y, \sigma_t, \sigma_{-1}$	*Aircraft industry. Transport. Hydropower engineering*
σ^s	**Dynamics and reliability of machines**
σ_y, σ_t, E	*Aircraft industry. Cars. Technological equipment*

1930 1940 1950 1960 1970 1980 1990 2000 2010

Figure 3. Stages of development of investigations of strength and safety

$$\sigma_a^y = f(P^y, t^y) \leq \left\{ \frac{S_K}{n_s K_\sigma} \right\}, \qquad (3)$$

where K_σ is the coefficient of stress concentration with allowance for redistribution of stresses at the expense of local plastic deformations.

Here, it was important to study the local structural physical-mechanical processes of formation of microdeformations and microdamages in material using methods of radiography and microscopy.

In the 1960s the systematic investigations on low-cycle fatigue were carried out for the intensively progressing aircraft, power and petrochemical machine-building. Creation of regions of non-elastic cyclic deforming in the zones of action of concentration and temperature stresses required the transition from calculations in local stresses to calculations in local strains:

$$\{\sigma^y, e^y, N^y\} = f(P^y, N^y, t^y, m) \leq$$
$$\leq \left\{ \left[\left(\frac{\sigma_{\hat{e}}}{n_\sigma} \right) \left(\frac{e_{\hat{e}}}{n_{\hat{a}}} \right) \left(\frac{N_{\hat{e}}}{n_N} \right) \right] f(\sigma_y, \sigma_t, \psi_{\hat{e}}, m_p, m_e) \right\}, \qquad (4)$$

where σ_k, e_k, N_k are the limiting stresses, strains and numbers of cycles ($\sigma_k = S_K$, $e_k = 1/(1 - \psi_k)$); m is the characteristic of strengthening in elasto-plastic region; ψ_k is the reduction in area at single fracture; m_p, m_e are the characteristics of a low-cycle fracture curve.

Local characteristics of strength σ_y, σ_t and ductility ψ_k were introduced into calculation for zones of welding and surfacing. Residual stresses after welding and surfacing in combination with dissimilarity in weld mechanical properties created three-dimensional stressed states, thus changing the ductility in the zone of fracture and leading to the effect of a contact strengthening. To determine σ^s, e^s the methods of photoelastic patches, moire, small-base grids and small-base tensometry were developed.

As regards to new problems of aerospace engineering, starting complexes, supersonic aviation, heat power engineering, petrochemistry, metallurgy, the investigations were carried out on creep, high-temperature short-time, long-time and cyclic (up to 500--3000 °C) strength, including those at programmed two-frequency conditions of loading. When designing machine parts the equations of initial long-time (by time of service τ^y) strength σ_{l-t}^τ were added to equations (1), (2) and (4):

$$\{\sigma^y, e^y, \tau^y, N^{py}\} = f(P^y, \tau^y, N^{py}, t^y) \leq$$

$$\leq \left\{\left(\frac{\sigma^{\tau}_{1.-t}}{n_{\sigma}}, \frac{e^{\tau}_k}{n_e}, \frac{\tau_k}{n_{\tau}}, \frac{N_k}{n_N}\right) f(m_{\tau})\right\}, \qquad (5)$$

where n_{τ} is the time margin τ; m_{τ} is the characteristic of curve of long-time strength.

It was assumed for zones of welding and surfacing that high temperatures create the relaxation of residual stresses and change local mechanical properties. Measurement of the local stresses and strains were made by high-temperature methods of tensometry and moire on different technical objects.

Development and generalizing of a large number of works on strength and fatigue life in the 1960--1970s led to the formation of one of the important chapters of designing, manufacture and service of machines, i.e. assurance of their reliability and service life. This, first of all, referred to the products of aircraft and general machine-building, operating at alternating conditions of thermocycling loading. To update equations (1) and (2), the coefficients of variation of service loading v_{σ}, endurance limits v_{σ_a} and also design-technological factors (K_{σ}, ε_{σ}, ψ_{σ}) are introduced into calculation by fatigue curves σ--N. These approaches were further spread also for initial low-cycle fatigue.

At the end of the 1960s and the beginning of the 1970s a great attention was paid to the development of the linear and non-linear mechanics of static, cyclic and dynamic fracture. Here, the calculations of crack resistance of the machines became to be based on local stresses σ^y and strains e^s, on allowance for sizes of defects l^s, coefficients of intensity of stresses K_I and strains K_{Ie}, temperature conditions of loading t^s:

$$\{\sigma^y, e^y, K_I^y, K_{Ie}^y\} =$$

$$= f(P^y, t^y, l^y) \leq \left\{\frac{\sigma_{\hat{e}}}{n_{\sigma}}, \frac{e_{\hat{e}}}{n_e}, \frac{K_{Ic}}{n_{\hat{e}}}, \frac{K_{Iec}}{n_{\hat{e}e}}\right\}, \qquad (6)$$

where n_k, n_{ke} are the margins by coefficients of intensity of stresses and strains.

Equation (6) found a standardized application in calculations of initial strength of nuclear reactors, pressure vessels, pipelines. In this case characteristics σ_k, e_k, K_{Ic} and K_{Ie} were determined for welded joints and deposits on special specimens, in which the initial cracks were located in welds and transition zones. The cracks created noticeable redistribution of residual stresses and change in coefficients of intensity K_I. A special interest in experimental mechanics for welded joints of structures was the physical simulation of fields of efficient and residual stresses at the tip of propagating cracks (using methods of photo-elasticity, holography, tensometry, radiography).

Methods of analysis of initial strength, service life in characteristics of crack resistance and survivability of machines with allowance for damages of technological and service origin were developed on the basis of earlier integrated investigations taking into account the new tasks in the field of the aircraft and aerospace engineering, nuclear and thermonuclear power engineering. In the last case the residual strength and service life were dealt with.

Equations (1)--(6) were added with equations for evaluation of initial and residual life with allowance for a long-time static and cyclic propagation of cracks in load-carrying structures:

$$\{\sigma^y, e^y, K_{Ie}^y, N^y, \tau^y, t^y\} = f(P^y, t^y, l^y) \leq$$

$$\leq \left\{\frac{\sigma_{\hat{e}}}{n_{\sigma}}, \frac{e_{\hat{e}}}{n_e}, \frac{N_{\hat{e}}}{n_N}, \frac{\tau_{\hat{e}}}{n_{\tau}}, \frac{t_{\hat{e}}}{n_t}, \frac{l_{\hat{e}}}{n_l}\right\}, \qquad (7)$$

where K is the index of critical characteristics; n_N, n_{τ}, n_t, n_l are the margins by number of cycles, time, temperature and sizes of cracks, respectively.

The calculated characteristics N_k and τ_k are determined by integrating kinetic diagrams of fracture:

$$\{N_k, \tau_k\} = F\left\{(\Delta K_I^y, \Delta K_{Ie}^y), \left(\frac{dl^y}{dN}, \frac{dl^y}{d\tau}\right)\right\}, \qquad (8)$$

where ΔK_I^y, ΔK_{Ie}^y are the ranges of coefficients of intensity of stresses and strains.

To analyze the processes of damage in parent metal and welded joints, the methods of a pulsed holography, thermovision, tenso-sensitive coatings, radiography, microstructural analysis, vibrometry were used.

Results of investigations to justify the equations (1)--(8) are reflected in appropriate fundamental manuscripts [5, 13--32].

Over the last decade the investigations on survivability and safety of machines and on mechanics of catastrophes were started. As regards to potentially hazardous objects with allowance for complexes of damaging factors these developments include calculation-experimental investigations on all above-mentioned directions using analytical, numerical and experimental methods of analysis of stress-strain and limiting states for initial residual parameters of serviceability. Actuality of the problem of determination of residual strength and life, and also problem of extension of service life became evident for most complex and potentially hazardous objects of nuclear and heat power engineering, aerospace and aircraft industry, objects of oil and gas complex, transport systems. Their peculiar feature consists in complexity and, in some cases, impossibility of replacement by the new objects with initial parameters of strength and service life. The presence of zones of welding and surfacing very complicates here the accurate determination of strength, service life and survivability due to non-linear redistribution of local stresses and strains in them and changing mechanical properties in the process of service.

It follows from data of Figures 1--3 that with complication of objects of an increased hazard the technologies of prevention of accidents and catastrophes should be based on integrated methods of substantiation, maintaining and increase in service life, survivability and, finally, safety of structure load-carrying elements.
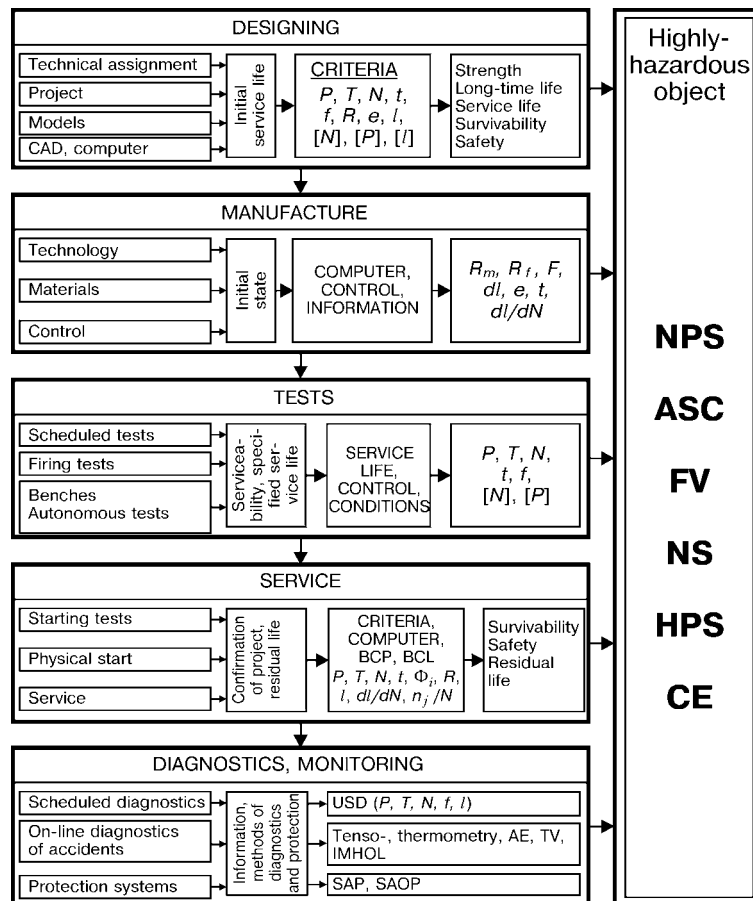
Figure 4. Schematic diagram of analysis of initial and residual strength, service life and safety of machines and structures

Development of methods of experimental mechanics for evaluation of strength, service life and survivability. The major tasks of developments on determination and substantiation of initial and residual strength, service life, survivability and safety of technical systems are as follows [1]:

• fundamental investigations on mechanics of deforming and mechanics of catastrophes being the basis of creation of criteria and methods for the solution of interindustry problems of strength, service life, survivability and safety of CTS with an increased potential hazard of occurrence of technogeneous emergency situations;

• applied investigations and developments of engineering methods, algorithms, programs, models, stands, hardware for calculation-experimental grounding of design-technological decisions in designing, manufacture, service and putting out of service of operating and radically new highly-hazardous machines and structures using the complex criteria of strength, service life, survivability and safety, first of all, for most loaded zones (concentration of stresses, welds, deposits).

Figure 4 shows an integrated schematic diagram of solution of problems for prevention accidents and catastrophes on the basis of formation of principles and requirements for strength, service life and safety of such potentially hazardous objects as nuclear power stations (NPS), aerospace complexes (ASC), flying vehicles (FV), nuclear submarines (NS), heat power

stations (HPS), chemical enterprises (CE). These problems cover all stages of life cycle of the objects: designing, manufacture, testing and service (with putting into and out of service), all types of emergency situations and damaging factors.

Designing includes development and coordination of technical assignment with introducing of basic requirements for initial strength, service life and safety. Development of the project consists of several stages (schematic diagrams, pre-sketch, technical and working projects). At this stage the physical and mathematical models are developed using computer engineering and systems of automated designing (CAD). At the stage of designing the analysis of strength is made and initial service life is grounded using standardized and additional calculations. Major criteria and characteristics of these calculations are: service loads P, temperature $t(\tau)$, number of cycles N, frequency f, characteristics of resistance of materials $R(\sigma_y, \sigma_t, \sigma_{l\text{-}t})$, deformations e, defects l. Values $[N]$, $[P]$, $[l]$ are justified with preset safety factors n as admissible using equations (1)--(8). Using the integrated calculation and service investigations the conclusion is made about the strength, service life, survivability and safety. Thus, at the stage of designing the bases of prediction and prevention od emergency and catastrophic situations are established.

At the stage of manufacture the problems of formation of requirements, selection, grounding and development of technologies, materials and control are

solved. To manufacture elements, systems and objects as a whole, the initial states in zones and out of zones of welding are established: real mechanical properties and their deviations from technical requirements, level of real defectness of load-carrying members, geometric shapes and their deviations. The accurate data of control are put into certificates and databases in the computer. All these data are initial information about characteristics of strength $R_m(\sigma_y)$, $R_f(S_K)$ deformability Δl (elongation), ψ (reduction in area), deformations e, temperature t, crack growth rate dl/dN (or $dl/d\tau$). Using them the clarification of design parameters of initial strength, service life, survivability and safety are made. In accordance with above-mentioned, the bases of prediction and prevention of severe accidents and catastrophes for real objects with allowance for a complex accepted design-technological solutions at the stage of manufacture are provided.

Stage of tests includes different their types and combinations: autonomous testing of sub-assemblies, bench test of sub-assemblies, units and products, firing and simulation tests. Final tests are the regular tests of main samples with reproducibility of real service and extremal conditions. Using the same criteria as for the stages of designing and manufacture, the additional clarification of admissible limiting loads $[P]$ and life time $[N]$ is made. The clarified conclusion about initial service life, methods of successive control is made and clarified service conditions are designed on this basis.

For the stage of putting into and out of service the pre-start and start tests (hydro-, pneumatic tests, cold and hot running), physical start (with correction of all systems of service support) and putting into service are realized. Here, the system of scheduled diagnostics of main parameters: loads P, temperatures t, cycles N, frequences f, defects l is designed and specified (using mainly the regular systems of ultrasonic diagnostics (USD)). For the objects of high potential hazard the methods and systems of on-line diagnostics of emergency situations are developed,

Figure 5. Scheme of limiting and admissible states in evaluation of strength, service life and survivability

manufactured and applied, using tenso- and thermometry, acoustic emission (AE), thermovision (TV), impulsed holography (IMHOL). Volume and level of flaw detection control is, as a rule, abruptly increased in the zones of welded joints and deposits. Data, obtained in this case, can provide initial information for connection of systems of automatic protection (SAP) and systems of automatic on-line protection (SAOP). From results of investigations the conclusion is made about specified initial strength and designed initial service life when putting into service.

At the initial stage of service the most important information should be obtained to confirm or to correct design decisions about the strength, life time, service life, survivability and safety. With exhausting of specified design service life the estimation of residual life of safe service is made. For approval of all the information for all the stages of a life cycle of the object the unified criteria and computer programs should be used. In this case, the data about the initial, used and residual service life can be displayed on block-type control panels (BCP) and board counters of life (BCL) ---- n_i/N.

With exhaustion of service life the problem of estimation of survivability, extension of service life, recovery and increase in residual strength becomes actual. As to the stage of service, then the problem of safe putting objects out of service (especially in case of accumulated residual radioactive radiations Φ, chemical, operating and emergency effects on objects, personnel and environment) becomes important scientific-technical and economical problem.

The feasibility to prevent accidents and catastrophes on the highly-hazardous objects is supported by definite system of design, technological and service measures using the new methods of diagnostics of load-carrying elements in scheduled and emergency conditions of functioning. In a general case the three-dimensional surfaces of limiting and admissible states can be constructed on the basis of equations (1)--(8). Coordinate axes for these surfaces are as follows:

• axis of characteristics of service load (forces P, rated stresses σ_r, coefficients of stress intensity K_I, given local maximum stresses $(\sigma_g)_{\max c}$ in zones of concentration);

• axis of temperature-time and cyclic parameters of service (temperature t, time τ, number of loading cycles N);

• axis of defectness condition (sizes l of defects with allowance for their shape and space location).

Formation of fractures, inadmissible plastic deformations or cracks corresponds to reaching limiting state (surface of limiting states). Limiting load P in this case is a vector passing through the beginning of coordinates with angles corresponding to the given state of the structures (by l, t, τ, N, σ_r, K_I, $(\sigma_g)_{\max c}$). If to introduce the necessary safety factors n on the basis of relations (1)--(8), then it is possible to transfer from the surface of limiting states to the surface
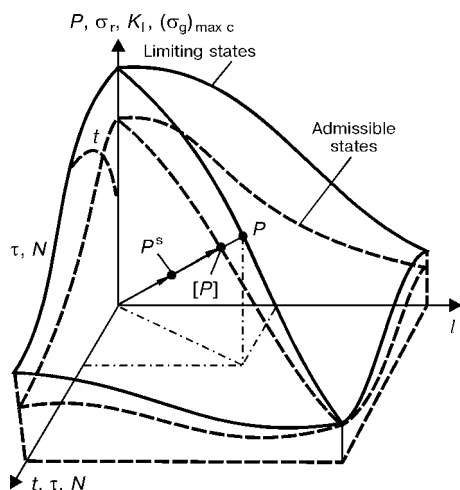
of admissible states and load [P]. On this base, the strength, service life and survivability can be considered provided, if the vector of service load P^s will be lower or equal to the vector of admissible [P] -- ($P^s \leq \leq [P]$).

Classical (traditional) methods of calculation of strength and service life were developed in the assumption of defectless structural material ($l = 0$). In this case it is possible to transfer from limiting and admissible surfaces to limiting and admissible curves (in plane «P, σ_r, K_I, $(\sigma_g)_{max\,c}$--t, τ, N»), i.e. static (at preset temperature t), long-time static (by preset time τ) and cyclic (by preset number of cycles N) strength. Strength and survivability were determined at the first stages by criteria of linear fracture mechanics (static crack resistance) for plane «P, σ_r, K_I, $(\sigma_g)_{max\,c}$--l».

For the modern calculations of strength, service life and survivability using limiting and admissible states (see Figure 5), it is important to adopt standard equations of states, standard criteria of fracture and standard complexes of rated characteristics in equations (1)--(8), independent of the type of structure, properties of structural materials and conditions of service loading. Here, the stage-by-stage transition from calculations in stresses [5, 13--16] (that was accepted in most standardized documents) to calculations in strains is most promising [17--32].

In the development and conducting of integrated calculations for strength, service life in a determinative statement, all initial information is used about averaged characteristics of service loading, about average or guaranteed criterial characteristics of fracture resistance of structural materials (parent metal, metal of welds and deposits), about averaged characteristics of initial defectness determined by standards of flaw detection control (in particular, in places of welds and deposits).

If for the stages of designing or service the statistic characteristics (functions of distribution and their parameters) of loading, mechanical properties of materials and defectness of parts are introduced into calculations, then it seems possible to determine the probability initial characteristics of strength, service life and survivability, reliability, risk and safety of structures.

For specified estimates of residual strength, service life, survivability and safety, the basic initial equations should include stresses and limiting states, changing in the process of service, with allowance for their dependence on service conditions, i.e. number of cycles, time, temperatures, working media.

1. (1998) *Safety of Russia. Legal, socio-economic and scientific-technical aspects. Functioning and development of complex national economy, technical, power, transport systems and communication systems.* Moscow: Znanie.

2. Makhutov, N.A., Osipov, V.I., Gadenin, M.M. et al. (2002) Scientific principles of safety of Russia. In: *Problems of safety in force-majeure situations.* Moscow: VINITI.

3. Vorobiov, Yu.L. (2002) *Principles of formation and realisation of public policy in the field of reduction of force-majeure risks.* Moscow: Delovoj Express.

4. (2002) *Safety of Russia. Safety of industrial complex.* Moscow: Znanie.

5. (1997) *Problems of fracture, life and safety of technical systems.* Ed. by V.V. Moskvichyov, M.M. Gadenin. Krasnoyarsk: KODAS-SibERA.

6. (2000) *Strength, life and safety of machines and structures.* Ed. by N.A. Makhutov, M.M. Gadenin, Moscow: IMASh RAN.

7. (2002) *Safety of Russia. Safety of pipeline transportation.* Moscow: Znanie.

8. (2002) *Complex safety of Russia: researches, management, experience.* Moscow: Informizdat.

9. (1999) *Safety of Russia. Protection of population and territories in case of force-majeure situations of natural and man-caused nature.* Moscow: Znanie.

10. (2000) *Safety of Russia. Environmental diagnostics.* Moscow: Mashinostroenie.

11. (1998) *Safety of Russia. Fundamental official acts.* Moscow: Znanie.

12. (2000) *Disasters and society.* Moscow: Kontakt-kultura.

13. Serensen, S.V. (1985) *Selected works.* Kyiv: Naukova Dumka.

14. Malinovsky, B.N. (2002) *Academician Boris Paton: The lifetime work.* Moscow: PER SE.

15. Troshchenko, V.T., Lebedev, A.A., Strizhalo, V.A. et al. (2000) *Mechanical behaviour of materials under different kinds of loading.* Kyiv: IPP.

16. Serensen, S.V., Shnejderovich, R.M., Makhutov, N.A. et al. (1975) *Strength in low-cycle loading. Principles of design and testing methods.* Moscow: Nauka.

17. Serensen, S.V., Shnejderovich, R.M., Makhutov, N.A. et al. (1979) *Deformation fields in low-cycle loading.* Moscow: Nauka.

18. Gusenkov, A.P. (1979) *Strength in isothermal and non-isothermal low-cycle loading.* Moscow: Nauka.

19. Makhutov, N.A., Gadenin, M.M., Gokhfeld, D.A. et al. (1981) *Equation of state in low-cycle loading.* Moscow: Nauka.

20. Makhutov, N.A., Vorobiov, A.Z., Gadenin, M.M. et al. (1983) *Strength of structures at low-cycle loading.* Moscow: Nauka.

21. Makhutov, N.A., Burak, M.I., Gadenin, M.M. et al. (1986) *Mechanics of low-cycle fracture.* Moscow: Nauka.

22. Kogaev, V.P., Makhutov, N.A., Gusenkov, A.P. (1985) *Calculations of strength and service life of machine parts and structures.* Moscow: Mashinostroenie.

23. Romanov, A.N. (1988) *Fracture at low-cycle loading.* Moscow: Nauka.

24. Makhutov, N.A., Zatsarinny, V.V., Gadenin, M.M. et al. (1989) *Statistical principles of low-cycle fracture.* Moscow: Nauka.

25. Makhutov, N.A., Stekolnikov, V.V., Frolov, K.V. et al. (1987) *Structures and methods of design of WWPR.* Moscow: Nauka.

26. Makhutov, N.A., Frolov, K.V., Gadenin, M.M. et al. (1988) *Strength and life of WWPR.* Moscow: Nauka.

27. Makhutov, N.A., Frolov, K.V., Stekolnikov, V.V. et al. (1990) *Experimental investigations of strains and stresses in WWPR.* Moscow: Nauka.

28. (1994) *Design of machines.* Refer. Book. Ed. by K.V. Frolov. Moscow: Mashinostroenie.

29. Makhutov, N.A., Frolov, K.V., Gadenin, M.M. et al. (1999) *Problems of life and safety of power equipment.* Moscow: IMASh RAN.

30. Makhutov, N.A. (1981) *Strain criteria of fracture and calculation of strength of structure components.* Moscow: Mashinostroenie.

31. Serensen, S.V., Kogaev, V.P., Shnejderovich, R.M. (1975) *Load-carrying capacity and strength design of machine parts.* Moscow: Mashinostroenie.

32. Makhutov, N.A., Frolov, K.V., Dragunov, Yu.G. et al. (2001) *Model investigations and full-scale tensometry of power reactors.* Moscow: Nauka.

REVIEW OF FATIGUE DESIGN RULES
FOR WELDED STRUCTURES

S.J. MADDOX
TWI, Abington, Cambridge, UK

Current fatigue design rules are reviewed in the light of recent research and the changing needs of industry. Available evidence indicates that many revisions are required and the scope can be extended. Topics addressed included classification of butt and cruciform joints, the inclusion of non-arc welds, size effect corrections, the hot-spot stress approach, the treatment of complex combined loading and cumulative damage calculation methods.

There is a fair measure of agreement world-wide between fatigue design rules for welded structures [1, 2]. Thus, they present a number of S--N curves obtained from fatigue tests on actual welded components, expressed in terms of nominal stress range independently of applied mean stress, that are used in conjunction with Miner's rule to predict the fatigue lives of structures subjected to random loading in service. However, research continues to lead to improved understanding of the factors affecting the fatigue lives of welded joints, and industrial priorities change. This paper reviews issues requiring attention and ways in which rules can be improved.

In the review, the IIW design S--N curves [3] are chosen as a basis for comparison with new fatigue data since they are in an easily recognisable format and are consistent with many other design S--N curves. They have the commonly-used form $S^m N = A$, where S is the applied stress range; N is the fatigue life in cycles; A is a constant; and m is usually 3, but may be 5. Each design curve is referred to as FAT x, where x is the value of S in N/mm^2 at $N = 2 \cdot 10^6$ cycles on the design curve. Furthermore, for ease of comparison, any curves fitted to the data presented are assumed to have the same slope as the relevant design curve.

Some of the weld details addressed in this review can embody compressive residual stresses due to welding, even in structural components. In contrast, most design S–N curves relate to the more usual situation of welded structures containing high tensile residual stresses, resulting in effectively high tensile mean stress conditions. However, since tensile residual stresses can also be induced during manufacture or assembly, and, of course, the fatigue loading might produce high tensile mean stress conditions, it is clearly prudent to continue to base design on fatigue test results obtained under high tensile mean stress conditions.

Detail classification. *Transverse butt welds made from both sides.* A weakness with the database used to establish current design curves for transverse butt welds was that no account was taken of possible misalignment in the test specimens. Subsequent research showed this to be highly significant and probably the main source of the wide scatter in the database. There is now an extensive database from transverse butt welds instrumented with strain gauges to measure any misalignment-induced bending [3] that suggests FAT 100. It covers a wide range of geometries, from aligned joints to joints axially-misaligned by up to one plate thickness. Hence, this classification could be assumed to apply to any arc welding conditions or process, regardless of weld profile. This contrasts with current rules which, for example, down-grade submerged arc welds or link the design classification to specified weld profiles, conditions that prove to be somewhat impractical for many industries. A condition on the use of FAT 100 is that allowance must be made for any misalignment (e.g. the maximum allowed by the fabrication Standard) in the calculation of the stress experienced by the welded joint, for example using published formulae [3]. With this approach, the manufacturer can gain commercial advantage, in terms of higher allowable stresses, by using good fabrication practice to minimise misalignment.

Transverse butt welds made from one side. There is mounting evidence that full penetration butt welds made from one side could be upgraded from the current low classification in most rules, sometimes as low as FAT 45, a fillet weld classification. The low classification reflects concern over the ability to produce and inspect full penetration welds with satisfactory weld root bead profiles. Relevant published data from pipe girth welds failing from the root, presented in [4], suggest FAT 80, as shown in Figure 1. As before, this would be applicable to perfectly aligned joints. The wide scatter reflects variations in pipe dimensions, weld type, joint quality, residual stress and the loading conditions. In this respect, a feature of girth welds is that, depending on the pipe dimensions and welding conditions, the residual stresses at the root may be compressive. However, as noted earlier fatigue design rules should not incorporate any benefit from compressive residual stress and therefore test data obtained under high tensile mean stress con-
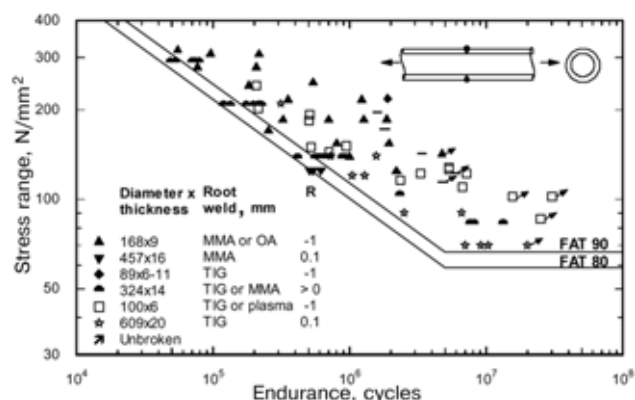
Figure 1. Fatigue test results for steel pipes with girth welds [4]

Figure 3. Influence of surface imperfections on fatigue of electron beam butt welds ([1], unless stated otherwise)

ditions are the most useful. There is no reason to suppose that FAT 80 could not be assigned to full-penetration single-sided butt welds in plates or other sections.

Non-arc transverse butt welds. Fatigue data obtained from arc welded specimens are the main basis of current design *S--N* curves. Appropriate rules for non-arc welds are long overdue. Power beam welding (electron beam or laser) in particular offers great potential for increased productivity, being capable of rapidly welding thick sections from one side in a single pass. An update of results presented previously [1, 5] (Figure 2) provides good support for FAT 100, comparable with the best two-sided arc butt welds. Full penetration welding must be achieved, with identifiable cap and root beads. Their profiles are less critical and the following ranges are all consistent with the data in Figure 2: weld toe angle from 10--50°; weld toe radius from 0.4--4.0 mm; weld bead height from 1.0--2.5 mm; weld bead width from 5--25 mm. However, an important limitation is that all the data were obtained at $R_\sigma = 0.1$ from relatively small-scale specimens that may not have incorporated high tensile residual stresses.

Therefore, it may be prudent to adopt lower FAT 90 for the design of real structures. In such rapid «one-shot» welds there is clearly the danger that it may be difficult to ensure full penetration and incomplete penetration, underfill and undercut are potential flaws. The data in Figure 3 show that flaws up to 1.4 mm deep can reduce the classification to FAT 71
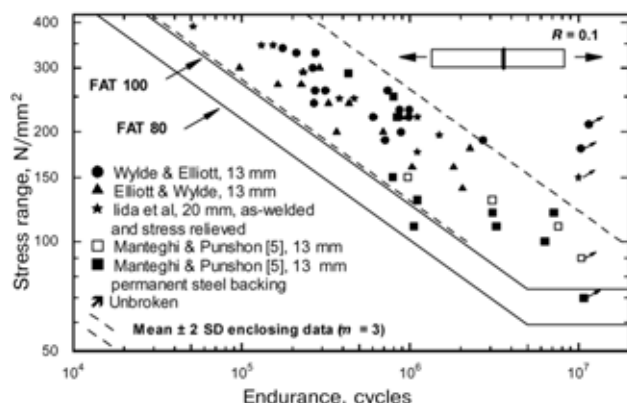
[1, 5]. However, FAT 80 satisfies all the results for flaws less than 1 mm in depth. Clearly, partial penetration welds would not be used deliberately, but such data help in setting acceptance levels for flaws.

Less information is available from laser welds but, as expected, transverse butt welds behave in a similar fashion to electron beam welds (Figure 4) [6--8]. Published data for fillet-type laser welded joints [2] are also consistent with the arc weld design curves.

Friction welding can also be used to make butt joints, usually between rods or tubes, and published data [9, 10] shown in Figure 5 again support FAT 100. However, with such a limited database this needs further confirmation; FAT 80 seems more reasonable at this stage.

A relatively new process that deserves mention is friction stir welding. This is capable of producing butt welds with exceptionally high fatigue strengths (Figure 6), potentially similar to that of the unwelded material [11], and lap joints. Most attention has been focussed on aluminium alloys, but the process is now being developed for application to steel. It is probably premature to provide fatigue design data for friction stir welds, except to note that they perform at least, as well as similar joints made by other welding processes.

Transverse load-carrying fillet welds. An extensive review of published data for cruciform joints failing in the weld throat, performed as part of the revision of UK fatigue rules, indicated that some cur-

Figure 2. Fatigue test results for transverse full penetration electron beam butt welds in steel plate ([1], unless stated otherwise)

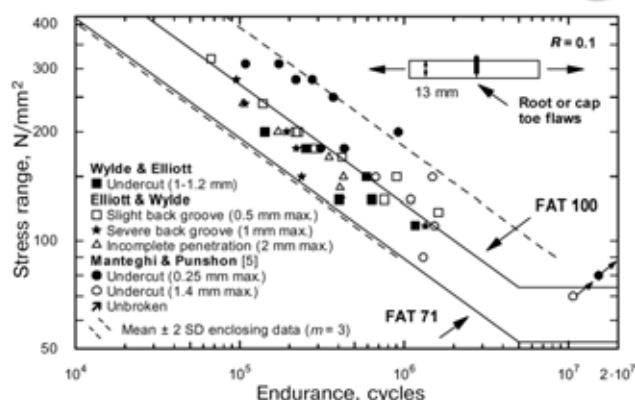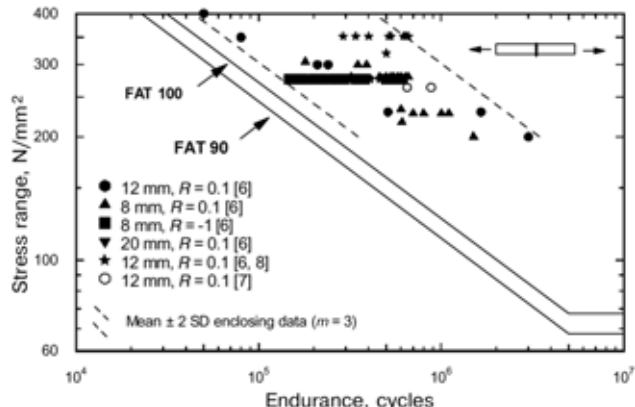**Figure 4.** Fatigue test results for transverse full penetration laser butt welds in steel plate
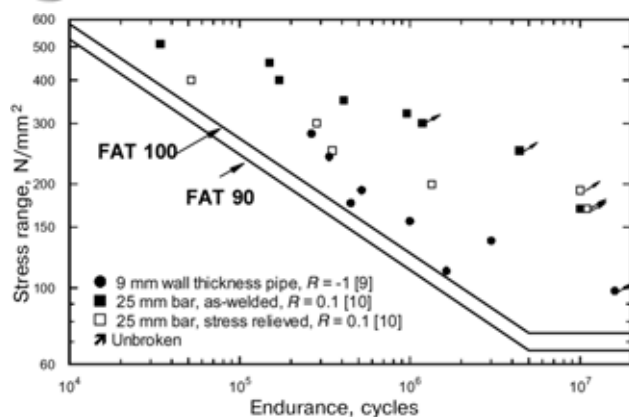
Figure 5. Fatigue test results for friction welds in round-section steel pipes and bars

rent design curves (e.g. IIW FAT 45) were too high [2, 12]. Instead, FAT 36, as used in Eurocode 3 [13], was more consistent with the data. However, closer examination showed that many low results were obtained from welds containing defects and that there was a case for neglecting them and thus retaining FAT 45. However, the review was confined to results obtained at stress ratios (R_σ) close to zero. An important finding subsequent to the review is that cruciform joints are very likely to contain compressive residual stresses at the weld [14], which would serve to improve their fatigue lives at $R_\sigma \approx 0$. Clearly, cruciform joints in real structures might also contain compressive residual stresses. However, as noted earlier, this should be discounted and design based on data obtained under high tensile mean stress conditions. Such data [12, 14–18] (Figure 7) again show that FAT 36 would be the most appropriate classification.

Design data. *Material.* The most comprehensive fatigue design guidance for welded structures relates to steel, although rules are also available for aluminium alloys [19]. Other weldable metals have been rather neglected. Amongst these, stainless steels are widely used. There is growing evidence that the design data for welded joints in typical carbon and carbon-manganese steels are directly applicable to welded stainless steels [20]. A condition is that environmental effects, such as the potentially different corrosion fatigue behaviour of welded carbon steels and stainless steels, would need to be considered separately.
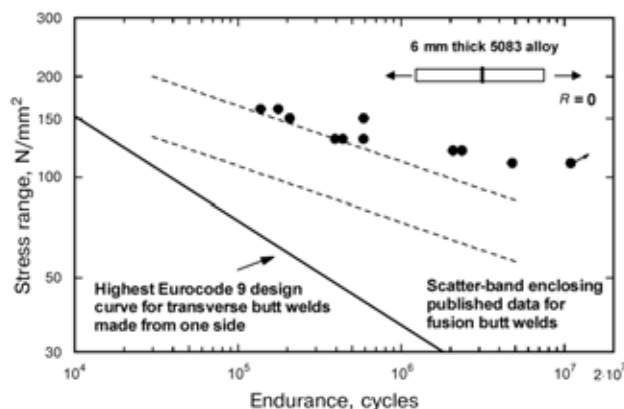
Corrosion fatigue. There is a wealth of fatigue data obtained in sea water. Most relate to North Sea conditions, that is sea water temperatures of 6–10 °C and the wave loading frequency of 0.17–1 Hz. However, they still offer useful guidance that could be relevant in other circumstances. Correction factors to be applied to basic *S–N* curves have been published, notably by the UK HSE [21]. In general, the effect of free corrosion is to reduce fatigue life by a factor of 3 and to eliminate the fatigue limit. Cathodic protection can inhibit corrosion, but it can also be detrimental to fatigue performance as a result of hydrogen embrittlement. Consequently, there is still a design penalty of 2.5 on life at relatively high applied stresses and in-air performance is only achieved at stress levels close to or below the fatigue limit.

Scale effect. It is now generally accepted that there is a geometric scale effect, such that fatigue performance tends to decrease with increase in the dimensions of a welded joint. Since design *S–N* curves tend to be based on data from relatively small-scale specimens, a consequence is that they may need to be reduced when designing real structures. Attention has focussed mainly on the effect of the main plate thickness in welded joints failing from the toe. The resulting well known «thickness effect» is now a feature of most fatigue design rules. It has the form $(T_{ref}/T)^k$, where T is the plate thickness; T_{ref} is the reference plate thickness up to which the design *S–N* curves are directly applicable (typically 13–25 mm); and $k \approx 0.25$. However, a more general scale effect is now recognised, such that the exponent k depends on the severity of the welded joint stress concentration and the scale effect itself is due to more than just plate thickness. As a result, some design rules incorporate the following:

• k varying from 0.1 for mild stress concentrations to 0.3 for severe ones;

• use of an effective thickness T_{eff} which depends on the actual plate thickness and the proportions of the welded joint (Figure 8).

A third effect, neglected in all fatigue design rules, is the potential benefit of smaller dimensions than those associated with the design *S–N* database. Experimental data are still are very limited, but those

Figure 6. Fatigue data obtained from friction stir butt welds in 6 mm 5083 aluminium alloy [11]
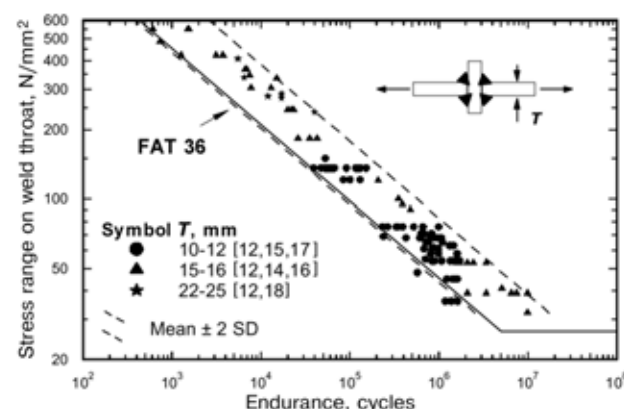

Figure 7. Fatigue data for fillet-welded cruciform joints obtained under either high tensile mean stress or high tensile stress range

in Figure 8 for aluminium [22], which confirm the general trend predicted by fracture mechanics calculations, are expected to be typical. A scale factor of the type shown for $T < 12$ mm would represent a design bonus.

Another scale effect relates to potential fatigue failure in the throats of transverse load-carrying fillet welds. In such cases, fatigue strength depends on, amongst other things, the weld throat size and the extent of incomplete weld penetration. In fillet welded joints (zero penetration), the latter equates to the main plate thickness. Thus, a plate thickness correction will probably be required. However, no such correction has yet been introduced into fatigue rules, the design curves being dependent only on the stress range on the weld throat. Several studies of the size effect in cruciform joints have been performed [12, 23, 24], most based on fracture mechanics fatigue crack growth calculations, sometimes validated by reference to limited test data. A common finding [23, 24] is that fatigue strength decreases with increase in plate thickness in accordance with the factor $(T_{ref}/T)^{0.15}$. Published data, such as those in Figure 7, show no systematic effect of plate thickness in the range 9 to 25 mm, suggesting that FAT 36 is applicable over this range and a thickness correction is only needed for thicker plates. If so, stresses obtained from the FAT 36 design curve would be reduced by applying the factor $(25/T)^{0.15}$ for $T > 25$ mm (with T in mm).

Hot-spot stress approach. A shortcoming of current fatigue design rules is that they have not kept pace with computing developments in design, notably the use of FEM. The basic design method embodied in current fatigue rules was actually developed over 30 years ago, when computers were something of a novelty and structural analysis relied mainly on the use of standard formulae and experience. Thus, it was entirely reasonable that the fatigue rules should be based on the use of nominal stresses. Computer-based analyses like FEM are now routine and, with increased computing power, their capabilities are increasing. Adoption of the hot-spot stress method for designing weld details from the viewpoint of potential failure from the weld toe could remedy the above shortcoming. Although the approach has been applied to tubular structures for over 25 years, only tentative guidance is available on its application to plate structures [25]. Two key issues are: (a) the definition of the hot-spot stress and how it is obtained from stress analysis; (b) the choice of hot-spot stress design S--N curves. In relation to (a), some work has developed the earlier IIW methods based on extrapolation to the weld toe from the surface stresses approaching the weld, for use with either measured or calculated stresses [26]. However, in the context of stresses calculated by FEM analysis another development has been a method based on the through-thickness stress distribution near the weld toe [27]. With regard to (b), tentative hot-spot stress design S--N curves have
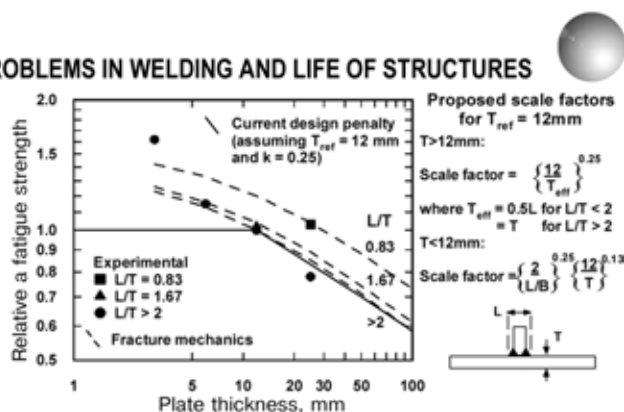

Figure 8. Evidence from an investigation of welded aluminium alloy to support a bonus scale effect factor for thin sections [22]

been proposed on the basis of available data [28]; an example is shown in Figure 9. However, a limitation is that the stress analysis information only allowed the IIW linear extrapolation method to be used to determine the hot-spot stress. Hot-spot stresses obtained by FEM, as would generally be used in design, are not available. Therefore, for the present, FAT 90 or 100 should only be used in conjunction with hot-spot stress values that correspond to the IIW definition. A rather more limited database for aluminium suggested FAT 40 as a suitable hot-spot stress S--N curve [28], but ideally more evidence is needed for a firm recommendation.

Complex loading. One aspect of fatigue design rules that has recently been identified as a weakness are the methods for assessing weld details subjected to complex, combined or multi-axial loading [29]. Of particular concern are situations in which the principal stress directions change during the fatigue loading cycle (i.e. non-proportional loading). The most common approach is to base design on the maximum principal or equivalent stress range with the design S--N curve for uni-directional loading conditions. Experimental data support such an approach for proportional loading, but can give much lower lives than expected under non-proportional loading [29]. In fact, an alternative method is given in the IIW and Eurocode 3 rules, which provide different S--N curves for assessing normal or shear stress, with slopes $m = 3$ or 5, respectively [3, 13]. This is
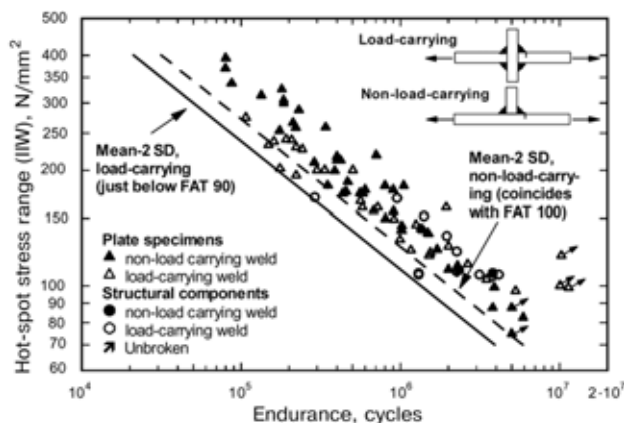

Figure 9. Fatigue test results for welded steel specimens and components expressed in terms of the hot-spot stress range determined using the IIW linear extrapolation method [28]
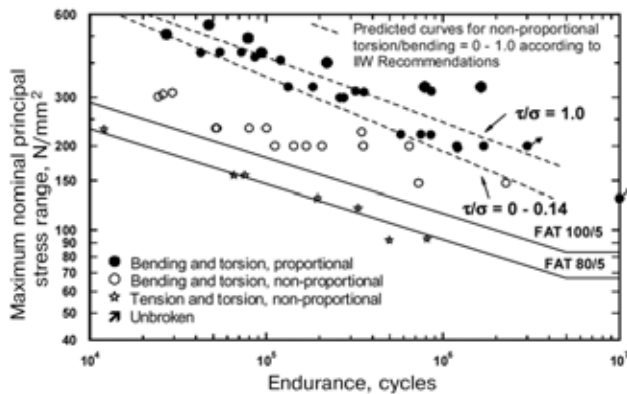
Figure 10. Evaluation of fatigue data for steel flange-pipe fillet welds failing from the toe, tested under combined bending or tension and torsion [30]

$$\left(\sum \frac{n}{N}\right)_{n.s} + \left(\sum \frac{n}{N}\right)_{s.s} \le 1 \quad \text{or} \le 0.5 \qquad (1)$$

in Eurocode 3 and in IIW, respectively, at the end of the fatigue life, where n is the number of applied stress cycles, and N is the endurance from the appropriate design curve at that stress. The lower IIW summation value reflects the preliminary indications that non-proportional loading was more damaging than proportional. However, as seen in Figure 10, even this approach can be unsafe when applied to actual data [30].

This problem has prompted a number of research studies and has led to alternative methods for correlating fatigue data for welded joints obtained under simple uni-axial and complex combined for multi-axial loading conditions. However, these are still considered to be too complex for general application in design and an alternative, interim approach was sought on the basis of a review of available fatigue data [30]. It was found that non-proportional loading conditions were only a problem if the applied shear stress contribution could give rise to a shear fatigue failure mode (i.e. mode III in fracture mechanics terms), as is the case with torsion applied to tube to plate joints. Otherwise, as in the case of beams subjected to combined bending and torsion, the normal stress contribution seems to dominate and the principal stress range is sufficient for correlating combined
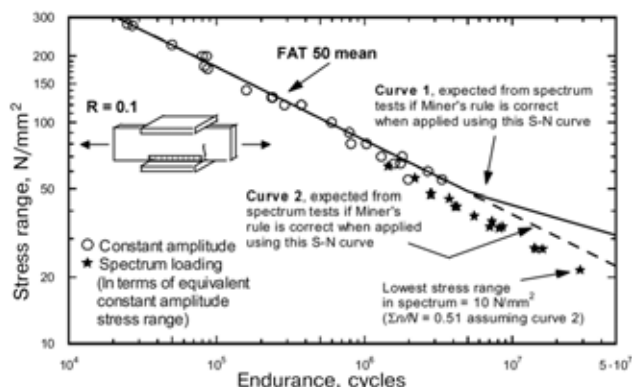

Figure 11. Fatigue test results that illustrate the damaging effect of stresses below the fatigue limit and the inaccuracy of Miner's rule [33]

stress data with data obtained under uni-directional loading, even under non-proportional loading [30]. However, if the applied shear stress component causes mode III fatigue failure, this is the stress that seems to dominate and the resulting fatigue performance is more in line with that obtained under shear loading alone, resulting in a shallower S–N curve than that for normal stress conditions. The data are lower than those obtained under shear stress alone, covered by FAT 100 / 5 (i.e. FAT 100 with $m = 5$), and consequently the final proposal for an interim design curve is FAT 80 / 5, as shown in Figure 10. A practical problem when choosing the appropriate design curve is the need to assess whether or not mode III fatigue fracture is likely to occur. It is clear that it can be induced under applied torsion and, for the present, it is suggested that FAT 80 / 5 is confined to cases of combined torsion and axial or bending loads. Otherwise, FAT 80 / 3 would be appropriate.

Cumulative damage. The final topic of major practical importance is the validity of the current method of assessing cumulative fatigue damage under variable amplitude loading. All the main fatigue rules specify Miner's rule, namely at failure

$$\frac{n_1}{N_1} + \frac{n_2}{N_2} + \frac{n_3}{N_3} + \dots = \sum \frac{n_i}{N_i} \le 1, \qquad (2)$$

where n_i are the numbers of applied stress cycles at stress ranges S_i, and N_i are the endurances obtained from the design curve at S_i. In addition, allowance is made for the fact that once fatigue cracks have started to propagate under stress levels above the constant amplitude fatigue limit (CAFL), stresses below that limit will gradually become damaging and hence cannot be neglected. The common method is to extrapolate the S–N curve beyond the CAFL at a shallower slope, typically $m = 5$ instead of 3.

However, there is mounting evidence from fatigue tests performed under random fatigue loading that there are two potential errors in the above approach:

• the majority of experimental data show that $\Sigma n / N < 1$ at failure, typically around 0.5 [31];

• stress levels below the CAFL appear to be more damaging than assumed using the above «bent» S–N curve approach [32].

Recent fatigue test results that illustrate both these points [33] are shown in Figure 11. In that case, under spectrum loading stresses as low as 10 N / mm², around 25 % of the CAFL and corresponding to $N = 5.7 \cdot 10^7$ cycles on the extrapolated constant amplitude S–N curve, were just as damaging as implied by that curve. Furthermore, the spectrum-loaded specimens all failed after around 50 % of the expected life according to Miner's rule. As discussed previously [2], it is thought that the basic concept of the linear cumulative damage rule does not apply because the crack closure conditions for a given stress fluctuation are different under variable and constant amplitude loading, being more damaging under the former. An argument to explain why stresses below the CAFL are more damaging than expected is that they depend

on the fracture mechanics threshold stress intensity factor which, in general, predicts a lower effective fatigue limit than constant amplitude testing [32]. However, there are still no sound quantitative explanations for the two deficiencies in the current cumulative damage method. Further research is clearly needed but, meanwhile, it is suggested that, as an interim solution, the constant amplitude S--N curve should be extrapolated without a slope change down to an effective fatigue limit corresponding to $N = 10^8$ cycles. At the same time, it would seem prudent to adopt a lower Miner's rule summation 1.0, perhaps 0.5.

CONCLUSIONS

Based on a review of fatigue of welded structures, the following changes to design rules are recommended:

• FAT 100 is a suitable design curve for any full-penetration transverse butt weld made from both sides, provided allowance is made for misalignment-induced bending;

• growing evidence from tests on pipes supports an upgrade to FAT 80 for full-penetration transverse butt welds made from one side, but tight control over alignment is required;

• FAT 90 is recommended for full penetration transverse butt welds made from one side by electron beam welding. Root flaws up to 1 mm deep are tolerable if FAT 80 is used;

• design curves for arc welded joints are applicable to laser welds;

• published data suggest that friction and friction stir welds exhibit superior fatigue properties to arc welds. However, the database is too small to justify upgrades yet;

• FAT 36 is the appropriate design curve for transverse load-carrying fillet welds with respect to potential weld throat failure, used with the correction term $(25/T)^{0.15}$;

• excluding environmental considerations, the design rules for carbon steel are equally applicable to welded stainless steels;

• the «thickness effect» factor should be revised to introduce a bonus for thin sections;

• FAT 90 and 100 are recommended for assessing potential weld toe failure in load-carrying and non-load-carrying steel welds respectively using the IIW hot-spot stress range;

• the IIW and Eurocode damage summation methods for assessing combined normal and shear stresses are unsafe for non-proportional loading. The alternative use of FAT 80/5 in conjunction with the maximum nominal principal stress range is recommended instead for combined torsion and bending or tension, or FAT 80/3 for other cases;

• Miner's rule should be used with S--N curves extrapolated down to an effective fatigue limit at 10^8 cycles without a slope change and assuming a summation value of 0.5.

1. Maddox, S.J. (1992) Fatigue design of welded structures. In: *Engineering design in welded constructions*. Oxford: Pergamon Press.

2. Maddox, S.J. (1997) Developments in fatigue design codes and fitness-for-service assessment methods. In: *Proc. of IIW Conf. on Performance of Dynamically Loaded Welded Structures*. New York: WRC.

3. (1996) *Fatigue design of welded joints and components*. Abington: IIW.

4. MacDonald, K.A., Maddox, S.J., Haagensen, P.J. (2000) Guidance for fatigue design and assessment of pipeline girth welds in free span. *OTH 2000 043*. Bootle: HSE.

5. Manteghi, S., Punshon, C.S. (1995) Fatigue tests on electron beam welded C–Mn steel butt joints. *TWI Research Report 520/1995*.

6. (1994) Analytical and experimental examinations of the fatigue of thick plates. *L-SHIP/WG2(94).20*.

7. Nielsen, S.E. (1994) Laser welding in ship construction. *L-SHIP/WG2(94).24*. TWI.

8. Weichel, F., Petershagen, H. (1995) Fatigue strength of laser welded structural steels with thicknesses between 8 and 20 mm. *IIW Doc. XIII-1590--95*.

9. Knight, J.W. (1976) Fatigue tests on friction welded pipes. *TWI Report 3/1976/E*.

10. Manteghi, S. (1997) Some fatigue tests on friction welded steel bars. *IIW Doc. XIII-1681--97*.

11. Threadgill, P.L. (1998) Friction stir welding — the state of the art. *TWI Research Report 7417.01/98/1012.02*.

12. Gurney, T.R., MacDonald, K.A. (1995) Literature survey on fatigue strengths of load carrying fillet welded joints failing in the weld. *Offshore Technology Report OTH 91 356*. HSE.

13. (1992) *Eurocode 3: Design of Steel Structures. prENV 1993-1-1*. Brussels: ECS.

14. Mori, T., Kainuma, S., Ichimiya, M. (2000) A study of fatigue crack initiation points in load-carrying type of fillet welded joints. *IIW Doc. XIII-1832--2000*.

15. (1979) Fatigue investigation of typical welded joints in steel Fe E460 as compared to Fe E355. *EUR-Report No.6340*. Luxembourg: EC.

16. Friis, L.E., Sperle, J.O., Wallin, L.E. (1971) Fatigue strength of welded joints ---- some Swedish results during recent years. In: *Proc. of Conf. on Fatigue of Welded Structures*. Abington, Cambridge: TWI.

17. (1975) Etude due comportement en fatigue classique de joints types soudes qualite industrielle. *EUR-Report No.5266*. Luxembourg: EC.

18. Watanabe, M., Nagai, K., Hioki, S. (1973) An elasto-plastic fracture mechanics approach to fatigue crack propagation and its application to the estimation of the fatigue life of transverse fillet welded cruciform joints. *IIW Doc. XIII-694–73*.

19. *Eurocode 9: Design of Aluminium Alloy Structures*. Part 2. Structures Susceptible to Fatigue. prENV 1999. Brussels: ECS.

20. Branco, C.M., Maddox, S.J., Sonsino, C.M. (2001) Fatigue design of welded stainless steels. *ECSC Report EUR 19972*. Luxembourg: EC.

21. (1995) Offshore installations: *Guidance on design, construction and certification*. 4th ed. London: UK HSE.

22. Maddox, S.J. (1995) Scale effect in fatigue of fillet welded aluminium alloys. In: *Proc. of 6th Int. Conf. on Aluminium Weldments*. AWS.

23. Nykanen, T. (1998) Geometric dependency on fatigue strength in transverse load-carrying cruciform joint with partial penetration K-welds. *IIW Doc. XIII-1709--98*.

24. Mori, T., Kainumu, S. (2001) A study of fatigue strength evaluation method for load-carrying fillet welded cruciform joints. *IIW Doc. XIII-1884–01*.

25. Niemi, E. (1996) *Stress determination for fatigue analysis of welded components*. Abington: IIW.

26. Fricke, W. (2001) Recommended hot-spot stress analysis procedure for structural details of FPSOs and ships based on round-robin FEM analysis. In: *Proc. of 11th Int. Offshore and Polar Eng. Conf*.

27. Dong, P. (2001) A structural stress definition and numerical implementation for fatigue analysis of welded joints. *Int. J. Fatigue*, **23**, 865--876.

28. Maddox, S.J. (2001) Hot-spot fatigue data for welded steel and aluminium as a basis for design. *IIW Doc. XIII-1900a–01*.

29. Sonsino, C.M. (1997) Multiaxial and random loading of welded structures. In: *Proc. of IIW Conf. on Performance of Dynamically Loaded Welded Structures*. New York: WRC.

30. Maddox, S.J., Razmjoo, G.R. (2001) Interim fatigue design recommendations for fillet welded joints under complex loading. *Fatigue Fract. Eng. Mater. Struct.*, **24**, 329.

31. Gurney, T.R. (1992) A summary of variable amplitude fatigue data for welded joints. *OTH Report No. 91 395*. London: HMSO.

32. Niemi, E. (1997) Random loading behaviour of welded components. In: *Proc. of IIW Conf. on Performance of Dynamically Loaded Welded Structures*. New York: WRC.

33. Gurney, T.R. (2001) Exploratory investigation of the significance of the low stresses in a fatigue loading spectrum. *IIW Doc. XIII-1899–01*.

EVALUATION OF CORROSION FATIGUE STRENGTH OF WELDED JOINTS AS HETEROGENEOUS SYSTEMS

V.V. PANASYUK and **I.M. DMYTRAKH**

G.V. Karpenko Physical-Mechanical Institute, NASU, Lviv, Ukraine

The paper describes experimental-analytical methods of evaluation of local corrosion and local fracture of welded joints of the type of «anticorrosion cladding–casing steel». The constructed diagrams of electrochemical resistance and corrosion crack resistance of multilayer welded joints may be the basis for evaluation of the residual life of the considered joints.

Problem of effectively ensuring the reliability and fatigue life of critical welded structures, which are exposed to aggressive corrosive media in service, is still urgent for power generation, chemical engineering and other industrial sectors. This is attributable to the fact that such materials or structural elements are ever wider used, which are heterogeneous systems in terms of electrochemistry, and initiation and running of corrosion processes in them is of a complex multi-stage nature. A typical example are welded joints of dissimilar materials and structural elements with protective anticorrosion cladding. As indicated by engineering practice [1] such structural elements are characterized by a somewhat unpredictable nature of the processes of corrosion and corrosion-mechanical damage, which result from sudden changes in the operating conditions, violation of technological modes, etc.

A significant drawback of the existing approaches [2, 3] to evaluation of fatigue life of structural elements of welded joints is a formalized and rather limited allowance for the factor of the aggressive operating medium. Corrosive medium is regarded as a constant (independent) parameter, which characterizes only the testing conditions, but does not adequately reflect the physico-chemical situation in the weld zone, which is the determinant one in the significant lowering of the operating reliability of welded joints under the impact of working media. A whole range of physico-chemical processes, often competing with each other, may run in such a heterogeneous

Figure 1. Schematic of the welded joint

system with varying degrees of probability. These processes lead to degradation of the mechanical properties of the welded joint, both through intensive anode dissolution of the material (initiation of pittings, corrosion pits, etc.), and through hydrogen embrittlement of the weld zone (acceleration of the processes of microcrack formation and initiation and propagation of macrocracks).

Considering these features, the paper suggests methods for evaluation of the corrosion resistance and corrosion fatigue strength of such a specific welded joint as two-layer anticorrosion cladding--casing steel (ACC--CS) [4], which is widely used for anticorrosion protection of casing structures in power engineering and petroleum processing.

Object and aim of investigations. The base of the welded joint was 15Kh2MFA casing steel (1), on the surface of which two layers of anticorrosion cladding were applied: first of 07Kh25N13 steel (2) of ≈ 4 mm thickness and the second of 04Kh20N10G2B steel (3) of ≈ 3.5 mm thickness (see Figure 1 and Table 1).

The purpose of these investigations was determination of electrochemical behaviour of individual components of the welded joint and their fusion zones, as well as determination of basic parameters of its corrosion cyclic crack resistance. Procedural basis of the investigations were original methods of physico-chemical and chemical-mechanical studies, developed in Physical-Mechanical Institute of the NAS of Ukraine [5]. All the investigations were conducted in 1 % water solution of H_3BO_3 with KOH addition up to pH 8 ($T = 25$--80 °C), which was the model of the so-called boron-controlled reactor water [6]. Frequency of corrosion fatigue testing was $f = 0.017$ Hz at the coefficient of asymmetry of the loading cycle $R = 0$. Testing in air was also conducted ($f_1 = 1$ Hz, $R = 0$, $T = 25$ °C) for comparative evaluation of the influence of corrosive medium on fatigue crack growth in the studied joint.

Since in the studied welded joint, as in the respective inhomogeneous (heterogeneous) system the fusion zones between the materials are potentially the most critical ones, it is first of all important to evaluate their real size (thickness). Used for this purpose was X-ray structure analysis of the fusion zones to establish the distribution in them of such basic ele-
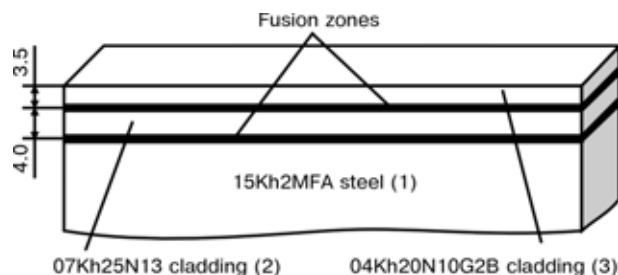
Table 1. Composition of components of the welded joint of two-layer ACC–CS

| No.	Steel	Element content, wt.%						
		C	Cr	Ni	Mn	Cu	V	Fe
1	15Kh2MFA	0.15	2.0	--	--	< 1.0	< 1.0	Balance
2	07Kh25N13 cladding	0.07	25.0	13.0	--	--	–	Same
3	04Kh20N10G2B cladding	0.04	20.0	10.0	2.0	--	–	»

ments as chromium, nickel and manganese. Scanning was conducted in the range of 1 mm (±0.5 mm from the visible line of separation of the joint materials). Scanning results were used to plot the dependencies of weight fraction of the element in percent versus scanning range. These dependencies were the basis for evaluation of the extent of the respective fusion zones. It was established, that the thickness of the zone of fusion between 04Kh20N10G2B and 07Kh25N13 cladding is $\approx 300~\mu m$, and for the fusion zone of 07Kh25N13 cladding–casing steel 15Kh2MFA it is in the range of 150 μm.

Electrochemical characteristics of materials and fusion zones. Volt-ampere studies [5, 7] of individual materials of the joint and their fusion zones were performed by layer-by-layer sectioning of the sample. Obtained potentiodynamic polarization curves were used to determine the following electrochemical characteristics: corrosion potential E_{cor} and corrosion current density i_{cor}, as the parameters, which describe the condition of the metal surface in the case of free corrosion, as well as anode b_a or cathode b_c Tafel coefficients, as qualitative parameters of implementation of initial electrochemical mechanisms at potential deviations from the sample surface to the anode or cathode side [8, 9].

It is established that all the determined basic parameters are indicative of a high electrochemical activity of casing steel 15Kh2MFA compared to the cladding materials. Parameters of the fusion zone between the casing material and 07Kh25N13 cladding have intermediate values in relation to materials, which form it. Material in the fusion zone between the two claddings layers has much lower indices of

corrosion resistance than the cladding materials proper. In this case, it was found that values of corrosion potential (Figure 2, *a*) for the base steel are lower by 250--300 mV than similar parameters of the cladding. Fusion zone between the base steel and 07Kh25N13 cladding has corrosion potential close to that of the base steel. Value of corrosion potential of the fusion zone between the two cladding layers reaches the value of --0.490 V, which is by 100--170 mV lower compared to those for the cladding proper (--0.320 V for steel 04Kh20N10G2B and –0.390 V for 07Kh25N13 steel, respectively). Analysis of the density of corrosion current (Figure 2, *b*) showed that for the base casing steel its value varies close to 0.0057 A/m^2, and for 04Kh20N10G2B cladding its value does not exceed 0.0054 A/m^2. The lowest values of density of corrosion currents were registered for the case of 07Kh25N13 cladding (i_{cor} = = 0.0023 A/m^2). It should be noted that in the zone of fusion between the two cladding layers the density of corrosion current is up to 0.0067 A/m^2. Therefore, in this zone the electrochemical processes will proceed at the highest rate, and it is a potentially critical zone in terms of corrosion resistance.

Electrochemical behaviour of joints of ACC--CS at crevice corrosion. Cases of crevice corrosion in structural elements are rather wide-spread in service and are believed to be some of the most hazardous in terms of corrosion damage of metals [10]. In order to study the conditions of crevice corrosion in the welded joint of ACC--CS, a flat slot was simulated, which was formed by two surfaces of the studied material [4]. The fixed width of the slot (0.12 mm) was achieved by using an inert film. In testing one surface
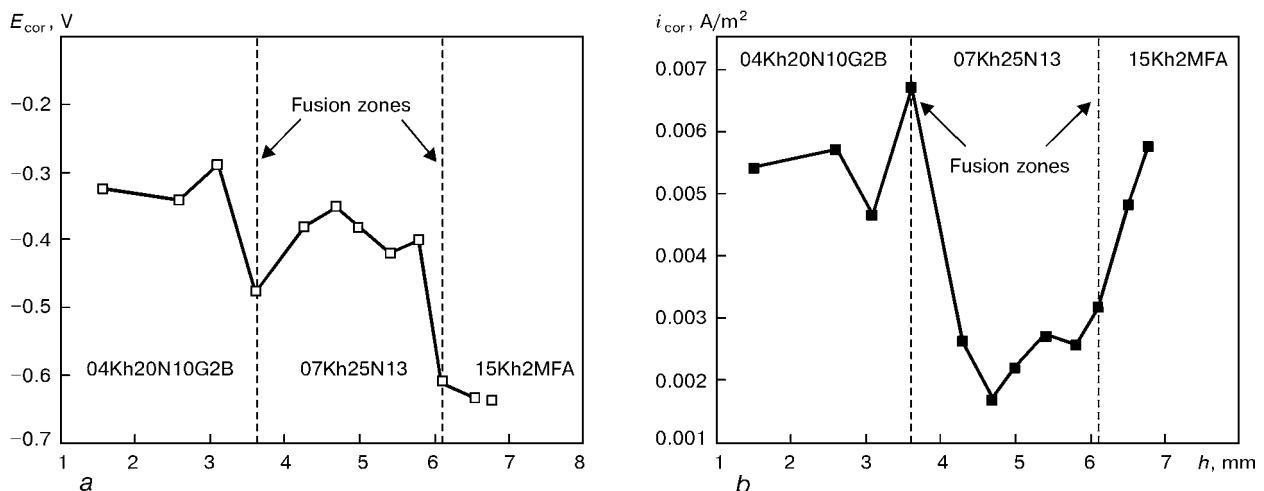
Figure 2. Change of corrosion potential (*a*) and density of corrosion current (*b*), depending on the section depth *h* of welded joint of ACC–CS
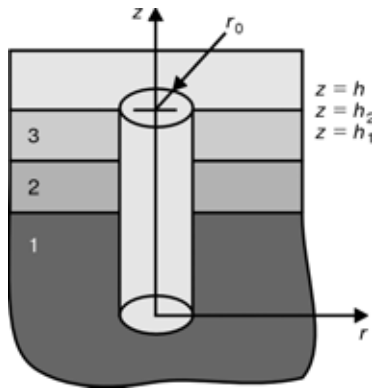
Figure 3. Schematic of a corrosion pit

Table 2. Comparison of the values of corrosion potentials E_{cor} and densities of limit currents i_l for the cases of studying an open surface and a crevice

Steel	Object of study	E_{cor}, V	i_l, A/m^2	$\dfrac{i_l \text{ (slot)}}{i_l \text{ (surface)}}$
15Kh2MFA	Surface	−0.539	0.0334	5.31
	Slot	−0.467	0.1772	
07Kh25N13	Surface	−0.330	0.0102	5.34
	Slot	−0.397	0.0545	
04Kh20N10G2B	Surface	−0.422	0.00995	14.27
	Slot	−0.469	0.1423	

of the slot was connected to the potentiostate and was the main electrode (the working potential of which varied), and the other remained in the free corrosion condition. As a result, anode polarization curves were obtained for the component materials of the studied welded joint (07Kh25N13 and 04Kh20N10G2B cladding, 15Kh2MFA casing steel) at crevice corrosion, which were compared to similar polarization curves, obtained under the conditions of an open surface. These curves were the basis to determine the respective values of corrosion potential E_{cor} and densities of limit currents i_l [5] for the cases of an open surface and a slot (Table 2).

Obtained results show that for the studied joints of ACC--CS the anode processes in the slots proceed much more intensively, compared to the open surface (Table 2). Special attention should be given to the case of crevice corrosion for 04Kh20N10G2B cladding, where the intensity of anode processes in the crevice is higher by an order of magnitude, compared to the intensity of these processes on an open surface.

Mathematical model and analytical evaluation of electrochemical corrosion of a welded joint as a multielectrode system. Let us analyze [11, 12] a corrosion pit of a circular cylindrical shape, which penetrates through a two-layer cladding into the base material (Figure 3).

Let us write the two relationships for determination of density of corrosion current, i, which are required for subsequent analysis. First of them [8, 9] is as follows:

$$i = (E_{st} - E)/b, \qquad (1)$$

where E and E_{st} are the equilibrium and stationary (i.e. established at electric current running) electrode potentials; b is the specific polarization resistance.

On the other hand, in keeping with the definition of electrode potential as a difference of electric potentials of the metal surface and the electrolyte on the boundary of a double electric layer, we may write that

$$E_{st} = \psi_m - \psi_c, \qquad (2)$$

where ψ_m and ψ_c are the potentials of the metal and electrolyte. As the electric conductivity of metal is approximately 10^6 times higher than that of the electrolyte, we may assume that

$$\psi_m = \text{const} \cong 0. \qquad (3)$$

Proceeding from equalities (1)--(3), we obtain the second relationship to determine i:

$$i = -(E + \psi_c)/b. \qquad (4)$$

The internal surface of the pit is a three-electrode system. To study the corrosion currents in it, let us introduce as it is done in [13], z ---- component of the total current across the pit cross-section $i(z)$ and averaged electric potential $\psi(z)$, i.e. in terms of electric processes, we will regard the pit as a long line. Such an approach is acceptable, if the cross-sectional dimensions of the pit are small, compared to its depth [13]. Let us constitute balance equations for $i(z)$ and $\psi(z)$. With this purpose, let us consider the change of values $i(z)$ and $\psi(z)$ when $J(z)$ and z increases by dz. In this case, change di of the total current, when z shows an increment, is due to sink (outflow) of current along the side surface of the pit, and in keeping with relationship (4), we may write that

$$di(z)/dz = -2\pi r_0 [E(z) + \psi_c(z)]/b(z). \qquad (5)$$

In equation (5) and further on the electric potential of the medium is taken to be equal across the cross-section, i.e. $\psi_c(r, z) = \psi_c(z)$. From Ohm's law for a column of the medium of height dz, we have

$$d\psi_c/dz = -i(z)/(\pi r_0^2 k), \qquad (6)$$

where k is the specific electric conductivity of the medium.

Let us now consider value $\psi_c(z)$. Let us differentiate with this purpose equality (6) with respect to z and substitute $di(z)/dz$ into it from equality (5). We will have

$$[d^2/dz^2 - s^2(z)]\,\psi_c(z) = s^2(z)\,E(z), \qquad (7)$$

where

$$s(z) = \sqrt{2/[r_0 k b(z)]}. \qquad (8)$$

In our case we will assume the equivalent electrode potentials E_n and specific polarization resistances b_n to be constant for each n-th region ($n = 1, 2, 3$ for regions $0 < z < h_1$, $h_1 < z < h_2$, $h_2 < z < h$). Let us introduce into analysis the following new functions:

$$\psi_n = \psi_c + E_n. \qquad (9)$$

Then, from equation (7) we have

$$(d^2/dz^2 - s_n^2)\,\psi_n = 0,\ n = 1,\ 2,\ 3, \qquad (10)$$

where

$$s_n = \sqrt{2/[r_0 k b_n]}. \qquad (11)$$

Density of corrosion current, in keeping with relationships (4) and (9) becomes:

$$i_n = -\psi_n/b_n. \qquad (12)$$

Specific values of coefficients s_n and respective solutions of equations (10) depend on what are the polarization resistances, namely anode or cathode, and this is determined by the relationship between the equilibrium electrode potentials and polarization resistances of individual materials and geometrical parameters of the system.

If the anode and cathode resistances of each individual electrode are equal to each other, then substituting their values into relationships (10)--(12) it is possible to find from them at the appropriate boundary conditions (which will be defined below), the corrosion currents, including their sign, and thus determine, whether a certain electrode is the anode or cathode. In the general case, when the anode and cathode resistances are different for a specific n-th electrode when selecting b_n, it is necessary to know in advance, what this electrode is in the considered system: anode or cathode. This issue is partially solved, based on comparison of the values of equilibrium electrode potentials of individual electrodes. Let us illustrate it for the case when $E_1 < E_2 < E_3$. From here it follows that the base material is the anode, the upper layer of the coating is the cathode, and the lower layer can in the general case be partially the anode and partially the cathode. Let us consider this case. Let z_0 be the interphase of these regions. It is obvious that the cathode region of the second material should be the one, adjacent to the first ($h_1 < z < z_0$), and the anode region should be the one, adjacent to the third material ($z_0 < z < h_2$). Then, the region of the crevice ($0 < z < h$) will be divided into four subregions, for which the solutions of equation (10) will be as follows:

$$\psi_{1a}(z) = c_1 \exp(-s_{1a}z) + d_1 \exp(s_{1a}z),\ \ 0 < z < h_1,$$
$$\psi_{2k}(z) = c_{2k} \exp(-s_{2k}z) + d_{2k} \exp(s_{2k}z),\ \ h_1 < z < z_0,$$
$$\psi_{2a}(z) = c_{2a} \exp(-s_{2a}z) + d_{2a} \exp(s_{2a}z),\ \ z_0 < z < h_2, \qquad (13)$$
$$\psi_3(z) = c_3 \exp(-s_{3k}z) + d_3 \exp(s_3z),\ \ h_2 < z < h.$$

Here

$$s_{1a} = \sqrt{2/[r_0 k b_{1a}]};\ \ s_{2k} = \sqrt{2/[r_0 k b_{2k}]};$$
$$s_{2a} = \sqrt{2/[r_0 k b_{2a}]};\ \ s_{3k} = \sqrt{2/[r_0 k b_{3k}]}; \qquad (14)$$

b_{na} and b_{nk} ($n = 1,\ 2,\ 3$) are the specific anode and cathode polarization resistances of n-th material. Thus, equations (13) include nine unknown values: c_1, d_1, c_{2k}, d_{2k}, c_{2a}, d_{2a}, c_3, d_3, z_0. They are defined from boundary conditions at $z = 0$ and $z = h$, conditions of continuity at $z = h_1$, h_2, z_0.

1. *Condition at $z = 0$ (bottom of the pit)*. In keeping with relationship (4) full current from the bottom will be $i_{(z=0)} = -\pi r_0^2(E_1 + \psi_{c(z=0)})/b_{1a}$. Let us substitute into this equality $i_{(z=0)}$ from equation (6) and allowing for equality (9), we obtain

$$(d\psi_1/dz - \nu_0\psi_1)\,|_{z=0} = 0,\ \ \nu_0 = (\kappa b_{1a})^{-1}. \qquad (15)$$

2. *Condition at $z = h$ (top of the pit)*. According to [9] (formula (19)) and the above (9), we have

$$(d\psi_3/dz + \nu_h\psi_3)\,|_{z=h} = 0,$$
$$\nu_h = (1 - 2I(q))/(2\kappa b_{3k}I(q)),$$
$$F(q) = \int_0^\infty \frac{I_1^2(\lambda)\,d\lambda}{\lambda(1 + q\lambda)},\ \ \ q = \kappa b_{3k}/r_0, \qquad (16)$$

where, $I_1(\lambda)$ is the Bessel function of the 1st kind 1st order. It should be noted that equality (16), as shown in [9], integrally takes into account the electric neutrality of the system pit + end face ($r_0 < r < \infty$, $z = h$).

3. *Conditions at $z = h_1$, $z = h_2$* express the continuity of potential $\psi_c(z)$ and $d\psi_c(z)/dz$. Taking (9) into account, these conditions have the following form:

$$(\psi_1 - \psi_{2k})\,|_{z=h_1} = E_1 - E_2,\ \ d((\psi_1 - \psi_{2k}))/dz\,|_{z=h_1} = 0, \quad (17)$$

$$(\psi_{2a} - \psi_3)\,|_{z=h_2} = E_2 - E_3,\ \ d((\psi_{2a} - \psi_3))/dz\,|_{z=h_2} = 0. \quad (18)$$

4. *Three conditions at $z = z_0$*. Two of them follow from the equality of zero density of the anode and cathode currents in this point. In keeping with relationships (12) they have the following form:

$$\psi_{2k}(z_0) = 0,\ \ \psi_{2a}(z_0) = 0, \qquad (19)$$

the third follows from continuity of $d\psi_c(z)/dz$:

$$[d\psi_{2a}(z)/dz - d\psi_{2k}(z)/dz]\,|_{z=z_0} = 0. \qquad (20)$$

Thus, the system of relationships (12)--(20) determines the density of corrosion currents on the inner surface of the pit. System of equations (15)--(20) may have no real solutions. This means that the second electrode (lower layer of the coating) is a complete anode or complete cathode. Such a situation will mostly be in place in the case considered below. It is obvious, that when the coating has more than two layers, the above method may also be used, if on the new interphases we take into account the conditions, similar to conditions (17) and (18).

The above analytical-numerical method cannot be applied, when the pit bottom is on the level of metal interphase (for instance $h_1 = 0$). In this case region $0 < z < h_1$ falls out, and ψ_{1a} should be excluded from relationships (13), and the process in the pit should be described by functions ψ_{2a}, ψ_{2k} and ψ_3. In this case, it is necessary to take into account the impact of the first material only through the pit bottom ($z = h_1 = 0$) by definition only for the bottom of the boundary condition, which is derived below.

Full current from the bottom, in keeping with relationships (4) and (9) will be equal to

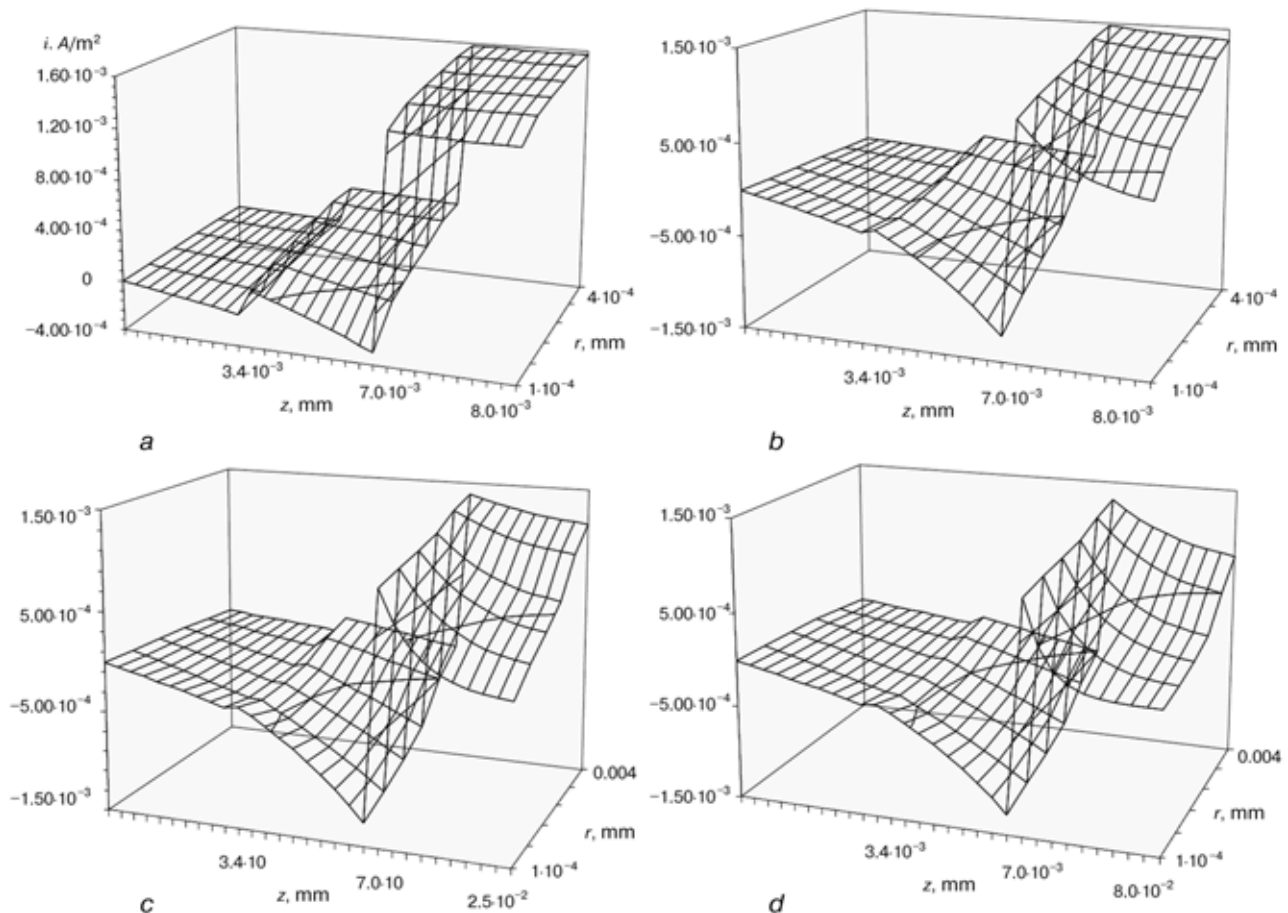$$i_{(z=0)} = -\pi r_0^2(E_1 + E_{2(z=0)} - E_2)/b_{1a}, \qquad (21)$$

Figure 4. Density of corrosion current from the surface of a cylindrical pit of variable radius r and constant depth h in the welded joint of ACC--CS: a — $h = 8$; b — $h = 16$; c — $h = 25$; d — $h = 40$ mm

and in keeping with (6) and (9)

$$i(z = 0) = - (\pi r_0^2 \kappa) d\psi_2 / dz |_{z = 0}. \qquad (22)$$

From equalities (21) and (22) we obtain the condition for the pit bottom:

$$(d\psi_2 / dz - \nu_0 \psi_2) |_{z = 0} = \nu_0 (E_1 - E_2), \ \nu_0 = (kb_{1a})^{-1}, \ (23)$$

which replaces condition (15). Equalities (17) are excluded from the system of conditions.

Let us demonstrate the implementation of the described method for evaluation of the density of corrosion current from the surface of a cylindrical pit of variable radius r and constant depth h in a welded joint of ACC–CS. Pits of various dimensions were considered, namely of radius $r_0 = (0.1$--$4.0)$ mm and total depth $h = 8, 16, 25$ and 40 mm. Working medium was 1 % water solution of $H_3BO_3 + KOH$ with up to pH 8 with the electric conductivity $k = 1 / 6$ $(Ohm \cdot m)^{-1}$, which is the model of boron-controlled reactor water [6]. The methods of standard potentiostatic measurements [7] were used to determine the equilibrium electrode potentials of welded joint materials: $E_1 = $ --0.345 V, $E_2 = $ --0.165 V, $E_3 = $ --0.149 V and their specific polarization resistances in $Ohm \cdot m^2$: $b_{1a} = 120$, $b_{2k} = 130$, $b_{2a} = 45$ and $b_{3k} = 80$ in order to perform calculations.

Calculation results are given in Figure 4, where distribution of density of corrosion currents from the side surface of the pit along axis z is given from the opening (extreme left points) to the bottom (extreme right points). Obtained data indicate that irrespective of the pit depth, the base material always is the anode, and the anode current density decreases with the increase of the pit depth. At a small penetration of the pit into the base material, both the cladding layers are the cathodes, but at the total depth of the pit $h \geq 15$ mm the cladding layer, adjacent to the base material partially becomes the anode. In this case, in the entire range of variation of the pit radii ($0.1 \leq r_0 \leq 4.0$ mm), the anode current density rises with increase of r_0.

Therefore, various combinations of anode–ca-thode can be implemented in the welded joint as a multielectrode system, depending on the pit dimensions. Thus, development of various electrochemical conditions is exactly what will determine the nature of corrosion fatigue fracture of such a heterogeneous system.

Electrochemical conditions in corrosion fatigue cracks in the case of their different location in the welded joint of ACC--CS. Electrochemical conditions, which may arise in corrosion fatigue cracks with their different location relative to the materials of the joint and fusion zones, were studied to evaluate the electrochemical mechanisms of the influence of the environment on the process of corrosion fatigue fracture of this welded joint. For this purpose five batches of samples were tested, which differ by the length of

the initial fatigue crack: in the first batch the crack tip was located in 04Kh20N10G2B cladding, in the second batch it was located between 04Kh20N10G2B and 07Kh25N13 cladding, in the third batch in 07Kh25N13 cladding, in the fourth batch in the fusion zone between 07Kh25N13 cladding and casing steel 15Kh2MFA, in the fifth batch in casing steel 15Kh2MFA. This permitted establishing the electrochemical conditions at the tip of a stationary crack separately for each component of the welded joint of ACC--CS.

Local electrochemical studies in the fatigue crack cavities were conducted by a special procedure, using measurement minicapillaries [5]. Investigation results allowed establishing the time dependencies of variation of pH_B value of the medium and electrode potential E_B at the crack tip with their different location relative to the joint components and fusion zones. Proceeding from them, the constant (stabilized) values of the above electrochemical parameters pH_{BC} and E_{BC} were determined on the basis of 100 h (Table 3).

Based on the obtained pH_{BC} and E_{BC} values the electrochemical conditions in corrosion fatigue cracks with their different location were plotted on the diagram of thermodynamic resistance of the water [14]. This enabled evaluation of the probability of running of certain electrochemical reactions in the crack tip and, thus, assessment of the probability of implementation of the mechanism of anode dissolution of the metal and hydrogen embrittlement in corrosion fatigue fracture of components of ACC--CS welded joint. It was established (see Table 3) that in all the studied cases, the electrochemical conditions at the tip of a stationary statically loaded crack promote running of electrochemical corrosion, and, hence, running of the anode dissolution mechanism, its intensity being the highest for casing steel 15Kh2MFA. Hydrogen evolution as a result of electrochemical reactions at the crack tip, and, therefore also manifestation of the mechanism of hydrogen embrittlement is only possible in terms of thermodynamics for cracks, the tips of which are located in the fusion zone of 07Kh25N13 cladding--casing steel 15Kh2MFA, as well as in casing steel 15Kh2MFA proper.

Special features of fatigue crack propagation in a welded joint of ACC--CS and generalized diagrams of its cyclic corrosion crack resistance. As is known preventive inspections of power reactors demonstrated that corrosion fatigue cracks develop in the anticorrosion cladding in reactor service [15], which, while propagating, may penetrate into the base material of reactor casing. For this reason, data on cyclic

Table 3. Stabilized values of electrochemical parameters pH_{BC} and E_{BC} based on 100 h testing

Steel	ðÍ $_{ÂÑ}$	Å$_{ÂÑ}$, ì V	Dissolution mechanism	
			HE	AD
04Kh20N10G2B	10.9	--500	--	+
Fusion zone I	9.6	--495	--	+
07Kh25N13	9.2	--505	--	+
Fusion zone II	6,0	--500	+	+
15Kh2MFA	9.8	--525	+	+

N o t e . HE — hydrogen embrittlement; AD — anode dissolution of metal.

crack resistance of the materials and fusion zones of the welded joint of ACC--CS are required, in order to assess the operating safety (serviceability) of such facilities, as well as specify the terms of timely preventive inspections.

The following tests were conducted with this purpose. A special procedure [5], which ensured stable electrochemical conditions at the tip of a corrosion fatigue crack, was used to experimentally establish the invariant [16, 17] diagrams of cyclic crack resistance (da/dN -- ΔK_I diagrams) of the studied materials and fusion zones of the welded joint of ACC--CS. During the experiments the frequency of cyclic loading of the specimens was $f = 0.017$ Hz, which is the closest to the actual service conditions of power reactors [15]. As a reference point, also diagrams of cyclic crack resistance of materials of ACC--CS welded joint in air were determined at the loading frequency $f = 1$ Hz and coefficient of cycle asymmetry $R = 0$ (Figure 5). Investigation results were represented by dependencies of a fast growth of fatigue crack da/dN on the range of stress intensity factor ΔK_I. Obtained experimental data are described analytically, using the known Paris's power dependence [16]:

$$da/dN = C(\Delta K_I)^n, \qquad (24)$$

where C and n are the constants of material--environment system and test conditions. For the above test conditions, their values are given in Table 4.

Proceeding from these data generalized diagrams of cyclic crack resistance were calculated, which allow evaluation and forecasting of fatigue cracks propagation, both in this welded joint as a whole, and in its individual elements, depending on test conditions (Figures 5 and 6).

It follows from the obtained results, that presence of a hydrogen working medium significantly changes the parameters of cyclic crack resistance of the mate-

Table 4. Values of constants in equation (24) to describe the diagrams of cyclic crack resistance of materials and fusion zones of ACC–CS welded joint under different test conditions

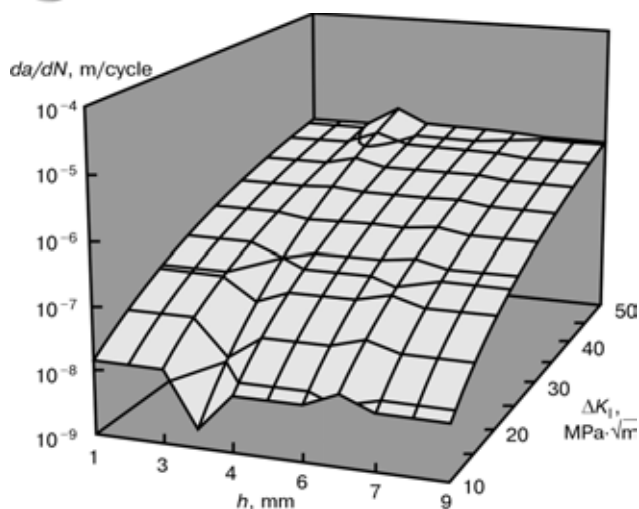| Steel	Air, f = 0.1 Hz			ðÍ 8, f = 0.017 Hz		
	$\tilde{N}$	n	R^2	C	n	R^2
04Kh20N10G2B	$3 \cdot 10^{-11}$	2.68	0.98	$1 \cdot 10^{-13}$	4.67	0.92
Fusion zone I	$8 \cdot 10^{-14}$	4.37	0.99	$2 \cdot 10^{-14}$	5.05	0.84
07Kh25N13	$5 \cdot 10^{-12}$	3.17	0.98	$1 \cdot 10^{-13}$	4.45	0.91
Fusion zone II	$2 \cdot 10^{-11}$	2.79	0.98	$2 \cdot 10^{-16}$	6.08	0.88
15Kh2MFA	$7 \cdot 10^{-12}$	3.04	0.98	$2 \cdot 10^{-13}$	4.02	0.87

Figure 5. Generalized diagram of cyclic crack resistance of a welded joint of ACC--CS (air, $f = 1$ Hz and $R = 0$)

Figure 6. Generalized diagram of cyclic corrosion crack resistance of a welded joint of ACC--CS (medium pH 8, 80 °C, $f = 0.017$ Hz and $R = 0$)

rials and fusion zones of the welded joint, both in the qualitative and quantitative sense. In this case they have the features, characteristic for corrosion fatigue with a simultaneous impact of the process of stress corrosion cracking [5, 16]. Under these conditions the lowest cyclic crack resistance is found in 04Kh20N10G2B cladding, and the highest ---- in casing steel 15Kh2MFA. 07Kh25N13 cladding takes an intermediate position, and this is characteristic of the entire studied range of rates of corrosion fatigue crack growth. In this case, the cyclic crack resistance of the fusion zones is higher than that of adjacent materials. It is particularly obvious for fusion zones of 07Kh25N13 cladding--casing steel 15Kh2MFA in the low-amplitude region of the diagram. Increase of the level of applied load (increase of ΔK_{I}) leads to the fusion zone losing the strength characteristics also in the high-amplitude region of the diagram: crack propagation rate in it is higher than in 07Kh25N13 cladding and 15Kh2MFA steel.

In conclusion it should be noted that such generalized diagrams are the basic ones for evaluation of the residual life of welded joints of ACC--CS type and for development of engineering-technical measures to prevent their corrosion-mechanical damage in long-term service.

CONCLUSIONS

1. New experimental-analytical methods of evaluation of local corrosion and local fracture of welded joints of the type of ACC--CS have been developed, considering such structural elements as complex heterogeneous mechanical and electrochemical systems.

2. A calculation model and an analytical-numerical method have been developed for determination of the density of corrosion currents on the surface of a circular cylindrical pit in a welded joint, which is a multilayer body, and it is shown that the density of corrosion current from the cylindrical pit surface in such a body increases with the increase of pit radius, and it is decreased with the increase of the depth of pit penetration into the base material. It was further established that the base material is the anode at all depths of the pit.
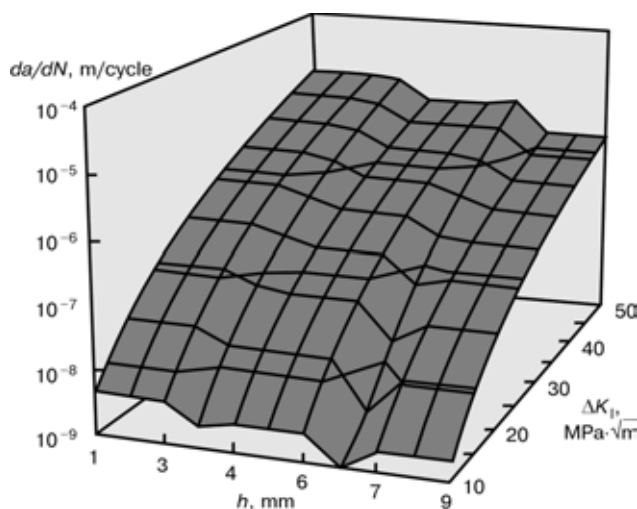
3. Diagrams of electrochemical resistance and corrosion crack resistance of multilayer welded joints of the type of ACC--CS have been constructed, which are the basic ones to evaluate the residual life of such joints and develop engineering-technical measures to prevent their corrosion-mechanical damage in long-term service.

1. (2002) Problems of corrosion and anticorrosion protection of materials. *Fizyko-Khimichna Mekhanika Materialiv*, **3**, 1--2.
2. (1996) Recommendations for fatigue design of welded joints and components. In: ISO Standard Proposal. *IIW Doc. XIII-1539--96--XV-845--96*.
3. (1992) *Eurocode 3 «Design of Steel Structures and National Application Document»*. Part 1-1. General rules and rules for buildings. Chapter 9. Fatigue. 22-311-9.
4. (2002) *Studies and evaluation of corrosion damage processes of different geometry welded joints on the base of examination of local synergetic factors of stress concentration and operating environment in weld zone*. Lviv: FMI.
5. Dmytrakh, I.M., Panasyuk, V.V. (1999) *Influence of corrosive media on local fracture of metals near stress concentrators*. Lviv: FMI.
6. Nikitin, V.I. (1980) Investigation of corrosion resistance of steel in aqueous heat carrier WWR with boron control. *Energomashinostroenie*, **3**, 21--24.
7. Frejman, L.I., Makarov, V.A., Bryskin, I.E. (1972) *Potentiostatic methods used in corrosion investigations and electrochemical protection*. Leningrad: Khimiya.
8. Scorceletti, V.V. (1963) *Theoretical electrochemistry*. Leningrad: Goskhimizdat.
9. Scorceletti, V.V. (1973) *Theoretical fundamentals of metal corrosion*. Leningrad: Khimiya.
10. Rozenfeld, I.L. (1970) *Corrosion and protection of metals (local corrosion processes)*. Moscow: Metallurgiya.
11. Kolody, B.I., Dmytrakh, I.M., Bily, O.L. (2002) Method of equivalent electrode for determination of corrosion currents in cracks and crevices. *Fizyko-Khimichna Mekhanika Materialiv*, **5**, 27--31.
12. Dmytrakh, I.M., Kolody, B.I., Bily, O.L. (2003) Determination of electrochemical current density from the surface of corrosion pits in three-layer material. *Ibid.*, **3**.
13. Turnbull, A., Ferris, F.H. (1987) Mathematical modelling of the electrochemistry in corrosion fatigue cracks. In: *Proc. of Int. Conf. on Corrosion Chem. Pits, Crevice and Cracks*, Teddington, Oct. 1--3, 1984. London.
14. Pourbaix, M. (1966) *Atlas of electrochemical equilibrium in aqueous solution*. Oxford: Pergamon Press.
15. Anikovsky, V.V., Ignatov, V.A., Timofeev, B.T. et al. (1982) Analysis of defect sizes in welded casings of power units and their influence on rupture strength. *Voprosy Sudostroeniya*, Series Welding, **34**, 17--32.
16. Panasyuk, V.V. (2002) *Strength and fracture of solids with cracks*. Lviv: FMI.
17. Panasyuk, V.V., Ratych, L.V., Dmytrakh, I.N. (1986) Determination of base diagrams of cyclic corrosion crack resistance taking into account the extreme electrochemical conditions in a crack. *Doklady AN SSSR*, **5**, 1128--1131.

IMPROVEMENT OF METHODS FOR ESTIMATION OF RESIDUAL LIFE OF WELDED JOINTS IN DURABLE STRUCTURES

V.I. MAKHNENKO

E.O. Paton Electric Welding Institute, NASU, Kyiv, Ukraine

Characteristic peculiarities of welded joints in durable critical structures requiring certain approaches to estimation of specified service life, residual safe life in particular, are considered. The possibility of using modern fracture mechanics approaches combined with rapidly developing risk analysis methods is examined.

The up-to-date durable critical welded structures (main pipelines, bridges, large oil and gas storage tanks, nuclear power rector bodies, reactive and radioactive material storage tanks etc.) are expensive facilities. High requirements for operational safety are imposed on these structures, which are met through appropriate measures taken in design and especially in operation. Among these measures we have to distinguish that which relates to estimation of residual safe life of a given structure.

In a general case, such estimation is made on the basis of results of monitoring of actual load on a structure, diagnostics of state of a material and presence of defects, as well as appropriate calculation diagrams (codes) for estimation of critical states at «hot spots» in the structure. Statistics show that welded joints account for almost 70--80 % of failures of welded structures, although the volume of the zone comprising welded joints in current structures is no more than 1.0--1.5 % of the total volume. In other words, welded joints account for a considerable part of the hot spots. This makes the procedural issues of estimation of residual life of welded joints, allowing for peculiarities of the latter, very topical. In terms of strength, welded joints have the following peculiarities:

• formation of residual welding stresses which may play a very important role under conditions of brittle fracture [1], alternating loads [2], corrosion fracture [3] etc.;

• presence of high stress raisers (Figures 1 and 2) associated with design characteristics (e.g. adjoining sharp cavities) or technological defects (lack of penetration, undercuts, hot and cold cracks etc.), the role of which is also very significant under the brittle and fatigue fracture conditions;

• non-homogeneity of physical-mechanical properties in the welded joint zone (Figure 3), resulting from differences in chemical compositions (between fusion zone and HAZ) and welding thermal cycles, which requires special approaches to be applied for diagnostic measurements and selection of computed values [4, 5].
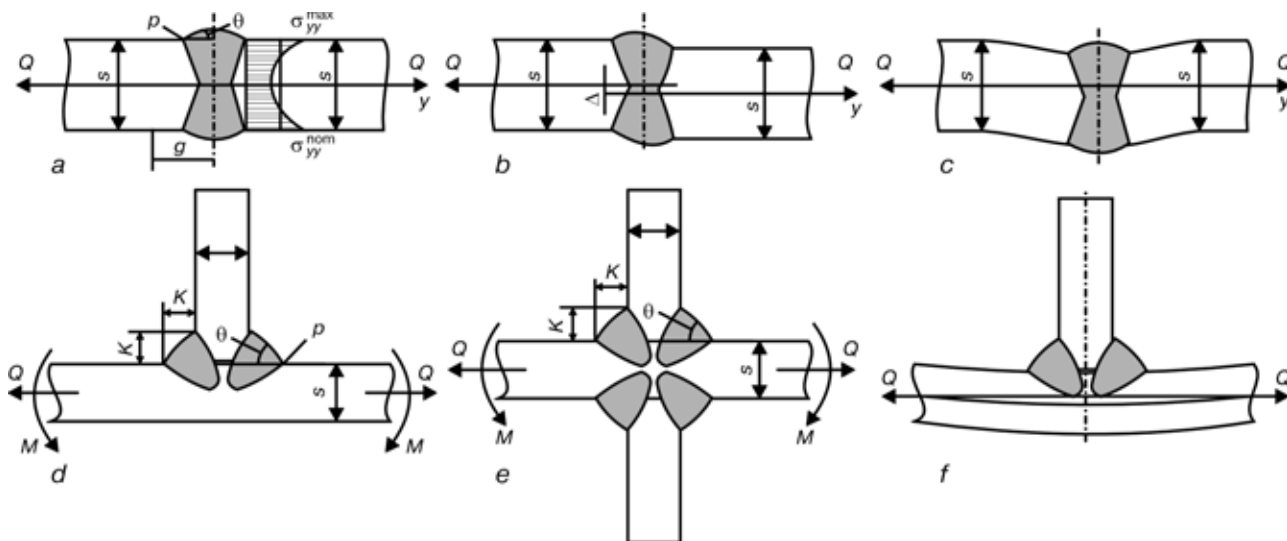

Figure 1. Geometric peculiarities of welded joints with butt (*a--c*) and fillet (*d--f*) welds
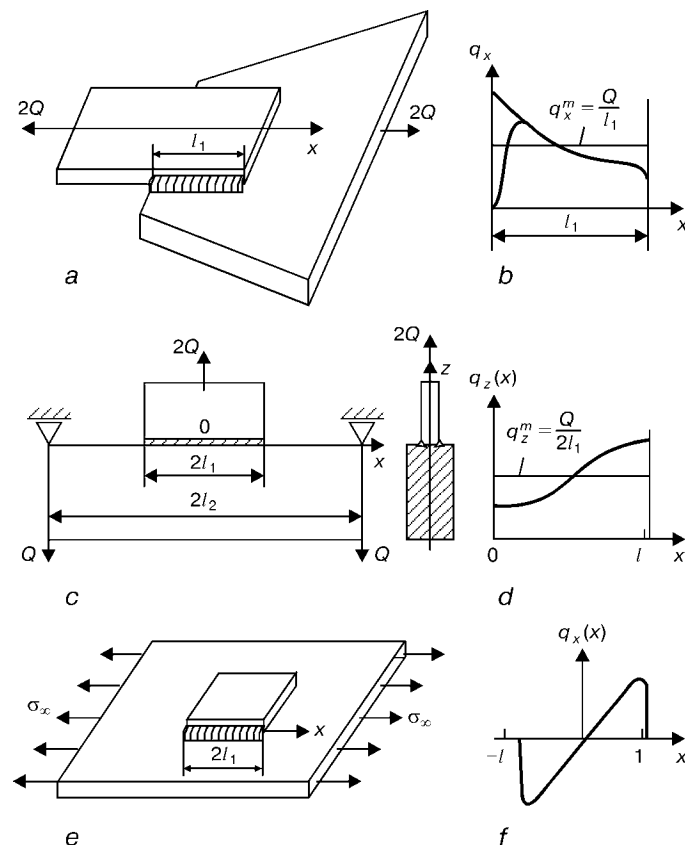
Figure 2. Geometric peculiarities caused by shape of a welded assembly with fillet welds (*a, c, e*) and diagrams of distribution of loads along the weld (*b, d, f*) [4]

It should be noted that much has been done during the last 10--15 years in the field of strength design of welded joints to allow for the above peculiarities [4--6 etc.]. This became possible in many respects owing to the progress in computer facilities. A number of studies were performed on this basis in such fields as thermomechanics of welding [7, 8 etc.], use of fracture mechanics for bodies with cracks for design of welded joints [6, 9 etc.], as well as probability methods to reflect stochasticity in quantitative estimation of a number of characteristic parameters related to geometry of a joint, its loading and resistance to corresponding deformation or fracture [10, 11 etc.]. The not less favourable factor was the development of methods for diagnostics of welded joints, intended both for detection of defects by determining their shape and size and for quantitative estimation of the degree of degradation of resistance of a material to this or that type of fracture [12, 13 etc.].

Nevertheless, much is still to be done to efficiently apply the developed approaches for practical utilisation of structures under consideration, the major part of which was designed as far back as the 1950--1960s of the last century, and the operational codes of which are based on the scientific-and-technical level of that time.

This paper provides some information on the efforts of the E.O. Paton Electric Welding Institute in the field of improvement of methods for estimation of residual life of welded joints on the basis of the advanced approaches that allow for the above peculiarities.

In particular, below we will consider the following issues: criteria of limiting states, residual stresses, diagnostics of defects and degradation of properties, probability approaches and risk analysis.

1. Criteria of limiting states of welded joints in structures under consideration. This issue has been sufficiently well covered in current literature [4]. Wide acceptance within the framework of approaches to local strength, allowing for a high risk of crack-like defects (adjacency of sharp cavities) was received by the criterion of non-violation of equilibrium of a crack-like defect of a corresponding origin (design, technology, service, hypothetical), having the form of a function of two parameters [14]:

$$f(K_r, L_r) = 0, \qquad (1)$$

where K_r characterises only brittle fracture in the studied zone of a welded joint with a given crack-like defect, and L_r characterises, respectively, tough fracture of the same zone with the same type of defect. K_r and L_r are complex parameters that include characteristics (invariant) of the stress-strain state, shape and size of the defect, as well as properties of material in a hot spot determining resistance to brittle or tough fracture, respectively [14].

Expression (1) can be presented in different forms, based mostly on generalisation of experimental data of the type of those shown in Figure 4, taken from

[14]. Curves in Figure 4 can be well approximated by the following dependence [14]:

$$K_r(L_r) = (1 - 0.14L_r^2) \, [0.3 + 0.7 \exp(-0.65L_r^6)]$$

$$\text{at } L_r < L_r^{\max};$$

$$K_r(L_r) = 0 \text{ at } L_r < L_r^{\max}, \qquad (2)$$

where $K_r = K_I / K_{I_c} \eta$ and $L_r = P/P_L(\sigma_y)$ (here K_I is the stress intensity factor on the crack-like defect profile; K_{I_c} is the brittle fracture resistance of a material, i.e. the critical value of K_I; $\eta \geq 1$ is the correction allowing for a partial difference of the defect considered from a crack under the planar deformation conditions; $P(a, \sigma_y)$ is the value of parameter P_L leading to plastic instability in the zone of the same crack with geometric size a on an assumption of the ideal plasticity of a material having yield stress $\sigma_y = \sigma_{0.2}$; $L_r^{\max} = \dfrac{\sigma_t + \sigma_y}{2\sigma_y}$; and σ_t is tensile strength of the material.

In a case of multiaxial stressed state at the crack apex, dependence (2) can be used within the framework of the generalised normal tear theory [1, 5] by substituting $K_{\omega\theta}^{\max}$, i.e. maximum value of the stress intensity factor at a corresponding apex point according to [15], for K_I. Allowing for non-relaxed residual stresses σ_{ij}^r, the value of $K_{\omega\theta}^{\max}$ can be calculated from (3):

$$K_{\omega\theta} = \left[(K_I + K_I^r) \cos^3 \frac{\omega}{2} - 3(K_{II} + K_{II}^r) \cos^2 \frac{\omega}{2} \sin \frac{\omega}{2} \right] \times$$

$$\times \cos^2\theta + (K_{III} + K_{III}^r) \cos \frac{\omega}{2} \sin 2\theta \qquad (3)$$

at values of angles $\omega = \omega_*$ and $\theta = \theta_*$ determined from conditions

$$\frac{\partial K_{\omega\theta}}{\partial \omega} = 0; \quad \frac{\partial K_{\omega\theta}}{\partial \theta} = 0,$$

where K_I, K_{II} and K_{III} are the modes of the stress intensity factor due to external load determined by parameter P; and K_I^r, K_{II}^r and K_{III}^r are the same due to non-relaxed residual stresses.

The value of $P_L(a, \sigma_y)$ is also determined with allowance for the multiaxial stressed state with the occurrence of plastic instability.

It is significant that residual stresses do not affect the value of $P_L(a, \sigma_y)$, as they have time to almost completely relax before occurrence of plastic instability. The same situation holds also for service temperature stresses. That is why in [14] it is not recommended to allow for both residual and service temperature stresses in calculation of L_r.

Vector a of geometric size of a defect a grows, and certain degradation of properties (e.g. decrease in K_{I_c}) takes place during operation. This leads to increase in K_r and L_r, according to the fracture estimation diagram (FED) (Figure 5), i.e. the state in a
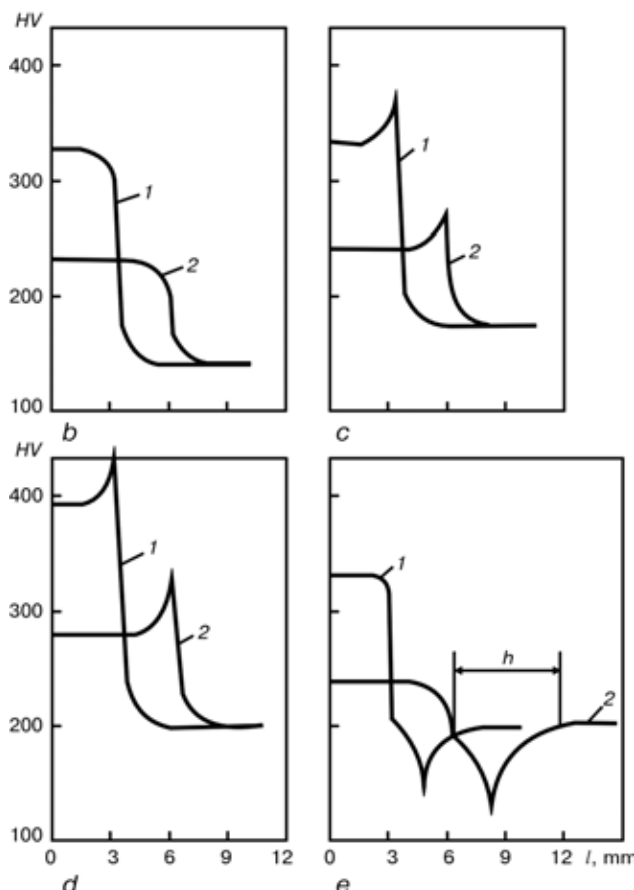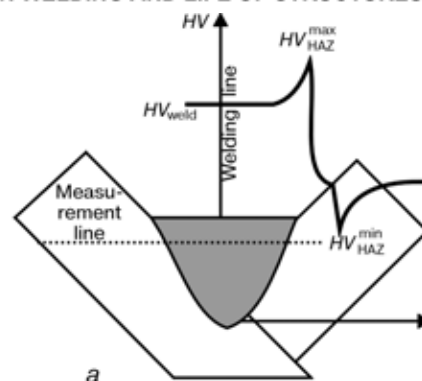
Figure 3. Distribution of hardness HV across the section of a joint with the fillet weld having leg 4 (1) and 8 (2) mm using the measurement diagram (a) in welding steels VSt3 (b), 10G2S (c) and 16G2AF (d) in a non-strengthened condition and steel VSt3 (e) in the strengthened condition

Figure 4. Diagrams of limiting state $K_r = \mathrm{f}(L_r)$ for different types of structural steels: A — high-strength steel EN408; B ---- pressure vessel steel A533B; C ---- low-carbon Mn-containing steel; D ---- austenitic steel; E — calculated curve according to (2)

Figure 5. FED and path *ABC* of the kinetics of propagation of fracture in hot spot

hot spot under consideration during operation will be determined by point *B* along path *ABC*.
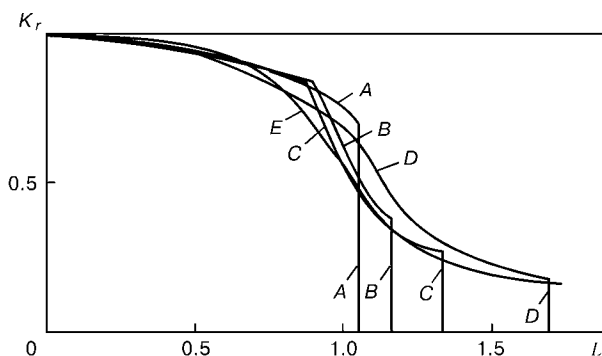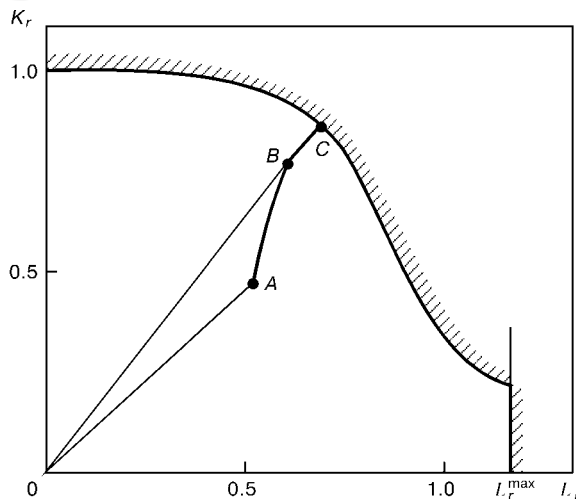
If the safety factor for strength, *n*, at point *A* is determined by length ratio $n = \dfrac{0C}{0A}$, then at point *B* $n = \dfrac{0C}{0B}$, and at point *C* $n = 1$. Therefore, with development of a defect and degradation of a material the risk of achieving the intolerable state for safe operation can be estimated from FED.

It follows from the above-said that in the case under consideration the estimation of the residual safe life is closely related to the estimation of the rate of development of the vector of defect geometric size, *a*, and degree of degradation of material properties, e.g. fracture toughness K_{I_c}.

The issues of growth of geometric size of a crack-like defect are well covered by the current literature. Three characteristic mechanisms of formation of this defect are distinguished in this case: fatigue under alternating loading, corrosion and creep under static loading.

For a general case, with a certain degree of idealisation (i.e. assuming that all these three mechanisms may occur independently of each other), the following holds for a normal tear crack:
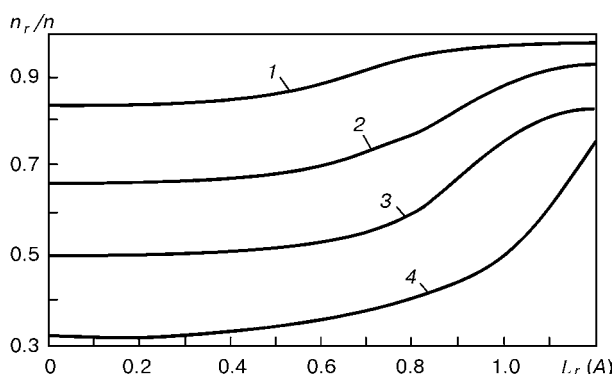

Figure 6. Effect of residual stresses on n_r / n depending upon $L_r(A)$: *1* ---- $K_r^r / K_r(A) = 0.2$; *2* — 0.5; *3* ---- 1.0; *4* ---- 2.0

$$\frac{\mathrm{d}a}{\mathrm{d}t} = \frac{C_y}{t_{\text{cycle}}} \Delta K_I^m (K_I^{\max})^s + C_{\text{cor}} (K_I^{\text{av}})^q + C_{\text{creep}} (K_I^{\text{av}})^p,$$

where t_{cycle} is the current cycle time; C_y, *m* and *s* are the experimental parameters of the cyclic crack resistance diagram; $C_y = 0$ at ΔK_{I_c}, i.e. amplitude of the stress intensity factor, lower than the threshold value of ΔK_{th} [4]; C_{cor} and *q* are the parameters of growth of a stress intercrystalline corrosion crack [16]; C_{creep} and *p* are the parameters of growth of a creep crack [17]; and $K_I^{\text{av}} = K_I^{\max} -- \Delta K_I / 2$. Peculiarities of a welded joint manifest themselves here only in the fact that it is necessary to allow for residual stresses to calculate $K_I^{\max}$, and that numerical values of the above parameters have very high degree of stochasticity.

2. Residual stresses. It follows from the above-said that the role of non-relaxed residual stresses in estimation of residual life of welded joints can be very significant, especially in the presence of defects, alternating cyclic loads and corrosive environment. Certain estimations of the effect of residual stresses can be made rather easily using FED (see Figure 5). As residual stresses have no effect on L_r, K_r^A at point *A* in FED can be assumed to be a sum of $K_r^A = K_r + K_r^r$, where K_r is determined by external load (force or temperature) and K_r^r ---- by residual stresses. Accordingly, the ratio of the safety factors for strength with, n_r, and without, *n*, allowance for residual stresses can be found from the following expression:

$$\frac{n_r}{n} = \frac{L_r^r}{L_r},$$

where $L_r(K_r^A)$ and $L_r(B_1)$ are the solutions of the following transcendental equation:

$$\frac{K_r}{L_r} = \frac{f_1(L_r)}{L_r}; \quad \frac{K_r + K_r^r}{L_r^r} = \frac{f_1(L_r^r)}{L_r};$$

here $f_1(x)$ is the right part of expression (2) at $x = L_r$, L_r^r. Figure 6 shows ratios n_r / n depending upon $L_r(A)$ and ratio K_r^r / K_r. It can be well seen here that the higher the value of $L_r(A)$, the lower the effect of residual stresses. At $L_r(A) < 0.7$, the role of residual stresses is noticeable as low as at $K_r^r / K_r > 0.2$. As even a high tempering of welded joints usually leaves non-relaxed stresses at a level of 50--120 MPa in the welded joint zone, under the service loads corresponding to operating stresses of 250--350 MPa the effect of non-relaxed residual stresses should not be neglected in estimation of life of welded joints for the given statement of the problem. In other words, estimation of non-relaxed residual stresses is one of the tasks of diagnostics of the state of welded joints in structures at different stages of their operation. Unfortunately, so far the majority of non-destructive (semi-destructive) testing methods [18] enables evaluation of residual stresses only in surface (accessible for measurements) layers or stresses averaged

through the plate thickness [19, 20], which is not always enough for calculation of K_r^r.

Modern methods of neutron diffraction [21] and high-energy synchrotron diffraction [22] are more informative from this standpoint. However, so far they can be used only under laboratory conditions, requiring expensive equipment.

In this connection, the most realistic for application is the combination of mathematical modelling of a history of formation of residual stresses, including welding and relaxation effects (tempering, force loading), and experimental measurements at individual points on the surface using non-destructive (semi-destructive) methods. The purpose of such an experiment is to validate calculated data used to determine K_r^r.

Examples of application of the above combination are shown in Figures 7--9. Results shown in Figure 7 correspond to estimation of residual stresses in the zone of a circumferential joint in piping with D_n 300 at unit 3 of the Chornobyl Nuclear Power Plant. This work was performed because it was necessary to substantiate permissibility of some defects revealed in the HAZ (of the type of intercrystalline corrosion cracks) for a period of operation to a forthcoming scheduled repair. The results obtained are described in detail in [9], and there is no need to dwell on them here.

We have to note only that the work was completed in 1998, i.e. over 5 years ago. Since then the capabilities of computer facilities have markedly grown ---- available now are accessible commercial software packages, e.g. SISWELD.

Figures 8 and 9 show data on estimation of residual stresses within the zone of circumferential welds in piping with D_n 850 at the South-Ukrainian Nuclear Power Plant. These data generated in 2002 are indicative of availability of solution to a more complicated problem, i.e. multilayer welding in 112 passes, deposition of a corrosion-resistant layer, high tempering at 650 °C, steel 10GN2MFA which is very sensitive to microstructural variations in welding used as the base metal, etc.

No doubt that in the near future we might expect greater advances in the field of calculation methods based on the capabilities of computer facilities. Therefore, the above way of estimating non-relaxed residual stresses within the zone of welded joints holds high promise.

3. Diagnostics of defects and degradation of properties. Diagnostics of the state of welded joints include detection of different geometric defects and evaluation of variations in mechanical properties responsible for safe operation.
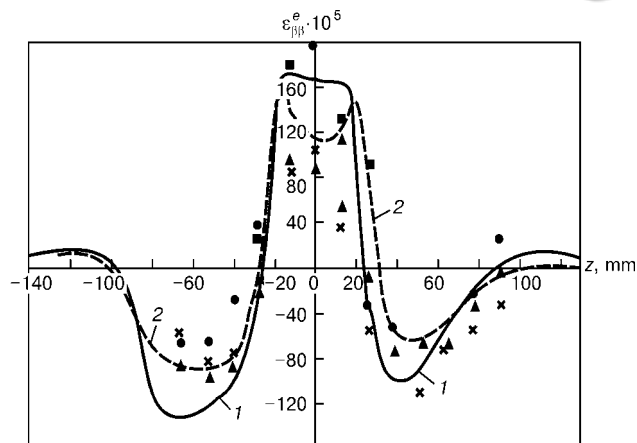
Figure 7. Comparison of calculated (curves) and experimental (points) data on distribution of residual strains $\varepsilon_{\beta\beta}^e$ over the internal (1) and external (2) surfaces of a pipe (gap 4--6 mm) along axis z

Figure 8. Calculated data on distribution of residual stresses after welding and tempering of a circumferential joint in pipeline with D_n 850: a — $\sigma_{\beta\beta}$; b — σ_{zz}; c — σ_{rr}; d — σ_{rz}
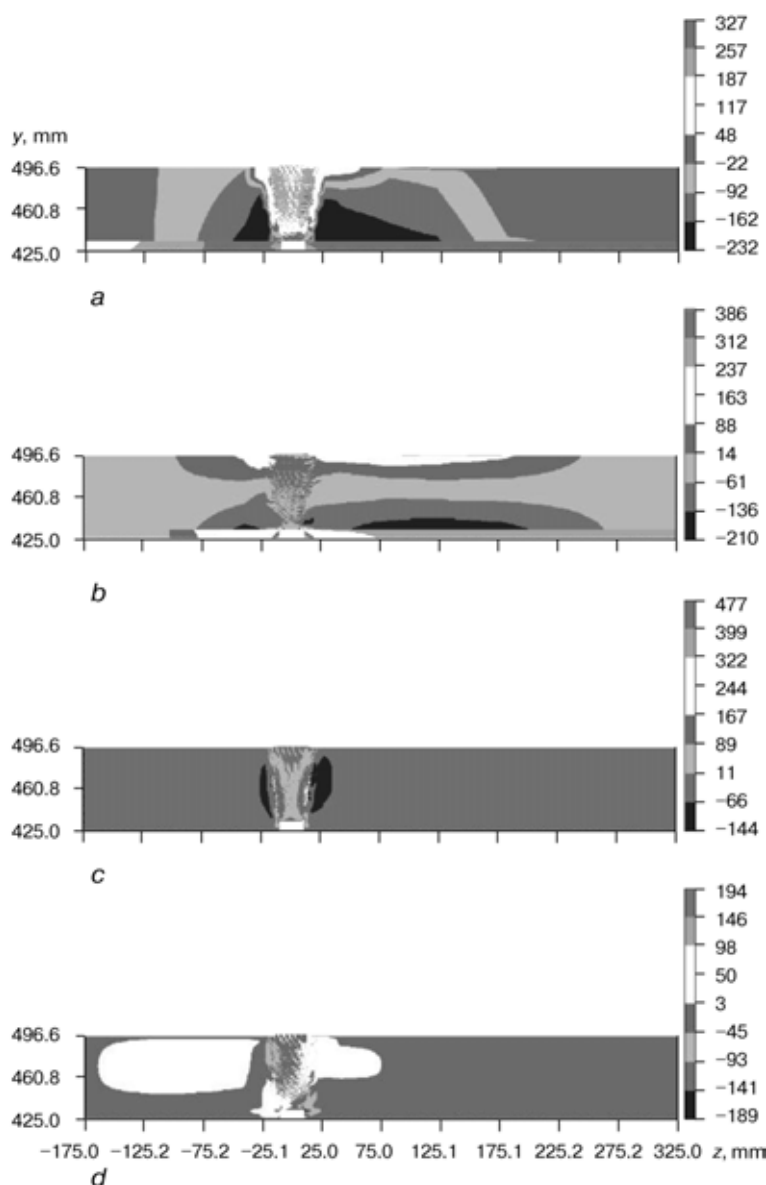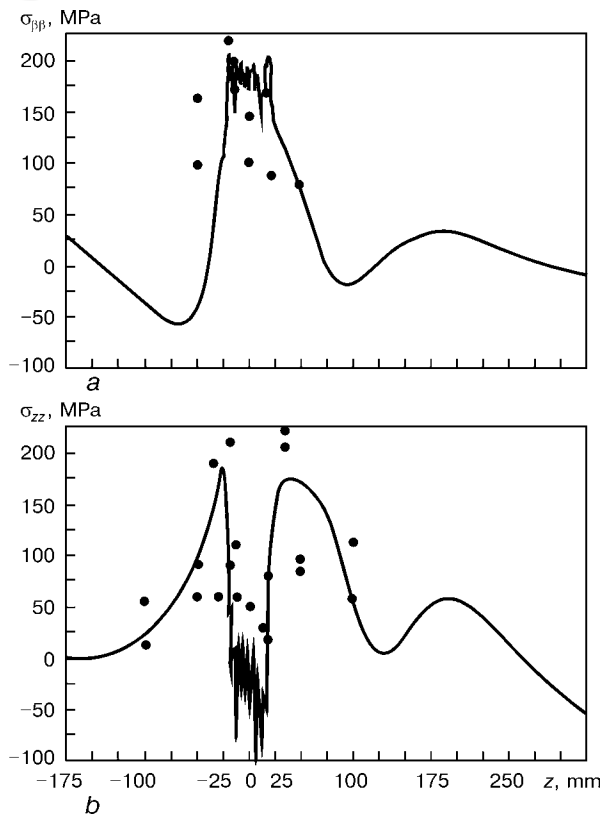
Figure 9. Comparison of calculated (curves) and experimental (points) data on residual stresses $\sigma_{\beta\beta}(z)$ (*a*) and $\sigma_{zz}(z)$ (*b*) on the external surface in the zone of a butt joint after high tempering

Geometric defects are usually revealed by non-destructive methods. Many specialists from different countries all over the world focus their attention particularly on this area. Geometric defects are usually subdivided into two big groups. The first group includes shape defects caused by changes in designed geometric sizes occurring during operation or manufacture (service dents or angularities in the zone of butt welded joints occurring during manufacture etc.). The second group includes defects of continuity of a material, which are characterised by local violation of the latter (service or technology defects, undercuts, lacks of penetration, pores, corrosion defects etc.).

In terms of estimation of performance of a welded assembly (joint) containing defects, it is very important to know geometric size and location of a defect, as well as its origin. There are still many problems in modern diagnostics regarding this area, especially the crack-like continuity defects, the discussion of which is beyond the frames of this study. What should be noted is just that the world science and technology community is very active in this field. This fact is evidenced by annual international conferences on NDT methods (normally held in Europe), as well as quantitative non-destructive evaluation methods (usually held in the USA), at which hundreds of papers associated with improvement of methods for detection and identification of geometric continuity defects are presented and discussed.

The situation in diagnostics of quantitative characteristics of resistance of a material to these or those types of fracture is much worse. In particular, determination of characteristics of the FED (see Figure 5) is related to the necessity to derive data on material fracture toughness K_{I_c}. Moreover, this requires the use of large samples, the manufacture of which in many cases from a material of the structure examined is physically impossible. Usually, if it is the case, the use is made of the results of indirect tests of small specimens, such as impact toughness tests of Charpy specimens. However, this should include certain recalculations based on an assumption that degradation of properties causes changes in critical brittle temperature value ΔT_{cr} and a corresponding shift of temperature curve $K_{I_c}(T)$ by the same value. The ΔT_{cr} value is determined by comparing curves $KCV(T)$ plotted for the initial state and state at a given stage of operation (Figure 10). Unfortunately, this approach is by no means universally applicable and eligible. Therefore, the search for the methods for estimation of K_{I_c} on small-size samples is of considerable practical interest.
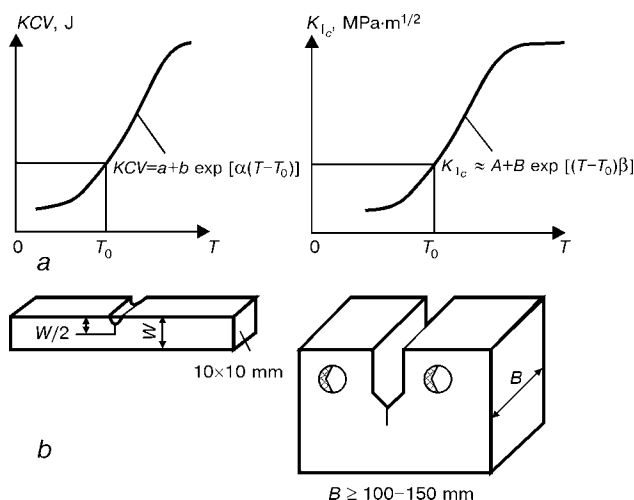

Figure 10. Results of impact toughness tests of Charpy specimens (*a*) and evaluation of K_{I_c} on a compact specimen with thickness B (*b*)
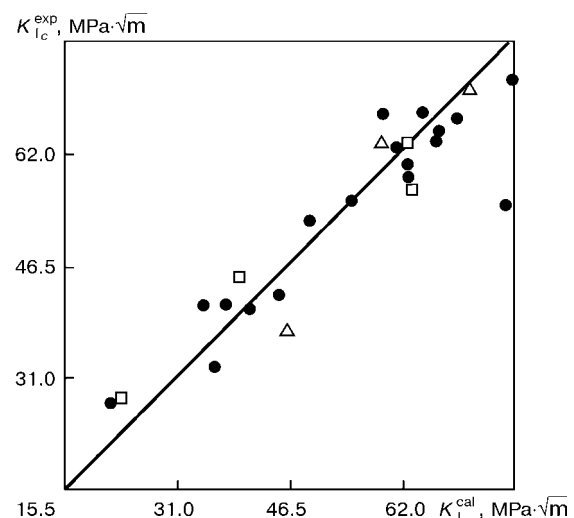

Figure 11. Comparison of calculated $K_{I_c}^{cal}$ from (4) and experimental $K_{I_c}^{exp}$ for steels 4340 ($\triangle$), 45KhN2MFA ($\blacksquare$) and 40X ($\bigcirc$)

It should be noted that there are many different suggestions of the type of $K_{I_c} = C\sqrt{KCV}$ in this area, where for steel with $C = 19$ KCV is measured in Joules and K_{I_c} ---- in MPa·m$^{1/2}$. Here only impact toughness tests are applicable.

There is a more complex relationship

$$K_{I_c} = \sqrt{\rho \ \tau_s \frac{E}{1 - \nu^2} \ln (1 - \psi)^{-1}}, \qquad (4)$$

where ρ is the linear size of a structural component; τ_s is the shear yield stress; E is the Young modulus; ν is the Poisson's ratio; and ψ is the reduction in area in tensile fracture of small-section standard specimens.

Examples of calculations in accordance with (4) are shown in Figure 11. Unfortunately, this dependence is not universal either. Like many other dependencies, it does not allow for physics of degradation of a material.

For example, in irradiation of hull steel at temperatures of about 300 °C the coarse microstructure persists, i.e. ρ = const, values of τ_s grow a little bit and ψ decreases to some extent. In this case it is very difficult to calculate from (8) how dramatically the value of K_{I_c}, associated with diffusion of phosphorus and leading to reduction in strength of grain boundaries etc. [23], decreased. In other words, characteristics ρ, τ_s, E, ψ and ν are insufficiently sensitive to the effect of redistribution of phosphorus in irradiation of hull steel, whereas the value of K_{I_c} does depend upon its effect. This example proves that with the non-destructive methods of measurement of mechanical properties the vector of measured parameters, X_i, should be sufficiently sensitive to physical changes in a material, determining a desired hard-to-measure characteristic, e.g. K_{I_c}.

The «Master Curve» method based on tests of specimens of a limited size has received acceptance in the last years for estimation of K_{I_c} for thin-walled structures. According to this method, the probability $P_f(K_{I_c}, B_1)$ that an experimental value of K_I at which fracture occurs is less than $K_{I_c}(B_1)$ is determined by testing specimens of limited sizes, e.g. 1T-CT with thickness $B_1 = 25$ mm, as shown in Figure 10.

It is assumed that this value is determined by the following form of three-parameter Weibull distribution

$$P_f = 1 - \exp\left[-\left(\frac{K_{I_c}(B_1) - K_{min}}{K_0 - K_{min}}\right)^\eta \frac{B_1}{B_0}\right], \qquad (5)$$

where K_{min}, K_0, B_0 and η are the parameters of the above distribution. If η = 4.0, then the following recalculation formula based on (5) is used:
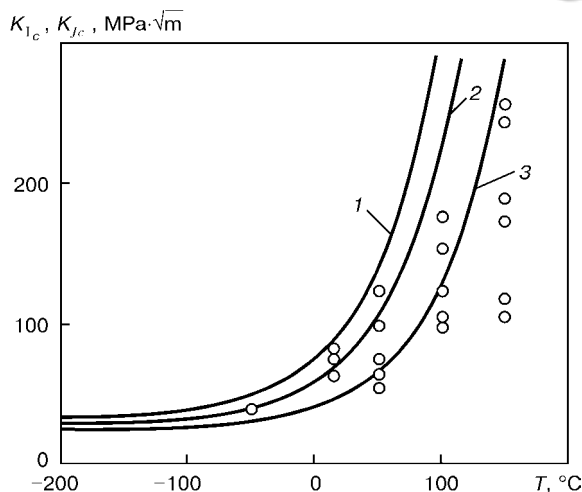
Figure 12. Comparison of results of calculations by the «Master Curve» method and experimental data derived on a specimen with thickness $B = 50$ mm [24]: $1 — P_f = 0.95$; $2 — 0.50$; $3 — 0.05$

$$K_{I_c}(B_1, P_f) = [K_{I_c}(B_1, P_f) - K_{min}]\left(\frac{B_1}{B_2}\right)^{\frac{1}{4}} + K_{min}$$

The use of this recalculation is also far from being always satisfactory for practical application. An example of such discrepancy is shown in Figure 12, which is indicative of the fact that the assumption related to dependence (9) has an insufficient physical grounding.

Noteworthy in this connection are the methods based on convenient measurements and sufficiently comprehensive mathematical models, which take into account physics of local changes in a material responsible for K_{I_c}. One of such methods being elaborated by Russian expert B. Margolin is worthy of a special notice.

Specimen for a standard tensile (see Figure 10) or three-point bending test is considered to estimate K_{I_c}. The stressed state in the zone of the crack apex (Figure 13) is unambiguously determined by loading conditions which are used to find current and critical values of K_{I_c} from standard dependencies [24].

Polycrystalline material of the specimen is assumed to be a set of elementary cell, the sizes ρ of which correspond to a mean size of grains of the polycrystalline material. This parameter can be deter-
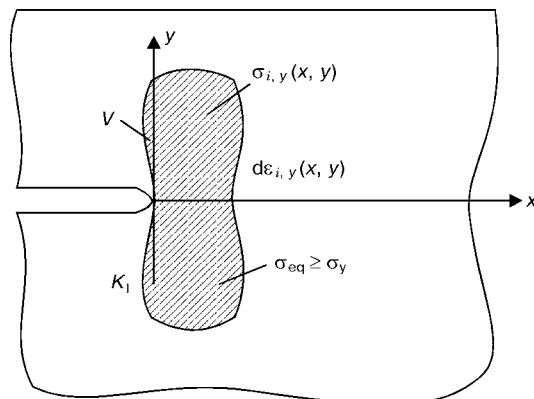
Figure 13. Schematic of deformation in zone V near the crack apex

mined by non-destructive methods within the zone of the hot spots.

The following form of local criterion of brittle fracture was assumed to hold for a cell

$$\sigma_1 \geq \sigma_d - m_I(T)m_\varepsilon(K)(\sigma_{eq} - \sigma_y); \quad \sigma_1 \geq S_C(K), \quad (6)$$

where σ_1 is the maximum principal stress; σ_{eq} is the equivalent stress (intensity of stresses); σ_d is the effective strength of initiation of cleavage microcracks in a given cell, which is a stochastic value. The following form of the three-parameter Weibull distribution is used to describe the function of distribution of this value

$$P(\sigma_d) = 1 - \exp\left[-\left(\frac{\sigma_d - \sigma_{d0}}{\overline{\sigma}_d}\right)^\eta\right],$$

where $P(\sigma_d)$ is the probability that minimum resistance to brittle fracture by the given mechanism in an elementary cell is lower than σ_d (here σ_{d0}, $\overline{\sigma}_d$ and η are the Weibull parameters).

In dependence (6) $m_T(T)$ allows for the effect of temperature. It is suggested in study [24] that $m_T(T)$ should be calculated as follows

$$m_T(T) = |\sigma_y(0) - \sigma_y(T)|m_0,$$

where $\sigma_y(T)$ is the yield stress of material at temperature T; $\sigma_y(0)$ is the same at $T = 0$; and m_0 is determined experimentally;

$$m_\varepsilon(K) = \frac{S_0}{S_C(K)} \cdots ,$$

where $S_C(K)$ is the critical brittle fracture stress; K is the Odquist parameter; and $K = \int d\varepsilon_{eq}^p$ (here $d\varepsilon_{eq}^p$ is the increment in the equivalent plastic strain, $S_0 = S_C(K)$ at $K \equiv 0$).

The $\sigma_y(T)$ and $S_C(K)$ values are determined on small-size specimens [24].

The stressed state of all the elementary cells within the crack apex zone at a given value of K_I being
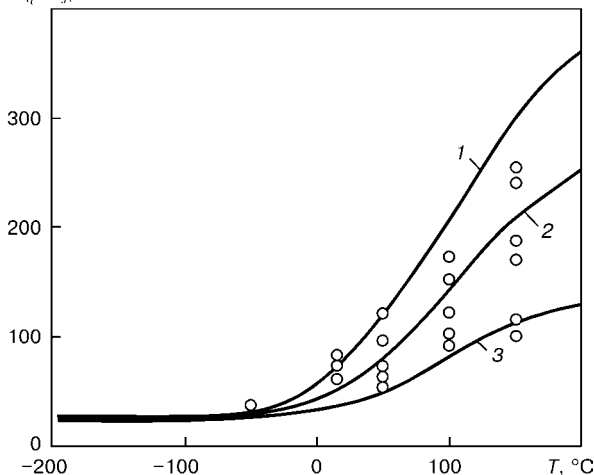
$K_{I_c}, K_{J_c},$ MPa·$\sqrt{m}$

Figure 14. Results of calculations by the Margolin's method (solid curves) compared with the experimental data taken from [24] (points) (*1–3* — see Figure 12)

known, it is possible to calculate the probability of brittle fracture of a specimen with a crack at temperature T:

$$P_f(K_I)_T = 1 - \exp\left[-\sum_{i=1}^M \left(\frac{\sigma_e^i - \sigma_{d0}}{\overline{\sigma}_d}\right)\right] =$$
$$= 1 - \exp\left[-\left(\frac{\sigma_W}{\overline{\sigma}_d}\right)^\eta\right], \quad (7)$$

where $\sigma_W = \left\{\sum_{i=1}^M (\sigma_e^i - \sigma_{d0})^\eta\right\}^{\frac{1}{\eta}}$ is the Weibull stress;

M is the quantity of the elementary cells within volume V under consideration (Figure 13).

Here $\sigma_e^{(i)} - \sigma_{d0} \equiv 0$, if conditions (6) are not met, i.e. such cells are characterised by a 100 % probability of non-fracture. If conditions (6) are met, then

$$\sigma_e^{(i)} - \sigma_{d0} = \sigma_1^{(i)} + m_T(T)m_\varepsilon(K)(\sigma_{eq} - \sigma_y) - \sigma_{d0}.$$

As condition (6) is met in a limited range of the V values near the crack apex, this allows the M value to be limited as well. Naturally, the thicker the specimen, the higher the M value. The use of the plane strain hypothesis, like in [23], makes it possible to consider the stressed state only in plane x, y (Figure 13), this resulting in decrease of B/ρ times in M. However, in this case the sum in (7) is preceded by the corresponding coefficient, like in [23]. In the model considered the Weibull parameters (σ_{d0}, $\overline{\sigma}_d$ and η) do not depend upon the temperature. They can be determined on small specimens containing a crack (see Figure 9) at a given temperature in the low-temperature range, resulting in brittle fracture, by modelling the deformation processes and processing the experimental results according to (7). This yields data for K_{I_c}, depending upon the specimen thickness and temperature, using the above procedure of modelling of the deformation processes, but this time on specimens of a given thickness and at given temperatures. Example of using this approach [23] is illustrated in Figure 14.

4. Probability approaches and risk analysis. As follows from the above-said concerning the level of residual stresses within the welded joint zone and diagnostics of geometric sizes of defects and degree of degradation of properties of a material, in the majority of cases the deterministic approach for estimation of residual life of welded joints and assemblies should be replaced by the probability one, allowing for stochastic character of values of residual stresses, sizes of defects and fracture resistance of the material. The probability approaches are successfully applied for strength design in advanced industries (aircraft engineering, some sections of machine building etc.). Theoretical background of such approaches is well known [24, 25 etc.]. In the last years these methods have been widely accepted also in welded fabrication [26].

Changes in values of safety factor n depending upon the probability of non-fracture, P_f, and coefficient of variation of initial parameters, ω, for fillet welds in a cruciform joint from [11]

P_f	ω	Fillet weld legs, mm		n
		K_y	K_z	
0.90	0.05	4.39	12.67	1.25
	0.10	7.33	14.12	1.50
	0.15	9.02	17.62	1.75
0.89	0.05	5.65	16.31	1.45
	0.10	10.00	19.72	1.90
	0.15	13.67	26.70	2.40

The E.O. Paton Electric Welding Institute developed a software package [27] for strength design of different welded joints with adjoining sharp cavities. Along with the deterministic calculations on the basis of the assigned safety factors n, including safety factor for service m, safety factor for material K_m, safety factor for application K_a and safety factor for loading K_p, the above package provides for computation of the probability of non-fracture, P_f, from the assigned load variations, geometric sizes and properties of a material. The conventional term for the calculated value of P_f is the calculation support [25, 26].

It is significant that the identical calculation support, i.e. value of P_f, depending upon variation coefficient ω of the above input parameters requires different safety factors, which is clearly demonstrated by the data of [11] given in the Table for fillet welds of a cruciform welded joint under static loading.

It can be seen from the Table that no one-to-one dependence exists between the values of safety factor n and calculation support P_f. An important role is played by variation in input data, which is far from being fully allowed for in assigning the safety factor. This example indicates that calculations based on the probability approach, i.e. allowing for variation in input data, are more advanced than deterministic calculations based on the safety factor.

Naturally, the probability calculations are more intricate. However, it is not that difficult to make such calculations with an up-to-date level of computing facilities. The most significant obstacles in a way of wide application of the probability approaches for design of welded joints and assemblies are associated with the absence of specifications for permissible values of the factor of calculation support P_f for different cases, as opposed to the safety factors.

In this connection it is of interest to try and use approaches based on risk analysis. The main point of such approaches in a reduced form is illustrated in Figure 15, as applied for estimation of residual safe life of a welded joint (assembly).

Two main curves are plotted in the coordinate system of operation time t and costs. Curve 1 shows the costs related to immediate repair of a given welded joint (assembly) of a structure at time moment t. Curve 2 corresponds to product $\Pi_{fail}(1 - P_f)$. Here
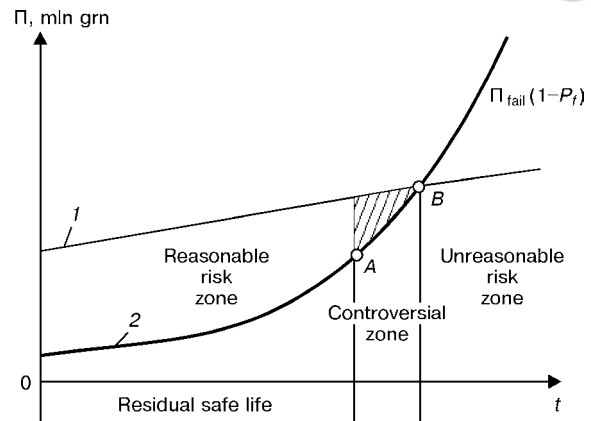

Figure 15. Diagram of estimation of residual life based on risk analysis

Π_{fail} are the costs for a case of failure of the given welded joint (assembly) at time moment t. Point B of intersection of these curves determines the boundary of zone $t < t_B$ of an unreasonable risk. Accordingly, zone $t < t_A$ is the zone of a reasonable risk or residual safe life of the welded joint (assembly).

CONCLUSIONS

1. Improvement of methods for estimation of residual safe life of welded joints (assemblies) in durable structures is closely related to the use of advanced approaches of fracture mechanics, probability methods and risk analysis.

2. Efficient methods for estimation of state of welded joints (assemblies) in a structure during operation in terms of the level of non-relaxed residual stresses, presence of geometric defects and degree of degradation of characteristic properties of a material determining resistance to fracture at the «hot spots» are very important.

3. Procedure for estimation of residual life is of an integrated character. With this procedure the issues of fracture mechanics, diagnostics of state concerning non-relaxed residual stresses, sizes of defects and material properties are closely related to economic and social problems of risk analysis.

4. It would be interesting to institute a corresponding speciality dealing with training of specialists in residual life of critical durable structures, which would allow practical problems to be effectively solved, including for welded joints and assemblies.

1. Wells, A.A. (1977) Influence of residual stresses on brittle fracture. In: *Fracture*. Vol. 4. Ed. by G. Libovits. Moscow: Mashinostroenie.
2. Trufyakov, V.I. (1973) *Fatigue of welded joints*. Kyiv: Naukova Dumka.
3. Steklov, O.I., Akulov, A.I. (1965) On influence of residual stresses and type of stressed state on corrosion cracking of welded joints. *Avtomatich. Svarka*, **2**, 38–43.
4. (1993) *Welded building structures*. Vol. 1. Principles of structure design. Ed. by L.M. Lobanov. Kyiv: Naukova Dumka.
5. Nikolaev, G.A., Kurkin, S.A., Vinokurov, V.A. (1982) *Welded structures*. Moscow: Vysshaya Shkola.
6. (1990) Guidance to assessment of fitness for purpose of welded structures. *IIW Doc. SST-1157–90*.
7. Makhnenko, V.I. (1976) *Computation methods for investigation of kinetics of welding stresses and strains*. Kyiv: Naukova Dumka.

8. Ueda, J., Murakawa, H., Nakacho, K. et al. (1995) Establishment of computation welding mechanics. *Transact. of JWRI*, **2**, 73–86.

9. Makhnenko, V.I., Makhnenko, O.V. (2000) Development of calculation procedures for assessment of allowable defects in welded joints of critical structures. *The Paton Welding J.*, **9/10**, 79--87.

10. Bokalrud, T., Koragren, P. (1979) Some aspects of the application of probabilistic fracture mechanics for design purposes. In: *Proc. of IIW Colloquium on Practical Applications of Fracture Mechanics to the Prevention of Failure of Welded Structures*, Bratislava, July 10, 1979.

11. Makhnenko, V.I., Ryabchuk, T.G. (1993) Calculation support and sizes of fillet welds of different joints. *Avtomatich. Svarka*, **1**, 3--6.

12. Troitsky, V.A., Radko, V.P., Demidko, V.G. (1983) *Defects in welded joints and means for their detection*. Kyiv: Vyshcha Shkola.

13. (1976) *Devices for non-destructive testing of materials and parts*. Refer. Book. Ed. by V.V. Klyuev. Moscow: Mashinostroenie.

14. Harrison, R.P., Looscmore, K., Milne, J. et al. (1980) Assessment of the integrity of structure containing defects. In: *Report R/H R6-Rev. 2 of Central Electricity Generating Board*. Bekeley.

15. Andrejkiv, A.E. (1982) *3D problems of crack theory*. Kyiv: Naukova Dumka.

16. Horn, R.M., Kass, J.N., Rangantath, K. (1984) Evaluation of the growth and stability of stress corrosion cracking in sensitised austenitic pipings. *J. of Pressure Vessel Techn.*, **2**, 201--208.

17. Makhnenko, V.I., Velikoivanenko, E.A., Rozynka, G.F. et al. (1995) Assessment of residual life of welded joints in structures operating at high temperatures. *Avtomatich. Svarka*, **1**, 3–9.

18. (1981) *Experimental methods for investigation of strains and stresses*. Refer. Book. Kyiv: Naukova Dumka.

19. Gushcha, O.I., Makhort, F.G., Chernoochenko, A.A. (1988) Application of acoustic elasticity of bulk waves for determination of stresses. In: *Proc. of 3rd All-Union Symp. on Technological Residual Stresses*, Kutaisi, 1998. Moscow.

20. Fuchs, P.A., Clark, A.V., Lozer, M.G. et al. (1998) Ultrasonic instrumentation for measuring applied stress on bridges. *J. Non-Destructive Eval.*, **3**, 129--140.

21. (1989) *Measurement of residual and applied stress using neutron diffraction*. Ed. by M. Hatchings, A. Krawitz. Dordrecht, Boston, London: Kluwer A.P.

22. Reimers, W., Broda, M., Brusch, G. et al. (1998) Evaluation of residual stresses in bulk of materials by high energy synchrotron diffraction. *J. Non-Destructive Eval.*, **3**, 129--140.

23. Margolin, B.Z., Shvetsova, V.A., Gulenko, A.G. et al. (2002) Prediction of crack resistance of reactor body steel on the base of the «Master Curve» concept and probabilistic model. *Problemy Prochnosti*, **1**, 5--21.

24. Bolotin, V.V. (1982) *Probability and reliability theory methods in design of structures*. Moscow: Strojizdat.

25. Rajzer, V.D. (1986) *Reliability theory methods in problems of regulation of building structure calculation parameters*. Moscow: Strojizdat.

26. *ISO SD 16708 Standard*. Petroleum and natural gas industries. Pipeline transportation systems. Reliability-based limiting state methods.

27. Makhnenko, V.I., Ryabchuk, T.G. (1991) Computerisation of design of welded joints with fillet welds. *Avtomatich. Svarka*, **11**, 1–6.

EFFECTIVE NOTCH STRESS METHOD IN COMPARISON WITH OTHER METHODS IN FATIGUE DESIGN OF WELDED STRUCTURES

A.F. HOBBACHER

University of Applied Sciences, Wilhelmshaven, Germany

Structures loaded by fluctuating forces are susceptible to fatigue damage. Besides the classical component testing, several calculative assessment methods have been developed. Most commonly used is the nominal stress method, which is based on the average stress in the section to be verified. With the oncome of the finite element method (FEM), more universal methods could be developed. The new method of effective notch analysis refers directly to the notch, at which a fatigue crack initiation is expected. On the basis of Neuber's theory and of more than 80 fatigue test series containing more than 1000 test specimens, it can be shown that the weld notch can be replaced by a fictitious, but consistent radius. For steel this radius is 1 mm. This method has been introduced to the IIW fatigue design recommendations.

Key words: *welded joint, fatigue, notch stress, structural steel*

Structures loaded by fluctuating forces are susceptible to fatigue damage. This damaging action is governed by a variety of parameters, e.g. size and type of load, frequency of occurrence and sequence of loads, material, surface, residual stress, geometry, internal imperfections etc. For most welded components, because of the severe notching effect of the weld bead and the residual stresses, fatigue considerations are dominant in design and analysis. Besides the classical component testing, several calculative assessment methods have been developed.

Conventional methods of fatigue assessment. Besides the classical component testing, several calculative assessment methods have been developed. Most commonly used is the nominal stress method, which is based on the average stress in the section to be verified. Allowable stresses have been tabulated for each structural detail (Table 1). New details or geometries cannot be directly assessed by this method.

Another problem is the definition of nominal stress for which up to now is no comprehensive definition is available (Figures 1 and 2).

With the oncome of the method of finite element analysis (FEA), more universal methods could be developed. Here the fracture mechanics and the structural stress methods have gained significance. The first requires complex and costly calculations, while the latter associated with some arbitrarity of the extropolation procedure to the hot spot. The advantage is a simple application of FEA.
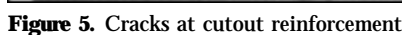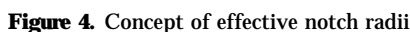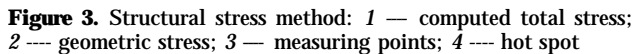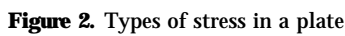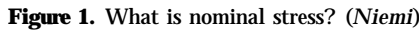
The structural stress method (Figure 3) is capable to calculate the stess level in the area of the weld toe, but it cannot assess the effects of the variation of the weld profile nor the of the weld root. Problems of imcomplete penetration or intended root gaps are not accessible by this method.

Effective notch stress method. *General procedure.* The new method refers directly to the notch, at which a fatigue crack initiation is expected, i.e. the weld root or the weld toe. The geometry of the notch cannot be directly modelled by FEA because of the irregularity of the weld. This problem has been overcome by the introduction of a fictitious effective notch radius, which can be modelled by FEA (Figure 4).

Application to welded joints. An extension of the Neuber theory of notches was made defining an universal effective notch radius. Besides these theoretical deliberations, the approach was verified by more than 80 fatigue test series containing more than 1000 test specimens of a variety of weld joints geometries and dimensional parameters. The probability plot of the results shows that a consistent effective notch radius can be found. For steel this radius is 1 mm. The plot also indicates that all results are originated by one statistical population [1].
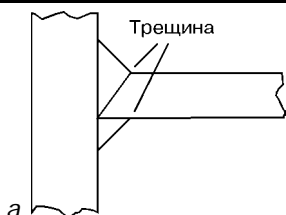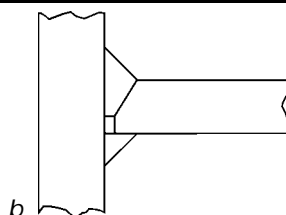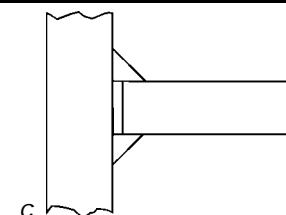
Table 1. Different methods for fatigue assessment

Loadings considered	Assessment procedure
Forces on components	Component testing
Average stress by simple formula	Nominal stress method
Membrane and shell bending stress at weld toe	Structural stress method
Total notch stress	Notch stress method
Stress intensity at crack tip	Fracture mechanics

Figure 1. What is nominal stress? (*Niemi*)

$$\sigma_{\Sigma} = \sigma_{mem} + \sigma_{ben} + \sigma_{n.pl}$$

Figure 2. Types of stress in a plate

Figure 3. Structural stress method: *1* — computed total stress; *2* ---- geometric stress; *3* — measuring points; *4* ---- hot spot

$R = 1$ мм

Figure 4. Concept of effective notch radii

Figure 5. Cracks at cutout reinforcement

Fatigue resistance for assessment. The first fatigue design code which has incorporated this method was the IIW fatigue design recommendations [2]. Here, the fatigue class for effective notch assessment was fixed to the value of 225 MPa, i.e. the effective notch stress range at $2 \cdot 10^6$ cycles at a survival probability of 95 % related to a confidence of the mean of 95 %. For practical evaluations this is equal to mean minus two standard deviations. The next code is the recommendations of the German Machine Manufacturer's Association (VDMA) [3].

With the assistance of this new method, parametric formulae can be developed considering the variation of the dimensional parameters of a joint type, e.g. cruciform load-carrying joints. One example is the parametric formulae for cruciform joints with varying root gaps and for butt welds, which may be found in [4].

Application example. The main load-carrying structure of a highly wind fatigue loaded steel tower is a conical tube with a diameter of 3.5 m at the bottom and 1.5 m at the top. The height of the tube tower is 60 m. Inside, the height is subdivided into several decks which can be accessed by ladders fixed from inside. For reasons of access and inspection several doors are provided. The cutouts of the doors are reinforced by door frames 200×20 mm, which should be welded to the shell plates of the tube tower by full penetration K-butt welds by design. A whole series of these towers of this design has been built. After a period of time of satisfactory operation, cracks have been observed at several towers (Figure 5). This failure was obviously caused by fatigue action. It had to frame and tower be analysed and the causes had to be found. Later proposals for a possible repair should be made. The welding of the steel structure was given to a subcontractor and so, the responsibility had to be established for reasons of recompensation of the financial loss.

After the detection of the first cracks, the welds have been gouged for a further inspection The crack

**Table 2.** Different executions of welds and weld types in code (DIN 4133)

Type 5 (butt welds)	Type 6 (lack of penetr.)	Type 8 (root gap)
Трещина		
a	*b*	*c*
Half V-butt weld with double fillets, no root gap	Half Y-weld with double fillets, unwelded gap 2 mm	Double fillet weld with root gap
Weld specified in drawing	Weld actually executed	Worst case weld

developed from inside of the tower to outside in the high stressed area (Figure 6). It started from the weld toe connecting the shell plate to the door frame and then propagated through the shell plate. Additionally, an incomplete penetration has been observed, which was also found by ultrasonic inspection in all the o ther steel towers of the same production batch. The situation may be seen in Table 2. The extention of the lack of penetration was from a line flush to the inner surface of the tower shell plate to the outside direction at a dimension in depth of 2 mm (see Table 2, *b*).

An overall FEA showed the areas of elevated stress in the tower (Figure 7). It is around 45° to the tower axis. This position coincides with the observed position of the crack.

For the present type of welded joints, the code provides three possibilities (see Table 2). Firstly, the weld type 5, which is a K-butt weld at full peneration (Figure 8). It is expected to fail from the weld toe. Secondly, the weld type 6, i.e. the K-butt weld with an incomplete penetration of maximum 2 mm. It is also expected to fail from the weld toe, but there is a reduced allowable stress. Thirdly, the weld type 8, which is a double fillet weld with a root gap by design. Here, the failure is expected to start from the root.

The present weld containing an incomplete penetration could be easily classified as type 6, but there are several drawbacks. The code provides a gap in the
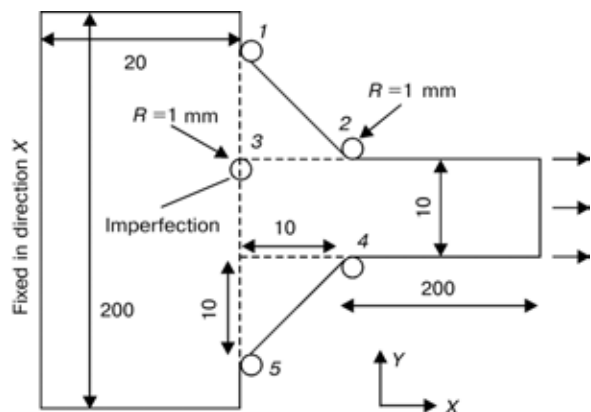
Figure 7. Model for FEA meshing

middle of the plate, whereas here the gap is assymmetric to the centerline of the plate. The more, a code has to cover the whole variation of dimensional parameters. Here the question was: Does this imperfection reduce the fatigue strength of this specific welded joint in comparison to a K-butt weld with full penetration?

The only existing fatigue assessment procedure which is capable to answer this question is the effective notch procedure. A plane model of the weld was established (see Figure 7) and used for a FEA analysis. All weld transitions, toe or root, have been modelled with an effective radius of 1 mm. The results may be seen in the stress plots (Figures 9 and 10).
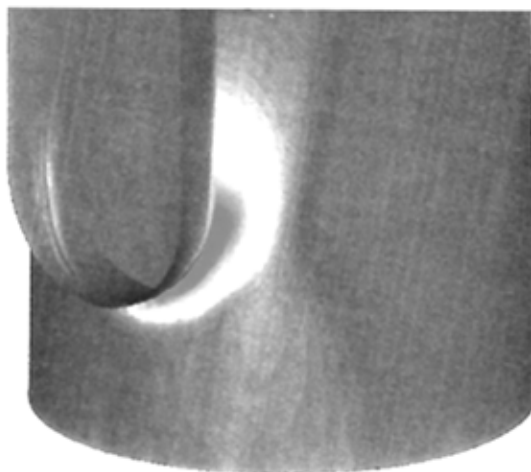
Figure 6. High-stessed area
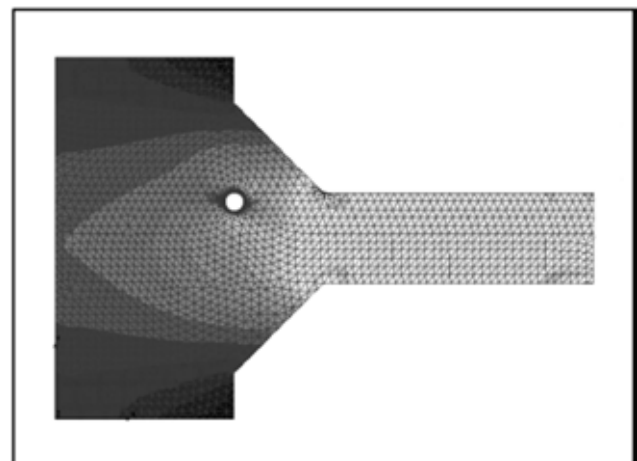
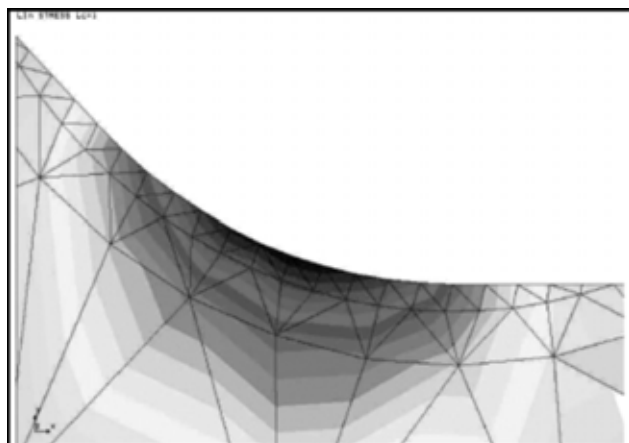**Figure 8.** Overall model of the joint

Figure 9. Weld toe notch

Table 3. Results of analysis

Spot	SCF	FAT
Toe	2.55	88
Root	1.6	140

The stress concentration factors (SCF) in relation to the stress in the plate is given in Table 3. The fatigue classes are also calculated by dividing the FAT 225 of notch stress by the stress concentration factor of the notch in consideration.

The results show that a failure from the root cannot be expected. Another analysis without imperfections shows that the fatigue strength of the weld toe is not affected by the incomplete penetration.

Many causes can influence the fatigue strength of a structure. Here, the possible causes have to be separated according to the responsibilities of the designer and the subcontractor. As will be shown below the fatigue resistance of the joint has not been affected by the unintended gap of the incomplete penetration. This poor manufacturing and inspection has to be attributed to the welding subcontractor. On the other side, the designer is responsible for proper load assumptions including the effects of dynamic response and for the proper design, at which all stress rising effects have to be considered. As a summary, which may be drawn now, the designer will be charged to carry the financial loss from these failures:

$$\text{FAT}_{\text{nom.str}} = \frac{225}{k}.$$

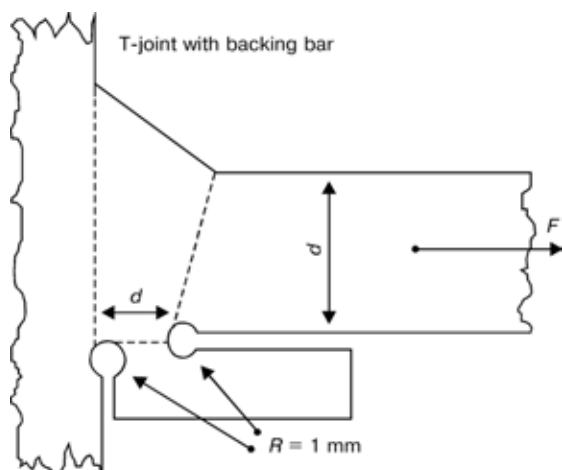A repair by gouging and removing the incomplete penetration is futile. The fatigue strength of the weld toe cannot be improved by this procedure. After a careful re-analysis of all loading parameters, a required fatigue strength of the welded joint should be specified. Then the notch stress method could be used again for the design of a joint with the required strength. Possible repair actions could be enlarging of the weld throat, reducing of the weld transition angle at the toe and applying the well established improvement techniques, e.g. TIG dressing and grinding.

Assessment of a nw structural detail. For a specific structural detail, the fatigue resistance class was to be determined [5]. It was a one-sided T-joint with a load-carrying one-sided narrow gap weld with a permanent backing bar. There are two sites of a possible crack initiation, namely the weld root notch directly adjacent to the transverse plate and the notch between the backing bar and the stressed plate. Preliminary calculations show that only the root notch is interesting. For the FEA model, the distance d between the two notches was varied. The wall thickness was kept constant at $t = 35$ mm. On this basis, the notch factors have been calculated. Later, the number of life cycles was determined with a Woehler S--N curve of FAT 225. The FAT class of the detail can be entered into the catalogue of details for the nominal stress procedure (Table 4).

No allowance for a linear or angular distortion is included in these values. They have to be considered additionally. A comparison with the fatigue classes of cruciform joints in the IIW fatigue recommendations show that the results fit well into the scheme.

Example of a parametric formula. The effect of dimensional variations of welded joints can be investigated using the effective notch stress procedure. In [3] a complete parametrisation of the dimensions at the example of a cruciform joint was elaborated. The dimensions which have been varied may be seen in Figure 11. The complex parametric formula has been simplified for fillet welds with a root gap equalling the wall thickness ($s = t$) and no bending loads and notch or weld transition radii equalling unity ($r = 1$ mm). With these conditions, the complex formula simplifies to the following equation:
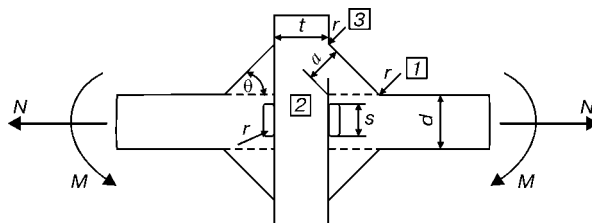

Figure 10. Detail with variation of parameters

Figure 11. Dimensions of a joint type

Table 4. Fatigue class FAT for nominal stress method

Wall thickness t	Distance d	FAT for root notch
35	2.0	80
35	2.5	67
35	3.0	65
35	5.0	62
35	6.0	60

$$k = 0.947 + [1 + 0.770 \left(\frac{a}{t}\right)^{-1.054} + 1.307 t^{0.093} -$$
$$- 2.315 \sin^{-0.029}\theta] \sin^{0.410}\theta \ t^{0.370},$$

where a is the weld throat; θ is the weld angle; and t is the wall thickness within the validity ranges: $a/t = 0.3\text{--}1.0$; $\theta = 0.26\text{--}1.57$ rad $\equiv 15\text{--}90°$; $t/r = 4\text{--}200$ (Figure 12).

The fatigue class FAT related to the weld throat area for the nominal stress method can be calculated by the following equation. The factor 1.2 was applied for a stress ratio $R_\sigma = 0$ at a low overall residual stress according to the IIW recommendations:

$$FAT_{\text{nom.str}} = (1.2 \cdot 225) / 2k(a/t).$$

CONCLUSION

Effective notch stress procedure is a new and effective way in assessing fatigue strength of welded joints. It can be universally applied, but it requires an elevated expense in calculative analysis. It will certainly not be the method for everydays calculations. But at few special critical points of a structure, the application might well be indicated.

In the near future, more experience will be collected, which will expand the application. The ex-
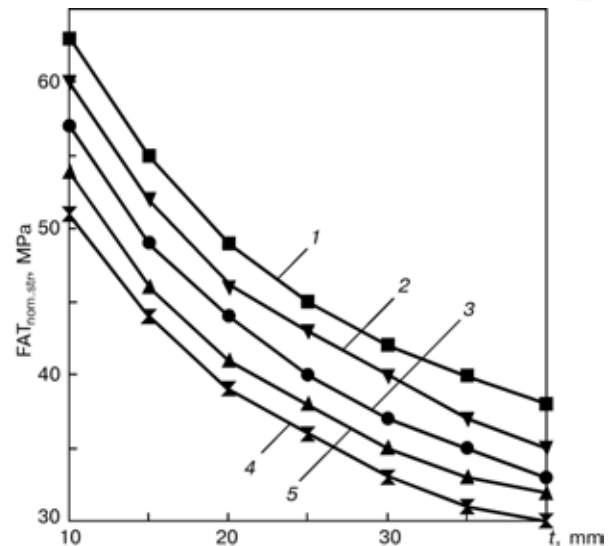
Figure 12. Parametric fatigue data: *1* — *a/t* = 0.3; *2* — 0.4; *3* ---- 0.5; *4* ---- 0.6; *5* ---- 0.7

pansion of the method to aluminium is on the way. It is expected for the next update of the IIW fatigue design recommendations.

1. Olivier, R., Kottgen, V.B., Seeger, T. (1989) Schwingfestigkeitsnachweis für Schweißverbindungen auf Grundlage örtlicher Beanspruchungen. Schweißverbindungen I. Vorhaben Nr. 105. *Forschungsheft. Forschungskuratorium Maschinenbau.* Frankfurt: VDMA.
2. Hobbacher, A. et al. (1996) *Fatigue design of welded joints and components.* Abington: IIW.
3. Haenel, B., Haibach, E., Seeger, T. et al. (1998) Rechnerischer Festigkeitsnachweis für Maschinenteile. *Richtlinie des Forschungskuratoriums Maschinenbau.* Frankfurt: VDMA.
4. Anthes, R.J., Kottgen, V.B., Seeger, T. (1993) Kerbformzahlen von Stumpfstößen und Doppel-T-Stößen. *Schweißen und Schneiden,* **12**.
5. Greuling, S., Steinmann, R., Seger, T. (2000) Betriebsfestigkeitsnachweis mit Kerbspannungen von nicht katalogisierten Schweißverbindungen und deren Einordnung in Kerbgruppen von Regelwerken. *Stahlbau,* **4**, 268--275.

FAILURE OF WELDED ALUMINIUM TUBES

K.J. MILLER

University of Sheffield, Sheffield, UK

A failure investigation concerning 6061-T6 aluminium tubes as produced by an extrusion process, required an extensive and detailed study. This involved ten aspects, namely the manufacturing process; 3D finite element stress analysis; microstructural fracture mechanics; metallurgical considerations; international codes and specifications; residual stresses; Raman spectra analyses; environmental factors an extremely long-life fatigue failure assessment; and recommendations as to how to avoid future failures. Obviously the investigation required a multi- and inter-disciplinary approach. At the start of the study the opinions of several experts were sought. At the termination of the investigation successful recommendations were made to the manufacturers that avoided future failures. The brief case history presented in this paper is a useful exercise for students of microstructural fracture mechanics and fatigue failure analyses.

Keywords: microstructural fracture mechanics, residual stresses, peripheral coarse grains, port-hole extrusions and fatigue failure analyses

The product of concern is a roller of cylindrical cross-section used in the construction of a conveyor belt system. This continuously transports coal from an inland open-cast mine, a distance of several miles, down to an ocean terminal at which one or two ships can be loaded without interruption. The roller is shown in Figure 1 along with its important dimensions. The spacing between rollers in the conveyor belt system is 1.5 m and the coal is transported on a rubber-composite belt, such that a uniformly distributed load of 718 kg (3.52 kN) is carried length-wise across the roller width. This load is spread from zero to a maximum value over $\pm 5°$ on the upper peripheral surface of the roller. The end plugs facilitate bearing lubrication, a necessary feature to inhibit seizure since the rollers rotate at 602 rpm, that is the 152.4 mm diameter roller sustains a belt velocity of 4.8 m/s. As shown later there are, unusually, four loading cycles per revolution which gives a total of 3.4 mln

cycles each day of continuous running. There are no mechanical or material property records that would provide information for a 10 year lifetime assessment for the rollers.

Problem. The product, although extensively and satisfactorily tested prior to its on-site introduction, frequently failed within a few days of installation. The plane of cracking was along the r–z plane and not the r–θ plane on which a cyclic axial tensile stress would exist due to bending of the roller. Some cracks zig-zagged a little in their axial growth direction while others meandered but only slightly. No cracks started at the end fittings, albeit these were interference fits. Many of the cracks had opened wide suggesting that residual stress played a significant role. Obviously a detailed finite element analysis was required.

A statistical analysis of failures per day/week/month was contemplated on the basis that the very long-life fatigue behaviour of a material is often considered to be a Weibull-type statistical phenomenon. This was not attempted since it would not explain the physical causes of the numerous and near instan-
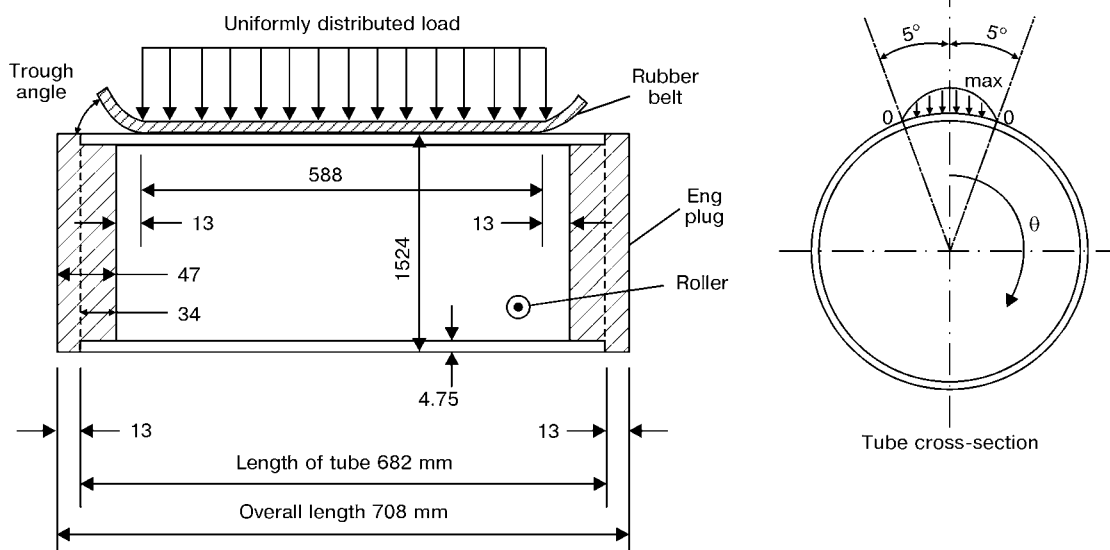

Figure 1. Cylindrical roller with key dimensions

taneous failures. Likewise a detailed chemical analysis was of little use since the material apparently met the required specification. Furthermore, mechanical properties were deemed to be satisfactory. Two possible environmental factors were considered, namely the close proximity of the sea, and the presence of small black particles which could, coupled with saline vapour, induce a corrosive attack.

Finite element analysis. Due to the cross-sectional symmetry of the roller only a quarter segment was analysed, i.e. one-half of the roller circumference with one half of the roller length. Figure 2 illustrates the 3D contours of one of the many parameters studied. 3D displacements were recorded and also maximum/minimum principal stresses together with radial, axial and hoop stresses. The FE solutions were derived from the ANSYS version 6.1 program using the H-element technique. A mapped quadrilateral mesh generates more accurate results in comparison to triangles or a mixture of triangles and quadrilaterals. The applied load was 1760.35 N (i.e. one half of 718 kg). The constrained end had a plug connection that provides a simply supported condition on the terminal 34 mm portion of the half cylinder. To simplify the belt pressure loading a triangular pressure distribution was assumed.

Figure 3 presents the main results in graphical form, while Table 1 presents the important numerical data. The major conclusions from the analysis are:

• cyclic stress levels are low and fatigue failures should not have occurred;

• as the cylinder rotates through 360°, both the inside and outside surfaces suffer two different cycles ---- a major and a minor cycle;

• this phenomenon occurs for both the circumferential and the axial stress patterns although the former is more important when compared to the axial stresses induced by rotary bending;

• radial stresses are negible;

• surfaces where initial cracking may be expected suffer a biaxial stress system;

• failures must be due to some other principal cause or causes.

Extrusion process. Aluminium lends itself to the extrusion process and a multiplicity of shapes can be produced. Figure 4 shows two examples of how the high thermal conductivity of aluminium can best be utilised for cooling systems by producing optimal but complex cross-sections. There are three basic methods for extruding products.
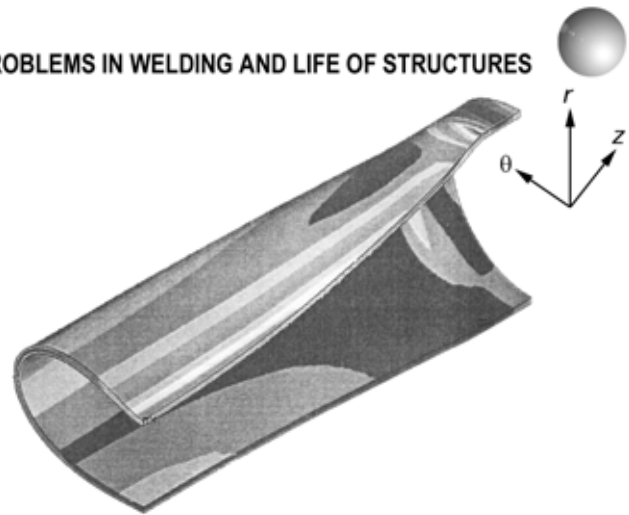

Figure 2. Equivalent von Mises 3D stress distribution

Direct seamless extrusion. Here a pre-heated billet is pushed through a die and consequently must slide along the inside wall of the container vessel. To overcome frictional forces high pressures have to be employed. The «back-end» or final part of the billet, i.e. up to 15 %, has to be discarded to avoid the introduction of various forms of defects into the extruded product.

Indirect seamless extrusion. Here in relative velocity terms the die is pushed by a hollow stem into the stationary billet and the product flows down the inside of the stem. The frictional load is therefore significantly reduced in comparison to the direct method and so is the preferred technique for the strong 2024 and 7075 aluminium alloys.

Port-hole extrusion method. This is a faster and cheaper method and is the preferred method for non-critical applications and for the softer alloys. It was used to produce the thin cylinders for the rollers in the case now being discussed and so further details are now presented.

Figure 5 shows how a solid cylindrical billet approaches a die. The bridge of the die is designed to split the billet into two halves. These halves then pass over the mandrel of a fixed outer diameter that equals the future bore of the tube. As the two halves pass through the die hole, which matches the extruded tube outer diameter, the two halves of the billet are pressure-welded together. The final product therefore has two diametrically opposite welds. Depending on the size and thickness of the tube to be produced there can be 3 (or 5) equally spaced bridges which split the on-coming stream of continuous billets into 3 (or 5) segments. Therefore the extruded tube will have

Table 1. Main results from the FEM analysis

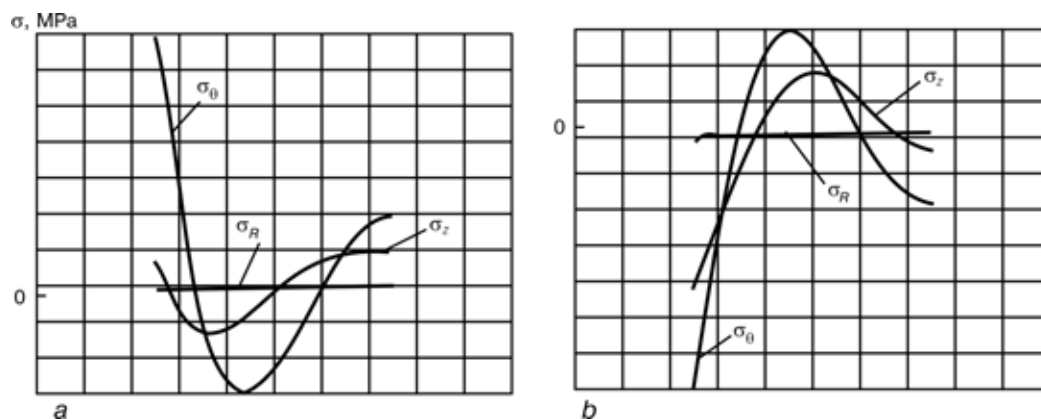|	Stress values, MPa					
	Circumferential (hoop) stresses			Axial stresses		
	σ_{min}	σ_{max}	$\Delta\sigma$	σ_{min}	σ_{max}	$\Delta\sigma$
Outside skin:						
major cycle	--45.6	18.6	64.2	--28.4	11.2	39.6
minor cycle	--12.1	18.6	30.7	--3.2	11.2	14.4
Inside skin:						
major cycle	--18.7	45.5	64.2	--8.1	6.0	14.1
minor cycle	--18.7	12.5	31.2	--8.1	5.1	13.2

Figure 3. Hoop σ_θ, axial σ_z and radial σ_R stress distributions over one-half of the roller circumference the outside (*a*) and inside (*b*) surface (for values see Table 1)

3 (or 5) weld zones equally spaced around the tube circumference.

The port-hole extrusion process can produce various forms of defects. It is vital that the surfaces to be welded are perfectly clean. The most common contaminant is colloidal graphite or boron nitride which are used to separate the aluminium billet from the steel components of the die tools. Contaminated welds can lead to easy splitting of the tube. Another defect is known as a transverse weld defect. This is created by the interface between the billet which is entering the die and the follow-up billet. This interface when extruded is a critical area for weld defects. Finally a peripheral coarse grain (PCG) structure can occur if the conditions for extrusion are not optimised, i.e. speed, temperature, pressure gradients and die geometry.

Post-extrusion processes. After leaving the die the hot-metal tube is treated to acquire maximum strength. This is achieved by a solution heat treatment followed by an immediate artificial ageing. However the final properties of the product are much dependent on the shape of the hot metal after it leaves the die. Should defects and/or faulty production processes have been introduced during the extrusion process then the thin, long, round cylinder can deform into an oval cross-section. Should this happen then the cylinders may have to be «reeled». In the reeling process the deformed tubes pass through a series of helically arranged cylinders that have a centred round core which produces the required final shape. Unfortunately, the reeling process can induce residual stresses and surface scratch marks.

Residual stresses. As stated previously the failed rollers exhibited open axial cracks indicative of the presence of residual stresses. Consequently several unused specimens were tested, some having been reeled and other not-reeled. The circumferential and axial residual stresses around the inner and outer circumferences were obtained from seventeen 90° strain gauge rosettes which provided data before and after cutting around each gauge to obtain, respectively, base-line and residual stress values.

In the carefully conducted tests reported above the maximum recorded values were 127 MPa (circumferential-outer surface), 38 MPa (axial-outer surface), --149 MPa (circumferential-inner surface) and --49 MPa (axial-inner surface). The crucial value is of course the +127 MPa but since this value was obtained on only one specimen it would not be surprising if the most heavily reeled cylinders had a much higher value. Additionally another peak of +103 MPa was recorded for the circumferential outer surface, this being displaced from the 127 MPa value by some 216°. Note, five equi-spaced weld zones exist at 0, 72, 144, 216 and 288°.

Mean stress effects. Residual stresses provide a very high mean stress onto which the smaller fatigue (cyclic) stresses must be added. Table 2 shows this data which includes the largest (127 MPa) and the smallest (103 MPa) tensile residual stress data previously obtained. Only the surface circumferential stresses are considered since these are normal to the failure crack plane. From this it follows that the two stationary tensile residual stress peaks (large and small being separated by 216°) combine with the two fatigue (major and minor) cyclic stress ranges to give four fatigue cycles per single revolution of the cylinder. Also provided in Table 2 are the ratio values R associated with each of the four fatigue cycles per revolution.
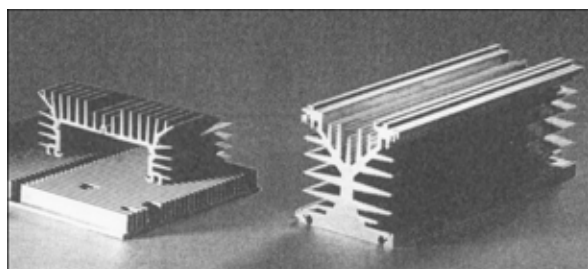

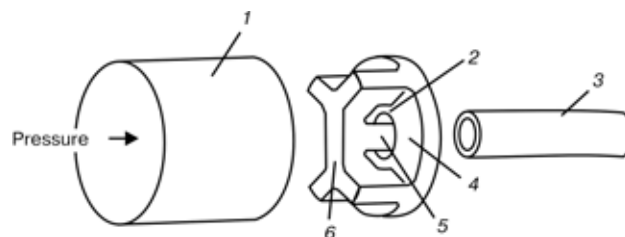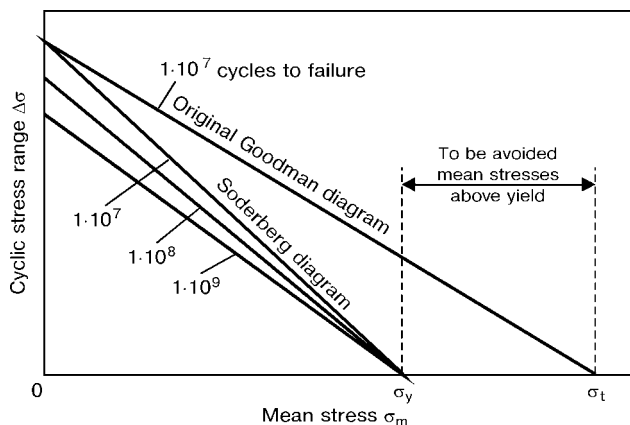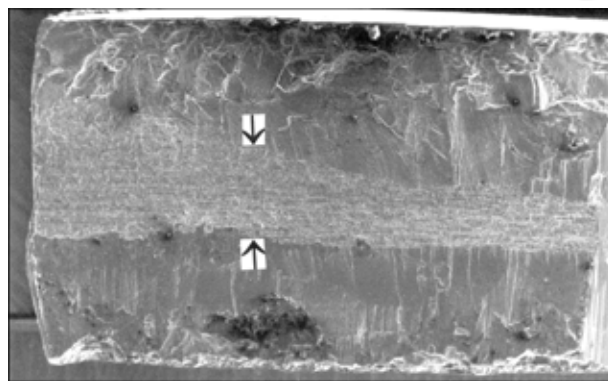**Figure 4.** Two examples of extruded products

Figure 5. Example of the port-hole die system showing two port-holes and welding chambers: *1* — solid billet; *2* — weld area; *3* — extruded tube; *4* — die; *5* — mandrel nose; *6* — bridge

Table 2. Fatigue stress values of the 4 cycles per revolution of the cylinder

Cycle	Tensile residual stress, MPa			
	σ_{max}	σ_{min}	σ	$R(\sigma_{min}/\sigma_{max})$
Major cycle:				
127	145.6	81.4	64.2	0.56
103	121.6	57.4	64.2	0.47
Minor cycle:				
127	145.6	114.9	30.7	0.79
103	121.6	90.9	30.7	0.75

Figure 7. Part of a fracture surface of the 4.75 mm thick cylinder wall

The Goodman--Soderberg diagram which plots the cyclic stress range ($\Delta\sigma$) as a function of mean stress (σ_m) for a given cyclic lifetime illustrates the high sensitivity to $\Delta\sigma$ values for very long-life fatigue when the mean (residual) stress approaches the yield stress of a material; this for plain (non-cracked) specimens is shown in Figure 6. Alternatively high positive values of the $R(\sigma_{min}/\sigma_{max})$ produce very low $\Delta\sigma$ (threshold) values in a linear elastic fracture mechanics type calculation for cracks which propagate by fatigue. In order to study which approach to adopt attention is drawn to Figure 7 which shows a fracture surface of a cylinder.

Fractography and microstructural considerations. Figures 7 and 8 show, respectively, the 4.75 mm thickness of the cylinder wall which is the fracture plane, and the PCG structure of the cylinder outer and internal surfaces. These two figures are complimentary. The two arrows of Figure 7 mark the boundaries of a fatigue fracture zone which is of very limited width. The outer and inner surface zones have cleavage-like facets indicative of fast fracture separation in this supposedly ductile metal. Figure 8 shows a mixture of surface coarse grains and a very fine interior grain structure; the latter providing a limited zone of excellent fatigue resistance with a high yield strength typical of the 6061-T6 alloy. The outer zone will have a neglible yield strength according to the Hall--Petch relationship linking yield stress to the reciprocal of the square root of the grain size i.e. $\sigma_y = k(1\sqrt{d})$. Considering that all metals will crack, should their grains be constrained from plastic deformation and that the low yield strength PCG zone is constrained both axially and circumferentially by a high elastic biaxial tension stress field due to residual stresses

then it is not surprising that the outer grains suffer deep cleavage-like cracks across whole grains which frequently have a size greater than 1.5 mm. Thereafter, once the mid-quarter of the cylinder wall has cracked by fatigue, the final ligament will rapidly fail.

One weld zone is shown in Figure 9 at a much larger magnification. This shows coarse grains at the weld interface and a fine grain structure below the surface and close to the weld zone. There can be five such weld zones around the circumference of the cylinder. It is highly probable that the PCGs cracked during reeling and before the rollers were subjected to cyclic forces.

Microstructural fracture mechanics. Microstructure fracture mechanics (MFM) has three main tenets:

• cracks begin to propagate immediately on cyclic loading;

• initial crack propagation rate is proportional to grain size (or the inverse of yield stress) which dictate the extent of the crack-tip plasticity;

• fatigue cracks slow down as they approach microstructural barriers, e.g. grain boundaries.

In the MFM equation

$$da/dN = C\Delta\sigma^m(d - a)$$

da/dN is the cyclic crack speed; C and m are the material constants; $\Delta\sigma$ is the cyclic stress range; d is the grain size; and a is the crack depth within the grain. Hence it can be seen that the larger the grain, the faster the initial crack will grow. At very high stress levels the crack will grow much faster. Additionally since the stress levels are greater than one-

Figure 6. Goodman--Soderberg diagram
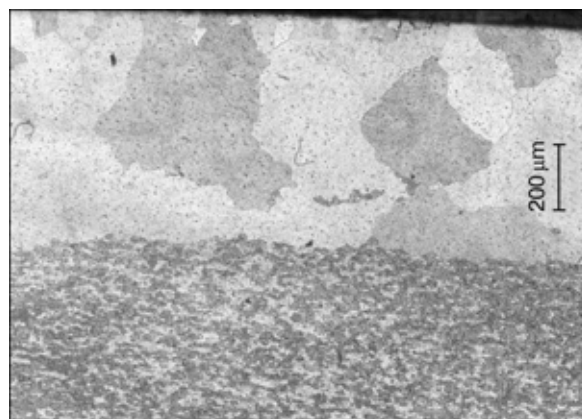
Figure 8. Sharp demarcation between the surface coarse grain zone (1 mm thick) and the inner fine grained zone

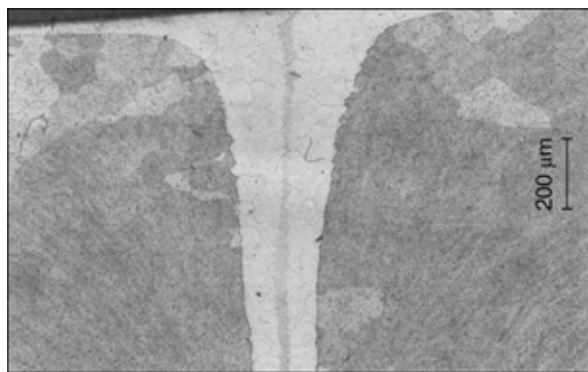**Figure 9.** Cross-section of a weld zone with a minimum thickness of 200 μm ≈ 1.8 mm below the outer surface

Figure 10. Relationship between MFM, EPFM and LEFM for different cyclic stress ranges, crack lengths and grain sizes

third of the yield stress of the material, linear elastic-fracture mechanics (LEFM) will not apply and elastic-plastic fracture mechanics (EPFM) should be considered. Under the present conditions of high maximum stress values (see Table 2) and large grains, should all the surface grains not have cleaved during reeling then the crack will certainly grow quickly across surface grains during the first day of operations when at least 3 mln cycles will have accumulated. In the mid quarter section of the tube wall the limited fatigue resistance will have to be quantified by EPFM. Hence threshold conditions according to LEFM principles are not applicable to this problem. Figure 10 encapsulates the above discussion.

Environmental considerations. Some corrosion pitting and intergrannular corrosion was in evidence on the surfaces of some failures. The questions was ---- did these contribute to the initial failure process or did they occur after the surface grains cracked following reeling. Since it is generally accepted that corrosion processes do not occur in this type of aluminium alloy which is frequently used in ocean environments, this possibility was not considered a priority issue. However, EDS and SEM techniques were used on surface products. Additionally Raman spectrum analyses were conducted on a black particle sample taken off a fracture surface and a sample of powdered coal. No definitive answer was achieved but the black particle sample was in all probability the graphite used to cover the billets prior to their extrusion. Coal dust would inevitably enter all surface cracks and due to its compressive strength, unlike graphite, would help prop open cracks thereby increasing fatigue crack propagation resistance. The major aspect of the failures, however, should always be remembered, namely that time-dependent processes, such as corrosion fatigue and stress corrosion, would have neglible effect since the majority of failures occurred soon after their installation.

CONCLUSIONS

The major factors leading to the failures were as follows:

1. The reeling process that followed extrusion introduced very large residual stresses. These stresses magnitude. The decrease in yield strength below international specifications is due to the large surface grains.
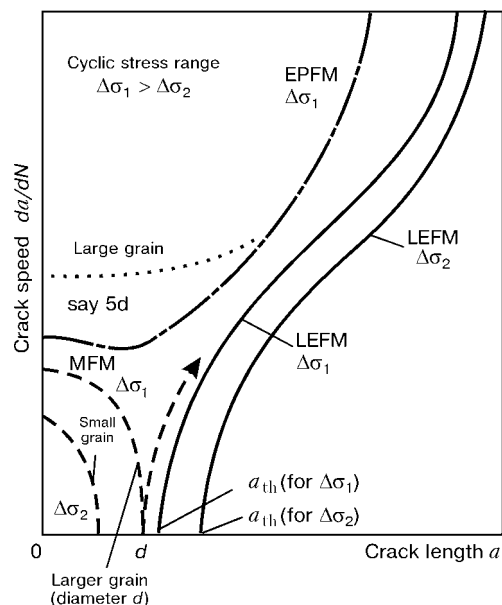
2. The peripheral coarse grain structure created due to insufficient plastic straining of the surface material during extrusion. Strains that are just above the yield stress but below a critical level do not create sufficient nucleation centres for the production of new and numerous small grains which give both strength and fatigue resistance to the rollers. Recrystalisation and grain growth at high temperature is assisted by the few nucleation sites that will exist within the weld zone of the die following extrusion but before reeling takes place.

3. Failures could have been avoided by introducing proper quality control systems during production, including drift tests on randomly selected samples. Here a drif tool of a slightly tapered profile is pressed into the cylinder bore which will cause splitting of the cylinder should weak zones exist.

4. This case-history shows that conveyor-belt rollers can accumulate 20 mln cycles in the first week of being placed in service. No long-term fatigue failure data exists in the literature for this aluminium alloy.

5. Microstructural fracture mechanics explains the important surface stage of cracking in the PCG zone. High biaxial tension stresses provide a constraint that will assist the introduction of deep cleavage-like cracks.

6. The fatigue fracture zone in the mid-quarter of the wall thickness is too small and the fatigue resistance of this 6061-T6 alloy has been severely compromised prior to service due to the PCG zones.

7. LEFM analyses, particularly those involving threshold values, are not appropriate to this failure analysis.

PREDICTION OF FRACTURE OF WELDED JOINTS IN DUCTILE STEELS CONTAINING DEFECTS

A.S. ZUBCHENKO, G.S. VASILCHENKO and **A.V. OVCHINNIKOV**
State Research Centre «TsNIITMASh», Moscow, Russia

Method for calculation of limiting loads for a structure comprising welded joints with defects is suggested. The method allows modelling of the process of quasi-static propagation of cracks in ductile steels. Examples of the calculation are presented.

Keywords: *welded joints, defects, static strength, limiting loads, fracture model*

The majority of calculations of a limiting state of ductile bodies containing defects is made by using *J*-integrals or crack displacement parameters. For example, the data on admissibility of defects of welded joints in the nuclear power plants (NPP) pipes at the stage of service given in the ASME code [1] were derived by using *J*-integrals. The popular method for estimation of integrity of a structure containing defects [2] known as *R*6 is based on the same principles. Approaches used by TWI [3] to calculate crack resistance are based on the crack displacement parameters.

Ductile materials during the fracture process have, as a rule, the stage of quasi-static increment in size of a crack. A current size of the crack in this case can be related to the effect of external forces. The similar relationship exists between the crack tip opening displacement (CTOD) δ_c and increment in its size.

Therefore, in contrast to conventional mechanical properties of materials (under assigned conditions), the critical values of *J*-integral and CTOD are functions of increment in the crack size, Δa, rather than numbers. These functions are designated as the J_R and δ_R curves. In turn, *J*-integral and CTOD δ_c, characterising the level of load applied on a body, also depend upon the crack size, $a = a_0 + \Delta a$, where a_0 is the initial crack size. In this case the share of the

crack size increment Δa in the current crack size is of no significance.

The limiting state of a body with a crack is reached under load P which provides simultaneous meeting of two conditions:

$$J(P, a) = J_R(\Delta a); \quad T(P, a) = T_{\text{mat}}(\Delta a), \qquad (1)$$

where $T = \mathrm{d}J/\mathrm{d}a \cdot E/R_{p\,0.2}^2$ is the applied rupture modulus; $T_{\text{mat}} = \mathrm{d}J_R/\mathrm{d}a \cdot E/R_{p\,0.2}^2$ is the material rupture modulus; E is the elasticity modulus; and $R_{p\,0.2}$ is the proof stress.

The value of Δa, at which condition (1) is met, corresponds to the ultimate subcritical increment in the crack size under soft loading.

Calculations using formula (1) can be replaced by a simple geometrical construction. Figure 1 shows the method for estimation of critical load $P_{\text{cr}} = P_2$ and the ultimate subcritical increment in the crack size by selecting the appropriate values.

The relationship between *J*-integral and CTOD δ is known [4]. Therefore, geometrical constructions shown in Figure 1 allow the P-δ loading diagram and the P-Δa relationships to be calculated (Figure 2).

Along with the traditional approach to description of the process of fracture of ductile bodies with cracks, we can suggest the model of fracture based on other premises. There is some value of opening of the crack
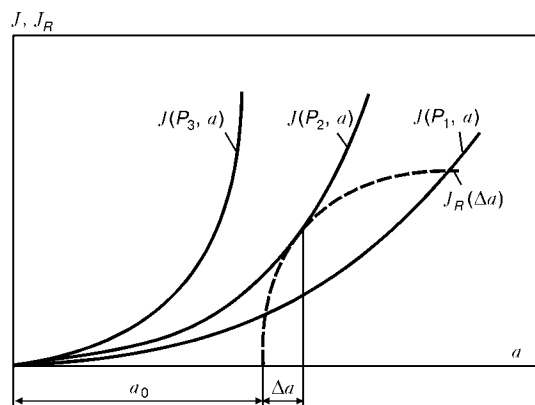

Figure 1. Estimation of critical load and static increment in size of a defect by the J_R curve method
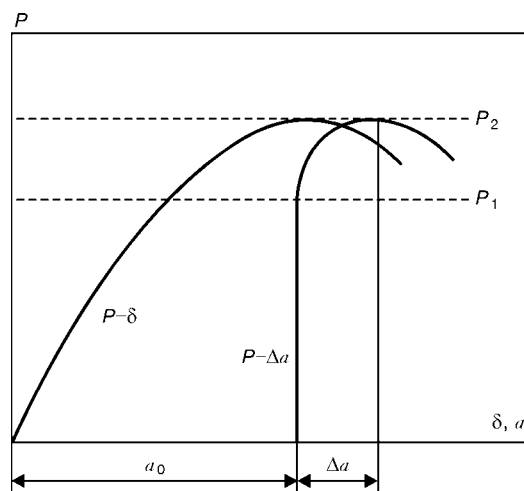

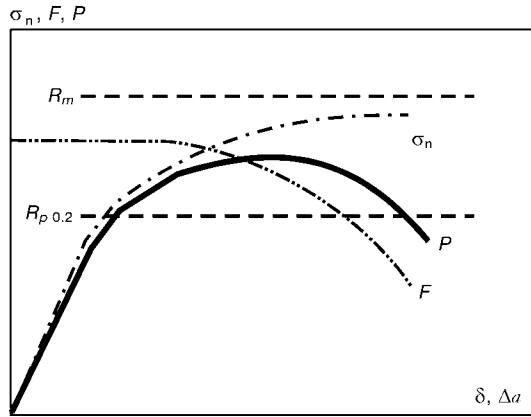**Figure 2.** Diagrams P–δ and P–Δa

Figure 3. Estimation of load as a function of plastic displacement and increment in crack size

centre, δ, corresponding to the starting point of displacement of the crack, at which the area of the section weakened due to the crack, F, decreases. Nominal (averaged) stress σ_n in this section increases with increase in δ, but it does not exceed ultimate strength R_m (or actual rupture resistance, if reduction in area is taken into account).

Therefore, the product of nominal stress by area that determines the applied load, $P = \sigma_n F$, has a maximum (Figure 3).

If we manage to determine relationships

$$\sigma_n = f_1(\delta) \quad \text{and} \quad F = f_2(\delta),$$

we can thus estimate the values of critical load P_{max} and corresponding variation in the crack size.

The authors of [5, 6] showed that the relationship of increment in plastic component δ_p of the crack opening displacement to the corresponding increment in its length (critical angle of plastic crack opening displacement)
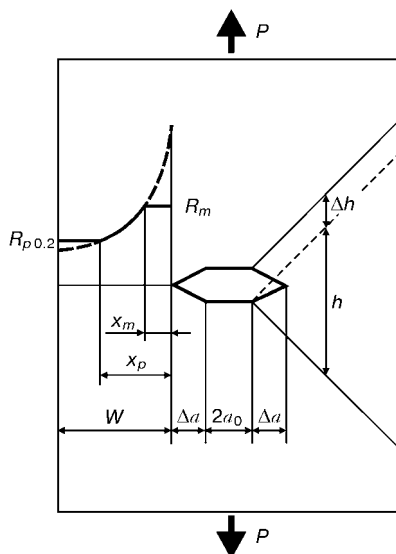
$$(2)$$

$$\chi = \frac{d\delta_p}{da}$$

Figure 4. Distribution of stresses (*to the left*) and diagram of deformation (*to the right*) of a plate with central crack

depends but to a much lesser degree upon the type of a specimen and its size than the J_R or δ_R curves. However, this fact had no effect on the calculation practice, as it remained unclear yet how the χ characteristic could participate in the criterial relationships.

In this study we suggest employing the value of χ to calculate critical loads and subcritical increment in crack size, based on a number of hypotheses using the so-called «plastic displacement method».

Quasi-static growth of a crack is accompanied by a relative plastic displacement of parts of a body located on different sides of the crack (Figure 4). However, this displacement causes plastic deformation of a certain zone in specimen. Knowing the shape of the plastic zone and plastic displacement $\Delta h = \delta_p$, we can estimate plastic strain $\varepsilon_p = \Delta h / h$ in each longitudinal element h of the plastic zone (see Figure 4).

The material strengthening law allows us to change from strains to stresses, while the integration of stresses for a section yields a load that corresponds to this or that value of the crack size increment.

The increment in plastic displacement dh corresponds to the increment in strain:

$$d\varepsilon = \frac{dh}{h} = \frac{dh}{2x}, \qquad (3)$$

where $x = h / 2$ is the distance between the element with length h and the end of a moving crack (angle at the apex of the plastic zone is about 90°). In turn, according to (2), $dh = d\delta_p = \chi da$.

By integrating expression (3) from the initial to final size of the crack, we can readily estimate the value of plastic strain depending upon increment Δa and coordinate x:

$$\varepsilon_p = \int_{a_0}^{a_0 + \Delta a} \frac{\chi da}{2x} = \frac{\chi}{2} \ln\left(1 + \frac{\Delta a}{x}\right) \approx \frac{\chi}{2} \frac{\Delta a}{x}. \qquad (4)$$

To proceed to stresses, let us use approximation of the Ramberg–Osgood deformation diagram:

$$\frac{\varepsilon}{\varepsilon_0} = \frac{\varepsilon_e}{\varepsilon_0} + \frac{\varepsilon_p}{\varepsilon_0} = \frac{\sigma}{\sigma_0} + \alpha\left(\frac{\sigma}{\sigma_0}\right)^n, \qquad (5)$$

where $\varepsilon_0 = \sigma_0 / E$; ε_e is the elastic component of strain; $\sigma = R_{p\,0.2}$; and α and n are the material strengthening characteristics.

Coming back to formula (4), we obtain relationship between stresses in the plastic deformation zone and increase in the crack size:

$$\sigma = \sigma_0 \left(\frac{\chi}{2\alpha\varepsilon_0} \frac{\Delta\alpha}{\chi}\right)^{1/n} = \sigma_0\left(B\frac{\Delta\alpha}{\chi}\right)^{1/n}, \qquad (6)$$

where $B = \chi / 2\alpha\varepsilon_0$ is the material characteristic ($B = 20$–400).

The stress diagram calculated from this formula is shown by the dashed line in Figure 4. While estimating load P, one should bear in mind that stresses exceeding ultimate strength R_m cause a substantial

reduction in section. Allowing for this factor makes the calculations using formula (4) with a logarithm much more accurate. The practice in engineering is to limit the maximum stress to the ultimate strength value, the value of reduction in area being ignored. As shown by comparison of the calculations and experimental data, this condition has almost no effect on accuracy of the calculations with a substantial simplification of the method.

As shown in [7], for the crack to move in tough materials it is required that stresses reach the yield point across the entire weakened section. Therefore, the minimum level of stresses can be limited to the $R_{p\,0.2}$ value (see Figure 4).

Integrating stresses across the section of bridge W (see Figure 4) and allowing for the fact that the initial size of the bridge is $W_0 = W + \Delta a$, we derive a formula for the calculation of load P depending upon the increment in the crack size:

$$P = 2R_{p\,0.2}tx_p \times$$
$$\times \left[\frac{R_m}{R_{p\,0.2}} \frac{x_m}{x_p} + \frac{n}{n-1}\left(\frac{B\Delta a}{x_p}\right)^{1/n}\left(1 - \left(\frac{x_m}{x_p}\right)^{n-1/n}\right) + \frac{W_0 - \Delta a}{x_p}\right], \quad (7)$$

where $x_m = \min \left\{ \begin{array}{l} B\Delta a\left(\dfrac{R_{p\,0.2}}{R_m}\right)^n \\ W_0 - \Delta a \end{array} \right.$; $x_p = \min \left\{ \begin{array}{l} B\Delta a \\ W_0 - \Delta a \end{array} \right.$;

t is the plate thickness.

The rule for the calculation of x_m and x_p reflects the fact that the boundary of a body with a crack may fall on any of the three regions of the stress diagram (Figure 4). Formula (7) can be simplified if conditions of its applicability are broken into three ranges of increment in the crack size:

for small increment $\Delta a \leq \dfrac{W_0}{B+1}$

$$P = 2R_{p\,0.2}t \times$$
$$\times \left\{ \frac{B\Delta a}{n-1}\left[n - \left(\frac{R_{p\,0.2}}{R_m}\right)^{n-1}\right] + W_0 - \Delta a(B+1) \right\}; \quad (8)$$

for large increment $\Delta a \geq \dfrac{W_0}{B\left(\dfrac{R_{p\,0.2}}{R_m}\right)^n + 1}$

$$P = 2R_m t(W_0 - \Delta a); \quad (9)$$

for intermediate values of $\dfrac{W_0}{B+1} \leq \Delta a \leq$

$\leq \dfrac{W_0}{B\left(\dfrac{R_{p\,0.2}}{R_m}\right)^n + 1}$

$$P = 2R_{p\,0.2}t \times$$
$$\times \frac{B\Delta a}{n-1}\left[n\left(\frac{W_0 - \Delta a}{B\Delta a}\right)^{(n-1)/n} - \left(\frac{R_{p\,0.2}}{R_m}\right)^{n-1}\right]. \quad (10)$$

The load calculated depending upon Δa using formulae (8) through (10) has a maximum, the location of which determines the critical values of P and Δa for soft loading. The plastic displacement method can also be applied for loading with an assigned compliance, as it allows not only the load but also the relative plastic displacement of the force application points (elastic displacement is calculated by traditional methods) to be estimated for a current value of Δa. The displacement being known, it is possible to correct the load and, using the iterative method, obtain the comprehensive description of the fracture process.

Tests of large specimens with a section of 300×65 mm were conducted at TsNIITMASh. The specimens of steel 15Kh2NMFA, containing central through and semi-elliptical cracks, were tested to quasi-static tension to rupture.

The specially developed procedure for marking the crack along its propagation front during loading allowed the increment in the crack size to be experimentally determined depending upon the load. The resulting values of the critical load ranged from 7 to 9 MN, and those of the subcritical increments in the crack size varied from 4 to 8 mm. The J_R curve and parameter χ were estimated on the basis of generalisation of experimental data for steel 15Kh2NMFA on specimens 65 mm thick.

Then the possibility of describing the fracture process by the plastic displacement method (formulae (8) through (10)), method of the J_R curves (formula (1)) and R6 method [2] was verified. This was done by using the most versatile version of the R6 method implying estimation of the J-integral. For a case of uniform tension this version of the R6 method formally coincides with the method of the J_R curves, although it has a limitation on a condition of plastic instability.

J-integrals were calculated using the following formula given in [2, 8]:

$$J = \frac{K^2}{E}\left[\frac{\varepsilon_i/\varepsilon_0}{\sigma_i/\sigma_0} + \frac{1}{2}\frac{(\sigma_i/\sigma_0)^3}{\varepsilon_i/\varepsilon_0}\right],$$

where K is the stress intensity factor calculated from the formulae given in [9] for through cracks and in [10] for semi-elliptical cracks; ε_i is the strain corresponding to the averaged stress σ_i; $\sigma_i = \sigma / k_F$ is the averaged stress in the weakened section; σ is the stress with no allowance for the presence of crack; $k_F = \dfrac{1}{1 + a/W}$ is the weakening coefficient for the central through crack; and $k_F = 1 - \dfrac{a/t}{\dfrac{4}{\pi} + \dfrac{2}{\pi}\dfrac{a/c}{a/t}}$ is that for the semi-elliptical crack with semi-axes a and c.

The experimentally evaluated Ramberg--Osgood approximation parameters (5) for steel 15Kh2NMFA are as follows: $\sigma_0 = 556$ MPa, $\alpha = 1.22$ and $n = 17.4$. The plastic displacement method for semi-elliptical cracks cannot be reduced to simple formulae of the
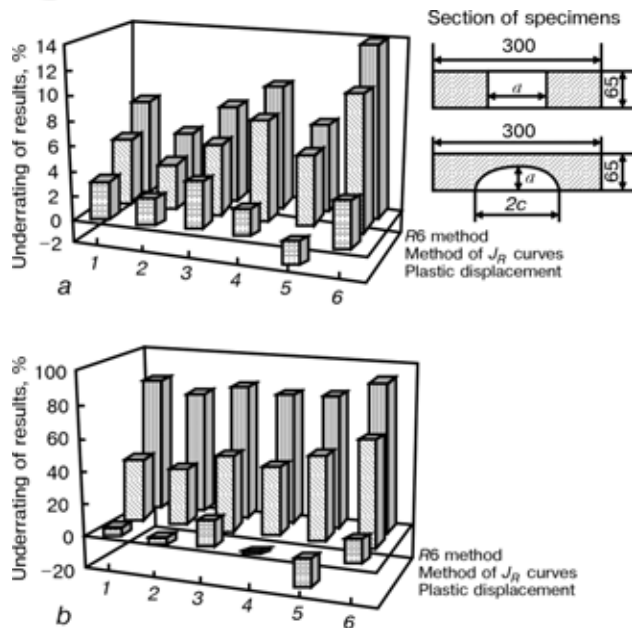
Figure 5. Estimation of error of the methods of calculation of critical load (*a*) and subcritical increment in crack size (*b*) for specimens with through (*1–3*) and semi-elliptical (*4–6*) cracks

type of (8) through (10), but it can be readily realised numerically.

The purpose of the calculations was to estimate the maximum load and a corresponding increment in the crack size. Comparison of the data obtained by the calculations using the above three methods (plastic displacement, J_R curves and $R6$) with the experiment is shown in Figure 5.

The comparison allows a conclusion of the applicability of all the three methods for estimation of the critical (maximum) load, as well as of the apparent advantage of the plastic displacement method for estimation of the subcritical crack growth. The method suggested can also be employed for description of the process of quasi-brittle fracture, although in this case the plastic displacement method is regarded as an element of the interpolation criterion described in [11, 12].

The use of the approach described to solve practical problems with boundary conditions set by strains or temperature fields opens up totally new prospects. Illustrate the above-said by an example of calculation of a pipe with length *L* and diameter *D*, comprising a coolant with temperature gradient ΔT in height (Figure 6). The pipe is fixed at the ends, which eliminates any angular and resolving longitudinal displacement.
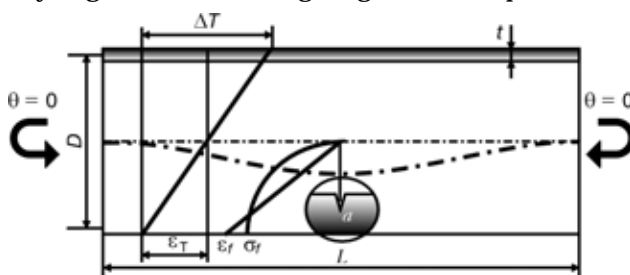

Figure 6. Temperature loading of pipe with a circular defect: *L* — pipe length; *D* — pipe diameter, θ — turning angle (bold dashed line shows impossible shape of bending)
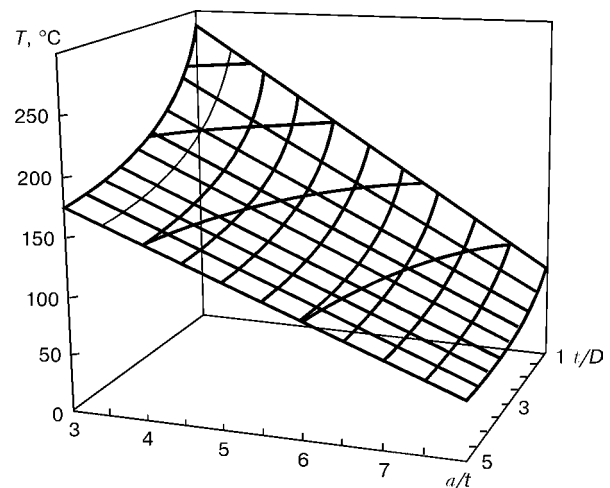

Figure 7. Critical temperature gradient *T* (*a/t* ---- depth of a defect)

Loads and internal pressure are ignored. There is no way for deflection of such a structure, as any shape of bending corresponding to boundary conditions requires the presence of a bending moment varying along the length. In our case the bending moment does not vary along the length. The temperature strain which is estimated as $\varepsilon_T \approx \alpha_T \Delta T / 2$ (α_T is the temperature coefficient of linear expansion) is fully compensated for by the bending moments at the pipe ends.

The pipe has a transverse crack. The pipe material is in the tough state. Traditional calculations by the plastic hinge method are not quite correct in this case, as there is no displacement of the neutral axis. The ultimate bending moment for such a structure can be readily calculated as the double moment due to stresses induced by a strain that linearly grows from zero at the centre of the pipe height to strain determined by the plastic displacement method. In the first approximation this formula can be written as follows

$$\varepsilon_f = \varepsilon_0 \left[\frac{\sigma_f}{\sigma_0} + \alpha \left(\frac{\sigma_f}{\sigma_0} \right)^n \right],$$

where $\sigma_f = \dfrac{R_{p\,0.2} + R_m}{2}$.

Distributions of stresses and strains are shown in Figure 6.

The ultimate moments corresponding to these stresses are much lower than the moments calculated by the plastic hinge method. For defects which lie deep to a quarter of the wall thickness the error of 20 % is not that high, but for a depth of half the wall thickness it equals 35 %, and for defects lying at a depth which is most interesting for analysis of actual fractures it amounts to 50 % and more (53 % for three quarters of the wall thickness).

Therefore, for pipes with defects the temperature bending moment is more dangerous than the force moment. This conclusion, corresponding with an accuracy to the inverse to the accepted system of assignment of the safety factors, can be disproved if the effect of unloading is caused by plastic deformation within the defect zone. It is most convenient to esti-

mate the unloading factor by using the plastic displacement method.

As follows from Figure 4, strain ε_f is realised on a linear size which is approximately equal to t--a that corresponds to a value of W. Given that starting from sizes of the defects approximately equal to 30 % of the wall thickness it is impossible to reach the yield point in undamaged sections, we will confine ourselves to consideration of a range of large cracks (calculations were made for steel 10GN2MFA).

Temperature tension of a lower generating line of the pipe is equal to

$$\Delta L_T \approx \alpha_T \Delta TL,$$

and the deformation one is equal to

$$\Delta L = \Delta L_e + \Delta L_p \approx \frac{M_c L}{\pi R^2 tE} + \varepsilon_f (t - a),$$

where ΔL_e and ΔL_p are the elastic and plastic components of variations in size L, respectively, and in the first approximation $M_c \approx 4\sigma_f R^2 (t -- a)$.

By equating them, we can readily estimate the critical temperature gradient

$$\Delta T_{cr} \approx \frac{1 - a/t}{\alpha_T}\left(\frac{4\sigma_f}{\pi E} + \frac{\varepsilon_f t/D}{L/D}\right) \qquad (11)$$

Dependence of the critical temperature gradient upon the depth of a defect and length of the pipe for a typical ratio of $t/D = 0.076$ (t/D is the pipe wall thickness) is shown in Figure 7.

Of interest is to estimate the effect of geometrical factors at a given temperature gradient. It follows from expression (11) that the critical length of the pipe can be determined from the following formula:

$$L/D \approx \frac{\varepsilon_f t/D}{\Delta T_{cr}\alpha_T/(1 -- a/t) - 4\sigma_f/(\pi E)}.$$

Combination of geometrical sizes of the pipe for which fracture occurs at a temperature gradient of 180 °C is shown in Figure 8.

It should be noted that the above results were obtained with no allowance for crack propagation and must be regarded as an initial qualitative estimation. At the same time, the plastic displacement method provides all the necessary conditions to come to much more accurate quantitative estimations

Note in conclusion that advantages of the above method include not only simplicity of the principles used for the calculations, but also the possibility of predicting fracture of the bodies containing cracks of an arbitrary shape (e.g. through cracks with non-linear fronts). The approach being kept unchanged, the numerical integration of stresses can be performed for
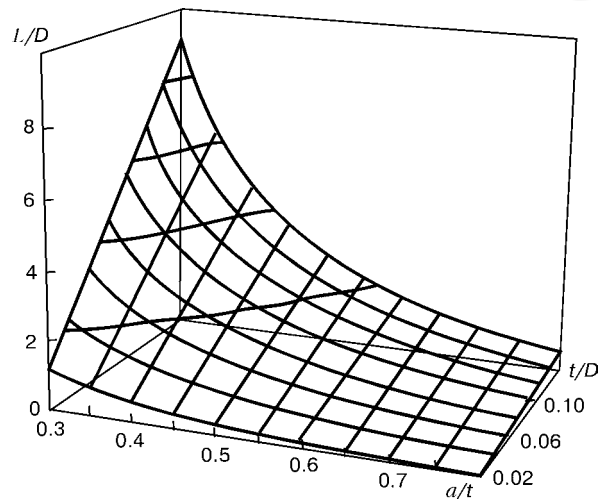

Figure 8. Critical sizes of pipe at a temperature gradient of 180 °C

a weakened section at different shapes of the crack front.

The approach suggested can be widely applied for modelling processes of damage of welded joints in critical structures. Verification calculations are underway now for the NPP structural members and pipes, the results for which were earlier obtained by using traditional methods.

1. (1986) *ASME*. Sect. 11. Boiler and pressure vessel code. N.Y., Wiley.
2. Milne, I., Ainsworth, R.A., Dowling, A.R. et al. (1986) *Assessment of the integrity of structures containing defects.* Berkeley.
3. (1979) *MEE/37*. British Standard Committee draft and IIW approaches on develop. pressure vessel technology. London.
4. (1981) *EPRI NP-1931*. An engineering approach for elastic-plastic fracture analysis. Research Project 1237-1. General Electric Co.
5. Vnuk, M.R. (1985) Problem of instability in plastic fracture. In: *Proc. of Int. Conf. on Fracture*, Cannes, Sept. 1981. Moscow: NIIinformenergomash.
6. Smith, E. (1983) The conditions for the onset of fracture at the tip of a part-through part-circumference crack in a pipe. *Int. J. Pressure Vessel and Piping*, **12**, 127--140.
7. Hasegawa, K., Shimizu, T., Shiga, N. (1984) Leakage and breakage estimation based on a net-stress approach for stainless steel pipes with circumferential cracks. *Nucl. Eng. and Des.*, **2**, 285--290.
8. Ainsworth, R.A. (1984) The assessment of defects in structures of strain hardening material. *End. Fract. Mech.*, **19**, 633--642.
9. Ovchinnikov, A.V. (1986) Approximation formula for determination of stress intensity factors K_I. *Problemy Prochnosti*, **11**, 41--47.
10. Newman, J.C., Raju, I.S. (1984) Stress-intensity factor equations for cracks in three-dimensional finite bodies subjected to tension and bending loads. *NASA Techn. Memorandum 85793*.
11. Zvezdin, Yu.I., Rivkin, E.Yu., Vasilchenko, G.S. et al. (1990) Application of non-destructive testing data for strength calculations. *Tyazh. Mashinostroenie*, **3**, 12--14.
12. Ovchinnikov, A.V., Rivkin, E.Yu. (1991) Interpolation criterion of fracture mechanics. In: *Proc. of Sci.-Techn. Seminar on Fracture Mechanics and Strength of Welded Joints and Structures*. Leningrad.

DEVELOPMENT OF FULLY AUTOMATIC WELDING TECHNIQUE FOR VESSELS AND PIPES

G. TAKANO and **K. KAMO**
Mitsubishi Heavy Industries, Ltd., Takasago R&D Center, Japan

The problem of quality assurance of welded joints in the conditions of TIG automatic welding of thin-sheet vessels and pipes is considered. It is shown that the alternative of high skill and experience of welder is the application of welding machines using the methods of read and adaptive control being developed. These machines can operate separately until now only during a certain period of operation. The next steps are necessary for the creation of logics of adaptive control of welding conditions with allowance for the difficulties in fulfillment of jobs.

Keywords: automatic welding, TIG method, vessels, pipes, joint quality, quality control, adaptive control

It has been a long time since a fully automatic welding technique had been requested to put in practice in order to secure a higher productivity and better quality without depending on master-welding skills, especially now that the aging of the welders at the fabrication shop is becoming inevitable. This document presents the efforts and undertaking of development of the fully automatic welding technique with GTAW as the object.

Background for fully automatic welding technique. Every production site confronts the problems of aging of the welders and shortage of young welders. The age groups of welders engaged in electric power plant in Japan are shown in Figure 1. As it shows, the largest group is at the ages between 45--49; this implies the fact that as these welders retire, not only the quality but also the productivity will reduce drastically in the near future.

To cope with the impending threat, fully automatic welding technique and related sensing and adaptive controlling techniques have been under development. However, in order to achieve a high quality welding in fully automatic welding technique, there laid some factors as obstacles, as shown in Figure 2. Thus, this had been an unapproachable field for some time.
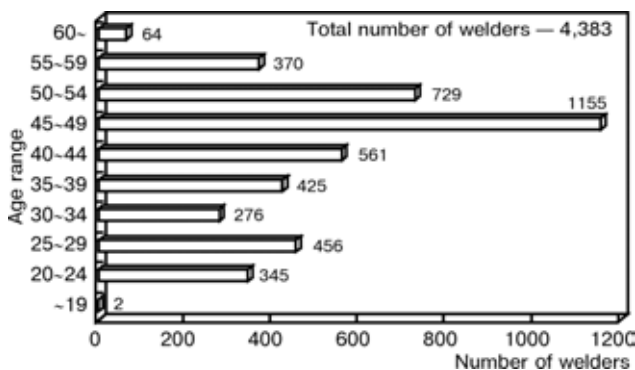

Figure 1. Age group of welders engaged in electric power plant at Japan (as of March 31, 2000)

© G. TAKANO and K. KAMO, 2003

Therefore, the following aspects have been investigated during the GTAW welding procedure: firstly, what welders observe and confirm and, secondly, what welding parameters welder adjust.

It was found that majority of the work was to adjust the positions of electrode and filler wire, but correction or adjustment of welding conditions, such as welding current, was rare in case of GTAW. Replacement of tungsten electrode, which is unique to GTAW, also took place several times. As these adjustment are practiced by visual information of welder, such as filler wire position, the position and shape of electrode, the position of grooves, the shape of molten pool and weld beads are practiced, it has been confirmed that visual sensor plays an important role in fully automatic welding system.

Developed examples of fully automatic welding technique. This chapter presents the developed examples of the fully automatic welding technique by using the visual sensor, with the observations mentioned in second chapter.

All position automatic welding system for pipes. In the case of development of the automatic welding system with all position welding of stainless steel pipe circumferential joint, the object of weld is shown in Table 1.

Table 1. Object of all position welding system for pipes

Material	Stainless steel
Outer diameter, mm	165.2–1000
Thickness, mm	7.1–35
Shape of the groove	Narrow gap (one pass, one layer)

The concept of the system is shown in Figure 3. The system is driven by each sensors, computer program and drive system that are replaced skill of welders replace the senses of skilled welders.

Figure 4 shows the adaptive control system for maintaining appropriate welding conditions, and the quality verification function for monitoring of weld quality. Also the Figure shows various installed sensors in order to ensure the quality of the weld joints. CCD camera, which is placed in front of the welding
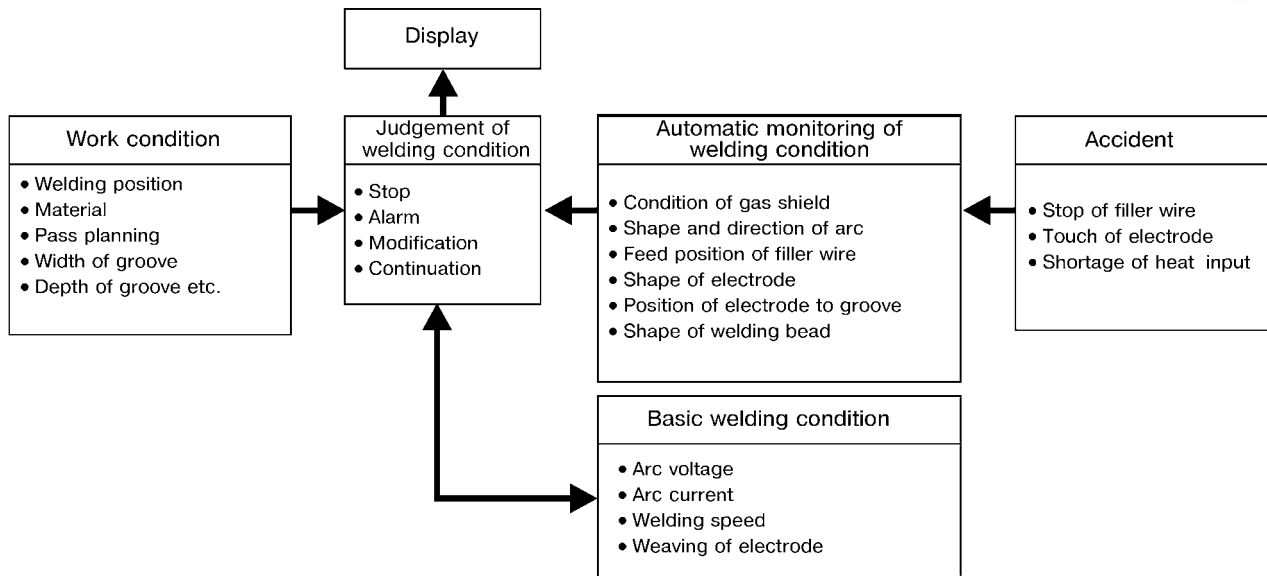
Work condition	Judgement of welding condition	Display	Automatic monitoring of welding condition	Accident

Display

Work condition
- Welding position
- Material
- Pass planning
- Width of groove
- Depth of groove etc.

Judgement of welding condition
- Stop
- Alarm
- Modification
- Continuation

Automatic monitoring of welding condition
- Condition of gas shield
- Shape and direction of arc
- Feed position of filler wire
- Shape of electrode
- Position of electrode to groove
- Shape of welding bead

Accident
- Stop of filler wire
- Touch of electrode
- Shortage of heat input

Basic welding condition
- Arc voltage
- Arc current
- Welding speed
- Weaving of electrode

Figure 2. Conception of intelligent control system in automatic welding
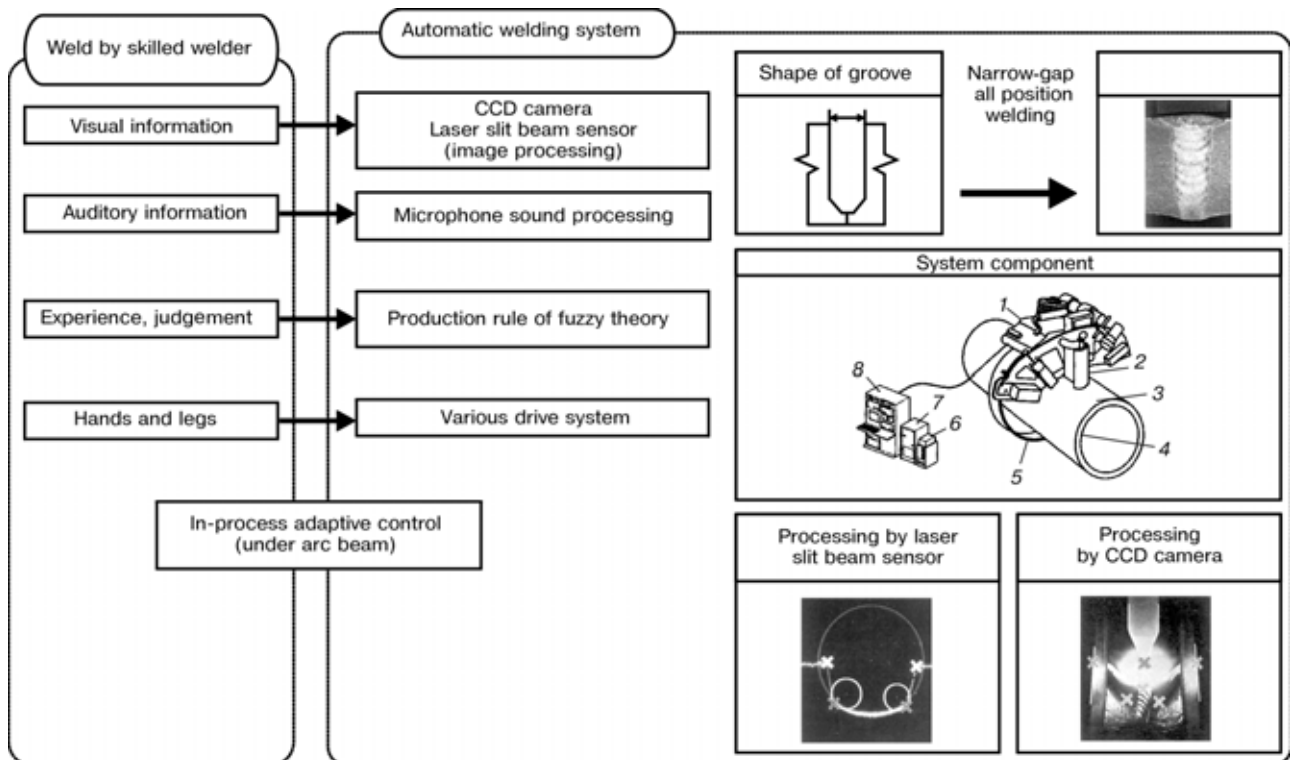

Figure 3. The concept of all position welding system: *1* — welding head; *2* ---- CCD camera; *3* — laser slit beam sensor; *4* — pipe; *5* ---- guide rail; *6* — cooling water unit; *7* — power source; *8* ---- weld control system
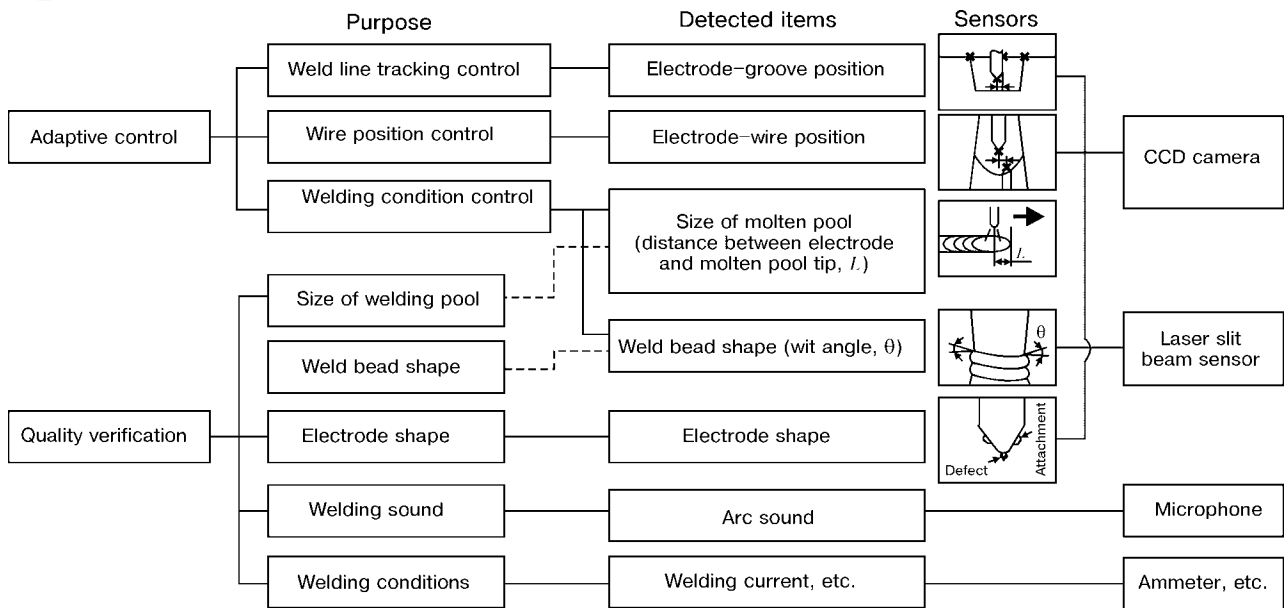
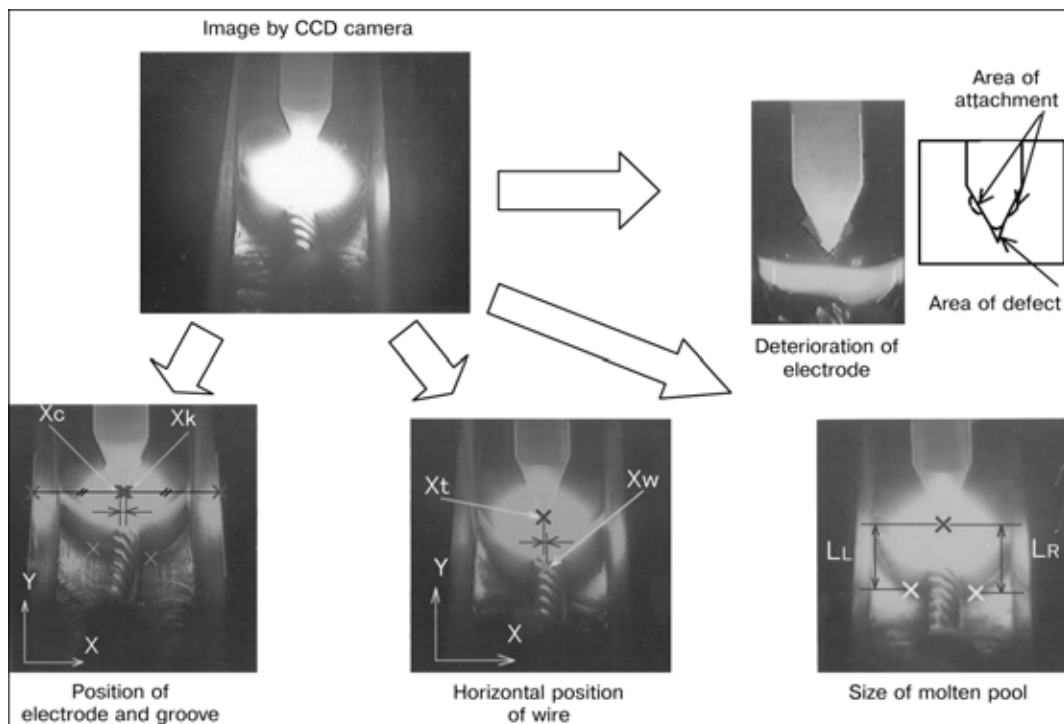**Figure 4.** Function and sensors of all position welding system

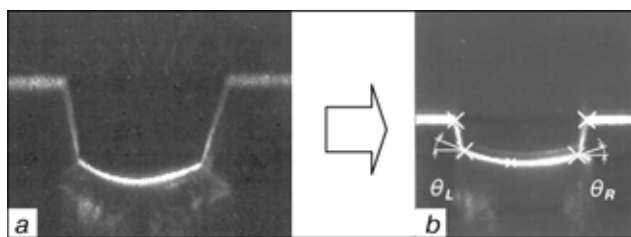**Figure 5.** Information from CCD camera images

Figure 6. Information from laser slit beam sensor images: *a* — images by laser slit beam sensor; *b* — wet angle of beads

torch, is mainly used to scan the images of welding and to obtain the necessary information. After the luminance distribution is analyzed by a computer using the images that are scanned by CCD camera, electrode position, groove position, horizontal position of wire, size of the molten pool and deterioration of electrode, are shown in Figure 5.

Also, wet angle between weld bead and wall of groove side are taken as a parameter to indicate the exterior of weld beads by using the images scanned by the laser slit beam sensor, which is placed at the rear of the weld torch (Figure 6).

Information obtained from CCD sensor and laser slit beam sensor is used to adaptive control of appropriate welding condition. One of the examples is shown in Figure 7.

Inputting the present shift length of electrode position and corrected rate of previous shift length, the electrode position to be adjusted is calculated by fuzzy theory.

Lastly, examples of the weld control system indication are shown in Figure 8. Figure 8, *a* shows the CRT indication of appropriate welding condition control as the images are being processed (position of electrode and groove) during welding. Figure 8, *b* indicates the welding record and quality judgement of the samples taken to verify the quality during welding.

Multi-head automatic welding system. This welding system welds the circumferential joints of piping in thermal and nuclear power plant, while the pipes are rotated and welding position is fixed to flat. The objects of the welding system are shown in Table 2, the component ---- in Figure 9. The main feature of this system is that the operation of five welding systems by one operator from the control room, through the arc monitor by using GTAW.
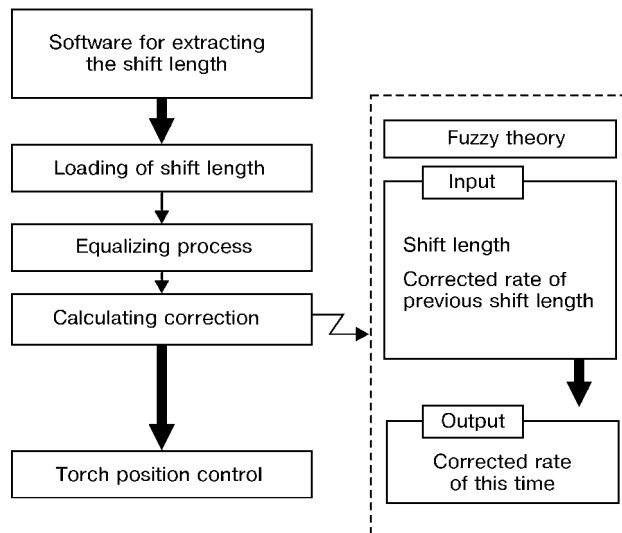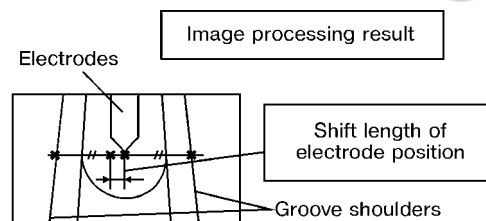

Figure 7. Weld line tracking control method

However, if the number of the welding system per operator should increase, time spent outside the control room increases for performing the task such as removing the welded pipe, carrying in the new pipe and replacing the tungsten electrode (Figure 10); the actual time for monitoring the welding condition decreases to 35 %. To ensure the welding quality even in such restriction, adaptive control, such as weld control, horizontal and vertical position control of

Table 2. Object of multi-head welding system

Welding position	Flat (rotating)
Groove	One side, narrow gap
Material	Carbon steel (Cr--Mo steel)
Pipe outer diameter, mm	139--558
Pipe thickness, mm	18--100
Pipe length, mm	> 1800

Figure 8. Display examples of welding control system: *a* — welding condition display; *b* — record of automatic welding

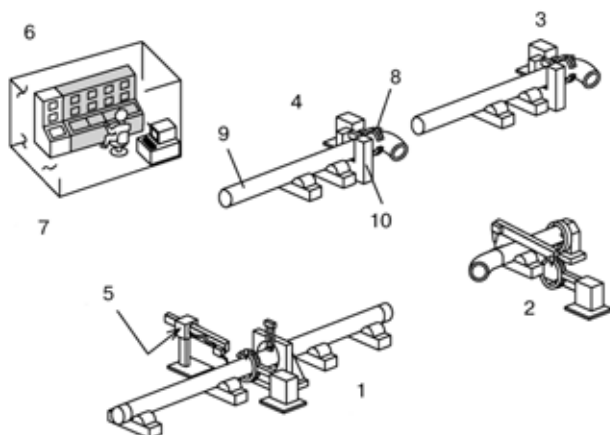**Figure 9.** Component of multi-head welding system: *1* — unit 1; *2* — unit 2; *3* — unit 3; *4* — unit 4; *5* — unit 5; *6* ---- control room; *7* ---- operating 5 units per one operator; *8* — welding head; *9* ---- pipe; *10* — chucking system

Table 3. Object of lap joint welding system

Welding position groove	Vertical and horizontal
Material	SUS304
Thickness, mm	2

Figure 10. Relationship between operating units and performance time at outside the control room

the wire that operator pays attention to are carried out (Figure 11) line tracking.

Of the sensors shown in Figure 12, detection method of the groove position by using a monochrome CCD camera is shown in Figure 13. This is a method that uses image by the monochrome CCD camera, and detects the luminance difference of inside (brighter) and outside (darker) of the groove by image processing. It automatically adjusts the shutter speed of CCD camera in order to get the suitable luminance, if welding conditions change to process. Welding line track system is adopted to maintain the position that is input at the beginning of welding.
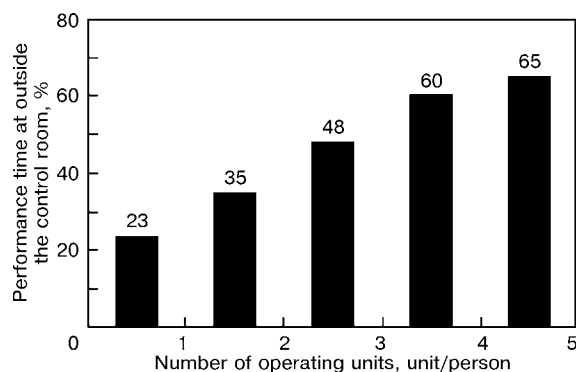
Due to the fact that the vertical position of the wire is hard to judge by the sampling image, wire heating electricity is used to perform the task: position of the wire is controlled by prediction the present wire vertical position from instability of heating electric current, which is caused while the wire droplets move to the molten pool, and from the electric value itself (Figure 14).

Automatic welding system for lap joint of thin sheets. The inner structure of underground LNG tank is formed by bonding some thin stainless steel sheets, therefore, it requires lap joint welding of straight and bent sheets, as shown in Table 3 and Figure 15. Plasma arc welding (PAW), which welding speed fast on thin vertical and horizontal plates, was adopted to lap joint for the subject with long straight weld line.

With the fact that the sheets being quite thin, weld defects, such as burn through, undercut and insufficient penetration, occur by a slight missmatch between a torch and weld line. As it is difficult to set the automatic welding machine along the weld line in accuracy, weld line tracking control is adopted. It is made possible by recognizing the weld line using the CCD camera image which includes step caused by the difference between upper and the lower plate.
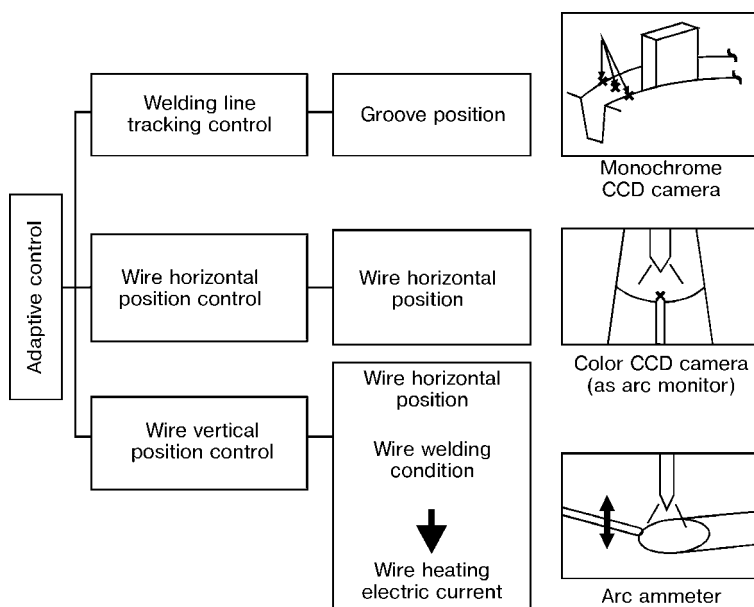
Figure 11. Controlled and monitored items and types of sensors
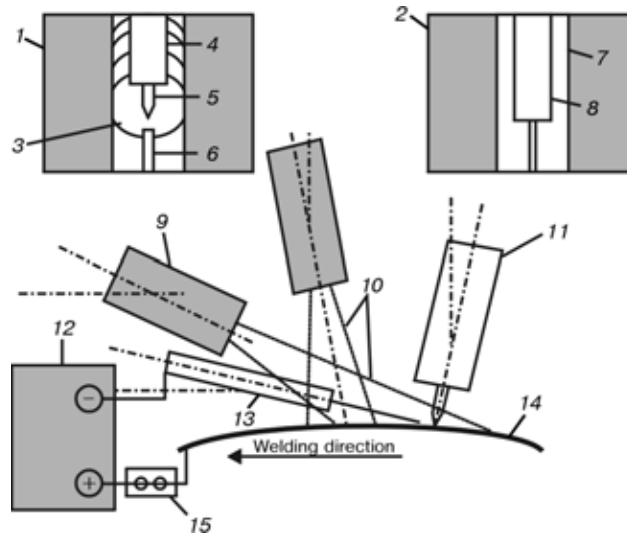
Figure 12. Sensor layout: *1* — image of color CCD camera; *2* — image monochrome CCD camera; *3* — molten pool; *4* — torch; *5* ---- electrode; *6* — wire; *7* — groove shoulder; *8* ---- wire nozzle; *9* ---- color CCD camera; *10* — monitoring range; *11* — welding torch; *12* — wire heating source; *13* — wire nozzle; *14* — pipe; *15* ---- heating current detector

$$U = (U_L + U_R)/2 \quad \Delta = U - B$$
$$B = (B_L + B_R)/2$$
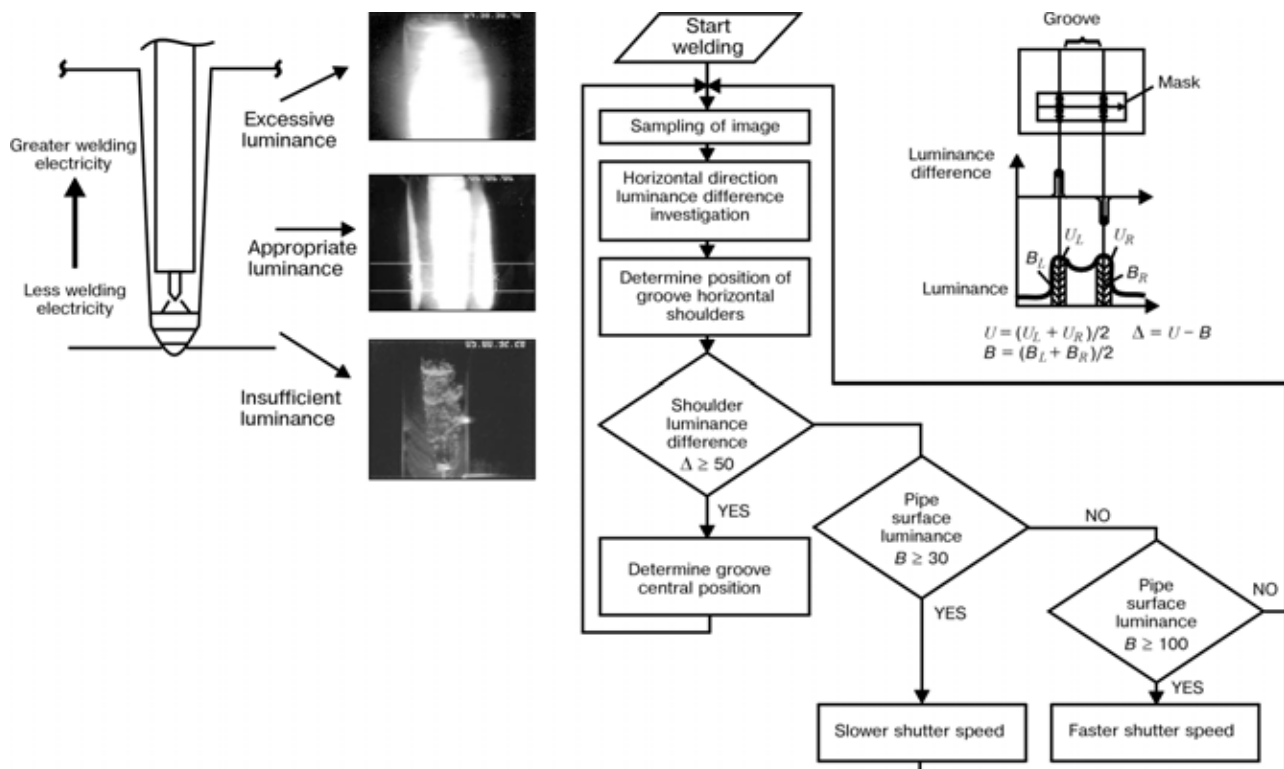
Figure 13. Processing method of CCD camera images
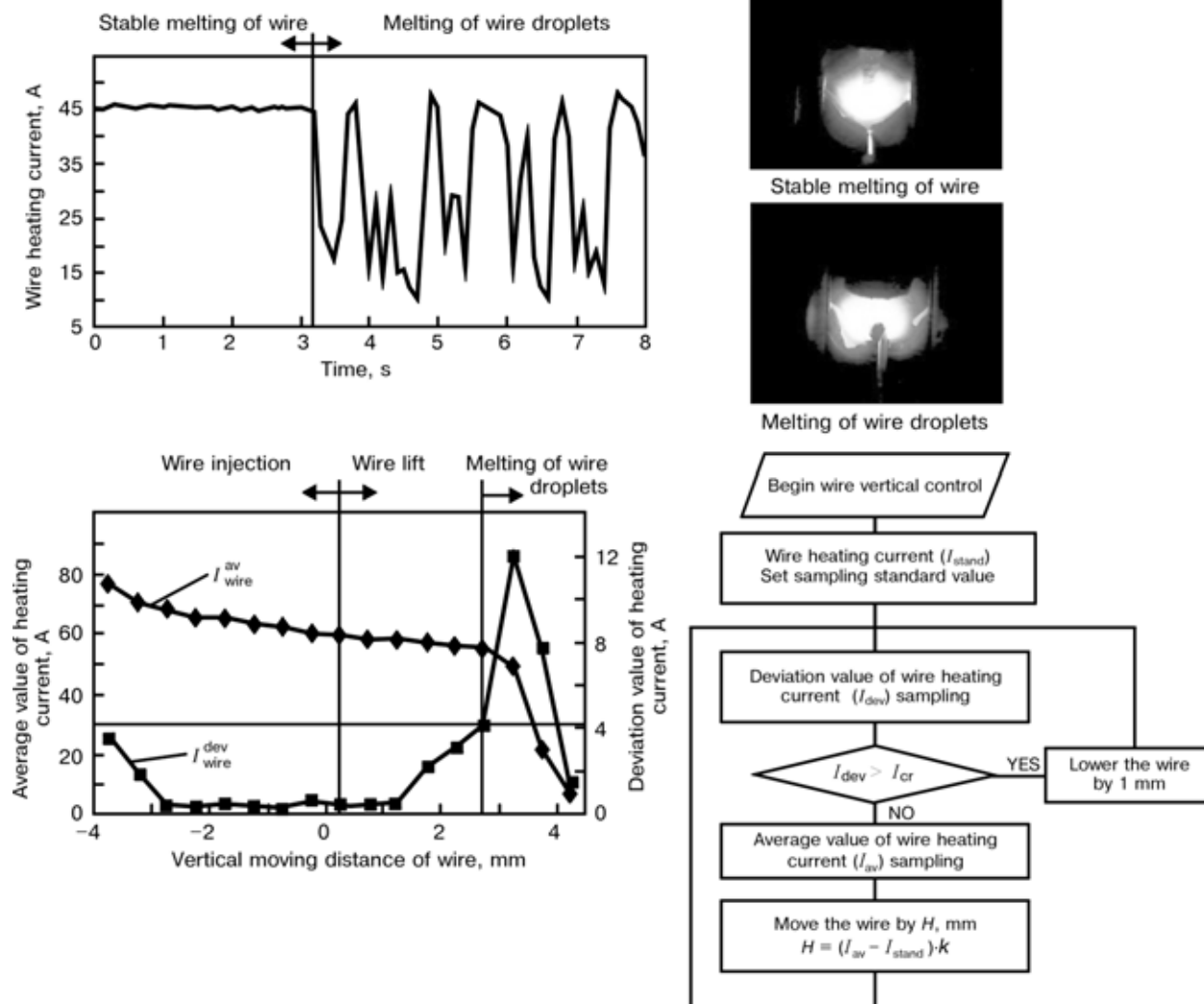
Figure 14. Relationship and detecting technique of wire vertical position and wire heating electric current

Figure 15. Example of the weld joint shape
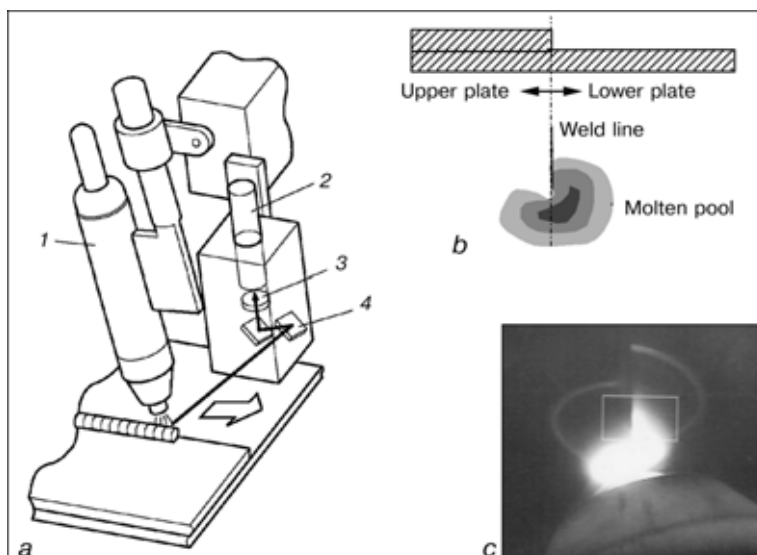
Figure 16. Layout of sensor and image processing: *a* ---- layout of welding torch and sensor; *b* — image processing to recognize weld line; *c* ---- image of sampling by CCD camera; *1* — plasma arc torch; *2* ---- CCD camera; *3* ---- filter; *4* — mirror
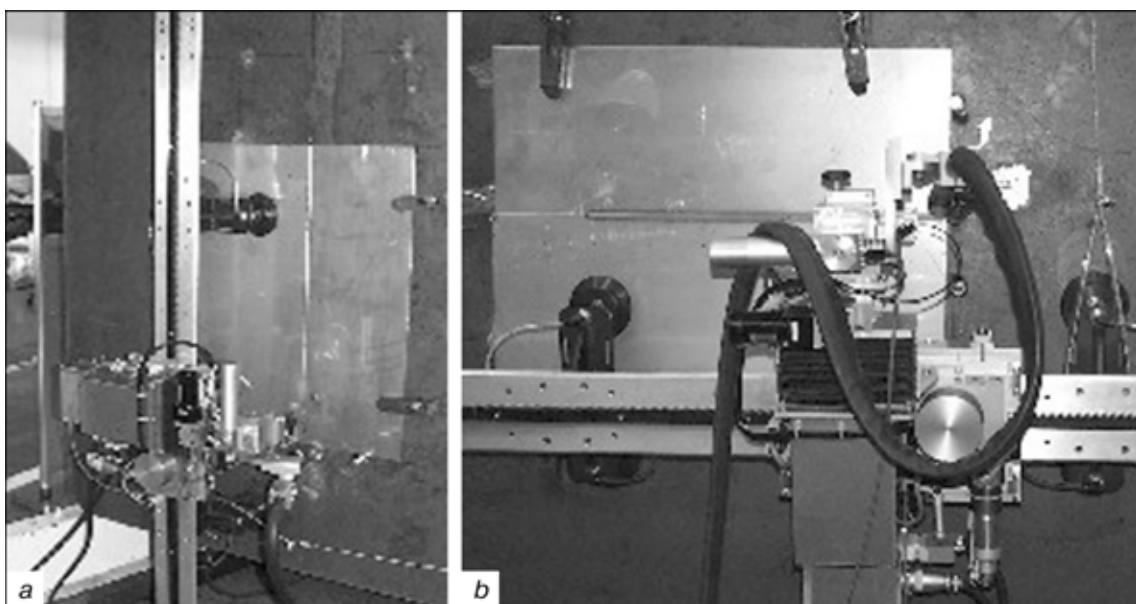
Figure 17. Welding work in vertical (*a*) and horizontal (*b*) position

With the help of those recognized weld lines, plasma arc torch can track weld line in accuracy (Figure 16).

Welding work in vertical and horizontal positions is shown in Figure 17.

CONCLUSION

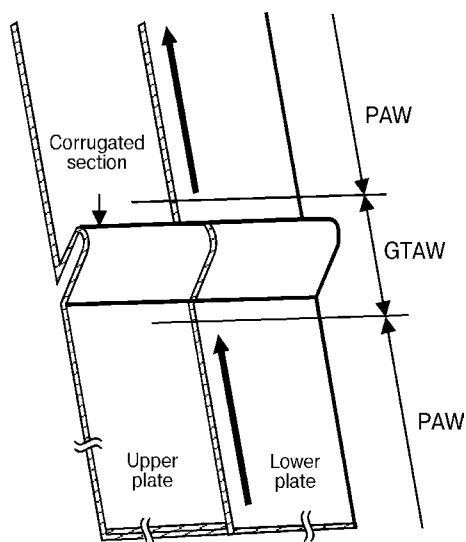**Further subjects.** In order to have machines do all the adjustments related to welding in place of skilled welders, various sensors have been developed so as to put them to practice. As CCD cameras and computers with higher performance become more inexpensive and accessible, using image processing for visual sensors in welding system becomes more available cost wise and time wise. These automatic welding systems can operate on its own for certain period of time under certain conditions. However, they are yet at the stage of controlling simple tasks, such as weld line tracking and determining wire position. Before they reach the level of controlling the welding conditions where they have to deal with all the variables, following techniques must be achieved:

1. Recognition of 3D shape of the molten pool which greatly affects the preventation of welding defects.

2. Relativity of 3D shape of molten pool and welding defect or quantification of criteria for judgement like that of welders.

3. Quantification of factors other than molten pool.

4. Adaptive control logic for welding condition in order to achieve appropriate welding.

STUDY OF LOW-TEMPERATURE STRENGTH OF MATERIALS AND THEIR WELDED JOINTS TO HANDLE PROBLEMS OF THE RUSSIAN NORTH

V.P. LARIONOV, O.I. SLEPTSOV, V.V. LEPOV and **S.P. YAKOVLEVA**
Unified Institute for Physical-Engineering Problems of the North,
Siberian Division of the Russian Academy of Sciences, Yakutsk, Russia

Problems associated with operation and repair of industrial facilities and metal structures under the Russian North conditions are considered. Areas of basic and applied research conducted by Yakut scientists with a purpose to develop new materials, welding processes and study behaviour of welded structures during operation are described. Promising lines for further research are presented.

Keywords: *welded structures, evaluation of state, life, extreme conditions, structural materials, mechanical properties, structure, cracks, materials science problems*

Problems associated with evaluation of state and extension of life of industrial facilities, equipment and metal structures are especially topical for the North regions, which is attributed to the specific effect on materials by low operating temperatures. Therefore, the oil-and-gas construction industry, which had never before been categorised as environmentally hazardous, now has become so in the sub-arctic and arctic regions. This puts in the forefront the problem of ensuring safety of engineering facilities in regions with a cold climate, i.e. European North, Tyumen North, Yamal etc.

The most important factors, which have to be allowed for from the moment of design and during the entire service life of a structure, include the seasonal factor, repairability under cold climate conditions, high costs of recovery works etc. For example, the seasonal factor shows up in the necessity to allow for low temperatures in winter, drastic daily temperature gradients in off-seasons, high flood hazards in spring, defrosting of frozen earth etc. Peculiarities of conditions in the Russian North regions under which the reclamation works, including repair and erection welding operations, are performed often determine performance and reliability of engineering systems [1--3]. The majority of accidents of a technogenous character occurring in the North results from mismatch of existing welding technologies and operational conditions, as well as non-compliance with welding codes and recommendations [1--5]. All these factors are closely related to the level of professional training of welding engineers and NDT specialists, their skill and qualification for regional climatic conditions.

This requires development of scientific-and-technical approaches to estimation and extension of life of engineering facilities and metal structures on the basis of an integrated analysis of all stages of their life cycle, including design, fabrication and operation.

Wide spectrum of extreme service conditions dictates elaboration of new technical requirements to materials, designs and technological processes. Their imperfection, showing up with decrease in ambient temperature, is known to be associated primarily with the cold shortness phenomenon. Therefore, one of the most important tasks in ensuring performance of machines and structures under the North conditions is to utilise right cold-resistance materials. A simple application of low-alloy cold-resistant steels, which has become a traditional way of tackling this problem, provides only a partial solution to the challenge of reducing the number of failures and catastrophic fractures of structures and machines. Safe operation and extension of life of process equipment, quarry facilities, pipelines and engineering structures in arctic regions require development of structural materials (including non-metallic ones) with high cold- and wear-resistant properties, which would retain their characteristics in long use at natural low temperatures and at drastic temperature gradients [2, 6, 7]. It is of no small importance that advanced materials allow reduction of weight of machines and structures and, at the same time, improvement in their performance.

Modern civilisation utilises a great amount of materials, each type being characterised by peculiar properties and applications [6]. New materials are being continuously developed. Structural materials can be subdivided into four main types: metals, ceramics, composites and polymers. However, despite emergence and continuous growth of output of non-metallic materials, steels and alloys will remain the most extensively employed structural materials for the next decades. This is attributed to a wide range of their strength and ductility properties, relatively low production costs and possibility of their recycling and regeneration. Good structural properties, low specific power consumption and price will determine the priority of metals and alloys. Development of cold-resistant materials is associated, first of all, with addressing the problem of investigation of the nature of

tough-brittle transition of metals, as well as the mechanism and peculiarities of degradation of their structure.

One of the decisive requirements for development of cold-resistant structural steels is to ensure that they have a fine-grained structure. Another important requirement is to provide their purity. For example, a metal should have a decreased sulphur content. Generally speaking, the ways and principles of making cold-resistant alloys are at a development stage so far. There are some theories of a phenomenological character describing mostly the effect of metallurgical factors. For instance, according to the available home and foreign studies of the effect of alloying elements on properties of steel, microalloying and modification with rare-earth elements lead to increase in strength properties of steel with a simultaneous increase in cold resistance. Meanwhile we can find answers only to individual questions, whereas no fundamental theories of a physical nature of the process of tough-brittle transition are available as yet. There are no theoretical bases enabling investigation of the physical nature of cold shortness at a level of collective electrons, the values of inter-atomic bonds, distortions and changes in the type of a crystalline lattice, which can be used for development of new structural alloys in particular. Therefore, of special significance under such conditions are the studies aimed at elaboration of theoretical principles of development of materials with new properties on the basis of knowledge of electron and microscopic structure of a material, as well as at investigation of fundamental aspects of a physical nature of the process of tough-brittle transition of materials at low temperatures.

Yakut scientists have been involved in development of cold- and wear-resistant structural materials for more than 30 years [8]. Based on investigation of some physical-mechanical characteristics (internal friction, microhardness, electrical conductivity, Mossbouer effect etc.), they showed that the tough-brittle transition of carbon steels is caused by an intensive formation of covalent bonds (change in the electron configuration of atoms), affecting the relaxation ability of a material [2]. It was concluded therefrom that cold resistance of steel could be increased through alloying it with certain chemical elements capable of decreasing a directed component of chemical bond of Fe-based materials. In the 1980s, scientists of the Institute for Physical-Engineering Problems of the North of the Siberian Division of the Russian Academy of Sciences, in collaboration with their counterparts from Tomsk, developed a new wear-resistant Ni-free alloy ISTs-1, which is high-chromium cast iron modified with an optimal amount of rare-earth metals. It was tested and applied at mines of Yakutia. In addition, the Uralchermet Company, in collaboration with the Siberian Division of the Russian Academy of Sciences, developed a cold- and wear-resistant steel which also passed experimental-industrial tests at the Yakut mines. Now, with revival of interest in funda-

mental, innovative developments, these studies have received extension under the Russian regional programs «Arctic», a number of task republican projects and the integrated combined project of the Siberian Division of the Russian Academy of Sciences.

Nanomaterials have received wide acceptance in the last years. As noted above, one of the methods for improving mechanical properties of metals and decreasing the tough-brittle transition temperature is refining of grains, and one of the most efficient methods for formation of metal structure is plastic deformation. An intensive plastic deformation may provide a mean grain size ranging from units to hundreds of nanometers, high strength being combined with a sufficient ductility. It is believed that the nanostructural state is a qualitatively new state of materials, the investigation of which is of high scientific and practical interest. Despite a large number of publications dedicated to this subject, processes and mechanisms leading to such changes in properties of materials have been little studied so far. A more comprehensive information on mechanical properties of metals with nano- and sub-microcrystalline structure, as well as on the mechanisms of formation of these properties, is required to practically apply these metals. We have started investigations in this area to study theoretical and experimental principles to ensure improvement in mechanical properties and cold resistance of structural steels through transforming them into the nanocrystalline structural state.

The most important area of fundamental research in modern materials science is investigation of the internal mechanisms of fracture at different structural levels of deformation, as well as experimental and computer modelling of the life cycle of a structure and its elements [9]. At the same time, until now mechanical engineers and materials scientists operate with just the phenomenological theories, which are not related to an actual arrangement and deformation structure of a material. On the other hand, solid-state physics has accumulated a large amount of knowledge of the internal structure of a matter, which is not called for by materials scientists.

Our Institute is active in research aimed at elaboration of the theory of development of materials, including investigation of macroscopic characteristics of strength in a wide range of temperatures, X-ray and diffractometry analyses of a fine structure of materials, optical, scanning and probe microscopy and fractography of fracture surfaces and deformation of metals, as well as metallography and chemical analysis of specimens. Much consideration is given to computer processing of experimental results and computer modelling [9, 10]. Plastic destruction aspects of failure of elements of real structures and model samples are being investigated, and integrated metallographic and microstructural studies are being carried out to reveal mechanisms of damage and fracture of metal at low temperatures. Unique data have been generated concerning behaviour of materials in hydrogen-in-
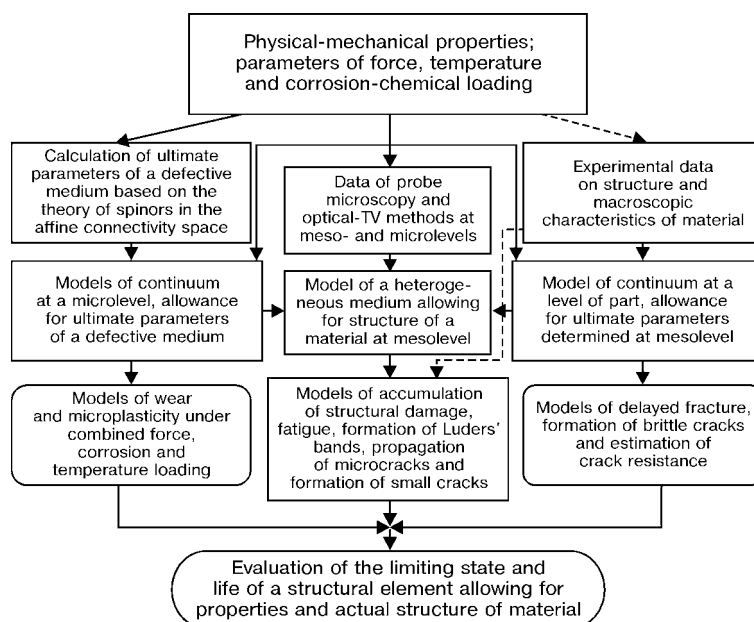
Figure 1. General diagram of integrated research of deformation and fracture processes for heterogeneous media based on hierarchical modelling

duced delayed fracture, effect of explosion loading on resistance of materials to cold cracking and propagation of brittle fracture [11]. Means and devices for evaluation and extension of life of machine parts under the cold climate conditions are being worked out. The hierarchical model is being deve-loped, based on consideration of the entire process of formation, deformation and fracture of a material in terms of arrangement of its internal structure at all deformation levels

Figure 2. Probe microscopy image of a central crack initiated from a carbide particle in martensite of steel 14Kh2GMR: *a* — profile of surface; *b* — 3D image (×16384)

under the combined effect of different force, temperature and corrosion loads (Figure 1). It was suggested that the systematic approach, based on the genesis of integrity, should be used for development of new materials with an optimal amount of covalent bonds in the initial state. Several models having an experimental confirmation were put forward to describe cold shortness.

Fracture surfaces of structural members and model samples were examined to reveal the mechanisms of fracture of metal at low temperatures. Optical and tunnel scanning fractography of fractures of specimens in different environments and under different impacts on metals, as well as their integrated metallography and microstructural examinations are being conducted.

Figure 2 shows surface of a sub-microcrack initiating from a carbide inclusion. This crack propagates over the crystallographic planes of martensite. The 2D image made it possible to measure parameters of the sub-microcrack. Size of the carbide inclusion was determined from the 3D image and profile of the surface.

The use of advanced materials in technical facilities implies also development of advanced technologies and welding in particular. For example, mechanical properties of the weld metal may substantially deteriorate because of high sensitivity of increased- or high-strength steels to thermal effect. In fact, as follows from the results of analysis of fractures of weldments at low temperatures, they occur or initiate mostly in welded joints. In addition, the welding arc burning in cold has special features, as proved by the pioneering studies conducted by the Institute. Temperature of the welding arc increasees due to contraction of the arc column [1]. Naturally, this leads to a change in the entire heat balance of the weld pool, kinetics of thermal and thermal-deformation cycles,
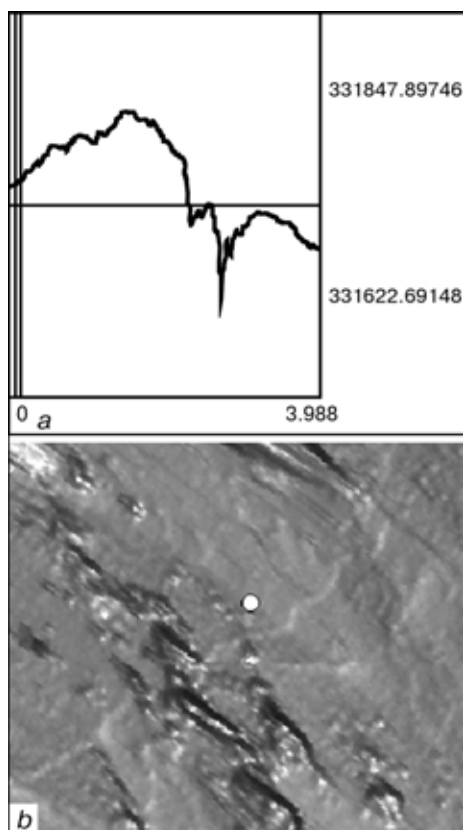
as well as phase and structural transformations. It is apparent that optimisation of the technologies of welding at low temperatures requires that all these factors be taken into account.

The problem of welding structural steels is related from the engineering standpoint to the necessity to ensure a package of properties to provide full-strength welded joints and prevent cold cracking and formation of internal structures that decrease resistance of welded joints to brittle fracture. The Institute developed physical nature of abnormality of the welding arc during welding of structural steels at low ambient temperatures, kinetics of welding strains and stresses, and processes of delayed fracture [1--3, 12]. This resulted in the development of fundamentally new principles of the welding technology, ensuring the process and service strength of welded joints. Its basis is the optimal welding heat input providing cha-racteristics of the weld metal as close as possible to those of the base metal, as well as the rational choice and development of welding consumables.

The need to avoid the preheating operation is considered to be one of the key problems in arc welding of high-strength low-alloy steels. In this connection, the special significance is attached to control of behaviour of hydrogen in welded joints, being one of the factors related to brittle fracture of welded structures [13].

The Institute uses the probe microscopy methods for microstructural and fractographic analysis of low-alloy steel specimens to study the role of dissolved hydrogen in delayed fracture. Fracture of 14Kh2GMR steel specimens saturated with hydrogen and tested to delayed fracture was studied at a temperature of 400 °C by tunnel microscopy (multi-microscope SMM-2000TA, scanner with a field of $6\times6\times1$ μm). Microcracks propagate in the notch zone along the boundaries of sub-structural martensite blocks (Figure 3). The surface of a sub-microcrack in fracture of a specimen exhibits splitting over the planes of sliding of sub-structural formations. The fracture profile makes it possible to measure sizes of individual blocks of a sub-structure and their disorientation relative to each other (Figure 4).

Application of new materials for upgrading of technical facilities leads to the need to make changes in practice of their designing and mass production. This stipulates the requirement for formation of a new system of criteria of strength, service life, viability and safety of structures to improve their reliability through a system of rules and regulations of design, manufacture and operation. For example, allowance for low temperatures, in addition to the most difficult topography and geology conditions (mountainous country, permafrost with ground ice mounds, marshy regions and land slides), is a major requirement for construction of railways under the natural-climatic conditions of the Russian North. We have the similar situation in construction of gas and oil pipelines, the wide deployment of which is anticipated in the first
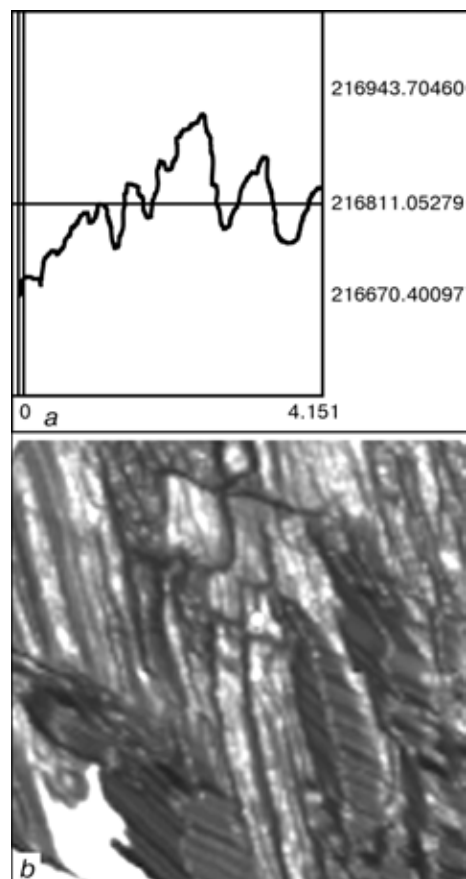

Figure 3. Sub-structural martensite blocks in a specimen simulating the overheated zone in steel 14Kh2GMR : *a* ---- profile of surface across the section; *b* — 3D image ($\times32768$)
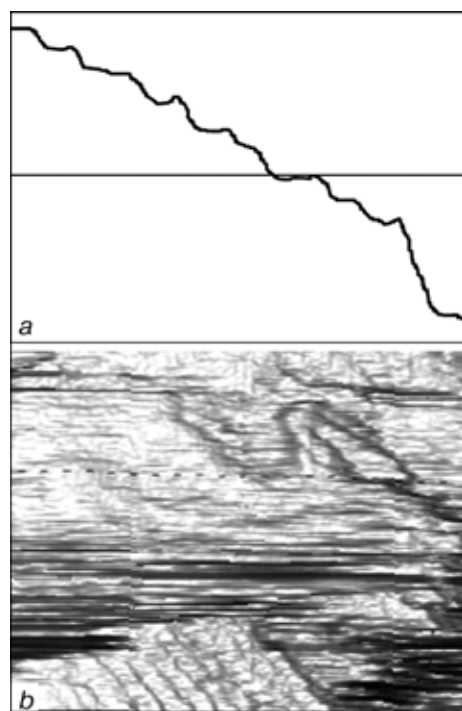

Figure 4. Image of laminated martensite of steel 14Kh2GMR obtained in the tunnel scanning mode: *a* — profile of surface across the section; *b* — 3D scan ($\times65536$)
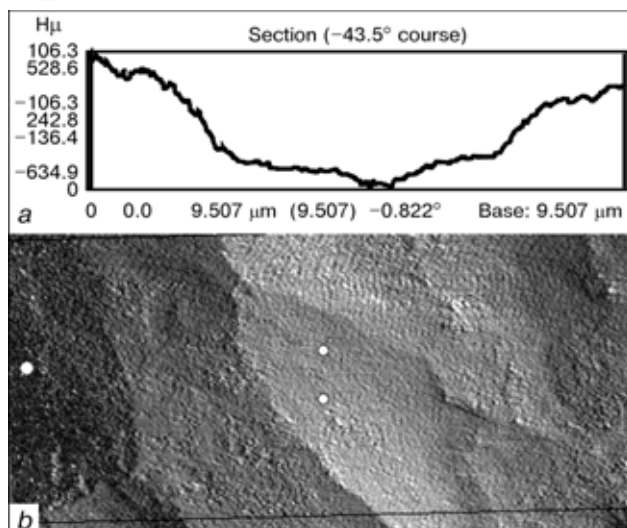
Figure 5. Initial state of the grain boundary in cold-resistant steel of an experimental composition: *a* ---- profile of surface across the section; *b* — 3D scan (scan size ---- 10×7 μm)

quarter of this century. Meanwhile, the minimum temperature assumed now in design of engineering structures is equal to about --40 °C, whereas the real temperatures may go down to --55 °C and lower. This means that it is necessary not only to develop new materials, but also to revise the existing design standards and specifications for metals used to manufacture rails, construct bridges etc.

The stage of design is the most important stage of practical application of fundamental research, providing for the basic technical-and-economic parameters of a part or structure. It is a known fact that values of such design characteristics of steels as tensile strength, yield stress and Young's modulus should be increase with decrease in temperature. At the same time, this is accompanied by increase in brittle frac-
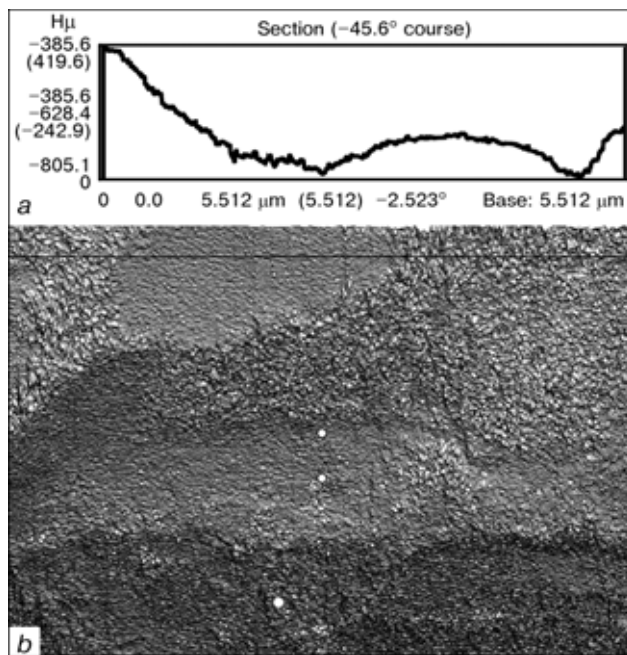

Figure 6. Grain boundaries in cold-resistant steel at a 5 % plastic deformation: *a* ---- profile of surface across the section; *b* ---- 3D scan (scan size — 5×5 μm)

ture. Traditional strength and ductility criteria fail to give positive results. These criteria are based on a postulate that the limiting state is determined by the stressed state at a point, and the effect of the rest of the volume of a material is assumed to be insignificant. However, there are cases where this effect may be very substantial. This contradiction is attributable to imperfection of available experimental procedures and approaches to evaluation of local properties of materials. The rational design and technology solutions determining performance of materials and elements of equipment and structures at low temperatures require improvement of strength design methods and elaboration of new strength and load-carrying capacity criteria. The new design methods should allow for and permit operation of structural elements containing cracks, which are inevitably present in them from the very beginning or formed during operation.

The challenge in design of facilities for extreme conditions can be effectively handled through using the strain and stress estimation methods. Thus, the Institute developed methods and equipment for investigation of behaviour of structures in a heterogeneous stress field by using moire and holographic interferometry. This enabled us to suggest criterion of a limiting state of structural elements, allowing for a non-uniform distribution of stresses and strains. Results of these investigations found practical application in optimisation of mining vehicles.

Investigation of limiting states of materials is directly related to estimation of service life of structures made from existing and new materials. The latest studies in this area are associated with investigation of the effect exerted by the condition of interfaces, such as segregation of impurities at the grain boundaries, on the mechanisms of fracture of heterogeneous polycrystalline and nanostructural materials. We used scanning electron microscopy to study «in situ» the evolution of surface damage in small-size samples of cold-resistant steel with an experimental composition during the deformation process. For this we employed a device with a tensile load of up to 4.5 kN and a tunnel probe with a scanning field of 20×20×2 μm. Figures 5 and 6 show results of scanning of the grain boundary zone before and after the deformation. Changes in surface relief and emergence of microcracks even before the formation of a macroplastic strain can be seen in the 3D image and profiles. The surface damage can be quantitatively estimated only by the methods of multi-fractal analysis [14], which requires more detailed experimental works.

Increasing interest is expressed now throughout the world to connected problems (multiphysics) and stochastic modelling. Results obtained in this area make it possible to solve the problem of estimation of life of weak elements (including those which comprise welded joints) of potentially hazardous objects. The model has been suggested to describe propagation of a crack in a tough-ductile heterogeneous material, allowing for a random character of its properties and

based on the mechanism of growth of the main crack as a result of pores and microcracks located ahead of it.

The most important task at the given stage of development of the economy of Russia is solution of the problem of renovation of the old fleet of machines that exhausted their designed life in potentially hazardous industrial facilities, such as oil and gas pipelines, storage tanks, water supply systems, steam power plants etc. In this connection, diagnostics and extension of life become especially important for such facilities. Therefore, the ability to predict and prevent emergency situations means control of the risk of disasters at engineering facilities.

To summarise, materials science, technology and engineering tasks of extending the life of technical facilities intended for different applications and having a different level of sophistication, and ensuring the efficiency and safety of their functioning in the North and Arctic regions can be formulated at follows:

• development of theoretical principles of strength, damage and fracture, and new cold-resistant materials characterised by a high resistance to delayed fracture;

• development of improved welding technologies;

• development of criteria for estimation of strength and life of technical facilities intended for the extreme North conditions;

• development of calculation-experimental methods for evaluation of cold resistance of large-size metal structures;

• development of advanced analytical, statistical and experimental methods for investigation of engineering systems.

1. Larionov, V.P. (1986) *Electric arc welding of structures in northern modification.* Novosibirsk: Nauka.
2. Larionov, V.P. (1998) *Welding and problems of tough-brittle transition.* Novosibirsk: SO RAN.
3. Sleptsov, O.I. (1985) *Process strength of welded joints at low temperatures.* Novosibirsk: Nauka.
4. Prokhorov, V.A. (1999) *Evaluation of parameters of safe operation of oil storage tanks under the North conditions.* Moscow: Nedra.
5. Makhutov, N.A., Kuzmin, V.R., Prokhorov, V.A. (2000) Expert evaluation of the state of tanks according to strength criteria. *Kontrol. Diagnostika*, **10**, 15–19.
6. Lyakishev, N.P. (1998) Structural and some functional materials. Present and future. In: *Proc. of Int. Conf. on Welding and Related Technologies for the 21st Century.* Kyiv: Naukova Dumka.
7. Larionov, V.P. (1998) Fundamental aspects of ensuring cold resistance, reliability and durability of welded structures under cold climatic conditions. *Ibid.*
8. Grigoriev, R.S., Larionov, V.P., Novikov, G.A. et al. (1969) *Cold shortness of metal structures and machine parts.* Moscow: Nauka.
9. Lepov, V.V., Lepova, K.Ya., Alymov, V.T. et al. (2002) Stochastic modelling of fracture of a heterogeneous damagable medium. *Fiz. Mezomekhanika*, **2**, 23--41.
10. Arkhangelskaya, E.A., Lepov, V.V., Larionov, V.P. (2001) Connected model of delayed fracture of a damagable medium. *Ibid.*, **5**, 81--87.
11. Sleptsov, O.I., Mikhajlov, V.E., Petushkov, V.G. et al. (1989) *Increase in strength of welded structures designed for North.* Novosibirsk: Nauka.
12. Larionov, V.P., Alymov, V.V., Mikhajlov, V.E. et al. (1999) *Delayed fracture of metal structures at low temperatures.* Novosibirsk: SO RAN.
13. Pokhodnya, I.K. (1998) Problems of welding high-strength low-alloy steels. In: *Advanced materials science of the 21st century*. Kyiv: Naukova Dumka.
14. Lepov, V.V., Achikasova, V.S., Ivanova, A.A. (2002) Investigation of damage of low-alloy steel and diamond crystals by fractal analysis methods. In: *Proc. of Euras. Symp. on Problems of Material Strength under Cold Climate Conditions*, Yakutsk, July 16--20, 2002. Yakutsk: SO RAN.

LATEST DEVELOPMENTS AND TRENDS IN HIGH-EFFICIENT WELDING TECHNOLOGIES

U. DILTHEY, L. STEIN, K. WOESTE and **F. REICH**

ISF Welding Institute, Aachen University, Aachen, Germany

Within the last couple of years, there have been several new developments in the field of high-efficient welding technology. This paper presents these developments, describing their principle, outlining their possibilities and giving examples for their application. Fields addressed are new arc welding processes, latest developments in electron beam welding, as well as trends in laser beam welding concerning processes and equipment.

Developments in arc welding processes. In the early 1960s, GMA welding methods were introduced into industrial manufacturing and they have been consequently developed further ever since. Recent advances do not only refer the power source technology, improved wire feed systems or new consumables, such as filler materials and shielding gases. Great efforts have been made to increase deposition rates and with this efficiency and welding speeds by extending the frontiers of known processes and by developing new ones.

GMA welding processes. Modern electronics and computer control, as well as improvements in wire feeding have led to digitally controlled power with high power/weight ratios with new features. Digital controllers allow the flexible implementing of several, very different power source characteristics containing complex control strategies. Pulsed-arc welding control strategies have been improved concerning process stability and avoiding and recovery from short circuits. Using digital controllers makes interfacing to external computers a lot easier, so that modern power sources provide multiple functions for adjusting process characteristics, parameter development and documentation, as well as for quality assurance.

These machines allow the use of all stable welding processes beginning with the well-known short arc welding process up to the high deposition welding processes such as the rotating-arc and high-deposition spray-arc welding processes.

Two-wire welding. GMA welding with one wire has, applying the mentioned types of arc, reached operating ranges, that probably can not be extended significantly by further developments of power sources, filler materials or shielding gases. Literature mentions welding speeds of up to 2 m/min for high deposition short arc welding, as well as deposition rates of up to 14 kg/h for the rotating arc. A further increase in deposition efficiency is, among other reasons, limited by the instable arc rotation.

This and the need for high deposition rates with reduced heat input led to the development of the two-wire GMA welding technology, combining two wire electrodes in one common gas nozzle. Early investigations on this field carried out in the 1975 failed as the power source technology at that time was not able to maintain a stable welding process. The application of a new generation of power sources, however, was able to overcome the witnessed difficulties and establish two-wire welding in two variations as a promising new production method in industry. Employing a second process has significant influence on the shape of the weld pool. Arranging the electrodes behind each other stretches the welding pool in the direction of the welding speed. The leading wire then causes adequate penetration while bead shape is determined by the trailing wire electrode. The longed weld pool allows better degasification, a fact which, especially in welding of aluminium and in welding through primer coatings, reduces porosity sensitivity. Twisting the electrodes slightly into a position next to each other enhances bridging abilities at reduced current levels. This, however, affects the weld speed. A twist by about 20° requires a reduction of weld speed by about 25--30 %.

Two-wire GMA welding processes are divided into two variants, i.e. twin GMA welding, which is the older process employing a common contact tube, and tandem GMA welding, which uses electrically isolated contact tubes for each wire (Figure 1).

Twin GMA technology. Developments started with the twin GMA technology, which is characterised by a common contact tube connected to one (or two coupled) power source (Figure 1, *a*). This results into the same voltage being applied to both wire electrodes. As two equi-directional current-carrying conductors are attracted to each other due to the magnetic forces, the arc roots of both electrodes form a common root (depending on the distance between them). At a spacing of 4 to 7 mm, depending on wire diameter and total current intensity, the detached droplets meet in one common weld pool. Smaller distances may lead to a droplet bridge between both electrodes, causing process instabilities. In case of a too large distance between the wires, the
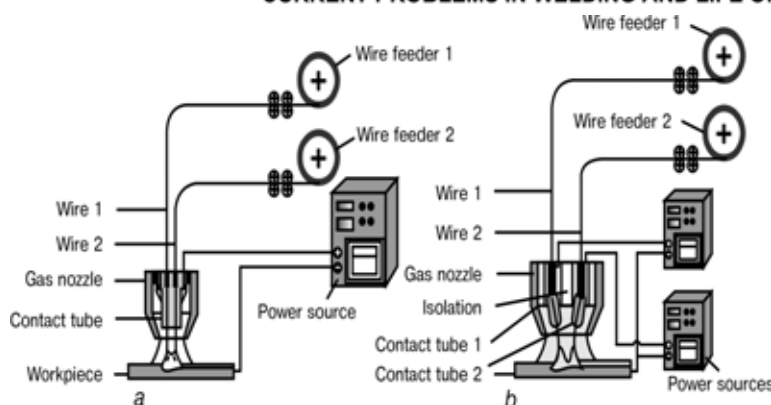
Figure 1. Two-wire welding technologies: *a* — twin GMA technology; *b* — tandem GMA technology

separate weld pools occur and because of heavy blow effects, heavy spatter occurs.

Main disadvantage of this process variant is that the welding parameters can not be set independently for each electrode, so that individual wire speeds and wire diameters cannot be used. Moreover, short circuiting of one arc will extinguish the other because of the common contact tube, making the overall process instable. This limits twin GMA welding to non-short circuiting processes, such as spray-arc or pulsed-arc.

Tandem GMA welding. In order to optimise process behaviour and to be able to control both arcs separately, torches with electrically isolated contact tubes are used and synchronized independently controllable power sources are employed (Figure 1, *b*). Such it is possible to use this process in short arc welding and to use different wire diameters and speeds, were necessary, featuring stable welding processes.

AC MIG welding. The need for lighter constructions leads to the use of thinner sheets, which in turn, results in difficult gap bridging ability. When GMA welding with reverse polarity, heat input into the base material, as well as penetration, is reduced and the ability to bridge gaps improves. Unfortunately, process stability is bad with reverse polarity. AC MIG powers sources combine a standard pulse process with an adjustable phase of reverse polarity. This leads to a stable welding process with adjustable penetration and gap bridging ability highly suited for thin sheets with gaps as often found in industrial applications.

GMA welding with strip electrode. A GMA process variation quite new on the market now is GMA welding with strip electrode. Using special wire feeding devices and special contact tips, narrow strip electrodes, approximately 4.0×0.5 mm, are employed. Because of their geometry, that has a greater surface than a round wire electrode of comparable cross section area, less energy is required to melt the material resulting in lower welding currents than for comparable round wires. There are two ways to make use of this effect. One is to increase the wire feed rate in order to improve deposition rate, the other is to lower heat input. Due to the rectangle cross section of the electrode the foot-point of the arc forms an ellipse. Depending on the orientation of this ellipse, it is possible to influence the penetration. Orientating the electrode in welding direction causes deep penetration well suited for fillet welds on thicker plates, orientating it across the seam yields into shallow penetration and optimum gap bridging ability.

GMA brazing. The principle difference between GMA welding and GMA brazing lies in the field of metallurgy. When welding, a certain amount of penetration is desired, to ensure fusion between base material and steel filler material. In brazing, there should be no melting of base material, if possible. GMA brazing equipment is the same as for GMA welding, merely a low-melting copper base bronze wire (900-- 1100 °C) is used. Processes used are short-arc, as well as pulsed-arc.
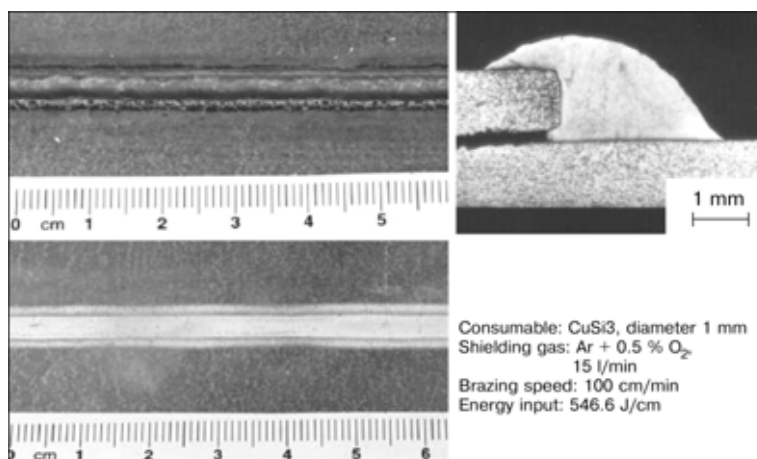

Consumable: CuSi3, diameter 1 mm
Shielding gas: Ar + 0.5 % O_2
15 l/min
Brazing speed: 100 cm/min
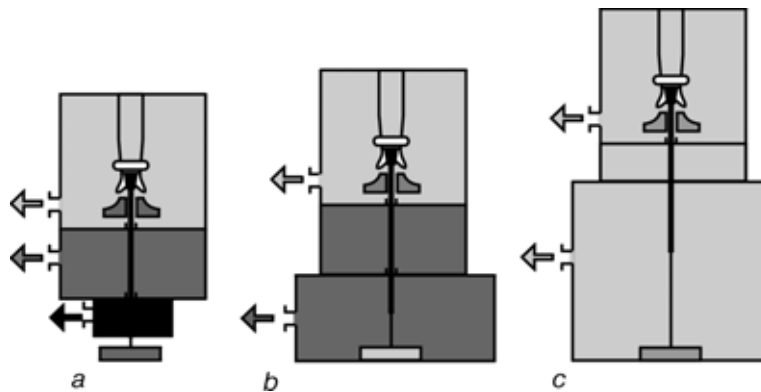Energy input: 546.6 J/cm

Figure 2. GMA brazing

Figure 3. Electron beam welding technologies: *a* ---- non-vacuum; *b* ---- low-vacuum; *c* — high-vacuum

GMA brazing has already become well established as a method for joining galvanised thin sheets. As no base material should be melted, heat input into the material is minimised and damage to the zinc coating is limited to a minimum with no negative influence on corrosion properties (Figure 2). Strength of the brazings is comparable to that of welds. Moreover, finishing of the brazed seam is easy. Due to this, GMA brazing is becoming more and more popular not only for car body building in automotive industry but everywhere where the advantages of low heat input, low distortion, less damage to galvanised coatings and high brazing speeds outrule the higher price of the required bronze electrode.

Plasma MIG welding. Plasma MIG welding is a welding process, that is experiencing a revival after being developed as a high deposition process in the past. New torch technology, as well as modern power sources are the reason for this. The plasma MIG process is a standard MIG process with a concentric plasma torch around it. Both processes are controlled by separate power sources. As the plasma process stabilises the MIG process and vice versa, parameters for both of them can be varied in a wide range. Thus possible applications reach from high-deposition aluminium and steel welding, making use from the wire preheating and the extra heat input from the plasma process to highly stable medium deposition processes with the extra benefit, that the additional plasma cleans the surface directly before material is deposited with benefits in aluminium welding down to plasma MIG brazing with very low heat inputs and the possibility of influencing bead shape.

Developments in beam welding processes. *Electron beam welding.* The range of joining tasks for EBW reaches from foil welding with plate thicknesses of just a few $1/10$ mm up to thick plate welding with achievable weld depths of 150 mm. Moreover, almost all electrically conductive materials are weldable, many of those materials may also be joined in material combinations. The high power density in the range from up to $1 \cdot 10^8$ W/cm^2 which is typical of EBW, and the connected depth-to-width ratio of the weld (up to 50:1) allows a large variety of possible applications of this joining process.

Standard EBW is normally carried out in a vacuum chamber under high or low vacuum, but there is also the possibility to use the electron beam at free atmosphere (Figure 3).

High-vacuum working chambers are used primarily when welds with large weld depths are demanded or when a beam with a maximum of power density and a minimum of beam diameter is requested. Thinner-walled parts are, as a rule, welded in low vacuum. The non-vacuum EBW (NV EBW) method is mainly used for the joining of plates; filler material is frequently applied and allows high gap bridging abilities.

New EBW technologies. As the electron beam is an almost mass-less welding tool which is deflectable, non-contacting and almost inertia-free, it is possible to oscillate the beam with extremely high frequency.

Modern electron beam machines frequently have the possibility to manipulate the beam with arbitrarily programmable deflection figures.

Using the same principle, the parallel deflection of the electron beam between several positions may be realised, thus leading to the simultaneous metallurgical influencing of the structure as a consequence of its thermal inertia. Depending on the achievable frequencies, accuracies and deflection distances, up to five electron beams may process the material simultaneously thus leading to the capillary to be always opened at all parts during welding (Figure 4). This technique holds a high future potential for different applications.

The easiest variation of this technique, with two parallel beams, has been used for many years now for the production of band saw blades consisting of a ductile backing layer in the middle and two hardened boundary layers in so-called conveyor machines.

A further interesting field of application for the multi-beam technology is the welding of axis-parallel, rotationally symmetrical bodies. As the material is melting simultaneously at several points of the axis-symmetrical weld and solidifies subsequently, the shrinkage stresses also occur simultaneously and symmetrically, thus avoiding disalignment of the axes. The last application example mentioned here is joining of material combinations. The multi-beam technique allows, by varying holding times at different points,
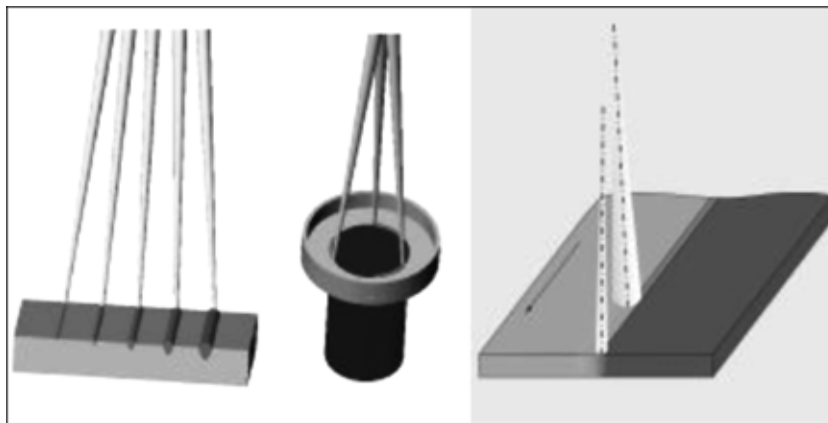
Figure 4. Parallel capillary technique

supling, one of the joining members at the welding point with a significantly higher energy than is the case for the second member. For example, one joining member is molten while the other one is just heated (diffusion welding). By this way, it is possible to join material combinations, where the joining members do not show complete solid solubility.

Equipment concepts. By adapted vacuum chambers the evacuation times may, for many applications, be reduced in a way that the necessary welding downtimes are not the decisive criterion against the use of EBW technology. Different working chamber systems are nowadays available to equip EBW machines. The most flexible variant is the universal working chamber, where the workpiece is moved in three directions. This vacuum chamber concept, however, entails comparatively high downtimes as the working steps «clamping the tool», «entering the recipient», «evacuation», «welding», «airing», «workpiece release» must be carried out one after another. In order to fulfil the demand for shorter cycle times, machine systems, such as cycle system machines, dual chamber machines, conveyor machines and lock chamber machines, have been developed. Double chamber machines have two working chambers which are placed side by side. The beam generator is either moved between those two chambers or the beam is deflected to one chamber at the time. Thus, welding may be carried out in one chamber while the other chamber is loaded or discharged, as well as evacuated. Should the welding time exceed the workpiece change and evacuation time, then the capacity of these chamber equipments is fully utilised. A disadvantage of these machines is that both chambers have to be equipped

with separate movement devices and pumping units (Figure 5, *b*) shows one of the variations of a double chamber machine.

The lock welding machines stand for another equipment concept (Figure 5, *a*). A high vacuum is permanently maintained in the chamber where the welding is carried out. Manipulation devices pass the workpieces through one or two pre-chambers. The machines have a position for loading and discharging, a lock for airing and deaerating as well as the welding lock. The most productive but also the most unflexible type of machine are the conveyor machines. These machines have the same operating principles as the lock welding machines, where the workpiece is continuously transported over centring lips through the pressure locks into the working chamber and from there again through a pressure lock. The inevitable leakage must be compensated by the vacuum technique.

Cycle system machines are the right choice for welding similar or equal parts with equal weld geometries and axial welds. Underneath the chamber (generally small volume), which is equipped with one or several loading stations with accordingly demands only short evacuation times, a rotating jig with vertical, horizontal or swivelling axes is fixed. Thus, loading and discharging, as well as welding, may be carried out at the same time.

Non-vacuum EBW. As in EBW in free atmosphere (NV EBW) a vacuum chamber is not necessary and thus evacuation times, as well as chamber-conditioned restrictions to the component dimensions may be set aside, this method is most advantageous. The technique has been developed in Germany in the 1960s.
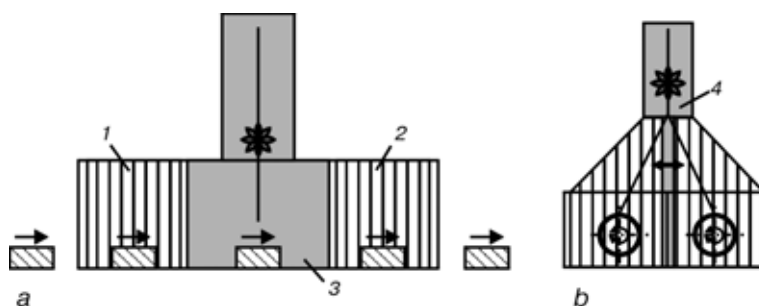

Figure 5. Different vacuum chambers principles: *1, 2* — vacuum lock; *3* — high vacuum; *4* — deflected beam
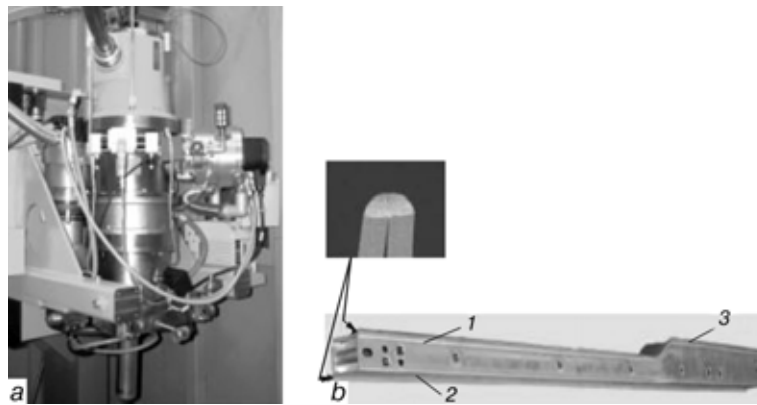
Figure 6. NV EBW generator (*a*), and cross-section and beam (*1, 2*) position in welding of aluminium hollow section (*3*) (*b*)

The beam generators are of the same design as those in vacuum EBW. Figure 6 shows a NV EBW generator and a typical application.

The half-shells of the depicted aluminium hollow sections are joined by the NV EBW method. Welding speeds of up to 12 m ⁄ min are applied which makes NV EBW also a highly profitable method. There are further reasons, besides the high welding speed, which make NV EBW applications highly recommendable.

In comparison with laser beam welding (LBW) methods which, for many applications, are directly competing with NV EBW methods, the electron beam is able to penetrate the workpiece surface independently from angles or surfaces. After leaving the beam generator, the beam is guided into ranges of higher pressure right to atmospheric pressure. Series-connected chambers generate the drop of pressure. The beam is focused onto the exit nozzle which has a diameter of 1--2 mm. With rising ambient pressure the electron beam is scattered through a collision with gas molecules and enlarges. In free atmosphere the beam maintains its initial power density over a short length only. During welding, a maximum working distance of approximately 25 mm must not be exceeded.

The beam diameter is between 1.5 and 2.5 mm, depending on the working distance and the accele-

rating voltage. This focused spot which is, compared with vacuum EBW and LBW, relatively large, allows a good gap bridging ability and a relatively coarse edge preparation in a combination with filler material.

Exactly as in vacuum EBW the NV EBW method allows using the deep penetration effect for the achievement of deeper welds. Depth-to-width ratios of 5:1 may be obtained with the NV EBW method. Thanks to the deep penetration effect the application possibilities of NV EBW are not limited to the thin sheet range but may be extended to weld depths of up to 10 mm. The use of filler wire helps to utilise the good gap bridging ability of NV EBW. A correlation between weld speed and weld depth is shown in Figure 7.

The utilisation of the energy density of the electron beam in free atmosphere and the high available machine powers allow achieving weld speeds of 20 m ⁄ min with steel materials and more than 50 m ⁄ min with aluminium alloys.

LBW. Developments in welding technology. Laser beam welds are characterised by a high depth-to-width ratio, resulting in a minimum influence on material properties and high welding speeds. On the other hand, the demands on seam preparation and positioning are high and gap briding ability is low. Recent developments mainly focus on optimising gap
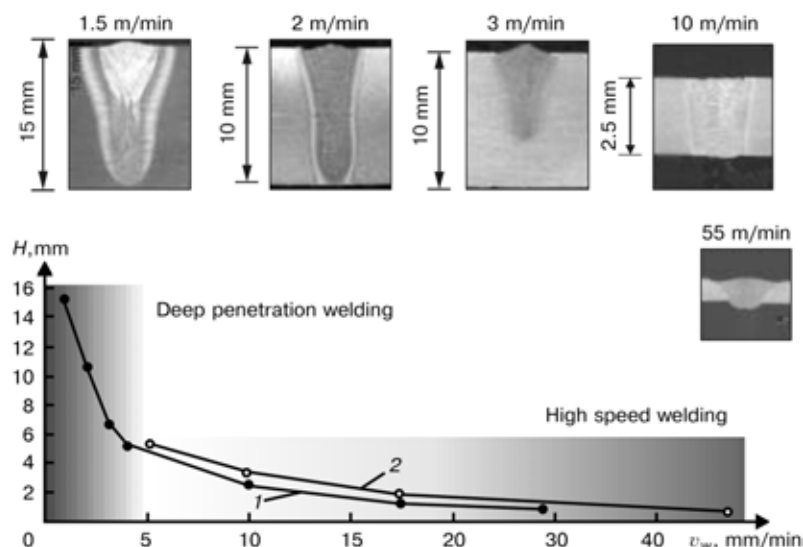

Figure 7. Correlation between weld depth H and welding speed v_w at a beam power of 15 kW
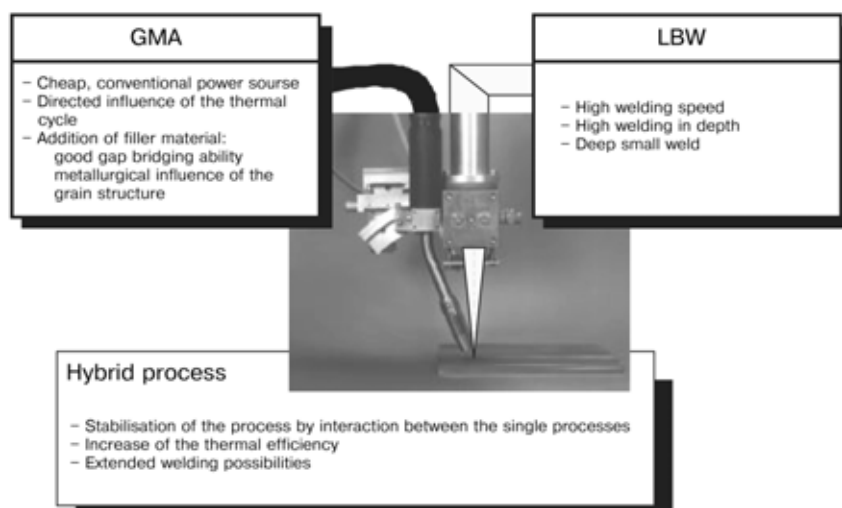
Figure 8. Hybrid laser-MIG welding

briding abilty and to lower demands on seam preparation and positioning.

LBW with filler wire. Adding a precise wire feeding device to the standard laser process is the simplest extension. By adding filler material, it is possible to fill gaps and take influence on the metallurgy of the weld. This qualifies LBW with filler wire also for material combinations with intermediate layers, as well as for materials tending to crack.

Hybrid laser-MIG welding. Hybrid laser-MIG welding is the combination of a laser welding process and a standard GMA process in one common welding zone (Figure 8). It combines the deep penetration of the LBW process with the good gap bridging ability of GMA welding. Furthermore, the laser process stabilises the GMA process. As filler material is applied as a liquid, high welding speeds can be achieved with low heat inputs. Applications for hybrid laser-MIG welding are steel (CO_2 lasers) and lightweight alloys (Nd:YAG lasers), plates thickness start from car body sheets and are limited by the available laser power. A rule of thumb estimates 1 mm plate thickness per kilowatt CO_2 laser power for steel. First industrial applications are in shipbuilding and in the production of aluminium car bodies.

Remote welding. When replacing spot welds by laser welds, this is usually done by short welds, that require long travel times between the welds when carried out with robot guided laser optics. To reduce these travel times, it is necessary to reduce the moved mass, only deflecting the laser beam itself is the ideal case. Figure 9 shows the principle of remote welding, which realises this ideal case. One or two mirrors deflect the laser beam, positioning the focus in height direction is done by moving the long-focus focussing lens along the axis of the beam.

The realisation of remote welding was only possible with a new laser generation with optimum beam quality, such as ROFIN-SINAR CO_2 slab laser. Together with a focussing lens of 1600 mm, this opens a considerable working field, which may be enhanced by mounting the remote welding unit to a 3D robot,

as demonstrated by COMAU. With remote welding, the travel time between the welds may be reduced to a few $1/100$ s reducing welding time by up to 25 %.

Developments in laser technology. Diode-pumped Nd:YAG laser. In the case of solid-state laser, the normally cylindrical rod serves only the purpose to pick up the laser-active ions (in the case of the Nd laser with yttrium-aluminium-garnet crystals dosed with Nd^{3+} ions). The excitation is usuallly done with flash or arc lamps, which are arranged as a double ellipsoid; with the rod positioned in their common focal point. The achieved efficiency is below 4 %.

In the mean time, diode-pumped solid-state lasers have been introduced to the market. Diode-pumped Nd:YAG lasers can be used as a reliable and economical tool for a wide range of industrial applications. The key features of the laser diode-pumped Nd:YAG lasers are the diode life time of more than 10,000 h, outstanding electrical efficiencies and excellent beam quality.

The optical excitation is done by high-power diode laser modules, which are radially arranged around the Nd:YAG rod. The resonator is coaxial with the laser rod, and consists of a high-reflectance mirror and a partial-reflective output coupler (Figure 10). Several
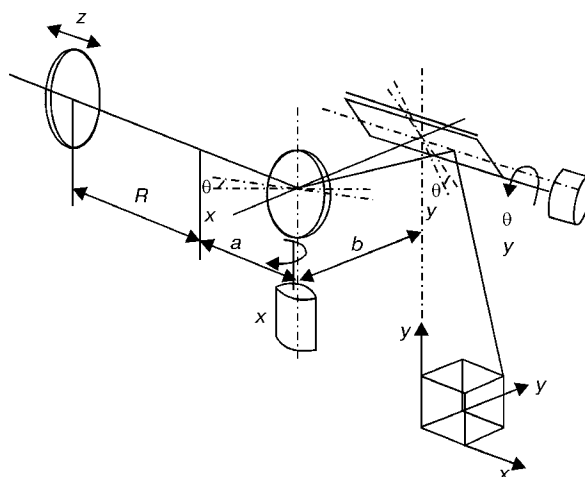
Figure 9. Principle of remote welding (COMAU welding system)
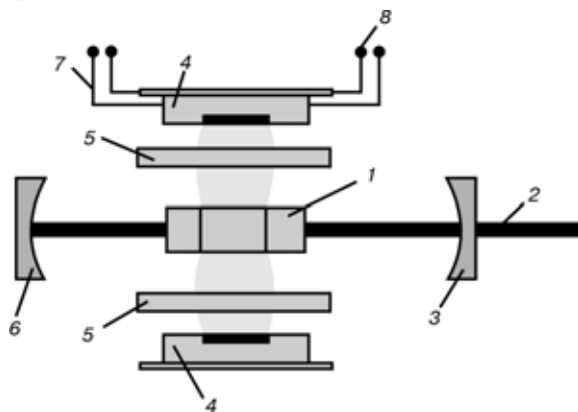
Figure 10. Principle of diode-pumped solid-state laser: *1* — Nd:YAG rod; *2* — laser beam; *3* ---- output coupler mirror; *4* — diode arrays; *5* — collimating optics; *6* ---- high-reflectance mirror; *7* ---- cooling; *8* — electrical supply

diode-pumped rods may be arranged in series in order to achieve output powers in the multi-kW range. The laser beam can be delivered by using one or several fibres.

Fibre lasers. The next step in laser development are fibre lasers. Diode-pumped active fibres provide highest beam quality, wall-plug efficiencies up to 20 %, robust design without alignable optics in compact design. Manufacturers, like IPG Photonics, the available laser power of the fibre laser 6.5 kW are reached rapidly at present, 25 kW are a medium-term target. Fibre lasers work at wavelengths similar to YAG laser, so that they have the same advantages as YAG lasers at welding lightweight alloys.

Diode lasers. Diode lasers are available up to 6 kW beam power now. To reach these powers, several laser diodes are combined to diode laser bars, which, in turn, are then put together to so-called stacks reaching several 100 W of beam power. By combining several stacks via optical systems, lasers in the region of kilowatts are realised. Other than with gas or solid-state lasers, the increasing of power cannot be achieved by longer resonators, but by increasing number and area of laser diodes. This leads to lower beam quality. High-power diode lasers deliver a rectangular focus spot of up to a few millimetres of edge length. For this reason, they are normally used for thermal surface treatment, powder transfer surfacing, and for heat-conduction welding. Advantages of diode lasers are electrical efficiencies up to 30 %, as well as compact dimensions, which makes integration into automated production systems easy. Wavelengths are the near infrared, resulting in good weldability for metals, as well as for plastics.

CONCLUSION

As well in arc welding, as in beam welding newly developed process technologies and process variants increase the field of application, welding speed and efficiency, weld quality and finally result in economical advantages.

RAPID FABRICATION OF REFRACTORY COMPONENTS BY THERMAL SPRAYING

D. DEHELEAN and **N. MARKOCSAN**

National R&D Institute for Welding and Material Testing, Timisoara, Romania

Using new technologies like near net-shape spray forming is possible to obtain quickly nozzle type refractory components. Material utilisation and very high and laborious machining can be avoided. In order to achieve nozzle type components plasma spray technique has been used to spraying molybdenum powder onto a preshaped substrate. The influence of plasma spraying parameters on the mechanical and physical properties of free-standing components has been studied. The residual stress was also evaluated in order to know their behaviour and working ability under difficult conditions.

Keywords: *thermal spraying, nozzles, burness, near net-shape components*

Today, due to the high dynamics of the market, the new products or subassemblies development is continuously subjected to a high competition pressures. That's why the reduction of the design, achievement and time-to-market for a product is a permanent desiderium for any manufacturer. From this reason, the new fabrication technologies able to fulfil the requirements of the market economy have known a rapid development and diversity.

One of these new technologies is near net-shape spray forming. In this family, an attractive method of fabricating refractory components is through the use of plasma spraying.

Plasma spray forming is a simple and relatively efficient method to produce radially symmetric net-shape parts. Parts manufactured to date include injector tubes that have been field tested in pyrometallurgical applications, converging / diverging gas burner nozzles, and submerged gas burners.

In general, the refractory metals and their alloys offer the desired high melting temperatures and inherent chemical stability, in non-oxidizing environments, needed for these applications. However, the difficulty of forming these materials into different shapes has limited their application in the past [1].

Recently, near net-shape forming by plasma spraying has been demonstrated as a viable fabrication tool for fabrication refractory metal furnace nozzles. A primary advantage of this technology over other powder metallurgy techniques is that near net-shape spray forming of components significantly simplifies and promises to reduce the cost of fabricating due to the high material utilization and reduction in laborious machining.

Experimental procedure. Molybdenum powder was sprayed to produce conical free-standing nozzles. The characteristics of feedstock powder are shown in Table 1.

In principle, the shape forming by thermal spraying consists in a support having the shape adapted to the given application a layer with the pre-established shape and size is deposited by thermal spraying. During the next phase, the deposited layer (component) is removed out of the support, so the desired component results.

The mandrel removing techniques can be divided in two families: removing by mandrel destroying (melting, burning or chemical dissolving of mandrel) and removing by mandrel saving, i.e. mandrel disassembling or removing by rapid contraction of the mandrel (can be used for much more free-standing component fabrication).

In this experimental program, the free-standing specimens were produced by spraying onto grit blasted and degreased brass substrates and subsequently removed from the mandrel. The removing was made by rapid cooling (contracting) of the brass mandrel. The principle of the procedure is presented in Figure 1.

The layers deposition was carried out by atmospheric plasma spraying, due to high spraying temperature of that technology, being able easily to deposit any refractory materials.

The fields of used thermal spraying parameters were as follows: plasma current 300--450 A, arc voltage 70--72 V, plasma gas flow rate 800--2200 l / h, powder flow rate 10--24 cm^3 / min, a mixture of Ar + 6 % H$_2$ was used as plasma gas.

Table 1. Powder materials used within the process

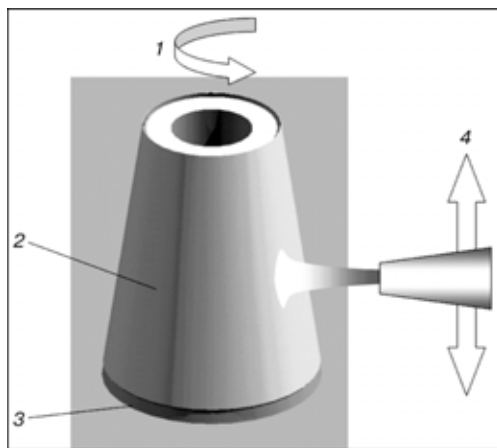| Material type	Chemical composition	Grain size, μm	Typical properties
Molybdenum (precipitated / sintered)	99.5 % Mo	--90--+45	Tough and hard, with excellent sliding properties, wear resistance and thermal barrier coatings Working temperatures 350--600 °C

Figure 1. Scheme of the spraying process: *1* — part rotation; *2* — ceramic part; *3* — aluminium support; *4* — plasma torch translation

Because the spray parameters have an important influence on the layer properties the experimental program has been focused on studying this influence on the nozzle properties.

The removing of the resulting component from the support was based, mainly on the dilatation ⁄ contraction differences of the materials (component and support, respectively).

In order to analyse the microstructure, the samples were prepared. Optical microscopy was performed on free-form samples mounted in epoxy and adequate prepared. The metallographic attack was carried out using a $K_3[Fe(CN)_6]$ solution in accordance with Romanian standards.

Porosity of the layers was determined by numerical calculus methods. So, specialised programmes were used, programmes which allow the numerical processing of the metallographic images, determining the porosity by colour selection, respectively.

The microhardness measurements were made with a hardness device Vickers type, and loadings of 300 g. Measurements were made in the cross section of the component. The zones where the indentations have been made were prepared consequently.

Fracture resistance was evaluated by tensile testing by adapting the standard procedures described in Romanian and European standards (SR EN 10002-1 ⁄ 95).

In order to determine the residual stress level into the components layers, X-ray diffraction measure-

ments were performed. It was used the CoK_α radiation, $\lambda = 1.7889$ Å and a circular slit on the X-ray beam with 1 mm in diameter.

The residual stress was measured in axial and tangential directions of conical components.

Results and discussions. By atmospheric plasma spraying and using the parameters shown above the nozzle type components (Figure 2) with dimensions of $D_{max} = 50$ mm, $D_{min} = 40$ mm, $L = 60$ were mm built-up.

The samples visual examination, respectively at ×10 increases, reveals conical components with compact walls, without cracks or large pores.

The wall thickness is constant on the whole of length, the measured values being included between 0.5 and 1.5 mm, function of different spraying conditions.

The visual examination reveals also different colours for the realised nozzles. Is been observed that a relationship exists between the nozzles colour and the spraying current. The different colours of samples result from the colours of molybdenum oxides that are formed at different temperatures. By modifying the current intensity value, the energy of plasma jet is modified too, and implicit his temperature. This colour difference of the nozzles surfaces could be an indicator about the oxidation degree, known being the molybdenum predisposition for oxidation between certain temperatures [2].

The main oxides, indicated by colours of sample surfaces, are molybdenum pentoxide Mo_2O_5 (dark-violet colour), molybdenum dioxide MoO_2 (dark-brown colour), molybdenum trioxide MoO_3 (yellowish colour).

The powder flow rate increasing has as the major effect the increase of the deposed coating thickness (at the same number of passing). The maximum coating thicknesses correspond to the maximum values of the powder flow rate.

The microscopically aspect of the layers deposited by plasma spraying can be observed in Figure 3.

The microstructures of molybdenum coatings produced by plasma spraying are well known [3]. However, the microstructure of thick free-standings de-
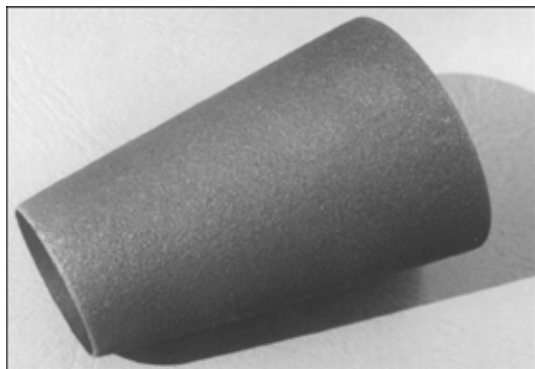

Figure 2. Molybdenum sample ($D_{av} = 47$ mm, $\delta_{wall} = 1$ mm)

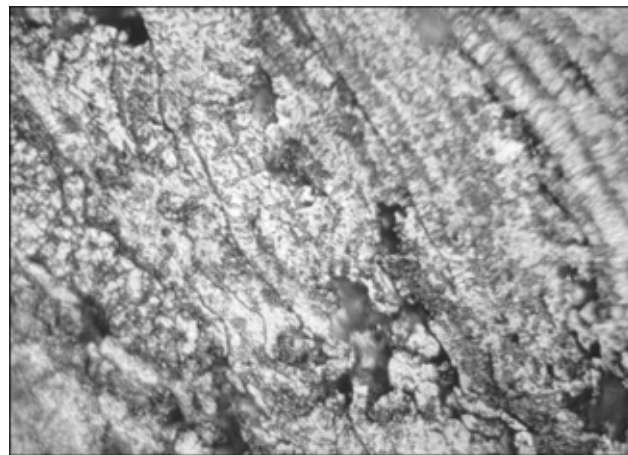**Figure 3.** Microstructure of deposited layer ($K_3[Fe(CN)_6]$ solution) (×500)

$$P = -0.0579\, I_p + 31.6$$
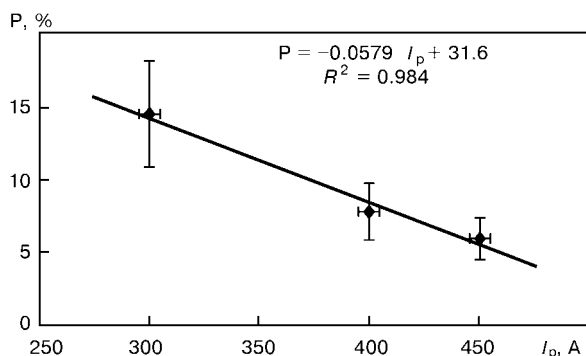$$R^2 = 0.984$$

Figure 4. Influence of plasma current on layer porosity

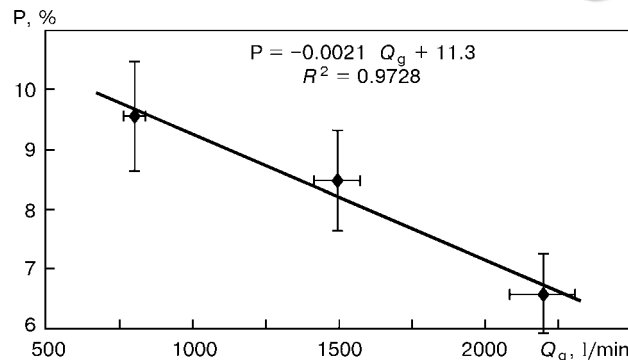$$P = -0.0021\, Q_g + 11.3$$
$$R^2 = 0.9728$$

Figure 5. Influence of plasma gas flow rate on layer porosity

posits produced need to be investigated. The free-forms are built-up from successive deposited layers of lamellae by plasma spraying. The microstructures typically exhibit distinct boundaries around splats and inter and intralamellar porosity. Rounded particles, indicating unmelted and/or partially feedstock powder may be found in the deposits.

The microstructure aspects of the all examined samples indicate an influence of spraying parameters on the microstructure of deposited layers.

The increase in value of parameters influencing the plasma jet energy (thermal and kinetic) (the current intensity in plasma arc and the plasma gas flow) leads to a higher compactness of the layer. The flattening degree of the particles in the layer is higher and the quantity of the unmelted or partially melted particle is decreased.

The increase of the powder flow has an inverse effect to the current in the plasma arc and the plasma gas flow, respectively.

The powder flow has a similar effect to the two working parameters analysed before on the microstructure of the sprayed layers. The obtaining of compact layers made out of thin lamella (having a high melting degree) has been observed when the powder flow is low.

Porosity. The values of the layer porosity determined by analytical calculus are between 2.3 and 14.4 % in thick cross-section.

Figures 4, 5 and 6 show the level of porosity in all deposits as the result of the spray parameters and process conditions, all influencing the built-up structures, i.e. deposit temperatures, particle velocities, re-solidified particles etc. Spherical pores were observed in all deposits, due to gases included during the flying time and released when the solidification occur. Porosity has also been observed around partially melted particles in the samples. This is reported to be a result of inadequate compact placement of particles due to low viscosities and/or low impact velocities.

The smallest values are to be noticed for low powder flows. Increasing the flow of the powder filler material the final temperature of the particle is reduced, their viscosity in the moment it reaches the substrate is higher; this leads to the increase of porosity.

The atypical values of porosity (over 10 %) [3--5] correspond to the layers deposited with low currents in plasma arc. The increase of the arc energy (by increase the current in the plasma arc and plasma gas flow, respectively) leads to the increase of the particles energy in the plasma jet; so the compactness of the layers increases and the porosity decreases.

From statistical point of view, it can be noticed a strong linear correlation between porosity and the spraying parameters, which means that there is a linear dependency between them, and their influence of these technological parameters on porosity is probably a direct one. The high values of the intensity coefficients in the linear correlation (R^2) between porosity and the spraying parameters indicate determinist linear dependencies.

Microhardness. The microhardness values of the layers within the experimental programme are between $HV_{0.2}$ 393 and $HV_{0.2}$ 467. The microhardness measured values of the layers are around the minimum values of the hardness intervals in the molybdenum layers deposited by plasma jet spraying [6]. These values come from the porosity of the layers; dependence can be noticed between the hardness of the layers and their morphology. Comparing the obtained values with those obtained on sintered components it can be found a higher hardness of the sprayed layers than of those made by sintering ($HV_{0.2}$ 260--360) [7].

Figures 7, 8 and 9 show the influence of thermal spraying parameters on the hardness of the layers of built-up components.

As shown in the above Figures the hardness is influenced by the thermal spraying parameters. In Figures 7 and 8 it can be observed that between hard-
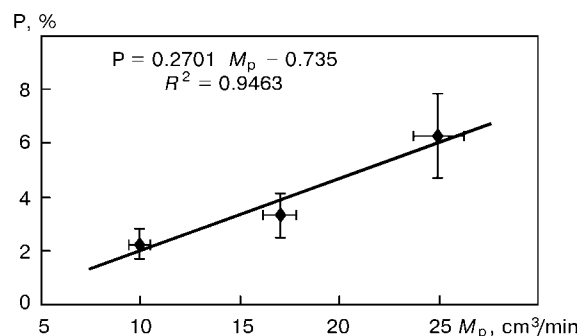

$$P = 0.2701\, M_p - 0.735$$
$$R^2 = 0.9463$$

Figure 6. Influence of powder flow rate on layer porosity

$$HV_{0.2} = 0.18 \; I_p + 332$$
$$R^2 = 0.99$$
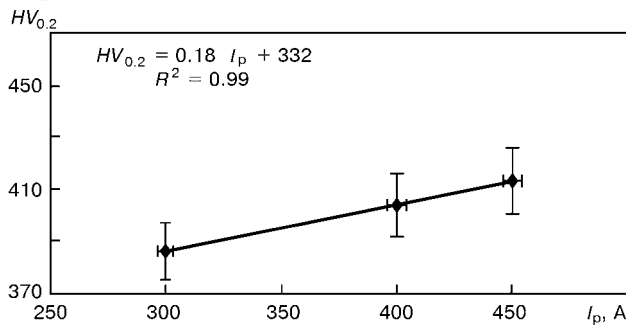
Figure 7. Influence of plasma current on layer hardness

$$HV_{0.2} = 0.04930 \; Q_g + 355.4$$
$$R^2 = 0.9753$$
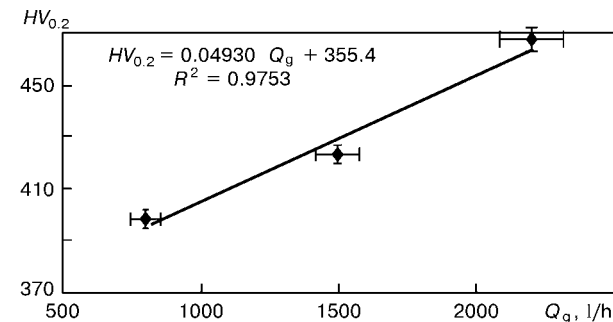
Figure 8. Influence of plasma gas flow rate on layer hardness
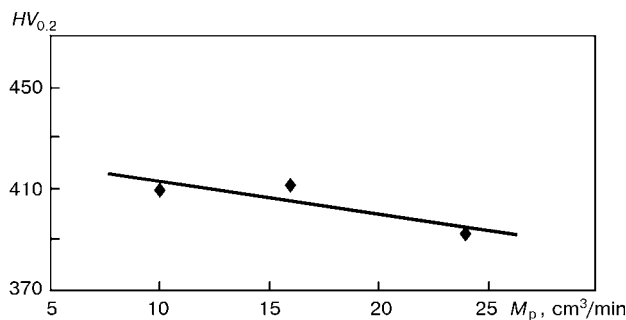
Figure 9. Influence of powder flow rate on layer hardness

$$R_m = 0.17 \; I_p + 20.5$$
$$R^2 = 0.9897$$
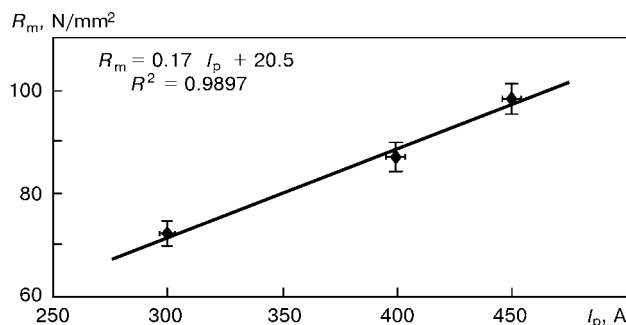
Figure 10. Influence of plasma current on tensile strength

$$R_m = 0.0207 \; Q_g + 52.262$$
$$R^2 = 0.9902$$
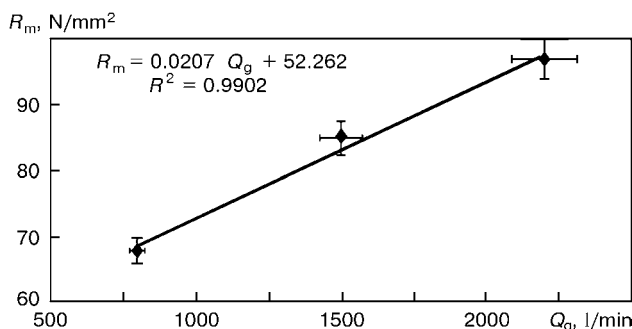
Figure 11. Influence of plasma gas flow rate on tensile strength

ness and plasma current, respectively plasma gas flow rate, is a direct proportionality.

The highest values of microhardness correspond to the high plasma gas flow rate; it leads to the conclusion that the kinetic energy of the particle has a higher influence than the thermal energy.

The high velocity, respectively the lower temperature of the particles, leads to a compact layer formed more by the plastic deformation of particles (at the substrate collision) and not due to the heat input of the gas jet. The compact layers, which are formed, determine a greater average of the measured hardness by reducing the negative influence, which the porosity has on the sclerometric measurements.

The variations of the powder flow rate do not lead to significant changes in the hardness of the layers (the range is $HV_{0.2}$ 17). The lower values of hardness at high powder flow rates can be the cause of compactness, respectively of the more reduced collision of layers, which in this case contain more unmelted particles.

From the statistical point of view, it can be seen that there is a strong linear correlation between hardness and the current in the plasma arc, respectively the plasmagen gas flow rate, which means that their dependence is linear. The existence of regression linear relations with high R^2 coefficients between hardness and the powder flow rate could not be established.

Tensile strength. The values of the tensile strength of nozzle type components made with different spraying parameters are between 68 and 105 N/mm².

The measured tensile strength values of free-standing nozzles made by thermal spraying are below that of the typical values registered for cast or sintered components having similar shapes [7, 8].

The low rupture resistance of thermal sprayed components is caused by the high fragility components (typical for refractory materials) respectively by specific morphology of layers characterised by high porosity and of low cohesion of layers.

Also, the dependence between the layer porosity and the component tensile strength can be easily observed.

The influence of thermal spraying parameters on the tensile strength of the components is shown in Figures 10, 11 and 12.

Analysing the Figures 10 and 11 the main conclusion is that the fracture resistance of the realised nozzle

$$R_m = -0.9257 \; M_p + 114.09$$
$$R^2 = 0.9986$$
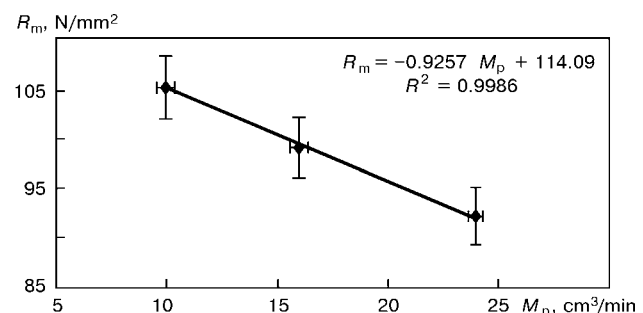
Figure 12. Influence of powder flow rate on tensile strength

type components depends on the energy of the plasma jet.

Variation of plasma jet current or plasma gas flow rate gives a proportional variation of measured tensile strength of components. These variations are almost linear, the high value of the coefficients of linear intensity correlation indicating determinist dependence between tensile strength and that two spraying parameters. The high energies of plasma jets give a high melting rate of the particles in the plasma jet, resulting in this way a layer with high compactness and low porosity. A decreased porosity increases the contact area between the splats and increases the strength of the sprayed deposits.

The powder feedstock influences the fracture resistance of the tested samples (Figure 12).

The high quantity of powder has a cooling effect on the plasma jet, the melting rate of particles is reduced, and the layers contain a bigger quantity of unmelted or partially melted particles. By this reason the allied processes of mechanical anchorage of the splats (diffusion, microwelding etc.) are reduced, and layer cohesion is reduced, too.

The high values of linear correlation coefficients show that the tensile strength can be controlled with high efficiency by a judicious adjusting of these three analysed thermal spraying parameters.

Residual stress. Regarding the evaluation of residual stresses it has to be noted that the results are affected (a little bit) by the measuring errors, which cannot be avoided.

The main reason is the anisotropy, respectively the unhomogeneity of the sprayed layers, which make the time to define a specific peak to be long. The dispersion of diffracted X-ray beam is high and the registering of specific data regarding the analysed peak to be difficult. From this reasons the data processing is affected by errors.

The measurements were carried out on nozzles, realised with following thermal spraying parameters: plasma current 450 A, arc voltage 72 V, plasma gas flow rate 2200 l/h, powder flow rate 16 cm^3/min.

The main results of residual stress measurements are shown in Table 2. The measurement directions are taken along the cone generator respectively tangential to it.

The level of residual stresses in the nozzle walls is low. The average of the residual stresses in free-standing components is below that of the residual stresses reported for layers deposed on a substrate (due to the differences in the physical properties of the layer and substrate) and it being between --60 -- +140 MPa [9].

The differences result from many reasons, the main are the physical properties of the layer material (thermal expansion, thermal conductivity), the geometrical configuration, the dimensions of components, the physical compatibility between the layer and substrate material, the substrate roughness, respectively the thermal history of components, while thermal spraying and substrate (support) removing.

Table 2. Residual stress values

Sample	Axial, MPa		Tangential, MPa	
	Stress	*Error*	*Stress*	*Error*
Nozzles	–22	7	54	8

CONCLUSIONS

1. Free-standing components can be easily fabricated by new techniques of plasma spraying. The great flexibility of the process allow performing of nozzle type components made from heat resistant materials, which are difficult to be processed by other fabrication methods.

2. The mechanical and morphological characteristics of the built-up layers (walls) do not differ from those of the layers deposited on a substrates.

3. The thermal spraying parameters have an important effect on the microstructure and mechanical properties of the nozzle type components.

4. The microstructure and porosity play an important role in the mechanical properties of the deposits, being a visible dependence between them.

5. The measured residual stress has a lower level in free-standing components than in the deposits on substrates.

6. The «near net-shape spray forming» type fabrication technologies can be developed for new types of materials, as well as for new type of shapes of the components, which will make the object of the new research work of the staff within ISIM, Timisoara.

1. O'Dell, J.S. et. al. (1998) Increasing performance of plasma spray formed components. In: *Proc. of 15th Int. Thermal Spray Conf.*, Nice, France, May 25--29, 1998.
2. Markocsan, N. et. al. (2000) Experimentation for near net-shape forming by plasma thermal spraying. *Research Report of Contract A8.* Timisoara: ISIM.
3. Markocsan, N. (2002) *Near net-spray forming.* Ph. D. Thesis. Timisoara.
4. Lugscheider, E. (1994) *Beschichtungstechnik, Vorlesungumdruck fur die Vertieferrichtung Werkstofftechnik.* Aachen: RWTH.
5. Pawlowski, L. (1995) *The science and engineering of thermal spray coatings.* J. Wiley&Soons.
6. Yntema, L.F., Percy, A.L. *Molybdenum. Rare metals.* Handbook.
7. Cheney, R.F. Production of tungsten and molybdenum powder. In: *Production of metal powders.*
8. (2000) GEM 2001 ---- Guide to engineered materials. *Advanced Materials&Processes*, 158 (**6**).
9. Lodini, A. (1996) *Analyse des contraintes residuelles par diffraction des rayons X et des neutrons.* Paris.

PROBLEMS OF WELDING AND FATIGUE LIFE OF WELDED STRUCTURES IN SHIPBUILDING

V.D. GORBACH, O.G. SOKOLOV and **V.S. MIKHAJLOV**
Central R&D Institute of Shipbuilding Technology, St.-Petersburg, Russia

Factors are considered, which determine the cyclic strength and fatigue life of shipbuilding welded structures. Design evaluations of welding deformations are given for the case of the hull of a tanker and catamaran ship. Methods to lower the local and total deformations, stabilization of the shape and accuracy of welded structures through their low-frequency vibration treatment are outlined. Examples are given of using fundamentally new types of welded joints, based on high-energy density sources and adaptive welding processes.

Keywords: *welding deformation, stress concentration, cyclic strength, laser technologies, adaptive welding processes, geometrical and process adaptation, honeycomb panels*

Welded structures of ships, off-shore platforms, deep-sea equipment are exposed to non-stationary alternating loads in service. Wind and water impact, as well as considerable pressures, applied to welded joints by ice fields in the arctic regions of the Ocean, in a number of cases are sources of fracture of individual elements of structures, which may lead to accidents. These circumstances require a very careful approach to allowing for all external impacts, as well as internal factors, which to varying degrees limit the initiation and nature of propagation of fatigue cracks in welded structures [1--5].

According to such an approach the full life time N of a welded joint is determined by fatigue life before fatigue crack initiation N_i and fatigue life N_c, which corresponds to the period of crack development up to its critical size a_{cr}:

$$N = N_i\{\alpha_\sigma,\ K_\varepsilon,\ \sigma_a^i(x,\ y)\} + \\ + N_c\{a_0,\ a_{cr}(t,\ \sigma_{res}(x,\ y),\ \sigma_a^i(x,\ y))\}, \quad (1)$$

where α_σ is the theoretical coefficient of stress concentration; σ_a are the local values of the amplitude of acting stresses; i is the power index determined experimentally; $x,\ y$ are the coordinates; $a_0,\ a_{cr}$ is the initial and critical crack size, respectively; K_ε is the coefficient of concentration of deformations, characterizing a defect or geometrical features of the welded joint; σ_{res} are the residual welding stresses.

Welding deformations and stresses, including the total and local deformations and residual stresses, have a significant influence on the quality, performance and labour content in fabrication of welded structures, including the ship hull structures.

Residual stresses have a negative impact on the fatigue life of structures, cyclic and corrosion-mechanical strength, corrosion and erosion condition of the ship hull [5].

In view of the above, Central R&D Institute of Shipbuilding Technology (TsNIIST) has conducted for many years the theoretical and experimental studies of the process of formation and forecast evaluation of welding deformations and stresses, which were the basis to develop the design and technological measures to prevent and lower the developing deformations and stresses [2--3].

Design evaluation of welding deformations and stresses. Calculation was based on the theory of heat propagation in welding, principles of structural mechanics and theory of elasticity. However, acceptable methods of calculation of welding deformations were developed only for the simplest welded structures (tee beams, finned panels, hull sections, tubular elements, etc.). Generalizations, made by experts of other enterprises, and our own studies and developments at TsNIIST were the basis to develop a branch standard OST5.9807--80, which specifies the methods of determination and prevention of residual welding deformations. Methods, included into this standard, are used to allow for the complex nature of development of welding deformations, which is influenced by three groups of factors, conditionally called thermal, physical and geometrical. These methods rather accurately allow for the influence of welding modes and sequence, as well as thermophysical characteristics of base and filler materials used in welding. The most complex is allowance for the geometrical factor, i.e. for the influence of the shape, dimensions and weight of structural elements on the magnitude of deformations, as well as the conditions of fastening the elements and structure as a whole [4].

For forecasting the formation and accumulation of welding deformations in fabrication of complex 3D structures (sections, beams and hulls of the ships as a whole) TsNIIST with participation of specialists of A.N. Krylov TsNII has over the recent years conducted a series of investigations and developed a computational method, based on the theory of welding deformations and finite element method (FEM). In calculations by the above method, the thermal processes of welding are used to determine the equivalent longitudinal and transverse forces, acting on the structure, and the structures proper are approximated by platen-column finite elements (FE) with six degrees of freedom in the node. Deformations are determined,
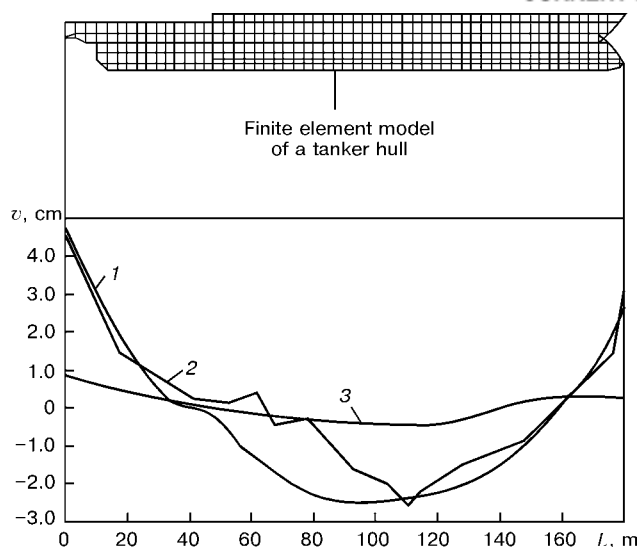
Figure 1. Results of calculation of the total bending of a tanker hull: *1* — calculated bending with the existing schematic of hull formation; *2* — actual bending of the keel line of a tanker hull; *3* ---- calculated bending with compensation of welding deformations (v — ship deflection; L — beam length)

taking into account the technological sequence of assembly and welding, weight of structural elements, reactions and sagging of berth supports (in hull assembly in the berth), structure rigidity and method of fastening of the elements being welded (tack welds or fittings), etc. Deformation analysis is performed, using ANSYS program in Pentium-III computer. Procedural approach to determination of residual welding deformations was optimized on sections, blocks and hull of a tanker, catamaran, as well as in calculation of deformations, resulting from welding-in internal parts into spherical and cylindrical structures.

In simulation of the tanker the number of FE on the blocks was up to 1.500, and of those on the hull as a whole ---- about 5000. Approximation of the tanker hull by the totality of plate and column FE as well as results of calculation of overalle bending of the hull, schematic of hull construction and calculation results are given in Figure 1 [4].

Curve of bending in Figure shows that at construction of the hull, as a rule, its bow and stern parts are raised, and the middle part is lowered below the main plane (sagging is observed). Hence, the main forces of supporting the hull in the berth are concentrated in its middle part. It is easy to forecast that at ship launching further bending of the ship hull occurs, because of redistribution of the forces of supporting the hull on the water and in the berth. Calculation procedure allows evaluation of the possible change of the elastic curve of the hull after launching, and, therefore, specifying the measures to compensate the deformations in hull assembly in the berth, taking into account additional changes of the elastic line of the hull after ship launching.

Figure 2 shows deformations of the catamaran, arising in welding on the bulkhead and upper deck. It is seen that during performance of welding-assembly operations the catamaran bodies are turned, both
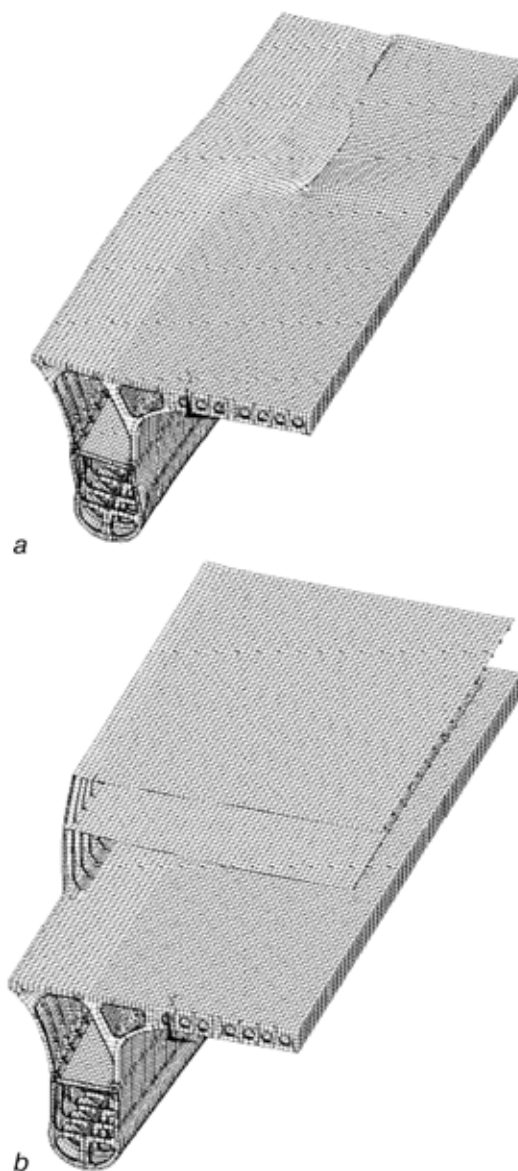
Figure 2. Deformation arising in mounting and welding-in the section of the bulkhead (*a*) and upper (*b*) deck of a catamaran

in the horizontal and vertical plane. Mounting the sections and blocks with appropriate preemptive tilts allows reducing the deviation of the catamaran shape and dimensions from design values.

Important is the problem of determination of local deformations, arising in welding in the internal parts into the spherical and cylindrical structures. Figure 3 shows a FE model of a spherical structure. Calculation of welding deformations with FEM application allows obtaining information about displacement of any point of the structure. Figure 4 shows the distribution of the displacements of points of a spherical structure and internal parts. Analysis was performed of the mutual influence of internal parts on the extent of their displacement relative to each other. Comparison of distortions of the central part for different technological stages, as well as for the variant of mounting and welding in the internal parts before mounting and welding in the platforms is shown in Figure 5. Analysis of the data given in the Figure, shows that

Figure 3. Finite element model of a spherical structure with internal parts

— — contour of coaming and spherical partition before performance of assembly-welding operations;
— — contour of coaming after performance of assembly-welding operations in the absence of platforms;
----- — same, after performance of work of 1st technological stage;
--- — same, for the 2nd technological stage;
— — same, for the 3rd technological stage

Figure 5. Comparison of displacements of the central coaming, arising at different technological stages and with different assembly sequences (DP and MP are the diametral and main planes, respectively)

welding in the upper internal part has a significant influence on the extent of displacement of the central part, whereas the influence of the availability or absence of the platforms on the magnitude of deformations is insignificant. Performance of such calculations, using the classical methods of structural mechanics is impossible.

In order to reduce the labour consumption in acquisition and entering the initial data for calculation of deformations of sections, blocks and the hull as a whole, it is rational to use the information, taken from the systems of CAD and technological preparation of production, available in the shipbuilding enterprises.

Lowering residual stresses. Heat treatment, which is a highly labour-consuming and expensive operation, is used for lowering the residual stresses, stabilization of the shape and dimensions of structures in shipbuilding and other industrial sectors. Low-frequency vibration treatment of structures is used as an

alternative process in shipbuilding and other industrial sectors [6--7].

The above method of lowering the residual stresses is based on applying the energy of forced oscillations, arising under the impact of periodical dynamic loads. Structure vibrations generate alternating stresses. At joint action of alternating and residual stresses the phase-structural stabilization is intensified, structure is refined, microplast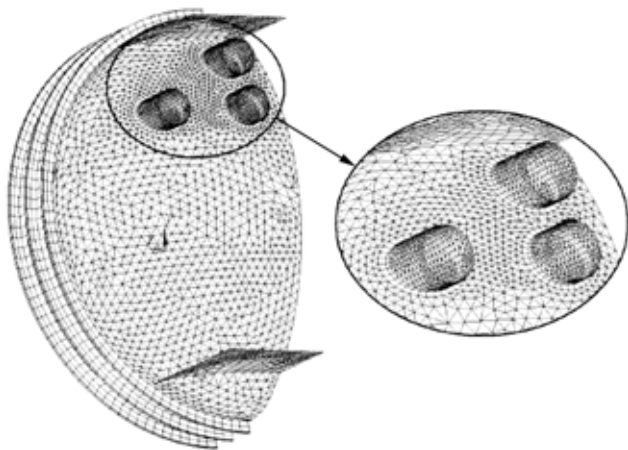ic deformations and other processes proceed in the metal, which lead to lowering of residual stresses, stabilization of the shape and dimensions of the structure as a whole. It is established that the degree of lowering of residual stresses depends on oscillation amplitude, duration of treatment, metal properties, structure rigidity, technology of vibration treatment and other factors [7].

Residual stresses are lowered the most intensively at vibration treatment of a structure under the resonance conditions, when the amplitude of forced oscillations rises abruptly, because of the frequency of natural vibrations of a structure becoming close to or coinciding with the frequency of external impact, applied to it. For a simplest beam the frequency of natural vibrations is given by the following dependence:

$$W = \frac{\pi^2 n^2}{L^2} \sqrt{\frac{EJ}{m}},$$

where $n = 1, 2, 3$ is the number of the mode of natural vibrations; L is the beam length; EJ is the flexural stiffness; m is the weight of a unit of beam length.

With the increase of n the elastic line of beam oscillation is broken into a number of half-waves and change of the elastic line is quite well approximated by the sinusoidal function. Bending moment and corresponding stresses, induced by bending, are distributed in keeping with the shape of beam bending.
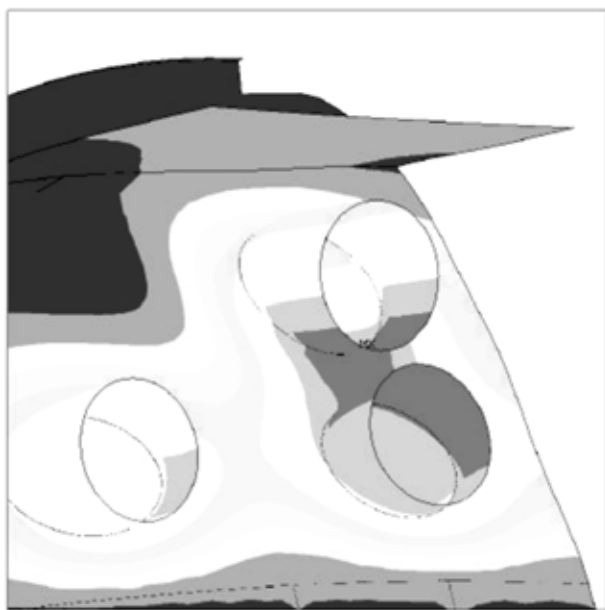

Figure 4. Distribution of displacements arising as a result of performance of assembly-welding operations over the surface of a spherical structure and internal parts
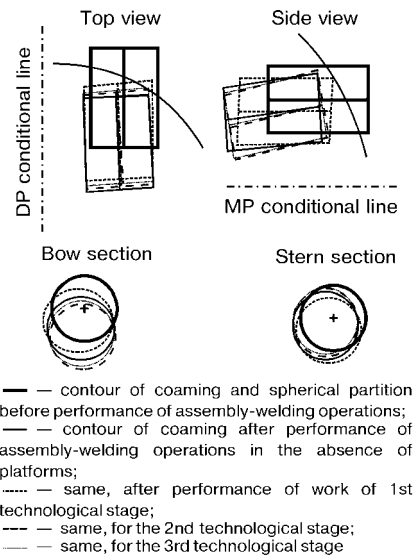
With the first shape of bending, the maximum stresses are in the middle part of the beam, with the second they are on one-fourth of beam length from its ends, etc. In this connection, in order to provide a uniform lowering of stresses, vibration treatment of the structure is performed on two-three resonance frequencies.

A series of investigations, performed at TsNIIST, and experience of introducing low-frequency vibration treatment in a number of shipbuilding factories showed that this method allows lowering the residual stresses in steel welded and cast-welded structures to 60--65 %, those in aluminium structures ---- to 70--75 %, those in titanium ---- to 60--65 %.

In order to lower the residual stresses, vibration treatment of structures is performed in unrestrained condition, and for stabilization of their shape and dimensions in the condition of fastening (in a fixture, jigs, or berth-jig). Pairing of similar structures during fabrication and subsequent vibration treatment is possible.

Portable vibration units, consisting of vibroexciter and control panel are applied to excite mechanical vibrations in ship structures (Figure 6).

Low-frequency vibration treatment allows stabilizing the structure and lowering of residual stresses in structures of material of dissimilar composition, and eliminates a number of operations (removal of scale after heat treatment, possible straightening of the structure, etc.). Moreover, it lowers the power consumption hundreds of times, reduces the labour consumption and duration of the process, and, therefore, lowers the cost of work performance as a whole, and improves the ecological situation.

Surface strengthening and redistribution of stresses in welded joints. It is known that residual welding stresses arise in any welded joint. Tensile residual welding stresses usually form along the welded joint. The latter are balanced by compressive stresses, which are distributed to both sides of the welded joint. In this case, gradual lowering of their magnitude is observed with greater distance from the weld. Values of longitudinal stresses are rather high and may reach the material yield point. Transverse stresses form alongside the longitudinal stresses in the welded joint. In welding of parts in an unrestrained condition, they are balanced in the welded joint proper. In the surface layer and HAZ tensile stresses form, which have rather high magnitude [5--7].

Thus, significant tensile residual stresses are present in the welded joint zone, both in the longitudinal and transverse directions. In order to reduce their adverse impact on the structure, the following various methods are used in many industries to reduce or redistribute the residual stresses (i.e. replacement of the tensile stresses by compressive stresses in the surface layers of welded joints). They include treatment by explosion, pneumatic hammer, ultrasonic beam hammer, treatment by a roller, shot peening, etc. Selection of the treatment method for lowering or

Figure 6. Vibration unit and device for stress measurement

redistribution of stresses depends on manufacturing conditions, kind of products, availability of equipment, etc.

In shipbuilding shot blasting, pneumatic or ultrasonic beam hammer, and pneumatic brushes are mainly used. TsNIIST conducted a series of investigations to determine the influence of the method and technology of treatment on the degree of lowering or redistribution of stresses. Figure 7 gives examples of distribution of residual compressive stresses by the depth of the processed steel sheets, depending on the method and duration of processing, dimensions of the shot, used for treatment and air pressure in the shot blasting machine, power of the pneumatic hammer, and modes of a special unit for surface strengthening of the welded joint, using the impact of needles strikers at ultrasonic frequency (Figure 8).
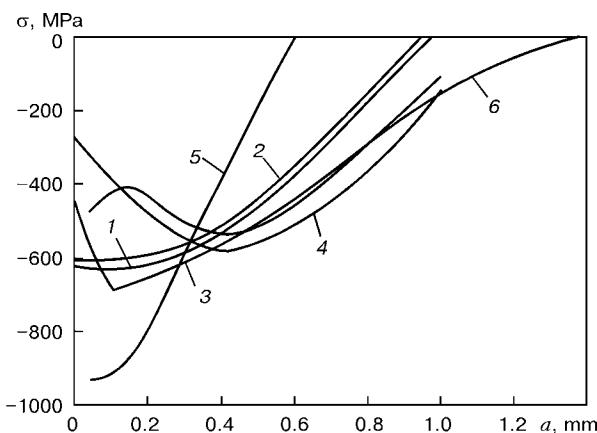

Figure 7. Distribution of residual compressive stresses in the metal surface layers depending on the method and modes of treatment: *1* — by a pneumatic hammer; *2--4* — by an ultrasonic hammer of 500, 800 and 1100 W power, respectively; *5* — shot blasting ($t = 15$ s); *6* ---- by a roller (σ — residual stresses; *a* — depth of layer strengthening)
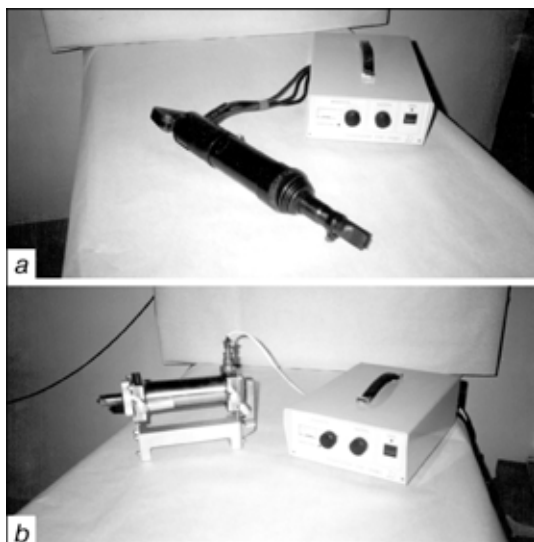
Figure 8. Unit for strengthening treatment of welded joints at ultrasonic frequency: *a* — ultrasonic hammer; *b* ---- device for impact treatment

During surface strengthening change of the width of the zone of strengthening of butt and fillet joints, degree of surface strengthening, geometrical elements of the stress raisers (butt and tee welded joints, welding on the inner parts) were studied. Butt samples with the width of the strengthening band of up to 70 mm were tested to determine the optimal zone of treatment. Figure 9 gives the results of fatigue testing, from which it follows that surface strengthening of welds allows improving the cyclic fatigue life of a structure 2 to 3 times. With the increase of the width of the strengthening band the corrosion fatigue strength of butt joints is increased up to a certain value. Further increase of the width of the strengthening zone has no effect on improvement of the corrosion fatigue strength. In this connection, the width
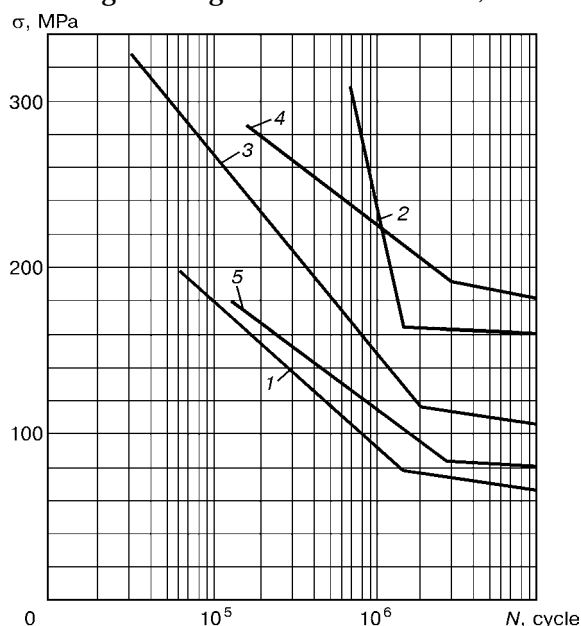
Figure 9. *S--N* curves of steel treated by different methods: *1* — without treatment; *2* — shot blasting at *P* = 0.5 MPa (*t* = 60 s); *3* — shot blasting treatment at *P* = 0.55 MPa (*t* = 5 s); *4* — shot blasting treatment at *P* = 0.55 MPa (*t* = 15 s); *5* — induction heating
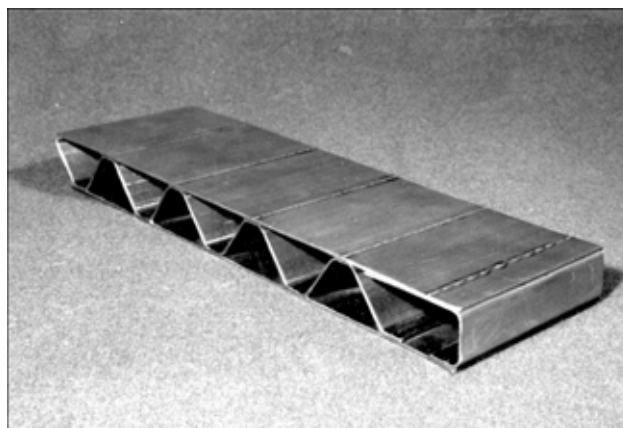
Figure 10. Example of the design of a honeycomb panel

of the strengthening zone should overlap the HAZ after welding and be equal to about 60 mm to one side of the welded joint, which is sufficient to achieve the required effect. Similar results were obtained in testing structures for corrosion and corrosion-mechanical strength.

TsNIIST, with participation of other enterprises, has developed and is producing equipment for surface strengthening, including beam pneumatic and ultrasonic hammers, shot blasting machines and other equipment.

Problems of design-technological improvement of welded structures in shipbuiding. Extension of the service life and reliability of ship hulls and offshore structures is possible not only by relaxation of the local residual stresses. Not less effective is using for this purpose the methods of welding based on high power density sources. Application of laser, electron beam and thin-plasma technologies in the operations of grooving, welding and processing of the metal, provides an abrupt lowering of the level of reactive welding stresses in structures, and also practically eliminates development of residual stresses due to the operations of fit up and straightening.

TsNIIST in cooperation with St.-Petersburg State University developed design solutions, fabrication technology, and performed testing of a sandwich panels based on computerized laser technology (Figure 10) [8].

Investigations at TsNIIST and A.N. Krylov TsNII demonstrated that application of the above panels not only ensures the service life of ships and vessels, but also essentially reduces the weight of structures, labour content and terms of their construction (Figure 11).

Adaptive welding processes. In 2001 PWI in cooperation with TsNIIST performed investigations of the means and methods of following the butt shape in welding parts of ship hull structures.

Analysis and evaluation of the design of technical vision systems was the basis for selection of the method of acquisition and processing of the initial information for welding tool control. A method of «light section» with subsequent processing by a triangulation procedure was selected for construction of
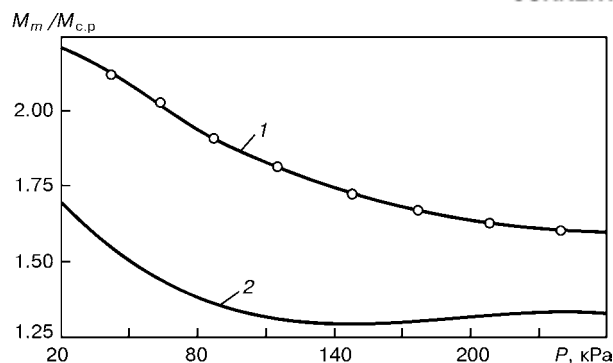
Figure 11. Relationship of the weight of a covering M_m designed on the basis of the traditional technology to the weight of covering $M_{c.p}$ designed using the honeycomb (corrugated) panels without a filler at different levels of calculated loading P on the covering: *1* ---- D40 steel; *2* — RSD32 steel

Figure 12. Schematic of scanning with the welding tool in uphill welding with electrode oscillation: *1* ---- initial position of the tool before welding; *2* — bisector of edge preparation

the technical vision system for the automatic welding machine. A module of optical videosensor was developed for automatic welding machines, fitted with systems of geometrical and technological adaptation.

A slot laser head and digital videocamera have small overall dimensions, thus providing the ability of placing them near the welding head. The videosensor block is rigidly coupled to the automatic machine transportation module. This provides fixed co-ordinates for the geometrical model of the welded joint, formed by the videosensor module. The vectors of speeds and values of corrective displacements of the actuators are assigned relative to the same co-ordinates. The data processing rate is several times higher than the highest values of welding speed (displacement of the transportation module). This eliminates any problems in the use of the videosensor module even under the conditions of high-speed arc welding processes. Such a system allows to completely solve all the problems of geometrical and technological adaptation.

As shown by the results of investigations, it is quite high. Under the condition of using the up-to-date hardware and modern technical means for the actuator drives, this permits, in parallel with solving the problem of a guaranteed level of welding quality, also solving that of resources saving. Calculations showed that 12 to 20 % welding consumables and power are saved just due to reducing the size of weld convexity. The considered welding process in conducted in the mode of «manlesss technology». Use of automatic machines with adaptive control systems allows effectively solving the problems of facilitating the conditions of welders' labour. A prototype of an automatic machine for performing uphill welding with electrode oscillations is currently being designed. The features of this technological variant consist in that the use of scanning by the pattern, shown in Figure 12, provides weld formation over the entire groove cross-section in one pass.
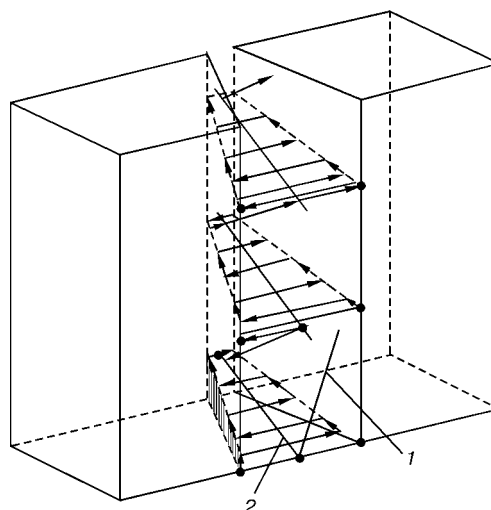
This technology is used in the Russia's shipbuilding sector and offers the following advantages: all-position welding, including roll butts at not more than 2 m radius of curvature; development of smaller angular deformations, compared to multipass welding; ability to perform welding of a broad range of steel grades and alloys, including Ti-based alloys; wider, compared to other technologies, range of admissible dimensions of the gap (±4 mm tolerance).

All of the above advantages of the developed automatic machine allow it to be applied under the conditions, when a manipulator or rotator is to be used for welding mechanization and automation.

1. Gorynin, I.V., Iliin, N.V., Leonov, V.P. et al. (1990) Calculated determination of welded joint fatigue life with allowance for specification requirements. *Sudostroit.* Prochnost, Series Materials Science. Welding, Issue 10, 3--14.
2. Kuzminov, S.A. (1984) *Welding strains of ship hull structures.* Leningrad: Sudostroenie.
3. *OST 5.9807--80.* Metal hulls. Methods of determination and prevention of welding strains. Introd. 1980.
4. Alfyorov, V.I., Mikhajlov, V.S. (1996) Mathematical simulation of the process of welding strain accumulation in fabrication of tanker structures using the finite element method. In: *Trans. of Acad. A.N. Krylov TsNII,* Issue 3 (287), 36--43.
5. Karzov, G.P., Margolin, B.Z., Shvetsova, V.A. (1993) *Physicomechanical simulation of fracture processes.* St.-Petersburg: Politekhnika.
6. Mikhajlov, V.S., Gorbach, V.D., Stegantsev, V.P. et al. (1999) Low-frequency vibrotreatment of structures and surface strengthening of welded joints as effective processes of decreasing and redistribution of residual stresses. *Vestik Tekhnologii Sudostroeniya,* **5,** 38–43.
7. Sokolov, O.G., Margolin, G.Z., Levshakov, V.N. et al. (2002) Prospects of application of new architectural-engineering solutions for ship hulls manufactured, using high power density sources. In: *Proc. of Int. Conf. on Welding and Related Technologies,* St.-Petersburg, 2001. St.-Petersburg: SPb GRU.
8. Gorbach, V.D., Suzdalev, I.V., Panikarovsky, R.F. et al. (2002) Adaptive control of the welding process as the method to ensure high quality and reliability of critical welded structures. *Ibid.*

NEW DEVELOPMENTS OF TECHNOLOGIES AND EQUIPMENT FOR FLASH-BUTT WELDING OF PIPELINES

S.I. KUCHUK-YATSENKO

E.O. Paton Electric Welding Institute, NASU, Kyiv, Ukraine

The paper describes new developments of technology and equipment for flash-butt welding of pipes, allowing enhancement of the technological features of application of this welding process in construction of various pipelines.

Keywords: *flash-butt welding, pipelines, quality, efficiency, welding machine design, welding technology, highly reliable pipeline transport*

In the world practice intensive search for technologies allowing one-position welding as the most promising in terms of organizing the construction flow in welding in site is still going on, alongside with improvement of various processes of electric arc welding of position butts in pipelines, using the traditional operational flow. TWI in co-operation with Cypem Company, Italy, developed technology and equipment for one-position electron beam welding of thick-walled pipes in a low vacuum [1]. In addition to this work, the interest to searching for various technologies of pressure welding of pipes is still high. Results of many years of work on deve-lopment of resistance welding of up to 320 mm pipes, using a unipolar generator, have been published [2]. This research, conducted in the University of Texas in co-operation with General Electric Company, USA, demonstrated the ability to produce high-quality pipe joints of various steels and alloys. Norwegian Company Stolt [3] developed a production unit for radial friction welding (using a deformed coupling) of high-strength casing pipes. Work is in progress on improvement of the process of welding small diameter pipes, using a magnetically-impelled arc (MIAB) [4].

Method of flash-butt welding (FBW), which allows performing one-position welding of pipes in site, may be regarded as one of the promising methods of pipe joining in new projects. Over the last decades the CIS countries have gained extensive experience of using FBW in construction of pipelines for various purposes. It is indicative primarily of the high stability of welded joint quality, achieved when working in the severe climatic conditions. FBW ensures a high output per team member, lowers the requirements to operator qualifications and welding consumables cost.

Available experience of application of FBW of pipelines, as well as analysis of inquiries from construction organizations, including foreign companies, allows determination of the following main directions of improvement of FBW technology and equipment, which should be pursued to further increase the effectiveness and competitiveness of this welding process:

• improvement of the technology of FBW in order to lower the power of the sources, metal losses in flashing and upsetting;

• development of technologies of FBW of higher strength pipes (X80--X100 type), providing the required mechanical properties;

• development of systems of automated non-destructive and on-line control of pipes joined by FBW;

• development of a new generation of FBW equipment, featuring a high manoeuvrability and lower power consumption;

• development of auxiliary equipment (flash removers), providing a higher accuracy of flash cutting, taking into account the requirements of modern methods of diagnostics.

Over the last years developments, aimed at solving the above problems, have been performed under an intergovernmental program.

Improvement of the technology of FBW of pipes. To achieve a stable continuous flashing, which is the base of the applied technologies of FBW of pipes, it is necessary for the set power of the power source to be 3 times higher than that consumed in welding [5]. When this proportion is decreased, the probability of short-circuiting of the parts being melted becomes higher, flashing stability is disturbed, which results in unstable heating. Application of various regulators of feed rate in flashing [5] allows reducing this ratio to 2.5. Increase of flashing stability at other conditions being equal is achieved also at lowering of the short-circuit resistance of welding machines. Conducted research demonstrated the possibility of a significant lowering of the set power of the source with development of new fast-response drives of FBW machines and lowering by 20--30 % the short-circuiting resistance due to improvement of the design of the machine welding circuit. An additional reserve for lowering the set power of the sources is also application of various power storage devices, providing the possibility of a short-term increase of the consumed energy.

Research performed over the last years at the E.O. Paton Electric Welding Institute permitted finding the methods for significant intensification of heating of the parts being welded during flashing [6]. The essence of these methods consists in that the resistance in the contact between the parts being welded is con-

Table 1. Main process parameters in pulsed and continuous FBW of pipes

Pipe material	Pipe diameter and wall thickness, mm	Welding time, s		Maximum consumed machine power, kV·A		Flashing and upsetting tolerance, mm	
		PF*	CF**	PF*	CF**	PF*	CF**
St20	219; 10	30	120	200	250	18	30
St20	219; 25	100	210	200	250	20	45
09G2S	530; 10	60	150	280	500	20	30
09G2S	630; 14	70	160	350	500	24	40
Õ65	920; 12	80	150	400	600	25	36
Õ65	920; 25	120	200	400	800	28	48
Õ65	1020; 14	90	160	500	800	20	38
Õ65, Õ70	1220; 16	110	180	550	800	23	45
Õ70	1420; 19.5	120	200	800	1100	25	50
Õ80	1420; 18.7	120	200	800	1200	25	45

*PF — pulsed flashing.
**CF — continuous flashing.

tinuously maintained on the level of limit power, which may be provided by the source of power supply. This is achieved by using automatic fast-response control systems, acting on the flashing drive of the welding machine and the mains voltage. Development of these systems was made possible by the application of modern components of the hydraulic drive and electronic control. A characteristic feature of the new flashing process, which was called pulsed flashing, is more intensive heating of parts than with continuous flashing. At the same power, the welding time and flashing allowances are reduced 2 --2.5 times. Depending on the set power, metal heating in pulsed flashing can be obtained in a wider range of set power values than with continuous flashing, also at lower specific powers. Depending on the set values of the source power the heating duration t_w and temperature distribution in the HAZ metal can be varied, which opens up new possibilities, particularly in welding thick-walled pipes, and pipes of high-strength steel. In particular, a feature of pulsed flashing is the possibility of achieving highly-concentrated heating, when the near-contact layers of the metal are heated up to a high temperature, and the total heating zone is relatively narrow (Figure 1). Due to that sound welding can be ensured with the smaller total heating zone and upsetting value, as all the deformation is concentrated in the near-contact layer. These advantages are particularly obvious in welding high-strength steels of X80--X100 type, highly sensitive to heating and prone to softening.

Pulsed flashing was used to develop the technology of welding pipes with different wall thickness. The main parameters of the modes of welding pipes with pulsed flashing are given in Table 1. For pipes of 114--325 mm diameters the data were obtained in welding in an upgraded K584 unit. For large-diameter pipes the data were obtained in welding large-diameter segments (up to 5000 mm²) cut out of pipes. Such a procedure was tried out in simulation of the modes of continuous FBW of pipes of 1420 mm diameter. The data given in the Table are for pipes with the wall thickness, which is the limit for the above wall diameter. For comparison the Table gives similar data obtained in continuous FBW. Application of pulsed flashing allows reducing the welding duration 1.5--2 times for pipes of less than 12 mm thickness and almost 2--2.5 times for pipes with 20--25 mm wall thickness. The set power of the source is taken to be at the same level as in continuous FBW.

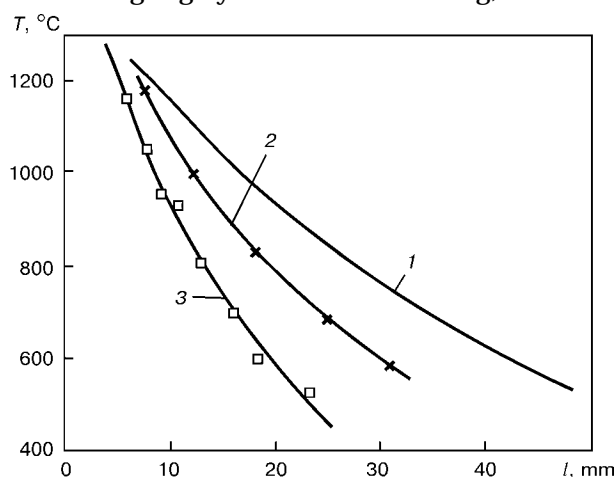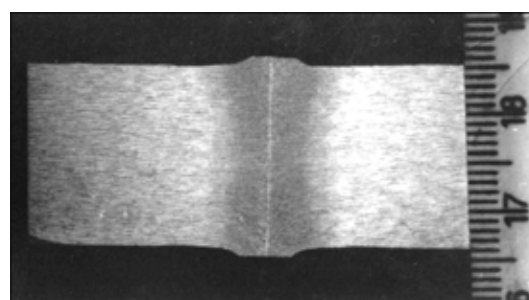**Figure 1.** Temperature distribution in the HAZ metal in welding by continuous (*1*) and pulsed flashing (*2, 3*): *1* — t_w = 180; *2* — 120; *3* — 30 s

Figure 2. Macrosection of a pipe joint of X80 steel

Table. 2. Technical characteristics of equipment for MIAB welding of pipes

Machine index	Diameter of welded pipes, mm	Wall thickness, mm	Productivity, butt/h	Upset force, kN	Consumed power, kV·A	Weight, kg
MD101	10–42	1--4	80	40	30	230
MD102	25–60	2--6	120	60	45	440
MD103	57--114	2--8	70	160	60	950
K872	70--219	2.5–16.0	30	300	100	2000

In pulsed FBW formation of sound joints is provided at a lower value of upsetting, and weld reinforcement is reduced, accordingly, the reinforcement having a slightly convex shape (Figure 2). Therefore, the labour consumption in machining of the welded butts is significantly reduced, and it is easier to achieve the required geometrical shape of welds during finish cutting off of flash. In this case it appears possible to cut off the flash, using a cutter system with radial displacement of cutters instead of the currently applied broach.

Pressure welding of pipes with preheating by magnetically-impelled arc (called MIAB). This welding process close to FBW as to the special features of joint formation, became applied on a commercial scale in CIS countries and abroad, mainly for joining pipes of small diameters (up to 50 mm) with the wall thickness of up to 6 mm [4]. It has a number of advantages compared to FBW, in particular, is characterized by lower losses of metal for flashing and consumed power. In MIAB method there is no need to protect the pipe surface before welding, weld reinforcement is lower, which allows in many cases elimination of the operation of flash removal after welding. Disadvantages of MIAB welding process include the requirements to more accurate alignment of pipes before welding and impossibility of producing sound joints with pipe thickness above 6 mm.

PWI has for many years conducted developments, aimed at widening the fields of application of this welding process, and designing a new generation of equipment of automatic control systems. Over the last five years systems of automatic control of the process have been developed, which allow a considerable improvement of the reproducibility of the specified welding parameters at variation of the accuracy of pipe alignment or geometrical dimensions of pipe ends. Systems of automatic on-line control and diagnostics of the quality of joints by the change of welding parameters and computerized systems of acquisition and storage of information on the joint quality have been developed. Main characteristics of the equipment, full-scale manufacturing of which has been mastered by the enterprises of the Scientific-Technological Complex «E.O. Paton Electric Welding Institute», are given in Table 2. Welding machines of MD type are used in various industries, MD1, MD2 machines are used by Tyumen construction organizations, Russia, K872 machine (Figure 3) is designed for welding thin-walled pipes of up to 219 mm diameter of 10 mm thickness, including piping of gas distribution networks.

Over the last years methods have been found to control the process of arc rotation in a magnetic field, which allow ensuring uniform heating in MIAB of pipes with the wall thickness greater than 6 mm. This is achieved by controlling the magnetic field components in the gap between the parts being welded, which induces arc scanning across the wall thickness. Pipes with the wall thickness of up to 16 mm have been welded by such a method. Equipment is currently being developed, which allows welding by MIAB

Table 3. Mechanical properties of joints in MIAB welding

Steel grade	Pipe diameter and wall thickness, mm	Ultimate tensile strength, MPa		Impact toughness KCV, J/cm²	
		Base metal	Welded joint	Base metal	Welded joint
St20	32; 5	488--509 / 502	488--509 / 502	94--100 / 98	88--94 / 90
St20	89; 10	488--509 / 502	488--509 / 502	92--100 / 97	86--94 / 90
St20	219; 6	488--509 / 502	488--509 / 502	90--100 / 95	84--92 / 88
St35	48; 4	538--565 / 551	538--565 / 551	56--64 / 60	52--96 / 70
St35	76; 16	536--565 / 550	536--565 / 550	56--64 / 60	42--68 / 55
12Kh1MF	32; 5	536--566 / 550	536--566 / 550	133--144 / 138	56--116 / 86
S75	48; 5	826--870 / 852	822--862 / 838	58--66 / 61	33--80 / 57

method pipes of 114--325 mm diameter, with up to 12 mm wall thickness. It may be used to weld various oil and gas pipelines.

Comprehensive mechanical testing has been conducted of pipe joints of various steels, welded by MIAB. As is seen from Table 3, strength and ductility characteristics of welded joints are quite close to similar characteristics of base metal.

Quality control of FBW joints. FBW application for many years in construction of pipelines in various regions, including Extreme North, is indicative of the high and stable quality of joints [7]. In keeping with the current specifications, quality of circumferential butts welded by FBW, is controlled by manual ultrasonic testing (UT) (in many cases selective) and on-line control (100 %) based on recording the main parameters of the process, which affect the joint quality. In addition, 1 % of the butts are cut out with subsequent mechanical testing of welded joints.

Mean statistical figures on the number of rejected butts, which are based on analysis of the results of control of ten thousand kilometers of welded pipelines of different diameter, are 0.4 %. Of the above number of rejected butts up to 80 % are rejected because of deviations of geometrical dimensions of welds (misalignment, poorly cut-off flash). Proceeding from the data obtained in control of individual sections of pipelines of 1420 mm diameter of 100 km length, the number of rejected butts is not more than 0.1 %.

Taking into account the gained experience of control of flash-butt welded pipe joints work has been conducted over the last years to improve the non-destructive and on-line methods of control. This work has been conducted together with R&D Institute of Shipbuiding Technology, Russia, under an Intergovernmental Program «Highly Reliable Pipeline Transport».

The main purpose of the work was automation of the control process and determination of the algorithms of quality assessment, using computerized systems. A key issue in development of automated UT is identification of various defects, which may appear in the joints made by pressure welding (including thin oxide films), using standards, universally accepted for arc welding processes, and determination of the validity of these defects detection. In the second stage of work performance investigation of the influence of various defect categories on mechanical properties of the joints was conducted. A procedure was widely used, which envisages testing wide samples (sectors cut out of full-scale pipes) under different types of loading, test temperatures and stress concentrations. These investigations allowed establishing the influence of various defect categories, reliably detected by UT, on mechanical properties of joints; determining the categories of inadmissible defects and limit dimensions of the admissible defects.

Shape of weld reinforcement can have a significant influence on UT results. According to technical requirements, the flash and partially the reinforcement
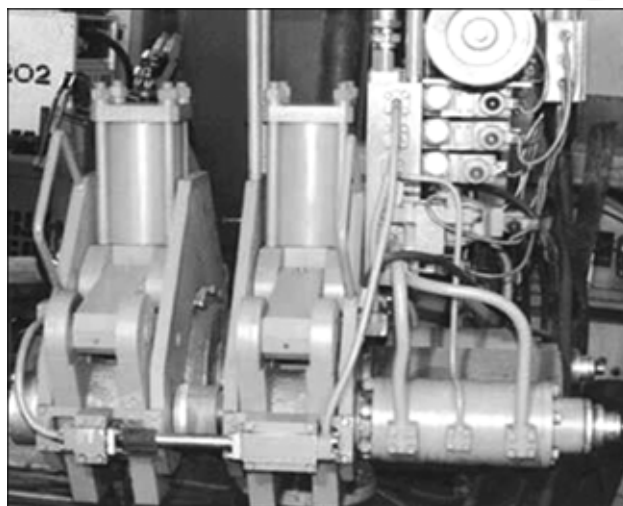
Figure 3. K872 machine for press welding of pipes of 60--219 mm diameter with heating by an arc rotating in a magnetic field

of the weld are removed after welding and weld reinforcement is not more than 2 mm. When universally accepted procedures are used, the above-mentioned protrusions on weld boundaries generate signals, which distort UT indications. Development of a system of sensors and transducers, functioning in a tandem, allowed eliminating the influence of signals received from weld boundaries on control results. UT studies were conducted by applying modern methods of diffracted waves, as well as pulse-echo and synthesized aperture methods. Control was performed using ZIPSCAN system.

During the above investigations also X-ray inspection of the joints was performed as specified for electric arc welding. This work provided comparative data on defect detectability by UT and X-ray method. It was established, that simultaneous application of «tandem» method and diffracted wave method allowed a significant reduction of the number of false signals, due to weld geometry, and improvement of the validity of detection of thin defects of oxide film type. Practically all the defects, influencing the mechanical properties of joints, generate signals, exceeding the accepted standard values, and are reliably detected at quite large deviations of geometrical dimensions of welds.

Comparison of the data given in Table 4 shows that UT results agree well with those of mechanical testing of full-scale samples with a notch along the joint line, where all the possible defects are revealed. Validity of UT results is higher than 0.95 in detection of inadmissible defects and 0.92 for all the defects. Presence of weld reinforcement and up to 3 mm misalignment does not influence the validity of control indications. Detectability of defects of oxide film type and non-metallic inclusions by X-ray inspection is low.

Results of the performed research were the basis to develop the basic technology of UT of flash-butt welded joints of pipes, which may be used to control the quality of circumferential welds in pipes with 8--30 mm wall thickness. Up-to-date UT systems, ap-

Table 4. Results of quality control of joints made by FBW

Batch No.	Butt No.	Geometrical shape of the weld	Type and dimensions of defects at rupture tests, mm²		
			X-ray inspection	Ultrasonic testing	Breaking tests
1	1	Without reinforcement, without displacement	D(12, 6)	D(12, 6), OF(136, 64)	D(12, 6)
	2		D(20, 8)	D(20, 8); OF(100, 90)	D(20, 8); OF(100, 30)
	3		–	D(1); OF(40); NMI(150)	D(1); OF(40); NMI(136, 64)
	4		–	D(10); OF(200); NMI(64)	D(10); OF(200)
	5		–	–	OF(6); OF(25)
2	1	Reinforcement of 2--3 mm	–	–	OF(48, 24, 20, 8)
	2		–	D(1) (cluster); OF(100)	D(1, 1, 1); OF(100)
	3		D(6)	OF(90)	D(6); OF(90)
	4		D(4)	–	D(4); OF(48, 28, 20, 8)
	5		–	D(4, 4, 2); OF(80, 40, 25, 25)	D(4, 4, 2); OF(80, 40, 25, 25)
3	1	Reinforcement of 2--3 mm, misalignment 2 mm	–	D(8, 6)	D(8, 6)
	2		–	D(16); OF(150)	D(16); OF(150)
	3		–	D(20); OF(200)	D(20); OF(200)
	4		–	–	NMI(100, 10)
	5		–	D(9); D(50)	D(9); D(50)
4	1	Reinforcement of 2–3 mm, misalignment 3.5--4.5 mm	–	OF(40)	OF(40)
	2		–	–	OF(20)
	3		–	OF(75)	OF(75)
	4		–	–	OF(75)
	5		–	OF(100)	OF(100)

N o t e . – — no defect; D — lack-of-penetration of discontinuity type; OF — lack-of-penetration of oxide film type; NMI — lack-of-penetration of non-metallic inclusion type.

plied in weld control in electric arc welding processes can be used in this case.

On-line control. On-line control was developed and introduced at the start of 1980s in connection with large-scale use of FBW in construction of critical pipelines. The main feature of the developed technology of FBW of pipes is use of the method of preheating by continuous flashing without resistance preheating with automatic regulation of the main process parameters. In this case, the latter are assigned by programs in combination with use of feedbacks, which permits automatic correction of the parameter values at the change of operating conditions. This enables ensuring a high reproducibility of the specified conditions of heating and deformation in welding. This further allows diagnosing the joint quality, depending on the value of deviation of the main parameters recorded during welding from those specified by the programs. During many years of the above technology application, a considerable databank has been accumulated, which demonstrates the interrelation between the joint quality and welding parameter deviations from the specified values, which occurred during operation. Processing of these data, as well as simulation of various conditions of welding with deviations

from the accepted modes, allowed determination of the criteria of evaluation of the joint quality by the results of comparing parameters recorded by the registering instruments with standard samples. Parameter recording was introduced into the current standard for acceptance of flash-butt welded joints as one of the mandatory methods of control. Interpretation of such diagrams requires the welding operators and controllers to have certain skills and does not eliminate subjective evaluation. Therefore, over the last years a computerized system has been developed for evaluation of the quality of joints, which is also based on measurement and comparison of the main parameters of the process.

Figure 4 gives a block-diagram of the system of control of the joint quality. It is based on PLC logical controller in combination with a computer. With such a design it allows controlling the welding process and supports the functions of on-line control. PLC program is constructed so, that first the controller analyzes the signals from the sensors, and then proceeding from their analysis a machine control command is generated. The algorithm of the control program allows tracing a number of possible undesirable situations, leading to disturbance of stable flashing, and

by acting on the flashing drive and power source, eliminating these situations or stopping their progress. The controller further incorporates some other sensors. Signals from these sensors are being continuously analyzed and in the case, if any of the parameters goes beyond the tolerance range, the system reacts to them, depending on their significance in the overall algorithm of quality assessment. Welding may be interrupted in the case of a gross violation of the process. At individual deviations the signals are analyzed and all the obtained information is immediately recorded into the computer memory and simultaneously displayed in the digital and analog form. After completion of the welding process, the stored data are read, process parameters are calculated and analyzed in keeping with the incorporated quality algorithm, and the computer takes a decision on this welded joint by the «fit--unfit» principle. Analysis result is displayed and automatically printed-out in such a way, that by the end of the shift a complete list is made of the welded butt joints with evaluation of their quality (Figure 5). A special program has been developed for the computer, which allows graphic representation of the progress of the welding process, both as a whole and of its individual fragments on a greater scale. Data on each butt joint is entered into the general data bank, accumulated during construction.
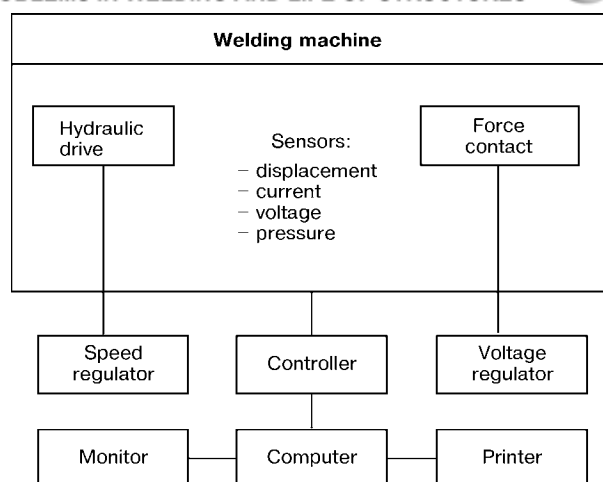
Figure 4. Block diagram of a system of control and monitoring of the process of FBW of pipes

The developed system of control of the parameters can be implemented as a separate attachment, which adapts easily to the currently used machines for FBW of pipes, in particular, K584, K700 machines. It is made up of a production or home computer with a printer and electronic block, as well as a set of current, voltage and displacement sensors. Such a system, based on a portable computer, was introduced in 2001 in an operating K700 machine.

Operator _____ Stamp _____ Controller _____

Butt No.	Time	U_w, V	V_{fl}, mm/s	$t_{pr.fl}$, s	V_1, mm/s	t_1, s	V_2, mm/s	t_2, s	t_{f}, s	Vfin, mm/s
xx00-000-1	14:41	1	0.15	50	0.15	55	*0.18	118	14	1.36
pc00-000-1	15:37	409	0.15	95	0.15	56	0.19	116	14	0.99
pc00-000-2	16:09	410	0.15	94	0.15	56	0.20	114	14	0.98
pc00-001-1	16:44	412	0.15	96	0.15	56	0.19	116	14	0.99
pc00-001-2	17:42	408	0.16	98	0.15	56	0.21	113	14	0.99
pc00-002-1	18:20	410	0.14	98	0.16	55	0.20	113	15	1.15
pc00-002-2	18:48	409	0.15	91	0.16	55	0.21	110	14	0.99

Butt No.	t_{fin}, s	V_{ups}, mm/s	L_{ups}, mm	$t_{(I)}$, s	Allow., mm	P, MPa	Z_{sh-c}, $\mu m \cdot Ohm$	Short-circ.	Total time	Slip	Conclusion
xx00-000-1	1.4	64	11	*0.0	50.0	14.9	--	Not	238.7	Yes	Cold run
pc00-000-1	1.4	42	11	0.8	50.6	14.9	15.9	Not	283.2	Not	Fit
pc00-000-2	1.4	41	11	0.9	51.4	14.7	17.3	Not	280.1	Not	Fit
pc00-001-1	1.4	45	11	0.8	50.9	14.4	16.8	Not	282.9	Not	Fit
pc00-001-2	1.4	43	11	0.9	52.0	14.6	17.1	Not	284.5	Not	Fit
pc00-002-1	1.4	42	10	0.8	51.6	14.6	16.3	Not	282.4	Not	Fit
pc00-002-2	1.3	44	11	0.8	50.8	14.8	17.4	Yes	272.4	Not	Reject

Total number of butts: 6

Acceptable: 5

Rejected: 1

Figure 5. Shift report with computerized control in the pipe welding Sever-1 system (K700)

Figure 6. External machine for FBW of pipes of 630 mm diameter (K1007)
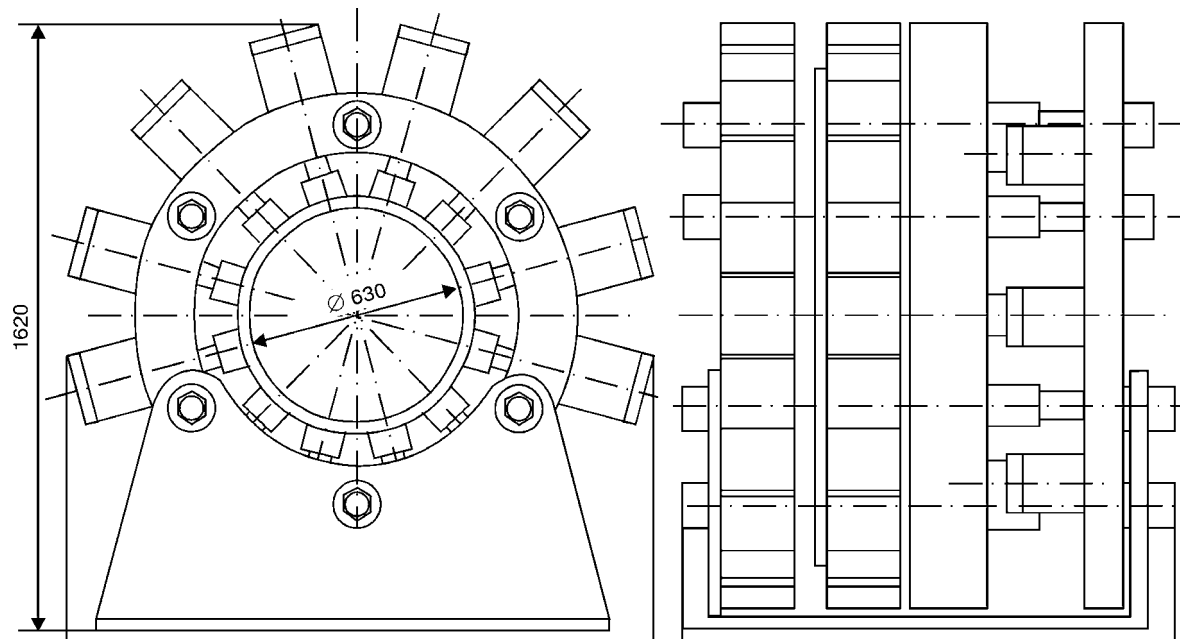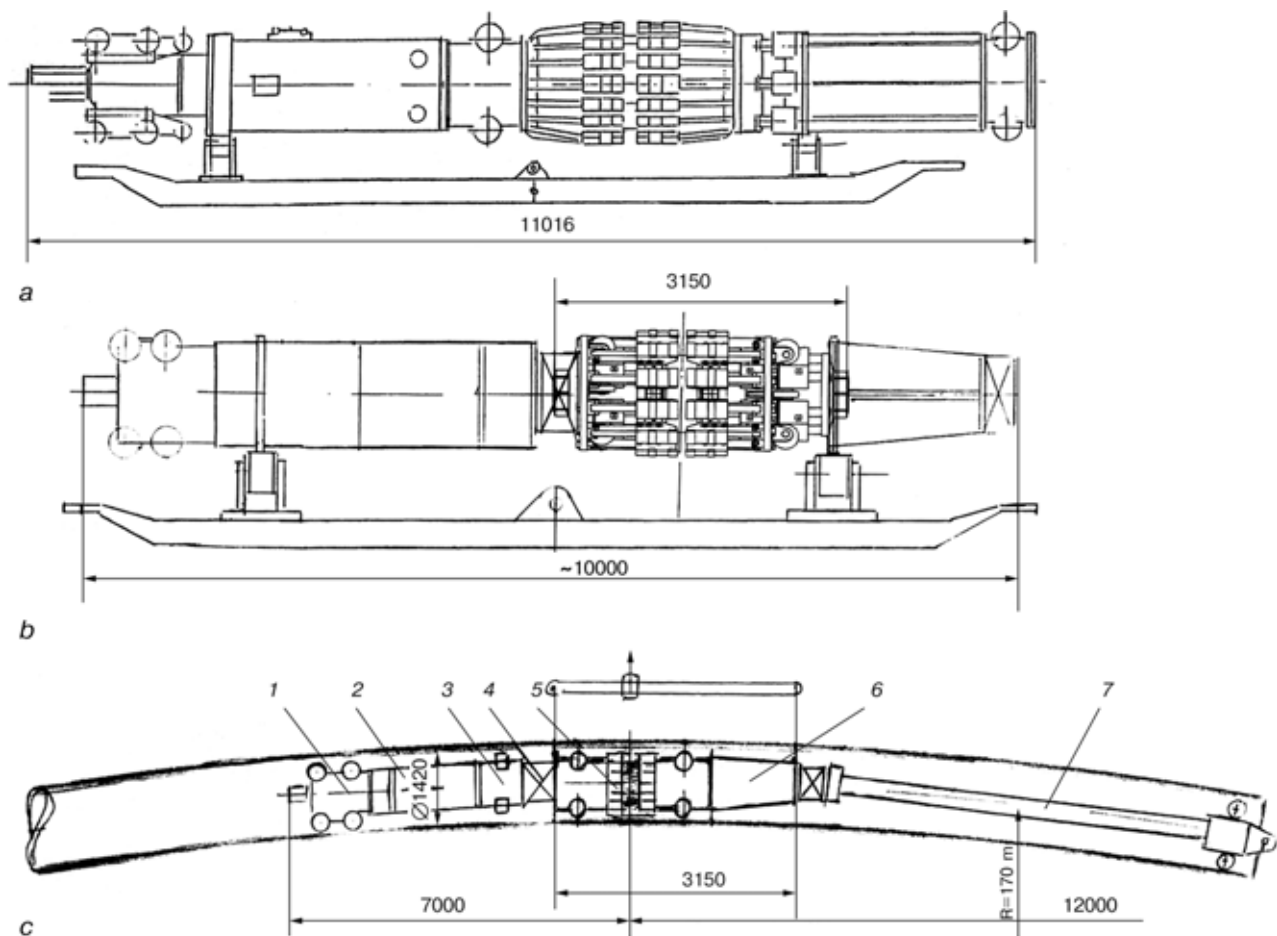
Figure 7. Diagram of in-pipe machines K700 (*a*) and K1007 (*b*) for FBW of pipes of 1420 mm diameter and their positioning in the pipe (*c*): *1* — displacement drive; *2* ---- pumping unit; *3* ---- flash remover; *4* ---- hinge; *5* — welding head; *6* — hydraulic block; *7* ---- rod

Table 5. Technical characteristics of machines for FBW of pipes

Machines type	Diameter and thickness of pipes, mm	Power at 50 % duty cycle, kV·A	Plant power, kV·A	Weight, t	Productivity, butt/h	Machine design
First generation machines						
Ê700	1420; 20	820	1000	26	6	In-pipe
Ê800	1220; 16	600	850	20	8	Same
Ê805	530; 8	300	500	12	10	External
Second generation machines						
Ê1006	1420; 20	650	800	16	10	In-pipe
Ê926	920--1020; 16	400	550	12	12	Same
Ê1007	630; 14	300	380	8	12	External

FBW equipment. Current experience of operation of external and in-pipe machines for FBW of pipes shows that in in site welding the effectiveness of their application is largely determined by the mobility of the entire equipment system, accuracy of alignment of pipe ends, which is provided by the machine alignment mechanism, and well as operation of the flash remover. In addition, in site welding it is often necessary to weld bent pipes. Implementation of the above developments enables a significant improvement of the technical and economic characteristics of FBW of pipes. However, this requires a significant change of the design of the main kinematic components of the electric circuit, hydraulic drive and control system, using modern components of the hydraulic system and electronics. This enables a significant reduction of the weight of the mechanical components of the machines, welding circuit impedance and consumed power, increase of the operating speed of the drive and implementation of advanced technology of pulsed FBW.

Development of a new generation of machines for FBW of pipes was based on the same concept of organization of welding operations in the shop and field conditions as that used for the first generation of machines. External design of the machines was selected for welding pipes of 114--325 and 377--630 mm diameters, and in-pipe design was used for large diameter pipes (710--1420 mm). External machines are fitted with built-in flash removers to remove the external flash in the hot condition and a separate flash remover of a new type for treatment of the internal flash, which is also performed in the hot condition. In-pipe machines have a built-in flash-remover to remove internal flash in the hot condition. External flash, similar to the first generation machines, is treated after welding in the cold condition by a separate mechanism.

For welding pipes of 114--320 mm diameter with up to 16 mm wall thickness an upgraded K584B machine can be used, manufacturing of which has been mastered in the Kakhovka Plant of Electric Welding Equipment. A new machine has been developed for pipes of 377--630 mm diameter with up to 14 mm wall thickness (Figure 6). It may be used both in the shop and in the field conditions.

A typical design of the in-pipe machine is shown in Figure 7, *a*. Its central part is an aligning device, hinged to two auxiliary blocks, which allows it to be moved inside bent tubes (Figure 7, *b*). A new type of flash removers is used in the machines, which provide finish treatment of the weld flash.

Table 5 gives the main technical characteristics of the new generation of the machines. For comparison it gives similar data for first generation machines. The new generation of equipment has an almost 2 times smaller weight, which increases its mobility, lower power plants can be used for feeding it, welding time is reduced 1.5--2 times, which is particularly important in welding thick-walled pipes. In 2003 it is intended to make pilot samples of some of the above machines.

1. Punchon, C., Saipen, A.B. (1999) Reduced pressure electron beam welding of steel pipelines. In: *Proc. of Int. Conf. on Advances in Welding Technology*, Houston, October, 1999.
2. Dorling, D.V., Loyer, A. (1999) Homopolar pulsed welding for pipeline application. In: *Proc. of Int. Conf. on Solid-Phase Welding*, Cambridge, September, 1999.
3. Huff, G. (1999) Radial friction welding for off-shore pipelines and rises. *Ibid.*
4. (1987) Pressschweissen mit magnetisch bewegtem Lichtbogen. In: *Proc. of DVS 2934*, May, 1987.
5. Kuchuk-Yatsenko, S.I. (1992) *Resistance flash-butt welding*. Kyiv: Naukova Dumka.
6. Kuchuk-Yatsenko, S.I., Didkovsky, A.V., Bogorsky, M.V. et al. *Resistance flash welding method.* Pat. 6297752B1 USA. Publ. 25.09.01.
7. Zagadarchuk, V.F., Kuchuk-Yatsenko, S.I., Kazymov, B.I. et al. (1991) Welding quality of X70 steel tubes produced by resistance flash welding. *Avtomatich. Svarka*, **4**, 27--32.

REVIEW OF QUALIFICATION AND CERTIFICATION SYSTEM FOR WELDING PERSONNEL IN JAPAN

H. KOGURE and **Yu. FUJITA**

Japan Welding Engineering Society, Japan

This paper summarizes the certification systems for welders and welding engineers established and implemented by the Japan Welding Engineering Society (JWES). The first issue for SMAW welders was appeared for carbon steel by JWES in 1944. After that, the various kind of issues for the different materials appeared with a variety of process has being introduced due to the request from the wide range of industries. The certification systems for welding engineers has been established in 1971. The scheme for the welders and the welding engineers are revised slightly in 1998 along with ISO Guide 61 ⁄ EN 45013 and also along with ISO 14731 (JIS Z 3410). The schemes are acrreditated by the Japan Accreditation Body for conformity assessment in 1999. Regarding the qualification system for welding engineer, welding technologist, welding specialist and welding practitioner, the Authorized National Body of Japan which are operated under JWES are established and approved by IIW in 2000, and the transition arrangements from the above certification holder has being implemented from 2001. There are unique Approved Training Body in Nagoya for the qualification system for welding engineer, welding technologist and welding specialist.

Keywords: welding personnel, systems of certification, classification, industrial standards, accreditation, center of training

The certification systems for welding personnel shown in Table 1 through Table 5 by JWES have been established and implemented with those people from academic organizations, research institutes and industries rather on a voluntary spirit to enhance welding technology in Japan.

The certification systems for welding engineer levels and six categories of welder have been accredited from Japan Accreditation Board (JAB) for conformity assessment in accordance with the procedures required in JAB standard CP 100 (equivalent to ISO Guide 61 ⁄ EN 45013) in 1999.

Under the support (including financial aspect) of Japanese industrial organizations, such as Japan Automobile Industry Association, Japan Machinery Industry Association, Japan Shipbuilding Association and so on, JAB was established in order to implement assessment and certification ⁄ registration in accordance with ISO standards, such as ISO 9000, in 1993 in Japan. JWES has also joined the foundation of this organization because the certification systems for welding personnel become very important in industry to assure the quality of welding products according to ISO 9000 and ⁄ or ISO 3834 «Quality Requirements for Welding» (JIS Z 3400).

Within the original version of ISO 9000 series of standards for quality management systems, welding is to be treated as a «Special Process» since the quality

Table 1. Classification and designation of welders certification for carbon steel welding

Grade, level and welding position					Welding process and joint type			
Plate	Plate		Plate		Welding process	Material thickness	Welding joint	
Flat	Vertical	Horizontal	Overhead	Horizontal fixed			Groove	Backing plate
N-1F	N-1V	N-1H	N-1O	N-1P	SMAW	Thin	H or V	No
A-2F	A-2V	A-2H	A-2O	A-2P		Medium	V	Yes
N-2F	N-2V	N-2H	N-2O	N-2P				No
A-3F	A-3V	A-3H	A-3O	A-3P		Thick		Yes
N-3F	N-3V	N-3H	N-3O	N-3P				No
C-2F	C-2V	C-2H	C-2O	C-2P	Combined process	Medium		Same
C-3F	C-3V	C-3H	C-3O	C-3P		Thick		
T-1F	T-1V	T-1H	T-1O	T-1P	GTAW	Thin	H or V	
G-1F	G-1V	G-1H	G-1O	G-1P	GAS			

Notes. N — without backing plate; A — with backing plate; 1 — thin plate thickness; 2 — medium plate thickness; 3 — thick plate thickness; F — flat position; V — vertical position; H — horizontal position; O — overhead position; P — pipe welding with horizontally fixed pipe. 2. Combined welding process, such as GTAW + SMAW. 3. According to JIS Z 3801–1997.

Table 2. Test items of certification testing

Grade of classification					Kinds of testing items			
F	V	H	O	P	VT	FB	RS	SB
N-1F	N-1V	N-1H	N-1O	N-1P	–	–	--	✳
A-2F	A-2V	A-2H	A-2O	A-2P	–	–	--	✳
N-2F	N-2V	N-2H	N-2O	N-2P	–	–	--	✳
A-3F	A-3V	A-3H	A-3O	A-3P	–	✳	--	--
N-3F	N-3V	N-3H	N-3O	N-3P	–	✳	--	--
C-2F	C-2V	C-2H	C-2O	C-2P	–	–	--	✳
C-3F	C-3V	C-3H	C-3O	C-3P	–	✳	--	--
T-1F	T-1V	T-1H	T-1O	T-1P	–	–	--	✳
G-1F	G-1V	G-1H	G-1O	G-1P	–	–	--	✳

Notes. 1. VT — visual test; FB — face bend test; RB — root bend test; SB — side bend test; – — to be carried out; ✳ — to be omitted. 2. According to JIS Z 3801–1997.

Table 3. Classification of certification of semi-automatic welders for carbon steels

Grade, level and welding position					Welding process and joint type			
Plate	Plate			Pipe	Welding process	Material thickness	Welding joint	
Flat	Vertical	Horizontal	Overhead	Horizontal fixed			Groove	Backing plate
SN-1F	SN-1V	SN-1H	SN-1O	SN-1P	SMAW (MAG)	Thin	H or V	No
SA-2F	SA-2V	SA-2H	SA-2O	SA-2P		Medium	V	Yes
SN-2F	SN-2V	SN-2H	SN-2O	SN-2P				No
SA-3F	SA-3V	SA-3H	SA-3O	SA-3P		Thick		Yes
SN-3F	SN-3V	SN-3H	SN-3O	SN-3P				No
SC-2F	SC-2V	SC-2H	SC-2O	SC-2P	Combined process	Medium		No
SC-3F	SC-3V	SC-3H	SC-3O	SC-3P		Thick		
SS-2F	SS-2V	SS-2H	SS-2O	SS-2P	GMAW (open arc)	Medium		Yes
SS-3F	SS-3V	SS-3H	SS-3O	SS-3P		Thick		

Notes. 1. S — semi-automatic welder (other designation are the same to Table 1). 2. Combined process, such as GTAW + GMAW. 3. Testing items: for thin and medium plate thickness VT, FB and RB; for thick plate thickness VT, RB and SB. 4. According to JIS Z 3841–1997.

Table 4. Classification of certification of welders for stainless steels

Grade, level and welding position					Welding process and joint type			
Plate				Pipe	Welding process	Material thickness	Welding joint	
Flat	Vertical	Horizontal	Overhead	Horizontal fixed			Groove	Backing plate
CN-F	CN-V	CN-H	CN-O	CN-P	SMAW	Medium	V	No
	--	–	CA-O	CA-P				Yes
	--	–	–	CN-PM	Combined			No
TN-F	TN-V	TN-H	TN-O	TN-P	GTAW	Thin		Same
MN-F	MN-V	MN-H	–	--	GMAW	Medium		»
MA-F	MA-V	MA-H	–	--				Yes

Notes. 1. Testing items are VT, FB and RB. 2. T — TIG (GTAW); M — MAG (GMAW). 3. Combined process, such as GTAW + GMAW. 4. According to JIS Z 3821–1997.

Table 5. JWES certification system for welders

Kind of certification	Standard referenced	Accreditation
SMAW for carbon steels (plates and pipes)	JIS Z 3801–97	JAB
Semi-automatic MAG, FCAW and combined with GTAW for carbon steels (plates and pipes)	JIS Z 3841–97	JAB
SMAW, GMAW, GTAW and combined with GTAW for stainless steels (plates and pipes)	JIS Z 3821–97	JAB
GTAW and GMAW for titanium and its alloys (plates and pipes)	JIS Z 3805–97	JAB
Manual hot gas welding for plastics (polyvinylchroride, polypropylene and polyethylene) (plates)	JIS Z 3831–97	JAB
Oxy-fuel gas brazing for copper, carbon steels and stainless steels (plates and tubes)	JIS Z 3891–97	JAB
SMAW, GMAW, GTAW and combined with GTAW for carbon steels, heat-resistant steels and stainless steels (plates and pipes)	JIS Z 3801, 3821, 3841	Voluntary with JPI[1]
SMAW filler welder for carbon steels (fillet only)	WES 8101–72	Voluntary
SMAW and GMAW for reinforced steel bars for PC construction	WES 8105–87	Voluntary[2]
SMAW, GMAW and FCAW for foundation pipe piles (vertically fixed pipes)	WES 8106[3]	Voluntary

Notes. 1. Tests are conducted by JWES, but qualification is made by JPI. 2. Tests are conducted by JWES, but qualification is made by the Architecture Pre-fabrication Association. 3. Carbon steel pipes with backing strip.

of welding cannot be fully verified by subsequent inspection and testing of the product to ensure that the required quality standards has been met. The special processes, at least, shall be validated to demonstrate their effectiveness and acceptability. The arrangements for validation shall be defined and shall address as following:

• processes to be qualified prior to use;

• qualification of equipment and personnel to be engaged;

• use of specific procedures and records;

• re-validation.

Certification systems for welders. The classification of the welding procedure specification and the related Japanese Industrial Standard (JIS) which are used for JWES certification for welders are shown in Tables 1--5.

The evaluation of the certification is performed based on a written examination for general welding technology, and also based on a practical test using sample material for the skill.

The test data banks for the written examination compose with 200 Q&A for a common welding technology field and about 30 Q&A for each specific field depending on a welding method by mainly multichoice form.

The practical test is evaluated by visual and bending test.

When the applicants pass the examination and the practical test, the certificate which is valid for one year will be issued.

After every one year, they have to submit a surveillance form which verify that they were engaged in the actual job during that one year of period less than six months interval, so that they can keep their skill through the engagement in the actual work.

After three year from getting the first certificate, they have to make a renewal application.

The number of applicants became in its peak as 120,000 in 1997 and the JWES certification systems become the most popular system in Japan, especially for frame structure industries, such as building construction, bridge etc.

But the number of applicants is decreasing after that due to the economic situation and other reasons.

One of the reason is that a welding robot is becoming popular in Japan, and now 3,000 units of welding robot for building construction are already shipped and become in operation.

JWES has established the certification system for robot operator in the field of building construction in 2001.

Other point is that welders from Asian countries come to Japan applying JITCO program which is supported by Japanese government, and many Japanese fabricators have employed these welders since they are good qualified person, and also they are good labor cost. They can stay in Japan for three years with JITCO program and during the period, they have to apply JWES welder certificate. Now up to 800 people come to Japan using JITCO program every year.

The purpose of JITCO program is to give a chance for the people of Asian countries to have a training and education during their stay as an employee of Japanese industries in Japan.

Certification system for welding engineers. *Background.* JWES established the certification standard for welding engineer according to JWES standard, WES 8103 in 1970, and the certification system started in 1972 based on the standard.

A major revision for the standard was made in 1998 so that the system meets the requirements of the

Table 6. Tasks, technical knowledge and job competence required for welding coordinators

Level	Tasks and activities	Technical knowledge and job competence
SWE	All activities described in Table 1 of ISO 14731	Comprehensive technical knowledge and job competence for providing supervising welding production and control of welding fabrication at a top level
L-1	Activities of items 1.3 and after parts described in Table 1 of ISO 14731	Specific technical knowledge and job competence for providing executing welding production and procedure control
L-2	Activities of 1.3, 1.6 and after parts described in Table 1 of ISO 14731	Basic technical knowledge and job competence assisting welding procedure control

international standard, e.g. ISO 14731 «Welding Co-ordination ---- Tasks and Responsibilities». The annex (informative) to ISO 14731 states that the following three groups of qualifications in the EWF scheme correspond to three levels of certification stipulated in ISO 14731:

- EWE (European Welding Engineer);
- EWT (European Welding Technologist);
- EWS (European Welding Specialist).

Through the above JWES standard, approximately 8100 number of Level 1 Welding Engineers, approximately 47,400 number of Level 2 Welding Engineers and approximately 1700 number of Senior Welding Engineers are certified by JWES until the end of 2000.

JWES has intended to become a certification / registration body accredited by JAB for welder and welding engineer and JWES has been accredited in accordance with JAB standards for personnel certification / registration body (CP-100 and CP-200) as the first certification body for personnel in Japan in 1999.

Thus, the JWES system has become more transparent, more objective, more impartial and internationally based on harmonizing with ISO standards.

The JWES certification system becomes popular especially for building construction and fabrication of steel frame industries in Japan since they have realized the importance of the role of welding coordinator for the quality of welding products and have adopted this certification system as a requirement. Then, the JWES certification system for welding engineers is becoming widely recognized in public.

Regarding senior welding engineers, the mutual recognition agreement was established between German Welding Society (DVS) and JWES though this agreement was terminated due to the establishment of IIW / EWF Diploma scheme.

The Japan International Cooperation Agency (JICA) has adopted JWES welding engineering system as one of the education and training course for the people of the development countries in Nagoya Training Center from more than twenty years ago.

The number of the people finished the education and training course becomes more than 200.

The transition arrangement for IIW Diploma from three groups of JWES welding engineer certificate holders has starts from 2001 and approximately 1000 of IIW Diploma has been issued until the end of 2002.

JWES certification system for welding coordination personnel. The levels of certification of welding coordinator are classified into three corresponding to ISO 14731 as shown in Table 5. Tasks, technical knowledge and activities required for each level is defined in Table 5.

The access conditions for the applicant for each level is required as shown in Table 6 which are based on the academic background and years of job experience relating to welding of the applicant. One of the features of the JWES system takes into account the academic career of the applicant, but not strictly limiting that of EWF or IIW qualification schemes. In the EWF or IIW scheme, for example, only the applicant who has a bachelor degree in the engineering is allowed to access the EWE or IWE examinations.

JWES conducts assessment examinations for each certification level twice a year. The examination consists of the written and oral examination. The technical knowledge and job competencies for the following modules will be examined:

- welding processes and equipment;
- materials and their behavior during welding;
- construction and design;
- fabrication and applications engineering

.The four modules are the same as those used in IIW (EWF) scheme, including the same syllabus (key words). The technical knowledge and job competencies which are necessary for the activities stipulated in ISO 14731 are included in module «Fabrication and applications engineering».

The oral examination is mandatory for the Senior Welding Engineer (SWE) level. On the other hand, applicants for level 1 and level 2 who have completed the education course which JWES has approved beforehand (not necessarily organized by JWES) may be exempted from the oral examination. If the score for the written examination of this candidate is around the border line (70 %), he / she shall take the oral examination.

When the candidate satisfies the acceptance criteria, JWES shall grant the certificate. The certificate is initially valid for two years.

Within six months prior to the expiry of validity, he / she shall submit a surveillance application form. JWES shall do the surveillance in which the written evidence of job engagement of welding is checked.

If the certificate holder is confirmed to be maintaining the competency by the surveillance, the va-

Table 7. Access condition for certification

Academic career or certification	SWE	Level 1	Level 2
BSc Degree (graduate of university) in welding engineering	1	1	1
BSc Degree (graduate of university) in engineering and science	3	2	1
Graduate of university in other than engineering or science	6	4	2
Graduate of college (two years education) in welding engineering	5	3	1
Graduate of two years college in engineering or science	7	5	1
Graduate of two years college in other than engineering or science	10	8	4
Graduate of college of technology	7	5	1
Graduate of engineering or science of vocational school	–	6	2
Graduate of technical high school	–	8	4
Graduate of high school other than technical or engineering	–	8	4
Academic career other than that of above columns	–	--	7
Level 1 Certificate holder	5	--	--
Level 2 Certificate holder	–	4	--

Note. Number is the minimum required years of job experience in welding engineering.

lidity of the certificate shall be extended by three more years.

Relation to the IIW qualification scheme. The International Institute of Welding (IIW) was established in 1948. At present, it consists of more than 40 member countries, including G8 countries, and its activities cover information exchanges in the annual assembly and intermediate meetings. It also include the preparation of the drafts for ISO standards, publication, organization of international conference and so on, in the fields of welding, cutting, joining and related engineering. It is planned the annual assembly in 2004 will be held in Osaka in Japan.

Based on the result of the discussion in the Commission 13 and Commission 14 of the IIW annual assembly held in Beijing in 1994, the decision was made to implement an IIW qualification scheme for welding personnel in world wide. After four years of further work, the IIW scheme was implemented.

In addition IIW and EWF agreed that the EWF scheme should be transferred to the IIW scheme within five years or as long as it is referenced in the EN 719 and ISO 14731 whichever is longer.

The EWF qualification scheme is referenced in the Annex of EN 719 and ISO 14731.

Under the Board of Directors in IIW, the International Authorization Board (IAB) was formed in order to implement the IIW schemes. This body consists of a supervisory board and two subsidiary Groups (A and B).

IAB defines the guidelines, rules and operating procedures that specify minimum requirements for the education, examination and qualification, rules and procedures for the implementation of the scheme.

These requirements, rules and procedures shall be applied uniformly by all countries involved. This shall be done by one appointed organization in each country to act for IIW, and these organizations shall be assessed and monitored in compliance with the rules.

These organization are defined as IIW Authorized National Bodies (ANBs). ANBs shall be responsible for ensuring that the standards of education, examination and qualification are maintained.

The objective of this system is that IIW qualified personnel at a certain level will be achieved to the same minimum level of knowledge, irrespective of the country in which they have been qualified.

IIW authorized only one organization related to welding technology for each IIW member country. Only the authorized ANB is allowed to join IAB activities.

It is the role of the ANB to act in its own country for IIW in respect of personnel qualification, including:

• the approval of Approved Training Bodies (ATBs) for the conduct of courses in accordance with IIW guideline;

• the conduct of the final examination;

• the qualification of the personnel and the recording of relevant information.

The ANB is able to extend qualification activities outside its country if the rules are strictly applied.

Comparing to JWES certification system, the features of the IIW qualification scheme are an education system based on hour basis and pay a great respect for the academic career. The education and minimum training hours and the syllabus are strictly adhered to for each level as follows:

• IWE: 446 hours;
• IWT: 340 hours;
• IWS: 222 hours;
• IWP: 146 hours.

If the candidate cannot fulfill the required academic career, he/she cannot enter the final examination. If the candidate obtain successful results in the examination, a diploma which is valid for life, is awarded by the ANB.

It is expected that the IIW scheme will be referenced in ISO 14731 in near future. When it is realized, the JWES system could be linked to IIW scheme through ISO 14731.

Transition arrangement from JWES certification to IIW qualification. Each country specific transition arrangements may be approved by IIW-IAB Group B if the country's system is correct. In case of Japan, if the candidates fulfill the access conditions which are already approved by IAB Group B, he / she may take the following transition arrangements to achieve different IIW qualification levels:

• JWES Senior Welding Engineer plus 5 years of work experience (WEx) in welding plus 24 hours case study training (CS) plus professional interview (PI);

• JWES Level 1 Welding Engineer plus 5 years WEx plus 24 hours CS plus PI;

• JWES Level 2 Welding Engineer plus 5 years WEx plus 24 hours CS plus PI;

• JWES Level 2 Welding Engineer (graduate from other technical high school) plus 8 years WEx plus 24 hours CS plus PI;

• JWES Welding Practitioner plus 10 years WEx plus 16 hours supplementary education plus PI;

• Professional Engineer in the fields of welding plus 7 years WEx plus PI.

The access condition of academic career for each case is adhered strictly to as well. The period of transition arrangements is limited up to 3 years for every case. Some of the above transition arrangements started in 2000 and others in 2001 in Japan.

CONCLUSION

Some of the JWES certification systems for welders and the JWES certification system for welding engineers were accredited by the Japan Accreditation Body for Conformity in accordance with ISO Guide 61 / 62. The welder's certification systems are based on the Japanese Industrial Standards. The welding engineer's certification system is based on ISO 14731 (JIS Z 3410). In Japan, the IIW qualification scheme was started for the welding engineers level and welding practitioner level in 2000.

APPLICATION OF MODERN HYBRID TECHNOLOGY FOR WELDING OF HIGH CORROSION RESISTANT Ni-BASED ALLOYS IN ENVIRONMENTAL TECHNOLOGY

H. HEROLD, M. ZINKE and **M. KARPENKO**
Otto von Guericke University of Magdeburg, Germany

The paper shows the advantages of application of a hybrid welding process (YAG laser + hot wire TIG) compared to TIG processes and laser welding, to produce reliable and sound joints of critical structures in high-nickel alloys. A great depth of penetration and high efficiency of the process can be achieved at a small input.

The public support for nuclear energy is relatively small in Germany. Therefore power plants using fossil fuel have been built in an increased number. Flue gas desulfurization (FGD) plants are prescribed in accordance with the valid law in Germany for limiting sulfur oxidation products, as well as accompanying gases (hydrochloric acid and hydrofluoric acid) from combustion processes of organic substances (hard and brown coal, oil). The consequence is that it is necessary to implement or retrofit such systems both in new and in existing power stations.

Different strong degrees of corrosion loads exist in a FGD plant. Especially areas, like untreated gas inlet, with a strong to very strong degree of corrosion load have to resist extreme corrosion attacks by sulfuric, hydrochloric and hydrofluoric acid, as well as by acid and halide-loaded water at partially extreme high temperatures and occurring erosion.

Although an intensive development of organic corrosion protection systems took place, tests with various special high-grade steels began in a larger extent in the 1970s. Based on experiences from the USA, the high-alloyed steels with the material No. 1.4429 (X2CrNiMoN17-13-3), 1.4439 (X2CrNiMoN17-13-5) and 1.4539 (X1NiCrMoCuN25-20-5) were applied in FGD. Because at components made from these materials corrosion damages occurred too, they are used only occasionally today.

Processing of high corrosion-resistant special high-grade steels and Ni-based alloys requires the development of flexible, reliable and efficient techniques to secure a high corrosion resistance of the welded structures, as well as an effective welding fabrication.

Welding processes. Due to the risks mentioned above, which exist when welding with Ni-based alloys, welds at composite materials within the medium-touched areas of FGD are executed almost exclusively by the TIG process. Various experiences showed that this process supplies very good weld quality necessary in the case of extremely high corrosion loads. A large disadvantage with the manual TIG welding process is its low productivity. A more effective version for wallpapering or joining of roll-cladded sheet metals represents the hot wire TIG welding process. This process is applicable in all welding positions, and welding speeds of ≈ 0.8 m/min can be achieved. A further advantage is the high deposit rate (about 5.8 kg/h at 100 % duty cycle, I_w = 300 A and wire diameter of 1.2 mm).

Also plasma-arc welding without keyhole effect shows always good prospects for a productive manufacturing of FGD from Ni-based alloys, since the pitting corrosion resistance of the plasma welded joints is not impaired. However, the welding speed has to be limited to maximum 0.33 m/min, in order to avoid weld imperfections due to the gap between the lap-joints.

Laser welds possess frequently characteristics, which are equivalent or even better than TIG joints. The heat influence on the material is around a multiple smaller due to the strongly concentrated energy input. The large disadvantages of the laser technology exist in its unfitness for field use and in the very high initial costs. Solid-state laser possesses good prerequisites for a site use compared to the gas lasers, since laser beams can be transported with low losses by fibre-optic cables up to 100 m and more. But the concentrated laser beam requires the adherence to small tolerances for joint preparation to avoid weld defects.

The hybrid technology, which has been known since the 1970s, opens a way out of this situation. It can offer a technically and economically interesting manufacturing possibility for wallpapering of extremely corrosively loaded industrial plants with corrosion-resistant high-performance materials.

From our current point of view, the process combination between Nd:YAG laser beam and TIG arc with hot wire feed offers itself with priority for a such welding of thin sheets under field conditions. On the one hand, the Nd:YAG laser beam is flexibly transportable by fibre-optic cables and TIG on the other hand, the TIG welding, indifferently whether with cold wire or hot wire feed, offers the most reliable and most frequently used high quality procedure for welding the materials mentioned above.

The equipment for hybrid welding consists of the TIG welding power source Magic Wave 2000 Fuzzy and the pulsed Nd:YAG solid-state laser HLS 622. For the combination of these two procedures a special hybrid welding head was developed (Figure), which guarantees the reproducible adjustment of all process-relevant parameters. The interaction between the three energy sources laser beam, TIG arc and hot wire causes an additional energy focusing in the process zone. Therefore a high welding depth and deposit efficiency can be achieved with smaller values of energy input. The procedure indicates very high welding speeds with very good weld qualities compared with non-hybrid TIG and laser welding processes and shows an example of a hybrid-welded lap-seam.

The maximal welding speed, achievable with the available equipment reaches 1.8 m / min. While using a solid-state laser with higher laser power (e.g. 1 kW) the welding speed could be increased above 2 m / min.

The processing of high performance materials requires the elaboration of flexible, reliable and efficient engineering processes. This necessity results from the requirements to guarantee a high quality of welded joints, as well as an effective manufacturing by welding. The combined hybrid Nd:YAG laser + hot wire TIG technology shows its superiority in re-
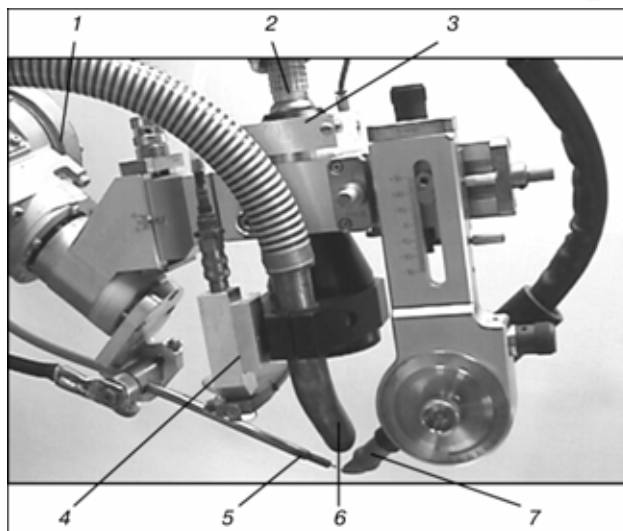
Hybrid welding head with integrated hot wire feeding, metal fume extraction and cross jet: *1* ---- robot arm; *2* — fibre optics; *3* ---- laser welding head; *4* — cross jet; *5* ---- hot wire feeding; *6* ---- extraction of metal fumes; *7* — TIG torch

lation to the single TIG welding, as well as the laser beam welding. The hybrid welding process could offer an economic problem solution for wallpapering FGD systems provided that appropriate site-suitable welding robot systems are developed.

ARC JOINING OF STEEL WITH ALUMINIUM

J. BRUCKNER

Fronius International GmbH, Wels, Austria

Latest investigations showed that joining of aluminium with steel would improve the characteristics of components used in industrial applications. Especially in the automotive industry joining of these two materials would minimize energy consumption. Until now mechanical joining of these two materials (clinching, screwing, etc.) was mostly done to attach or band them. Thermal joining is strongly restricted due to the formation of intermetallic phases. These phases are very brittle and therefore deteriorate the mechanical properties of such joints. Another attempt to join steel with aluminium is the use of laser systems combined with pressing devices. This paper describes a modified GMAW system to join Zn-coated steel with aluminium alloys of type 6000 (AlMgSi) and, with some restrictions, even with aluminium alloys of type 5000 (AlMg).

Keywords: *arc welding, steel, aluminium, strength properties, dissimilar joint*

Especially in transportation systems the reduction of weight and therefore reduction of energy is an important task. This task can be fulfilled by the use of materials with different characteristics. All the benefits of the two materials can be obtained, i.e. weight reduction, high thermal and electrical conductivity, etc. Steel and aluminium are used for technical industrial applications most often and therefore joining of these two materials leads to economic advantages.

Aluminium is already used in many fields of technology due to its good resistance against corrosion and good weldability. The low specific weight is also a very important property of aluminium, as it helps to decrease weight and fuel consumption in aviation and automotive industry. Many cars already have a spaceframe made of aluminium.

When joining aluminium with steel, the specific advantages of each of these materials can be utilized. Until now these materials were mostly joined by mechanical processes, e.g. clinching or riveting. Thermal joining processes, such as friction welding [1], spot welding or explosive welding [2] can only be used for very specific seam geometries and with many restrictions. Laser-welding [3] or laser-press welding [4] needs much effort.

Problems and demands. Thermal joining of aluminium with steel presents many problems. Differences in chemical and physical properties (e.g. melting point, thermal expansion coefficient, *E* modulus) and the insolubility of aluminium in steel lead to the formation of very brittle intermetallic phases (IMP), whose thickness depends on the heat input during

Figure 1. Overlap geometry for basic experiments

joining. This IMP deteriorates the static and dynamic tensile strength of the resulting joint.

As shows the binary Al–Fe phase diagram [2], only a few percent of aluminium can be in solid solution in iron. For 12 wt.% Al, a change in the crystal microstructure takes place and compounds, such as FeAl and Fe_3Al, are formed. These compounds are very hard and brittle. For a higher aluminium content the IMP Fe_2Al, Fe_2Al_5 and $FeAl_3$, which are also very brittle, are formed by volume diffusion of aluminium into iron and vice versa. This diffusion is caused by different chemical potentials.

Corrosion is also a very big problem. The larger the difference in galvanic potential, the larger amount of corrosion of the less noble component that can occur. As mentioned before, thermal joining of aluminium with steel can only be performed with many restrictions. For good joining, the thickness of the IMP should be less than 10 μm.

Tests and results. The work reported in this paper describes research conducted over a 12 year period to develop an arc joining process for Zn-coated steel sheets and aluminium in a thickness range of 0.8–3.0 mm. The process is a modified GMAW. In this process the Al-base material is welded with the filler metal, which has optimised properties for joining aluminium with steel to the surface of the Zn-coated steel.

Basic experiments were performed on an overlap geometry (2F position) with sheets of 1 mm thickness (Figure 1).

The tests were performed with a robot. The position of the torch was chosen so that the arc was concentrated on the melting of aluminium and the filler metal. Only small tolerances for torch position were allowed.

Further investigations were made with different torch positions and geometries. It is possible to braze overlap seams (2F, 3F (vertical down), 3F (vertical up)), filled seams (1F, 2F, 3F (vertical down)), flanged seams (1F, 3F (vertical down)) and butt seams (1G, 3G (vertical down)).

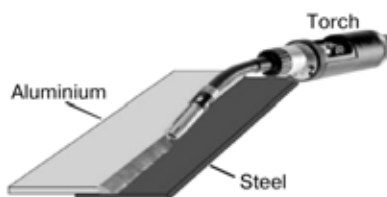The alloys tested are Al–0.4Mg–1.2Si (EN-AW 6016) and DDS 47G47GU (7.5 μm zinc coating on
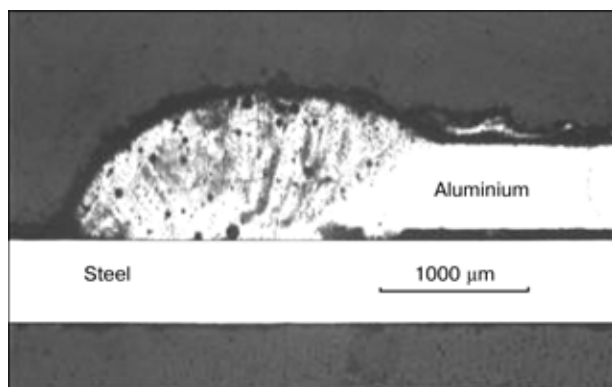
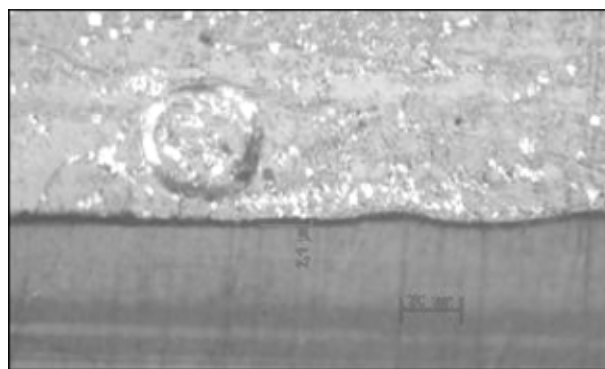**Figure 2.** Low magnification image

Figure 3. Intermetallic phase

each side). Further investigations were made with combinations of Al--0.8Mg--0.9Si (EN-AW 6120) and DDS G40 (10 μm zinc coating on each side), AlMg3 (EN-AW 5754) and DDS G40 (10 μm zinc coating on each side), Al--5Mg--Mn (EN-AW 5182) and CS G90 (20 μm zinc coating on each side).

Figure 2 shows a low magnification image, and Figure 3 ---- the IMP of an overlap joint (Al--0.4Mg--1.2Si∕DDS 47G47GU). Figure 2 clearly shows the different types of joining: aluminium is welded while steel is brazed. In Figure 3 the IMP has a thickness of 2.1 μm. In all experiments the thickness of the IMP was below 10 μm, and therefore the joint is more influenced by the properties of the base material than of the brittle IMP.

In tensile tests the break always occured in the HAZ of aluminium or sometimes even in the aluminium base material. Table 1 shows the average values of the tensile strength.

When joining heat treated alloys (type 6000), the tensile strength in the HAZ decreases due to precipitation processes. Therefore, the HAZ is the weakest zone with a loss of strength of about 30--40 %.

Diagram in Figure 4 shows the tensile strength of the material combination AW 6016 with DDS 47G47GU, each 1 mm thick. The lowest tensile strength is ≈ 60 % of the aluminium base material in condition T4 (tempered and age hardened).

Also for workable hardening alloys (type 5000), the tensile strength of the HAZ decreases due to recrystallization. The decrease of the strength depends on pre-treatment and on heat input during joining [5]. The break of the specimens mainly took place in the HAZ. The values of the tensile strength were lower than expected, probably due to decomposition
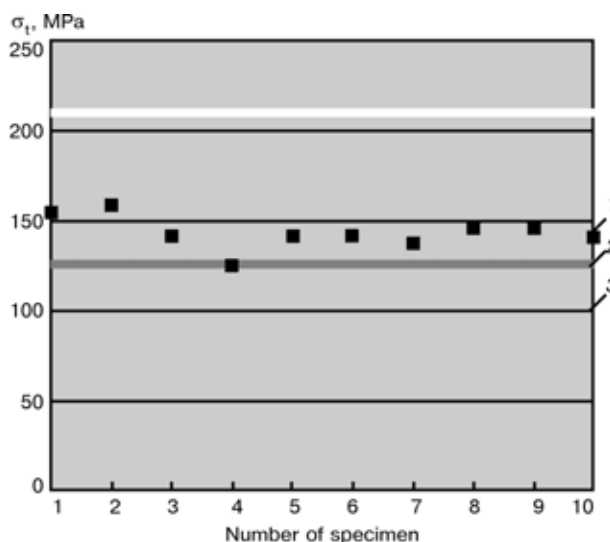

Figure 4. Diagram of tensile strength of AW 6016 in combination with DDS 47G47GU: *1* — tensile strength of specimen; *2* ---- tensile strength of aluminium base material in condition T4; *3* ---- 60 % of σ_t of aluminium base material in condition T4

Average values of tensile strength (DIN 50123)

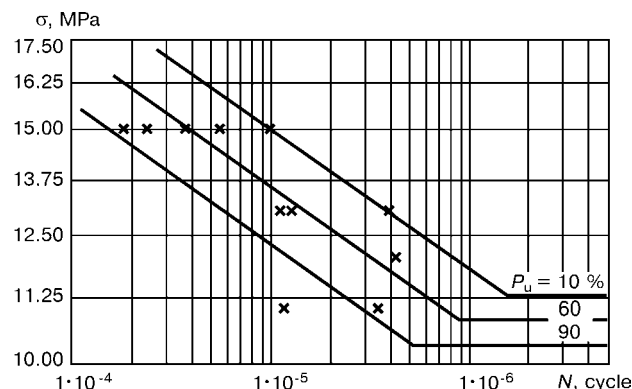| Base materials, thickness	Tensile strength, MPa
Al--0.4Mg--1.2Si∕DDS 47G47GU, 1.0 mm	145.00
Al--0.4Mg--1.2Si∕CS G90, 1.0 and 1.5 mm	166.70
AlMg3∕DDS G40, 1.0 mm	130.30
Al--5Mg--Mn∕DDS G40, 1.0 mm	134.50
Al--5Mg--Mn∕DDS G90, 1.0 and 1.5 mm	175.13

Figure 5. Diagram of fatigue cylce test of joint of aluminium sheet (1 mm thick) with steel sheet (1 mm thick)

in the vicinity of the weld. These data refer to the alloy Al--5Mg--Mn.

The welding speed depends on material thickness, torch position and seam geometry in the range of 30--70 cm ⁄ min. The welding is spatter-free, no special pre-treatment of the base material and no flux additive is needed. Corrosion tests (salt spray test, alternating climate test) showed that the surface treated specimen (e.g. cathodic immersion coating) do not corrode, neither intercrystalline nor contact corrosion. Choosing a proper weld geometry also reduces the corrosion tendency.

First limiting fatigue strength tests using overlap geometry showed even rather good results (Figure 5).

CONCLUSION

In general it was shown that joining of aluminium with steel is possible. Naturally, there are some re-strictions, e.g. certain zinc coating of steel, special filler metal, special GMAW process etc.

Preliminary tests showed rather good results for tensile strength, corrosion tendency and limiting fatigue strength. In addition it was proofed that it is possible to reduce the thickness of the intermetallic phase to values smaller then 2 μm. This fact is important for joining of steel with aluminium to minimize brittle failures.

1. Radscheit, R.R. (1996) *Laserstrahlfügen von Aluminium mit Staht*. Dissertation. Universität Bremen.
2. Kubaschewski, O. (1992) *Iron binary alloy phase diagramms*. Berlin: Springer.
3. Sepold, G. *Potenziale lasergefügte Mischverbindungen*.
4. Schör, H. (1998) *Schweißen und Hartlöten von Aluminiumwerkstoffen*. DVS.
5. Murti, K.G.K., Sundarsen, S. (1994) The formation of intermetallic phases in aluminium austenitic stainless steel friction welds. *Materials Forum*, **17**, 301--307.